

David Jin
Sally Lin (Eds.)

Advances in Computer Science, Intelligent System and Environment

 Springer

Advances in Intelligent and Soft Computing

Editor-in-Chief

Prof. Janusz Kacprzyk
Systems Research Institute
Polish Academy of Sciences
ul. Newelska 6
01-447 Warsaw
Poland
E-mail: kacprzyk@ibspan.waw.pl

Further volumes of this series can be found on our homepage: springer.com

Vol. 91. A. Abraham, J.M. Corchado, S.R. González, J.F. de Paz Santana (Eds.)
International Symposium on Distributed Computing and Artificial Intelligence, 2011
ISBN 978-3-642-19933-2

Vol. 92. P. Novais, D. Preuveneers, and J.M. Corchado (Eds.)
Ambient Intelligence - Software and Applications, 2011
ISBN 978-3-642-19936-3

Vol. 93. M.P. Rocha, J.M. Corchado, F. Fernández-Riverola, and A. Valencia (Eds.)
5th International Conference on Practical Applications of Computational Biology & Bioinformatics 6-8th, 2011
ISBN 978-3-642-19913-4

Vol. 94. J.M. Molina, J.R. Casar Corredra, M.F. Catedra Pérez, J. Ortega-García, and A.M. Bernardos Barbolla (Eds.)
User-Centric Technologies and Applications, 2011
ISBN 978-3-642-19907-3

Vol. 95. Robert Burduk, Marek Kurzyński, Michał Woźniak, and Andrzej Żołnierek (Eds.)
Computer Recognition Systems 4, 2011
ISBN 978-3-642-20319-0

Vol. 96. A. Gaspar-Cunha, R. Takahashi, G. Schaefer, and L. Costa (Eds.)
Soft Computing in Industrial Applications, 2011
ISBN 978-3-642-20504-0

Vol. 97. W. Zamojski, J. Kacprzyk, J. Mazurkiewicz, J. Sugier, and T. Walkowiak (Eds.)
Dependable Computer Systems, 2011
ISBN 978-3-642-21392-2

Vol. 98. Z.S. Hippe, J.L. Kulikowski, and T. Mroczek (Eds.)
Human – Computer Systems Interaction: Backgrounds and Applications 2, 2011
ISBN 978-3-642-23186-5

Vol. 99. Z.S. Hippe, J.L. Kulikowski, and Teresa Mroczek (Eds.)
Human – Computer Systems Interaction: Backgrounds and Applications 2, 2011
ISBN 978-3-642-23171-1

Vol. 100. Shoumei Li, Xia Wang, Yoshiaki Okazaki, Jun Kawabe, Toshiaki Murofushi, and Li Guan (Eds.)
Nonlinear Mathematics for Uncertainty and its Applications, 2011
ISBN 978-3-642-22832-2

Vol. 101. Darina Dicheva, Zdravko Markov, and Eliza Stefanova (Eds.)
Third International Conference on Software, Services and Semantic Technologies S3T 2011, 2011
ISBN 978-3-642-23162-9

Vol. 102. Ryszard S. Choraś (Ed.)
Image Processing and Communications Challenges 3, 2011
ISBN 978-3-642-23153-7

Vol. 103. Tadeusz Czachórski, Stanisław Kozielski, and Urszula Stańczyk (Eds.)
Man-Machine Interactions 2, 2011
ISBN 978-3-642-23168-1

Vol. 104. D. Jin and S. Lin (Eds.)
Advances in Computer Science, Intelligent System and Environment, 2011
ISBN 978-3-642-23776-8

David Jin and Sally Lin (Eds.)

Advances in Computer Science, Intelligent System and Environment

Vol. 1



Springer

Editors

Prof. David Jin
International Science & Education
Researcher Association
Wuhan Section
Special No.1
Jiangxia Road of Wuhan
Wuhan
China
E-mail: 30978376@qq.com

Prof. Sally Lin
International Science & Education
Researcher Association
Guangzhou Section
No.144, Jinheng Road
Jinbi Garden 85-1102
southern Road of Industry Avenue
Haizhu District
Guang Dong province
Guangzhou
China
E-mail: 864690186@qq.com

ISBN 978-3-642-23776-8

e-ISBN 978-3-642-23777-5

DOI 10.1007/978-3-642-23777-5

Advances in Intelligent and Soft Computing

ISSN 1867-5662

Library of Congress Control Number: 2011935562

© 2011 Springer-Verlag Berlin Heidelberg

This work is subject to copyright. All rights are reserved, whether the whole or part of the material is concerned, specifically the rights of translation, reprinting, reuse of illustrations, recitation, broadcasting, reproduction on microfilm or in any other way, and storage in data banks. Duplication of this publication or parts thereof is permitted only under the provisions of the German Copyright Law of September 9, 1965, in its current version, and permission for use must always be obtained from Springer. Violations are liable to prosecution under the German Copyright Law.

The use of general descriptive names, registered names, trademarks, etc. in this publication does not imply, even in the absence of a specific statement, that such names are exempt from the relevant protective laws and regulations and therefore free for general use.

Typeset & Cover Design: Scientific Publishing Services Pvt. Ltd., Chennai, India

Printed on acid-free paper

5 4 3 2 1 0

springer.com

Preface

International Science & Education Researcher Association (ISER) puts her focus on studying and exchanging academic achievements of international teaching and scientific research, and she also promotes education reform in the world. In addition, she serves herself on academic discussion and communication too, which is beneficial for education and scientific research. Thus it will stimulate the research interests of all researchers to stir up academic resonance.

CSISE 2011 is an integrated conference concentrating its focus upon Computer Science, Intelligent System and Environment. In the proceeding, you can learn much more knowledge about Computer Science, Intelligent System and Environment of researchers all around the world. The main role of the proceeding is to be used as an exchange pillar for researchers who are working in the mentioned field. In order to meet high standard of Springer, Advances in Intelligent and Soft Computing, the organization committee has made their efforts to do the following things. Firstly, poor quality paper has been refused after reviewing course by anonymous referee experts. Secondly, periodically review meetings have been held around the reviewers about five times for exchanging reviewing suggestions. Finally, the conference organization had several preliminary sessions before the conference. Through efforts of different people and departments, the conference will be successful and fruitful.

CSISE 2011 is co-sponsored by International Science & Education Researcher Association, Beijing Gireida Education Co. Ltd and Wuchang University of Technology, China. The goal of the conference is to provide researchers from Computer Science, Intelligent System and Environment based on modern information technology with a free exchanging forum to share the new ideas, new innovation and solutions with each other. In addition, the conference organizer will invite some famous keynote speaker to deliver their speech in the conference. All participants will have chance to discuss with the speakers face to face, which is very helpful for participants.

During the organization course, we have got help from different people, different departments, different institutions. Here, we would like to show our first sincere thanks to publishers of Springer, Advances in Intelligent and Soft Computing for their kind and enthusiastic help and best support for our conference. Secondly, the authors should be thanked too for their enthusiastic writing attitudes toward their papers. Thirdly, all members of program chairs, reviewers and program committees should also be appreciated for their hard work.

In a word, it is the different team efforts that they make our conference be successful on September 24–25, Guangzhou. We hope that all of participants can give us good suggestions to improve our working efficiency and service in the future. And we also hope to get your supporting all the way. Next year, In 2012, we look forward to seeing all of you at CSISE 2012.

July 2011

Helen Zhang
ISER association

Committee

Honor Chairs

Chen Bin	Beijing Normal University, China
Hu Chen	Peking University, China
Chunhua Tan	Beijing Normal University, China
Helen Zhang	University of Munich, China

Program Committee Chairs

Xiong Huang	International Science & Education Researcher Association, China
LiDing	International Science & Education Researcher Association, China
Zhihua Xu	International Science & Education Researcher Association, China

Organizing Chair

ZongMing Tu	Beijing Gireida Education Co. Ltd, China
Jijun Wang	Beijing Spon Technology Research Institution, China
Quanxiang	Beijing Prophet Science and Education Research Center, China

Publication Chair

Song Lin	International Science & Education Researcher Association, China
Xionghuang	International Science & Education Researcher Association, China

International Committees

Sally Wang	Beijing Normal University, China
LiLi	Dongguan University of Technology, China
BingXiao	Anhui University, China
Z.L. Wang	Wuhan University, China
Moon Seho	Hoseo University, Korea

Kongel Arearak Suranaree University of Technology, Thailand
Zhihua Xu International Science & Education Researcher Association,
China

Co-sponsored by

International Science & Education Researcher Association, China
VIP Information Conference Center, China

Reviewers of CSISE2011

Chunlin Xie Wuhan University of Science and Technology, China
LinQi Hubei University of Technology, China
Xiong Huang International Science & Education Researcher Association,
China
Gangshen International Science & Education Researcher Association,
China
Xiangrong Jiang Wuhan University of Technology, China
LiHu Linguistic and Linguistic Education Association, China
Moon Hyan Sungkyunkwan University, Korea
Guangwen South China University of Technology, China
Jack. H. Li George Mason University, USA
Marry. Y. Feng University of Technology Sydney, Australia
Feng Quan Zhongnan University of Finance and Economics, China
PengDing Hubei University, China
Songlin International Science & Education Researcher Association,
China
XiaoLie Nan International Science & Education Researcher Association,
China
ZhiYu International Science & Education Researcher Association,
China
XueJin International Science & Education Researcher Association,
China
Zhihua Xu International Science & Education Researcher Association,
China
WuYang International Science & Education Researcher Association,
China
QinXiao International Science & Education Researcher Association,
China
Weifeng Guo International Science & Education Researcher Association,
China
Li Hu Wuhan University of Science and Technology, China
ZhongYan Wuhan University of Science and Technology, China
Haiquan Huang Hubei University of Technology, China
Xiao Bing Wuhan University, China
Brown Wu Sun Yat-Sen University, China

Contents

Design and Study on Photovoltaic Array Simulator	1
<i>YongQiang Zhao</i>	
Design and Research of Battery Charged Intelligent System	7
<i>JiLin Jia</i>	
Accuracy Performances of Asymmetrical Right Circular Flexure Hinge	13
<i>Jianying Shen, Huawei Ji, Yun Zhao</i>	
The Application of the Pseudo Random Bit Index Sequence in the Image Encryption Algorithm	19
<i>Zongying Li</i>	
Research on the Method of Soft-sensing Intelligent Compensation for BOD Biosensors in Sewage	25
<i>Xiaoyi Wang, Zaiwen Liu, Shuoqi Dong, Xiaoping Zhao, Jiping Xu, Wandong Li, Xiaodong An</i>	
A New View on Regional Innovation System from Degree Distribution of Complex Networks Theory with Intelligent Attributes	33
<i>JiangBo Zheng</i>	
Research on a Modified Newton-Type Method with Fifth-Order Convergence for Solving Nonlinear Equations with Application in Material Science	39
<i>Han Li, Liang Fang</i>	
Image-Adaptive Watermarking Algorithm to Improve Watermarking Technology for Certain Watermarking Based on DWT and Chaos	43
<i>LingFeng Zhang, Xine You, YuPing Hu</i>	
An Intelligent System of Diagnosis Based on Associative Factor Uncertainty Speculation Inference	51
<i>Wenxue Tan, Xiping Wang, Xiaorong Xu</i>	
The Weather Disease Prediction Model Based on the Cognitive Map	57
<i>Yucheng Liu, Yubin Liu</i>	

Research on a Technology of Structural Equation Modeling Based Approach to Product Form Design Analysis	63
<i>Yongfeng Li, Liping Zhu</i>	
Discuss the Theoretical Rationale for the Existence of Banks	71
<i>Xiao Xiao, Songliang Cheng</i>	
Transmission Spectra of Liquid Surface Waves over Finite Graphene Structured Arrays of Cylinders	77
<i>Yong Wei, Sheng Li, GuoPing Tong, YouSheng Xu</i>	
Construction of Ontology Information System Based on Formal Concept Analysis	83
<i>LiuJie He, QingTuan Wang</i>	
The Electricity Information Acquisition Terminal Design Based on Linux Technology	89
<i>Yucheng Liu, Yubin Liu</i>	
New Prediction Algorithm for English Class Personnel Assignment Problem	95
<i>GuoYi Liu, ShuFang Wu, YanE Zhang</i>	
Research of E-Learning Intelligent Affective Model Based on BDI Agent with Learning Materials	99
<i>XueJing Gu, Qing Li, RuiJiang Diao</i>	
Quality Cost Optimization Problems Research Based on the Operating Station with Winning Machine	105
<i>WeiWei Liu, Lan Li</i>	
Method of the Road Lines Recognition in the Maps of Digital Material Based on Improved BP Neural Network	113
<i>Yunliang Yu, Tingting Zhang, Ye Bai, Jianqiang Wang</i>	
The Heavy Mineral Analysis Based on Immune Self-organizing Neural Network	119
<i>Yunliang Yu, Ye Bai, Tingting Zhang, Jianqiang Wang</i>	
Research on Mobile Electronically Published Materials Protection	125
<i>Sha Shi, Qiaoyan Wen, Mingzhu Li</i>	
Research on OCR Post-processing Applications for Handwritten Recognition Based on Analysis of Scientific Materials	131
<i>Zhijuan Hu, Jie Lin, Lu Wu</i>	
Research on Predicting Tool Wear Based on the BP Network	137
<i>Ping Jiang, ZhiPing Deng</i>	

Building the Internet of Things Using a Mobile RFID Security Protocol Based on Information Technology	143
<i>Tao Yan, Qiaoyan Wen</i>	
Study on Linear Regression Prediction Model of County Highway Passenger Transport Volume	151
<i>ShuangYing Xu, Lei Zhang, Jian Ma</i>	
Some Views of Chinese Construction of Modern Forestry	157
<i>Yuefen Wang, Yi Li</i>	
A Productive Time Length-Based Method for Multi-tenancy-Oriented Service Usage Metering and Billing	163
<i>Huixiang Zhou, Qiaoyan Wen, Xiaojun Yu</i>	
Comparison and Analysis of the Fusion Algorithms of Multi-spectral and Panchromatic Remote Sensing Image	169
<i>Chao Deng, Hui-na Li, Jie Han</i>	
An Approach for Plotting Reservoir Profile with the Rendering of Material and Texture of OpenGL	175
<i>Shaowei Pan, Husong Li, Liumei Zhang</i>	
A Nonmonotone Smoothing Algorithm for Second-Order Cone Programming in Failure Criteria	179
<i>XiaoNi Chi, WenLue Chen</i>	
The Research of Tobacco Leaf Roasting Control Tactics Based on Fuzzy PID	185
<i>Xifeng Liu, Chunxiang Xu, Chuanjin Huang, Wei Shiand</i>	
Advertising Marketing Communication Strategy under the Background of Media Convergence—Based on the Generation after 80s Advertising of Audience Behavior Changes	191
<i>Ye Bingqing</i>	
Building Smart Material Knowledge System Based on Ontology Bayesian Network and Grid Model	197
<i>Jing Li, XiuYing Sun</i>	
Research on Simulation of Electrostatic Discharge on Human Body Detonating the Gas	203
<i>Shengman Liu, Ying Zhang, Tingtai Wang, Jingchang Zhang</i>	
Delay-Dependent H_∞ Control for Uncertain Time-Delay Systems	209
<i>Cheng Wang</i>	
Statistical Analysis of Some Complex Censored Data	215
<i>Huanbin Liu, Congjun Rao</i>	

Application Study on Detection of Pipeline Weld Defects Based on SVMs . . .	221
<i>Wu Xiao Meng, Gao Wei Xin, Tang Nan</i>	
Analysis and Evaluation of Operation Mode for 35kV Loop-Network of Oilfield Distribution	227
<i>Wu Xiao Meng, Yan Su Li, Gao Wei Xin</i>	
An Improved Differential Evolution Algorithm for Optimization Problems	233
<i>Libiao Zhang, Xiangli Xu, Chunguang Zhou, Ming Ma, Zhezhou Yu</i>	
Case Study about City Brand Image Design Orientation of ZhangShu	239
<i>Guobin Peng</i>	
Maximum Power Point Tracking in Photovoltaic Grid-Connected Generation System by Using Fuzzy Control Algorithm	245
<i>Jie Liu, HaiZhu Yang</i>	
Research on the Power Marketing Technique Supporting System Based on Semantic Web Services	251
<i>Jun Liu, ChaoJu Hu</i>	
Design of Mechanics of Materials Study Monitor System Based on Distance Education Environment	257
<i>Ai Xiao Yan</i>	
An Improved Threshold Function for Wavelet De-noising	265
<i>Zhong Li, Dong-xue Zhang</i>	
A Modified MUSIC Algorithm Based on Eigen Space	271
<i>Qian Zhao, WenJuan Liang</i>	
The Theoretical Study of Paper Screening System	277
<i>Qingwen Qu, Chengjun Wang, Xiaodan Lou, Bo Zheng</i>	
Solving Method of Dimension Chain Based on Interval Analysis	285
<i>Jirong Yang, Weiyue Xiao, Yuehua Cai</i>	
Solving Method of Dimension Chain Based on ScientificErrorAnalysis Package	291
<i>Jirong Yang, Yuehua Cai, Weiyue Xiao</i>	
Feasibility Analysis on Tax Incentives Policy of Venture Capital	297
<i>Rong Jiang</i>	
Design and Simulation of Caterpillar Drive System for Multifunction-Paver	303
<i>Wu Guoyang</i>	

A Hybrid Biometric Personal Identification Method Based on Chinese Signature	309
<i>Yongjian Zhao, Haining Jiang</i>	
The Interference in Numerical Control Machine System and Response	315
<i>Hengyu Wu, Ling He, Minli Tang</i>	
A Structure for the Model of Intelligent Plan Agent	321
<i>Lei Wang</i>	
Tele-education Technology Eliminating Chinese Knowledge Poverty Based on Information Technology	327
<i>Lei Wang, Dan Han</i>	
Grey Clustering Evaluation for Road Traffic Safety Condition	333
<i>XiaoKun Miao, MingYang Li</i>	
Injection Material Selection Method Based on Optimizing Neural Network	339
<i>ZengShou Dong, YueJun Hao, RenWang Song</i>	
Collaborative Knowledge Management and Innovation Integration of Strategic Management Post Mergers and Acquisitions	345
<i>Yu Gu, Song Chen</i>	
Dispatch of Many Kinds of Fast Consumable Goods in Large-Scale Emergency	351
<i>WeiQin Tang</i>	
A Conformist Mechanism to Promote Collaboration Emergence	357
<i>Yi He, Jia-zhi He</i>	
Indefinite LQ Optimal Control for Systems with Multiplicative Noises: The Incomplete Information Case	363
<i>Guojing Xing, Chenghui Zhang, Peng Cui, Huihong Zhao</i>	
Chaos Memory Less Information Material Analysis and Modeling	371
<i>Feng Shan Pu, Ping chuan Zhang, Hangsen Zhang</i>	
An Approximate Retrieval of Uncertain Data in Data Sources	375
<i>Taorong Qiu, Haiquan Huang, Yuyuan Lin, Xiaokun Yao</i>	
Moving Object Detection through Efficient Detection and Clustering of Reliable Singular Points	381
<i>Jianzhu Cui, Ping Wang, Zhipeng Li, Jing Li, Yan Li</i>	
Study on Packaging Technology of Small-Type FED Panel with Cold Field Emitter	387
<i>Dong Yan, Li Qiang, Zhao Feng, Han Lifeng</i>	

Combining Stock Market Volatility Forecasts with Analysis of Stock Materials under Regime Switching	393
<i>Dong Jing-rong, Chen Yu-Ke, Zou Yan</i>	
Impulsive Consensus of the Leader-Following Multi-agent Systems	403
<i>Wanli Guo, Guoqing Wang</i>	
Application of Computer Aided Instruction Technology on Hydromechanics Experiment Teaching	409
<i>Bing Wang</i>	
Image Segmentation Technology of the Ostu Method for Image Materials Based on Binary PSO Algorithm	415
<i>Shuo Liu</i>	
Collection and Processing of the Point Clouds of Telephone Receiver by Reverse Engineering	421
<i>Dongsheng Wang, Yanru Zhao, Xiucui Chen</i>	
Characteristic Extraction of Chinese Signature Identification Based on B-Spline Function and Wavelet Transform	427
<i>Yongjian Zhao, Haining Jiang</i>	
Classification of Rice According to the Geographic Origin Based on Inductively Coupled Plasma Atomic Emission Spectrometry and Chemometrics	433
<i>Xiaoying Niu, Liya Xia, Xiao-yu Zhang</i>	
A Code Dissemination Protocol of Intelligent Wireless Sensor Network Based LEACH Algorithm	439
<i>HaiYan Li, KaiGuo Qian, ZuCheng Dai</i>	
Study on Photoelectrocatalytic Technology of Three-Dimensional Electrode	447
<i>Ying Liu, Honglei Du</i>	
Research on Process-Oriented Design Method and Technology	453
<i>Songbo Huang, Guangrong Yan, Sijia Yu</i>	
OPC Server Technology Development in the System Software Integration	461
<i>Yucheng Liu, Yubin Liu</i>	
Reliability Analysis for the Pareto Model Based on the Progressive Type II Censored Sample	467
<i>Feng Li</i>	

Study on the Technology of the Secure Computation in the Different Adversarial Models	473
<i>Xiaolan Zhang, Hongxiang Sun, Qiaoyan Wen, Shi Sha</i>	
The Research of Simulation and Optimization of Multimodal Transport System Based on Intelligent Materials on Container Terminal Job Scheduling	479
<i>Qing Yu, Changhui Zhang, Jinlin Wang</i>	
Design of Program-Controlled Micro-flow Feeding System Based on Single Stepping Motor	485
<i>Qing Song, Cunwei Zou, Yuan Luo</i>	
Static Hedging for the Prices of Raw Materials to Hedge Based on Poisson Jump-Diffusion Model	491
<i>YongMing Jiang, HangSheng Tan</i>	
Speech Material Recognition Technology on an Objective Evaluation System for the Rhythm of English Sentences	501
<i>Jing Zhang, Min Zhang</i>	
Research on the Equipment Maintenance Support Quality Index System . . .	509
<i>Xiang Zhao, Bing Feng, Qiangbin Yue</i>	
Modal Analysis and Optimization of Some Internal Rotor Radar Stabilized Platform	517
<i>Shan Xue, GuoHua Cao, YuLong Song</i>	
Research on the Methods of Constructing Perfect Binary Array Pairs to Explore New Material Uses	525
<i>Yuexia Qian, Guozheng Tao</i>	
Case-Based Reasoning for Data Verification with Data Structure in M&S	533
<i>Guozhen Xu, Peng Jiao, Yabing Zha</i>	
Discussion on Prioritization Method of Make-to-Order Corporation for Sales Products	539
<i>Hongyan Shi, Mei Chu, Man Liu, Tao Wang</i>	
Adaptive Pinning Synchronization of Delayed Complex Dynamical Networks	543
<i>Haiyi Sun, Ning Li, Yang Li</i>	
Travel Path Guidance Method for Motor Vehicle	549
<i>Ande Chang, Guiyan Jiang, Shifeng Niu</i>	

Research and Realization of Real-Time Ultrasonic TOFD Scan Imaging System	555
<i>Di Tang, Xingqun Zhao, Ling Xia</i>	
Study of Integrated Design Processing Methods of Surge Links in Loose Logistics Transportation System	561
<i>Xiaoping Bai, Yu Zhao</i>	
Collection System Implementation for Four TCM Diagnostic Methods Information of Hyperlipemia and Research on Intelligent Symptom Classification Algorithm	567
<i>YongQiu Tu, GuoHua Chen, ShengHua Piao, Jiao Guo</i>	
Experience of Nurbas Modeling Design Process	573
<i>Guobin Peng</i>	
Research on Coupling Characters of the Linear Polarized Mode between Two Multi-mode Silica Circular Waveguide	577
<i>Miao Yu, ZhiQiang Zhang, JianHua Ren</i>	
A Study on the Integration of Netblog and English Teaching with Reform of Teaching Materials	583
<i>Wenlong Wan, Ling Zhang, Yuzhuang Lu, Zhen Liu</i>	
A Corpus-Based Study with Corpus Materials on Conjunctions Used by Chinese and English Authors in English Academic Article Abstracts	589
<i>Wenlong Wan, Ling Zhang, Zhen Liu, Wenxian Xiao</i>	
Embedded Fingerprint Identification System Based on DSP Chip	595
<i>Fuqiang Wang, Guohong Gao</i>	
Temperature Monitoring System Based on AT89C51	601
<i>Xingrui Liu, Guohong Gao</i>	
A Simple Query Mechanism for the Compressed XML in Mobile Circumstance	607
<i>ShengBo Shi</i>	
Robust Audio Watermarking Algorithm Based on Audio Binary Halftone Pre-process	615
<i>Huan Li, Zheng Qin, XuanPing Zhang, Xu Wang</i>	
A Virtual Restoration Strategy of 3D Scanned Objects	621
<i>Guizhen He, Xiaojun Cheng</i>	
The Study of Multimedia Transmission IPv6 QoS	629
<i>Wenxian Xiao, Tao Zhang, Wenlong Wan, Zhen Liu</i>	

Character Istics Recognition of Typical Fractional Order Dynamical Systems via Orthogonal Wavelet Packet Analysis Method	635
<i>Tao Zhang, Wenxian Xiao, Zhen Liu, Wenlong Wan</i>	
A Novel Method Inpainting Insect Feathered Wing	641
<i>Minqin Wang</i>	
Research on Gender Differences of Trendy Online Behavior Patterns	647
<i>Tsui-Chuan Hsieh, Chyan Yang</i>	
Study on Affecting Factors of Time Domain Reflectometry Cable Length Measurement	653
<i>Jianhui Song, Yang Yu, Hongwei Gao</i>	
Input-to-Output Stability for One Class of Discontinuous Dynamical Systems	659
<i>Yang Gao, Wei Zhao</i>	
Finite Element Analysis of Pump Diesel Engine Connecting Rod	665
<i>Bin Zheng, Yongqi Liu, Ruixiang Liu, Jian Meng</i>	
A Multiscale Image Edge Detection Algorithm Based on Genetic Fuzzy Clustering	671
<i>Min Li, Pei-Yan Zhang</i>	
Research on Transitional Culture on Impulse Buying Intention in Mainland China	677
<i>Wang Jian-guo, Yao De-li</i>	
Finite Element Analysis of Marine Diesel Engine Crankshaft	683
<i>Bin Zheng, Yongqi Liu, Ruixiang Liu, Jian Meng</i>	
Design of Magnetic Separation Column Data Logger Based on PROFIBUS and USB Bus Control Chip	689
<i>Ying Sun</i>	
The Theory of Elastic Thin Plate Stability Problem Analysis with Approximated Daubechies Wavelets	695
<i>Gao Zhongshe</i>	
Design of Low Cost Human ADL Signal Acquire System Based on Wireless Wearable MEMS Sensor	703
<i>Ying Sun</i>	
A Fast Plotting Method for 3D Directional Marker	709
<i>Hongqian Chen, Yi Chen, Yuehong Sun, Li Liu</i>	
A Fast Rendering Method for Dynamic Crowd Scene	715
<i>Hongqian Chen, Yi Chen, Yuehong Sun, Jian Cao</i>	

Human Daily Activity Detect System Optimization Method Using Bayesian Network Based on Wireless Sensor Network	721
<i>Ying Sun</i>	
Support Vector Machine Based on Chaos Particle Swarm Optimization for Lightning Prediction	727
<i>Xianlun Tang, Ling Zhuang, Yanghua Gao</i>	
Extraction of Visual Material and Spatial Information from Text Description for Scene Visualization	735
<i>Xin Zeng, MLing Tan, WJing Chen</i>	
The Design of Elevator Control System Based on PLC and Configuration	743
<i>Shuang Zheng, Fugang Liu</i>	
Study on Module Partition Method for CNC Lathe Design	749
<i>ZhiWei Xu, YongXian Liu</i>	
Risk Control Research on Chang Chun Street Networks with Intelligent Materials Based on Complex Network	755
<i>Ling Zhang, Fan-sen Kong, Yan-hua Ma</i>	
Research on Semantic Web Services Composing System Based on Multi-Agent	761
<i>Junwei Luo, Huimin Luo</i>	
Approach of the Secure Communication Mechanism for the Off-Site Live Virtual Machine Migrations	767
<i>Xinnian Wang, Yanlin Chen</i>	
Author Index	775

Design and Study on Photovoltaic Array Simulator

YongQiang Zhao

Shaanxi University of Technology,
Shaanxi, Hanzhong, China, 723003
zyq0620@163.com

Abstract. Aiming at the characteristics of distributed power system and output capacity solar energy cell array, a photovoltaic generation simulator and Maximum Power Point Tracking (MPPT) controller were designed. An experimental investigation was conducted of the simulator. The result shows that the simulator can simulate the output power of the photovoltaic array with certain parameters, and has high precision.

Keywords: Solar energy, Photovoltaic array, Maximum Power Point Tracking (MPPT).

1 Introductions

Solar, is a energy of distributed widely, clean, inexhaustible, is compared with primary energy as coal, oil, natural gas, nuclear etc. while its shortcomings is scattered, random, intermittent. In China, Photovoltaic technology was started in 1970's. The total of photovoltaic generation power is 40MW, accounting for 2% of the world's total in 2002. The total of Combined to the grid, is about 50% of photovoltaic power generation, is the first in the world [1]. Solar cells are the foundation and core of PV power, it use battery to change light energy into electrical energy. Solar cells array is controlled by maximum power point tracking and obtain the maximum power output at any sunlight conditions.

2 Mathematics Model of Photovoltaic Array

The distributed power generation systems can be simulated by the output characteristics of photovoltaic arrays and wind turbines. The system scheme of photovoltaic Simulation is shown as Fig.1, the system is mainly made up of solar array simulators and the maximum power point tracking controller.



Fig. 1. System scheme of photovoltaic Simulation

The main circuits of Photovoltaic array simulator consist of DC stability power supply and BUCK converter. The Maximum Power Point Tracking controller is BOOST topology. Output terminal connects to DC bus of distributed power generation system, which replaced by the battery in Fig.1.

3 Principle of Maximum Power Point Tracking (MPPT)

Characteristic curve of solar cells array is shown as Fig.2. It shows that array output power increased with solar battery voltage V_{PV} increase when the array voltage is less than the maximum power point voltage V_{MAX} ; array output power decreased with solar battery voltage V_{PV} increase when the array voltage is greater than the maximum power point voltage. Substance of Photovoltaic system MPPT is a self-optimization process.

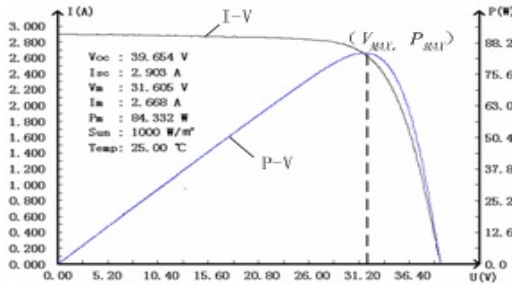


Fig. 2. Characteristics of solar array power-voltage

Shown as Fig.3, according to internal equivalent circuit, the solar photovoltaic array can be simplified an ideal DC source and variable resistor in series.

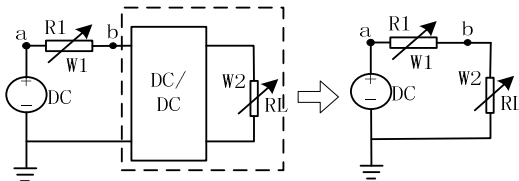


Fig. 3. Principle Diagram of the Maximum Power point Tracking (MPPT)

3.1 Main Circuit

The maximum output power of photovoltaic module is designed for 900W. The target array is JDG-M-45 photovoltaic arrays which made in the Green Energy Limited

Company of China. Two sets is parallel firstly, each sets was consist of 10 batteries in series. So the array maximum power point voltage and current were $V_m = 171V$, $I_m = 5.28A$. Main circuit of photovoltaic generation power simulator is shown as Fig.4.

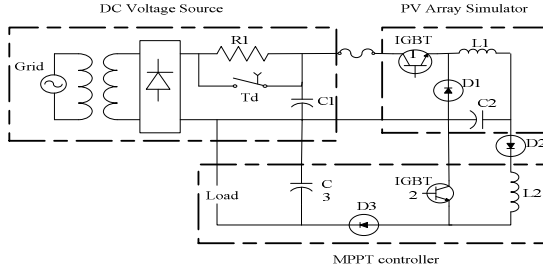


Fig. 4. Main circuit of photovoltaic generation power simulator

3.2 DC Source Module

DC source is a bridge made by VISHAY Company. Its model is KBPC3510/W. Its average current is 35A. The surge currents can withstand up to 400A. Filter capacitor C1 is $2200\mu F/630V$. Current limiting resistor is $R1 = 20\Omega$.

3.3 Select of Components Parameters

The mainly design of main circuit is selection of power switching and I/O parameter of LC.

1) Selection of power switch

The main circuit power switch of simulator is IGBT of the 1MBH60D-100, which parameters is 1000V/60A. Freewheeling diode is DESI30-10 produced by corporation of IXYS, which can withstand the positive current of 30A and reverse voltage of 1000V.

2) Design of filter inductance capacitance

To make the system working continuously, inductor L and capacitor C can be setting with equation (1) and (2).

$$L = \frac{V_{out}(1-D)}{2f_s I_{out}} \quad (1)$$

$$C = \frac{V_{out}(1-D)}{8Lf_s^2 \Delta V_{out}} \quad (2)$$

Maximum output voltage is 200V. Switch duty-cycle D is varies between 0 and 1. Switch frequency $f_s = 20kHz$, $I_{out} = 5.9A$, the critical inductance value is 0.85mH. Capacitor C is $74\mu F$. The electrolytic capacitor is 470V/100, in view of voltage surplus capacity [4].

4 Software Design

A mathematical model of photovoltaic array is stored in simulator based on the storage and computing power of DSP. According to the solar radiation, environmental temperature and photovoltaic array parameters (V_{oc} 、 I_{sc} 、 I_m 、 V_m) tested under standard conditions, the photovoltaic array output characteristics can be simulated. The structured flowchart of photovoltaic array simulator is shown as Fig.5.

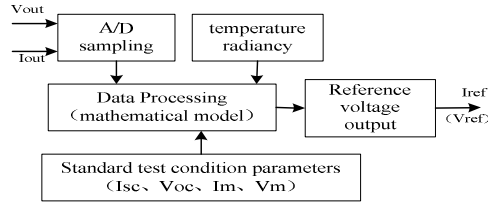


Fig. 5. Block diagram of simulator

4.1 Software Structure of MPPT Controller

Battery is charged through the diode in the photovoltaic generation simulation system. Output voltage of controller is tied down the battery rating voltage nearly. In fact, the battery voltage rate of change is a gradual process, relative to temperature and PV array current change caused by solar irradiance. After a change of direction for the new duty cycle to change the BOOST converter input voltage, the regulator output voltage PV array, so that approximate the maximum power point voltage value. Block diagram of Maximum Power Point Tracking Controller is shown as Fig.6.

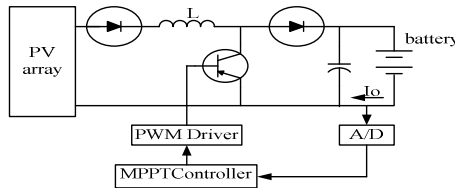


Fig. 6. Block Diagram MPPT Controller

4.2 MPPT Controller Software Process

Batteries are the load, which instead of DC bus of distributed power generation system. Algorithm flow of current feedback MPPT is shown as Fig.7.

5 Experimental Studies

JDG-M-45 photovoltaic cells, is experiment on Simulator, which produced by Shanghai Jiaotong University Guofei Green Energy Limited company. Load is

ST-SC6001 DC electronic load, which produced by Hangzhou super Tektronix electronic technology Co., Ltd. The range of load input voltage and current 1.0 ~ 50.0V, 0.10 ~ 50.0A.

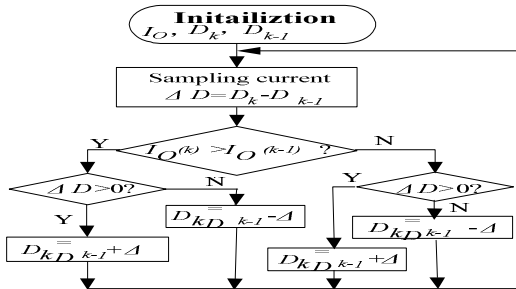


Fig. 7. Algorithm of current feedback MPPT

When $R1 = 25.6\Omega$, used MPPT algorithm and constant duty cycle operation. While constant duty cycle $D = 0.3$, the average output current is 0.812A, output voltage is 36.8V, output power is 29.88W. Using current feedback method MPPT algorithm, the average output current is 1.036A, output voltage is still 36.8V, output power of 38.12W. So maximum power point tracking controller can adjust the input impedance dynamically, output power has been improved.

BOOST converter output voltage is 36.8V and remains constant when the duty cycle is 0.6. The average output voltage of PV array simulators is 16.2V. When BUCK converter work in MPPT algorithm, the output voltage of PV simulator is dynamically adjusted to 17.2V. The BUCK and BOOST converter duty cycle adjusts dynamic at this time, battery charging current increased significantly than constant duty cycle.

6 Summaries

In this paper, solar photovoltaic array simulators and the maximum power point tracking controller are designed by the characteristics of solar distributed generation system. BOOST converter, control circuit and control software of MPPT controller are designed according to the requirements of photovoltaic generation. Comparing with the measured of solar panels and tested solar array simulator, shows that simulator characteristic is similar to output of photovoltaic array. MPPT algorithm is simple and the accuracy of simulation is higher.

References

1. Wang, C.: New energy generation technology, pp. 1–16. China Electric Power Press, Beijing (2003)
2. Zhu, T.: MPPT of photovoltaic cells based application system of power and design. Donghua University (2005)

3. Hua, C., Lin, J.: An on-line MPPT algorithm for rapidly changing illuminations of solar arrays. *Renewable Energy*, 1129–1142 (2003)
4. Yu-Gang: Modern power electronic magnetic technology, pp. 168–172. Science Press, Beijing (2003)
5. Lu, J.: Analytical model fitting with solar cells IV characteristics of test data. *SOLAR* (1), 44–49 (1996)

Design and Research of Battery Charged Intelligent System

JiLin Jia

Shaanxi University of Technology,
Shaanxi, Hanzhong, China, 723003
jjl_jyg@sohu.com

Abstract. The thesis researches on the theory on fast-charging method of lead-acid battery. A new type of charging pattern was proposed. The current can match the acceptance curve of the lead-acid battery proposed by J.A.Mas very well. With the intermission and discharge in the course of the charge, it avoids the gas-generation and overtemperature. About charging control methods, the system selects an integrated control method to judge whether batteries was full-charge or not. A Fuzzy control algorithm was used to realize charging course. The experiment result indicates that fuzzy control has a fast response speed, a good steady state precision and a strong anti-interference.

Keywords: Lead-acid battery, Polarization, Fast- charging, Fuzzy control.

0 Introduction

As following of continuous improvement, the technology of VRLA batteries has matured. VRLA batteries become secondary batteries, most widely used in the industrial, communications, transportation, electric power system, etc [1]. Although the battery updated constantly, but the charging method has not improved significantly. There is serious over-charging and gassing phenomena in the process of charging used methods of constant voltage charging, constant voltage current limiting charging and constant current, which lead to shortened battery life. So the actual life of batteries is less than the half of the nominal life. Even the nominal life of batteries is about 10 years; the actual service life is only 1 to 2 years. The proportion of damage batteries is very large because of unreasonable charge and discharge control. Because of many cells use simple methods of charging and discharging in the production and use, thus the batteries is insufficient charge and can't play its best power effects. So the life of batteries is shorter and shorter. There is a very important significance of increased battery life and power effects, the battery is charged efficiently, rapidly, non-destructively. Therefore, it is very necessary to design a more comprehensive system of battery charging and discharging for extending the battery life and ensuring the stability of battery's power system.

1 System Overall Design

1.1 The Basic Functions of the System

1) When battery charged, the charged system tests the battery voltage and temperature firstly. If the voltage and temperature is less than threshold value, the charging system is pre-charging. Otherwise, the battery voltage and temperature is more than threshold value, the charged system works automatically in the default method of fast charging.

2) If the tested voltage and temperature is more than the threshold value, system works in the fast charge method to charge and can convert the charged state according to battery voltage and charged current automatically. Though, it can work in the floating charged state when the battery is fully charged.

3) In charging process, the battery information, such as voltage, temperature and charge current status, can be test and shown in LED at real time.

4) There should be monitored circuit and warning light in the charging system to avoid output over-voltage, over-current, short-circuit and overheat detection etc.

1.2 Selection of Fast Charged Method

In order to charged fast, one hand to try to speed up the chemical reaction rate of the battery and charge with the most speed. On the other hand, must be ensured the negative absorptive capacity of the battery. So the negative absorptive capacity of the battery will be equal to the rate of positive oxygen. As possible is eliminate the polarization phenomena of the battery.

Through analysis of the traditional charging methods and several fast charging methods, four stages charged method is found based on variable current intermittent charge and pulse current charge. Four stages include pre-charge, variable current intermittent depolarization charged, threshold voltage complement charged and float charged. Dual closed-loop is made of charged equipment and batteries. When the battery charged, the equipment parameters will be adjusted in keeping with ideal current curve as following state of the battery charged. So, no gas precipitation and both to saving power and no damage to battery in the process of battery charged.

1.3 System Main Circuit Design

The charged system was used integrated control method of negative incremental control battery voltage and battery temperature control method. The system of charge management is intelligent because of the main circuit can be charged and discharged. So the energy can be flow in two-ways and the converter circuit is reversible. The main circuit is AC-DC-DC converter and is made up of input rectifier filter circuit (AC-DC) and Buck / Boost (DC-DC) convert circuits [2].

The system is AC-DC-DC conversion circuit and was made up of AC-DC and DC-DC. The transform results of AC-DC is DC voltage U1, be filtered and isolated of three-phase AC by rectifier transformer, and then rectified by three-phase uncontrolled bridge made up of six diode. DC-DC is Buck-Boost circuit (shown as Fig.1) to be charged and discharged the battery. So Buck circuit is charged and Boost circuit is discharged.

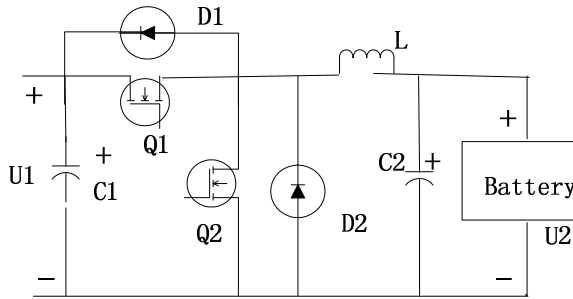


Fig. 1. DC-DC converts circuit

1.4 System Control Circuit Design

DSP is the core of hardware control circuit. The diagram of control block is shown as Fig.2. Control circuit includes DSP basic circuits, multiple voltage, current, temperature, signal acquisition, conditioning circuit, PWM signal power amplifier circuit, fault monitoring circuit and JTAG emulation interface circuit [3]. The master chip is TMS320LF2407A, which supplied voltage is 3.3V. The voltage of many chips used in control panel is +5V and 15V. So system control circuit includes multiple voltage conversion circuit.

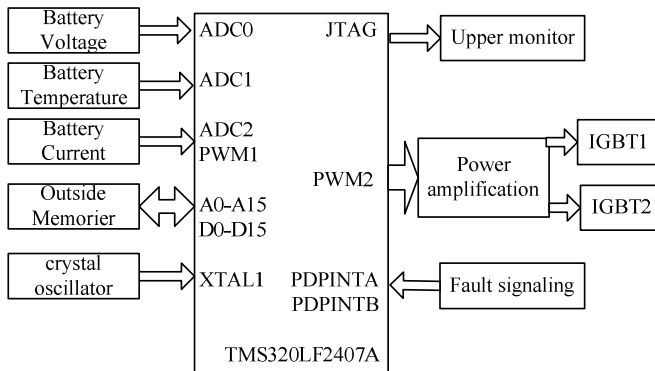


Fig. 2. System controller diagram

2 Battery Charged Experiment

2.1 Charged Parameters to Determine

The charged method is variable intermittent depolarizing current charging. The parameters are initial charged current, converter voltage, stop charging time and variable current method.

When battery has been charged, with higher of conversion voltage, the quantity of electricity charged in battery is more. But the conversion voltage is too high to short

the battery life. Otherwise the conversion voltage is too low to insufficient the battery. In order to solve this problem, the method of progressively increasing voltage used in system. Example of single cell, the first converter voltage $U_{t1} = 2.20V$, secondary converter voltage $U_{t2} = 2.25V$, the third converter voltage $U_{t3} = 2.30V$, and so on.

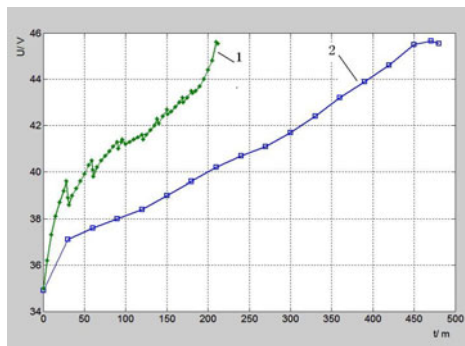
To determine the charged initiative voltage, variable current mode, the compared experimental was make with the battery of 12V/10Ah. The result is shown in Tab.1.

Table 1. Comparison of charging mode

Order	Current-variable current(A)	Charged time (min)	capacity(%)
1	10-7-5-3.5-1.8-1	150	73
2	10-5-2.5-1.25-1	168	65
3	7-5-3.5-2.5-1.8-1	230	93
4	7-4.2-2.5-1.5-1	238	90
5	5-3.5-2.5-1.8-1	253	88

2.2 Analysis of Experimental Results

It shows that in Fig.3, the voltage of constant current charged method rises rapidly initially and then slowly. At the end of the charged, voltage increased negatively, because of the battery voltage connected with electrolyte concentration. The battery voltage is high when electrolyte concentration is high. At beginning of charged, the reaction of sulfuric acid is too late to spread to outside of electrode, so the battery voltage increases quickly. With variable current intermittent depolarization, the battery voltage has been rapidly, because of charged current is higher during the charged process. During stage of intermittence discharging and intermittent depolarization, the battery voltage decreases gradually.



1—constant current charged
2—variable current intermittent charged

Fig. 3. The battery voltage curve

It shows in Fig.4, which the temperature decreases about 4 with variable intermittent depolarization current method than constant current charging method. Both battery charged method, the temperature rise slowly in the charged initial process, but increased rapidly in the later of charged process.

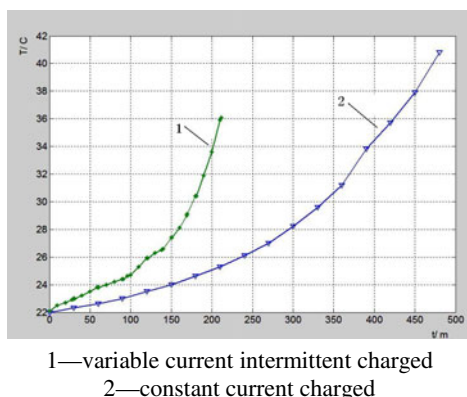


Fig. 4. Battery temperature curve

3 Summaries

The variable current intermittent depolarizing charged, that described in the paper, is a new battery charged method based on the variable current intermittent charging and pulse fast charging. The battery charge current can be adjusted to acceptable current closely by variable current charged. By intermittent, can be accelerated the spread of electrolyte ions, increased the reaction area of the electrode surface. While, by the impulse discharged can be eliminated chemical polarization, improved the acceptability current of the battery. Variable current intermittent depolarizing charged method has the merit of both all. It has the advantages, such as less time battery charged, lower temperature, higher charged efficiency. It is a good fast charged method of efficiently, rapidly and non-destructive, etc.

The battery charged system is designed in the paper, can effectively improve the battery life. However, different batteries have different charging the optimal management, especially different charging method is recommended by different batteries. In the battery charged system, each battery should be had a storage to stored each battery-related information. Battery management system can be communicated with the battery and different management methods can be loaded by different battery information. So the efficiency of the battery charged management system will be higher.

References

1. Zhou, Z., Zhou, J., Ji, A.: VRLA batteries, pp. 1–5. China Electric Power Press, Beijing (2004)
2. Wang, Z., Huang, J.: Power Electronics Technology. Mechanical Industry Press, Beijing (2002)

3. Ning changed Cindy: Principle and Application of DSP controller, pp. 6–17. Science Press, Beijing (2002)
4. Suyitnot, A., Fujikawa, J., Kobayashi, H., Dote, Y.: Variable-structured robust controller by fuzzy logic for Servomotors. *IEEE Trans. on Industrial Electronics* IE-40(1), 80–88 (1993)
5. Gao, P., Cheng, M.: Variable structure control system of quality control. *Control and Decision* 4(4), 1–6 (1989)
6. Liu, H., Wang, W.: TMS320LF240x DSP C language development and application. Beijing Aerospace University Press, Beijing (2003)

Accuracy Performances of Asymmetrical Right Circular Flexure Hinge

Jiaying Shen¹, Huawei Ji², and Yun Zhao³

¹ College of mechanical & electrical engineering, Jiaxing University, Zhejiang, China
zjjxsjy@163.com

² College of mechanical engineering, Hangzhou Dianzi University, Zhejiang, China
jhw76@163.com

³ College of mechanical & electrical engineering, Jiaxing University, Zhejiang, China
zhaoyun@mail.zjxu.edu.cn

Abstract. Flexure hinge has been widely used in high precision micro-positioning mechanism driven by piezoelectric ceramic and the most common type is right circular flexure hinge. According to the size of the cutting arc radius of both sides of right circular flexure hinge, the structure coefficient is introduced and asymmetrical right circular flexure hinges are summarized and classified. There is an offset value in the centre point of flexure hinge under a load, which will affect its displacement accuracy. So, the accuracy performance is analyzed by using finite element method. The program created by using a programming language named APDL in software ANSYS automatically builds the analytic model to achieve parametric analysis. The analytic result has an important significance to design flexure hinge.

Keywords: asymmetrical right circular flexure hinge, accuracy performance, structure coefficient.

1 Introduction

Flexure hinge has been widely used in micro-positioning stage and micromanipulator because of its many advantages[1,2]. It has no stick-slip friction, no clearance, smooth and continuous displacement, and has no need of lubrication and inherently infinite resolution. There are many kinds of flexure hinges, such as, right circular, right angle, elliptical, corner-filled, parabolic and hyperbolic flexure hinges[3,4,5]. The right circular flexure hinge is the most common type because it is simple to design and manufacture.

An ideal flexure hinge should be able to rotate freely around its central point, but for a real flexure hinge, there is an offset value in the centre point of flexure hinge under a load[4]. The positioning accuracy of micro-positioning stage is directly affected by flexure hinge due to the offset value. In this paper the displacement accuracy of asymmetrical right circular flexure hinge are studied. Then the relationship between the basic construction parameters of flexure hinge and the offset value is analyzed in software ANSYS.

2 Structural Type of Right Circular Flexure Hinge

As mentioned before, according to the contour maps of the notched-part flexure hinges may be divided into right circular, right angle, elliptical, corner-filled, parabolic and hyperbolic flexure hinges[3,4,5,6] illustrated in Fig. 1.

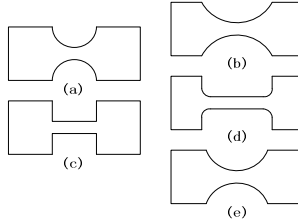


Fig. 1. Category of flexure hinges: (a) right circular ,(b) hyperbolic, (c) right angle, (d)corner-filled,(e) elliptical

The most common type of right circular flexure hinge is symmetrical in structure, where both sides of the notched arc radius are the same. The asymmetric structural type is introduced in the study, and both sides of the notched arc radius are R_1 and R_2 , respectively. So the structural coefficient e is employed in the following equation

$$e = \frac{R_2}{R_1} \tag{1}$$

Assuming R_1 is a constant and R_2 varies from zero to $+\infty$, thus, the structural coefficient e is varied from zero to $+\infty$. So the asymmetric flexure hinges are divided into the following five categories:

- (i) if $R_2 = 0$, then $e = 0$, shown Fig. 2 (a).
- (ii) if $0 < R_2 < R_1$, then $0 < e < 1$, shown Fig. 2 (b).
- (iii) if $R_2 = R_1$, then $e = 1$, shown Fig. 2 (c).
- (iv) if $R_1 < R_2 < +\infty$, then $1 < e < +\infty$, shown Fig.2 (d).
- (v) if $R_2 \rightarrow +\infty$, then $e \rightarrow +\infty$, shown Fig. 2 (e).

According to the above analysis and illustration in Fig. 2, the following conclusions can be drawn:

- (i) the height of flexure hinges in Fig. 2(a),(b),(c) and (d) equals to h and the height of one in Fig. 2(e) equals to $(h + t) / 2$.
- (ii) the geometrical structural shape of the flexure hinges in Fig. 2(a) and (e) is equivalent, which has the notched arc only on one side, so this kind of flexure hinge is called as single-notch flexure hinge. The height of flexure hinge are

different and are h and $(h+t)/2$, respectively, and the performance is considerably different.

- (iii) the flexure hinges in Fig. 2 (b),(c), (d) and (e) have the notched arc on each side, so this kind of flexure hinge is called as double-notch flexure hinge.
- (iv) the notched arc radius of both sides of flexure hinge is in the same size when the structural coefficient e equals to one, which is the most common type of right circular flexure hinge.

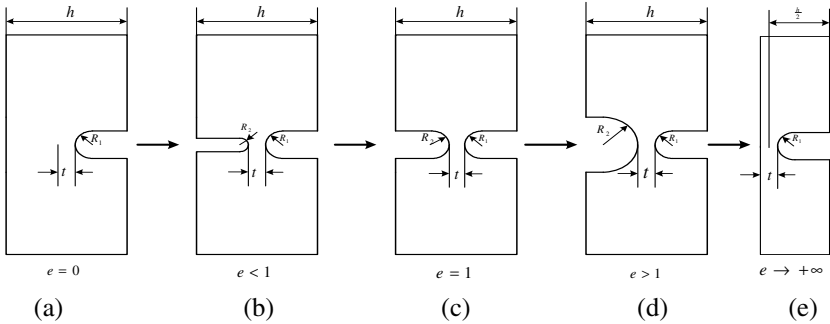


Fig. 2. Right circular flexure hinges with different value e

3 Accuracy Performances

Under an ideal condition, flexure hinge should rotate around its center point c (shown in Fig.3) and the center point has a steady position. However, flexure hinge has an offset value from its geometrical centre with the application of moment M . The offset value directly affects the accuracy performances of flexure hinge.

The lateral deformation of point p in the x -direction is to stand for the output displacement x_p in flexure hinge while the lateral deformation of point c in the x -direction is to stand for the offset value. In the same output displacement x_p , the larger the offset value x_c of point c is, the lower the accuracy performance of flexure hinge is.

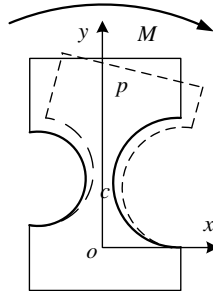


Fig. 3. Load and deformation of flexure hinge

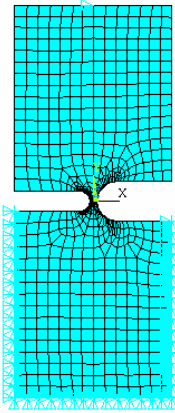


Fig. 4. Finite element model

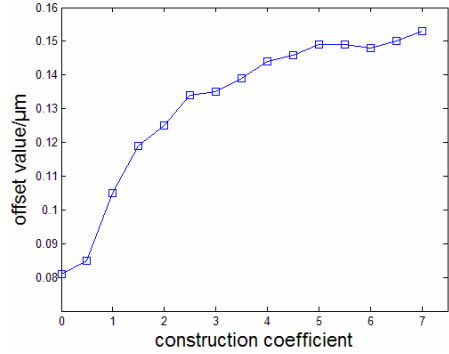


Fig. 5. Offset values with the different construction coefficient

To design flexure hinge better the relationship between the construction coefficient e and the offset value x_c needs to be studied. But it is complicated to theoretically calculate the offset value x_c due to the asymmetry of the notched-part of circular flexure hinge. So, the finite element simulation analysis is done to get the offset value x_c in advanced software ANSYS.

There are many models for flexure hinge as the basic construction parameters R , t , and b vary. It will take a large amount of time to create every model with human-computer interactive approach. To raise work efficiency and to save time a parametric modeling method is employed by using APDL language in ANSYS.

The geometric basic parameters of analytic model have a minimum hinge thickness t of 1 mm, a cutting radius R of 2 mm and a width b of 10 mm. Aluminium alloy is selected as the material of flexure hinge, and its elastic modulus E is 68 GPa. The meshes are generated using 3D eight-node element solid45 and the given displacement of point c is $10 \mu\text{m}$. The basic construction parameters R_1 , t , and b , of flexure hinge are regarded as the constant while the parameter R_2 is defined as a variable in program. Thus, the values of the construction coefficient e are obtained by changing the value of the parameter R_2 . So the corresponding offset values x_c are obtained by running the parametric programs repeatedly with the different values of the parameter R_2 in model. The finite element model of flexure hinge and the corresponding results are shown in Fig.4 and Fig.5, respectively.

From Fig.5, we know that the offset values increases as the construction coefficient e is increased and there are two cases divided by the boundary line corresponding to the construction coefficient $e=3$. One case is that the offset value increases rapidly as the construction coefficient e is increased when $e < 3$, another case is that the offset value increases slightly as the construction coefficient e is increased when $e > 3$.

4 Conclusions

According to the size of the cutting arc radius of both sides of flexure hinge, the structure factor is introduced and right circular flexure hinges are summarized and classified. Then, the accuracy performance is analyzed by using finite element method in software ANSYS by creating parametric model. The analytic result has an important significance to design flexure hinge.

Acknowledgements. This work was supported by National Natural Science Foundation of China, No.50805042 and by Key Foundation of Jiaying University, No. 70110X06BL.

References

1. Li, Y., Xu, Q.: Modeling and performance evaluation of a flexure-based XY parallel micromanipulator. *Mechanism and Machine Theory* 44, 2125–2152 (2009)
2. Nia, Z., Zhanga, D., Wub, Y., et al.: Analysis of parasitic motion in parallelogram compliant mechanism. *Precision Engineering* 34(1), 133–138 (2010)
3. Smith, S., Badami, V., Dale, J., Xu, Y.: Elliptical flexure hinges. *Rev. Sci. Instrum.* 68(3), 1474–1483 (1997)
4. Lobontiu, N., Paine, J., Garcia, E., Goldfarb, M.: Design of symmetric conic-section flexure hinges based on closed-form compliance equations. *Mech. Mach. Theory* 37, 477–498 (2002)
5. Lobontiu, N., Paine, J.S.N., O'Malley, E., et al.: Parabolic and hyperbolic flexure hinges: flexibility, motion precision and stress characterization based on compliance closed-form equations. *Precision Engineering* 26(2), 183–192 (2002)

The Application of the Pseudo Random Bit Index Sequence in the Image Encryption Algorithm

Zongying Li

School of Science, Linyi University,
Shandong, Linyi, China 276000
zongying_li@126.com

Abstract. In this paper, we firstly introduce a new scheme to acquire the pseudo random bit index sequence generation based on the Logistic chaotic system, then introduce a novel digital image encryption algorithm, which is based on the 2D Arnold map and the pseudo random bit index sequence. At last, the large number of simulations are carried on, and the results have shown that the proposed algorithm is a very good encryption algorithm.

Keywords: Image correlation, Entropy, Histogram, The pseudo random bit index sequence.

1 Introduction

With the development of information society, the security of transmitted digital information about the digital image [1,2,3] becomes more and more important. At present, many researchers proposed different image encryption schemes to the application [4,5,6,7,8], however, these traditional image encryption algorithm may still be improved.

In the following sections, we presents a whole novel digital image encryption algorithm, and the experimental results and analysis have both shown that the algorithm can achieve the goal of better encryption effect.

2 The Novel Image Encryption Scheme

The 2D Arnold Map. The Arnold map can be regarded as the process of tensile, compression, folding and stitching. The general 2D Arnold map [4] is an invertible chaotic map, which may be described by:

$$\begin{pmatrix} x_{n+1} \\ y_{n+1} \end{pmatrix} = \begin{pmatrix} 1 & 1 \\ 1 & 2 \end{pmatrix} \begin{pmatrix} x_n \\ y_n \end{pmatrix} \bmod N \quad (1)$$

The Arnold map is known to be chaotic, when $N = 1$, Eq.1 is a standard Arnold map, and with geometrical explanation shown in Fig.1, from which one can see that a unit

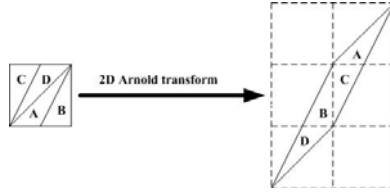


Fig. 1. Geometrical explanation of the generalized discrete 2D Arnold map

square is first stretched by the linear transform and then folded by the modular operation, which is abbreviated as mod.

The Logistic Chaotic System. One of the simplest and most widely studied nonlinear dynamical systems capable of exhibiting chaotic system is the logistic map [4] which can be written in its recursive form as:

$$x_{n+1} = \mu x_n (1 - x_n) \tag{2}$$

where $x_n \in (0,1)$, $n = 1, 2, 3, \dots$, μ is the controlling parameters, this map has a very sensitive dependence upon its initial value x_0 and the controlling parameter μ , when $3.5699456 \dots \leq \mu \leq 4$, the system dynamic shape is very complex, the system is a chaotic system, and when $\mu > 4$, its form is more complex systems dynamics.

In the paper we choose a floating number $x_1 \in (0,1)$ to be used as an initial condition to compute the logistic map in Eq.2, then another number $\mu \in [3.5699456 \dots, 4]$ to be used as a seed.

After iterating Eq.2 enough rounds, we can get a chaotic sequence $C = \{c_1, c_2, \dots, c_8\}$, and for $\forall i \in \{1, 2, \dots, 8\}$, let $t_i = \lceil 10000 * c_i \rceil \bmod 32$, where the symbol $\lceil a \rceil$ means that getting the smallest integer which is not smaller than a , then the new integral sequence $T = \{t_1, t_2, \dots, t_8\}$ is generated, and we name it the pseudo random bit index sequence.

The Generation of the Fictitious Pixel. In order to generate the integer sequence, firstly, for every grid (x, y) in the digital image, we can get a unique grid (x', y') by means of the 2D Arnold map and denote its adjacent pixel as P_1, P_2, P_3, P_4 shown in Fig.2. To assume their corresponding sequence of bits as: $P_i = \{p_{i1}, p_{i2}, \dots, p_{i8}\}$, where $i = 1, 2, \dots, 4$ and P_i is a boolean number sequence. And we construct a new bit sequence $S = \{P_1, P_2, P_3, P_4\}$ with the length of 32, which is expressed as follow and shown in Fig.3.

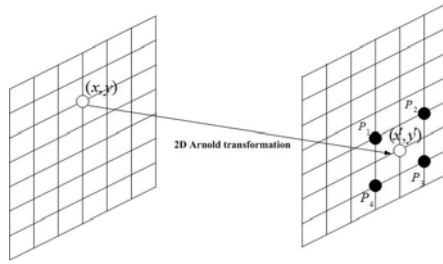


Fig. 2. The schematic diagram of the pixel coordinate map

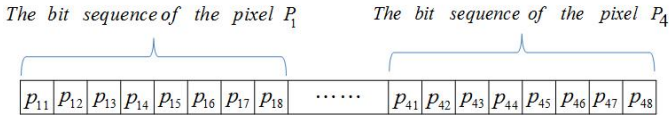


Fig. 3. The bit sequence of the adjacent pixels

At last, we construct a new sequence N by means of obtaining a subsequence of the sequence S , and which is defined as follow: $N = \{S_{t1}, S_{t2}, \dots, S_{t8}\}$.

It's obvious that $N_i = S_{ti}$, $i = 1, 2, \dots, 8$ is also a boolean number, so we may regard sequence N as the bit sequence of a fictitious pixel, and mark its gray value as Q .

The Pixel Gray Value Diffusion Equation. If we encrypt the digital image only by the scrambling transformation, we can't change the image statistical histogram, so the attacker will attack by using statistical histogram. Therefore, we must introduce the spread of pixel gray value transformation in order to make the statistical histogram of the encrypted image become more uniform. And the expression is given as follow:

$$f(x, y) = \text{bitxor}(f(x, y), Q) \tag{3}$$

where $f(x, y)$ means the gray value of the pixel at the grid (x, y) , and Q means the gray value of its corresponding fictitious pixel. We name Eq.3. as the diffusion equation based on the fictitious pixel, and it's obvious a reversible transformation.

The Encryption Algorithm Steps. The novel digital image encryption algorithm is presented which is based on the 2D Arnold map and the pseudo random bit index sequence, the integrated image encryption scheme consists of the following three steps of operations:

Step 1. Select the iteration rounds k and the initial value x_0 , the controlling parameter μ .

Step 2. For every image pixel, the previously Eq.3. is used to build a newly transformed image with the corresponding fictitious pixel.

Step 3. Repeat the 2D Arnold map and Step2 for k rounds to satisfy the requirement of security. Finally we can get the encrypted image.

3 The Experimental Results Analysis

In order to investigate the quality of encryption, a large number of digital simulations are performed. In the paper, the original image peppers of size 256×256 and 256 gray levels is employed as the experimental image. The simulation results and performance analysis of the proposed image encryption scheme are provided in the following section.

The Entropy Analysis. The entropy [3] is a measure of uncertainty. The smoother the image is, the smaller the entropy is. And the minimum entropy is zero while the picture has only one pixel value. In the contrary, the more disordered the image is, the bigger the entropy is. The entropy of the original image and the encrypted image is calculated as:

$$H = \sum_{i=0}^{255} p(i) \log_2 p(i) \tag{4}$$

Where $p(i)$ is the number of occurrence of a pixel/total number of pixel in the image.

The entropy of the original image selected in the paper is 7.5851, Fig.4 indicates the various values of the entropies for the different encryption rounds. It can be noted that the entropy of the encrypted image is very close to the max of entropy value of 8, which means a high confusion is achieved in the encrypted system.

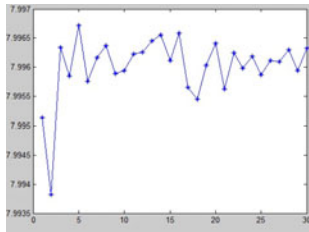


Fig. 4. Entropy vs. encryption rounds

The Histogram Analysis. Intensity transformation functions based on information extracted from image intensity histograms [1,2,3] play a basic role in image progressing. The experimental image is shown in Fig.5.(a) while its histogram is given in Fig.5.(b). After fifteen rounds of the confusion process, the ciphered image obtained is shown in Fig.5.(c), its corresponding histogram found in Fig.5.(d). As we can see, the histogram of the ciphered image is fairly uniform and significantly different from that of the original image.

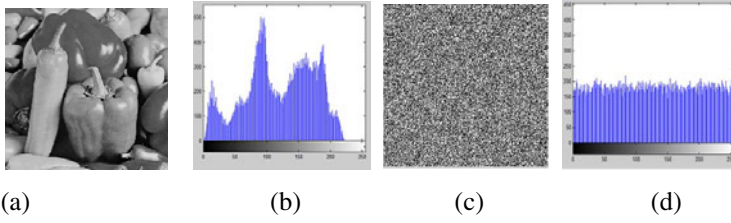


Fig. 5. Image and its histogram

The Correlation of Adjacent Pixels. To analyze the effectiveness of our cryptosystem in this aspect, the correlations between two adjacent pixels along horizontal, vertical and diagonal directions are calculated. The correlation coefficient is [4,5,6,7,8] defined as follows:

$$r_{xy} = \frac{\text{cov}(x, y)}{\sqrt{D(x)}\sqrt{D(y)}} \tag{5}$$

Where

$$E(x) = \frac{1}{N} \sum_{i=1}^N x_i, D(x) = \frac{1}{N} \sum_{i=1}^N (x_i - E(x))^2, \text{cov}(x, y) = \frac{1}{N} \sum_{i=1}^N (x_i - E(x))(y_i - E(y)).$$

In the paper, 1000 pairs of random digital image pixels were selected. And the correlation coefficients along the different directions of adjacent pixels are calculated, and their corresponding results are shown in Fig.6. The results imply that the proposed encryption algorithm can effectively make the adjacent pixels uncorrelated in the original image after fifth encryption round.

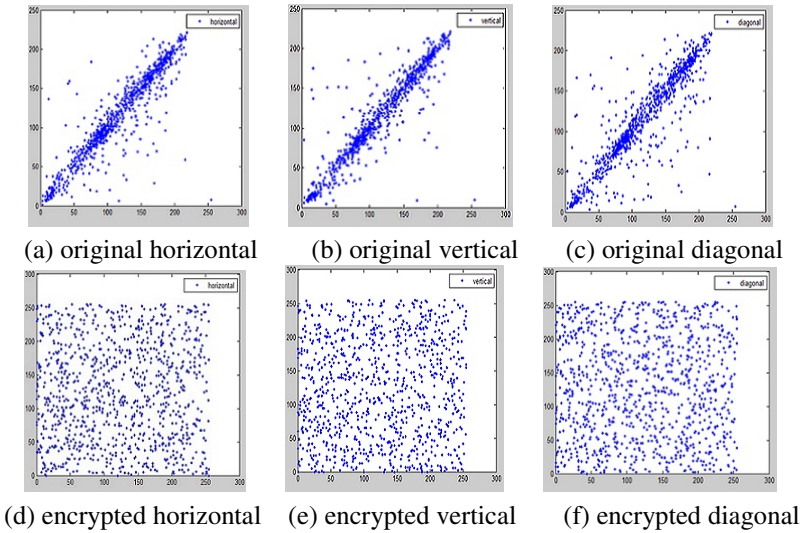


Fig. 6. Correlation of the neighboring pixels

4 Summary

In the paper, one new digital image encryption algorithm is proposed which is based on the 2D Arnold map and the pseudo random bit index sequence. And a large number of simulation experiments were carried out, all the experimental results and analysis have shown that the proposed encryption algorithm has very good diffusion properties, and is a very effective encryption algorithm.

References

1. Castleman, K.R.: Digital Image Processing. Prentice-Hall Inc., Englewood Cliffs (1996)
2. Gonzalez, R.C., Woods, R.E.: Digital Image Processing, 3rd edn. Prentice-Hall, Englewood Cliffs (2008)
3. Gonzalez, R.C., Woods, R.E., Eddins, S.L.: Digital Image Processing Using MATLAB. Electronic Industry Press (2004)
4. Chen, G.R., Wang, X.F.: Dynamical Systems Chaos Theory, Methods and Applications, pp. 80–105. Jiaotong University Press, Shanghai (2006) (in Chinese)
5. Qi, D.X., Zou, J.C., Han, X.Y.: A New Class of Scrambling Transformation and Its Application in the Image Information Covering. Science in China(Series E) 43(3), 304–312 (2000)
6. Zhang, Y.W., Wang, Y.M., Shen, X.B.: A chaos-based on image encryption algorithm using alternate structure. Science in China(Series F) 50(3), 334–341 (2007)
7. Zhang, L.H., Liao, X.F., Wang, X.B.: An image encryption approach based on chaotic maps. Chaos, Solitons and Fractals 24, 759–765 (2005)
8. Awad, A., Awad, D.: Efficient Image Chaotic Encryption Algorithm With No Propagation Error. ETRI Journal 32(5), 774–783 (2010)

Research on the Method of Soft-sensing Intelligent Compensation for BOD Biosensors in Sewage

Xiaoyi Wang¹, Zaiwen Liu¹, Shuoqi Dong¹, Xiaoping Zhao¹, Jiping Xu¹,
Wandong Li¹, and Xiaodong An²

¹ College of Computer and Information Engineering, Beijing Technology and Business
University, Beijing, China

sdwangxy@163.com, liuzw@th.btbu.edu.cn,
surecheer@hotmail.com

² Taiyuan Yi tai-hao Science and Technology Co. Ltd., Shanxi, China
ann_xiaodong@163.com

Abstract. PLS (Partial Least-Squares) is adopted to carry on non-linear compensation to the BOD (Biochemical Oxygen Demand) soft-sensing mechanism model on the basis of studying on Lawrence - McCarty formula's BOD mechanism model. Compared with BOD biosensors adopting different materials and the least squares compensation method, the method has obvious advantages, improves the soft-sensing accuracy of BOD markedly and provides an effective way for the accurate measurement of water quality BOD in the process of waste water disposal.

Keywords: BOD, soft sensor, Lawrence - McCarty formula, PLS, least-squares method.

1 Introduction

BOD is not only one important effluent index, but also a significant monitoring parameter during the process of biologically treating waste water. Traditionally, the method of measuring BOD is mainly to adopt chemical means with field sampling and cultivation in laboratories, and then measured value can be obtained after five days. However, this method cannot realize the functions of real-time on-line measurement and the closed-loop control of wastewater treatment. Recently, an important direction in BOD measuring is the use of biosensors with new materials, such as the organic-inorganic hybrid materials using sol-gel and grafted copolymer composition [1], but the process is relatively too complex to meet the real time requirement of wastewater treatment.

In recent years, some scholars have done a lot of researches on BOD soft-sensing modeling and obtained some achievements [2,3,4,5]; however there are still some deficiencies. The literature [6] puts forward the error compensation of BOD mechanism model using limited memory method of least squares to realize BOD Soft-sensing, but certain bias compensation accuracy is existed as a result of the linear compensation method. For the purpose of further enhancing the compensation

accuracy of the mechanism model, the characteristics of activated sludge is considered in this paper. Started from the mechanism of biological wastewater treatment process, through studying the BOD soft-sensing second-order mechanism model of the Lawrence - McCarty formula in depth, the non-linear error compensation between mechanism model and the true value is acquired by using partial least squares (PLS), and then an effective BOD soft-sensor hybrid model is set up to provide a theoretical basis for the realization of BOD on-line measuring instruments.

2 BOD Soft-sensing Model Formula

The BOD mechanism model formula is based on the classic Lawrence - McCarty chemistry formula in 1949, through the experimental study of the pure culture's cultivation by diluting solution with a continuous flow, Monod proposed the functional [7] relation between microbe multiplication rate and substrate concentration:

$$u = u_{\max} \frac{S}{k_S + S} \quad (1)$$

Where u is microbe multiplication rate, u_{\max} is the maximum microbe multiplication rate, and k_S is the saturation constant [mg/L]. When $u = u_{\max} / 2$, the substrate concentration is also known as half-rate constant; S is the concentration of organic substrate [mg/L].

In the wastewater biological treatment, the microbial growth has a certain relationship with substrate degradation. From this, the Lawrence - McCarty formula can be evolved into [8]

$$S = m_1 \frac{Q_a(DO_s - DO)}{X} t^2 + m_2 \frac{Q_a(DO_s - DO)}{X} t + m_3 \frac{Q_a(DO_s - DO)}{X} + m_4 t^2 + m_5 t + m_6 \quad (2)$$

Eq. 2 is the final model formula of BOD soft-sensing mechanism model in water treatment process. In the formula, the input variables are Q_a (aeration flow), t (temperature), X (the concentration of volatile sludge in mixed liquor, which is turbidity) and DO (dissolved oxygen concentration), and the output variable is S (substrate concentration), which is BOD. In the activated sludge process, the saturated concentration under the condition of half the depth of the pressure oxidation pond is usually used as DO_S in Eq. 3.

$$DO_S = (1 + H/20)(DO_S)_{760} \quad (3)$$

Where H is the depth of the aeration tank. The Eq. 4 is the saturation solubility:

$$(DO_S)_{760} = \frac{475 - 2.65Z}{33.5 + t}. \quad (4)$$

When the atmospheric pressure is 760mm Hg, $(DO_S)_{760}$ is the saturated solubility of oxygen in water [mg/l]. Z is the solid concentration of dissolved oxygen in water [g/L]. The parameters of mechanism model Eq. 2 are shown in Table 1 [9].

Table 1. Constant coefficient values of the mechanism model

Parameters	m_1	m_2	m_3	m_4	m_5	m_6
Values	0.000065 025	- 0.004335	0.1445	- 0.00000976 05	0.00065 07	-0.02169

However, sewage treatment process has poor production conditions and serious random disturbance with the characteristics of strong nonlinear, big time-variance and serious lag. Therefore, the big variance of data exists in the mathematical model built by the mechanism. It needs to use compensation methods for the mechanism model.

3 The PLS Compensation of BOD Soft-sensing Mechanism Model

The theory of partial least square. Supposing there are p independent variables x_1, \dots, x_p and q dependent variables y_1, \dots, y_q , observing n sample points, which constitutes the independent variable and dependent variable matrix $X = (x_{ij})_{n \times p}$ and $Y = (y_{ij})_{n \times q}$. In PLS regression, the components t_1 and u_1 are extracted from the X and Y matrix respectively. These two components should meet the following conditions [10]: (1) t_1 and u_1 need to carry their own variability information in the data table as far as possible; (2) the relevance between t_1 and u_1 can achieve the greatest degree.

The first component t_1 and u_1 have been extracted, PLS regression implement the return of X on t_1 as well as the return of Y on u_1 . If the regression equations have reached a satisfactory accuracy, then the algorithm is terminated; otherwise, it will be using the residual information from X interpreted by t_1 and Y interpreted by u_1 for the second extraction. So back and forth until it can reach a far more satisfactory accuracy. Finally, If m components t_1, \dots, t_m were extracted from X , PLS regression through implementing the return of y_k on t_1, \dots, t_m , and then expressed as y_k regression equation which on the original variables x_1, \dots, x_m , where $k = 1, 2, \dots, q$.

BOD mechanism compensation algorithm steps. Soft measurements obtained from BOD model have a certain degree of deviation compared with actual values, non-linear iterative PLS method can be used for an effective remedy about the mechanism model. The difference in BOD as the output, soft-sensing value of mechanism model as input of the regression equation, so concrete steps of BOD compensation algorithm can be described as follows:

Recorded the matrix consisted of auxiliary variable input (DO, X, Qa, t) as $E_0 = (DO, X, Qa, t)$ after standardization, and the deviation Δu between soft-sensing value obtained from the mechanism model and the true value is recorded as $F_0 = (VU)$.

t_1 is the first component of E_0 , w_1 is the first axis of E_0 , that is, $Pw_1P = 1$. u_1 is the first component of F_0 , $u_1 = F_0 \cdot c_1$. c_1 is the first axis of F_0 , that is, $Pc_1P = 1$. The Requirement is to maximize the covariance, that is

$$Cov(t_1, u_1) = \sqrt{Var(t_1)Var(u_1)} \cdot r(t_1, u_1) \rightarrow \max . \tag{5}$$

Adopting the Lagrange algorithm:

$$E_0' F_0 F_0' E_0 \overline{w_1} = \theta_1^2 \overline{w_1}, F_0' E_0 E_0' F_0 \overline{c_1} = \theta_1^2 \overline{c_1} . \tag{6}$$

Where $\overline{w_1}$ is characteristic vector of matrix $E_0' F_0 F_0' E_0$, and the corresponding characteristic value is θ_1^2 . θ_1 is the objective function value, $\overline{c_1}$ is the unit matrix eigenvector of the largest eigenvalue θ_1^2 corresponding to $F_0' E_0 E_0' F_0$. Thus, according to $\overline{w_1}$, ingredients $\overline{t_1}$ and $\overline{u_1}$ can be acquired, where $\overline{t_1} = E_0 \overline{w_1}$, $\overline{u_1} = F_0 \overline{c_1}$.

Calculating the two regression equations separately, one is E_0 on $\overline{t_1}$, the other is F_0 on $\overline{t_1}$.

$$E_0 = \overline{t_1} \overline{p_1}' + E_1, F_0 = \overline{t_1} \overline{r_1}' + F_1 . \tag{7}$$

Where, $\overline{p_1}, \overline{r_1}$ are the regression coefficient vectors. E_1 and F_1 are respectively residuals matrixes of the two regression equations. Using the residual matrix E_1, F_1 replace E_0, F_0 and then seeking the second axis $\overline{w_2}, \overline{c_2}$ and the second component $\overline{t_2}, \overline{u_2}$, repeat the previous calculation steps, if A is the rank of X , then there will be

$$E_0 = \overrightarrow{t_1 p_1} + \cdots + \overrightarrow{t_A p_A}, F_0 = \overrightarrow{t_1 r_1} + \cdots + \overrightarrow{t_A r_A} + F_A. \quad (8)$$

Since $\overrightarrow{t_1}, \dots, \overrightarrow{t_A}$ can be expressed as a linear combination of E_{01}, \dots, E_{0p} , F_0 can be written as the regression equations about E_0 , that is,

$$F_0 = \overrightarrow{t_1 r_1} + \cdots + \overrightarrow{t_A r_A} + F_A = E_0 \left(\sum_{j=1}^A w_j \overrightarrow{r_j} \right) + F_A. \quad (9)$$

So, the regression coefficient vector matrix is $B = \sum_{j=1}^A w_j \overrightarrow{r_j}$.

In order to achieve compensating the mechanism model, calculate compensation $S = E_0 * B + F_A$, and add it to mechanism model values.

Experiment and simulation results. In the waste water treatment process, the four inputs (DO, X, Q_a, t) and BOD measured values are measured at the same time from sludge concentration of different batches as a set of data. According to the aeration frequency changes, 19 groups sampled data are acquired for soft-sensing. It is shown in Table 2.

Table 2. Measured data sheet

No.	Oxygen solubility DO [mg/l]	Aeration flow Q_a [m ³ /s]	Turbidity X [mg/l]	Temperature t [°C]	Actual BOD [mg/l]
1	8.15	31	4.2	18.8	19.55
2	8.16	32	9.9	18.9	13.24
3	8.2	33	12.1	18.9	16.75
4	8.22	34	11.7	18.9	18.15
5	8.24	35	5.8	18.8	23.06
⋮	⋮	⋮	⋮	⋮	⋮
9	8.65	40	8.6	18.9	13.94
10	8.43	41	8.5	18.5	22.36
11	8.15	42	8.9	18.5	10.44
⋮	⋮	⋮	⋮	⋮	⋮
15	8.69	46	6.4	18.9	19.55
16	8.39	47	9.7	18.5	12.54
17	8.09	48	9.5	18.5	37.79
18	8.61	49	6.4	18.8	23.4
19	8.71	50	8.1	18.9	17.45

In the data processing process, the data is firstly normalized. And then, according to the compensation algorithm steps from the previous chapter, compensated results are shown in Fig. 1.

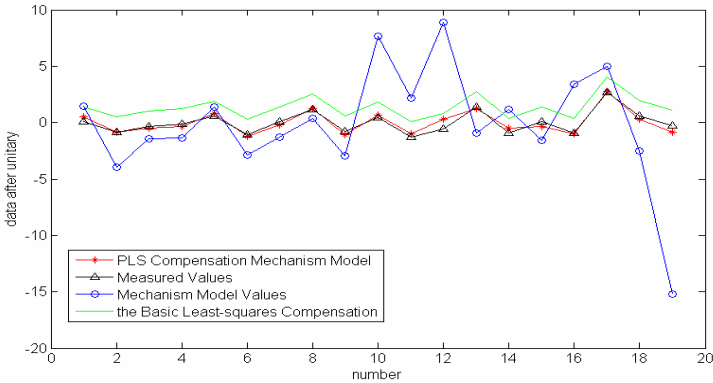


Fig. 1. Simulation results based on the PLS compensation mechanism model.

From Fig. 1, the deviation between soft measured BOD value and real BOD value is large, but the trend is basically the same, and compensation accuracy of the non-linear PLS compensation method has significantly improved compared with limited memory of least-squares method proposed in literature [6], the relative error of PLS compensation value is 0.0190, while the limited memory of least-squares method of compensation relative error is 0.9381. Therefore, the regression equations calculated by non-linear iterative partial least squares method achieved an effective compensation for mechanism model, greatly enhanced the accuracy of the model.

4 Summary

The problem that BOD is difficult to be on-line measured is the brief bottleneck of the closed-loop control of waste water disposal. Thus, the mixed model based on BOD soft measurement is built to resolve the problem. That is, on the basis of Lawrence - McCarty formula's BOD mechanism model, the compensation for mechanism model is achieved through non-linear iterative partial least squares method. Compared with Least squares linear compensation method, this method has higher accuracy. Compared with BOD biological sensors adopting different materials, it provides a reliable theoretical reference for further realization of the soft-sensing intelligent apparatuses and makes waste water's real-time closed-loop control become possible.

Acknowledgment. This study is supported by Beijing Natural Science Foundation, the Shan xi Technologies R&D Program, the Beijing Education Committee and Beijing science and educational Foundation (4112017, 20100321022, PHR201007123, PHR201008238). Those supports are gratefully acknowledged.

References

1. Liu, C., Qu, J., Xia, J., Qi, L., Dong, S.: Soft-sensing method research based on neural network for Sewage treatment indicators. *Chinese Journal of Analytical Chemistry* 33, 609–613 (2005)
2. Guan, Q., Wang, W., Xu, X., Chen, S.: Soft-sensing method research based on neural network for Sewage treatment indicators. *Environmental Pollution and Control* 28, 156–158 (2006)
3. Qi, G., Liu, Z., Cui, L.: The soft measurement method based on RBF neural network for municipal waste water treatment. *Journal of Beijing Technology and Business University: Natural Science Edition* 22, 36–38 (2004)
4. Massimo, C.D.I., Saunders, A.C.G., Morris, A.J., Montague, G.A.: Nonlinear estimation and control of mycelia fermentations, pp. 1994–1999. ACC, Pittsburg (1989)
5. Mcacvoy, T.J.: Contemplative stance for chemical process control. *Automatic* 28, 441–442 (1992)
6. Qi, J., Liu, Z., Wang, X.: Compensation of restrictive memory least square method for wastewater BOD soft measurement mechanism model. In: ICNC 2009, pp. 115–118.
7. Rongsen, D.: *Oxidation Channel Waste Water Treatment Principle and Technology*. Chemical Industry Press, Beijing (2006)
8. Qi, J., Liu, Z., Wang, X.: Research on waste water biologic process soft measurement mechanism model. In: 19th Meeting Chinese Process Control Conference Proceedings, China, pp. 95–99 (2008)
9. Zhang, Y.: *Waste water analysis soft measurement method and application and research*. Zhe Jiang University, China (2001)
10. Wang, H.: *Partial Least-squares Regression Method and Application*. National Defense Industry Press, Beijing (1999)

A New View on Regional Innovation System from Degree Distribution of Complex Networks Theory with Intelligent Attributes

JiangBo Zheng

School of management, Jinan University, Guangzhou, China
zhengjbjnu@126.com

Abstract. This paper views Regional Innovation System as a complex network. The complex features of the entities in this system as well as the interaction between the entities, which show the attributes of intelligent materials, are discussed. Based on the Degree Distribution of Complex Networks theory, this paper proves the feasible degree distributions in practical networks through mathematical reasoning and analyzing. Then, an empirical case of degree distribution characteristics of Regional Innovation System is tested by using the statistical data of Guangdong Province. Coupling Complex Networks theory with the practical conditions of Guangdong province, this paper deeply analyzes the data. The results show that the methodologies and conclusions of this paper are proper.

Keywords: Regional Innovation System, Degree Distribution, Complex Networks, Intelligent Materials.

1 Introduction

The world-famed physicist Stephen Hawking once said that the 21st century will be the Century of Complexity. This statement is widely recognized, and the researches on complexity have been carried out in many fields in recent years. Among many new researches on complexity science, one of the most representative theories is Complex Networks Theory. According to this theory, a complex network is a highly abstract complex system. In fact, complex networks can be found in natural, engineering, and even our social field. For instance, the metabolism in cells, neural networks in brains, food chain networks forming the ecological system, social relationship networks, science research cooperation networks, trade networks, internet, and electric power networks, etc[1~6]. Recent years, with the rapid development of network and computer technologies, researchers are able to obtain abundant data from major real networks to conduct statistical analysis. Such results show that complex networks are not homogeneous; on the contrary, they are heterogeneous. Their degree distribution does not follow Poisson distribution, but power-law distribution. A network that follows power-law distribution is called a scale-free network [7]. Because of the scale-free feature possessed by complex networks, its degree distribution is completely determined by its power-law index (degree distribution index). For instance, the degree distribution indexes

of most artificial networks are between 2 and 3. And some key natures (like transmission threshold) of network dynamics (like transmission of infectious disease, transmission of virus) are directly related with degree distribution index.

All of the achievements have shown the successful application of complex networks theory. However, there are not yet specific researches utilizing this theory into the important academic field--regional innovation. According to this situation, this paper first analyzes the connotation of the degree distribution based on complex network theory. Then, taking Guangdong Province as the object of demonstration, this paper calculates the degree distribution with the related data and tries to explain the calculation results. It is believed that this paper will offer important reference for future studies related to regional innovation.

2 The Definition of Regional Innovation System in the Sight of Networks

The innovation theory initially emphasizes on the technological innovation within corporations. For instance, American economist Joseph Alois Schumpeter's book *The Theory of Economic Development: An inquiry into profits, capital, credit, interest and the business cycle* pointed out that technological innovation is a linear process including developing, designing, manufacturing and selling [8]. However, as researches deepened, innovation was no longer confined to a linear model within corporations or between corporations. Now people generally consider it in a higher level--regional innovation system.

In 1987, British economist Christopher Freeman introduced the concept of "National Innovation System" [9]: the network of institutions in the public and private sectors whose activities and interactions initiate, import, modify and diffuse new technologies. The OECD report "Managing National Innovation Systems" [10] in 1999 pointed out: "innovation performance depends on the way in which the different components of the 'innovation system' -- businesses, universities and other research bodies - interact with one another at the local, national and international levels, and concludes that the public authorities must change their approach to the promotion of innovation." Throughout the researches published, although regional innovation systems have drawn great attention in the academic fields, there is no plausible explanation about it given by mainstream Economics, Industrial Economics, or Evolutionary Economics [11]. The researches in managerial fields are in worse situation.

Based on the previous studies, this paper defines regional innovation system as a complex network constituted by corporations, research institutions, universities and colleges, government and institutions with intermediary functions within a given region, which develop the ability of regional innovation by interacting with each other.

3 Theoretical Analyses on Degree Distribution

Based on the principles of complex networks, the degree of a node refers to the number of the sides to which link the node. Suppose that there is no isolated node in networks, no self-circled phenomenon, and there is at most one side between any two given nodes, then the definition of degree distribution should be:

$$P(k) = \frac{\text{the number of nodes whose degrees are } k}{\text{the total number of nodes}} \quad (\forall \text{ positive integer } k)$$

Set the total number of nodes as N , and the total number of sides as W . Then the minimum degree of every node is 1, the maximum is $N-1$. So the relationship of degree distribution can be expressed as equation (1) which is called completeness:

$$\sum_{k=1}^{N-1} P(k) = 1 \tag{1}$$

For a scale-free network [12~13], $P(k)$ is a power function, namely $\gamma > 0$ and $C_N > 0$, making

$$P(k) = C_N \cdot k^{-\gamma} \tag{2}$$

In the equation above, γ is called degree exponent; C_N is a Power law coefficient, whose value can be calculated according to the completeness of degree distribution in equation :

$$C_N = 1 / \sum_{k=1}^{N-1} k^{-\gamma} \tag{3}$$

In order to further discuss degree distribution, set the first moment and second moment of degree distribution as d_{M1} and d_{M2} respectively, expressed as followed:

$$d_{M1} = \sum_{k=1}^{N-1} k \cdot P(k) = C_N \cdot \sum_{k=1}^{N-1} k^{1-\gamma} \tag{4}$$

$$d_{M2} = \sum_{k=1}^{N-1} k^2 \cdot P(k) = C_N \cdot \sum_{k=1}^{N-1} k^{2-\gamma} \tag{5}$$

Set the average value and standard deviation as μ and σ respectively, then:

$$\mu = d_{M1} \tag{6}$$

$$\sigma^2 = d_{M2} - \mu^2 = d_{M2} - d_{M1}^2 \tag{7}$$

As we can see, with γ increasing, both d_{M1} and d_{M2} will decline. When reflecting on network topology, that means the network transits from heterogeneity to homogeneity. And when $\gamma \rightarrow +\infty$, there would be $\mu \rightarrow 1$, $\sigma \rightarrow 0$, which means the network is completely homogeneous. Since the length of this paper is limited, only one situation is discussed to demonstrate the relations between the range of γ and network topology. When $0 \leq \gamma < 1$, there are:

$$\sum_{k=1}^{N-1} k^{-\gamma} = o(N^{1-\gamma}), \quad \sum_{k=1}^{N-1} k^{1-\gamma} = o(N^{2-\gamma}) \tag{8}$$

$$d_{M1} = o(N^{2-\gamma} / N^{1-\lambda}) = o(N) \tag{9}$$

Obviously, when N is abundantly large, d_{M1} is divergent. The same:

$$d_{M2} = o(N^{3-\gamma} / N^{1-\lambda}) = o(N^2) \tag{10}$$

So d_{M2} is also divergent. Therefore based on the equation (6) and (7), it can be proved that the average and variance of degree distribution are divergent. And the total number of sides in the network is:

$$W = N \cdot \mu = N \cdot d_{M1} = o(N^2) \quad (11)$$

The equation (11) shows that the number of sides in the network is of the same magnitude with $N \cdot (N-1)/2$, the number of sides in a **complete network**. The calculation does not quite fit the real evidence obtained by other researchers since many researches with real evidence show that large networks are almost sparse networks, therefore the network where γ lies does not exist in the real world.

Specially, when $\gamma=1$, $\sum_{k=1}^{N-1} k^{-\gamma} = o[\ln(N)]$, $\sum_{k=1}^{N-1} k^{1-\gamma} = o(N)$, $\sum_{k=1}^{N-1} k^{2-\gamma} = o(N^2)$, so:

$$d_{M1} = o[N/\ln(N)], \quad d_{M2} = o[N^2/\ln(N)] \quad (12)$$

$$W = N \cdot \mu = N \cdot d_{M1} = o[N^2/\ln(N)] \quad (13)$$

Based on the principle above, a large network with $\gamma=1$ does not exist in the real world either.

4 Demonstration and Analyses Based on Data Calculation

In the view of complex network theory, different types of degree distribution of networks can reflect the nature of the whole structure. Moreover, nodes with different degrees have different status and functions within the network. Besides, the degree distribution of complex network theory is built on the hypothesis that sides and weights are equal. But practically, what matters is the overall weight. When we look into degree distribution, we can pass the source of degrees and sides or the direction of the sides and just focus on the calculation of input and output distribution of nodes.

5 Decisions of Nodes and Sides in Networks

Ideally, universities, corporations and government sectors can be identified as the innovation subjects in a region because these subjects meet with the requirements of complex network theory well. But since data that completely fits theoretical requirements is unavailable, we instead employ rough method to define nodes. That is, to see Guangdong Province as an innovation network and the 21cities of Guangdong as nodes.

Then we choose some statistics data with temporal continuity of nodes, and calculate its relevance with time, to gauge whether and at what degree they are related. The method is to subjectively define the critical value of the correlation coefficient between nodes as R_0 , then to conduct a correlation analysis between every two different nodes. When the correlation coefficient is larger than R_0 , we consider there is a side between the two nodes. This assumption is built on such theoretical basis. If two cities, at a particular time period, have a relatively consistent development trend, it means that they have similar policies and other internal and

external elements. The reason they have such similarities is generally due to communications and interactions between cities (for instance, cities often learn from other cities and promote the experience of development). So, this method avoids subjectivity, as well as better reflecting the connections between cities.

6 Selection of Data and Calculation Results

Table 1 shows statistics of the number of patents of 21 cities of Guangdong Province (data from statistics yearbook, only part of the data is shown below), which is calculated to see if a side is formed between any 2 cities. When the given $R_0=0.97$, the degree distribution (by computing programming) is shown in Fig.1.

Table 1. Domestic patent application of the main cities in Guangdong

City/year	2000	2001	2002	2003	2004	2005
Guangzhou	4410	4998	6288	8206	8230	11012
Shenzhen	4447	6177	8337	12344	15088	20943
.....	
Jieyang	498	346	331	504	539	523
Yunfu	28	43	84	94	152	148

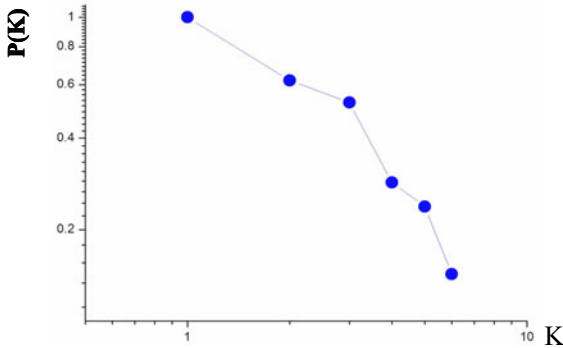


Fig. 1. Distribution of domestic patent application

As seen in figure 1, the network built by numbers of patents in Guangdong cities is a typical scale-free network. It is found that the degree distribution is negative power law distribution with $2 < \gamma \leq 3$. Based on the complex network theory, its network architecture is highly self-similar and divergent, meaning that most nodes' degree have low values, but a minority of nodes are central nodes with pretty high degree values. There subject to fore, these central nodes with high degree values are obviously of great importance, like Guangzhou, Shenzhen, Zhuhai and Foshan. The results fit the actual situation of Guangdong Province quite well, in a way demonstrating the correctness of our research.

7 Summary

The major conclusions of this paper are as follows:

- (1) A regional innovation system can be considered as a complex network. The definitions of nodes and sides reflect the features of a complex network.
- (2) The calculations show that the Guangdong Province regional innovation network follows the negative power law distribution and the degree index is between 2 and 3.
- (3) The calculations show that degree distribution theory is able to reflect the status of nodes and their relationships with one other.
- (4) The complex network theory brings new views, new tools and new methodologies to the research fields of regional innovations. Such researches worth going even further.

Acknowledgements. This paper is financially sponsored by Sponsored by: (1) the Philosophy and Social Science Fund of Chinese Ministry of Education, foundation item 09YJC630103; (2) the Fundamental Research Funds for the Central Universities, foundation item 10JYB2041.

References

1. Wasserman, S., Faust, K.: *Social Network Analysis*. Cambridge University Press, Cambridge (1994)
2. Watts, D.J., Strogatz, S.H.: Collective Dynamics of Small-World Networks. *Nature* 393, 440–442 (1998)
3. Amaral, L.A.N., Scala, A., Barthelemy, M., Stanley, H.: Classes of Small-World Networks. *Proc. Natl. Acad. Sci. USA* 97, 11149–11152 (2000)
4. Newman, M.E.J.: The Structure of Scientific Collaboration Networks. *Proc. Natl. Acad. Sci. USA* 98, 404–409 (2001)
5. Scott, J.: *Social Network Analysis: A Handbook*. Sage Publications, London (2000)
6. Barabási, A.L., Albert, R.: Emergence of scaling in random networks. *Science* 286(10), 509–512 (1999)
7. Albert, R., Barabási, A.L.: *Statistical Mechanics of Complex Networks*. *Rev. Mod. Phys.* 74(1), 47–97 (2002)
8. Schumpeter, J.A.: *The Theory of Economic Development: An inquiry into profits, capital, credit, interest and the business cycle*. Oxford Press, Oxford (1961)
9. Freeman, C.: *Technology Policy and Economic Performance: Lessons from Japan*. Pinter, London (1987)
10. OECD. *Managing National Innovation Systems*. OECD, Paris (1999)
11. Cooke, P.: Regional innovation system: an evaluation of six European cases. *Urban and Regional Development in the New Europe*, 133–154 (1993)
12. Diez, M.A.: The evaluation of regional innovation and cluster policies: towards a participatory approach. *European Planning Studies* 9(7), 907–923 (2001)
13. Jacobsson, C.B., Holmen, S., Rickne, M.: An innovation system: analytical and methodological issues. *Research Policy* 31, 233–245 (2002)

Research on a Modified Newton-Type Method with Fifth-Order Convergence for Solving Nonlinear Equations with Application in Material Science

Han Li¹ and Liang Fang²

¹ Department of Mathematics, Heze University, 274015, Heze, China
lihan9529@163.com

² College of Mathematics and System Science,
Taishan University, 271021, Tai'an, China
fangliang3@163.com

Abstract. Numerical solution methods of nonlinear equation have very broad application prospect in materials science. In this paper, we present and analyze a fifth-order convergent method for solving nonlinear equations. The method is free from second derivatives and permits $f'(x)=0$ at some iteration points. Several numerical tests demonstrate that the sixth-order method given in this paper is more efficient and performs better than classical Newton's method.

Keywords: Nonlinear equations, Iterative method, Newton's method, efficiency index, Order of convergence.

1 Introduction

The design of iterative formulas for solving nonlinear equations is a very interesting and important task in numerical analysis. Numerical solution methods of nonlinear equation have very broad application prospect in many fields, such as materials science, computer science, physics, art design, etc. In this paper, we consider iterative method to find a simple root x^* of a nonlinear equation $f(x) = 0$, where $f: D \subseteq \mathbb{R} \rightarrow \mathbb{R}$ for an open interval D is a scalar function and it is sufficiently smooth in a neighborhood of x^* .

It is well known that classical Newton's method (NM) is a basic and important method for solving non-linear equation (1) by the iterative scheme

$$x_{n+1} = x_n - \frac{f(x_n)}{f'(x_n)}, \quad (1)$$

which is quadratically convergent in the neighborhood of x^* .

In recent years, much attention has been given to develop iterative methods for solving nonlinear equations and many iterative methods have been developed [2-12]. Some fifth-order iterative methods have been proposed and analyzed for solving nonlinear equations. These methods improve some classical methods such as Newton's method, Cauchy's method and Halley's method. It is said that the improved methods are efficient and can compete with Newton's method. However, many of

these fifth-order methods depend on the second derivative, and most of existing methods need $f'(x_k) \neq 0$ at the iterate x_k which strictly reduce their practical applications.

Motivated and inspired by the on going activities in this direction, in this paper, we present a fifth-order convergent method. Several examples are given to illustrate the efficiency and advantage of the method.

2 The Method and Its Convergence

Let us consider the following iterative method.

Algorithm 1. For given x_0 , we consider the following Newton-type method for non-linear equation [1] by the iterative scheme

$$y_n = x_n - \frac{f(x_n)}{\lambda_n f(x_n) + f'(x_n)}, \tag{2}$$

$$z_{n+1} = y_n - \frac{f(y_n)}{\lambda_n f(x_n) + f'(x_n)}, \tag{3}$$

$$x_{n+1} = z_n - \frac{f(z_n)}{\mu_n f(z_n) + f'(y_n)}, \tag{4}$$

where λ_n are real numbers chosen such that $0 \leq |\lambda_n|, |\mu_n| \leq 1, n=1,2,\dots$ and $\text{sign}(\lambda_n f(x_n)) = \text{sign}(f'(x_n)), \text{sign}(\mu_n f(z_n)) = \text{sign}(f'(y_n))$, where $\text{sign}(x)$ is the sign function.

For Algorithm 1, we have the following convergence result.

Theorem 1. Assume that the function $f: D \subseteq \mathbb{R} \rightarrow \mathbb{R}$ has a single root $x^* \in D$, where D is an open interval. If $f(x)$ has first, second and third derivatives in the interval D , then Algorithm 1 is fifth-order convergent in a neighborhood of x^* and it satisfies error equation

$$e_{n+1} = 2c_2(\lambda_n + 2c_2)(\lambda_n + c_2)^2 e_n^5 + O(e_n^6), \tag{5}$$

where $e_n = x_n - x^*, c_k = \frac{f^{(k)}(x^*)}{k!f'(x^*)}, k=2,3,\dots$

Proof. Let x^* be the simple root of $f(x), c_k = \frac{f^{(k)}(x^*)}{k!f'(x^*)}, k=2,3,\dots$ and $e_n = x_n - x^*$. Consider the iteration function $F(x)$ defined by

$$F(x) = z(x) - \frac{f(z(x))}{\mu_n f(y(x)) + f'(y(x))}, \tag{6}$$

where $z(x) = y(x) - \frac{f(y(x))}{\lambda_n f(x) + f'(x)}, y(x) = x - \frac{f(x)}{\lambda_n f(x) + f'(x)}$.

By some computations using Maple we can obtain

$$F(x^*) = x^*, F^{(i)}(x^*) = 0, i=1,2,3,4,$$

$$F^{(5)}(x^*) = \frac{30f''(x^*)[f'(x^*) + 2\lambda_n f(x^*)]^2 [f''(x^*) + \lambda_n f'(x^*)]}{f'(x^*)^4}, \tag{7}$$

Furthermore, from the Taylor expansion of $F(x_n)$ around α , we get

$$\begin{aligned} x_{n+1} &= F(x_n) \\ &= F(x^*) + F'(x^*)(x_n - x^*) + \frac{F''(x^*)}{2!}(x_n - x^*)^2 + \frac{F'''(x^*)}{3!}(x_n - x^*)^3 + \frac{F^{(4)}(x^*)}{4!}(x_n - x^*)^4 \\ &\quad + \frac{F^{(5)}(x^*)}{5!}(x_n - x^*)^5 + O((x_n - x^*)^6). \end{aligned} \tag{8}$$

Substituting (7) into (8) yields

$$x_{n+1} = x^* + e_{n+1} = 2c_2(\lambda_n + 2c_2)(\lambda_n + c_2)^2 e_n^5 + O(e_n^6). \tag{9}$$

Therefore, we have

$$e_{n+1} = 2c_2(\lambda_n + 2c_2)(\lambda_n + c_2)^2 e_n^5 + O(e_n^6), \tag{10}$$

which means the order of convergence of the Algorithm 1 is five. The proof is completed.

3 Numerical Results

Now, we employ Algorithm 1 presented in the paper to solve some nonlinear equations and compare it with NM. Displayed in Table 1 are the number of iterations (ITs) required such that $lf(x_n) < 1.E-14$.

In table 1, we use the following functions.

- $f_1(x) = \sin(x+1) - x + 2, x^* = 2.07076672709785.$
- $f_2(x) = x^3 + e^x - x + 1, x^* = -1.38070588484698.$
- $f_3(x) = x^3 - 10, x^* = 2.15443469411846.$
- $f_4(x) = (x-1)^3 - 1, x^* = 2.$

Table 1. Comparison of Algorithm 1 and classical NM

functions	x_0	NM	Algorithm 1
f_1	-1	Failure	5
	0	70	3
f_2	0	Failure	6
	-1	6	3
f_3	0	Failure	7
	0.02	26	5
f_4	1	Failure	7
	1.01	26	10

The computational results in Table 1 show that Algorithm 1 requires less ITs than NM. Therefore, the present fifth-order convergent method is of practical interest and can compete with classical Newton's method. The study will be used in material design and some other aspects.

Acknowledgements. The work is supported by Project of Shandong Province Higher Educational Science and Technology Program (J10LA51).

References

1. Traub, J.F.: *Iterative Methods for Solution of Equations*. Prentice-Hall, Englewood Cliffs (1964)
2. Noor, M.A., Noor, K.I.: Fifth-order iterative methods for solving nonlinear equations. *Appl. Math. Comput.* 188, 406–410 (2007)
3. Muhammad, A.N., Khalida, I.N.: Modified iterative methods with cubic convergence for solving nonlinear equations. *Appl. Math. Comput.* 184, 322–325 (2007)
4. Kou, J.: The improvements of modified Newton's method. *Appl. Math. Comput.* 189, 602–609 (2007)
5. Fang, L., He, G., Hu, Z.: A cubically convergent Newton-type method under weak conditions. *J. Comput. Appl. Math.* 220, 409–412 (2008)
6. Fang, L., He, G.: Some modifications of Newton's method with higher-order convergence for solving nonlinear equations. *J. Comput. Appl. Math.* 228, 296–303 (2009)
7. Fang, L., Sun, L., He, G.: An efficient Newton-type method with fifth-order for solving nonlinear equations. *Comput. Appl. Math.* 27, 269–274 (2008)
8. Fang, L., He, G., Hu, Y., Sun, L.: Some modified Newton-type methods with order of convergence varied from two to six under weak conditions. In: *IEEE CSO 2009*, pp. 637–640 (2009)
9. Hu, Y., Fang, L., He, G.: Two new three-step predictor-corrector type iterative methods with fifth-order convergence for solving nonlinear equations. In: *CINC 2010*, vol. 2, pp. 16–19 (2010)
10. Hu, Y., Fang, L.: A seventh-order convergent Newton-type method for solving nonlinear equations. In: *CINC 2010*, vol. 2, pp. 13–15 (2010)
11. Muhammad, A.N., Faizan, A.: Fourth-order convergent iterative method for nonlinear equation. *Appl. Math. Comput.* 182, 1149–1153 (2006)
12. Grau, M., Diaz-Barrero, J.L.: An improvement to Ostrowski root-finding method. *Appl. Math. Comput.* 173, 450–456 (2006)

Image-Adaptive Watermarking Algorithm to Improve Watermarking Technology for Certain Water Marking Based on DWT and Chaos

LingFeng Zhang¹, Xine You¹, and YuPing Hu^{2,3}

¹ Loudi Vocational and Technical College, Loudi, 417000, China

² HangZhou Key Lab of E-Business and Information Security
Hangzhou, 850922, China

³ Guangdong Province Key Lab of EC Market Application Technolog,
Guangzhou, 510320, China
okhyp@yahoo.com.cn

Abstract. In this paper, a digital image watermark algorithm to improve watermarking technology for certain watermarking materials based on discrete wavelet transform and chaos theory is proposed. During the watermarking embedding, discrete wavelet transform is done firstly and the chaotic sequence is produced for the watermark. Before the watermark is embedded, a correlation mask for every lowest coefficient is confirmed by the characteristic and tree structure relation of the wavelet coefficients. Then, the hidden watermarking strength of every lowest coefficient is controlled by its corresponding mask. The experimental results show that the proposed algorithm is effective and robust to common image processing operations and some geometric operations such as JPEG compression, JPEG2000 compression, Filtering, Adding Gaussian noise and so on. The effect of watermarking image is very well.

Keywords: Wavelet transform, chaotic sequence, Watermark.

1 Introduction

With the development of the Internet, more and more digital media products become available through different online services. The rapid growth of the multimedia services has created a potential demand for the protection of ownership since digital media is easily reproduced and manipulated. Digital watermarking has been introduced for solving such problems. One of the most prominent applications of watermarking is using robust and practical watermarking to protect image and video data [1].

There are a number of desirable characteristics that a digital watermarking technique can offer, including security, imperceptibility, and robustness. Roughly speaking, the digital watermarking technology includes spatial-domain methods (embedding the watermark into the grey values directly) and transform-domain methods (performing a special transform to the original image and then embedding

the watermark into part of the transform-domain coefficients). Embedding the watermark into the transform-domain generally helps to increase the imperceptibility, security, and robustness. Therefore, this approach is very common, where DFT, DCT, DWT are three main transform methods used[2]. In 1963., Chaos evolved from the work of Edward Lorenz,a meteorologist at Massachusetts Institute of Technology [3].An overview of early chaotic watermarking techniques can be found in [4][5][6].In this paper, we propose a Image-adaptive Watermarking algorithm based on DWT and chaos.

2 The Wavelet Trees and Chaotic Key Sequence

2.1 The Wavelet Trees

For convenience, we will use 3-level wavelet transform of a 512×512 image as example. With 3 level decomposition, we have 10 subbands as shown in Fig 1,the coefficients are grouped according to wavelet trees We will use the coefficients in band LL (I_3) as roots to form wavelets trees. At the forth it can be defined as follow:

$$tree(I_3(x, y)) = \bigcup_{\theta=1}^3 tree(I_3^\theta(x, y))$$

$$tree(I_l^\theta(x, y)) = \bigcup_{i=1}^2 \bigcup_{j=1}^2 tree(I_{l-1}^\theta(2x-2+i, 2y-2+j)) \quad (l=3,2) \quad (1)$$

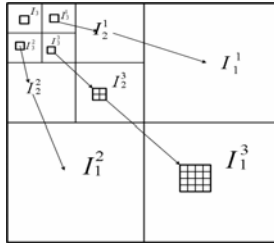


Fig. 1. Tree structure of wavelet coefficients

2.2 Chaotic Key Sequence

In recent years, chaotic maps have been used for digital watermarking to increase the security. The most attractive features of chaos in information hiding are its extreme sensitivity to initial conditions and the outspreading of orbits over the entire space. These special characteristics make chaotic maps excellent candidates for watermarking and encryption [7].

The model here is chaos 1-D Logistic:

$$x(n+1) = \mu x(n)[1-x(n)] \quad (2)$$

Here, $\mu \in (0,4)$; $x(n) \in (0,1)$. By setting μ and initial value $x(0)$, we get chaotic signal.

In order to get chaotic sequences, the chaotic $x(n)$ must be transformed into binary signal sequence $x(s)$. So quantized function $W[x(n)]$ is used, its definition is[8]:

$$W[x(n)] = \begin{cases} 0 & x(n) \in \bigcup_{k=0}^{2^m-1} I_{2k}^m \\ 1 & x(n) \in \bigcup_{k=0}^{2^m-1} I_{2k+1}^m \end{cases} \quad (3)$$

Here, $m > 0$ and m is random integer, $I_0^m, I_1^m, I_2^m, \dots$ is continuous equal interval in $[1,0]$, the interval is divided by 2^m . If the value is in the odd interval of the quantized function, the quantized value is 1, or else, the quantized value is 0. The binary sequences generated were tested of good pseudo-random sequence characteristics, such as long period, 0-1 equivalence and non correlation.

2.3 Watermarking Algorithm

Due to the excellent time-frequency features and the well matching to the human visual system (HVS) characteristic, wavelet has been widely used for digital watermarking, especially after the wavelet transform becoming the basic technology in JPEG2000 standards. In this scheme, the watermark is embedded into the DWT low frequency coefficients, where perceptual considerations are taken into account by setting the amount of modification proportional to the strength of the coefficient itself. Here take a initial value of Logistic equations key, produce a chaos sequence for watermark.

2.4 Watermarking Embedding

Step 1: Make three-level harr wavelet decomposition to the original image I of the size $M \times N$ and the low frequency LL_3 as the embedded domain.

Step 2: Use the author signature K as the initial value of Logistic equations key, produce a chaos sequence for watermark

$$W = \{\omega(x, y) \mid \omega(x, y) = \pm 1, 1 \leq x \leq M/8, 1 \leq y \leq N/8\}$$

Step 3: Compute every perceptual mask of low frequency coefficient according to the following formula:

$$M(x, y) = d_3(x, y) + \sum_{\theta=1}^3 [d_3^\theta(x, y) + \sum_{i=1}^2 \sum_{j=1}^2 d_2^\theta(2x-2+i, 2y-2+j) + \sum_{i=1}^4 \sum_{j=1}^4 d_1^\theta(4x-4+i, 4y-4+j)] \quad (4)$$

Here $d_3(x, y)$ is the power quotient of the low frequency coefficient $I_3(x, y)$ in its corresponding band. $d_l^\theta(x, y)$ is the power quotient of the high frequency coefficient $I_l^\theta(x, y)$ in its corresponding band, the computing formula of them is as follow:

$$d_3(x, y) = \frac{I_3(x, y)^2}{\sum_{i=1}^{M/8} \sum_{j=1}^{N/8} I_3(i, j)^2} \quad (5)$$

$$d_l^\theta(x, y) = \frac{I_l^\theta(x, y)^2}{\sum_{i=1}^{M/2^l} \sum_{j=1}^{N/2^l} I_l^\theta(i, j)^2} \quad (6)$$

Step 4: Modify every low frequency coefficient $I_3(x, y)$ to embed watermark into original image

$$I'_3(x, y) = I_3(x, y) + \alpha M(x, y) \omega(x, y) \quad (7)$$

Here $I_3(x, y)$ is the low frequency coefficient before embedding. $I'_3(x, y)$ is the low frequency coefficient after embedding. α is the parameter for controlling the watermarking strength which is determined by experiment.

Step 5: Use all modified coefficients of low band and non-modified coefficients of high bands to make a wavelet reconstruction of the watermarking embedded image I' .

2.5 Watermarking Checking

Step 1: Make same three-level harr wavelet decomposition to the detected image I' as the watermarking embedding.

Step 2: Use the author signature K as the initial value of Logistic equations key, produce a chaos sequence for watermark.

Step 3: Compute the correlation relative coefficient of the detected image and watermark W according to the following formula:

$$\rho = \sum_{x=1}^{M/8} \sum_{y=1}^{N/8} I'_3(x, y) \omega(x, y) \quad (8)$$

If we can obtain the original image, the correlation relative coefficient is computed according to the following formula:

$$\rho = \sum_{x=1}^{M/8} \sum_{y=1}^{N/8} [I'_3(x, y) - I_3(x, y)]\omega(x, y) \quad (9)$$

Here $I_3(x, y)$ is the low frequency coefficient of original I .

Step 4: Using a defined decision threshold ρ_T , if $\rho > \rho_T$, we can conclude the detected image contain watermark, otherwise it do not contain watermark.

The ρ_T is determined as following[9]:

$$\rho_T = 3.3 \sqrt{\frac{2 \times 64^2}{(MN)^2} \sum_{x=1}^{M/8} \sum_{y=1}^{N/8} [I'_3(x, y)]^2} \quad (10)$$

3 Experiment Results

In this paper, the performance of the proposed algorithm is evaluated with respect to watermark imperceptibility, robustness, and watermark fidelity. The 512×512 image “Baboo” is used for our experiments. The quality metric is based on the Peak Signal to Noise Ratio (PSNR). The watermarked image in this experiment has PSNR=38.2db which means the watermark is almost imperceptible.

To test the reliability of the blind detection algorithm, we design 1000 different watermarks by sequence randomizer, and with the original watermark replace the 500th watermark, embed these watermarks into the original image, so can get 1000 different watermarked images. Then decompose each image with DWT and extract low frequency component, calculate the correlation value between w and each wavelet coefficient, then plot the curve, it can be seen that only when the watermark is the original watermark, the peak value $\rho(500) = 17.53$ is produced in the correlation curve, otherwise the correlation value is near to 0. According to the formula (10) $\rho_T = 2.01$ and $\rho(500) > \rho_T$. The correlation value of watermark images is seen in Figure 2.

The correlation value between original watermarked image and the attacked images is listed in Table 1. It can be seen, when using this scheme to embed the watermark into the image, the correlation value between the attacked images and the watermark is more than 0. So by using calculate the correlation value, it can be detect whether the image embed the watermark.

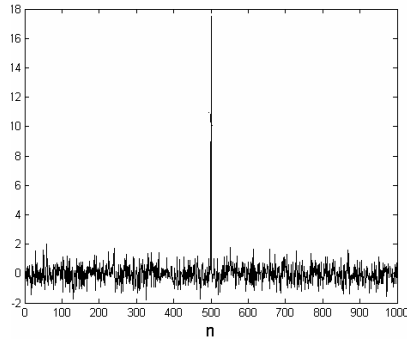


Fig. 2. Correlation value of watermark images

Table 1. Correlation value of attacks

Attacks	Correlation value $\rho(500)$
JPEG(QF=70)	12.93
JPEG2000(0.40bpp)	13.81
Average filter (3×3)	9.52
Median filter.(3×3)	8.34
Adding Gaussian noise(variance=30)	11.68
Crop(cut 15% from top left corner)	14.32

4 Conclusions

In this paper, a image-adaptive watermarking algorithm improve watermarking technology for certain watermarking materials based on DWT and chaos is proposed an algorithm based on discrete. The security is enhanced by chaotic binary and. a correlation mask for every lowest coefficient is confirmed by the characteristic and tree structure relation of the wavelet coefficients. Then, the hided watermark strength of every lowest coefficient is controlled by its corresponding mask. The results in this paper demonstrate that it is effective and robust to common image processing operations and some geometric operations such as JPEG compression, JPEG2000 compression, Filtering, Adding Gaussian noise and so on.

Acknowledgment. This work was by Guangdong Provincial Science and Technology Planning Project of China (No. 2010B01060036); Natural Scientific Research Fund of Guangdong (No. 2011023960). Research Fund of Hang Zhou Key Lab of E-Business and Information Security; (HZEB201003).

References

1. Thomas, T., Emmanuel, S., Subramanyam, A.V., Kankanhalli, M.S.: Joint Watermarking Scheme for Multiparty Multilevel DRM Architecture. *IEEE Transactions on Information Forensics and Security* 4(4), 758–767 (2009)
2. Petitcolas, F.A.P., Anderson, R.J., Kuhn, M.G.: Information hiding – A survey. *Proc. IEEE* 87(7), 1062–1078 (2006)
3. Peterson, G.: Amol’s cat map survey. *Math 45-Linear Algebra* (Fall 1997)
4. Zhao, J.-L.: Watermarking algorithm based on chaotic sequence and DWT. In: *DWT Proceedings of the Seventh International Conference on Machine Learning and Cybernetics, Kunming, July 12-15*, pp. 3052–3055 (2008)
5. Nikolaidis, N., Tsekeridou, S., Nikolaidis, A., Tefas, A., Solachidis, V., Pitas, I.: Applications of chaotic signal processing techniques to multimedia watermarking. In: *Proceeding of the IEEE Workshop on Nonlinear Dynamics in Electronic Systems Cantania, Italy, May 18-20*, pp. 1–7 (2000)
6. Keyvanpour, M.R., Farnoosh, M., Keyvanpour, M.R., Merrik-Bayat, F.: A new Encryption method for secure embedding in image watermarking. In: *2010 3rd International Conference on Advanced Computer Theory and Engineering (ICACTE)*, pp. V2-403 –V2-407 (2010)
7. Kuribayash, M., Tanaka, H.: A new digital watermarking scheme applying locally wavelet transform. *IEEE Trans. Fundam.* E84- A(10), 2500–2507 (2004)
8. Wang, Q., Ding, Q., Zhang, Z., Ding, L.: Digital Image Encryption Research Based on DWT and Chaos. In: *ICNC 2008. Fourth International Conference on Natural Computation*, pp. 494–498 (2008)
9. Liu, T., Qiy, I.U., Zheng-Ding: An Image-Adaptive Digital Watermarking Algorithm Based on Wavelet Transform. *Chinese Journal of Computers* 25(11), 1195–1199 (2002)

An Intelligent System of Diagnosis Based on Associative Factor Uncertainty Speculation Inference

Wenxue Tan¹, Xiping Wang², and Xiaorong Xu³

¹ Institute of Network Technology, Hunan University of Arts and Science,
Changde, P.R. China
papertwx@163.com

² College of Economy and Management, Hunan University of Arts and Science,
Changde, 415000
xpwang@sina.com

³ College of Computer Science and Technology, Hunan University of Arts and Science
rortyrong@163.com

Abstract. Along with the development of computer technology and Artificial Intelligence, it has been a highlight of Intelligent Diagnosis System how to solve diagnosis problem more accurately and smoothly by the help of AI system. In this paper, some novel concepts such as Key Factor, Associative Factor and Uncertainty Speculation are initiated. Furthermore, we pioneer a method so-called Uncertainty Inference based on Key-Associative Uncertainty Speculation, into which an innovative speculation mechanism is proposed and integrated. Study of cases and experiment statistics makes it clear that our scenario is practical, effective, and with a satisfying accurate rate of diagnosis.

Keywords: AI, Associative Factor, Uncertainty Speculation, Intelligent Diagnosing, Disease.

1 Introduction

Disease Intelligent Aid system, which is based on digital technology and normalized expert experience knowledge, expands human's diagnostic ability, and it is widely used in diagnosing as a practical instrument. But, some systems, of which expert knowledge is only based on the traditional Uncertainty factor-Inference, abbreviated by U-Inference obviously manifests 2 faults as follows. 1. A low efficiency of Knowledge-Rule. 2. The mechanism of traditional U-Inference based on the static Certainty Factor Vector while short of Correction or Speculation process disagrees with the human's habit of thinking and diagnosing, and always results in one-sided diagnosis, even misdiagnosis [1, 2].

What is the cause? In fact, it goes without saying that the role of symptoms manifested in the life span of disease haven't been equal, while some of them haven't developed and been observed at the same time. It is intelligible that the traditional *U-Inference* overlooks both respects and returns a one-sided even mistake conclusion. So, we try to overturn the situation by researching the *Uncertainty Inference* based on *Associative Uncertainty Speculation*.

Previous work. On the basis of the theory of certainty, EH Shortliffe and his partners pioneered the Uncertainty Inference algorithm which was successfully applied in the intelligent system named "MYCIN". On the application of U-Inference method in the intelligent systems, some scholars did a lot of related researches. For instances, the Research on the Application of Multi-combined Technologies of Fault Diagnosis on Missile Seekers [3], in which a mechanism of locating the faults of missile seekers based on U-Inference is proposed. A Sheep Disease Intelligent System based on production rules [1], and a Grape Disease Diagnosis System based on Fuzzy Neural Network [4], etc.

Our Contributions. We pioneer Uncertainty Inference based on Key Associative Uncertainty Speculation in order to improve computational intelligence of diagnosis. Concepts of Key-Associative Factor and Uncertainty Factor Speculation are initiated and defined. An innovative Certainty speculating mechanism is brought forward and integrated into the algorithm of Uncertainty Inference based on Key-Associative Uncertainty Speculation, which improves things better.

2 Related Fundamental s of Key-Associative Factor Uncertainty Speculation

Randomicity and chanciness, uncertainty is universe phenomena in the nature and the same thing are in the area of disease diagnosing. Concepts of Certainty are often used to depict indeterminate causality between cause and effect, which is taken into consideration when we select AI methods to lay foundation for disease intelligent diagnosing mechanism.

However, after a long span of practice, it is made clear because the traditional Certainty Factor method doesn't take the associativity between the observed clinic symptom and those so far not occurring and unobserved symptom which are listed in the standardized description of corresponding disease into account. Thus, some knowledge rules which should have been available while Inferring have no opportunity to be activated and applied. As a result, misdiagnosis or fail of diagnosis is ended. As to the case, we pioneer the concepts of Key-Factor, Associative Factor and Uncertainty Speculation and devise the algorithm so-called Uncertainty Inference based on Associative Uncertainty Speculation, abbreviated by *UIAUS*.

Uncertainty Rule. It refers to the knowledge rule denoted as equation (1), $CF(E,H)$ denotes the Certainty Factor depicting the knowledge intensity, the greater its value, the more intensively the precondition denoted by E supports the Hypothesis conclusion denoted by H . In other words, the bigger is the probability of conclusion H to be true. λ is a threshold of certainty, calculation of $CF(E,H)$ referred in [5].

$$\text{if } E_1(w_1) \text{ AND } E_2(w_2) \text{ AND} \cdots \text{AND } E_n(w_n) \text{ then } H(CF(H,E),\lambda) \quad (1)$$

Associative Factor and Key-Factor. In the life span of disease, the development of clinic manifestation is a phasic course, which varied by the different symptoms [5, 6, 7]. Symptom E_i of a disease, it has a big weight w_i in a certain knowledge rule as

equation (1). If E_i has occurred, the symptom E_{i+1} also will appear in succession if no action is taken and let the diseased subject be. Furthermore, E_{i+1} has a weight as big as E_i even greater than E_i , then we define E_{i+1} as an Associative Factor, and define E_i as Key Factor. A case of associative factor rule is exhibited as Table 1.

In reality, it is often that if the E_{i+1} isn't observed, and the CF vector composite value of E_{i+1} is assigned 0, which produces a very low resultant macro CF -value of all the evidences. As a result, the match between the evidences and rules fails, and a misdiagnosis or fail of diagnosis occurs. As viewed from the above, the appropriate measures should be taken to counteract it [6,7].

Table 1. A Case of Associative Factor Rule about Lamb-dysentery

Name of disease	type	Symptoms	Prevention and treatment	Set of Normalized Clinic		
				Code	description	CF
Lamb-dysentery	Infectious	Shortness breath; anorexia; and diarrhea; and stool being brown yellow; or yellow-white or dark-red, watery, a lightly bloody, Lying land unable to afford to getup.	be care of keeping warm, breastfeeding; keeping sheep-shed disinfection, isolating the sick lamb; pre-injection vaccine of anaerobic bacteria detail operation following as follows...	01	the lamb not to suck colostrums	[0.65]
				02*	anorexia even slowly or cease to eat	[0.77]
				03*	Diarrhea; with brown yellow fecal matter.	[0.82]
			
			

Uncertainty Factor Speculation. According to the description above, some steps should be taken to correct the Certainty Factor of E_{i+1} which is an associative factor relative to key factor E_i , not to let it be 0 and denote it by $CF(E_{i+1})$. We define these steps and their corresponding process as *Uncertainty Factor Speculation*. Definitely, there are 3 methods designed and introduced in this research as follows. Taking the lowest of CF vector is called the *Lowest-Speculation* method. If taking the highest weight of CF vector be called the *Highest-Speculation* method. Taking a midpoint of confidence-interval between the lowest and the highest is called the *Midpoint-Speculation* method.

3 Experimentation Statistics and Analysis

Individual Experiment. In the course of the experiment, the Black Goat is singled out as a subject. The disease named "Sheep-Pox" is highlighted as an example, of which the clinic manifestations are standardized and segmented into 8 atomic clinic items. A veterinary inputs the clinical symptom data sampled from the diseased goat into both

software prototypes, one of which is based on *UIAUS*, the other is based on the Traditional U-Inference (abbreviated by *TUI*). Meantime, by diagnosing system several paper copies of the clinical report are printed and distributed to some human experts for diagnosing in order to determine the disease infecting the goat. The data from human expert and about the disease Sheep-Pox are listed in [6] in detail.

Average of human experts' results is 0.64, which falls into the interval [0.6, 0.8]. Results of *UIAUS* is listed in Table 2. 5 knowledge rules about Sheep-Pox are activated on machine diagnosing, each of which has a weight vector of clinic characteristics, and the no. 5,6,7 symptoms are the *Associative Factors* assigned with bigger weights. As to uncertainty factor speculation, the *Highest-Speculation* method is introduced to speculate the *Uncertainty Factor of Key-Associative Factors*. The conclusion interval of *UIAUS* is about [0.63, 0.77]. It is in a good agreement with the conclusion interval [0.6, 0.8] drawn by human experts. However, the result of *U-Inference* is [0, 0.53], last column of Table 2, and only is the first rule activated. Mistake is obvious while its reliability is very low.

Mass Experiment. This system, an other system based on U-Inference, and 4 human experts (denoted by A,B,C,D) respectively diagnose about 60 typical cases which are arranged and chosen out from the recent medical records. Accuracy evaluation standard of results makes a reference to the finding recorded in the medical records.

Comparison of diagnosis performance is shown in Fig 1. It reveals that the diagnosis of the system with the highest accurate rate, the lower misdiagnosis and uncertainty ratios, and this system demonstrates an overall diagnosing efficiency better than any single human expert. Whereas, thing is nearly reverse as to traditional system based on *U-Inference*.

Table 2. Statiscis of *URKAUS* Inference

No of Clinic	CF	Weight vectors					
		1	2	3	2	4	4
0	1	1	2	3	2	4	<u>4</u>
1	0.9	3	3	5	3	3	<u>1</u>
2	0.8	11	16	4	3	1	<u>3</u>
3	0.6	15	16	5	3	3	<u>5</u>
4	0.9	5	8	7	9	7	<u>11</u>
*5	0	9	7	10	9	6	<u>5</u>
*6	0	7	4	9	7	9	<u>3</u>
*7	0	3	5	8	5	5	<u>3</u>
λ		0.6	0.5	0.55	0.75	0.6	<u>0.6</u>
Result of 5 <i>UIAUS</i> rules							
CF(D, L)		0.77	0.71	0.74	0.71	0.63	<u>0.53</u>

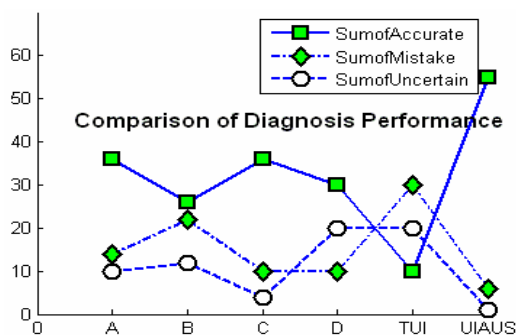


Fig. 1. Parallel of Diagnosis Performance

4 Summary

We pioneer the mechanism of *UIAUS* based on classic certainty factor method. Because of overlooking the associativity between the observed factors and prospective ones, the certainty factor inference widely used in intelligent system often ends a blank reply or a mistake diagnosis. Firstly, concept of Key-Factor is initiated and defined, and a novel certainty speculation mechanism is brought forward and integrated into the algorithm of *UIAUS*, which improves things better. Secondly, uncertainty inference based on *Associative Uncertainty Speculation* can be used in the Intelligent Diagnosis System and behaves best with a satisfying effect, and we devise a hierarchy architecture of intelligent system, in which function subsystems such as Knowledge Rule System, AI-component System ,etc. are isolated effectively. Meantime, the architecture causes a convenient reconstruction and update of traditional system. At last, as to implementation, the algorithm is introduced into Intelligent Diagnosing system. After studying case and field experimentation statistics, it is made clear that our scenario is practical and effective, and it does improve diagnosing efficiency and increase accuracy. On the whole, the favorable performance demonstrates it is a promising scheme.

Acknowledgments. This work is partially funded by Hunan Natural Science Foundation, Hunan, with Grant No. 10JJ5063 and School Foundation of Hunan University of Arts and Science, with No.JJZD1002.

Wenxue Tan (1973-). He is an Associate Professor engaging in teaching in Computer Science and Technology. His current research interests include AI and Intelligent Computing.

Xiping Wang (1979-). She is a Lecturer engaging in teaching in Economy and Management. Her current research interests include Intelligent Decision of Economy and E-Commerce.

Xiaorong Xu (1979-). She is a Lecturer engaging in scientific researching and teaching in Hunan University of Arts and Science. Her research interests include: Artificial Intelligence.

References

1. Hu, J.-d., Yu, Y.-c.: Technology of a fertilizing expert system PDA for crop growing. *Transactions of The Chinese Society of Agricultural Engineering* 22, 149 (2006)
2. Tan, w.-x., Wang, x.-p., Xi, j.-j., et al.: Research on diagnosing disease method based on back propagation neural network. *Computer Engineering Design* 32, 1070 (2011)
3. Liao, Y., Liang, J., Liao, C., et al.: Research on the application of multi-combined technologies of fault diagnosis on missile seekers. *Journal of Astronautics* 3, 30 (2006)
4. Liu, S.-w., Wang, Q.-w.: Grape disease diagnosis system based on fuzzy neural network. *Transactions of the Chinese Society of Agricultural Engineering* 18, 144 (2006)
5. Tianhong, L.: Integration of large scale fertilizing models with GIS using minimum unit. *Environmental Modeling and Software* 18, 221 (2003)
6. Xi, J.-j., Li, S.: Research on sheep disease diagnostic expert system based on subjective Bayesian algorithm with self-learning. *Journal of Hunan University of Science and Technology* 24, 95 (2009)
7. Yang, P., Zhuang, C.-l.: Design and implementation of Web-based teleconsultation system for fish disease diagnosis. *Transactions of The Chinese Society of Agricultural Engineering* 22, 127 (2006)

The Weather Disease Prediction Model Based on the Cognitive Map

Yucheng Liu¹ and Yubin Liu²

¹ School of Electrical & Information Engineering, Chongqing University of Science & Technology, Chongqing, China
lych68782763@163.com

² Computer Science School, Panzhihua University, Panzhihua, China
lybwxy1zh@163.com

Abstract. The weather disease Prediction is a complex process. In order to improve the accuracy of the forecast process, the paper proposed a sort of forecast model based on the cognitive map. The cognitive map has the intuitive information expression and reasoning ability. It is often used to complex system modeling. In this paper, we built the cognitive map to show the impact of the weather factors on various diseases by training. We selected some weather factors and the treatment records of the disease cases as the sample. The research shows that this model has good prediction effect and can provide the scientific decision-making basis for preventing and controlling the occurrence of various diseases.

Keywords: Data sample, Cognitive map, Model, Disease prediction, Disease diagnosis.

1 Introduction

Medical studies show that the common diseases such as respiratory, digestive and cardiovascular diseases are related to some specific climatic conditions [1]. The paper used the cognitive map theory to analyze the causal relationship between a variety of common diseases and key meteorological indicators and to build the weather disease prediction the model which provides decision support for the common diseases pre-control and health management.

2 Forecasting Model Based on Cognitive Map

Cognitive Map Model. The cognitive map model can be denoted with $E=(C, V, U, W)$. In which, $C = \{c_1, c_2, \dots, c_n\}$ represents the collection of nodes in cognitive maps. It describes the properties of main data. Nodes can be divided into reason node and result node. For example, there are nodes C_1 and C_2 , if the changes of C_1 results in the changes of C_2 , then we say C_1 is the reason node of C_2 , and C_2 is the result node [2]. $V=\{v_i|v_i(t)$ shows the node status of i at the time t }; $U=\{<c_i, c_j>|c_i, c_j \in C\}$ is a direction arc which shows the causal relationship between two nodes. $W=\{w_{ij}\}$, w_{ij} is

the weight of the direction arc $\langle c_i, c_j \rangle$. W is a weight matrix of cognitive map, the j of w_{ij} shows the weight of node i influence to node j . If $w_{ij} > 0$, changes of node i leads to change in node j in the same direction; if $w_{ij} < 0$, does in the opposite direction; if $w_{ij} = 0$, there is no causal relation between nodes i and j .

Reasoning Process of Cognitive Map Model. The reasoning process depends on the weight matrix W and the node status, and it can be expressed by Eq. 1 as follow.

$$v_i^{(t+1)} = f(v_i^{(t)} + \sum_{j \neq i}^n v_j^{(t)} \bullet w_{ij}). \tag{1}$$

Here, $v_i^{(t+1)}$ is the status of a concept node C_i in the iteration $t+1$; $v_i^{(t)}$ is the status of a concept node C in the iterations t ; w_{ij} is weight of causal relation between concept node C_i and the concept of the node C_j ; The f is a S-type threshold function, such as the Eq. 2 below. f is used to ensure that the status value of concept node is in provision interval.

$$f(x) = \frac{1}{1 + e^{-\lambda x}}. \tag{2}$$

After the certain iterations, if the state value of the concept node is the following one of the fixed value, periodic changes and chaotic state, the system reached a steady state. The state value of the node is affected by the other nodes in the cognitive map. The impact is reflected in the weight w_{ij} . According to reasoning process, topology structure of the cognitive map can be described as shown in Fig. 1. To guarantee the validity of the model needs to renew the weight matrix.

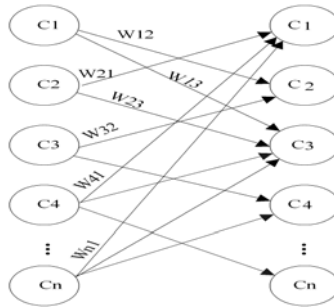


Fig. 1. Topology structure of the cognitive map

Cognitive map learning algorithm. Cognitive map learning algorithm is the weight matrix calculation method, its goal is finding the most superior weight coefficient and making the model output result restrain in the expectation steady state. The concrete algorithm description is as follows:

The first step. Read all property variable’s record value $o_j^{(i)}$ ($j=1,2,\dots,m$; $i=1,2,\dots,n$) from the primary data resources.

The second step. Standardize all recording value according to Eq. 3 as follow. Where, M_j and L_j respectively is the maximum value and minimum value of the j th attribute variable's all records in the primary data resources; $O_j^{(i)}$ is the i th record value which Corresponds in the j th attribute variable in the primary data resources.

$$d_j^{(i)} = \frac{O_j^{(i)} - L_j}{M_j - L_j}. \quad (3)$$

The third step. Establish initial weight matrix W (w_{ij} in $[-1, 1]$ scope).

The fourth step. Hypothesis circulation iteration variable $q=0$, then execute next steps.

(1) Calculate the second input value $x_j^{(i)}$ according to the Eq. 4 as follow.

$$x_j^{(i)} = \sum_{i=1}^m w_{ij} d_i^{(i)}. \quad (4)$$

(2) Calculate the second output value $y_j(i)$ according to the Eq. 5 as follow. Here, f is the S form function in the Eq. 2

$$y_j^{(i)} = f(x_j^{(i)}). \quad (5)$$

(3) Calculate weight matrix error Δw_{ij} according to Eq. 6 as follow.

$$\Delta w_{ij} = y_j(1 - y_j)(d_j - y_j)y_i \quad (6)$$

(4) Renewal weight matrix W according to the Eq. 7 as follow. Here, p is the learning coefficient, its value is the real number between $[0, 1]$.

$$w_{ij} = w_{ij} + p \bullet \Delta w_{ij}. \quad (7)$$

(5) Calculate the value of the objective function $g(w)$ according to Eq. 8 as follow.

$$g(w) = \frac{1}{2} \sum_{i=1}^m \sum_{j=1}^n (d_j^{(i)} - y_j^{(i)})^2. \quad (8)$$

(6) If $g(w)$ is smaller than the threshold value which was given, then the cognitive map model has reached to the steady state, the execution next step. Otherwise, $q=q+1$, transfers step (1).

The fifth step. Output the final weight matrix W .

3 Experiments and Result Analysis

In order to confirm the validity of the algorithm, take some local meteorological calculus material and the same time respiratory disease's treatment record as the

sample to carry on the experiment. First, carry on training the chosen sample data, analyze the causal relation between various attribute variable and obtain the cognitive map weight matrix, thus establishment cognitive map. Then, carry on the forecast to the respiratory disease diseased population by means with the formed model, thus examine model validity [3]. In the experiment, we collected an area’s meteorological statistics data of 7-8 months within three years from 2007 to 2009 and data records of 186 cases of the local respiratory disease during the same period. By consulting experts, we take the following cognitive map concept nodes: (1) The air temperature difference a day is represented by C1 so as to simplify operation; (2) Relative humidity is represented by C2; (3) Air pressure is expressed by C3; (4) Wind speed is showed by C4;(5) Sunshine time is showed by C5; (6) The number of respiratory disease is expressed by C6 [4]. In the test the data in 2007 and 2008 were used to train and to get all the causal associated value between the concept nodes in order to build cognitive maps model, while the data in 2009 were used to achieve prediction based on the model. Samples were first standardized so that all the data would be normalized to the interval [0, 1]. The standardized method can be seen in the Eq. 4. The result of normalization is shown in the Table 1.

Table 1. Standardized results of the original data resources

C1	C2	C3	C4	C5	C6
0.3711	0.3902	0.9348	0.6602	0.3011	0.309
0.3563	0.5075	0.9343	0.2812	0.3402	0.248
⋮	⋮	⋮	⋮	⋮	⋮
0.3802	0.7513	0.9505	0.3291	0.1201	0.198

According to the cognitive map learning algorithm described above, the cognitive map weight matrix can be obtained as Eq. 9 as follow.

$$W = \begin{bmatrix} 0 & 0.6411 & -0.4148 & 0 & 0 & 0.1068 \\ 0 & 0 & -0.8458 & 0 & 0 & 0 \\ 0.2168 & 0.0468 & 0 & 0 & 0 & 0 \\ 0 & 0.6251 & -0.8128 & 0 & 0 & 0.1957 \\ -0.3878 & -0.2857 & -0.4559 & 0 & 0 & 0 \\ 0 & 0 & 0 & 0 & 0 & 0 \end{bmatrix} \tag{9}$$

According to the weight matrix W, cognitive map model can be obtained as shown in Fig. 2. Using the 62 data records in 2009 into the model can be obtained the predicted results as shown in Fig. 3. Fig. 3 has shown that the change trends of the people number of respiratory disease which were predicted by model calculation are consistent with the actual situation.

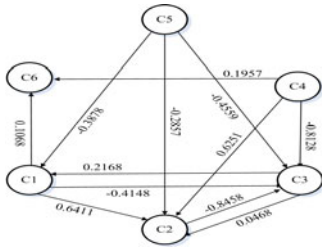


Fig. 2. Cognitive map of medical data

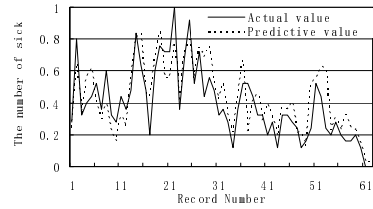


Fig. 3. Model prediction value and actual value

4 Conclusions

Arming at the characteristics of weather disease, the paper built a sort of weather prediction model based on cognitive map. By means of the sample data learning, we used the model to build cognitive maps so as to complete the experiment on predicting the meteorological factors to result the respiratory disease. The model can predict respiratory diseases trend affected by weather factors. It can provide the scientific reference for making decision of preventing weather disease occurrence.

Acknowledgment. This research is funded by Chongqing Natural Science Foundation (NO.CSTC, 2010BB2285) and science & technology project of Chongqing municipal education committee (No. KJ111417).

References

1. Fan, C.-Y.: A hybrid model combining case-based reasoning and fuzzy decision tree for medical data classification. *Applied Soft Computing* (11), 632–644 (2010)
2. Jiang, J., Trundle, P., Ren, J.: Medical image analysis with artificial neural networks. *Computerized Medical Imaging and Graphics* (11), 543–551 (2010)
3. Yang, Y.-p., Hu, J.-j.: Application of Fuzzy Cognitive-map in Collaborative Medical Diagnosis System. *Computer Engineering and Applications* (7), 218–220 (2006)
4. Stylios, C.D.: Fuzzy cognitive map architectures for medical decision support systems. *Applied Soft Computing* (8), 1243–1251 (2008)

Research on a Technology of Structural Equation Modeling Based Approach to Product Form Design Analysis

Yongfeng Li and Liping Zhu

College of Mechanical and Electrical Engineering,
Xuzhou Normal University, Xuzhou, 221116, China
yfli_xznu@yahoo.com.cn, zhuliping@yahoo.cn

Abstract. Affection and practicality are two important aspects of product design. To improve competitiveness of product, the two aspects are combined to study. A structural equation modeling based approach to product form design analysis is proposed. Firstly, morphological analysis and orthogonal experimental design are chosen to determine the experimental samples. Secondly, taking affection and practicality as latent variables, the related manifest variables are set and measured. Finally, the relationship among the form design elements, affection, practicality and consumer's purchase intent are analyzed. Based on this, the structural equation model is built, solved, and evaluated. A case study of office chair is conducted based on the presented method, and the results suggest that this method is valid and feasible.

Keywords: Industrial design, Product form design, Structural equation modeling, Office chair.

1 Introduction

With the increasingly fierce market competition, product design should not only meet affection, but also have certain practicality. Nagamachi [1] proposed kansei engineering which is a translating technology of a consumer's affection for a product into design elements. Many research studies have been carried out on the theory. Product practicality is a hot topic in product design field. It includes various aspects, such as usability, comfort, convenience, etc. Kim [2] researched the consumer electronic products usability. Groenesteijn [3] studied the influence of chair characteristics on comfort. Affection and practicality are two important factors of product design. However, few attempts have been done on combining affection with practicality to research. In order to increase the competitiveness of product and improve consumer's purchase intention, we will integrate the two factors through structural equation modeling to study product form design.

The purpose of this paper is to study the impact of office chair's form on affection and practicality. Furthermore, we will also discuss the extent to which affection and practicality impact on consumer's purchase intent.

2 Structural Equation Modeling and Product Design

Structural Equation Modeling (SEM) was proposed aiming at the shortcomings of traditional statistical methods. From the point of statistics, SEM has the following main advantages [4]. (1) The introduction of latent variables makes research more in-depth. Let multiple latent variables and their identification in the same model of analysis to study the structural relationship between them. (2) There aren't strictly limited assumed conditions, and allow the independent variable and dependent variable both have measurement errors. (3) The advantages of path analysis are developed. Application of the path map makes the complex relationship between multiple variables clear. In addition to the direct effects of variables can be calculated, the indirect effects and total effects can be derived, and the role of intermediate variables can also be expressed. (4) It can estimate the entire model's fitting degree.

Due to structural equation modeling having the merits which traditional statistical methods cannot reach, its applications in the research field of product design are increasing in recent years. Tsao [5] applied SEM to research the reasons of generating negative emotions during the process of product use. Seve [6] studied the relationship between apparent usability and affective quality of mobile phone based on SEM. Conci [7] adopted SEM to explore the empirical model of acceptance of mobile phones by elderly people.

This paper will take office chair as an example, based on SEM to study the impact of product design elements on affection and practicality, and explore their effects on consumer's purchase intention so as to provide guidance on product design.

3 The Construction of SEM

Determining the test samples. 125 samples of office chair pictures were collected. After deleting peculiar and similar form samples, 62 samples were selected to do multidimensional scaling and cluster analysis [8]. Finally, 6 typical samples of office chairs were determined which are illustrated in Fig.1.
















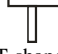







Fig. 1. Typical samples of office chairs

Morphological analysis is a project design method based on elements and form analysis using concepts and principles of morphology. It is widely used in main domains, including product design, manufacturing, and architectural design, among

others [9]. We use morphological analysis to divide the 6 representative samples into 8 elements, such as headrest, back frame, chair-back, lumbar support, seat cover, combining way, arm-rests, and legs, afterward divide every design element into 2 to 4 types [10] [11]. The results are shown in Table 1.

Table 1. Form design elements of office chairs

Design elements	Type 1	Type 2	Type 3	Type 4
Headrest (X1)	 With back integrated	 Independent	 Without	
Back frame (X2)	 Square	 Arc	 Oblate arc	
Chair-back (X3)	 With network	 Without network		
Lumbar support (X4)	 With	 Without		
Seat cover (X5)	 Square	 Rounded square	 Circular	
Combining way (X6)	 Integrated	 Detached		
Arm-rests (X7)	 T-shaped	 L-shaped	 Annular	Without
Legs (X8)	 Five-Star feet	 Arched	 Four-leg style	

Using the above design elements, we can produce 2592 (3×3×2×2×3×2×4×3=2592) kinds of form. But building 2592 models and letting subjects assess are not realistic. So we adopt orthogonal experimental design to reduce the number of models [12]. This method can select representative points to test which are chosen from comprehensive experiments according to orthogonality. We adopted mixed level orthogonal table $L_{32}(4 \times 2^3 \times 3^4)$ and full-profile method to construct product cards. Consequently, 2592 forms were compressed to 32 forms. In this study, the 32 office chair forms were taken as the experimental samples.

Setting variables. Affection refers to human sensitivity of a sensory organ where sensation or perception take place in response to stimuli from external world [13]. Generally, it is described using adjectives. A total of 162 words that describe office chairs were collected from magazines, literatures, manuals, and experts. According to KJ method, four adjectives were finally used to specify customers' perception of office chairs. They are lively, light, luxury and simple. We take these four indicators as manifest variables of latent variable of affection.

Practicality of office chairs is mainly reflected in functionality, convenience and comfort. The meaning of functionality is whether the chair’s height can be adjusted, and whether the chair provides arm-rests, lumbar support, headrest, etc. Comfort includes stationary comfort and operating comfort in the operating process. Convenience means that when people use chair whether he can be easily in and out the seat, and move the location of chair. In this study, functionality, convenience and comfort are taken as manifest variables of hidden variable of practicality.

Purchase intention refers to whether consumer is willing to buy the chair and the intensity of desire. In this research, it is regarded as a manifest variable.

Measuring manifest variables. For the 32 chairs identified by orthogonal experimental design, we adopt 8 evaluation factors which are lively, light, luxury, simple, functionality, convenience, comfort and purchase intention. To obtain the evaluation, 7-grade-Likert scale is used, where 1 is not at all and 7 is very much. 140 subjects (72 male and 68 female; average age 22) were invited to the experimental study. Every subject needs to evaluate 256 ($32 \times 8 = 256$) items. A total of 134 valid questionnaires were obtained. Cronbach’s α coefficient of the survey data is 0.823, which indicates the reliability is good.

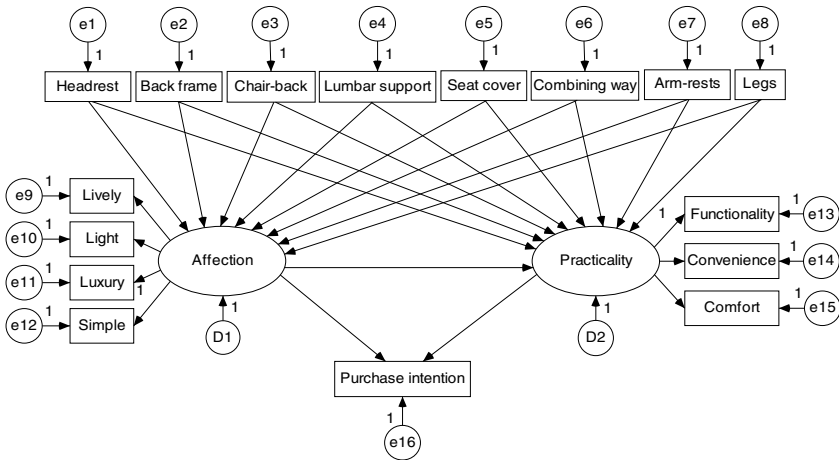


Fig. 2. Structural equation model

Establishing model. Product design elements have a direct impact on affection and practicality. Affection and practicality are two important aspects for choosing products. Sonderegger [14] found that affection affects practicality. Norman [15] thinks beautiful product works better. Therefore, this research hypothesizes affection and practicality exist certain relationship. According to the above analysis and hypothesis, the model was built and modified, and the final model is depicted in Fig.2. Amos 16.0 software is applied to construct structure equation modeling. Maximum likelihood estimation is used to estimate the parameters.

4 Model Evaluation

The evaluation of model fitting degree. We chose Chi-square, Comparative Fit Index (CFI), Bentler-Bonett Normal Fit Index (NFI), Incremental Fit Index (IFI), Root Mean Square Error of Approximation (RMSEA), Akaike Information Criterion (AIC), Browne-Cudeck Criterion (BCC) and Expected Cross-Validation Index (ECVI) to evaluate the model fitting degree. The final model's fitting indexes are presented in Table 2. Chi-square value and degree of freedom are 149.5 and 94 respectively, which are reasonable. CFI, NFI, and IFI are close to 1, and RMSEA is less than 0.1. Information indexes including AIC, BCC and ECVI are relatively small. The above data suggest that the model fitting degree is good.

Table 2. Computational results of common fit indexes

Fit index	Chi-square Value (df)	CFI	NFI	IFI	RMSEA	AIC	BCC	ECVI
Index value	149.5(94)	0.857	0.791	0.882	0.078	233.465	335.465	1.531

The evaluation of model path coefficients' significance. The estimated values of model's path coefficients are shown in Table 3. According to statistics test associated probability p , we can find the p value of path "Affection <--- Legs" is less than 0.001. Its path coefficient has significant difference with 0 at 99.9% confidence level, so there is no reason to believe it is 0, and reject the null hypothesis. The standardized path coefficient is 0.595, which implies that the type of office chair legs changes from "five-star" to "bow", or from "bow" to "four-legged" will increase its affection. The standardized path coefficient of "Practicality <--- Affection" is -0.882, and the p value is less than 0.001. Minus sign indicates when affection promotes, the usability will reduce. So the design of office chair should obtain balance between practicality and affection.

The p value of "affection<---Combining way" is less than 0.05, this suggests that it has significant difference with 0 at 95% confidence level. Its standardized path coefficient is -0.227, which indicates the type of combining way changes from "Integrated" to "Detached" will decrease its affection. The p values of "Affection <--- Headrest", "Practicality <--- Back frame", "Practicality <--- Headrest", "Practicality <--- Seat cover" and "Practicality <--- Chair-back" are also less than 0.05, and their analyses are similar to the above approach.

The p values of path coefficients of latent variables "Affection" and "Practicality" with their manifest variables are all less than 0.05, which indicate the selections of manifest variables are reasonable. The p value of path coefficient of "Purchase intention <--- Practicality" is less than 0.001, and "Purchase intention <--- Affection" is less than 0.005. Therefore, comparing affection with practicality, practicality's impact on purchase intentions is more significant.

Table 3. Estimate of the model's path coefficients

Path	Not standardized path coefficient estimates	S.E.	<i>p</i>	Standardized path coefficient estimates
Affection <--- Legs	0.588	0.146	***	0.595
Affection <--- Back frame	0.103	0.131	0.430	0.104
Affection <--- Chair-back	0.148	0.216	0.493	0.091
Affection <--- Lumbar support	0.038	0.215	0.861	0.023
Affection <--- Seat cover	0.023	0.131	0.862	0.023
Affection <--- Combining way	-0.454	0.221	0.040	-0.277
Affection <--- Arm-rests	0.141	0.097	0.148	0.192
Affection <--- Headrest	0.232	0.133	0.048	0.235
Practicality <--- Legs	-0.063	0.060	0.295	-0.062
Practicality <--- Arm-rests	-0.024	0.031	0.431	-0.033
Practicality <--- Back frame	-0.111	0.058	0.043	-0.111
Practicality <--- Headrest	0.108	0.058	0.045	0.108
Practicality <--- Combining way	-0.089	0.077	0.250	-0.054
Practicality <--- Seat cover	-0.125	0.062	0.042	-0.125
Practicality <--- Lumbar support	-0.06	0.067	0.368	-0.036
Practicality <--- Chair-back	0.154	0.087	0.047	0.093
Practicality <--- Affection	-0.894	0.167	***	-0.882
Simple <--- Affection	1			0.829
Luxury <--- Affection	-0.516	0.079	***	-0.909
Light <--- Affection	0.326	0.080	***	0.660
Lively <--- Affection	-0.205	0.120	0.049	-0.307
Functionality <--- Practicality	1			0.899
Convenience <--- Practicality	0.376	0.109	***	0.517
Comfort <--- Practicality	0.471	0.073	***	0.797
Purchase intention <--- Affection	2.309	0.827	0.005	1.866
Purchase intention <--- Practicality	3.061	0.808	***	2.507

Here “* * *” denotes $p < 0.001$.

The causal effects of model's variables. The impact of causal variable on result variable is called total effect, which is the summation of direct and indirect effects. Total effects between the model's variables are shown in Table 4. Among them, the total effects of lumbar support impact on affection and practicability are 0.023 and

-0.057 respectively. This implies when other conditions remain unchanged, lumbar support increase 1 unit (from with lumbar support to without lumbar support), affection will increase 0.023 units, but practicality will decrease 0.057. The total effect of legs impact on convenience is -0.303, which suggests when legs increase 1 unit (from five-star feet to arched or from arched to four-leg style), convenience will decrease 0.303 units. The impacts of other design elements on every variable can be analyzed according to the above method. The total effects of latent variables affection and practicality on purchase intention are -0.346 and 2.507 respectively, which indicate when affection increase 1 unit, purchase intention will decrease 0.346 units, but when practicality ascend 1 unit, purchase intention will increase 2.507 units. Therefore, practicality of office chairs is more important than affection.

Table 4. Standardized total effects

	Legs	Arm-rests	Combining way	Seat cover	Lumbar support	Chair-back	Back frame	Head-rest	Affection	Practicality
Affection	0.595	0.192	-0.277	0.023	0.023	0.091	0.104	0.235	0.000	0.000
Practicality	-0.587	-0.202	0.190	-0.145	-0.057	0.013	-0.203	-0.099	-0.882	0.000
Purchase intention	-0.362	-0.149	-0.039	-0.321	-0.099	0.201	-0.314	0.189	-0.346	2.507
Comfort	-0.468	-0.161	0.152	-0.116	-0.045	0.010	-0.162	-0.079	-0.703	0.797
Convenience	-0.303	-0.105	0.098	-0.075	-0.029	0.007	-0.105	-0.051	-0.456	0.517
Functionality	-0.528	-0.182	0.171	-0.130	-0.051	0.011	-0.182	-0.089	-0.793	0.899
Lively	-0.183	-0.059	0.085	-0.007	-0.007	-0.028	-0.032	-0.072	-0.307	0.000
Light	0.392	0.127	-0.182	0.015	0.015	0.060	0.069	0.155	0.660	0.000
Luxury	-0.541	-0.175	0.251	-0.021	-0.021	-0.082	-0.095	-0.213	-0.909	0.000
Simple	0.493	0.159	-0.229	0.019	0.019	0.075	0.087	0.194	0.829	0.000

5 Conclusion

Structural equation modeling allows for considering measurement error of the complex concept, at the same time establishing of the relationship between variables, especially the causal relationship. This characteristic is that all traditional statistical methods are difficult to achieve. In this paper, we took office chair as an example, based on structural equation modeling to study the influence degree of design elements on evaluation indexes and the relationship among affection, practicality and purchase intention. We found that for office chair, design elements can affect evaluation indexes, and practicality's impact on purchase intention is more significant than affection's. Although office chair was used as a case study, this approach can be applied to other products.

It should be noted that evaluation indexes of product design include affection, practicability, economics, environmental protection and innovation, etc. and we only concentrate on affection and practicality. In the future, we will combine other factors to study in-depth.

Acknowledgment. Financial support from the Natural Science Foundation of the Jiangsu Higher Education Institutions of China (Grant No. 10KJD460002) is gratefully acknowledged by the authors.

References

1. Nagamachi, M.: *TQM Journal* 20, 290 (2008)
2. Kim, J., Han, S.H.: *International Journal of Industrial Ergonomics* 38, 333 (2008)
3. Groenesteijn, L., Vink, P., de Looze, M., Krause, F.: *Applied Ergonomics* 40, 362 (2009)
4. Bollen, K.A., Long, J.S.: *Testing Structural Equation Models*. SAGE Publications Ltd, Newbury Park (1993)
5. Tsao, Y.C., Chan, S.C.: *Applied Ergonomics* 42, 503 (2011)
6. Seva, R.R., Gosiaco, K.G.T., Santos, M.C.E.D., Pangilinan, D.M.L.: *Applied Ergonomics* 42, 511 (2011)
7. Conci, M., Pianesi, F., Zancanaro, M.: 12th IFIP TC 13 International Conference on Human-Computer Interaction, INTERACT 2009, p. 63 (2009)
8. Wang, K.C., Huang, C.C., Lin, Y.C.: *Journal of Grey System* 11, 205 (2008)
9. Hsiao, S.W., Chiu, F.Y., Lu, S.H.: *International Journal of Industrial Ergonomics* 40, 237 (2010)
10. Hsiao, S.W., Liu, E.: *Integrated Computer-Aided Engineering* 11, 323 (2004)
11. Ostrosi, E., Tié Bi, S.: *International Journal of Advanced Manufacturing Technology* 49, 13 (2010)
12. Liao, C.S., Lee, C.W.: *International Journal of Clothing Science and Technology* 22, 211 (2010)
13. Yanagisawa, H., Murakami, T.: ASME International Design Engineering Technical Conferences and Computers and Information in Engineering Conference, p. 791 (2008)
14. Sonderegger, A., Sauer, J.: *Applied Ergonomics* 41, 403 (2010)
15. Norman, D.A.: *Emotional Design: Why We Love (or Hate) Everyday Things*. Basic Books, New York (2004)

Discuss the Theoretical Rationale for the Existence of Banks

Xiao Xiao^{1,2} and Songliang Cheng^{3,4}

¹Economics and Management School, Wuhan University, Wuhan, P.R. China

²School of International Education, Wuhan University of Technology, Wuhan, P.R. China
nesteaboyxiao@yahoo.com.cn

³Law School, Wuhan University, Wuhan, P.R. China

⁴School of literature, law and economics,
Wuhan University of Science and Technology, Wuhan, P.R. China
hendry_ch@sina.com

Abstract. The essay reviews the theoretical and practical content circumventing the essence of banks, the functions of banks and analyses the development trend to construct a modernized and multinational banking in conjunction with the role of banks in European financial system.

Keywords: financial intermediaries, essence of banks, theoretical rationale.

1 Nature and Necessity of Existence of Banks

As a representative intermediary in indirect finance, bank issues to surplus economic units claims on itself that are relatively safe and easy to exchange for money, and in purchases claims issued by deficit units – claims that are relatively risky and scheduled to mature at relatively distant dates. The advanced economic growth has been caused by the financial intermediaries especially the existence of banks subsequently, because both saving and capital investment are freed from certain institutional limitations and investment tends to be directed into the most productive projects through the banking system. As shown, figure 1 indicates the options of traders. Figure 2 summarizes the transaction of banks.

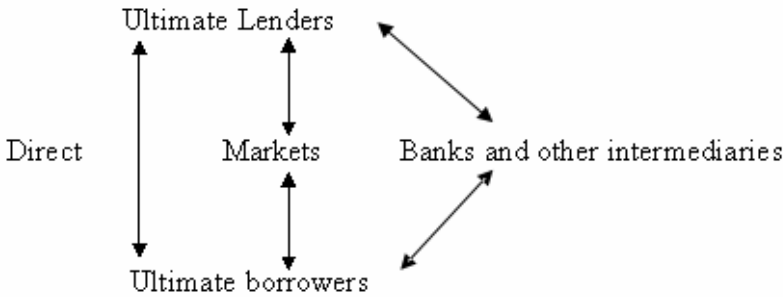


Fig. 1. The options of traders

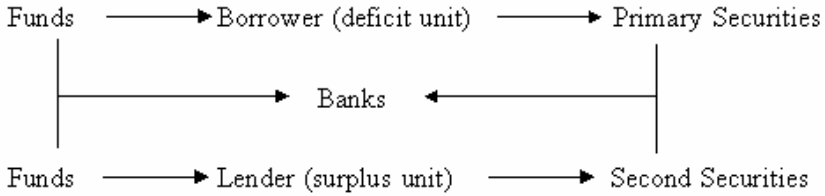


Fig. 2. The transaction of banks

It is argued by the historians that the existence of banks has enlarged the banking system. The emergence of the banking system, which has been placed predominately, pushed Britain's economic development during the eighteenth and early nineteenth centuries. Officially, in 1979, the criteria which the bank of England adapted to were determined by the United Kingdom Act. [1] And it reflects what a bank's basic function. It is as follows: 1.a good reputation must exist for the deposit-taking institution; 2.a wide range of banking services, specialist or otherwise must be provide such as: a.current and deposit account facilitates, or accepting funds in the wholesale market; b.provision of loans and overdrafts, or lending in the wholesale money markets; c.foreign exchange facilities; d.the handling of bills of exchange and promissory notes including financing foreign trade; e.financial advice and the provision of facilities for the purchase and sale of investments; 3. a minimum account of capital and reserves.

2 Theoretical Rationale for the Existence of Banks

Financial intermediation through the bank can be defined as the purchase of primary securities from ultimate borrowers and users of funds and the issue of indirect claims to ultimate lenders and investors. Then, essentially, banks come between lenders and borrowers not as agents for one or the other but as independent financial operators, seeking profits themselves and making separate contracts between themselves and the different counterparties. Thus, a vast flow of credit is created or produced by banks. The significance of the existence of banks was discussed using the production theory, liquidity preference theory, portfolio theory, theory of innovation and 'market' theory.

A Production Theory

Commercial banks are by far the largest financial intermediaries in the system, function to channel monetary assets through the economy. They create deposit liabilities when an asset, such as cash or a deposit held at another institution, is deposited into the bank. Assets required by the banks when they create their liabilities are then used to satisfy reserve requirements, maintain sufficient liquidity and generate a profit for the bank's owners. Alternatively, banks delegate consumers to make loans for the optimal unity of the deposits according to the contracts in the terms of indirect capital flow. The process of intermediation requires that something

be created by the transformation of inputs into outputs. Through the services created by banks, as to the depositors, first, their funds can be withdrawn at any time without incurring a substantial penalty. Second, their funds can be placed in deposits with a fixed dollar value (plus interest), and since the funds are claims against the bank so that the depositor is largely insulated from default risk. As to banks, indirect finance involves certain costs to the intermediary naturally. The wherewithal to meet these costs is provided mostly by the “spread” between the yields on assets held by the intermediary and the interest rates paid on its obligation. It can be explicable that optimize the profit through the mismatch between the maturity of assets and liabilities could be highly concerned by the banks. At its simplest we might say that what banks do is to create assets for lenders and liabilities for borrowers which are more attractive to each than would be the case if the parties had to deal with each other. [2] This kind of mechanism adopted to the production theory. (See figure 3)

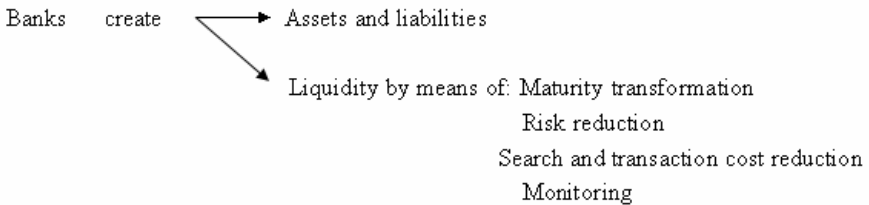


Fig. 3. Creation of money and liquidity

Within the market-orientated approach, the services in commercial banks are not simply concentrated on the basic services, instead, abounding in providing many other banking-related services because the force of the competitive market would induce bankers to engage in other business activities. Such as Credit cards, Wire transfer of funds, Foreign exchange, Traveler’s check, Equipment leasing, etc. In many case these services are incentive for people to use the commercial bank’s deposit services. Commercial banks, alternatively, are multi-product firms [3], adjusting to the changes of markets consistently.

B Liquidity Preference Theory

From an economic point of view, banks inevitably have a significant impact both on the velocity of circulation and the quantity of monetary assets available by serving to bring together the funds made available by both small and large lenders with borrowers desiring those funds. This essence allows banks to create liquidity. Liquidity is defined as an asset immediately for cash without taking a capital loss and relies upon maturity transformation, risk reduction, the reduction of search and transaction costs and monitoring. It is a key factor, not only because of the consumers’ preference to the efficient capital liquidity, but also because the prior function is able to meet both normal and abnormal shortfalls in anticipated cash flow. A liquid portfolio enables the concern to safety by limiting the uncertainty. For example, the behavior of withdrawing the funds readily guarantees the depositors that

the banks are the safe storehouses. In theory, the much more appropriate ratio of liabilities to equity capital banks carried, the much more efficient liquidity of capital generated, and then it is the lower risk to promote safety. Liquidity and safety together determine the solvency of the banks. Bank would not be considered safe if there is high probability of insolvency and failure. Liquidity tends to promote solvency. Strikingly, liquidity makes banks unique and provides the prior guarantees to the consumer compared with other intermediaries. It also guarantees the existence and circulations of banks themselves.

C Portfolio Theory

As the growth, banks differ in their relative expertise in specific markets and tend to specialize in specific markets. This specialization leads to differences in banks' portfolio and to somewhat different choices in solving the fundamental problem of financial intermediation. Portfolio theory primarily describes how the banking business of portfolio management should be conducted to generate sufficient earnings while still providing for adequate liquidity and safety. At a microeconomic level, that is, how well match the deposit with a loan even the due maturity differs from the deposit. Commonly, banks establishing general rules that move closely approximate the portfolio with the greatest return for a given risk will realize greater profitability at lower risk and will tend to survive in the long run. [3] The use of general rules for selecting portfolios is optimizing behavior such that the commercial bank is economizing on the use of resources in selecting approximate assets. To avoid risk, to stabilize earnings, to increase soundness of banks, the greater the degree of portfolio diversification, the lower will be the level of risk. And portfolio management is so practical that adjusting the banks much more to the financial system.

D Theory of Innovation and 'Market' Theory

Since the existence of banks links buyers and sellers together, a financial market has been organized wherein the payment mechanism created. Traditionally, it is a fact that banks have attracted significant public regulation, mainly because of the important role they have to play. As the flourishing growth of financial market, bank regulation is usually justified by a policy to ensure that banks are safe so as to help preserve the overall financial stability of the economy, to provide adequate 'consumer protection' particular in the enforcement of contracts to depositors and desire to control the monetary system and sometimes imposed on the grounds that it is necessary to protect financial markets from being inherently uncompetitive. In general terms, the variable banking regulations have authorized banks in the aspects of reserve requirement, qualitative controls including moral suasion, quantitative controls and indirect controls, which assist to the survival of banks in the competitive market. While the forces in social market has leads to the continuous modification of banking regulation over time, the mutual effects achieves the consumers' demands to some extend so that banks has been placed predominantly in financial market whatever bank- orientated, market- orientated or consumer- orientated.

One of the cornerstones of market competition is the ability to enter the industry. Have been specialized in the market strategies included expansion of banking through branches, centralization, globalization and internationalization during a new era, banks take a comparative advantage to survive against local competition and significantly influenced in leading industrial economies. Banks to expand into other geographic locations would allow a greater choice of banks and tend to lower the costs of the services offered. Since the international operations has occurred, a great increase in international lending led to the globalization of the banking industry. Meantime, the banking industry is highly regulated at both local and federal levels for controlling the possibility of risk that the collapse of a bank in one country could cause serious losses for banks in other countries. These regulations basically are concerned with attempting to assure that the proper amount of banking and financial activity is provided. The regulations presume that the operations of the free market would provide either too much banking, which would lead to instability, or too little, with a resulting concentration of market power. The regulations imposed on commercial banks have served to determine the structure of banking industry.

As economic conditions change, innovation has been a fundamental driving force in the development of banking, which covers products that product a novel or unique experience for bank customers encompasses the systems, procedures and Instruments. The immediate cause of innovation is the prospect of profit. Typically relevant changes are those involving regulation, technology and volatility of financial flows. For example, banks are assumed to maximize utility subject to a balance sheet constraint, this in turn creates the regulation for bank runs; cash dispensing automated teller machines (ATMs) first appeared in the mid-1970s and have spread rapidly ever since as to give customers easier access to their accounts; in 1990s, the technology of combining the ATMs into networks was extended to electronic funds transfer (EFT) with the result that stores can provide cash withdrawal facilities. With the application of technology, the costs of transactions become lower; the ability to access to current balance information is more quickly and cheaply. Equally, people will be willing to hold larger simultaneous debit and credit positions leading to a larger money stock and lower velocity than hitherto.

3 Summary

“It is the conglomeration of all various services and functions that sets the commercial bank off from other financial institutions. Each then is an integral part of the whole, almost every one of which is dependent upon and would not exist but for the other.” J. Clary said. As growth, today’s banks are far more sophisticated in their knowledge of, and response to, changes in the politico-economic environment. Although the banks have their own identifying characteristics, there are the problems in common involved in attempting to achieve particular objectives through management of their portfolios and acquisition of financing. The management of banks seeks to reconcile these sometimes conflicting objectives in the light of its perception of the economics and regulatory environment and its own preferences.

References

1. Brown, C., Mallett, D.J., Taylor, M.G.: Banks. The Institute of Chartered Accountants, England and Wales (1993)
2. Howells, P., Bain, K.: The Economics of Money, Banking and Finance, 2nd edn., p. 41. Personal Education Limited, London (2002)
3. Johnson, I.C., Roberts, W.W.: Money and Banking: A Market-orientated Approach. CBS College (1982)
4. Dahm, T.E.V.: Money and Banking. D.C. Heath and Company (1975)
5. Llewellyn, D.T., Green, C.: Survey in Economics, vol. 2. Oxford Basil Blackwell, Malden
6. Weston, R.: Domestic and Multinational Banking. Croom Helm Ltd (1980)
7. Diamond, D.: Financial Intermediation and Delegated Monitoring Review of Economics Studies (1984)

Transmission Spectra of Liquid Surface Waves over Finite Graphene Structured Arrays of Cylinders*

Yong Wei, Sheng Li, GuoPing Tong, and YouSheng Xu

Department of Physics, Zhejiang Normal University, Jinhua, 321004, China
weiyong@zjnu.cn

Abstract. The transmission spectra of liquid surface waves over finite graphene(or honeycomb) structured arrays of bottom-mounted cylinders with a uniform height on a level with liquid surface or below of it are investigated by multiple scattering method. Comparing the transmission spectra of the graphene structure with the square and triangle structures, we find that the finite graphene structure can produce more complete band gaps than the other finite structures.

Keywords: Transmission spectra, Liquid surface waves, Array.

1 Introduction

When a light wave or acoustic wave propagates inside a periodic structure, it is modulated with a periodic structure. The corresponding lattice structure is called a photonic crystal [1] or sonic crystal[2]. Similarly, once a liquid surface wave propagates over a periodic structure, due to multiple Bragg scatterings, it is also modulated with the introduced periodicity. As a result, many interesting phenomena found in photonic crystals or sonic crystals may also exist in liquid surface waves. However, a unique advantage of using liquid surface waves lies in the fact that many interesting phenomena can be observed visually [3,4]. Because of the reason above, liquid surface waves propagating over periodically and randomly structured bottoms are both investigated by theories [5-15] and experiments[16,17]. Some important phenomenas on liquid surface waves, such as the complete band gap[7-9], localization[10] and negative refraction[16], are found.

In 2004, Geim's team found that electronic waves propagating inside graphene appear an unusual propagation pattern[18,19]. For a liquid surface wave being one kind of classical waves, what is the propagation pattern when it propagates inside a graphene(or honeycomb) structure? In 2002, Ha et al investigated the propagation of water surface waves through square structured, triangle structured and graphene structured arrays of vertical cylinders, and found that the finite graphene structure can produce a complete band gap at a lower filling fraction than other finite structures[7].However, in their paper, the investigation of water surface waves through the graphene structure is insufficient, because they didn't compare the graphene structure with other finite structures in detail.

* This work was supported by the Young Foundation of Zhejiang Normal University under Grant No. KJ20100001.

In this paper, first we will calculate the transmission spectra of liquid surface waves over finite graphene structured arrays of bottom-mounted cylinders with a uniform height on a level with liquid surface or below of it using multiple scattering method. Then, comparing the transmission spectra of the graphene structure with the square and triangle structures, we will show the different band gaps of three kinds of structures.

2 Theory Model

Before calculating, let us present some conclusive equations which are used in our calculation.

These conclusive equations have been derived rigorously in Ref[6]. If $x - y$ is set in the calm liquid surface and z is set to the vertical and upward axis, the displacement of the liquid surface waves at any point $\eta(\vec{r})$ can be expressed as

$$\eta(\vec{r}) = i\pi H_0^{(1)}(k|\vec{r} - \vec{r}_s|) + \sum_{i=1}^N \sum_{n=-\infty}^{\infty} i\pi A_n^i H_n^{(1)}(k|\vec{r} - \vec{r}_i|) e^{in\phi_{\vec{r}-\vec{r}_i}}, \quad (1)$$

where n and i are the indexes of order and cylindrical steps respectively, \vec{r}_s denotes the place of the source, $\phi_{\vec{r}-\vec{r}_i}$ is the azimuthal angle of the vector $\vec{r} - \vec{r}_i$ relative to the positive x axis. $H_0^{(1)}$ and $H_n^{(1)}$ are the zeroth order and the n th order Hankel functions of the first kind. k denotes the wave number of liquid surface waves over the bottom and satisfies

$$\omega^2 = gk \left(1 + \frac{\sigma}{\rho g} k^2 \right) \tanh(kh), \quad (2)$$

where ω is the angular frequency, g is the gravity acceleration, σ is the liquid surface tension, ρ is the liquid density, h denotes the depth of liquid over the bottom. The eq.(2) is also suitable for the wave number k_i at the i th step and the depth of liquid over the i th step h_i . In eq.(1), the coefficient A_n^i can be obtained from the matrix equation

$$\Gamma_n^i A_n^i - \sum_{j=1, j \neq i}^N \sum_{l=-\infty}^{\infty} G_{l,n}^{i,j} A_l^j = T_n^i, \quad (3)$$

where $\Gamma_n^i = \frac{H_n^{(1)}(ka)J_n'(k_i a) - \beta H_n^{(1)'}(ka)J_n(k_i a)}{\beta J_n'(ka)J_n(k_i a) - J_n(ka)J_n'(k_i a)}, \quad (4)$

$$T_n^i = H_{-n}^{(1)}(k|\vec{r}_i - \vec{r}_s|) e^{-in\phi_{\vec{r}_i - \vec{r}_s}}, \quad (5)$$

$$\text{and } G_{l,n}^{i,j} = H_{l-n}^{(1)}(k|\bar{r}_i - \bar{r}_j|)e^{i(l-n)\phi_{\bar{r}_i - \bar{r}_j}}, i \neq j. \quad (6)$$

In Eqs.(3-6), $\beta = \tanh(kh)/\tanh(k_i h_i)$, l and j are also the indexes of order and cylindrical steps respectively, J_n is the Bessel's function of the first kind, the prime refers to the derivative.

Making the calculational results experimentally testable, we pick the capillary length of liquid $b = \sqrt{\sigma/\rho g} = 0.93\text{mm}$, the depth of liquid over the bottom $h = 2.5\text{mm}$, the radii of each cylindrical step $a = 0.875\text{mm}$, and the filling fraction $f_s = 0.296$.

3 Results and Discussion

Here, according to the conclusive equations above, we calculate the transmission spectra of the finite graphene structured, square structured and triangle structured arrays. Our calculation is along the ΓM and ΓK directions. The ΓM and ΓK directions of the graphene, square and triangle structures are shown in Fig.1.

We arrange the cylinders in an about $6.3\text{cm} \times 6.5\text{cm}$ rectangular area which has the graphene structure or the square structure or the triangle structure, and set the ΓM or ΓK direction of the structure to parallel the short side of rectangle. The stimulating source is set in the centric place about one lattice constant away from one long side of rectangle, whereas the detector is placed in the centric place about one lattice constant away from the other long side of rectangle.

The numerical results are shown in Fig.2. In these numerical results, the transmission spectra are normalized, and its are expressed as $\ln|T|^2 = \ln|\eta/\eta_0|^2$ ($\eta_0 = i\pi H_0^{(1)}(k|\bar{r} - \bar{r}_s|)$). In Fig.2, when the depth of liquid over the steps h_i equals 0mm, that is to say, the top of the steps is on a level with liquid surface, for the finite graphene structured array, the normalized transmission spectra along

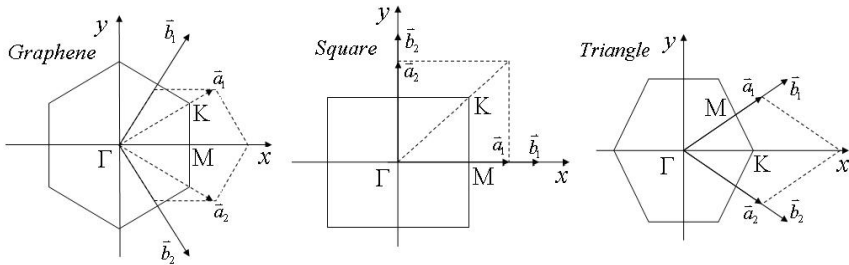


Fig. 1. The symmetry directions, the first Brillouin zone(the solid line zone) and the unit cell(the dotted line zone) of graphene, square and triangle structures. The ΓM and ΓK denote the symmetry directions, \bar{a}_1 and \bar{a}_2 are the unit vectors, \bar{b}_1 and \bar{b}_2 are the reciprocal lattice unit vectors.

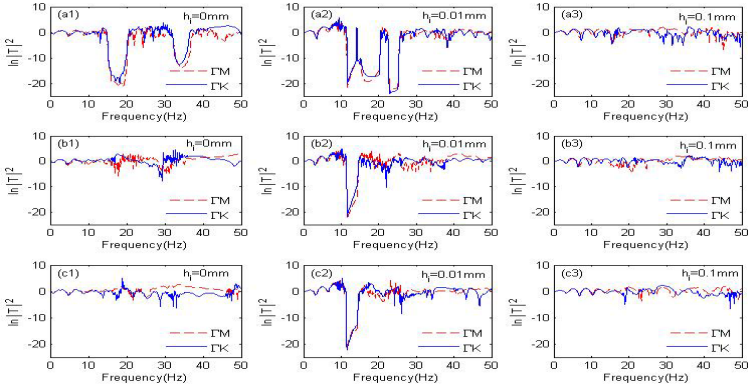


Fig. 2. The normalized transmission spectra $\ln|T|^2$ of liquid surface waves over the finite graphene structured arrays(Fig.a), square structured arrays(Fig.b) and triangle structured arrays(Fig.c) along the symmetry directions for the identical filling fraction $f_s=0.296$. The left, middle and right column denote the depth of liquid over the steps $h_l=0\text{mm}$, 0.01mm and 0.1mm , respectively. The liquid capillary length is 0.93mm .

the ΓM and ΓK directions both have two troughs which can insulate well, which indicates the liquid surface waves have two complete band gaps. The two complete band gaps locate at the region of frequency about between 15Hz and 20Hz and the region about between 32.5Hz and 36Hz , respectively. While for the finite square structured and triangle structured arrays, the normalized transmission spectra along the ΓM and ΓK directions don't have the trough, which means the liquid surface waves don't have the complete band gap.

When h_l equals 0.01mm , for the finite graphene structured array, the transmission spectra along the ΓM and ΓK directions both have three troughs which can insulate very well, which means the liquid surface waves have three complete band gaps. The three complete band gaps locate the region of frequency about between 11.5Hz and 14Hz , the region about between 14.4Hz and 20.4Hz and the region about between 22.5Hz and 25.5Hz , respectively. As for the finite square and triangle structured arrays, the normalized transmission spectra show only one complete band gap. What's more, the complete band gaps in the finite square and triangle structured arrays locate the same region about between 11.4Hz and 14.5Hz , and the region nearly coincides with first gap region in the finite graphene structured array.

When h_l equals 0.1mm , for the finite graphene, square and triangle structured arrays, the liquid surface waves all don't have the complete band gap, which illustrates that the steps no longer affect well the propagation of liquid surface waves. Besides the complete band gaps, we also can study the partial band gaps of liquid surface waves according to the transmission spectra in Fig.2. In Fig.2, all transmission spectra don't have the obvious deviation between the ΓM direction and ΓK direction, which indicates the partial band gaps over three kinds of finite structured arrays are inconspicuous.

In a word, the finite graphene structure can produce more complete band gaps than the finite square and triangle structures, which is another important phenomenon besides the phenomenon that the graphene structure has the complete band gap at a lower filling fraction than other structures in Ref.[7].

4 Summary

In this paper, we have investigated the transmission spectra of liquid surface waves over finite graphene structured arrays of bottom-mounted cylinders with a uniform height on a level with liquid surface or below of it. We compared the transmission spectra of the graphene structure with the square and triangle structures, and found that the finite graphene structure can produce more complete band gaps than the other finite structures.

References

1. Yablonovitch, E.: Phys. Rev. Lett. 58, 2059 (1987)
2. Martínez-Sala, R., Sancho, J., Sánchez-Pérez, J.V., Llinares, J., Meseguer, F.: Nature 378, 241 (1995)
3. Torres, M., Adrados, J.P., Montero de Espinosa, F.R.: Nature 398, 114 (1999)
4. Torres, M., Adrados, J.P., Montero de Espinosa, F.R., Garcia-Pablos, D., Fayos, J.: Phys. Rev. E 63, 011204 (2000)
5. McIver, P.: J. Fluid Mech. 424, 101 (2000)
6. Ye, Z.: Phys. Rev. E 67, 036623 (2003)
7. Ha, Y.K., Kim, J.E., Park, H.Y., Lee, I.W.: Appl. Phys. Lett. 81, 1341 (2002)
8. Hu, X.H., Shen, Y., Liu, X., Fu, R., Zi, J., Jiang, X., Feng, S.: Phys. Rev. E 68, 037301 (2003)
9. Chen, L.S., Kuo, C.H., Ye, Z., Sun, X.: Phys. Rev. E 69, 066308 (2004)
10. Chen, L.S., Ye, Z.: Phys. Rev. E 70, 036312 (2004)
11. Chen, L.S., Li, S., George, T.F., Kuo, C.H., Sun, X.: Appl. Phys. Lett. 89, 011905 (2006)
12. Li, Y., Mei, C.C.: J. Fluid Mech. 583, 161 (2007)
13. Li, Y., Mei, C.C.: Phys. Rev. E 76, 016302 (2007)
14. Farhat, M., Guenneau, S., Enoch, S., Tayeb, G., Movchan, A.B., Movchan, N.V.: Phys. Rev. E 77, 046308 (2008)
15. Tabaei, A., Mei, C.C.: Phys. Rev. E 79, 026314 (2009)
16. Hu, X.H., Shen, Y., Liu, Z., Fu, R., Zi, J.: Phys. Rev. E 69, 030201 (2004)
17. Shen, Y., Chen, K., Chen, Y., Liu, X., Zi, J.: Phys. Rev. E 71, 036301 (2005)
18. Novoselov, K.S., Geim, A.K., Morozov, S.V., Jiang, D., Zhang, Y., Dubonos, S.V., Grigorieva, I.V., Firsov, A.A.: Science 306, 666 (2004)
19. Novoselov, K.S., Jiang, D., Schedin, F., Booth, T.J., Khotkevich, V.V., Morozov, S.V., Geim, A.K.: PANS 102, 10451 (2005)

Construction of Ontology Information System Based on Formal Concept Analysis

LiuJie He and QingTuan Wang

Modern Education Technology Center, Huanghe science and technology college,
Zhengzhou, 450063, China
heliujie@sina.cn

Abstract. As the foundation of the semantic web, ontology is a formal, explicit specification of a shared conceptual model and provides a way for computers to exchange, search and identify characteristics. The aim of ontology is to obtain, describe and express the knowledge of related domain. However, there are some defects between several kinds of existing ontology construction methods in many aspects. After analyzing and comparing, this paper makes up these defects by applying formal concept analysis theory to construct concept hierarchies of ontology. This paper puts forward formal concept analysis method applied in ontology learning based on non-structured of source data. The experimental results have shown our suggested information system will increase precision and performance.

Keywords: Information system, Formal concept analysis, Domain ontology.

1 Introduction

Many ontology-based information sharing approaches rely on mapping between ontologies from different sources. Mapping tools use different techniques to suggest matches between ontology elements, and vary in input requirements, output formats, and modes of interaction with the user. Ontologies are formal, explicit specifications of shared conceptualizations of a given domain of discourse. But this field is still being discussed today. Such cooperation may involve agents belonging to different organizations. Therefore it is necessary for these agents to have common knowledge of these exceptions and their causes[1]. To address this problem, clustering algorithm is introduced first. Clustering is a popular unsupervised classification technique which groups the input space into K regions based on some similarity or dissimilarity metric.

Due to the decentralized nature of the Web, there usually exist multiple ontologies from overlapped application domains or even within the same domain. Comparative evaluation of appropriate mapping techniques with real ontologies from the public safety community allows us to study them in detail and take a few more steps to the goal of seamless connectivity between information sources. As a branch of applied mathematics, formal concept analysis comes of the understanding of concept in philosophical domain. The user then has to spend more time waiting for query

responses. A more refined range is used for the function that represents the meaning of a proposition. This is usual in natural language when words are modeled by fuzzy sets [2]. Ontologies are used in federated database systems because they are capable of containing the meaning and context of the terms whereas schema is simply a collection of terms. The information is available over the Internet, published by various travel information providers.

Finally, Ontologies play an essential role in the semantic web by enabling knowledge sharing and exchange. Ontology is also an essential component of collaborative computing. The ontological model, along with the coordination model and user interface model form a collaborative system. Ontologies present semantics for interpreting data instances. If an ontology is substituted by a new version, its data instances may become non-interpretable. In this study, we survey public safety information sharing initiatives and discuss the ontological implications of the systems and standards. We also perform a survey of ontology mapping and evaluate commonly used tools that use various techniques to map ontologies. Consequently, how to help users to find out user-oriented solutions; furthermore, to obtain, learn, and predict the best solution through user feedback, or how to support incremental maintenance of the solution database becomes an important research topic. We construct a prototype implementing the method to provide a proof on the validity and feasibility. The ontology-based method described in this paper can help retrieve and save the complex relations, support the reasoning, integrate heterogeneous data resources and offer users more accurate, proper and comprehensive data.

2 The Information System Based on Ontology Model

The aim of ontologies is to formalize domain knowledge in a generic way and provide a common understanding of a domain, which may be used and shared by applications and groups. In addition, we design a mapping tool that uses WordNet and mutual information between data instances and compare its performance to other techniques. In order to make collaborative systems communicate with each other, it is required to build a common terminology. A precisely defined common terminology enables applications to communicate with each other. Ontology is a conceptualization of a domain into a human understandable, machine-readable format consisting of entities, attributes, relationships, and axioms.

2.1 Using Formal Concept Analysis Build Ontology

As a branch of applied mathematics, FCA (formal concept analysis) comes of the understanding of concept in philosophical domain. It is to describe the concept in formalization of symbol from extent and intent, and then realize the semantic information which can be understood by computer. It is to extract all connotative concepts and connections between them from formal context according to the binary relationship so as to form a hierarchical structure of concept[3]. This paper puts forward formal concept analysis method applied in ontology learning based on non-structured of source data. In particular, for $x \in X$ and $m \in M$, denote xIm to express that an object x is in a relation I with an attribute m . Let G be a set of objects and M be

a set of fuzzy or crisp attributes. $\forall g_1, g_2 \in G$, one can define τ as follows, we define Eq. 1.

$$\begin{aligned} \forall A_1 \subseteq A : f(A_1) &= \{y \in B \mid \forall x \in A_1, xRy\} \\ \forall B_1 \subseteq B : g(B_1) &= \{x \in A \mid \forall y \in B_1, xRy\} \end{aligned} \quad (1)$$

Eq. 1 express that the set of attributes common to the objects in A and the set of objects which have all attributes in B , respectively. According to the goal of ontology, the pivotal problem of ontology constructing is to find the concepts and relationship among concepts after confirming the field, but these are connotative in the brain or store the file of this field in actual life.

If no confusion arises, we use the subset $R \subseteq C$ to represent its corresponding similarity relation in the following. In this paper, the ‘MIN’ operator is chosen as the aggregation operator, thus if $P \subseteq R$, then $P(x, y) \geq R(x, y)$ always holds.

After analyzing and comparing, this paper makes up these defects by applying formal concept analysis theory to construct concept hierarchies of ontology, and expresses the relevancy of concepts and documents in combination with probabilistic model for ontology presentation. Users can easily search for the most relevant information using the order of the related documents and concepts, so that search efficiency is improved. For any subset $X \subseteq U$, the β lower approximation of X with respect to f is defined as Eq. 2.

$$f_{jk} = \text{relevancy}(T_j, T_k) = \frac{\sum_{i=1}^n d_{ijk}}{\sum_{i=1}^n d_{ij}} \times \text{WeightingFactor}(T_k) \quad (2)$$

Ant colony optimization was introduced in the early 1990s as a novel technique for solving hard combinatorial optimization problems and inspired by the behaviours of ants in finding paths from the colony to food.

The construction method of ontology is mainly divided into two kinds at present: One is manual ontology building, in which the problem is: (1) In a complicated field it is time-consuming and strenuous;(2) We adopt different standards and modeling methods while building ontology, so that ontology is not currency;(3) It's of great subjectivity. It will lead to the disunity of ontology construction because different domain experts adopt different views. It is the most important that the methods which we adopt are distinct when searching concepts and relationship between concepts in domain.

Ontology-based interoperability techniques have been used in many domains including e-commerce. Finally, the User Interface receives a user query, expands the query using ontology, and sends it to Webpage Retrieval, which in turn returns a list of ranked webpages. Table 1 gives a formal context with $U=\{1,2,3,4,5,6,7,8\}$, $C=\{a,b,c,d,e,f,g\}$, $D=\{e\}$, In the next step, we attempt to reduce the superfluous values of the condition attributes in whole decision rules.

Users can easily search for the most relevant information using the order of the related documents and concepts, so that search efficiency is improved. A case is given to demonstrate how to construct and present ontologies. Figure.1 denotes ontology figure based on formal concept analysis $\text{Sim}[(D,E,G),(r,t)],(A,E,G),(r,s)]$ and

Table 1. Formal context U

U	a	b	c	d	e	f	g
1	×		×	×		×	
2	×	×	×	×		×	
3	×		×				×
4	×	×					×
5	×	×					×
6	×	×	×				×
7	×	×		×		×	
8	×		×	×	×		

attribute oriented concept lattice associated with formal context $(U \setminus \{5,6\}, A, R \cap (U \setminus \{5,6\} \times A))$.

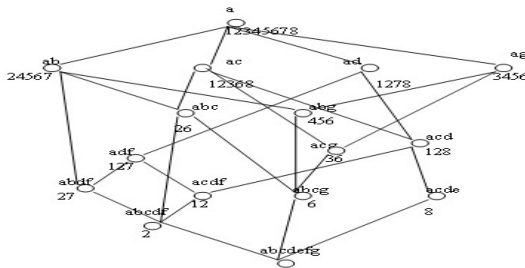


Fig. 1. Ontology figure based on concept lattice

2.2 The Knowledge Based on Ontology

As the foundation of the semantic web, ontology is a formal, explicit specification of a shared conceptual model. The aim of ontology is to obtain, describe and express the knowledge of related domain. Ontology provides common understanding of the domain knowledge and confirms common approbatory vocabulary in the domain, as well as gives specific definition of the relation between these vocabularies from formal model of different levels. Therefore, it becomes a pivotal issue on ontology application to build ontology. But this field is still being discussed today. There is no any mature methodology to guide ontology constructing[4]. Ontologies play a key role in information retrieval from nomadic objects, Internet and heterogeneous data sources. These knowledge assets are indexed in terms of consultancy, innovative products, expert reports, and intellectual properties.

Step 1: The classes of the ontology correspond to the tables of the database, load the knowledge base which is in the OWL file, therefore, JTP queries the knowledge base, reasons and gets the result.

Step 2: Each concept c has a set of instances $I(c)=\{i_1, \dots, i_n\}$. Note that a data instance of concept c can instantiate any property whose domain is concept c , or any of its equivalent or superclass concepts.

3 Constructing Ontology Information System Based on FCA

In order to reduce cost of manual ontology constructing, it is very meaningful that how to utilize technology of knowledge acquisition to obtain the ontology automatically or semi-automatically. This is the second method - Ontology Learning. By this way we can simplify the manual workload of ontology building. But the technology can't search concepts and the relation among all connotative concepts in the field, moreover, it can't present the concepts and conceptual model with definite formalized way. As to Web search, current general search engines use the concept of crawlers (spider or soft-robots) to help users automatically retrieve useful Web information in terms of ad-hoc mechanisms.

According to the goal of ontology, the pivotal problem of ontology constructing is to find the concepts and relationship among concepts after confirming the field, but these are connotative in the brain or store the file of this field in actual life. According to above-mentioned theory, ontology prototype system based on FCA is designed and developed. Figure. 2 describes the drawing of ontology based on concept lattice. The concept lattice displays more intuitively in the form of concept lattices visualizing in three-dimensional space. Formal concept analysis generated conceptual structures provide to the students a user friendly natural presentation of the semantic web evolved. Moreover, domain ontology is constructed by a case, which has perfect hierarchical structure of concept and semantic information to retrieval. So that search efficiency is improved.

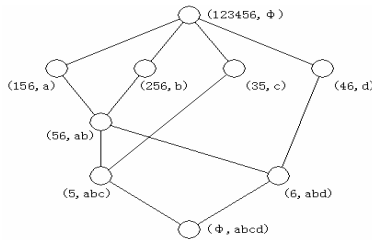


Fig. 2. Ontology pictures based on FCA

4 Summary

The paper probes into ontology information system based on formal concept analysis in order to constructing the ontology model of e-commerce system, and to suffice the needs of theory and application in e-commerce recommendation system. This paper puts forward formal concept analysis method applied in ontology learning based on non-structured of source data. Ontology and FCA model is proposed based on integrating of ontology model and formal concept analysis, and the experimental results have shown our suggested information system will increase precision and performance.

References

1. Berners-Lee, T., Hendler, J., Lassila, O.: The Semantic Web. *Scientific American*, 5 (2001)
2. Lee, C.S., Kao, Y.F., Kuo, Y.H., Wang, M.H.: Automated ontology construction for unstructured text documents. *Data & Knowledge Engineering* 60(3), 547–566 (2007)
3. Xu, H.-S., Shen, X.-J.: Construction and Presentation of Ontology on Semantic Web Based on Formal Concept. *Journal of Computer Science* 34(2), 171–174 (2007)
4. Formica, B.A.: Ontology-based Concept Similarity in Formal Concept Analysis. *Information Sciences* 176, 2624–2641 (2006)

The Electricity Information Acquisition Terminal Design Based on Linux Technology

Yucheng Liu¹ and Yubin Liu²

¹ School of Electrical & Information Engineering, Chongqing University of Science & Technology, Chongqing, China
lych68782763@163.com

² Computer Science School, Panzhihua University, Panzhihua, China
lybwxy1zh@163.com

Abstract. To meet the requirement of the intelligent energy measurement, the paper introduced the electric energy data acquisition terminal which implemented an intelligent energy acquisition by exchanging information with the hub, collecting information from voltage transformer and current transformer and communicating with the electrical energy meter. The paper also described the function, hardware composition and software design of the system. The system used Linux multiprocessing technology to acquire and process the data. It can acquire meter data conveniently with standard communication protocols and submit the data to the master as basis for fee. It can be used widely in the electric energy calculation in industries such as the electric power, oil field, mining, mechanical and chemical industry.

Keywords: Embedded system, Intelligent, Electric energy acquisition terminal, Linux.

1 Introduction

With the increasing demand for electricity, the requirements for the quality and reliability of the power supply are getting higher and higher. Relying on traditional technologies and management tools, that power supply units have been unable to provide a safe and high quality electric energy to the users. In the electricity market reform, smart grid technology has been put forward the new demands. In the field of electricity supply and distribution, it is very important to achieve the intelligence, automation and scientific of the electric energy management and distribution [1]. Currently, power enterprises and electricity companies have widely established the billing system for the electric energy. The electricity information collection terminal is the devices for the electricity information collection to each information collection point. It is device which is between the master and the electric energy meter. It is mainly used for the real-time data collection to the examination electric power meters and the user electric power meters in the electric power distribution system to provide the strong technical support and data basis for the electricity demand management so as to achieve electric energy acquisition, multi-rate pricing, power quality monitoring and line loss analysis, distribution transformer monitoring and anti-tamper, load

forecasting and other functions. Its function and the distribution data's type and accuracy of the data acquisition directly affect the function and reliability of distribution automation systems. Basing on the importance of the power information collection terminal and the development of the new technologies, the Nation Power Grid Corporation provided the new statute of the information collection system to the electric power user in the end of 2009. What this article discussed is the Linux information collection terminal design based on the new statute.

2 Electric Energy Information Acquisition Terminal System Structure

The power information collection terminal which was designed in this paper used AT91SAM9G20 as microprocessors. The operating system used Linux 2.6.27. Although Linux is a soft real-time operating system, but in the kernel body, Linux2.6 has been improved in the interrupt performance and response time. It uses more efficient scheduling algorithm to increase its synchronization. In the real time, it fully meets the needs of terminal equipment. The system is composed of the acquisition module, communication interface module, input and display module and other components, as shown in Fig. 1. In the external communication interfaces, the terminal is divided into four functional interfaces: (1) Remote Communication Interface: The interfaces between the terminal application software and a variety of remote master, such as the TCP / IP communication interface, GPRS functional interface and carrier communication interface. (2) Local Communication Interface: The interfaces are between the terminal application software and a variety of the local communication software, they complete the data exchange in the byte stream manner. (3) Interface between human-machine interface and the terminal application software: The data exchange between human-machine interface and the terminal application software is completed with according to the prescribed index manner and the data model. (4) Other Interface: Including the interface of control, AC and DC analog acquisition, pulse acquisition and other parts, such as the SPI data acquisition A / D conversion interface and USB terminal maintenance upgrade interface.

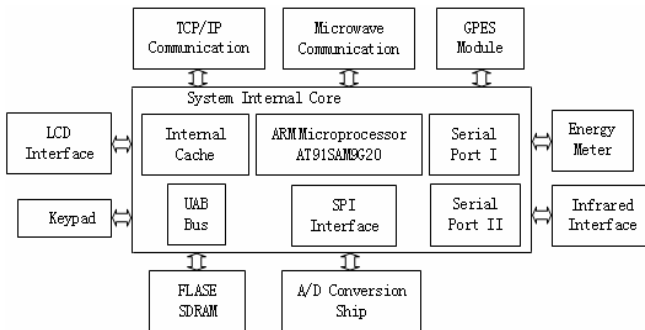


Fig. 1. System hardware frame structure

3 Software Design of Power Data Acquisition System the Terminal

Acquisition Terminal Software Function. According to the function, the acquisition terminal software can be divided into the following sections:

Data Acquisition. to acquire meter data, smart devices data, pulse data and other data.

Data Management. to achieve the reasonable check of the records for the real-time data and current data, historical daily data and events, historical of monthly data and events and the analysis of the storage and remote transmission.

Data Control. including the power setting control, setting control and remote control of the electric energy and fee rate.

Integrated Use. automatic meter reading management, cost management administration, and orderly power management, statistical analysis of electricity consumption, abnormal power analysis, power quality data statistics, the line loss, variable loss analysis, value-added services.

Operation and Maintenance Management. the management of the system privileges and password, terminal management, parameter settings and queries, file management, communication and routing management, run status management, management of maintenance, fault records and report, software upgrades management, and so on.

System Interface. through a unified interface specifications and interface technology, the business application systems of the marketing management is connected to receive collection tasks, control tasks and tasks such as assembly and disassembly information so as to provide the data support and background security for meter reading management, orderly power consumption management, collection of electricity charges , electricity inspection ,and other marketing business.

Acquisition Terminal Software. The core parts of the terminal application software design should include three parts: remote communication module, the main task control module and the local data processing.

Remote Communication Module. Terminal communication protocols request messages and process messages, and then report the processing results to the master station in the form of the message. When the master station does not send messages, if the bottom remote channels support, according to need, it initiatively send the log, important events and cascade terminal uplink packet to the master station.

Main Task Control Module (Multi-Task Acquisition). As shown in Fig. 2, multi-task acquisition modules running in the way of independent processes, they are

mainly responsible for the regular acquisition task management of the data measurement points. After running, the module completed the initialization of message queues, shared memory, timing acquisition cycle time, generated meter reading queue and data entry queue, set acquisition task time point according to parameters of the acquisition cycle and entered the acquisition main cycle. In the main cycle, the system judges whether the current time is acquisition task time. If the current time is acquisition task time, the system starts a new round of meter reading tasks and sends the concentrator communication protocol which is used for communication with downlink communication module local interfaces and performs meter reading. After completing a recycling collection, additional meter reading acquisition process achieves additional meter reading to the measuring points of the acquisition failure. In the main cycle, the program real-timely monitors meter reading task at any time and request of the pass through command issued by the main station communication module. When the multi-task acquisition module receives the other acquisition request, it immediately terminates the current timing acquisition task and sent meter reading at any time and the pass through command acquisition task to DL / T 645 communication module. After having completed all work of the acquisition cycle, it viewed whether the measuring point parameters and the task cycle parameters change. If they have changed, it implemented re-initialization and started the next timing acquisition task cycle [2].

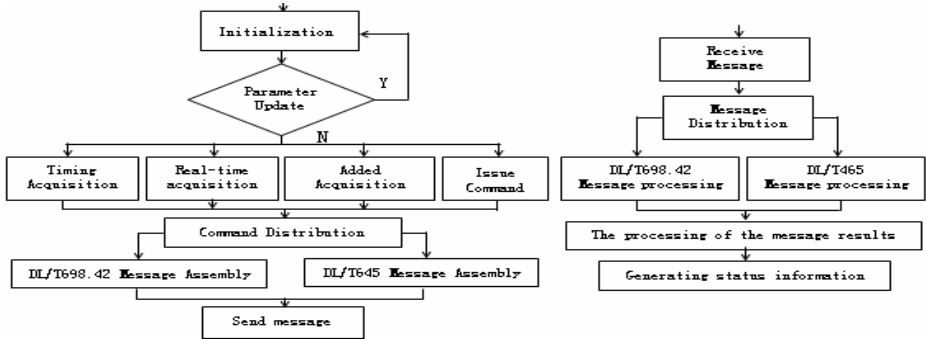


Fig. 2. The main task control program flow diagram

Local Data Processing. Linux supports multi-channel program design, time-sharing processing and real-time processing. The local data processing module can be divided into two processes running, the basic data processing module and the total data processing module, as shown in Fig. 3 and Fig. 4. The basic data processing module is responsible for the abnormal analysis on the data of the measurement points and generates the corresponding event. The total data processing module, is responsible for the statistics of the total add group and sends the total add data to the data storage module for storage according to the set frozen cycle of the total add group.

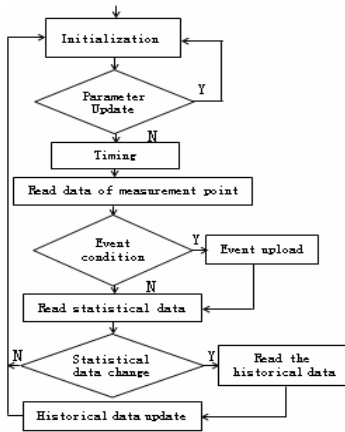


Fig. 3. Basic data flow diagram

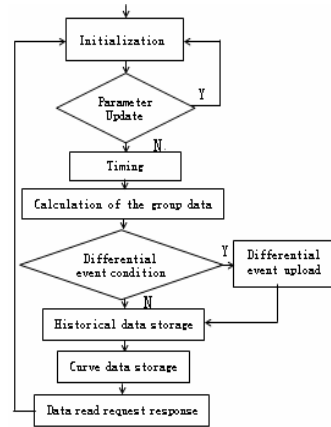


Fig. 4. Total additional group data

4 Conclusions

The paper used the embedded Linux operating system to design the electric energy information automatic acquisition terminal system. Combining with the intelligence measurement main station, the intelligence acquisition terminal can achieve the acquisition of the electricity Information and monitoring of load status. The system has a positive meaning in the enhancing electricity system management, improvement of the power grid reliability and the achievement of electricity management automation.

Acknowledgment. This research is funded by Chongqing Natural Science Foundation (NO.CSTC, 2010BB2285) and science & technology project of Chongqing municipal education committee (No. KJ111417).

References

1. Cui, K., Wu, Z.: Research and implementation of remote monitoring system based on real-time uClinux. In: Proceedings of Services Systems and Services Management, ICSSSM 2005, vol. 2, pp. 1182–1187 (2005)
2. Teng, J.-H., Tseng, C.-Y., Chen, Y.-H.: Integration of networked embedded systems into power equipment remote control and monitoring. In: 2004 IEEE Region 10 Conference, vol. 3, pp. 566–569 (2004)

New Prediction Algorithm for English Class Personnel Assignment Problem

GuoYi Liu¹, ShuFang Wu², and YanE Zhang³

¹ Department of Preventive Medicine and Health Service
Administration, Hebei University, Baoding, China

² Information Engineering Department, HeBei Software Institute,
Baoding, China
arthurzhujie@yahoo.com.cn

³ Department of Information Management, The Central Institute for Correctional
Police, Baoding, China
zhyane@sina.com

Abstract. This paper presents a new intelligent prediction algorithm for English Personnel assignment problem. In order to make the most adaptive education to every student from all over the country, many colleges try to divide the students into two or even more groups depends on their English level to perform the different teaching schedules. English entrance examination score which is usually used to be the standard of it has shown its defects during the past few years' practices. In this paper, the clustering data mining algorithm and fuzzy mathematics theory are applied to find hidden rules which make the English class personnel assignment scientific and rational not only depend on their scores but also other characteristics.

Keywords: English class personnel assignment, Data Mining, Cluster Analysis, membership degree theory.

1 Introduction

Reasonable class personnel assignment methods not only help students acquire knowledge better and more beneficial to the students depending on the situation of Teachers' teaching schedules. But it has been the standard of English class classification in the school only once, as measured by test scores of students were divided into A, B class, this way is clear shortcomings and deficiencies: one-sided and absolute. To reduce the disadvantage taking by the wrong classification, and assign the right student to the right class, this paper proposed a theory based on cluster analysis and the concept of membership degree to make the sample into the maximum possible class.

The new statistical prediction algorithm needs basic information to create database. When students should be classified, simply enter the new basic information, including the new name, sex, source location, exam type, English test results, enter their English test scores can be.

2 Data Mining

Generally, data mining is the process of analyzing data from different perspectives and summarizing it into useful information that can be used to increase revenue, cuts costs, or both. Data mining algorithm is one of a number of analytical tools for analyzing data. It allows users to analyze data from many different dimensions or angles, categorize it, and summarize the relationships identified. Technically, data mining is the process of finding correlations or patterns among dozens of fields in large relational databases. Information can be converted into knowledge about historical patterns and future trends. Mining information and knowledge from large databases has been recognized by many researchers as a key research topic in database systems and machine learning, and by many industrial companies as an important area with an opportunity of major revenues[1].

3 Cluster Analysis

Clustering analysis is an unsupervised learning technique used to discover group structure of a data set. The goal of clustering is to group a set of patterns, points, or objects into meaningful subsets whose in-class members are “similar” in some sense and whose cross-class members are “dissimilar”. Over the past few decades, significant progress has been made in clustering high-dimensional data sets distributed around a collection of linear and affine subspaces[2].

Generally speaking, clustering algorithms can be categorized into hierarchical and partition algorithms. Hierarchical algorithms deliver a hierarchy of possible clusters while partitioned clustering algorithms divide the data up into a number of subsets. In partitioned clustering analysis, many algorithms, such as the K-means [3], assume the number of clusters to be known a priori. Other algorithms partition clusters by minimizing the cluster scatter with a constraint on certain measures, such as cluster variance. Cluster analysis is one of the main tasks of data mining. It is based on correlation between selected samples of the standard can be divided into several categories, high similarity of the sample, different categories are different. According to different clustering criteria, the more common is the distance method.

Distance method is adopt to measure the distance between the variable clustering in the similarity. The shorter the distance, similarity, the better, you can merge into one group. In the distance method, the variable is seen as a point in multidimensional space, commonly used Euclidean distance formula is

$$d_{ij} = \sqrt{\sum_{k=1}^n (x_{ik} - x_{jk})^2} \quad (1)$$

Clustering algorithm in the cluster center is an important concept, is the midpoint of all the clusters in each dimension vector and the mean, is this class which is the most typical representative of the point, usually used to represent the whole class.

4 Membership Degree

Membership belongs to the concept of fuzzy evaluation function in: Fuzzy comprehensive evaluation is affected by many factors and make a comprehensive assessment of things as a very effective multi-factor decision-making method, this method is that: if U in the study area any element x , there is a number $A(x) \in [0,1]$ In response, it claimed that A is the fuzzy set U , $A(x)$ as x on the A 's membership. When the change in x in U , $A(x)$ is a function, called the A 's membership function. Membership degree $A(x)$ the more close to 1 that the higher the degree of x belonging to A , $A(x)$ the more close to 0 indicates that x belongs to A , the lower level. With values in the interval $[0,1]$ the membership function $A(x)$ characterize the degree of x belonging to A level.

5 Algorithm Based on Clustering and Membership Degree

Construct two clustering through data analysis; data within the same class have similar characteristics, differences between the two clusters. Computational method to determine the degree of membership from the complete predicted in Figure 1, the algorithm is as follows:

The feature space of the samples is $U = (\text{sex, source location, exam type, National College Entrance English Examination score, Score of the first exam})$. It is described as $U = \{u_1, u_2, u_3, u_4, u_5\}$

(1) Calculate the cluster centers of the two classes (Class A and Class B) O_1, O_2 based on the samples.

(2) Calculate the distances between the new sample and O_1 described as R_a between the new sample and O_2 described as R_b .

(3) Calculate the membership degree of new sample to Class A

$P_1 = (1/R_a) / (1/R_a + 1/R_b)$. The membership degree of new sample to Class B $P_2 = (1/R_b) / (1/R_a + 1/R_b)$, the membership degree of new sample to the nearest sample of A is $P_3 = (1/r_a) / (1/r_a + 1/r_b)$ the membership degree of new sample to the nearest sample of B is $P_4 = (1/r_b) / (1/r_a + 1/r_b)$

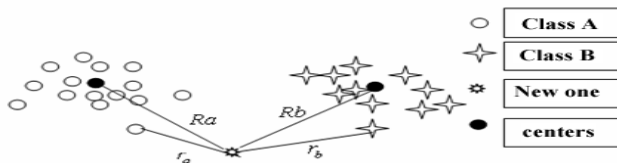


Fig. 1. Proposed algorithm

(4) If $P_1+P_2>P_3+P_4$, the new sample belongs to A, if $1 P_1+P_2<P_3+P_4$, the new sample belonging to B, the new sample can both be A or B when $P_1+P_2=P_3+P_4$.

If the algorithm only considers the distance between the center and the class will result in the following situation in Figure 2, when A, B class in any of the cluster radius is too large, the new data point will be closer to the edge of the radius of a large cluster. In this case, a small cluster radius will be unfair for making classification. Therefore, it is necessary to introduce membership degrees which new data points belong to the nearest point of the clusters. Shown in Figure 2, the new data clearly should belong to the A class, but the data itself because the radius of A class is too large, leading to the wrong classification.

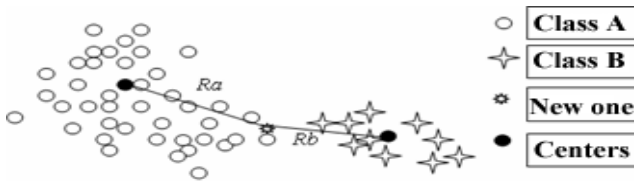


Fig. 2. Only considering the cluster centers

6 Experiment

400 samples are selected, 80% of them are recognized as the training set, and the remaining percent is the testing set. The testing precision is 84.36%.

The experiment results showed that there are still some defects in this algorithm. The reasons are as follows: First, the weight of all the attributes may not be equal. Second, the weight of P_1, P_2, P_3, P_4 are considered equal to each other. Because the weights are not given, the testing precision may decrease.

7 Conclusion

This paper presents a theory based on clustering and the concept of membership to forecast sample should be in class A or B, to some extent solved the problem of English class personnel assignment, and was verified by experiment, the algorithm is feasible and effective. How to assign the weights is still a question.

References

1. Chen., M.-S., Han, J.: Data mining: an overview from a database perspective. Knowledge and Data Engineering, 866–883 (2002)
2. Vidal, R.: Subspace Clustering. Signal Processing Magazine 28(2), 1053–5888 (2011)
3. Turaga, D.S., Vlachos, M., Verscheure, O.: On K-Means Cluster Preservation Using Quantization Schemes. In: 2009 Ninth IEEE International Conference on Data Mining, pp. 533–542 (2009)

Research of E-Learning Intelligent Affective Model Based on BDI Agent with Learning Materials

XueJing Gu^{1,2}, Qing Li³, and RuiJiang Diao⁴

¹ School of Electrical Engineering, Hebei United University, Tangshan

² School of Information Engineering, University of Science & Technology Beijing, Beijing
guxuejing@sina.com

³ School of Information Engineering, Hebei United University, Tangshan
qinger_li@126.com

⁴ School of Mechanical Electronic & Information Engineering,
China University of Mining and Technology (Beijing), Beijing
diaoruijiang@126.com

Abstract. Although E-learning system had become a popular intelligent teaching system in the world, with the development of artificial psychological technologies and the demand of people, it become a hot research topic that intelligent system combined with affective model. The paper proposed an affective model based on BDI Agent with E-learning system. It got teacher's subjective affective data in the form of questionnaire and obtained affective transfer matrix with the method of fuzzy statistic. By designing the interpreter based on constructing Bayesian Network, it achieved the deduction on the changes of virtual teacher's emotion, finally realizing the harmonious E-learning teaching environment.

Keywords: BDI Agent, Affective model, BBN, Fuzzy statistics.

1 Introduction

With the unceasing innovation and development of science and technology, the intelligent teaching system is increasingly unable to satisfy the requirement of people. Though it meets learners' demands for knowledge, learners' affective needs which still play an important role in the teaching environment are ignored. The positive emotions can improve the students' cognitive ability. On the contrary, the negative ones will limit it.

E-learning system is a new kind of intelligent system with more perfect interactive function than ever before, but in the E-learning environment, teachers and learners are still spatially separated and lack the affective communication and feedback.

As the artificial psychological technologies develop, it is possible that E-learning system combines with affective model [1]. Nijholt, A. and others[2] investigated the introduction of haptics in a multimodal tutoring environment, provided an affective model in the tutor agent and introduced the haptic tasks and how different agents are made responsible for them; Ma Xirong [3] made true the identification and catch of students' affective signal in affective computing through monitoring the message of

facial expression and speech sounds in time and used this as a basis for the judgment of students' study state; Luo Qi [4] constructed effective model of e-learning system with facial expression recognition, emotion recognition of speech and motion recognition techniques; Xie Yinggang [5] presented a method using approach-withdrawal and attention to recognize learners' affective state of learning, obtained affective classification with fuzzy mathematics and realized E-learning system based on Agent.

Now the affective model research applied in the E-learning system is underway. As the factors the emotion involved are extensive, we can explore other ways but what I mentioned above. A.R. Abbasi and others [6] performed two experiments indicating that sometimes emotion which should be shown is invisible, or there was not one-to-one correspondence between facial expression and action. That is to say, external affective expression could not be detected subtly (*such as slight face and tone changes*). Thus the paper lays emphasis on the research of people's purely subjective affective changes, establishes the affective model based on BDI Agent, gets teachers' affective changing data in the form of questionnaire, realizes the inference of their emotion through designing the interpreter and finally makes the E-learning system more humanized and intelligent.

2 The Structure Overview of BDI Agent

In the recent years, with the development of intelligent Agent technology, the researches of Agent and Multi-Agent have become a hot topic. Agent is an entity in certain environment. It apperceives the environment with sensors and effects on the environment with effectors. It has autonomy, responsiveness, adaptability and sociality. BDI Agent is a kind of intelligent Agent structure with Belief, Desire and Intention. Although Agent doesn't have explicitly definition, Bratman insists that belief, desire and intention should be the mental states of Agent and having BDI Agent structure would effectively realize the reasoning process according to the changes of resource [7, 8].

In the structure of BDI Agent, belief database is used to store the current facts, belief and demands; desire database is used to plan the method of responding to environmental changes; intention structure is used to perform the final planning; the interpreter is used to get the final planning according to belief and desire database and sent it to intention structure. The structure of BDI Agent is shown in Fig.1.

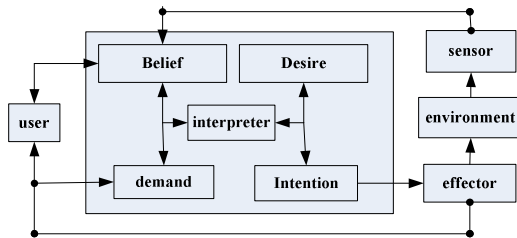


Fig. 1. The structure of BDI Agent

The system sends the affective data to the interpreter and gets affective output. Finally the intention structure responds. In the designing of system the most important part is the process of realizing the interpreter of BDI Agent, thus we complete the establishment of E-learning affective model with the realization of interpreter.

3 The Affective Model of E-Learning System

In the affective model of E-learning system, we regard current affective state of children and teachers as model input and obtain the next emotional output of teacher through the BDI Agent interpreter, so the designing of the BDI Agent interpreter becomes the most important part of the establishment of affective model.

The changes of Children’s emotion result in the changes of teachers’ emotion. That is to say, if the children’s emotion changes, the teachers’ emotion would transfer from i to j state. Thus problem can be expressed by Bayesian Network [9].

Given a mood set $X = \{joy, angry, sad\}$, then

$$B = \langle G, \theta \rangle \tag{1}$$

G is a directed acyclic graph. Its vertex corresponds to the affective variables joy, angry and sad. Its arc represents a function dependency. If $joy \rightarrow angry$, joy is parents of angry and angry is offspring of joy.

Supposing that X_i represents i state of teacher’s initial emotion and X_j is the next j affective state of teacher during which X_i and X_j can be each element in the mood set, the affective transition probability of X_j in case that X_i occurred is:

$$\theta_{X_j|X_i} = P(X_j | X_i) \tag{2}$$

As the mood is fuzzy, the probability of X_i is represented by the probability component of every emotion in X :

$$P(X_i) = [joy \quad angry \quad sad] \tag{3}$$

$$P(X_j) = \theta_{X_j|X_i} P(X_i) \tag{4}$$

Affective transition probability matrix

The article obtains the original data through questionnaires, processes all data with fuzzy statistical method and gets affective shift probability finally.

According to children’s learning state of teaching system, the questionnaires classify children’s emotions into three categories: joy, anxiety, sad. Teacher’s emotions are divided three classes: joy, angry, sad. Every question is designed with teachers’ and children’s current affective state and each option represents the next affective state which teacher will transfer to under the topic environment.

For example: Today you are happy, look at the wistful appearance of Xiao Ming in the English class, you will feel:

- i. Very gratified and more abundant;
- ii. Angry because of his obtrusiveness and let him sit down;
- iii. Not be respected;

The paper investigates 100 people, including 30% male and 70% female, their ages ranging from 20 to 40 years old. Because of the limitation of the survey data and uncertainty of emotion itself, we'll use fuzzy statistic method to get the state shift matrix.

First, questionnaires are classified according to children and teacher's current emotion; here we suppose that they have K kinds of affective states. Then we start to reckon each kind of topic.

Bernoulli theorem concludes that: In n times of repeated independent trails, if the frequency of happening event A is n_A , there is a random number $\epsilon > 0$:

$$\lim_{n \rightarrow \infty} P\left\{\left|\frac{n_A}{n} - p\right| < \epsilon\right\} = 1. \tag{5}$$

In the enough times of repeated independent randomized trials, the frequency of random events will always be stability near to probability value. That is, the probability of event can be identified approximately by enough statistical experiments.

Supposing that the total number of some certain topic is S, the statistical number of the next shift affective state is T, then the membership frequency of X_i belonging to the next fuzzy affective sets:

$$A(X_i) = \frac{T}{S}. \tag{6}$$

$A(X_i)$ is the shift probability that the next emotion is X_i .

$$P_{ij} = \frac{T_j}{S_i}. \tag{7}$$

The Eq.7 represents the probability that teacher's emotion transfers from i to j state.

As above, we process other topics in the same way and obtain teacher's affective shift probability matrix P:

$$P_{ij} = \begin{bmatrix} p_{11} & \cdots & p_{1k} \\ \vdots & \ddots & \vdots \\ p_{k1} & \cdots & p_{kk} \end{bmatrix}. \tag{8}$$

The realization of system

In accordance with the changes of children's emotion, we can get the conditional shift probability matrix.

When the excitation condition of teacher's affective shift is A,

$$P_{ij} = \begin{bmatrix} 0.88 & 0.10 & 0.02 \\ 0.43 & 0.44 & 0.07 \\ 0.87 & 0.04 & 0.09 \end{bmatrix}.$$

When the excitation condition of teacher's affective shift is B,

$$P_{ij} = \begin{bmatrix} 0.65 & 0.26 & 0.09 \\ 0.24 & 0.49 & 0.27 \\ 0.23 & 0.46 & 0.31 \end{bmatrix}.$$

When the excitation condition of teacher's affective shift is C,

$$P_{ij} = \begin{bmatrix} 0.15 & 0.05 & 0.80 \\ 0.07 & 0.15 & 0.78 \\ 0.19 & 0.12 & 0.69 \end{bmatrix}.$$

A, child is happy; B, child is anxiety; C, child is sad.

Therefore, we can assume a teaching scene: teacher's current status $P(X_i) = [0.2 \ 0.5 \ 0.3]$, at this time child has a great improvement in his marks, and then the next emotion of teacher is

$$P = P(X_i) * P_{ij} = [0.2 \ 0.5 \ 0.3] \begin{bmatrix} 0.88 & 0.10 & 0.02 \\ 0.43 & 0.44 & 0.07 \\ 0.87 & 0.04 & 0.09 \end{bmatrix} = [0.6520 \ 0.2520 \ 0.066]$$

It can be seen clearly that the improvement of child's score has a positive effect on teacher. Teacher's emotion transfers from angry to joy status. That is to say, "teacher is glad to see the improving of his student's score".

Fig.2 is the test interface of teacher's affective reaction.

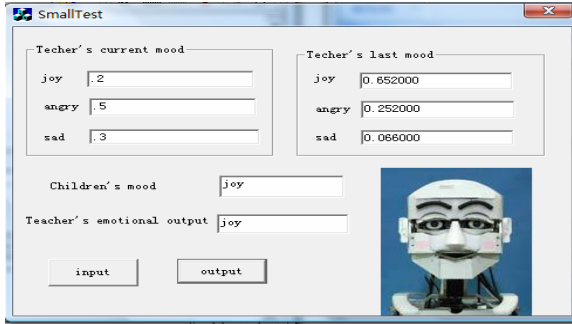


Fig. 2. The test interface of teacher's affective reaction

4 Conclusion

The paper puts forward the new design of BDI Agent interpreter. It investigates different affective shifting rules in different group, handles affective data with fuzzy statistical method and finishes the conclusion of teacher's emotion by the Bayesian Network. Finally it realizes a harmonious interaction environment and provides a theoretical method for the establishment of affective model.

Acknowledgment. This research thanks the National Natural Science Foundation of China (60573059), the High Technology Research and Development Program of China (2007AA01Z160), Beijing Municipal Natural Science Foundation (KZ200810028016), Foundation of Tangshan Science and Technology Bureau(08110201A-1-1-2) and Hebei Polytechnic University Teaching Reform Fund.

References

1. Wang, Z.: Artificial Emotion. Machinery Industry Press, Beijing (2009)
2. Nijholt, A.K., Zwiers, S.: J. Multimodal interaction in a haptic environment. In: Haptic Interfaces for Virtual Environment and Tele-operator System, Japan (2005)
3. Ma, X., Liu, L., Sang, X.: Researching on E-learning System based on Affective computing. Computer Science (2005)
4. Luo, Q., Wan, L., Wu, Y.: Application of Affective Computing in e-learning System. Open Education Research (2006)
5. Xie, Y.: The Research of Intelligent E-learning System Based on Artificial Psychology. University of Science & Technology, Beijing (2007)
6. Abbasi, A.R., Uno, T., Dailey, M.N.: Towards Knowledge-based Affective Interaction: Situational Interpretation of Affect. In: Affective Computing and Intelligent Interaction, Lisbon, Portugal (2007)
7. Jaques, P.A., Vicari, R.M.: A BDI approach to infer students' emotions in an intelligent learning environment. Computers & Education 49 (2007)
8. Gu, X., Shi, Z., Wang, Z.: Research of Affective Robot Based on BDI Agent. Application Research of Computers (2003)
9. Sun, Z.: Research on the Bayesian Networks Methods for Situation Assessment. National University of Defense Technology (2005)

Quality Cost Optimization Problems Research Based on the Operating Station with Winning Machine

WeiWei Liu^{1,2} and Lan Li³

¹ School of Mechanical Engineering, Shenyang University of Technology,
Shenyang, P.R. China

² School of Management of Dalian University of Technology, Dalian, P.R. China
vivianliu0616@163.com

³ Industrial engineering postgraduate, Shenyang University of Technology,
Shenyang, P.R. China

lilan19841209@yahoo.com.cn

Abstract. Based on the quality level requirements of coal mining enterprises for winning machine products, this paper studied the relationship between reliability and quality cost, according to the combination of fuzzy neural network and genetic algorithm established the quality cost optimization model. The case of the operating station with winning machine shows that the optimization model has the advantages of rapid searching, high accuracy, effective and brings the economic benefits for the enterprise.

Keywords: Reliability, Quality cost optimization model, Genetic algorithm, Fuzzy neural network.

1 Introduction

Recently, more and more scholars do research on how the time schedule, quality and costcontrol targets to achieve a balanced three best. They mainly classify the CoQ model into 4 categories: P-A-F model[1], Crosby model[2], opportunity cost model[3], process cost model[4] or ABC model. However, all these are almost all on the research on the theme of quality cost, for the quality cost optimize, there are not so many discussions or just the conceptive discussion. This paper based on the operating station with winning machine uses the genetic algorithmf and the fuzzy neural network method into the quality cost optimization process and establishes the quality cost optimization model based on those methods.

2 Quality Cost Optimization Model

A. Relationship of reliability and the quality cost

Generally, the coordination of reliability and economy, mainly related to the following questions [5]:(1) Limit the total cost of the system to find the optimal reliability (for enterprises, it is the performance of quality levels); (2) In a given system reliability conditions, find the minimum cost for system; (3) Defined the total

cost of the system, then allocate the cost properly; (4) Based on different reliability and cost, compare different programs. In the actual operation of the enterprise, firstly set a quality goal, then optimize and control the cost under it. The relationship model of reliability and the quality cost as follow:

$$y = \sum_{i=1}^n C_{x_i}(R(x_i)) \tag{1}$$

$$s.t: R = \xi(R(x_1), R(x_2), \dots, R(x_n)) \geq R_s \quad 0 \leq R(x_i) \leq 1 \quad i=1,2,\dots,n$$

y is the total quality cost. $C_{x_i}(R(x_i))$ is the cost when reliability of subsystem x_i is $R(x_i)$. $R(x_i)$ is the reliability of subsystem x_i . R is the system reliability. R_s is the limit of the system reliability. $\xi(R(x_1), R(x_2), \dots, R(x_n))$ is the total system reliability when the system reliability is $R(x_1), R(x_2), \dots, R(x_n)$.

the formula of system reliability R [6]:

$$R = P\{S\} = P\left\{\bigcup_{i=1}^n L_i\right\} \tag{2}$$

S is the successful event of system. L_i is the minimal path set of i th line.

B. Quality cost optimization model

This paper uses a tangent function to simulate the relation of every subsystem cost and reliability as in

$$C_{x_i}(R(x_i)) = C_a(x_i) \left[\operatorname{tg} \left(\frac{\pi}{2} * R(x_i) \right) \right]^{k_i} \tag{3}$$

$i=1,2,\dots,n$.

$R(x_i)$ is the reliability of subsystem x_i . $C_a(x_i)$ is the basic cost value of subsystem x_i . k_i is the index of cost increasing.

Based on the analysis of reliability and quality cost model, quality cost optimization model is as in

$$Q(x_i) = \min y = \min \sum_{i=1}^n C_{x_i}(R(x_i)) \tag{4}$$

$$s.t: \begin{cases} R(x_i)_{\min} < R(x_i) < 1 \\ R_{s \min} < R < 1 \end{cases} \quad i=1,2,\dots,n$$

$Q(x_i)$ is the lower total quality cost of system. $R(x_i)_{\min}$ is the lower limit of reliability of subsystem x_i . R_{\min} is the lower of limit of total reliability of system. Other variable are same as before.

3 Resolving Quality Cost Optimization Problem Based on Fuzzy Neural Network and Genetic Algorithm

A. Genetic Algorithm

1) Coding: As the problem of quality cost optimization is a numerical optimization, we adopt floating numbers in order to solve the problem more direct and more efficient. A chromosome or individual representing each code corresponds to a solution of the problem, and a gene represents a real number which on the

chromosome. In this paper, we make genes constitute a chromosome by a uncertain structure.

2) Fitness function: Fitness function is the individual fitness evaluation function by the combination of objecting and fitness function, it as follows:

$$f_i = \frac{1}{Q(x_i)} \tag{5}$$

f_i is the fitness of the i th chromosome. $Q(x_i)$ is the lower total quality cost of system.

The best individual chromosomes choice basis:

$$p_i = \frac{f_i}{\sum_{i=1}^n f_i} \tag{6}$$

n is population size. P_i is the probability of the i th chromosome.

3) In order to ensure convergence of the algorithm and more suitable for floating coding, we chose the part of the arithmetic crossover P_c and uniform mutation P_m .

B. Fuzzy Neural Network

1) Fuzzy neural network consists of input layer, fuzzification layer, rules layer and output layer. The fuzzy neural network structure is as shown in Figure 1.

a) Input layer. It takes the acceptable variables to the next layer.

$$f_1(i) = x_i \tag{7}$$

$i=1,2,\dots,n$

i is a Input variable.

b) Fuzzification layer. it put each input variables into fuzzy linguistic value. Each node in this layer represents a fuzzy language value.

$$f_2(i, j) = \exp[-(f_1(i) - \theta_{ij})^2 / \sigma_{ij}^2] \tag{8}$$

θ_{ij} is the center value of the function. σ_{ij} is the mean value of the function.

c) Rules layer. Realizing the function of fuzzy set operations.

$$f_3(m) = \prod_{j=1}^n \prod_{i=1}^n f_2(i, j) \tag{9}$$

$m=1,2,\dots,M$ M is the nodes of the third layer.

d) Output layer. Calculated to achieve clarity.

$$f_4(k) = \sum_{m=1}^M w_j * f_3(m) \tag{10}$$

w_j is The center value of membership function of the j th language value in $f_4(k)$.

$k=1,2,\dots,K$ K is the nodes of the forth layer.

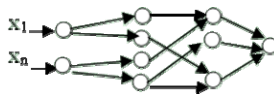


Fig. 1. Fuzzy neural network structure

2) In this paper, we adopt the fuzzy rules and the error of fuzzy neural networks as follows:

The fuzzy rules: If x_1 is A_1 and x_2 is $A_2 \dots$ and x_n is A_n , then y is B

$$E(i) = \frac{1}{2} \sum_N \sum_L (V_L - T_L)^2 \tag{11}$$

$E(i)$ is the error of fuzzy neural network. N is the number of study samples. L is the nodes of output subset. V_L is the network desired output T_L is the network actual output.

Adjusting the error by gradient descent method, Parameters shall be adjusted as follows:

$$\frac{\partial E}{\partial w_j} = -(V_L - T_L) \frac{\partial T_L}{\partial w_j} \tag{12}$$

$$\frac{\partial E}{\partial \theta_{ij}} = -(V_L - T_L) \frac{\partial T_L}{\partial f_3(m)} \frac{\partial f_3(m)}{\partial f_2(i, j)} \frac{\partial f_2(i, j)}{\partial \theta_{ij}} \tag{13}$$

$$\frac{\partial E}{\partial \sigma_{ij}} = -(V_L - T_L) \frac{\partial T_L}{\partial f_3(m)} \frac{\partial f_3(m)}{\partial f_2(i, j)} \frac{\partial f_2(i, j)}{\partial \sigma_{ij}} \tag{14}$$

C. Fuzzy neural network and genetic algorithm

1) Steps of the fuzzy neural network and genetic algorithm as follow:

- a) Substitute $R(x_i)$ and Randomly initialize population.
- b) According to formula (5) calculation of population fitness of each chromosome, and fitness sorting, select the largest fitness value of chromosomes as the optimal chromosome.
- c) Using formula (6) to calculate choice probability for each chromosome. Select the larger fitness value of chromosomes to generate new chromosomes.
- d) Setting the crossover probability and the mutation probability.
- e) After genetic algorithm, the optimize parameters as the initial value of fuzzy neural network parameters.
- f) According to formulas (7)-(10) computing the output node of each layer in fuzzy neural network.
- g) Using formula (11) to calculate the error of fuzzy neural network.
- h) Using formulas (12)-(14) to adjust the parameters of fuzzy neural network.
- i) If reach the number of iterations, then end.
- j) Repeat steps (f) to (h), until meet the end condition.

2) Based on the above content, the flow chart which is the combination of fuzzy neural network and genetic algorithm is shown in Figure 2.

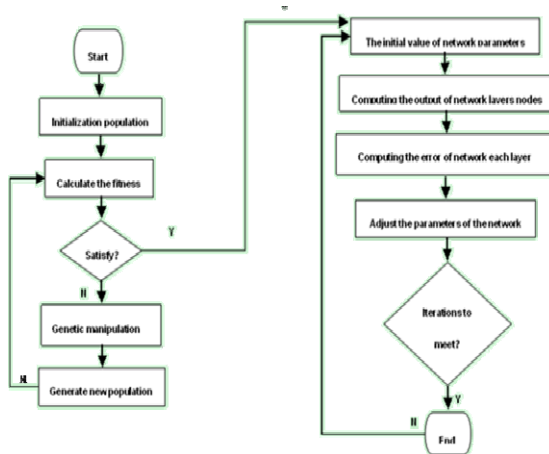


Fig. 2. The flow chart of the combination of fuzzy neural network and genetic algorithm

4 Example

The operating station with winning machine as an example, structure chart as figure 3. Network system chart which included 12 subsystems is as Figure 4. Basic quality cost values and reliability of these subsystems are as Table 1.

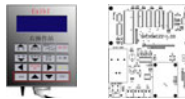


Fig. 3. The structure chart of operating station with winning machine



Fig. 4. The network system chart

In this paper, group size N is 30, the crossover probability P_c is 0.65, the mutation probability P_m is 0.01, the number of iterations is 100. Assume the low limit of reliability of system is 0.5, the low bound of reliability of each subsystem is 0.45, and the index of cost increasing is 0.1.

First, put the data in Table 1 into formulas (1)-(2), we can get the total reliability R is 0.4571, and the total quality cost C is 371.46 thousand. This shows that R is lower than 0.5, so the plan can not meet the demand and must to be optimized.

The reliability of subsystems optimized by the quality cost optimization model which based on fuzzy neural network and genetic algorithm is in Table 2. Then, put $R(x_i)$ in Table 2 and $C_a(x_i)$ in Table 1 into formula(3), we can get $C_{x_i}(R(x_i))$ in Table 2.

Table 1. Basic quality cost values and reliability of these subsystems

[cost unit: thousand]

x_i C R	x_1	x_2	x_3	x_4	x_5	x_6	x_7	x_8	x_9	x_{10}	x_{11}	x_{12}
$C_a(x_i)$	41	8	60	20	30	50	53	28	40	45	16	20
$R(x_i)$	0.72	0.70	0.68	0.67	0.65	0.60	0.79	0.69	0.71	0.73	0.61	0.74

Table 2. The reliability of subsystems optimized

[cost unit: thousand]

x C R	x_1	x_2	x_3	x_4	x_5	x_6	x_7	x_8	x_9	x_{10}	x_{11}	x_{12}
$C_a(R(x_i))$	37	6	60	20	28	50	40	35	45	38	15	23
$R(x_i)$	0.79	0.56	0.69	0.54	0.65	0.52	0.59	0.70	0.78	0.68	0.60	0.76

Take the data of Table 2 into formulas (1)-(2), we obtain the total reliability R is 0.5024, and the total quality cost C is 343.65 thousand. The value is higher than 0.5, so this plan can meet the demand.

In conclusion, the quality cost optimization model which based on fuzzy neural network and genetic algorithm not only meet the restricted condition, but also reduce the cost of quality to 371.46-343.65=27.81 thousand.

5 Summary

The research method of quality cost optimization which based on fuzzy neural network and genetic algorithm can meet the constraints, reduce the cost of quality, and make the cost control more precise. This method is general to understand, and provides a new way for the coordination of reliability and the cost of quality.

Acknowledgement. National Natural Science Foundation: Complex production process is based on the optimization scheduling theory and methods of the data and its application in metallurgical industry. (61034003).

References

1. Albright, T.L., Roth, H.P.: The measurement of quality costs: an alternative paradigm. Accounting Horizons (1992)
2. Allen, N., Oakland, J.S.: Quality assurance in the textile industry: Part I. International Journal of Quality & Reliability Management (1988)
3. Chung, K.J.: A necessary and sufficient condition for the existence of the optimal solution of a single-vendor single buyer integrated production-inventory model with process unreliability consideration. International Journal of Production Economics (2007)

4. Atkinson Jr., J.H., Hohner, G., Mundt, B., Troxel, R.B., Winchell, W.: Current Trends in Cost of Quality: Linking the Cost of Quality and Continuous Improvement. NAA Publication (1991)
5. Guo, Y.: Reliability Engineering Principles, ch. 7. Qinghua university Press (2002)
6. Shi, Y.: Comprehensive control technique of reliability in construction project management. Changan University, Xian (2005) (in press)

Method of the Road Lines Recognition in the Maps of Digital Material Based on Improved BP Neural Network

Yunliang Yu¹, Tingting Zhang², Ye Bai¹, and Jianqiang Wang¹

¹ College of Earth Sciences, JiLin university, ChangChun, China
yuyunliang@sina.com, baiye2196@sina.com, 281181026@qq.com

² SINOPEC Northeast Oil and Gas Company, ChangChun, China
53366544@qq.com

Abstract. Maps made of paper material are required to be digital, the necessary step is to recognize and trace the road lines in the maps of digital material. But there are so many crossing points of the road lines in the digital map. In order to recognize a complete road line, the tracing direction at the crossing point must be solved at first. According to present roads crossing points recognition algorithm has not obtained good effects. This paper describes the calculation principle of road lines recognition using BP neural network in maps of digital material, and method has been improved. It was proved by experiment that the improved algorithm of the crossing point recognition method is highly effective.

Keywords: crossing lines recognition, BP neural network, false saturation, average square root error.

1 Introduction

In the recent years, with the sharply increasing number of the geography and geology map made in paper material, which is needed to save the maps as digital material, and the massive road lines are used to recognize and trace from the saved maps of digital material. BP neural network has good pattern recognition and clustering function. This advantage makes it become optimal selection for recognizing and tracing the road lines from the scanned digital maps. But BP algorithm exists some problems, make the recognition speed slow, and success rate low. In order to improve the precision and speed of the road lines from the scanned digital maps, the training convergence rate of the tracing directions at crossing point should be improved. This paper improves BP neural network to solve false saturation and net oscillation problem during road lines recognition process.

2 Existing Crossing Lines Recognition Method

Chen Yi[1] puts forward a new idea of crossing lines recognition with BP neural network, and overcome the disadvantages of the limited storage capacity of Hopfield

network. Its idea is to make one digital map seen as a synthesized scalar field overlapped by some independent scalar field, but just one related scalar is researched. Some line is seen as a contour of corresponding scalar field. Thus the problem transforms into finding the point in the contour of the scalar field, it is also to find the point of the contour $F(X,Y)=C$. Using the BP neural network approaches to this function. The neural network is designed three-layer structure. The input layer has two neurons, corresponding to x, y ; and the output layer has one neuron, because we just want to output one real number. Collect the points of line as the training sample from the beginning of the line until crossing point. When the crossing point is detected, train the sample with BP neural network algorithm. After training, make the coordinate value of the standby point as net input value, calculate the output. Choose the best point from the input points as the next point, which is the minimum error, to pass over the crossing point and continue to tracing the road line automatically.

3 False Saturation in Road Lines Recognition Using BP Neural Network

According to the gradient method, the RMS error should have decreased gradually during BP neural network is training. Such as fig1, the classic error curve of BP algorithm is the process of convergence study, in which the net RMS error decreases gradually.

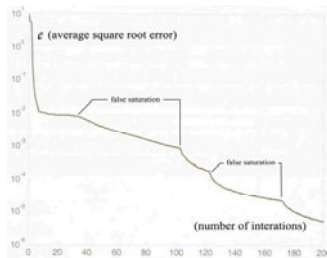


Fig. 1. Error curve of Classical BP training until convergence

But in a long period, the error keeps invariant with the increasing number of the superposition, after this period, the error decreases gradually, this phenomenon is called the false saturation. The false saturation is not accidental, which is related to the initial weight of net, modification of the weight, distribution of the samples and so on.

The given input model under the initial weight, if it is far away between the total input of the input unit layer and the threshold value, we called the unit goes in the saturation region, and there are errors between input and expectation output, the weight is needed to modify to make the unit drop out the saturation region. The value of threshold function is small in the saturation region, so we must modify the weight during every time of training. When the outputs stay in the saturation, the error of net RMS does not change or turns small, which leads to false saturation. With the sustained net training, when the processing unit dropped out the saturation region, the

error and derivative of action function are bigger, the weight correction value increases gradually, and the RMS error decreased rapidly in the training curve.

4 Improved Crossing Line Recognition Algorithm

The improvement of modified weight and threshold value

During the fact training process, select the minimum integrate of the η as the training rate. The gradient search step has effect greatly with the η training process. η is greater, the changing of weight is stronger.,and select the bigger η when the range is stable. To make the training speed is fast and stable, we always insert a ‘‘Situational items’’ [2] into ‘‘weight regulation’’ and ‘‘threshold value regulation’’,as formula (1) and (2):

$$\Delta\omega_{ji}(t+1) = \eta\delta_{kj}o_{ki} + \alpha\Delta\bar{\omega}_{ji}(t) \quad (1)$$

$$\Delta\theta_j(t+1) = \eta\delta_{kj} + \alpha\Delta\theta_j(t) \quad (2)$$

α is a constant, it decides the influence degree on the change of the past weight from the change of the present weight.

The improvement of avoiding falling into the minimal point

When the map is complex and the crossing lines is too many, the selected samples increased greatly, if the training fall into the minimal point, the process is too long, the recognition always is failure.

Aiming at the convergence speed of BP algorithm being slow which leads to the crossing lines recognition being slow, we take the batch processing into the BP algorithm. When the all input samples have completed, sum all errors[3], then, modify the weight once, as formula (3):

$$E = \sum_k E_k \quad (3)$$

According to (4)、(5) ,modify the weight and threshold value,

$$\Delta\omega_{ji}(t+1) = \eta\delta_{kj}o_{ki} + \alpha\Delta\bar{\omega}_{ji}(t) \quad (4)$$

$$\Delta\theta_j(t+1) = \eta\delta_{kj} + \alpha\Delta\theta_j(t) \quad (5)$$

and:

$$\left\{ \begin{array}{l} \eta = \eta \cdot \varphi \quad \alpha = \alpha \quad \Delta E < 0 \\ \eta = \eta \cdot \beta \quad \alpha = 0 \quad \Delta E > 0 \end{array} \right. \quad (6)$$

$$\Delta E = E(t) - E(t-1) \quad \varphi > 1 \quad \beta < 1 \quad (7)$$

In addition to avoid occurring the calculation overflow, we can modify like this:

$$\eta = \eta_0, \quad \alpha = 0 \quad \Delta E > 0$$

further: $\eta = \eta \cdot \left(1 + \frac{c}{p}\right)$

C is a constant, p is a learning cycle. The two ways of the correction could avoid oscillation during training because of the bigger training rate to some extent.

The neural network can be divided into input layer, hiding layer and output layer with BP algorithm training[4]. The input layer has two neurons, corresponding to x, y. Because BP neural network approaches to the contour $F(X, Y)=C$, so the output layer only designed a neuron. The original hiding layer neuron is 5, if the train is convergence, decrease the number then to decrease the order of space complexity of the neural network; if the training is not convergence before it reaches the maximum, increase the number of the neurons until convergence. The value of the convergence is 0.001 or 0.005 for considering to convergence speed and precision.

Snapping from part of digital map (fig 2), collect the colors, grayscale and width data of each road for input of BP net, and use improved cross line recognition algorithm to automatical track this snapshot, result shows in fig3.



Fig. 2. Part of digital map before recognition



Fig. 3. Part of digital map after recognition

This improved algorithm could finish training in a short time, and error curve, as showed in fig 4.

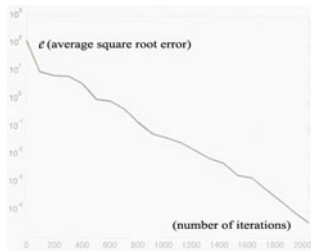


Fig. 4. Error curve of BP training until convergence

Experiments show that the improved algorithm plays well at oscillation preventing and trapping in minimum value, thus improved road recognition method has two improvements:

Reducing weight modify frequency, makes adjustment to minimum globe error, avoiding turning back;

The learning speed is obtained according to circumstances, learning speed η and momentum α , so that learning efficiency can be greatly increased.

5 Conclusion

Using improved BP algorithm to recognize road lines in the maps of digital material can not only solve the problem of Hopfield model's lack of storage capacity which leads to low identification ability, but also insure the original advantage of tracing the lines across the crossing points without manual intervention, and aim at BP algorithm's oscillating and trapping in minimum value, improved BP algorithm give a major increase to recognition speed and accuracy. Based on experimental results, the improved BP algorithm makes the reconition degree to a new level.

References

1. Chen, Y., Wang, Y., Zhang, J.-k.: Research on Combined Artificial Neural Network and Its Application in Earthquake Prediction 1(28), 190–193 (2011)
2. Hopfield, J.J.: Nerual NetWorks and Physical systems with emergeat collective computational abilitical. Proc. Natl. Acad. Sci. USA 79, 2554–2558 (1982)
3. Hopfield, J.J., Tank, D.W.: Computing with neural circuits,a model. Science 233, 625–633 (1986)
4. Liu, G., Xia, X., Jiang, D.: Structure random response analysis based on artificial neural net. Journal of Guilin University of Technology 2(26), 205–208 (2006)

The Heavy Mineral Analysis Based on Immune Self-organizing Neural Network

Yunliang Yu¹, Ye Bai¹, Tingting Zhang², Jianqiang Wang¹

¹ College of Earth Sciences, JiLin university, ChangChun, China
yuyunliang@sina.com, baiye2196@sina.com, 281181026@qq.com

² SINOPEC Northeast Oil and Gas Company, ChangChun, China
53366544@qq.com

Abstract. The heavy mineral analysis is the important content of the oil and gas exploration in sedimentary basin, and the provenance data can be clustered according to the theory of sedimentary heavy mineral composition similar to its characteristic value. But self-organizing neural network can not determine its own clustering number, thus we introduce the immune algorithm, which can better adjust the number of competitive layer neurons and the size of the adjustment of the neighborhood. Classify the provenance data with immune self-organizing neural network, and compare the result of clustering with sedimentary facies, which confirms the reliability of the method.

Keywords: heavy mineral, self-organizing neural network, immune algorithm, provenance analysis.

1 Introduction

The heavy mineral analysis is the important research area of basin reconstruction of ancient geography, and lithology sandstone reservoir prediction. In recent years, neural networks have been widely applied in many areas, whose advantage is to learn to adjust itself, and able to establish the nonlinear relationship between data, but it need prior knowledge[1], in the actual analysis, some of the exploration area or areas of complex mineral assemblages is difficult to obtain reliable and complete sample data, which brings heavy mineral classification difficult[2], We combine self-organizing neural network and immune algorithm in the cloning and mutation mechanism to judge on the heavy mineral analysis of provenance information automatically.

2 Existing Self-organizing Neural Network

Multi-layer perceptron learning and classification is based on priori knowledge of a certain condition, and the adjustment of network weights is carried out under the supervision. In practice, sometimes it can not provide the necessary prior knowledge, which requires neural network to have the ability to self-learning. Kohonen's self-organizing feature map is the self-learning neural network[3]. Compared with other

clustered neural network, SOM has the advantage of real-time self-learning, self-stability, and evaluation function is not necessary all the time, which can recognize the most significant features of the vector space.

3 Immune Algorithm to Better Adjust Self-organizing Neural Network

The number of heavy mineral classification has effect on the final results of the analysis. Less classification number will lead to omission provenance types, and more classification number will have effect on the tracing of the provenance[4]. Thus, the introduction of the immune algorithm will improve the number of competitive layer neurons and adjust to the size of the neighborhood[5].

The input model In immune self-organizing neural network is $P_k = (P_1^k, P_2^k, \dots, P_N^k)$, $k = 1, 2, \dots, q$, q is the sample number. Competitive layer neurons is $A = \{a_1, a_2, \dots, a_M\}$, M is the number of neurons. Competition layer neurons j and Input layer neuron weight matrix is $W_{ij} = (w_{1j}, w_{2j}, \dots, w_{ij}, \dots, w_{Nj})$, $i = 1, 2, \dots, N$, $j = 1, 2, \dots, M$.

Define the distance of the input sample L relative to the winner neurons j in the classification process:

$$\Phi(a_j) = \frac{1}{\|P_i - W_j\|} = \frac{1}{\left[\sum_i (p_i^l - w_{ij})^2 \right]^{1/2}} \quad (1)$$

a_j is the number of neurons in the neighborhood:

$$N_j = g(M^*, \Phi(a_j)), \quad j = 1, 2, \dots, M \quad (2)$$

M^* is the number of cloning sample.

$$W_{ij} = (t+1) = W_{ij}(t) + \eta(t) \cdot (P_j^1 - W_{ij}(t)) \quad (3)$$

$$\eta(t) = N_t(0, \sigma^2); \quad \sigma = \sqrt{\frac{1}{\Phi(a_j(t))}}$$

Rule of weight adjustment: after the introduction of immune algorithm, adjust the weight of neighborhood neuron in the adjustment process[6]. Formula as follows:

$$W_{ij} = (t+1) = W_{ij}(t) + \eta(t) \cdot (P_j^1 - W_{ij}(t)) \quad (4)$$

$$\eta(t) = N_i(0, \sigma^2); \quad \sigma = \sqrt{\frac{1}{\Phi(a_j(t))}}$$

The average of $N_i(0, \sigma^2)$ is zero, standard deviation σ is the random variable of normal distribution.

Choosing the winning neuron after adjusting neighborhood neurons, re-calculate the weights of neurons, and the Euclidean distance of input vector, $\forall_i = 1, 2, \dots, M$, If there exists neurons after weight adjusting $b = \{a_{ij}(t+1) \max \Phi(a_{ij}) j = 1, 2, \dots, (N_i - 1)\} \quad i = 1, 2, \dots, M$ allows $\Phi(a_i) < \Phi(b), a_i \in A$, so replace the original winning neuron a_i with b to update the winning neuron group. Through the above process makes the whole output of the network more optimized.

4 The Automatic Analysis of Multi- Heavy Mineral

According to the principle of heavy mineral has similar characteristics on combination and rich degrees, we analyze the ratio using self-organizing neural network with five terrestrial stable heavy minerals like garnet, zircon, tourmaline, rutile, magnetite of three sub-layers such as Sha- I and Sha- II in Shahejie Formation of Kongnan area of Huanghua depression. The input data of Sha- I and Sha- II trained through 500 times, the centers of clustering derives from various types of the heavy mineral content, as shown in Table 1 and Table 2, the clustering result shown in fig 1.

Table 1. Clustering centre of heavy mineral content of Sha- I

	Mineral content of the cluster center (%)			
	First kind	Second kind	Third kind	Forth kind
Rutile	1.13	1.18	2.02	88
Zircon	28.46	5.68	23.95	12.90
Electrical stone	2.44	1.83	3.51	1.57
Magnetite	1.90	11.78	14.03	15.51
Garnet	51.38	12.55	8.80	56.15

The division of the sedimentary facies is based on the grain size analysis, the core structure, the structure observation and logging characteristics, and the results is accurate and reliable, which has certain instructions to provenance direction. Eventually compare the clustering results with sedimentary facies shown in fig 2.

Table 2. Clustering centre of heavy mineral content of Sha- II

	Mineral content of the cluster center (%)					
	First kind	Second kind	Third kind	Forth kind	Fifth kind	Sixth kind
Rutile	1.20	63	75	51	25	89
Zircon	28.18	16.16	13.84	13.56	9.79	23.45
Electrical stone	2.95	1.88	1.28	93	90	1.35
Magnetite	6.43	9.61	7.58	21.76	43.99	5.38
Garnet	27.43	42.35	69.73	53.65	28.92	53.83

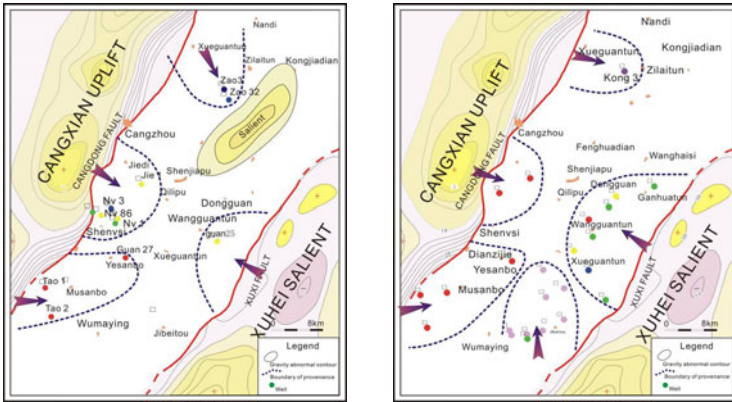


Fig. 1. Clustering centre of heavy Mineral content of Sha- I (left) and Sha- II (right)

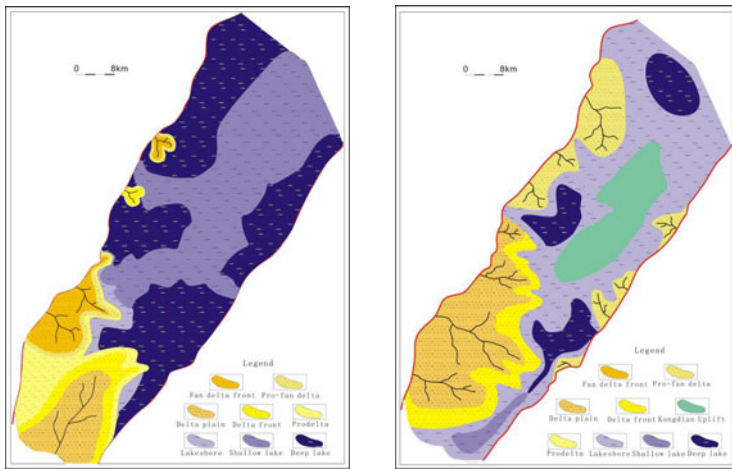


Fig. 2. Sedimentary facies of Sha- I (left) and Sha- II (right)

5 Conclusion

(1) Combine self-organizing neural network with the cloning and mutation mechanisms of immune algorithm, and make the heavy minerals clustered more rational and effective.

(2) The clustering of heavy minerals feature in three layers at Shahe jie Formation of Kongnan area of Huanghua depression, which compares with gravity detection and the clustering diagram, confirms that classify multi-provenance using heavy minerals data by immune self-organizing neural network is reliable and accurate.

References

1. Zhao, T.: The Distribution of Biolimestone and Igneous Rock in Dagang Area and the Research for Its Hydrocarbon Reservoir. *Logging Technology* 12(3), 41–46 (2001)
2. Linfu, X., Baozhi, P.: Identify lithofacies automatically using self-organizing neural network. *Journal of Changchun university of science and technology* 29(2), 144–147 (1999)
3. Li, G., Shao, F., et al.: Research of the clustering algorithm based on neural network. *Journal of Qingdao University Engineering & Technology Edition* 16(4), 21–24 (2001)
4. Wu, X.: Contrast of SOM Neural Networks and Cluster Analysis Using in Grain-size Analysis, pp. 48–51 (2006)
5. Jiang, Z.: *Sedimentology*, pp. 101–102. Petroleum Industry Press, Beijing (2003)
6. Liu, X., Wen, J., et al.: A Fuzzy Clustering Method to Recognize Coherent Generator Groups Based on Self-Organizing Neural Network. *Power System Technology* (7), 98–102 (2010)

Research on Mobile Electronically Published Materials Protection

Sha Shi¹, Qiaoyan Wen², and Mingzhu Li³

¹ State Key Laboratory of Networking and Switching Technology Beijing University of Posts and Telecommunications Beijing, 100876, China
shisha1980@126.com

² State Key Laboratory of Networking and Switching Technology Beijing University of Posts and Telecommunications Beijing, 100876, China
wqy@bupt.edu.cn

³ Siemens Ltd., China Corporate Technology Beijing, China
mingzhu.li@siemens.com

Abstract. This article presents a new solution of portable electronically published materials protection. The solution uses strict data security authentication and strong encryption protocols to improve security features with division of mobile storage device functional domains. And a security protection code to generate a new portable document format is used to prevent the attackers disclose the document information illegally.

Keywords: electronically published materials, authentication and encryption, protection code.

1 Introduction

Some leakage protection technologies have been proposed to prevent the information from being illegally disclosed to competitors. There are two kinds of information leakage prevention technologies: network based and host based. Network-based technologies are used to prevent users from leaking out information through various network applications by deploying security gateway at the network entry/exit. Host-based technologies usually use security agent in the user terminals to monitor the terminals and prevent information leakage through host peripheral interface, printer or mobile storage.

While document can not be protected when it is stored in mobile storage device in plaintext and sent to those whose computers do not installed host-based document protection agent. Some secure mobile storage device support to encrypt the document which avoids the plaintext document being accessed by malicious attacker. But this can not prevent the receiver from disclosing the plaintext document unconsciously or intentionally to the malicious attacker because the target computer does not install the host-based document security system. In some case, it is inconvenient or impossible to install the host-based document security system in the target computer. For example, in a partner meeting, the presider does not expect the confidential documents to be disclosed by some partners since it is inconvenient to install the protection system in those partner computers.

Herein, a new mechanism to protect the portable document leakage is proposed. This method improves the secure mobile storage device to support the strict authentication and strong encryption and prevent illegally disclosure from the target computer with a secure portable document format.

2 Design

Herein, a mobile storage device comprising security control module, data area and security area is designed as the secure electronically published materials. The document is encrypted and appended to the Security Protection Code which makes a portable security document before storing in the device. The device can work in two modes: online and offline. In online mode, the Portable Document Security Device can authenticate and get key material from Document Security Server. In offline mode, the key material is stored in the security area of the Portable Document Security Device. The following technology description takes online mode as sample.

2.1 Portable Document Leakage Protection System

The Portable Document Leakage Protection System is shown as Fig 1. The system comprises a Document Security Server, Management Terminal. The protected document is transferred to the target computer via the Portable Document Security Device. The protected document should be encrypted with $Dkey$, and access password and security policy are set before the document is transferred to the other computer via the Document Security Device. Then the document is appended to an executable protection code and makes a portable security document. Finally, the document is copied to the data area of the Portable Document Security Device.

The encryption key and security policy will be transferred to the Document Security Server. The user can request the key by security protection code.

When user accesses the document from the Portable Document Security Device in the target computer, the device will require the user to perform password-based authentication, and then the target computer can access the data area to find the portable security document. The security protection code will run when user open the document. Then the protection code can protect the document according to the security policy during the document access. The enforcement security policy can include: document Read, Write, Print Screen, Print, Change Permission, Change Location, etc.

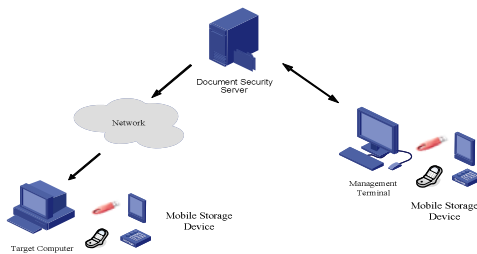


Fig. 1. Portable Document Leakage Protection System

2.2 Portable Document Security Device

The Portable Document Security Device is shown as Fig 2.

The Portable Document Security Device comprises a Security Control Module, Data Area and Security Area. The Security Control Module perform authentication, access control and cipher computation. The Security Area stores the Key shared with the Document Security server which is used for secure validation protocol. The user access password can also be stored in the Security Area. The Data Area will become accessible when user passes the password authentication.

The USB Document Security Device communicates with the target computer via Mobile Storage Media interface. The target computer can not access the data area until the user enters the correct password (Pwd). After the user opens the document, the Security Protection Code will run in the target computer and request the authentication information. The Security Control Module will reply with the following message:

$$UID\|Hash(Key\|Pwd) \quad (1)$$

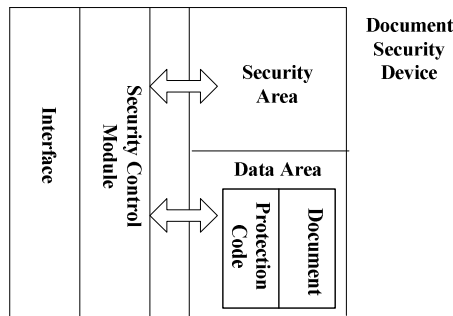


Fig. 2. Secure Mobile Storage Device Structure

Key is the shared secrecy between Portable Document Security Device and Document Security Server. Pwd is the password set when the document is encrypted and copied to the device.

Then the Security Protection Code can use the message to perform the secure validation protocol and get the key and policy of the document from the Document Security Server.

2.3 Secure Validation Protocol

The Security Protection Code will perform the following secure validation protocol to get the key and policy of the document after the user passes password-based authentication of the Portable Document Security Device. The Security Protection Code computes the following message and sends it to the Document Security Server:

$$UID\|SEQ\|Hash(Key\|Pwd\|SEQ) \quad (2)$$

The SEQ is the increment sequence number to resist the replay attack. Hash () is a kind of hash function such as SHA, etc. The Document Security Server validates the SEQ and $Hash(Hash(Key\|Pwd))$ by computation. If valid, the Server sends the following message to the Security Protection Code:

$$UID\|Esk(SEQ1\|Dkey\|Policy)\|Hash(Hash(Key\|Pwd)\|SEQ1) \quad (3)$$

$$sk = Hash(UID\|Key\|Pwd\|SEQ1) \quad (4)$$

Where $Dkey$ is the encryption key of document which is encrypted by session key: $sk.SEQ1 = SEQ + 1$, and $Policy$ is the document's protection policy for the user. The Security Protection Code validates the message after receiving it. Then it computes the sk and decrypts the encryption key: $Dkey$ and security policy: $Policy$. The Security Protection code can decrypt the document with the $Dkey$ and then allow the user access the document.

3 Security Analysis

The existing security Portable Document Security Device only stores the encrypted document and does not take the security protection code. In this solution, the protected document can be protected not only in the computer installed document security system but also in those without document security system because the document is accompanied with the Security Protection Code.

The document can also be protected by the Portable Document Security Device during it is transferred from one computer to the other computer since those steal the Portable Document Security Device can not access the document without the access password.

A Secure Validation Protocol is used to guarantee the validation process security which avoids the document key to be stolen when user accesses the document.

4 Application Case

One embodiment of Portable Document Security Device is online mode shown in Fig.1. The device's internal structure is shown in Fig. 2. The module of the portable document leakage protection system is shown in Fig3. The Security Protection Code uses the secure validation protocol to get the document key and security policy from the Document Security Sever.

The other embodiment of Portable Document Security Device is offline mode when the target computer can not access the Document Security Server. The device's

internal structure is shown in Fig. 2. In offline mode, the protected document should be encrypted with *Dkey*, and the access password and security policy are set before the document is transferred via the Document Security Device. Then the document is appended to an executable protection code and makes a portable security document. Finally, The Document encryption key and security policy are stored in the security area of the Portable Document Security Device and the document is copied to the data area of that.

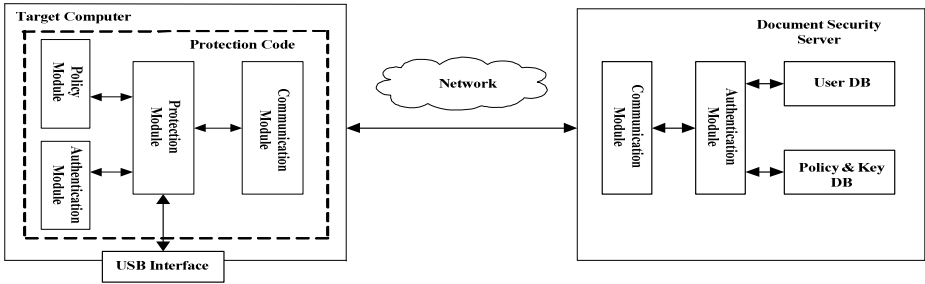


Fig. 3. Schematic Diagram of Mobile Document Protection System

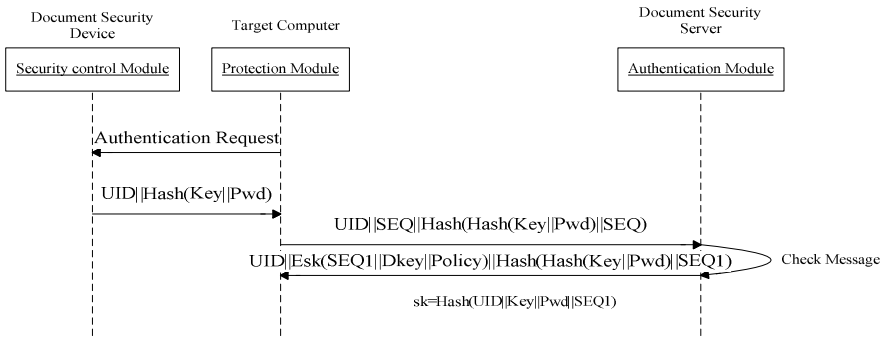


Fig. 4. Flow Diagram of Mobile Document Security Protection

5 Summary

This article presents a new solution of mobile and portable electronically published materials protection which using function area and algorithm to ensure the mobile electronically published materials security and secure authentication protocols to protect communication between data in electronically published materials and document server, on condition that no security system installed on the target computer, the theft of mobile electronically published materials, and key stolen when user access to the documents etc.

The solution also could be used for network-based information protection system and host-based information protection system.

Acknowledgement. This work is supported by National Natural Science Foundation of China (Grant Nos. 60873191, 60903152, 61003286, 60821001) and the Fundamental Research Funds for the Central Universities (Grant Nos. BUPT2011YB01, BUPT2011RC0505).

References

1. Papadimitriou, P., Garcia-Molina, H.: Data Leakage Detection. *IEEE Transactions on Knowledge and Data Engineering* 1, P1–1 (2010)
2. Wikipedia. Data Loss Prevention (2009), <http://en.wikipedia.org/wiki/datalossprevention>
3. Yoshihama, S., Mishina, T., Matsumoto, T.: Web-based Data Leakage Prevention
4. Borders, K., Prakash, A.: Quantifying information leaks in outbound web trace. In: *IEEE Symposium on Security & Privacy* (2009)
5. Microsoft Technet. Protecting Data by Using EFS to Encrypt Hard Drive (EB/OL), http://www.microsoft.com/technet/security/smallbusiness/topics/cryptographyetc/protext_data_efs.aspx
6. Huang, C.-M., Hsu, T.-H., Hsu, M.-F.: Network-aware P2P File Sharing over the Wireless Mobile Networks. *IEEE Journal On Selected Areas In Communications* 25(1), 204–210 (2007)
7. Claudio, E., Bujari, P.A., Cervi, E.: P2P File Sharing on Mobile Phones: Design and Implementation of a Prototype. *IEEE*, 136–140 (2009)
8. Noponen, S., Karppinen, K.: Information Security of Remote File Transfers with Mobile Devices. In: *Annual IEEE International Computer Software and Applications Conference*, pp. 973–978 (2008)
9. Whitman, M.E., Mattord, H.J.: *Information Security Principles*. Tsinghua University Press, Beijing (2006)
10. Japan Network Security Association. Information Security Incident Survey Report ver.1.0, <http://www.jnsa.org/result/index.html>

Research on OCR Post-processing Applications for Handwritten Recognition Based on Analysis of Scientific Materials

Zhijuan Hu¹, Jie Lin², and Lu Wu³

¹ Room 3022, 17th Building, NO.4800, Caoan Road, Jiading District, Shanghai, China
huzhj2008@yahoo.cn

² Room 506, YunChou Building, NO.1239, SiPing Road, Yangpu District, Shanghai, China
jielinfd@163.com

³ Room 918, NO.95, West Beijing Road, Jingan District
wulu@fangdi.com.cn

Abstract. This paper studied the application of OCR post-processing techniques in Real estate transactions registration and proposed a dictionary-based post-processing method. This paper introduced briefly the design of database and post-processing program of this system. Average accuracy rate was enhanced largely compared to that of pretreatment when the system conducted models test. The experimental results showed that this model was very practical, and can significantly improve the recognition accuracy rate, which verified the validity of the approach.

Keywords: OCR, Post-processing, Handwritten recognition.

1 Introduction

In recent years, OCR study for Chinese character recognition has made great progress. At the same time, many OCR software systems have been commercialized successfully to market and achieved a great deal of economic and social benefits. However, for Chinese text recognition, during to its complicated structure and considerable variability in written, character recognition rate is subject to certain restrictions. In particular, for offline handwritten Chinese characters, OCR recognition rate is not good enough, some good OCR software generally keep accuracy rates of about 50-60%. At present, a considerable part of the key information in the registrations of real estate transactions needs to be identified and extracted from the offline handwritten, it is of great significance to improve the recognition rate of the text by verifying and correcting through OCR post-processing techniques which based on character recognition and integrated professional fields knowledge, probability statistics and statistical language model.

2 OCR Post-processing Techniques

OCR[1] post-processing method is by analyzing the syntax, semantics and phrase of OCR recognition pretreatment results in which every single character may be

represented by several candidates through using certain language and knowledge models, in order to rectify some incidental mistakes and finally to realize the purpose of improve recognition accuracy rate. A common goal of OCR post-processing systems [2] is to ensure that the words or sentences generated by corrections to the OCR output are correct in the sense that they belong to the language of the task and the specialty. The key issue of post-processing is how to use context information to determine a plausible word from multiple candidate word as a final result to be outputted.

Most widely used OCR post-processing method [3] are those based on probability and Statistical models, based on dictionary and mixed method. In terms of specific implementation technology, probability and statistical-based models can be classified into two categories: Hidden Markov Method and n-gram methods (especially Bi-gram and Tri-gram). A hidden Markov model (HMM) [4] is a statistical model in which the system being modeled is assumed to be a Markov process with unobserved state. An n-gram [5] model models sequences, notably natural languages, using the statistical properties of n-grams. N-gram models are widely used in statistical natural language processing. Bigrams or digrams are groups of two written letters, two syllables, or two words, and are very commonly used as the basis for simple statistical analysis of text. They are used in one of the most successful language models for speech recognition [6]. They are a special case of N-gram. Trigrams are a special case of the N-gram, where N is 3. They are often used in natural language processing [7] for doing statistical analysis of texts.

The dictionary-based post-processing method is constituted by two main steps: the first one is to choose candidate characters; secondly, calculate the similarity between the candidate and the terms in the dictionary, and output the most similar terms as plausible results. This paper adopted a dictionary-based post-processing method to recognize and distinguish key information in original property files which were scanned in daily registration in every district of Shanghai Real Estate Trading Center. By saving recognition results, the database can be enriched. For clerks they can also compare and identify the content while entering data manually, hence, improving the accuracy further.

3 OCR Post-processing System

The post-processing system, which is a combination of post-processing program and DBMS, is responsible for processing pre-results. The system will offer post-processing results to the user after retrieving the dictionary database by post-processing program. DBMS is maintained by DBA is a less important part in this whole system. Since in this system we adopted dictionary based method, the design of dictionary is also an important component of the system. We will introduce the two important parts: Dictionary database design and post-processing program in the following.

4 Dictionary Database Design

A key problem of dictionary-based post-processing method is how to build Chinese terms database. The database should meet some requirements. First, it should

performance perfect term storage and maintenance functions; Secondly, it must reflect the frequency of words being used; Thirdly, it should help to improve the search speed as much as possible, only by this way, it will facilitate post-processing program. For different industries, the content of the professional entries in the dictionary is changing greatly.

This paper conducted a study in Real estate industry. Accordingly every term in the dictionary contain name of the term, its type and also its used frequency. We also group the dictionary by type so that when executing similarity calculation, the program will search terms of a specific type which is known already. In this way, recognition accuracy rate can be enhanced by avoiding the confusion of different types which is not the same as the given one.

5 OCR Post-processing Model

1. Define a String: $S=S_1+S_2+\dots+S_m$,

Where S_i ($i=1\dots m$; m represents the length of the string) is the characters to be identified. For each S_i there are several candidate characters which are denoted as X_{ij} . This definition can be described as following:

S_1	S_2	S_3	\dots	S_m
(λ_{11}, X_{11})	(λ_{21}, X_{21})	(λ_{31}, X_{31})	\dots	(λ_{m1}, X_{m1})
(λ_{12}, X_{12})	(λ_{22}, X_{22})	(λ_{32}, X_{32})	\dots	(λ_{m2}, X_{m2})
\vdots	\vdots	\vdots	\dots	\vdots
(λ_{1n}, X_{1n})	(λ_{2n}, X_{2n})	(λ_{3n}, X_{3n})	\dots	(λ_{mn}, X_{mn})

Where: X_{ij} is candidate word j for S_i ; λ_{ij} is the similarity degree of candidate word j for S_i .

2. Set s string $W= X_{11}+ X_{21} +X_{31} \dots +X_{m1}$;

Where we get the first candidate for every S_i , that is those have the most similarity, and form a string. Then we search in the dictionary to find whether there a same string, if there is one, output it as the most possible results.

3. if there is none term which is the same as string W , then search all the terms in the database for those contain at least one of the first candidates, and compose entries $Record=\{T_1, T_2, T_3, \dots, T_L\}$ (where L is the number of eligible terms). Then introduce a variable $TValue$.

$$\text{Set } TValue = \sum_{i=1}^m \sum_{j=1}^n \lambda_{ij}$$

Where n is the length of every term; When the character in the term is the same as the candidate word, λ_{ij} is the similarity degree of candidate word j for S_i ; When the character in the term is different from the candidate word, set $\lambda_{ij}=0$.

4. For every term $T_k(k=1\dots L)$, calculate corresponding the value of $TValue$, order by value and then output several front T_k , which has relatively bigger $TValue$ value, as temporary results.

The prerequisite of above way to select record is that at least one of the first candidate word is the correct final results. If all of $X_{11}, X_{21}, X_{31} \dots, X_{m1}$ are wrong,

two situation will happen as following:(1)There are temporary results, however, they are wrong. When this happens, the corresponding TValue of terms are relatively low. So when the biggest TValue is very low, there is a need for reselect terms. (2)There is no term at all, the searching results are empty.

We adopted the same way to handle those two instances. Firstly, search in the database for all terms that contain at least one of the candidate words, not the first ones, but all candidates; secondly, calculate corresponding TValue for every selected terms; thirdly, output those terms with the highest values.

The biggest disadvantage of this mean is large computation; therefore, it would be adopted on when those two situations happen.

6 Experiment and Analysis

In this paper, we recognized four common templates, each contain about 100 proofs. Therefore, this experiment is universality in some degree.

1. Experiment result:

Table 1.

templates	Total number	Pretreatment accuracy rate	The first temporary result accuracy rate	The second temporary result accuracy rate	The third temporary result accuracy rate
Template 1	102	35.33%	65.55%	68.02%	70.57%
Template 2	90	31.43%	63.06%	69.76%	70.03%
Template 3	95	39.26%	67.57%	71.79%	73.34%
Template 4	105	27.75%	58.92%	62.34%	65.89%
Average:		33.44%	63.78%	67.98%	69.96%

2. Analysis

- (1) This approach has very high accuracy rate, which could enhance accuracy rate by nearly 30 percent. Two main reasons contribute to this success. One is that we give the most similar terms instead of the exact ones; the other one is the correct result is in the database without any exception. In this way, we limit search range, therefore, we improve accuracy rate greatly.
- (2) A higher pretreatment accuracy rate will lead to a higher post-processing rate. This is because post-processing program use pretreatment results as query conditions to search in the database. Consequently, only high pretreatment accuracy rate can improve query results.

7 Conclusion

In conclusion, this paper adopted word-based language model to realize post-processing program. Experiment results show that this program is effective in enhancing recognition accuracy rate. However, since this approach is an application in specific industry, some limitations still exist, and further study is needed. At the same time, post-processing resulted is closely related with pretreatment results, there is a lot work to be done in increasing pretreatment results.

Acknowledgement. The authors would like to thank the fund: Application of OCR techniques in Real estate transactions registration (FG2009019).

References

1. http://en.wikipedia.org/wiki/Optical_character_recognition
2. Perez-Cortes, J.C., Amengual, J.-C., Arlandis, J., Llobet, R.: Stochastic error-correcting parsing for OCR post-processing. In: Proceedings of the International Conference on Pattern Recognition, pp. 4405–4408 (2000)
3. Long, C., Zhuang, L., Zhu, X.-y.: A Post-processing Approach for Handwritten Chinese Address Recognition. *Journal Of Chinese Information Processing* 20(6), 69–74 (2006)
4. Wang, X., Yang, Y., Xie, B.: HMM-based off-line handwritten Chinese characters recognition using Krawtchouk moments. In: 6th World Congress on Intelligent Control and Automation, WCICA 2006, pp. 10068–10072 (2006)
5. http://en.wikipedia.org/wiki/N-gram#n-gram_models
6. Collins, M.: A new statistical parser based on bigram lexical dependencies. In: Proceedings of the 34th Annual Meeting of the Association of Computational Linguistics, Santa Cruz, CA, pp. 184–191 (1996)
7. Manning, C.D., Schütze, H.: *Foundations of Statistical Natural Language Processing*. MIT Press, Cambridge (1999)

Research on Predicting Tool Wear Based on the BP Network

Ping Jiang¹ and ZhiPing Deng²

¹ School of Mechanical Engineering & Automation, Xinhua University,
Cheng Du, Si Chuan, China
jp_529@yahoo.com.cn

² School of Mechanical Engineering & Automation, Xinhua University,
Cheng Du, Si Chuan, China
zhipingdeng@mail.xhu.edu.cn

Abstract. Established 3D turning model by the solid works, based on DEFORM-3D software for turning process simulation with intelligent materials, obtained the data in the process of turning the intelligent materials, curve fitting the tools wear by BP neural network, and obtained the prediction curve of tool wear based on the BP network.

Keywords: Intelligent Materials, turning simulation, BP neural network, tool wear.

1 Introduction

Intelligent materials is a kind of material that can through the system to response function and effect to event, place and environment. intelligent material is a new material and different from the traditional structure of materials and functional materials, it blurs the material concept both bounds and realizes the structure and function diversification. It is a gradual rise up and will become mainstream material science branches soon.

In intelligent materials cutting process, because intelligent materials reacts sensitively to the external conditions, some subtle change of external conditions can cause intelligent materials reaction. so, it becomes difficult to control the high cutting quality. But, with the development of society, machinery industry for the accuracy requirement of turning becomes more and more high, in order to adapt to the social development and Improve turning quality, we must pay more attention to every subtle factors which will influence turning quality, reducing bad influence because of these factors, so as to improve the quality of turning. At present, people research turning mechanism mainly are cutting angle, amount of cutting, cutting speed, cutting force and cutting method in the process of cutting, and have made great achievements, greatly improving the cutting quality. For example, the paper *Study on Diameter Errors of Slender Bar Turning based on Neural Network* have predicted size errors in turning processing by change amount of cutting, cutting speed and cutting depth[1], finally greatly improves turning quality; the paper *Mechanical Analysis of Machining*

Error in Turning Slender Shafts by Reversible Turning Techniques and the paper *Design of Slender Shaft Turning with Two Tools Machining*, both improve the cutting quality through changing the processing technology[2]. But, the present studies rarely have aimed at tool wear in the process of intelligent materials cutting to improve the cutting quality.

In intelligent materials cutting process, tool wear has always been a problem that doesn't allow ignoring; it can make a significant impact on cutting quality, if we can solve the processing error that because of tool wear, we can greatly improve the cutting quality. This article established 3D turning model by the solid works, based on DEFORM-3D software for turning process simulation, obtained the tool wear in the process of turning, curve fitted the data by BP neural network, obtained the prediction curve of tool wear, according to the forecast graph we got a precise tool wear compensation, thus greatly improved the cutting quality.

2 DEFORM Modeling

DEFORM-3D is a set of based on process simulation system, specifically designed for analysis of various kinds of metal forming process, it provides valuable process analysis data for the three-dimensional flow, DEFORM-3D powerful simulation engine can analyze metal forming process multiple connection object coupling large deformation and thermal characteristic, system integrations self trigger automatic grid redrawing generator, generating optimized grid system, the typical DEFORM-3D applications include forging, extrusion, heading head, rolling, free forging, bending and other forming machining method[3]. Due to DEFORM software cannot directly establish a 3d turning model, this paper establishes a 3d turning model by solid works, then put the model in importing DEFORM software, this article uses the turning simulation parameters such as table1[4]. WC-Co cermet is a kind of tool materials of good performance. Especially, the ultra-fine WC-Co has both high strength and high hardness. Using the WC powder and bonding metals into the WC sintering and cemented carbide, it can be widely used in making special items, tiny bits, print needles and other precision abrasive. In addition, WC in some catalytic reaction also has peculiar catalytic activity. Determined WC-Co cermet for the cutting tool and AISI-1045 material for the work piece, established three-dimensional models as shows in Fig. 1[5].

Table 1. Parameters of cutting processing and cutter's installation

Tool cutting edge angle	90
Rake angle	20
Clearance angle	10
Tool cutting edge inclination	3
Cutting speed	400mm/min
Cutting depth	0.5mm
Feed Rates	0.3mm/r
Work piece diameter	50mm

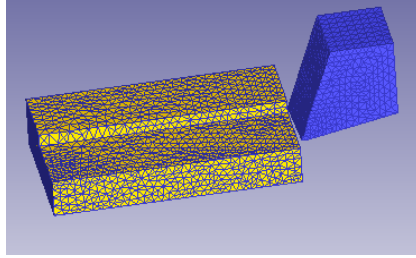


Fig. 1. Turning model gridded

3 The Simulation Results

After the completion of the program, run into post-processing, tool wear amount shows in Fig. 2:

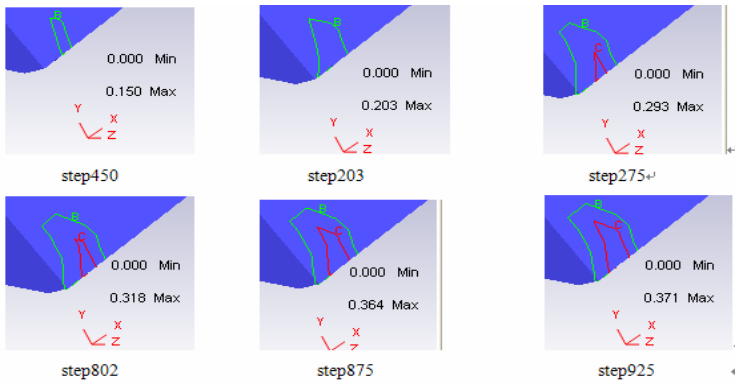


Fig. 2. Tool wear under different time

We can know from Fig. 2, tool wear is increasing as time increases. In step45 when wear position limits in a smaller range, but, with the cutting going, tool wear is diffusion around and initial tool wear is deepening[6]. The whole simulation tool wear changes as shows in Table 2:

Table 2. Tool wear during simulation(mm)

Step	50	100	150	200	250	300	350	400	450	500
Tool wear	0	0.025 2	0.031 3	0.062 0	0.079 3	0.092 9	0.101	0.129	0.150	0.163
Step	550	600	650	700	750	800	850	900	950	1000
Tool wear	0.17 8	0.234	0.253	0.274	0.304	0.318	0.355	0.367	0.383	0.391
Step	1050	1100	1150	1200	1250	1300	1350	1400		
Tool wear	0.40 8	0.458	0.493	0.526	0.529	0.543	0.548	0.548		

4 Establish the BP Network and Curve Fitting

In 1974, P. Werbos first put a learning algorithm that suit of multilayer network in his doctoral thesis, but this algorithm were not enough attention and extensive application, until the 1980s, the book *Parallel Distributed Processing* published, the algorithm was applied to neural network, just to be the most famous multi-layer network learning algorithm-BP algorithm, thus neural network trained by this algorithm called BP neural network [7].

BP neural model shows as Fig. 3:

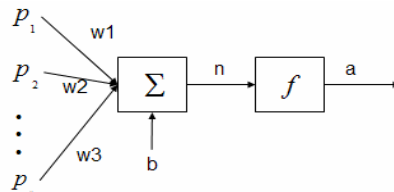


Fig. 3. The general model of BP neuron

We often encounter some complex nonlinear system in engineering, these systems have complex state equation, and it is difficult to use mathematical methods to accurate modeling. In this situation, we can build the BP neural network, this method of nonlinear system to express the unknown system as a darkroom, first with the input/output data of system trains the BP neural network, the network can express a unknown function, and then you can use the trained BP neural network prediction system output.

Based on experimental data, set *step* for input, *tool wear* as output, established a BP network to train these inputs and outputs, and then use trained function to predict tool wear. Based on this experiment that the method process of nonlinear function fitting by BP network can be divided into the BP network construction, the BP neural network training and the BP neural network forecast three steps, as shows in Fig. 4 shows:

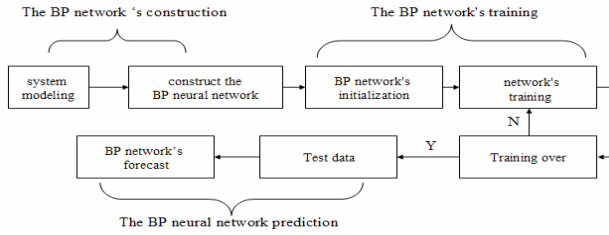


Fig. 4. Algorithm processes

During the training, TF uses *tansig* function, BTF uses *traingdx* function and BTF uses *learnqdm* function. Through comparing the neural network model output and the actual expected output, we can know both of data are very close, the simulation accuracy is satisfactory. Effect screenshots as shows in Fig. 5

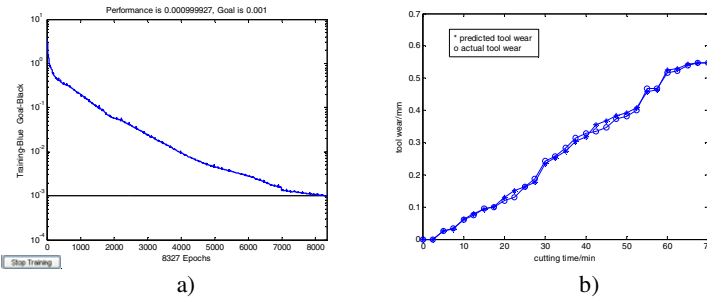


Fig. 5. Effect screenshots a) Training error's performance curve of The BP neural network b) The forecast result and the actual inspection

5 Summary

Through this simulation we can see, in WC-Co material cutting process, cutting tools can achieve maximum wear such as 0.1 mm level, and tool wear is increasing as time increases, it makes a bad impact on cutting quality. This article through the finite element simulation, obtained the data of tool wear during processing, predicted tool wear by BP neural network with intelligent materials, provided precise error compensation caused by tool wear for cutter, and improved the cutting quality.

References

1. Han, R., Cui, B.: Study on Diameter Errors of Slender Bar Turning Based on Neural Network. *Tool Engineering* 5 (42), 9–11 (2008)
2. Dai, H., Deng, Z.: Design of Slender Shaft Turning With Two Tools Machining. *Machine Tool and Hydraulics* 6, 88–92 (2010)
3. Li, C., Wang, X., et al.: *Finite Element Analysis Example Guide Tutorial of DEFORM5.03 Metal Forming*. China Machine Press, BJ (2007)

4. Deng, Z.: Mechanical Manufacturing Technology Foundation. Southwest Jiaotong University Press, CD (2008)
5. Wu, W., Huang, M.: Finite Element Simulation of High-speed Turning Using Deform-3D. Modern Manufacturing Engineering 11, 91–94 (2009)
6. Deng, Z., Sun, D., Cao, K., Xie, X.: Finite Element Analyses of Tool Wear in High-speed Cutting. Tool Engineering 44, 22–25 (2010)
7. Shi, F., Wang, X., Yu, L., Li, Y.: Mat lab neural network's case analysis. Beijing Aerospace University Press, BJ (2010)

Building the Internet of Things Using a Mobile RFID Security Protocol Based on Information Technology

Tao Yan and Qiaoyan Wen

State Key Laboratory of Networking and Switching Technology,
BUPT, Beijing, 100876, China
yantao1982@hotmail.com, wqy@bupt.edu.cn

Abstract. The Internet of Things as an emerging global, information service architecture facilitating the exchange of goods in global supply chain networks is developing on the technical basis of the present Domain Name System. In this paper, we assume that all the communication channels among Tag, Reader, and Server are insecure. We implement a TTP (Trust-Third-Party) based key management protocol to construct a secure session key among the tag, reader and server to construct a security Mobile RFID (Radio Frequency Identification) service based on the IOT(Internet of Things). The proposed idea is security and efficiency and supply three advantages for a secure IOT architecture.

Keywords: The Internet of Things, RFID, Mobile RFID, RFID Security, Key Management Protocol, Trust Third Party.

1 Introduction

The Internet of Things (IOT) is a technological phenomenon originating from innovative developments and concepts in information and communication technology associated with: 1) Ubiquitous Communication/Connectivity, 2) Pervasive Computing and Ambient Intelligence.

These concepts have a strong impact on the development of the IOT [1]. Ubiquitous Communication means the general ability of objects to communicate (anywhere and anytime). Pervasive Computing means the enhancement of objects with processing power (the environment around us becomes the computer). Ambient Intelligence means the capability of objects to register changes in the physical environment and thus actively interact in a process. Typically, objects fulfilling these requirements are called “smart objects” [2]. Hence, the IOT is defined as the ability of smart objects to communicate among each other and building networks of things, the Internet of Things.

The IOT architecture is technically based on data communication tool, primarily Radio Frequency Identification (RFID) tagged items. A smart mobile phone with a RFID reader can provide Mobile RFID (MRFID) services [3] based on RFID tagged objects. All these IOT services need to be carefully designed so that they can be

intuitively used by humans, devices and things, to mash up services, to federate new services along with others and overcome the future technological challenges.

This paper introduces a mobile RFID Architectural for IOT. Chapter 2 introduces related work. Chapter 3 describes the mobile RFID network. In Chapter 4 we describe TTP (Trust-Third-Party) based secure mobile RFID system and Chapter 5 proposed our key management protocol. We analyze security and privacy problems of our scheme in efficiency and security in the chapter 6 and conclude in Chapter 7.

2 Related Work

Despite vast literatures have been reviewed on several occasions and new secure communication mechanisms have been proposed [4,5,6,7,8,9], none of which considered the security and privacy issues of M-RFID as a whole system. This scheme only considered the privacy of readers and it would greatly increase the burden on system for the practical application if key agreement occurred for each tag access.

3 Mobile RFID Network

Besides these privacy threats, we introduce a mobile RFID network consists of a tag, a mobile RFID reader and network servers which will be more security.

RFID Tag. A tag receives a query from a reader and transmits EPC (Electronic Product Code), unique information of an object using RF signals. The tag is composed of an antenna for a RF communication and the microchip which stores information of objects and implements operation function. The tag is divided into a passive tag and an active tag in power supply method.

Mobile RFID Reader. In mobile RFID systems, the mobile device plays a role as a reader of the RFID systems. The mobile reader is the mobile including reader of the RFID systems. It transmits a query to a tag and identifies the received information from the tag. In some case, the mobile reader rewrites new information to some tag. The mobile reader has a high computation ability and a large storage capacity unlike the reader of previous RFID systems.

Network Server [10,11]. ONS(Object Name Service) server : When a base-station requests information of URL for EPCs, the server informs the URL(Uniform Resource Location) of server which manages information related to EPC to the base station (similarity DNS (Domain Name Server)).

OIS (Object Information Service) server: The server stores the information related to EPC of tags. When the base station requests the information of the tags, the server sends it to the base station.

4 TTP Based Secure Mobile RFID System

The architecture for TTP (Trust-Third-Party) based secure mobile RFID system. When a mobile RFID user possesses a RFID tagged product, TTP enables the owner to control his backend information connected with the tag such as product information, distribution information, owner's personal information, and so on. TTP ensures the owner to communicate with the tag and application server in secure channel through the key agreement among the tag, reader and server.

In our system, a consumer reads the tag from the tagged product with his or her mobile RFID reader. The consumer then browses the product-related information from the application server and purchases the product using one of payment methods. Then the consumer becomes the tag owner. Next, the security and privacy protection will be provided by TTP. TTP requests the owner defined privacy profile such as privacy protection level used in [8] to access the application server. The TTP server receives and forwards the owner's privacy protection policy for his application service to the application server and distributes certificates to the owner and server, respectively. The tag, reader and server then set up the key for secure transmission. Anyone requesting information associated with this tag can browse all information provided by the application server in secure channel if the requestor is the owner, but otherwise, the requestor only has access to a limited amount or no information according to the limits established by the owner in insecure channel. Step (1) - (6) in Figure 1 depicts the process. In the following section we will elaborate on the distribution of certificates and key agreement.

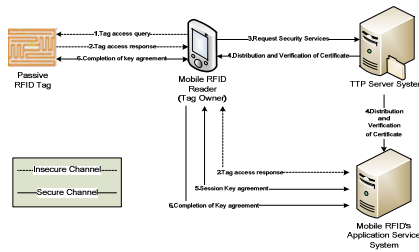


Fig. 1. Data transmission and filtering

5 Proposed Key Management Protocol

In our scheme, a trusted third party server is introduced as a key distribution authority to solve the privacy disclosure problem for mobile RFID-enabled devices.

Preliminary Notations. We use the same way in generation and distribution of certificates as [9]. We assume each tag, reader and server is hard coded a unique identity ID_T , ID_R and ID_S . An one-way hash function $H(\)$ and a stream cipher algorithm are utilized among the tag, reader, server and TTP. We assume the tag has the computation power to do hash function and stream cipher encryption. To realize the anonymity of reader, the protocol is based on the elliptic curve cryptosystem [12].

We assume the reader has the computation power to do elliptic curve cryptography algorithm. Another two reasonable assumptions are that the application server shares symmetric key k_{ST} and k_{TPS} with the tag and TTP, respectively.

The symbol $E_k(M)$ denotes the encryption of message M using key $Cert(\)$ denotes a certificate. The protocol is divided into three parts, key initialization, key agreement and key update. The process of proposed scheme is shown in Figure 1.

Key Initialization. Once label a RFID tag on certain product, the tag ID_T will be bundled with an application server ID_S . The tag and server will set up shared symmetric key k_{ST} . The application server will provide default privacy protection. The TTP server set up shared symmetric key k_{TPS} with all RFID application servers. To avoid tag tracking, it is required to establish an ID flag, denoted by ID_{T-FLAG} , which will be used to show whether the corresponding ID_T is possessed by fixed users. If the tagged product isn't belong to private users, ID_{T-FLAG} will be closed. That is, the identity of the tag ID_T remains unchanged, any mobile RFID user obtain the same information according to the default privacy protection policy using the fixed ID_T to access the information server. The process is:

Step 1: *reader* \rightarrow *tag* : Access query.

Step 2: *tag* \rightarrow *reader* \rightarrow *server* : $ID_T || ID_S || ID_{T-FLAG} || E_{k_{ST}}(T_n)$.

Where the symbol $||$ denotes concatenation and the value of ID_{T-FLAG} is False. T_n is a random number generated by tag to protect its identity at the next steps.

Key Agreement. The user purchases the product using one of payment methods and requests security services to TTP server.

Step 3: *reader* \rightarrow *TTP* : $E_{P_{k_{TP}}}(ID_T || ID_S || ID_{T-FLAG} || ID_R || k_R || t_i)$ Reader applies elliptic curve encryption with the public key

$$P_{k_{TP}} = i_1 B_1 + i_2 B_2 \quad (1)$$

to protect its own identification ID_R , its secret key k_R , the current timestamp t_i to TTP server. Where (i_1, i_2) is the sect key $s_{k_{TP}}$ of TTP and randomly selected from the interval $[1, n-1]$.

Step 4: *TTP* \rightarrow *reader* : $E_{k_R}(R_C || Cert(R_C) || r)$

$$TTP \rightarrow server : E_{k_{TPS}} (ID_T \| ID_S \| P_C \| Cert(P_C) \| r)$$

$$\text{Step 5: } reader \rightarrow server : E_{p_{ks}} (P_i \| Cert(P_i) \| r \| n_1 G \| t_{r_2})$$

$server \rightarrow reader : P_i \| n_2 G \| E_{k_{auth}}(t_{r_2}) \| E_{k_{ST}}(k_{auth} \| Cert(P_i) \| T_n)$ Once reader verified the certificate of

$$R_C = (c_1, c_2), \quad (2)$$

a pseudonym

$$P_i = (p_1, p_2) \quad (3)$$

of reader is generated for the usage of future communication. Reader compute

$$Cert(P_i) = (e'', S_{e_1''), S_{e_2''}), \quad (4)$$

where

$$e'' = H(P_i, R_S), S_{e_1''} = d_1 + c_1 e'' \pmod{n},$$

$$S_{e_2''} = d_2 + c_2 e'' \pmod{n}, R_S = d_1 B_1 + d_2 B_2, \quad (5)$$

d_1 and d_2 is randomly selected from the interval $[1, n-1]$.

$$\text{Step 6: } reader \rightarrow tag : E_{k_{auth}} (Cert(P_i)) \| E_{K_{ST}} (k_{auth} \| Cert(P_i) \| T_n)$$

$$tag \rightarrow reader \rightarrow server : ID_T \| ID_S \| ID_{T-FLAG} \| E_{k_{ST}} (T_n \| Cert(P_i)) \| k_{auth} (Cert(P_i))$$

Key Update. The session key k_{auth} update is very simple, repeat Step 5 and Step 6, reader, server and tag will renegotiate the session key.

Security Analysis

In this section, we analyze our scheme as follow:

Session Key Security. Attackers can't know the message content, because every message is enciphered by session key k_{auth} . Based on the *ECDLP* problem [12],

the session key $k_{auth} = n_1 n_2 G$ cannot be derived without knowing the value n_1 and n_2 .

Impersonation Attack. Attacker can intercept the transmitted message under the wireless communication environment and attend to impersonate any communication party in a normal operation. However, unknowing the secret key k_{ST} , k_R and k_{TPS} , attacker can't obtain any information from eavesdropped messages. Furthermore,

based on the value ID_{T-FLAG} stored in server, attacker can't engage the Step 3 to apply for the key pair (P_C, R_C) and corresponding certificates. Thus, the impersonation attack can be prevented.

Forward Security. The benefit of forward security is to protect the new session key even if the current session key is leaked, the backward security is just the opposite. Since the session key k_{auth} is dynamic and the key is generated by the random selection of n_1 and n_2 , the attacker can't derive the previous or new session key from the current session key.

6 Conclusion

A mobile RFID system is a new service using a mobile device like RFID reader and wireless internet. In this paper, we propose a scheme that protects personal privacy. This paper introduces a mobile RFID Architectural for IOT and introduces a key management protocol for secure mobile RFID service to protect data privacy against the threats of replay attack, impersonation attack and provide excellent privacy protection features forward and backward security at the same time. In conclusion, the proposed scheme can offer data security enhancement and privacy protection capability at reader side under an insecure and wireless mobile RFID system.

Acknowledgments. This work is supported by National Natural Science Foundation of China (Grant Nos. 60873191, 60903152, 61003286, 60821001).

References

1. Kim, H., Kim, Y.: An Early Binding Fast Handover for High-Speed Mobile Nodes on MIPv6 over Connectionless Packet Radio Link. In: Proc. 7th ACIS International Conference on Software Engineering, Artificial Intelligence, Networking, and Parallel/Distributed Computing (SNPD 2006), pp. 237–242 (2006)
2. Information Society Technologies Advisory Group (ISTAG): Revising Europe's ICT Strategy, Report from the Information Society Technologies Advisory Group, ISTAG (2009)
3. Seidler, C.: RFID Opportunities for mobile telecommunication services. ITU-T Lighthouse Technical Paper (2005)
4. Chang, G.C.: A Feasible security mechanism for low cost RFID tags. In: International Conference on Mobile Business (ICMB 2005), pp. 675–677 (2005)
5. Osaka, K., Takagi, T., Yamazaki, K.: An efficient and secure RFID security method with ownership transfer. In: International Conference on Computational Intelligence and Security, vol. 2, pp. 1090–1095 (2006)
6. Kim, H.W., Lim, S.Y., Lee, H.J.: Symmetric encryption in RFID authentication protocol for strong location privacy and forward-security. In: International Conference on Hybrid Information Technology, vol. 2, pp. 718–723 (2006)

7. Yang, M.H., Wu, J.S., Chen, S.J.: Protect mobile RFID location privacy using dynamic identity. In: 7th IEEE International Conference on Cognitive Informatics (ICCI 2008), pp. 366–374 (2008)
8. Park, N., Won, D.: Dynamic privacy protection for mobile RFID service. In: RFID Security: Techniques, Protocols and System-on-Chip Design, pp. 229–254. Springer, US (2009)
9. Lo, N.W., Yeh, K.H., Yeun, C.Y.: New mutual agreement protocol to secure mobile RFID-enabled devices. Information Security Technical Report (2008)
10. EPCglobal Inc: EPCglobal Network: Overview of Design, Benefits, and Security (2004)
11. EPCglobal Inc: EPCglobal Object Name Service (ONS) 1.0 (2005)
12. Miller, V.S.: Use of elliptic curves in cryptography. In: Williams, H.C. (ed.) CRYPTO 1985. LNCS, vol. 218, pp. 417–426. Springer, Heidelberg (1986)

Study on Linear Regression Prediction Model of County Highway Passenger Transport Volume

ShuangYing Xu, Lei Zhang, and Jian Ma

School of automobile, Chang'an University, Shaanxi, Xi'an 710064
xsying@chd.edu.cn, zhanglei@chd.edu.cn

Abstract. County highway passenger transport occupied an important position in China highway transportation system. Correct forecast growth of county highway passenger transport volume was the key for county passenger planning and optimizing transport resource allocation. This paper analyzed the influence factors of county highway passenger transport volume and constructed eight regional economic and social development indexes as explanatory variables of passenger transport volume linear model. The model was calibrated by using specific county data. Linear simulation showed that the relationship between county highway passenger transport volume and explanatory variables was quantified, formation characteristics of the calibration data sources of the county highway passenger transport volume was revealed and the future years of highway passenger transport volume could be predicted.

Keywords: Highway passenger transport volume, Explanatory variables, Demand forecast linear regression prediction model.

1 Introduction

Correct forecast growth of county highway passenger transport volume is the key for county passenger planning and optimizing transport resource allocation. This paper analyzed the influencing factors of county highway passenger transport volume and established the linear regression model of passenger transport volume using the practical county history data of 12 consecutive years.

2 The Influence Factors of County Highway Passenger Transport Volume

County highway passenger transport volume means the number of passengers by vehicles using the at least one endpoint in county regional in a certain period. How effectively choice of highway passenger transport volume explanatory variables is the key to the analysis and prediction of regional highway passenger transport volume. The explanatory variables selection is based on the correct understanding of the influence factors of highway passenger transport volume growth. Influence factors of

highway passenger transport volume growth regional were studied in many papers. In opinion of HeQing Chen [1], the main influence factors of highway passenger transport volume is the development of social economy, population change, urbanization level and freight rate. DeFeng Bao[2] proposed urban households per capita annual disposable income, annual population, industrial index, the total tourist income, freight rate as explanatory variables of the multivariate linear regression model of highway passenger transport volume and used practical data to demarcate model parameters. He found that annual population, industrial index and total tourist income played significant role on the passenger transport volume, while the other two factors were not significant.

County highway passenger travel is the derivative of county population economic, social activities. County economies of scale and industrial structure reflect the regional economic activity demand on highway passenger travel. The bigger of county economic scale, the secondary and tertiary industries is the more developed and the more highway travel demand is produced. The more of county population and higher disposable income will produce more travel opportunity. Therefore, GDP, eight parameters of the first industrial output, the second industry GDP, the third industry GDP, gross industrial output, residents' per capita income, rural per capita net income and total population were selected as the explanatory variables of county highway passenger transport volume growth.

The counties with different economic structure and economic development will produce different passenger travel industry activity and different passenger travel opportunities derived from population participation in social and cultural activities.

Therefore, counties with different economic social structure and economic activity level will have different economic and social explanatory variables. In this point, passenger transport volume models of specific counties should be calibrated with actual data. The calibrated model will be able to accurately reflect the reasons and characteristics of county passenger transport volume generated with different economic and social development.

3 Linear Regression Prediction Model of County Highway Passenger Transport Volume

Using the mentioned 8 with explanatory variables as independent variables and county passenger transport volume as the dependent variable, the initial multiple linear regression model of county passenger transport volume is as follows:

$$Y = b_0 + \sum_{i=1}^8 b_i x_i \quad (1)$$

where:

Y — county passenger transport volume, unit is person-time.

x_i — the i th explanatory variable of passenger transport volume.

b_i — the coefficient of the i th explanatory variable of passenger transport volume.

A group of successive year historical data of 8 explanatory variables and county passenger transport volume was gain by survey as the data sample to calibrate linear regression model. Multiple regression model intercept traffic and the coefficients of explanatory variables were calculated by the sample data. Then linear equation of the model was obtained. The standard error was calculated to judge matching degree of the equation. Using F statistics, we test whether the role of explanatory variables in passenger transport volume was notable. The coefficients of the explanatory variables recognized as the not significant role in passenger transport volume by t test should be eliminated and only variables played significant role in passenger transport volume would be retained in the model equation.

To gain required linear equation excluding remarkable effect explanatory variables, we could adopt "out not only into" method, i.e. firstly, a regression equation was established including all independent variables, then remarkable independent variables were eliminated one by one, at last, the regression equation only contained independent variables played significant role.

4 Calibration of Regression Equation

As the research object, the county near the regional central cities is Ping Yuan County which lies in the GuanZhong region of ShaanXi province in China with an area of 3081.48 square kilometers. A group of successive year historical data in Ping Yuan County of 8 explanatory variables and county passenger transport volume was gain to calibrate linear regression model. The specific county data was shown in table 1.

All 8 explanatory variables were selected as independent variables, eight variables coefficients calculated by data analysis tool of EXCEL was 0.003941, 0.000528, 0.00644, 0.017157, - 0.20219 0.00012, 0.376079 and 4.461349. Fitting coefficient R^2 was 0.9950 and standard error was 19.6556. That means equation fitting well. Significance $F = 0.002243 < 0.05$, means the coefficient of explanatory variables having significant role in passenger transport volume. The coefficients of explanatory variables appeared minus and the coefficients of explanatory variables the probability values were greater than 0.025. So we could believe that there were certain correlations among explanatory variables, and therefore some variables should be eliminated. The absolute value of explanatory variable x_2 coefficient was smallest and should be eliminated firstly [3]. We used the remaining seven explanatory variables to new regression analysis and obtained equation 2. Equation 2 was test and the explanatory variable should be eliminated which coefficient absolute value was smallest. The process was iterated until all variables in the model are significant. The concrete process was shown in table 2.

So, linear model of county highway passenger transport volume was selected as equation 8. Equation as follow:

$$Y=848.4482+0.010365X_4 \quad (2)$$

Table 1. Highway passenger transport volume and explanatory variables of Ping Yuan County

Year serial number	Passenger transport volume (million person-time)	GDP (million yuan)	Where			Gross industrial output (billion yuan)	Residents ' per capita income (yuan)	Rural per capita net income (yuan)	Year-end total population (million peapole)
			The first industrial	The second industry	The third industry				
1	942	60210	17179	30492	12539	10264	950	517	63.9
2	964	68219	19459	35392	13368	82959	1141	589	64.6
3	995	68795	21004	33708	14083	121513	1295	707	67
4	1054	71974	21675	32236	18063	118900	1476	714	67.6
5	1079	78951	23594	35299	20058	151696	1651	724	68.6
6	1121	96521	27493	43974	25024	190323	1915	782	69.3
7	1191	120253	34762	55044	30483	245545	2411	913	69.9
8	1286	145768	36058	72352	37358	274733	2805	1023	70.2
9	1291	172006	36851	92229	42926	345552	3317	1214	70.5
10	1219	177682	31985	103178	42519	363574	3573	1307	70.7
11	1319	178010	31000	101000	46000	334000	3696	1393	72.2
12	1363	188000	310000	101000	490000	363000	4000	1445	72.7

5 Prediction of Passenger Transport Volume

According to the need of the forecast, 10 years and 20 years later of the statistical year were future features years. The tertiary industry in GDP of the future features years were gain used 3 times exponential smoothing predict and were generated into the equation (2) , and then the passenger transport volume of future features years could be obtained. The specific calculation type as follow:

$$Q_{t+10}=848.4482+0.0010365 \times 96161=1844 \quad (\text{person-times}) \tag{3}$$

$$Q_{t+20}=848.4482+0.0010365 \times 159801=2504 \quad (\text{person-times}) \tag{4}$$

6 Summary

Counties with different economic social structure and economic activity level will have different economic and social explanatory variables. In this point, passenger transport volume models of specific counties should be calibrated with actual data.

The empirical result indicates that:

The calibrated model will be able to accurately reflect the reasons and characteristics of county passenger transport volume generated with different economic and social development.

The calibrated model reveals the forming reasons of highway passenger transport volume and has a good explanatory forecast of the highway passenger transport volume growth.

Table 2. Regression model calibration process table

Item	Intercept	X ₁	X ₂	X ₃	X ₄	X ₅	X ₆	X ₇	X ₈
1									
	Equation 1		R ² =0.9950			Standard error		=19.6556 sig	
F=0.002243									
coefficient	401.3364	0.003941	0.000528	-0.00644	0.017157	-0.00012	-0.20219	0.376079	4.461349
t _i	0.229041	0.531047	0.082469	-1.46278	1.206287	-0.18952	-1.06314	1.226602	0.161859
p-value	0.833563	0.632189	0.939468	0.23971	0.314159	0.861782	0.36571	0.307462	0.881704
2									
	Equation 2		R ² =0.9950			Standard error		=17.0415 sig	
F=0.00019									
coefficient	350.6471	0.004365	-0.00667	0.016993	-0.00011	-0.21206	0.368616	5.344301	
t _i	0.24647	0.938751	-2.27372	1.391693	-0.19941	-1.65554	1.451334	0.242692	
p-value	0.81745	0.401008	0.085376	0.236411	0.851667	0.173156	0.220315	0.82018	
3									
	Equation 3		R ² =0.9950			Standard error		=15.31 sig	
F=1.7E-05									
coefficient	599.6199	0.003597	-0.00657	0.019035	-0.21414	0.38888	1.549804		
t _i	0.978081	1.534025	-2.52978	3.181353	-1.86605	1.858627	0.155566		
p-value	0.372954	0.185607	0.052544	0.024501	0.121026	0.122186	0.882461		
4									
	Equation 4		R ² =0.9949			Standard error		=14.01 sig F=8.17E-07	
F=8.17E-07									
coefficient	694.3391	0.003609	-0.00682	0.019156	-0.20891	0.400065			
t _i	10.60631	1.682519	-3.70705	3.528662	-2.08087	2.225036			
p-value	4.14E-05	0.143459	0.010004	0.012388	0.082635	0.067727			

Table 2. (continued)

5 Equation 5		$R^2=0.9926$	Standard error =15.47 sig F=1.53E-07		
coefficient	781.60 79	-0.00397	0.02463	-0.14458	0.246564
t_i	17.422 45	-4.93057	5.046514	-1.38668	1.416852
p-value	5.05E- 07	0.001693	0.001486	0.208093	0.199458
6 Equation 6		$R^2=0.9906$	Standard error =16.62 sig F=1.9E-08		
coefficient	831.27 1	-0.00413	0.018346		0.03908
t_i	29.133 36	-4.91004	9.584229		0.41643 4
p-value	2.09E- 09	0.001179	1.16E-05		0.68804 1
7 Equation 7		$R^2=0.9904$	Standard error =15.84 Sig F=8.27E-10		
coefficient	842.1016	-0.00393	0.018822		
t_i	75.29291	-5.94403	12.85397		
p-value	6.51E-14	0.000217	4.28E-07		
8 Equation 8		$R^2=0.9906$	Standard error =16.62 Sig F=1.9E-08		
coefficient	848.4482		0.010365		
t_i	36.19484		14.20371		
p-value	6.16E-12		5.9E-08		

References

1. Chen, H.: Economic Metrology. China business press Publications, China (1987)
2. Bao, D., Lu, R.: Inner Mongolia autonomous region passenger forecasting model. Journal of Inner Mongolia on Rural University 28 (2007)
3. Ma, F., Yu, M., Fan, J.: Applied Probability and Statistics (Rudin). Higher Education Press, China (1984)

Some Views of Chinese Construction of Modern Forestry

Yuefen Wang and Yi Li

Northeast Forestry University, Harbin, 150040, Heilongjiang, China
mlbwyf@126.com

Abstract. In this paper, explore the main ideas of the construction of modern forestry to promote the development of Chinese forestry. This paper proposes to establish the dominant position of forestry ecological construction, develop sustainable forestry, set up forestry in the whole society, reform the management system of Forest property and state-owned forest resources, Forest classification management to build Chinese modern forestry.

Keywords: Modern forestry, ecological construction, sustainable forestry, reform.

1 Introduction

The 21st century is Chinese sustainable social and economic development period. It gives the forest more than ever an important role. Since the Party Congress of Sixteen, Party central committee has established development concept of "people-oriented, comprehensive, coordinated and sustainable." In 2003, the CPC Central Committee, State Council issued a decision on the development of forestry. Not only pointed out the direction for forestry, but also has been given a very important task to forestry. Therefore, how to understand forestry and how to promote the construction of modern forestry have very important significance.

2 Establish the Dominant Position of Forestry Ecological Construction

Forestry is organized for conducting forest management and it conducts timber and forest products business production and protection of resources and the latter based on the basic industries and public welfare. Modern forestry must adapt to level of modern technology and equipment and social development. Based on modern scientific knowledge, Modern forestry armed with modern technology and equipment, produced with Modern process methods and Managed with modern scientific methods, is the sustainable forestry. Some people even said that modern forestry is sustainable forestry. Its objection is that Economic development and utilization of forest ecology and protection make Forest Ecology seek a steady growth in economic productivity to meet the needs of human society's overall economic needs of forest.

We know that forests are the main terrestrial ecosystems, and in maintaining the balance of terrestrial ecosystems play a supporting role. However, in the past, we did not recognize that the people have the forest for long-term and large-scale over-exploitation and destruction, so that human life on Earth must to face with the difficult issues to deal with any serious ecological crisis than ever, which will be possible to replace nuclear war as the greatest threat facing humanity. So it is recognized that Environmental degradation, such as soil erosion, desertification, grassland degradation, desertification and salinity, and biodiversity destruction and aggravating the greenhouse effect, have directly related with over a large area of forest exploitation, forest decline and even loss of ecological function. Sharp drop led to a series of forest ecological crisis, actually constitute a strategic threat to the global.

A large number of forests in China are still being over-harvesting, and state-owned forest enterprises have severe forest resources crisis and economic midst of these difficulties, destruction of forest ecosystems is continued, and the damage of sand-water and other natural disasters is increased, which cause the serious floods in the Yangtze River, Songhua River and Nen river and severe sandstorms in some areas. Therefore, we must give the forest to re-positioning, to be implemented mainly by the timber production to ecological construction to change. Forestry ecological construction should work on the most important and most central location, to strengthen environmental protection, maintenance of ecological balance, to establish a complete, stable and efficient construction of forest ecological system as the main task of forestry. Thus guide the establishment of forestry management on the basis of the ecological balance.

3 Sustainable Forestry Is the Strategic Goal of Building a Modern Forestry

Sustainable forestry is that in the human sense of time and space scales, have no space, time, activity on non-economic nature, irrational, unscientific and non-development of forestry. It is in a particular area, do not harm and weaken the present and future generations to meet on forest ecosystems and their ability to demand products and services of forestry.

Sustainable forestry is a strategic goal of modern forestry development, and is a necessary requirement for modern forestry development, and is sustainable development in forestry applications. In 1992, United Nations Conference on Environment and Development adopted the "Declaration of Principles on Forests," stated: "Forest resources and forest lands should be sustainably managed to meet this generation and future generations in the social, economic, cultural and spiritual needs. These needs are for forest products and services, such as wood and wood products, water, food, fodder, medicine, fuel, accommodation, employment, recreation, wildlife habitat, landscape diversity and other forest products. Should take measures to protect forests, prevent it from the harmful effects of pollution, including air pollution, fires, pests and diseases, in order to maintain the value of all its variety. Sustainable forestry does not mean that the traditional natural regeneration is made, and use the inefficient outdated forestry technology, but for modern eco-forestry, that the use of modern

scientific knowledge, practical design and implementation of forestry, forest ecology and reasonable technical measures. "[1]

Sustainable Forestry far beyond the traditional forestry development and seek only the amount of forest growth and harvesting of sustainable use principles of equilibrium, but all the functions related to forest ecosystem maintenance and development, It also defined the sustainable forestry development and the sustainable development of human society cannot be separated. Therefore, to achieve sustainable development of forestry need to do a full range of deep-level work, you need to get the whole community.

Its goal is to establish sustainable forestry in the social, economic, technical support system to meet the needs of our society and the formation of Chinese economic and social development to adapt to temporal and spatial characteristics, and sustainable management of resources, environment and industrial base.

4 Reform Is the Inevitable Modern Forestry Road Construction

Since Third Plenum of the Eleventh Party, all walks of life are under reform, no exception for forestry. Only can the reform have power, dynamic, viable. At present, the forestry reforms were mainly forest property rights reform, focusing on reform of state forest management of forest resources, forest classification and forest management system reform of comprehensive law enforcement.

First, the reform of forest ownership. Deepen the reform of property rights, clear property rights, make the ownership, management rights, the right to use and management responsibility to protect unified. Active stakeholders, mobilize and motivate the enthusiasm of the operators and the investors, have individuals and private companies can invest in a bold, daring operation. In the course of business, to long-term planning, long-term business objectives, to avoid the quick success of the short-term behavior, to develop non-public economy. To achieve the outside world, economic and technical co-investment, and promote the rational flow of factors of production forestry, to take stock, public private, private business, joint ventures and other forms to promote the economic development of non-public forestry.

Second, the reform of state-owned forest resources management system. Strengthen the asset management of forest resource, adhere to valuable resources, the use of paid, scientific assessment, reasonable fees, equal competition, the principle of unity rights and obligations of responsibility. Ownership of resources and the transfer of shares in business, investment associate, mortgage loans and other forms of economic activities, management and supervision of state-owned forest resources to prevent the transfer of business assets in the course of the loss of forest resources to ensure that state-owned assets.

Third, the reform of forest classification and management system. The key is in accordance with the nature of forestry production and business activities to determine the unit of economic nature, to take a different value of economic operation and implementation, the Council part of the rule, as a whole into one. In our public forestry and commercial forestry should adopt a different operating mechanism. Forest Construction, should be included in the public welfare, into the scope of government functions, the implementation of the government's unified plan and the

main cause of macro-control management system, according to the division of power between central and local governments the principle, established by governments at all levels, mainly through financial means to solve the funding, the state invested with wide community to raise funds to run a combination of input compensation mechanism. Commercial forest development should be market-oriented, as a corporate act, the implementation of the country under the control of regulated mainly by the operation of market mechanism, market operators, mainly through financing, market-oriented, autonomous, self-financing, national and local Government under certain circumstances to give policy support. [2]

Fourth, the comprehensive reform of forestry law enforcement. Insist on administering the forest, follow the laws and regulations, and effectively protect the forest resource owners, operators of the legitimate rights and interests, to strengthen forest ownership, forest management; improve the quality of law enforcement officers and law enforcement capacity, strengthen supervision and management of law enforcement personnel, increase law enforcement and severely punish the destruction of forest resources, truly sound the alarm bell.

5 The Whole Community to Do Forest Is an Important Guarantee for the Construction of Modern Forestry

Since reform and opening, the entire community to do forest, the deepening of all the people engaged in green development, particularly in the six project started, but the increase in forestry as a whole society is very concerned about the high degree of public participation require strong cooperation and support in all aspects of social engineering.

The whole community to do forest, the first change is the main forestry. Forestry decision to the task of building the forestry sector alone is not enough, must be the whole society to care, support and participation. The second is to further and more in all areas open. Determined to overcome long-standing forestry front of the drawbacks of a single public ownership, attract a wide range of social funds, various forms of ownership and actively participate in forestry development, to fully mobilize the enthusiasm to make a difference in the forestry sector. Third, further transform government functions. Governments at all levels from the economic and social development of the overall situation, assume the responsibility of the social construction of public services, which is at all levels of government to take primary responsibility for forestry. Fourth, further the nationwide voluntary tree-planting campaign, and constantly enrich and improve the forms of voluntary tree-planting efforts to improve the rate of responsible citizens, to promote the nationwide voluntary tree-planting campaign to the depth and breadth. Fifth, we should step up publicity efforts to create a strong public opinion, so that every citizen participation in forestry into a conscious action, so that attention of the community forestry, forestry support, from their own living environment and the vital interests of the construction of forestry, to join the forestry.

Modern forestry is a long and arduous task, as long as we are able to correctly understand the importance of forestry to develop guidelines for the development of modern forestry policies, practical strategies to determine the goals, take positive and

effective way to mobilize the enthusiasm, so that the whole society to care for forestry, support for forestry, construction, forestry, forestry a new vibrant scene will be presented in front of us, they will make full play to its forestry role and function.

References

1. China Daily compilation environment. In: The 21st century - the United Nations Conference on Environment and Development literature compilation of. China Environmental Science Press, Beijing (1992)
2. Zhou, S.X.: China Forestry historic change. China Forestry Publishing House, Beijing (2003)

A Productive Time Length-Based Method for Multi-tenancy-Oriented Service Usage Metering and Billing

Huixiang Zhou, Qiaoyan Wen, and Xiaojun Yu

State Key Laboratory of Networking and Switching Technology,
BUPT, PO Box 305#, No. 10, Xitucheng Road, Haidian District, Beijing, 100876, China
zhouhuixiang@bupt.edu.cn, wqy@bupt.edu.cn,
yuxiaojun@bupt.edu.cn

Abstract. Currently, most of the service computing-related platforms provide services free of charge or simply charge users fees based on storage occupation or processor capacity as tradition. For the services themselves, which almost the only functional elements in a service computing environment [1,2], the usage metering and billing is still a not well-solved but important problem. To solve the Multi-tenancy-oriented [3] service usage metering and billing problem, this paper presents a productive time length-based method, compared to the traditional method for multi-tenancy -oriented service usage metering and billing, the productive time length-based method is more discriminative and can improve the accuracy of the metering process. It can avoid the mis-metering of services that return failed or contribute little to the final output user-obtained.

Keywords: service computing, cloud computing, Multi-tenancy, indirect service, valid invoking process, productive time. Usage Metering, Usage Billing.

1 Introduction

As an innovative computing paradigm shifting from mainframe computing and desktop computing, service computing and its variations have been becoming more and more widely utilized and deeply influenced the design patterns of IT solutions and the business models of IT services. Among a plurality of variations, Service-Oriented Architecture (SOA) [4] and cloud computing [5,6] are two well-known ones.

Currently, as business logic-centric services or public service orchestration platforms are rarely provided, the usage metering and billing methods of the services themselves are seldom discussed. In addition, Multi-tenancy issues are also rarely addressed in the public products & platforms.

This paper presents a productive time length-based method for Multi-tenancy -oriented Service usage metering and billing, and the metric possesses two advantages: First, the metric is designed based on the definition of “*valid invoking process*” and “*productive time length of services*”, in which, only when all the correlated services in one invoking process return successfully, the services involved are considered for

usage metering and billing. The metric can avoid the mis-metering of services that return failed or contribute little to the final output user-obtained. Second, the metric is built on the productive time length of a service and can quantitatively differentiate two invoking processes of the same service.

2 Related and Public Products and Platforms

Nowadays, most of the software architects build their enterprise-level solutions more or less based on the SOA techniques or certain tools. Meanwhile, more and more cloud computing platforms are launched by big companies, and their products & platforms conduct the usage metering and billing issues show as table1.

Table 1. Products & platforms conduct the usage metering and billing issues.

Products & Platforms	service usage metering and billing
<i>Google App Engin</i>	Google App Engine platform conducts the usage metering and billing issues based on the computing resources [7], including outgoing bandwidth (gigabytes), incoming bandwidth (gigabytes), CPU Time (CPU hours), stored data (gigabytes per month), recipients emailed.
<i>Microsoft Windows Azur</i>	Microsoft Windows Azure platform gives a detailed resource classification. the usage metering is performed as: compute (hours), storage (GB), storage transactions (transaction number), and content delivery network (GB based on source/destination location).
<i>Salesforce forcecom platform</i>	Salesforce force.com platform is released as several editions (free, enterprise, unlimited) based on the service capacity, and then performs pricing and billing in terms of per user per month (/user/month) for each edition (the free edition is free of charge).
<i>Amazon Web Services</i>	Amazon Web Services include several types of products, such as compute (EC2), database (simpleDB, RDS), storage (S3, EBS), and so on. Most of the products provide resource-centric services, and the service usage metering is conducted based on resources.

As a conclusion, most of the services provided by public products & platforms are resource-centric services, such as processor, memory, storage, networks, database, and so on, and the service usage metering and billing processes are usually simplified as the quantity measurement of resource used.

3 Productive Time Length-Based Method

To solve the problem of Multi-tenancy -oriented service usage metering and billing, the metering & billing metric should be defined first, based on which, the service usage metering and billing scheme can be designed.

3.1 Pre-definition (Service Classification)

In a service computing environment, the correlations of services are usually formed based on the service orchestration or the interoperations between them. According to

the correlations, for a given service invoking process, services can be classified as the *Direct Service (DS)* and *Indirect Service (IS)*.

- *Direct Service*: a service directly invoked by the Multi-tenancy Access Server (MAS, providing the service access interface for users belonging to different tenants) or the Business Process Management System (BPMS [8], serving as the supporting platform for service orchestration) through the Service Gateway (SG, the gateway for service invoking, the invoking process of each service must pass through the gateway);
- *Indirect Service*: a service invoked by other services (direct or indirect) through the service gateway.

In the service invoking process, for an invoked service S, if S is a DS, its direct service is itself, if S is an IS, its direct service is the direct service that initiates the service invoking process.

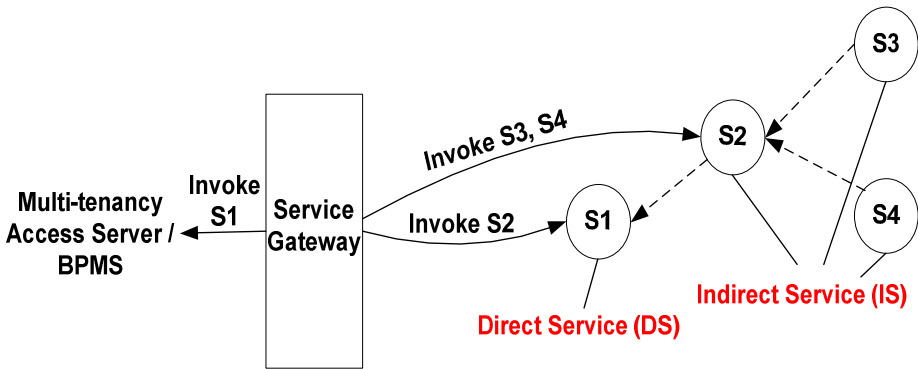


Fig. 1. The service invoking process

As an example shown in Fig.1, to fulfil a service requirement, the Multi-tenancy access server or BPMS invoke service S1 through the service gateway. As there are inherent correlations between services S1~S4 (interoperations denoted by dashed arrows), S2, S3 and S4 are invoked successively through the service gateway (denoted by solid arrows). In this service invoking process, service S1 is a direct service/DS, and the services S2, S3 and S4 are indirect services/IS. Furthermore, S1 can be called the direct service of S2, S3 and S4.

3.2 Method for Service Usage Metering

In a service invoking process, only direct services are invoked by the Multi-tenancy access server or BPMS directly, and the returned results, which serve as the output of the invoking process, will be forwarded to users. A service invoking process can be defined as a *valid invoking process* when the direct service and all the indirect services invoked return successfully and the output of the invoking process can be obtained finally.

For any service S invoked in a service invoking process P, if P is a valid invoking process, the length of time consumed by the invoking process of S can be defined as the *Productive Time Length (PTL)* of S in P.

For a tenant T, the service usage can be metered by the productive time length of each service invoked directly or indirectly by the users belonging to T, in the form of $\langle \text{TenantID}, \text{ServiceID}, \text{Productive Time Length} \rangle$. As the price of each independent service may be different, for billing purpose, the service usage metering should be performed based on each service respectively.

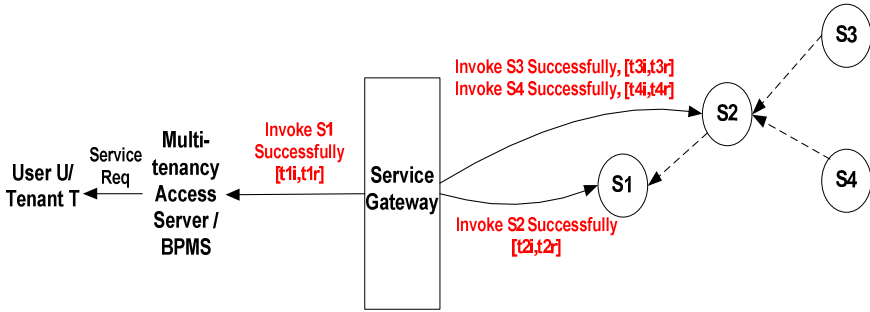


Fig. 2. An example of service usage metering

As an example shown in Fig.2, the user U belonging to tenant T submits a service requirement, based on which, the Multi-tenancy access server or BPMS invokes service S1 directly, and then S2~S4 are invoked indirectly through the service gateway, i.e. $\text{MAS/BPMS} \leftarrow \text{S1} \leftarrow \text{S2} \leftarrow \text{S3 \& S4}$. Finally, all the services return successfully, i.e. $\text{S3 \& S4} \rightarrow \text{S2} \rightarrow \text{S1} \rightarrow \text{MAS/BPMS}$. And thus, this service invoking process can be treated as a valid invoking process. For any service SX in the process, the points of time when SX is invoked and returned are respectively denoted as tXi and tXr , and thus the productive time length of SX can be denoted as $tXr-tXi$. Then for this process, the service usage metering of Tenant T can be represented as $\{ \langle T, S1, t1r-t1i \rangle, \dots, \langle T, S2, t2r-t2i \rangle, \dots, \langle T, S3, t3r-t3i \rangle, \dots, \langle T, S4, t4r-t4i \rangle \}$.

For the service usage metering results generated by two users U1 and U2 belonging to the same tenantT: $\{ \langle T, S1, \Delta t11 \rangle, \langle T, S2, \Delta t12 \rangle, \langle T, S3, \Delta t13 \rangle, \dots, \langle T, SX, \Delta t1X \rangle \}$ and $\{ \langle T, S1, \Delta t21 \rangle, \langle T, S2, \Delta t22 \rangle, \langle T, S3, \Delta t23 \rangle, \dots, \langle T, SX, \Delta t2X \rangle \}$, they can be merged and together meter the service usage of tenant T, as $\{ \langle T, S1, \Delta t11 + \Delta t21 \rangle, \langle T, S2, \Delta t12 + \Delta t22 \rangle, \langle T, S3, \Delta t13 + \Delta t23 \rangle, \dots, \langle T, SX, \Delta t1X + \Delta t2X \rangle \}$.

3.3 Method for Service Usage Billing

In a service computing environment, the billing process should be performed based on the service usage metering process and service pricing results.

With the productive time length-based service usage metering metric, the pricing of each service should be performed based on the running time, i.e. for a service S, its

service fee can be charged based on a basis of per second or per minute. In a service computing environment, the pricing issues are conducted by each service (or the provider) independently, and then collected by the billing-related module.

Given the service usage metering results for the tenant T as $\{ \langle T, S1, \Delta t1 \rangle, \langle T, S2, \Delta t2 \rangle, \dots, \langle T, SX, \Delta tX \rangle \}$, and the service pricing results (per second or per minute) as $\{ P(S1), P(S2), \dots, P(SX) \}$, the Tenant T should be charged as $P(S1) \times \Delta t1 + P(S2) \times \Delta t2 + \dots + P(SX) \times \Delta tX$.

For the example shown in Fig.2, with the service usage metering result $\{ \langle T, S1, t1r-t1i \rangle, \langle T, S2, t2r-t2i \rangle, \langle T, S3, t3r-t3i \rangle, \langle T, S4, t4r-t4i \rangle \}$, the tenant T will be charged a service fee. $P(S1) \times (t1r-t1i) + P(S2) \times (t2r-t2i) + P(S3) \times (t3r-t3i) + P(S4) \times (t4r-t4i)$

4 Scheme Design

4.1 Scheme of Service Usage Metering & Billing

Based on the service usage metering & billing metric above, the service usage metering & billing architecture is shown as Fig.3.

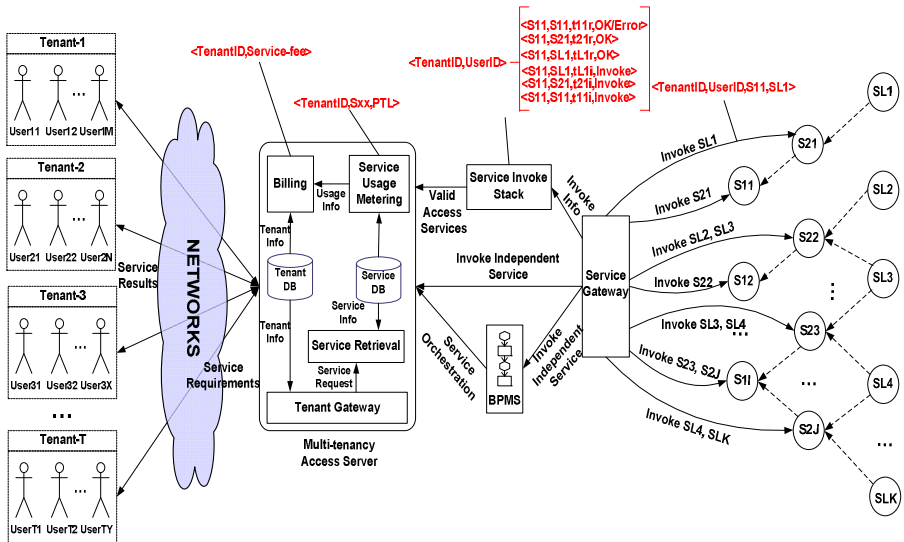


Fig. 3. The service usage metering & billing architecture

To provide a Multi-tenancy -oriented service environment, a Multi-tenancy access server is deployed. In the server, a Tenant Gateway (TG) takes charge of tenancy management issues, including maintaining the tenant information. The Service Retrieval (SR) module mainly retrieves the service or service orchestration which fulfils user requirements. The Service Usage Metering (SUM) module is deployed to perform the service usage metering process and the Billing module performs the

billing process based on the service usage information. In addition, a service gateway is deployed to conduct the service invoking issues and the invoking process of each service must pass through the service gateway. In addition, two database modules, i.e. tenant DB and service DB, are placed in the Multi-tenancy access server, and keep the information of tenants and services respectively.

And a BPMS platform is included to support the service orchestration. The service orchestration running on the BPMS platform is invoked by the Multi-tenancy access server and each independent service involved is invoked by the BPMS platform through service gateway according to the business process of the orchestration. To support the service usage metering process, a Service Invoke Stack (SIS) module is deployed to record each service invoking/return action and the result information. With the productive time length-based method for multi-tenancy -oriented service usage metering and billing, the service usage metering and billing process can be performed completely, finally the service usage metering and billing results will be produced.

5 Conclusion

By considering the correlation of services formed by the service orchestration and interoperation, this paper presents a tenant-oriented service usage metering and billing method for the service computing environment. It can solve the usage metering and billing problem of business logic-centric services in a multi-tenancy service environment, compared to the traditional, the productive time length-based method is more discriminative and can improve the accuracy of the metering process.

Acknowledgment. This work is supported by Natural Science Foundation of China (Grant Nos. 60873191, 60903152, 61003286, 60821001).

References

1. Maric, D.M., Meier, P.F., Estreicher, S.K.: Mater. Sci. Forum 83-87, 119 (1992), http://en.wikipedia.org/wiki/Services_computing
2. Zhang, L.: The Lifecycle of Services Computing Innovations (2005)
3. <http://en.wikipedia.org/wiki/Multitenancy>
4. <http://searchsoa.techtarget.com/definition/SOA-governance>
5. <http://www.infoworld.com/d/cloud-computing/what-cloud-computing-really-means-031>
6. <http://bx.businessweek.com/cloud-computing-/reference/>
7. <http://code.google.com/appengine>
8. <http://www.auraportal.com/EN/EN0-AP-What-is-BPMS.aspx>

Comparison and Analysis of the Fusion Algorithms of Multi-spectral and Panchromatic Remote Sensing Image

Chao Deng¹, Hui-na Li¹, and Jie Han²

¹ College of Computer Science & Technology
Henan Polytechnic University, China
superdeng5@163.com, lihuina851013@163.com

² College of Surveying & Land Information Engineering
Henan Polytechnic University, China
rainbow871027@163.com

Abstract. Keeping the spectral information and improving spatial resolution of the fused image is a crucial research topic recently. PCA transform, High Pass Filtering and SFIM transform of three methods are analyzed and compared by multi-spectral and panchromatic remote sensing images fusion in qualitative and quantificational aspects. The assessment of experimental results indicates that PCA algorithm will lose some useful information, the image is relatively large deviation, but maintaining a good spectral information definition; High Pass Filtering has better spatial resolution and spectral characteristics, but short of the whole spectral characteristics of image is not good; SFIM algorithm is not good at improving the spatial texture detail and has a great spectrum distortion.

Keywords: Fused Image, PCA transform, High Pass Filtering, SFIM transform, Evaluation.

1 Introduction

As is well known, the technology of remote sensing is developing with each passing day, toward the multi-platform applied in various fields, multi-temporal and high space resolution multi-spectral satellite remote sensing imagery system came forward in great numbers in all fields. Corresponding to the remote sensing data processing and analysis theory, methods are emerging, image fusion is one of the important methods, and it can be different together the advantages of remote sensing data, data refinement, reduce redundancy, improve remote sensing image efficiency [1].

Remote sensing image fusion most attention has been focused on the multi-spectral with high spatial resolution panchromatic image fusion. Multi-spectral image has a wealth of spectral information but low spatial resolution, image is rather fuzzy. High spatial resolution image of its rich details but the spectral information poor. Good spectrum quality and the spatial resolution to let image has the advantage of both. For this reason, of which by combining useful information in the different images. But different fusion algorithm will always produce different effect. The

development of PCA conversion, High Pass Filtering and SFIM transformation in this paper was studied by using Average grads, Standard Deviation combined with Entropy that an experiment has been carried out High Pass Filtering fusion for multi-spectral and panchromatic image fusion is a better method.

2 Fusion Algorithms

PCA transformation. PCA is also called primarily component analysis, k-l transformation, eigenvector transform etc, is based on the relationship between variables, with minimal loss of information on the premise of a linear transformation method of mainly used for data compression and information enhancement [2]. The process is: First, do multi-spectral image PCA transform get component independent of each other, then the high-resolution panchromatic image with principal component of by PCA transform on histogram matching, so that high-resolution panchromatic image and the principal component as the same histogram, and finally will pass the histogram match high-resolution panchromatic instead of principal component with other components of principal component together for PCA inverse transformation, get merged image.

HPF transformation. Since the purpose of remote sensing image fusion is to preserve low-resolution multi-spectral images with high resolution panchromatic images based on the details, therefore, it is workable to use high-pass filter operator to extract high-resolution image detailed information, then simply add the method by pixel, the details will be extracted to the low-resolution image overlay [3]. The integration of the expression as follows:

$$F_k(i, j) = M_k(i, j) + HPH(i, j) \quad (1)$$

Where $F_k(i, j)$ is the k band pixel (i, j) the integration of values; $M_k(i, j)$ is the low-resolution k band multi-spectral image pixel (i, j) values; $HPH(i, j)$ is the high pass filter for high spatial resolution images obtained by high-frequency filtering image pixel (i, j) values.

SFIM transformation. SFIM transformation is also known as gray scale modulation method, which is mainly used for integration of low-resolution multi-spectral images and high-resolution panchromatic image is a spectral type of integration to maintain algorithm. The fusion algorithm is defined as follows:

$$IMAGE_{SFIM} = \frac{IMAGE_{low} \times IMAGE_{high}}{IMAGE_{mean}} \quad (2)$$

Where $IMAGE_{SFIM}$ is the fused image; $IMAGE_{low}$ is the low resolution image; $IMAGE_{high}$ is the high-resolution image; $IMAGE_{mean}$ is simulation low resolution image.

3 Fusion Algorithm Evaluations

The subjective qualitative evaluation. Qualitative evaluation is subjective evaluation of visual observation. Based on technical experience, observers judge

fused image matching, whether there is ghosting, the target is blurred edges, the texture and color information is rich, there is an obvious color distortion.

Objective quantitative evaluation index. In order to quantitatively for the analysis of fused image, this paper presents some major evaluation index simple introduction [4-6].

Average grads. The size of the average grads express the average size of image pixels, the average size of human eye for average brightness, as reflected in the mean moderate (grayscale value 128 controls), and visual effect is good, the image of the average grads defined as:

$$\mu = \frac{1}{M N} \sum_{i=1}^M \sum_{j=1}^N F(i, j) \tag{3}$$

Where F (i, j) is the image in the (i, j) at pixel; M, N are image width and height.

Standard Deviation. Reflecting the standard deviation of the average image intensity relative to gray discrete situation. If the standard deviation of a large images, the image of the gray-scale dispersion, the larger the image contrast, the information contains richer. The formula is:

$$std = \sqrt{\frac{\sum_{i=1}^M \sum_{j=1}^N (F(i, j) - \mu)^2}{M N}} \tag{4}$$

Entropy. According to Shannon information theory proposed in 1984, the principle of entropy reflects the amount of information available how much. Image Entropy is defined as:

$$H = - \sum_{i=0}^{L-1} P_i \log P_i \tag{5}$$

Where L is the total gray scale image series, Pi is always gray value for the probability of the pixel i appeared. Entropy is a measure of the richness of the image information, an important indicator of the fused image entropy the greater the amount of information carried by the fusion image shows the more the better integration of quality, the fused image entropy smaller, then the fused image carrying less information.

4 Analysis of the Experiment Result

Fusion experiments. This paper adopts multi-spectral (band 3, 2, 1) and the panchromatic image fusion as an example, image size for 1431×1431, as showing in Fig. 1, Fig. 2. And then comparing different fusion methods, the results are showing below:

Visual effects from the point of view, three methods of fusion fused image texture information after all have been enhanced, the spatial resolution get a certain degree



Fig. 1. Original multispectral image



Fig. 2. Original panchromatic image



Fig. 3. PCA Transform



Fig. 4. HPF Transform



Fig. 5. SFIM Transform

of enhancement, the fusion than the original image makes the image clearer and easier to interpret. Which, PCA transformation the traditional image fusion has high definition and good spatial resolution, better preserving the image of the spectral features, however, PCA algorithm will lose multi-spectral some of the first principal component will be reflected in the spectral characteristics of useful information, and makes the results of some of the deviation of the fused image; HPF transform fusion image is not only good to retain the vast majority of multi-spectral image spectral information but also image color close to natural color, contrast surface features better; SFIM transformed the most obscure image texture, the feature not obvious.

Analysis and comparison of different fusion. Based on the fusion images, each image the Average grads, Standard Deviation, Entropy are calculated respectively (Table 1).

Table1 is the quantitative result of that comparison of multi-spectral with panchromatic image fusion method. You will see in the Table1: Spatial detail information to reflect the Standard Deviation of two types of parameters and information Entropy, the three fusion methods showed obvious differences. PCA

Table 1. Comparisons and quantity analyses of three different fusion methods

	Average grads	Standard Deviation	Entropy
PCA321	190.968664	82.895909	4.190430
	292.888675	64.304679	4.306835
	329.673439	36.605254	4.145418
HPF321	382.256149	74.494133	5.365165
	442.739788	58.739931	5.458258
	414.935930	34.670791	5.533333
SFIM321	382.176121	73.457551	4.152605
	442.577926	60.114808	4.324505
	414.739214	38.760807	4.077404

transformed Standard Deviation and HPF transformed is considerable, but the HPF transformed Entropy larger than PCA transformed, so the HPF transformed average gray more concentrated, retained more detail information, the space of less distortion.

5 Summary

Image fusion is an efficient method of image enhancement technique. Experimental results show that: Whether in subjective visual or in objective statistical data, three algorithms have got better fusion result. Specifically, PCA transform fusion method and the HPF transform fusion method better retain spectral image of the spectral information, highlighting the image hue, makes the detail the image characteristics of the target more clearly, particularly in the HPF transform the best; High Pass Filtering has better spatial resolution and spectral characteristics; SFIM algorithm is not good at improving the spatial texture detail and has a great spectrum distortion. The experimental result proves that HPF is a comparatively good method for multi-spectral and panchromatic image data fusion.

References

1. Zhu, S., Zhang, z.: Remote sensing image acquisition and analysis, vol. 53-57, pp. 68–73. Science Press, Beijing (2000)
2. Yang, X., Tang, K., Deng, D.f., et al.: ERDAS remote sensing digital image processing experiments Tutorial. Science Press, Beijing (2009)
3. Xu, Q., Zhang, Y., Geng, Z., Xing, S., Tan, B.: Remote sensing image fusion and resolution enhancement technology, vol. 31-34, p. 76. Science Press, Beijing (2007)
4. Zhong-Liang, J., Gang, X., Zhenhua, L.: Image Fusion - Theory and Applications, vol. 26-27, p. 10. Higher Education Press, Beijing (2007)
5. He, G., Chen, S., et al.: Multi-sensor image fusion evaluation. Journal of Computers 3, 31 (2008)
6. Yang, F.L., Yang, G., Yang, f.b.: Pixel level image fusion evaluation method. Mapping Technology 16, 276–279 (2008)

An Approach for Plotting Reservoir Profile with the Rendering of Material and Texture of OpenGL

Shaowei Pan¹, Husong Li², and Liumei Zhang¹

¹ School of Computer Science, Xi'an Shiyou University, Shanxi Xi'an, 710065, China
dennis_pan@163.com, rikrun@gmail.com

² Yulong Computer Telecommunication Scientific (Shenzhen) Co., Ltd, Guang Dong Shen Zhen, 518040, China
lihusong@yulong.com

Abstract. This paper proposes an OpenGL approach with the rendering of material and texture for plotting reservoir profile. Such approach realizes the plotting along X or Y axis and arbitrary direction. At last, the application example shows correctness and intuitiveness of plotting reservoir profile by illustrating sectional drawing from subzone sedimentary facies between S1 and S2 in 106 well of one oil field.

Keywords: reservoir profile, material, texture, OpenGL, cutting plane.

1 Introduction

Plotting reservoir profile is one of the key research contents in reservoir 3D visualization. The material and texture are the basic function of OpenGL. Our research topic is focused on two section plotting methods with the rendering of material and texture of OpenGL: the cutting line along with the X/Y axis and vertical to strike direction, the cutting line in arbitrary direction and vertical to strike direction[1].

2 Material and Texture of OpenGL

OpenGL is a high performance three dimensional programming interface and software infrastructure for graphics hardware, which was developed by SGI [2]. And it is possible to apply a material and texture to rendered primitives. OpenGL provides tools to handle this task. User can set a texture itself and its properties. For example user can set whether the texture is repeated on the surface or not, how it is combined with rendered primitives and textures, etc.

3 OpenGL Approach for Plotting Reservoir Profile

Cutting Plane along X or Y Direction. Reservoir model hereby referred as reservoir profile model. Such model composites with the overlaying reservoir profiles. A point

determined by mouse click may further define the linear equation on two dimensional surfaces which further defines reservoir profile that vertically associated with the strike direction. Therefore, it transforms the complex cross area problem between cutting plane and reservoir body into a simplistic multi-reservoir-plane line intersection problem.

Cutting Plane along arbitrary direction. In Fig. 1(a), polyline $ABCD$ is the projection of cutting plane on XOY plane. Grid plane is the projection of some plane on XOY plane. Where the coefficient value and attribute value has firstly been obtained. Q is defined as the section point which start from point B nesting i (a positive integer) times. Each time when moving the point took a fixed step length d . B, C is selected by mouse cursor then be inverse transformed. $(X_b, Y_b), (X_c, Y_c)$ represents the result coefficients also defines liner equation.

$$y = (Y_c - Y_b) / (X_c - X_b) * (x - X_b) + Y_b \tag{1}$$

The X, Y coefficient of $Q(x, y, z, a)$ is defined.

$$\alpha = \arctg((Y_c - Y_b) / (X_c - X_b)) \tag{2}$$

$$x = X_b + (i * d) * \cos \alpha \tag{3}$$

$$y = Y_b + (i * d) * \sin \alpha \tag{4}$$

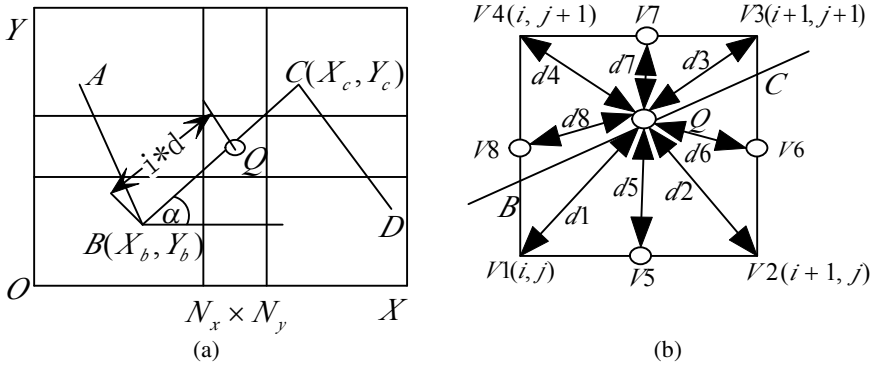


Fig. 1. The projection of Q when cut along the arbitrary direction and the indication of the relationship of Q and grid node

Once x, y coefficient of Q has been obtained, all node in reservoir profile grid will be traversed. Q then can be proved inside a grid formed by four grid nodes, they are $(i, j), (i + 1, j), (i + 1, j + 1)$ and $(i, j + 1)$, of the reservoir profile as shown in Fig.4(b). $V1(x_1, y_1, z_1, a_1), V2(x_2, y_2, z_2, a_2), V3(x_3, y_3, z_3, a_3), V4(x_4, y_4, z_4, a_4)$ are the grid nodes. $V5(x_5, y_5, z_5, a_5), V6(x_6, y_6, z_6, a_6),$

$V7(x_7, y_7, z_7, a_7)$, $V8(x_8, y_8, z_8, a_8)$ are the points respectively allocated on centroid of four edges of the grid. Thus:

$$x_5 = x_1 + \frac{(x_2 - x_1)}{2}, y_5 = y_1 = y_2, z_5 = z_1 = z_2, a_5 = \frac{(a_1 + a_2)}{2}. \tag{5}$$

$$x_6 = x_2 = x_3, y_6 = y_2 + \frac{(y_3 - y_2)}{2}, z_6 = z_2 = z_3, a_6 = \frac{(a_2 + a_3)}{2}. \tag{6}$$

$$x_7 = x_4 + \frac{(x_3 - x_4)}{2}, y_7 = y_3 = y_4, z_7 = z_3 = z_4, a_7 = \frac{(a_3 + a_4)}{2}. \tag{7}$$

$$x_8 = x_4 = x_1, y_8 = y_1 + \frac{(y_4 - y_1)}{2}, z_8 = z_4 = z_1, a_8 = \frac{(a_4 + a_1)}{2}. \tag{8}$$

By Ordinary Kriging interpolation, the Z coefficient value of point Q can be obtained.

According to the principle of Ordinary Kriging interpolation, in order to obtain the Z coefficient value of point Q , the weight coefficient towards Z coefficient value of points $V1, V2, V3, V4, V5, V6, V7$ and $V8$ should be obtained first. The solution is as follows.

$$\begin{cases} \sum_{j=1}^8 \lambda_j c(z_i, z_j) - \mu = c(z_i, z) \\ \sum_{i=1}^8 \lambda_i = 1 \end{cases} \quad (i = 1, 2, \dots, 8) \tag{9}$$

Where μ is the Lagrange multiplier. Once when obtained $\lambda_1, \lambda_2, \lambda_3, \lambda_4, \lambda_5, \lambda_6, \lambda_7$ and λ_8 , the Z coefficient value of point Q can then be obtained from below.

$$z = z_1 * \lambda_1 + z_2 * \lambda_2 + z_3 * \lambda_3 + z_4 * \lambda_4 + z_5 * \lambda_5 + z_6 * \lambda_6 + z_7 * \lambda_7 + z_8 * \lambda_8. \tag{10}$$

With a same method, one could easily obtain the attribute value a of point Q . The above calculation only focuses on one point of the reservoir profile. But once when all section point set been calculated, this point set would contribute to the reservoir profile with cuts in arbitrary directions. In contrast with inverse distance weighting, Kriging interpolation needs more memory space for calculation. Thus reflects well topographical changes. Inverse distance weighting specialized in calculation efficiency. The interpolation of inverse distance weighting requires less memory space but with a relatively poor interpolation result[3]. When all the Algorithms are finished, the reservoir profile could be rendered by material and texture of OpenGL.

3.1 Application Example

Fig.2 shows the section of sedimentary facies rendered by material and texture of OpenGL along the arbitrary direction between the subzone of S1 and S2 in a 3D

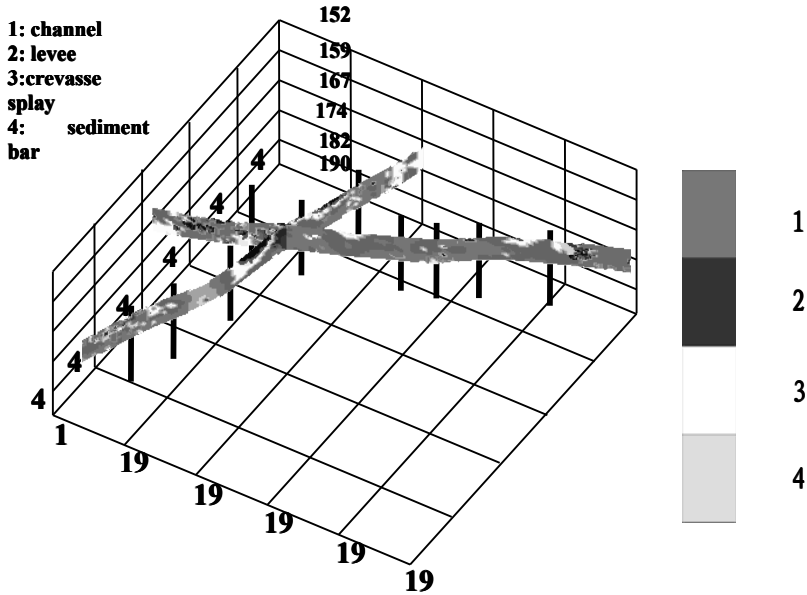


Fig. 2. The section of sedimentary facies along the arbitrary direction between the subzone of S1 and S2

space. This 3D sectional graphic fit close with practical situation due to real data from seismic, well drilling and etc. Thus further verifies the correctness and practicability of our method.

4 Summary

Material and texture are the basic function of OpenGL. This paper proposes an approach for plotting reservoir profile with the rendering of material and texture. It opens new gate for quantification geology structure and reservoir research.

Acknowledgement. This paper is supported by National Natural Science Foundation of China, its number is 50874091. The 3D visualization code was provided by Husong Li.

References

1. Bloomenthal, J.: Polygonization of Implicit Surfaces. *Computer Aided Geometric Design* 46(6), 73–77 (1998) (published in Chinese)
2. Wu, H.-x., Wu, J.-h., Xue, H.-f.: Application research for interactive 3D modeling based on OpenGL. *Computer Engineering and Design* 27(3), 376–378 (2006) (published in Chinese)
3. Jin, G.-d., Liu, Y.-c., Niu, W.-j.: Comparison between Inverse Distance Weighting Method and Kriging. *Journal of Changchun University of Technology* 24(3), 53–57 (2003) (published in Chinese)

A Nonmonotone Smoothing Algorithm for Second-Order Cone Programming in Failure Criteria

XiaoNi Chi and WenLue Chen

College of Mathematics and Computer Science, Huanggang Normal University,
Huanggang 438000, Hubei, P.R. China
chixiaoni@126.com

Abstract. It is shown that a wide variety of material failure criteria can be represented as second-order cone problems. In this paper, we present a nonmonotone smoothing Newton algorithm for solving the second-order cone programming (SOCP) in material failure criteria. Based on a new Fischer-Burmeister smoothing function, our smoothing algorithm reformulates SOCP as a nonlinear system of equations and then applies Newton's method to the system. The proposed algorithm solves only one linear system of equations and performs only one nonmonotone line search at each iteration. It is shown that the algorithm is globally and locally quadratically convergent under suitable assumptions.

Keywords: second-order cone programming, smoothing Newton method, nonmonotone line search, global convergence, material failure criteria.

1 Introduction

Second-order cone programming is widely used in materials, such as lower bound limit analysis of cohesive-frictional materials, material failure criteria [7, 8] and so on. It is shown that a wide variety of material failure criteria can be represented as systems of second-order cone constraints, giving rise to respective second-order cone programming problems.

The second-order cone (SOC) K of dimension k is defined by

$$K = \{x = (x_0, x_1) \in R \times R^{k-1} : x_0 - \|x_1\| \geq 0\},$$

where $\|\cdot\|$ stands for the Euclidean norm of vectors. It is well-known that the SOC K is self-dual.

The second-order cone programming (SOCP) problem is to minimize or maximize a linear function over the intersection of an affine space with the Cartesian product of a finite number of second-order cones. Since our analysis can be easily extended to the general case, we may consider a single SOC in the following analysis. Consider the following SOCP problem

$$(P) \quad \min\{c^T x : Ax = b, x \in K\}, \quad (1)$$

where $x \in K$ is the variable, $A \in R^{m \times k}$, $c \in R^k$, and $b \in R^m$ are the data and K is the SOC of dimension k . The dual to (1) can be written as [1]

$$(D) \quad \max \{b^T y : A^T y + s = c, s \in K\}, \tag{2}$$

where $y \in R^m$ is the variable and $s \in K$ is the dual slack variable.

Then the set of strictly feasible solutions of (1) and (2) are

$$F^0(P) = \{x : Ax = b, x \in K^0\}, \quad F^0(D) = \{(s, y) : A^T y + s = c, s \in K^0\}$$

respectively, with $K^0 = \{x = (x_0, x_1) \in R \times R^{k-1} : x_0 - \|x_1\| > 0\}$.

Throughout this paper, we assume that $F^0(P) \times F^0(D) \neq \emptyset$. Under this assumption, it can be shown that both (1) and (2) have optimal solutions and their optimal values coincide [1].

Recently great attention has been paid to smoothing Newton methods for solving some mathematical programming problems, such as complementarity problems, variational inequality problems, and so on [3]. However, there is little work on smoothing methods for the SOCP. Moreover, some algorithm [3] depends on the uniform nonsingularity condition. without uniform nonsingularity, some algorithms [2] need to solve two linear systems of equations and to perform two or three line searches at each iteration.

In this paper, we present a nonmonotone smoothing Newton method for the SOCP. Based on the new Fischer-Burmeister smoothing function [6], the algorithm reformulates the SOCP as a nonlinear system of equations and then applies Newton's method to this system. Our algorithm is shown to possess the following good properties: (i) if A has full row rank, the algorithm is well-defined and globally convergent; (ii) the algorithm can start from an arbitrary point and solve only one linear system of equations at each iteration; (iii) any accumulation point of the iteration sequence generated by our algorithm is a solution of the SOCP without uniform nonsingularity; (iv) the nonmonotone line search is used to improve the performance of our algorithm.

2 Nonmonotone Smoothing Algorithm

It is well-known that solving the SOCP problems (1) and (2) is equivalent to [1] finding $(x, y, s) \in R^k \times R^m \times R^k$ such that

$$\begin{cases} Ax = b, & x \in K \\ A^T y + s = c, & s \in K \\ x \circ s = 0. \end{cases} \tag{3}$$

Here the Euclidean Jordan algebra for the SOC K is the algebra [1,4] defined by

$$x \circ s = (x^T s, x_0 s_1 + s_0 x_1), \quad \forall x, s \in R^k.$$

The element $e = (1, 0, \dots, 0) \in R^k$ is the unit element of this algebra. Moreover, for any $x \in K$, let $x^2 := x \circ x$, $x^{1/2}$ denote the unique vector such that $(x^{1/2})^2 = x^{1/2} \circ x^{1/2} = x$, and $L_x = \begin{pmatrix} x_0 & x_1^T \\ x_1 & x_0 I \end{pmatrix}$.

To design our algorithm, let $\phi : R_+ \times R^k \times R^k \rightarrow R^k$ denote the new smoothing function [6]

$$\phi(\mu, x, s) = x + s - [(x \sin^2 \mu + s \cos^2 \mu)^2 + (x \cos^2 \mu + s \sin^2 \mu)^2 + 2\mu^2 e]^{1/2}.$$

By Theorem 3.1 in [6], $\phi(\mu, x, s)$ is a smoothing function of Fischer-Burmeister function $\phi_{FB}(x, s) = x + s - (x^2 + s^2)^{1/2}$ and satisfies

$$\phi(0, x, s) = 0 \Leftrightarrow x \circ s = 0, x \in K, s \in K. \tag{4}$$

Let $z := (\mu, x, y) \in R \times R^k \times R^m$ and define the function $G : R_+ \times R^k \times R^m \rightarrow R_+ \times R^m \times R^k$ by

$$G(z) = \begin{pmatrix} \mu \\ b - Ax \\ \phi(\mu, x, c - A^T y) + \mu x \end{pmatrix}, \tag{5}$$

and $\Psi(z) = \|G(z)\|^2$. According to (3), (4) and (5), $z^* := (\mu^*, x^*, y^*)$ is a root of the system of equations $G(z) = 0$ if and only if $(x^*, y^*, c - A^T y^*)$ is the optimal solution of (1) and (2).

By Theorem 3.2 in [5] and Theorem 4.1 in [6], we obtain the following properties of $G(z)$.

Lemma 2.1. Let $G : R_+ \times R^k \times R^m \rightarrow R_+ \times R^m \times R^k$ be defined as in (5).

(i) G is globally Lipschitz continuous and strongly semismooth everywhere in $R_+ \times R^k \times R^m$.

(ii) G is continuously differentiable at any point $z := (\mu, x, y) \in R_{++} \times R^k \times R^m$ with its Jacobian

$$G'(z) = \begin{pmatrix} 1 & 0 & 0 \\ 0 & -A & 0 \\ M(z) & N(z) & -P(z)A^T \end{pmatrix},$$

where

$$\begin{aligned}
 M(z) &= L_w^{-1}[(L_q - L_p)(x - c + A^T y) \sin 2\mu - 2\mu e] + x, \\
 N(z) &= (1 + \mu)I - L_w^{-1}(L_p \sin^2 \mu + L_q \cos^2 \mu), \\
 P(z) &= I - L_w^{-1}(L_p \cos^2 \mu + L_q \sin^2 \mu), \\
 \bar{p} &= x \sin^2 \mu + (c - A^T y) \cos^2 \mu, \\
 \bar{q} &= x \cos^2 \mu + (c - A^T y) \sin^2 \mu, \\
 \bar{w} &= \sqrt{\bar{p}^2 + \bar{q}^2 + 2\mu^2 e}.
 \end{aligned}$$

(iii) If the matrix A has full row rank, $G'(z)$ is nonsingular for any $\mu > 0$.

From Lemma 2.1, $G(z)$ is continuously differentiable at any point $z := (\mu, x, y) \in R_{++} \times R^k \times R^m$. Thus, for any $\mu > 0$, we can apply Newton's method to the smooth system of equations $G(z) = 0$ at each iteration and make $G(z) \rightarrow 0$ so that a solution of (1) and (2) can be found.

Algorithm 2.1

Step 0 Choose $\delta \in (0, 1)$, $\sigma \in (0, 1/2)$, and $\bar{\mu} > 0$, $\tau \in (0, 1)$ such that $\tau\bar{\mu} < 1$. Let $(x_0, y_0) \in R^k \times R^m$ be an arbitrary point and $z_0 := (\bar{\mu}, x_0, y_0)$. Choose η_{\min} and η_{\max} such that $0 \leq \eta_{\min} \leq \eta_{\max} < 1$. Take $R_0 := \|G(z_0)\|^2 = \Psi(z_0)$ and $Q_0 := 1$. Set $\beta(z_0) := \tau \min\{1, \Psi(z_0)\}$, $e_0 = (1, 0, \dots, 0) \in R^{1+k+m}$, and $k := 0$.

Step 1 If $\|G(z_k)\| = 0$, stop.

Step 2 Compute a solution $\Delta z_k = (\Delta \mu_k, \Delta x_k, \Delta y_k) \in R \times R^k \times R^m$ of the linear system of equations

$$G'(z_k)\Delta z + G(z_k) = \bar{\mu}\beta(z_k)e_0. \tag{6}$$

Step 3 Let $\lambda_k = \max\{\delta^l \mid l = 0, 1, 2, \dots\}$ such that

$$\Psi(z_k + \lambda_k \Delta z_k) \leq [1 - 2\sigma(1 - \tau\bar{\mu})\lambda_k]R_k. \tag{7}$$

Step 4 Set $z_{k+1} := z_k + \lambda_k \Delta z_k$. If $\|G(z_{k+1})\| = 0$, stop.

Step 5 Choose $\eta_k \in [\eta_{\min}, \eta_{\max}]$. Set

$$\begin{aligned}
 Q_{k+1} &:= \eta_k Q_k + 1, \\
 \beta(z_{k+1}) &:= \min\{\tau, \tau\Psi(z_k), \beta(z_k)\}, \\
 R_{k+1} &:= (\eta_k Q_k R_k + \Psi(z_{k+1}))/Q_{k+1},
 \end{aligned}$$

and $k := k + 1$. Go to Step 2.

By Algorithm 2.1, we state the following lemma which will play an important role in the well-definedness and convergence analysis of our algorithm.

Lemma 2.2. Let the sequences $\{R_k\}$ and $\{z_k\}$ be generated by Algorithm 2.1. For any $k \geq 0$, we have: (i) both $\{R_k\}$ and $\{\beta(z_k)\}$ are monotonically decreasing; (ii) $\Psi(z_k) \leq R_k$; (iii) $\bar{\mu}\beta(z_k) \leq \mu_k$; (iv) $\mu_k > 0$ and $\{\mu_k\}$ is monotonically decreasing.

Theorem 2.3. If A has full row rank, Algorithm 2.1 is well-defined.

Proof. Since $\mu_k > 0$ by Lemma 2.2(iv) and A has full row rank, it follows from Lemma 2.1 that $G'(z_k)$ is nonsingular. This demonstrates that Step 2 is well-defined.

Now we show that Step 3 is well-defined. For any $\alpha \in (0, 1]$, let

$$r(\alpha) := \Psi(z_k + \alpha\Delta z_k) - \Psi(z_k) - \alpha\Psi'(z_k)\Delta z_k. \tag{8}$$

Then by (6), we have

$$\begin{aligned} \Psi(z_k + \alpha\Delta z_k) &= r(\alpha) + \Psi(z_k) + \alpha\Psi'(z_k)\Delta z_k \\ &\leq r(\alpha) + \Psi(z_k) + 2\alpha G(z_k)^T[-G(z_k) + \bar{\mu}\beta(z_k)e_0] \\ &\leq r(\alpha) + (1 - 2\alpha)\Psi(z_k) + 2\alpha\bar{\mu}\beta(z_k) \|G(z_k)\|. \end{aligned} \tag{9}$$

If $\|G(z_k)\| > 1$, then

$$\beta(z_k) \|G(z_k)\| \leq \tau \|G(z_k)\| \leq \tau\Psi(z_k);$$

and if $\|G(z_k)\| \leq 1$, then

$$\beta(z_k) \|G(z_k)\| \leq \tau\Psi(z_k) \|G(z_k)\| \leq \tau\Psi(z_k).$$

Since $G(g)$ is continuously differentiable for any z_k with $\mu_k > 0$, it follows from Lemma 2.1 (ii) and (8) that

$$|r(\alpha)| = o(\alpha). \tag{10}$$

Thus, according to (9), (10) and Lemma 2.2(ii), we know that there exists a constant $\sigma \in (0, 1/2)$ such that

$$\begin{aligned} \Psi(z_k + \alpha\Delta z_k) &\leq r(\alpha) + [1 - 2\alpha(1 - \tau\bar{\mu})]\Psi(z_k) \\ &\leq [1 - 2\sigma(1 - \tau\bar{\mu})\alpha]R_k. \end{aligned}$$

Hence Step 3 is well-defined.

3 Convergence Analysis

As a consequence of Lemma 2.2 and Theorem 2.3, we have the following global convergence and local Q-quadratic convergence for Algorithm 2.1.

Theorem 3.1. Suppose that A has full row rank and that the iteration sequence $\{z_k\}$ generated by Algorithm 2.1 has at least one accumulation point. Then the sequence $\{\mu_k\}$ converges to 0, and any accumulation point of $\{z_k\}$ is a solution of $G(z) = 0$.

Theorem 3.2. Suppose that A has full row rank. Let z^* be an accumulation point of the iteration sequence $\{z_k\}$ generated by Algorithm 2.1. If all $V \in \partial G(z^*)$ are nonsingular, then

(i) $\lambda_k \equiv 1$ for all z_k sufficiently close to z^* ;

(ii) $\{z_k\}$ converges to z^* quadratically, i.e.,

$$\|z_{k+1} - z^*\| = O(\|z_k - z^*\|^2); \text{ moreover, } \mu_{k+1} = O(\mu_k^2).$$

Acknowledgment. This research was partially supported by the Scientific and Technological Innovation Team Project (No.T201110) of Hubei Provincial Department of Education, Excellent Youth Project of Hubei Provincial Department of Education (No. Q20092701), and the Doctorial Foundation of Huanggang Normal University (No. 08CD158), China.

References

1. Alizadeh, F., Goldfarb, D.: Second-order cone programming. *Math. Program.* 95, 3–51 (2003)
2. Burke, J., Xu, S.: A non-interior predictor-corrector path following algorithm for the monotone linear complementarity problem. *Math. Program.* 87, 113–130 (2000)
3. Chen, B., Xiu, N.: A global linear and local quadratic non-interior continuation method for nonlinear complementarity problems based on Chen-Mangasarian smoothing functions. *SIAM J. Optim.* 9, 605–623 (1999)
4. Faraut, J., Korányi, A.: *Analysis on Symmetric Cones*. Oxford University Press, Oxford (1994)
5. Sun, D., Sun, J.: Strong semismoothness of Fischer–Burmeister SDC and SOC complementarity functions. *Math. Program.* 103, 575–581 (2005)
6. Fang, L., He, G.P., Hu, Y.H.: A new smoothing Newton-type method for second-order cone programming problems. *Appl. Math. Comput.* 215, 1020–1029 (2009)
7. Bisbos, C.D., Pardalos, P.M.: Second-order cone and semidefinite representations of material failure criteria. *Journal of Optimization Theory and Applications* 134, 275–301 (2007)
8. Makrodimitopoulos, A., Martin, C.M.: Lower bound limit analysis of cohesive-frictional materials using second-order cone programming. *International Journal for Numerical Methods in Engineering* 66, 604–634 (2006)

The Research of Tobacco Leaf Roasting Control Tactics Based on Fuzzy PID

Xifeng Liu, Chunxiang Xu, Chuanjin Huang, and Wei Shiand

The College of Engineering Technology, Zhongzhou University,
No.6 of Yingcai Street, Huiji, Zhengzhou, Henan Province, China, 450044
comin999@126.com, xchx_2002@126.com,
huang_chuan_jin@sina.com.cn, shiwee@163.com

Abstract. In connection with different require of temperature and humidity of five roast period during tobacco leaf roasting, propose control tactics of tobacco leaf roast based on Fuzzy PID. In order to increase the color grade, savory grade and quality grade of tobacco leaf, the control tactics used Fuzzy PID technology, decrease difference in temperature between roast house top and bottom, achieve fundamental leveling of temperature through adjusting rotate speed of axle flow draught fan, the control tactics can achieve heating up and steadying temperature through controlling oxygen quantity of coal burning by adjusting rotate speed of oxygen fan, the control tactics can keep humidity smooth in roast house by controlling quantity of air entering roast house. In fact, the control tactics can affectively control running states of object, it has good characteristics such as high controlling precision, good stability, this is the reason that ensure the quality of tobacco leaf roasting.

Keywords: Tobacco Leaf Roasting, Fuzzy PID, Temperature Control, Humidity Control.

1 Preface

The quality of fresh tobacco is the basic of manufacturing tobacco products in high grade, while the advanced technology and control system for leaf roasting ensures the accomplishment of good products. The process of roasting leaves generally contains five parts of color fading, shape shrinking, edge drying, mesophyll drying and leafstalk drying, each of which needs different conditions for temperature and humidity with the value and gradient. It is very difficult for the traditional process of taking care of the roasting departments with workers to control the speed gradient of increasing temperature, the real-time temperature accurately, and to keep the temperature steadily, therefore, it is also difficult to guarantee tobacco leaves in high quality, which will affect the product manufacture and the market competition strength of cigarette. As a result, it is significant to design and develop an advance system for controlling temperature and humidity.

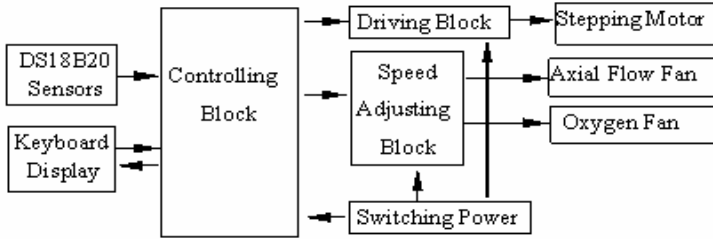


Fig. 1. System Diagram

2 Hardware Architecture [1]

The system described in the paper is designed in the way of modularization showed in Figure 1, which contains the controlling block, the keyboard-display block, the driving block for stepping motor, the speed adjusting block for single phase AC asynchronous motor, and the switching power supply block. The input of sampled temperature is achieved with the digital temperature sensor of DS18B20.

The displayed information contains the setup temperature parameter, the setup coasting time, the processing state, the keyboard state, the expert program number, the sampled value from four groups of sensors, the state of air flowing gate and oxygen motor, the running time etc. The air flowing gate is driven by the stepping motor; the oxygen fan and the axial flow fan are driven by the single phase asynchronous AC motor, the rotating speeds are controlled by the speed adjusting block to achieve the effect of the stepless speed changing.

3 The Static of Adaptive Fuzzy PID Controlling [2][3][4]

The PID Model is widely used in the industrial control system because of the simple algorithm, good robust performance and high reliability. The general PID controller is linear with the mathematic model showed below.

$$\begin{aligned}
 u(t) &= K_p[e(t) + \frac{1}{T_i} \int_0^t e(t)dt + T_d \frac{de(t)}{dt}] \\
 &= K_p e(t) + K_i \int_0^t e(t)dt + K_d \frac{de(t)}{dt}
 \end{aligned} \tag{1}$$

The controller output is indicated by $u(t)$ in the formula, and the input $e(t)$ of the difference between the setup and real temperature. K_p , K_i and K_d are the corresponding coefficient for proportion, Integration and differentiation.

3.1 The Principle of Adaptive Fuzzy PID Controller

In the control system based on the hardware of micro-controllers, inputs and outputs are sampled in period, so it is a discrete system with the mathematic formula as the following.

$$\Delta u(k) = K_p \Delta e(k) + K_i e(k) + K_d [e(k) - 2e(k-1) + e(k-2)] \tag{2}$$

In the formula, K_p is the proportion coefficient, $K_i = K_p \frac{T}{T_i}$ the integration coefficient with the sample period of T and integration constant of T_i , and $K_d = K_p \frac{T_d}{T}$ the differentiation coefficient with the differentiation constant of T_d .

The schematic diagram of adaptive fuzzy PID controller is showed in Figure 2.

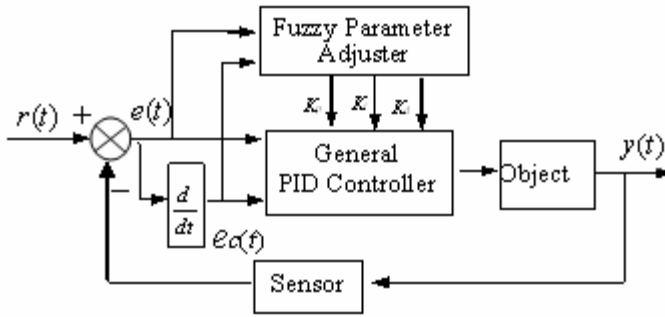


Fig. 2. Schematic Diagram of Adaptive Fussy PID Controller

The adaptive fuzzy controller is made up of the general PID controller and the fuzzy reasoning part, which is factually a fuzzy controller with the input of error indicated by e and variance rate by e_c . The fuzzy controller fixes the fuzzy relation of PID coefficients, e and e_c , and adjusts the coefficients of K_p, K_i and K_d online to make object get the good static and dynamic performance.

3.2 The Design of Adaptive Fuzzy PID Controller

3.2.1 Variables and Membership Function

According to the basic principle of fuzzy controlling, as temperature or humidity values from the coasting house are input to the fuzzy parameter adjuster as the error of E and the variance rate of E_c , the PID parameter's related information such as the language variable, basic discussion domain, fuzzy subset, fuzzy discussion domain, quantificational factor are obtained and showed in Table 1.

In the condition of the uniform trigonometric function chosen as the membership function for all the variables, the language variable values of variables will be obtained, and then after the process of fuzzy reasoning, fuzzy subset will be also gotten. With the fuzzy solution to the fuzzy subset, the values of all the controlling parameters will be available.

Table 1. Related Information of PID Parameter of K_p , K_i and K_d

Variable	e	e_c	k_p	k_i	k_d
Language Variable	E	E_c	K_p	K_i	K_d
Basic Discussion Domain	[-1.2,1.2]	[-0.3,0.3]	[-0.6,0.6]	[-0.012,0.012]	[-1.2,1.2]
Fuzzy Discussion Domain	[-6,6]	[-6,6]	[-6,6]	[-6,6]	[-6,6]
Fuzzy Subset	{NB, NM, NS, Z0, PS, PM, PB}				
Quantificational Factor	6/1.2=5	6/0.3=20	6/0.6=10	6/0.012=500	6/1.2=5

3.2.2 Rule of Fuzzy Controlling

The function and relationship of the three parameters of K_p , K_i and K_d in fuzzy parameterized self-tuning PID controller must be discussed in different periods, and results follows below.

① K_p determines the system responding speed, and large K_p brings fast responding speed, however, if K_p is too large, it will cause over adjustment and a unstable system. In contrast, small K_p brings slow responding speed, and if too small, it will long the time for adjusting the system and cause a bad static and dynamic performance.

② The function of K_i is to eliminate the steady state error. Large K_i can eliminate error fast, and contrarily slow. However, if K_i is too large, it will cause over saturated integration at the beginning of responding process, and quite large adjustment during the responding process. If K_i too small, it will be hard to eliminate the static error and meanwhile reduce the precision.

③ K_d affects the system dynamic performance, mainly restrains the system change in any direction and predicts possible changes. However, If K_d is too large, it will cause the system to brake ahead, long the adjusting time and reduce the system performance of anti-interference.

The fuzzy rule will be able to be designed referring to the function of PID parameters and the influence to PID parameters by different errors of e and variance rates of e_c .

3.2.3 Fuzzy Reasoning and Solution

The fuzzy reasoning is one of uncertain reasoning methods based on the fuzzy logic and has many implementing ways. The way of Mamdani of maximum and minimum values is applied in the paper.

Principle: If A_i and B_i , then the fuzzy relation of C_i will be showed below.

$$[\mu_{A_i} \wedge \mu_{B_i}] \wedge \mu_{C_i} \tag{3}$$

The opposition side is indicated by “or”, and expressed in the way of union sets in the reasoning process.

As a result, the membership function will be expressed below.

$$\mu = \vee \{ \mu_{A'} \wedge [\mu_{A_i} \wedge \mu_{C'}] \} \quad (4)$$

$$\cap \vee \{ \mu_{B'} \wedge [\mu_{B_i} \wedge \mu_{C'}] \}$$

The fuzzy subset of ΔK_p , ΔK_i and ΔK_d will be achieved in the reasoning process, and then the system output parameters also achieved with the fuzzy solution. The weighted average function is used as the fuzzy algorithm in the paper.

$$u_1 = \frac{\sum_{i=1}^{13} x_i \mu_{u_1}(x_i)}{\sum_{i=1}^{13} \mu_{u_1}(x_i)} \quad (5)$$

4 Experimental Analysis

The design system of tobacco leaf roasting control tactics based on Fuzzy PID has passed the testing program in Yiyang Tobacco Leaf Roasting Base in 2007.

Experimental method: taking the roasting system made in Kewei co. as the reference system, put fresh tobacco leaves with identical parts from same positions of some field into corresponding places in roasting houses controlled by the reference system and the designed system in the paper for 5x24 hours; and measure the weight of fresh and roasted leaves.

Experimental Process: record data every hour, including real temperature, controlled temperature by the system, the difference between them. Results show the precision of temperature controlling is $\pm 0.3^\circ\text{C}$.

Experiment Result: after roasting process, compare objective leaves in two houses by sense quality showed in Table 2 and economic benefit in Table 3.

Table 2. Appraisal of Sense Quality

Increment	Fragrance Quality	Fragrance Quantity	Density	impurity	Strength	Pungent Smell	Left Smell	combustibility	grayness	Summary
Unit 1	1.00	0.00	0.00	0.50	0.00	0.50	1.00	0.00	0.00	3.00
Unit 2	0.40	1.20	0.40	0.20	0.10	0.00	0.20	-0.20	0.00	2.30
Unit 3	0.56	0.89	0.06	0.53	-0.08	-0.08	0.61	0.17	0.00	2.64
Average	0.65	0.70	0.15	0.41	0.01	0.14	0.60	-0.01	0.00	2.65

Data shows that comparing to the reference, the fragrance improves, the mouth feeling is more comfortable, and the pungent smell reduces.

Table 3. Economic and Efficiency Analysis

Increment	Av.(CNY/ KG)	Scale of Good Leaves (%)	Scale of Orange Leaves (%)	Benefit (CNY/Load)
Unit 1	2.46	0.00	14.20	123.18
Unit 2	1.67	17.88	-0.35	83.50
Unit 3	1.90	5.78	16.06	95.11
Average	2.01	7.89	9.97	100.60

Comparing to the reference, the leaf average price increases by 2.01CNY/KG, the average scale of good leaves and orange leaves increases by 7.89% and 9.97%, and the benefit per load increases averagely by 100.60 CNY.

The designed system has applied and gotten the intellectual property with the patent number of 200720148702.X.

5 Conclusion

The tobacco leaf roasting control tactics based on fuzzy PID applies the fuzzy control theory and PID control technology to achieve the adaptive fuzzy PID control algorithm and is able to adjust the PID parameters in real mode. The experimental results show that the designed system is able to steadily control object's processing states in a high precision and also can be planted into other fields such as heating system, hydromechanics control system etc.

References

1. Limin, H.: Advanced Tutorial of Micro-Controller. Beihang University Press (2007)
2. Zhang, H., He, X.: Fuzzy Adaptive Theory and Application. Heihang University Press (2002)
3. Li, Y., Lun, S.: Temperature Meter Based on Fuzzy PID, Meters and Sensors 1, 20–21 (2003)
4. Zhai, X., Xie, S., Yang, W.: Constant Pressure Air Supply System Based on Adaptive Fuzzy PID Controlling, Hydraulic Pressure and Aerodynamics 2, 21–23 (2008)

Biography: Liu Xifeng (1965--), male (Han nationality), Henan Tanghe, University regular college course, labor BA, associate professor, engage in electromechanical integration.

Advertising Marketing Communication Strategy under the Background of Media Convergence----Based on the Generation after 80s Advertising of Audience Behavior Changes

Ye Bingqing

1289 Tianxiang Avenue, Nanchang HI-Tech Development Zone, China
ybcq827@gmail.com

Abstract. With the continuous development and spread of computer technology, information technology and network technology, the media convergence formed gradually, which makes the advertising industry has undergone tremendous changes. This paper analyzed the characteristics, causes and trends of media contact behavior and information received behavior and consumer behavior of post-80s under the background of media convergence. And it proposed mode of transmission of converged media, advertising content' innovative models, the use of new media prominent feature of open advertising. Audience interaction and to enhance literacy training of advertising audience and make the products and brands are accepted by AD audience in the new advertising strategy materials environment.

Keywords: Media Convergence, the Behavior of AD Audience, AD Literacy, Marketing Materials.

1 Introduction

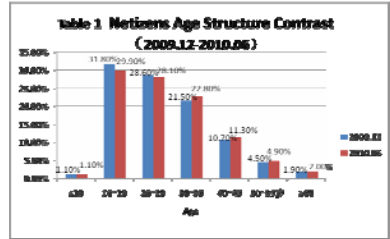
With the development of digital communication and network technology, the forms of information dissemination and media dissemination become more diversified, media convergence become an unstoppable trend and the reality. In this context, the audience who mainly through the passive acceptance of advertisements on television and turn to segmented customer in the 21st century. The post-80s advertising audience is a very representative group, they are likely to change Chinese consumer trends and the consumption structure of Chinese families because of the change of their media contact behavior, information receive behavior and consumer behavior.

2 Changes in Ad Audience's Behavior

2.1 The Media Contact Behavior

Growth time of the generation after 80s is coincided overlap with reform and opening for thirty years in China. In these years, the form and pattern of Chinese media has

undergone tremendous changes, it evolved fast. In this period, the generation after 80s was still in the stage of 0-10 years of age, they don't have the ability of media exposure and consumption. They only read book, listen to the radio and watch TV. Until 1994, China officially became a full-featured Internet country, and at that time, the mobile phone also appeared. Since the 21st century, the internet has been rapid development. During this time that new media occurs and grow popular that widely linked to the globe, it is just the golden age that the generation after 80s forms the values from high school to college. And they have time and conditions access to the Internet. The post-80s netizen is the main force of Internet users (see Table 1). In addition to the Internet, the generation after 80s watch digital television, read mobile newspaper, play PSP, talk on iPhone.

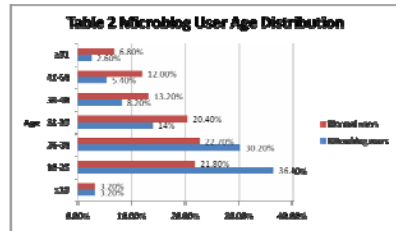


It can be say that media contact behavior of post-80s is changed by the development of Chinese media technology and the ecological change.

2.2 The Behavior of Receive Information

Media Contact behavior' change means change in the way of information received. In the past, people obtain information through radio, newspaper and television program. In the 21st century, the advantages of new media like internet and mobile phone are more obvious. Internet, it is the major channels that generation after 80s receive information, whether it is through the internet or mobile computer, Internet access. Internet has become an indispensable tool for generation after 80s in their life. A website did a network survey in 2010, "Which media do you get the news?" The survey showed that 39.4% of users believe that the network is essential to the media way of life, followed by TV, cell phones, newspapers, radio and magazines.

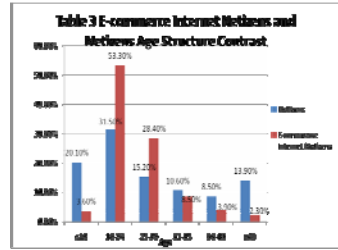
In recent two years, microblog sprung up. Data shows that, during March 2010 to 2010 in June, microblog coverage of the number of months increased from 54,521,000 to 10,307 million in domestic market. Up to February in this year, Sina and Tencent microblog registered users have already reach billions of people. The generation after 80s has owned a lot of seats in this group. In August 2010, according to data released by Swiss "microblog media usage characteristics and user research " shows that microblog user age dominated by 18-30 year olds, accounting for up to 67%(see Table 2).



2.3 Consumption Behavior Change Analysis

The characteristics of consumer behavior of post-80s can be summarized as follows: excessive consumption, brand advocates, pursue fashion, personality self, focus on consumer experience.

When post-80 consumers were shopping, the purchasing behavior at last is not only related to product itself and the convenience of products purchased. They also considered whether the décor is beautiful, parking lot and other hardware facilities are complete. In addition to hardware conditions, the level of service of mall staff also affects post-80s an important factor when they are shopping.



Recently, online shopping has become a new consumption pattern is represented by 80 users of the ages. This consumer is mainly to meet quick, convenient needs. It can be seen from the "online shopping market research report in China in 2009". Look from the age composition of online shoppers, online shopping population is more biased than the average younger Internet users. It is the main power of online shopping users that they are from 18 to 30-year-old, online shopping accounted for 81.7% of total number of users. Among them, 18 to 24 years of age also increase the proportion of online shoppers, the annual increase of 15.4 percent (see Table 3).

3 The Advertisement Audience Behavior Changes Cause Analysis

3.1 The Reason of Advertising of Audience Behavior Changes

The causes of behavior changes in Ad audience are in the following main aspects.

From a technical point of view, innovation of diffusion technology is the most direct reason of ad behavior in audience that occur changes. In the past, you should have a radio when you listened to the radio. But with the development of semiconductor technology, radio volume becomes smaller, and now we can listen to the radio from mobile phone, MP4 and other equipment. From the earliest black-white TV to color TV, and now there are various types of TV sets in the store, even Internet TV set. A few years ago, internet and mobile phones are still seemingly denied their status as a new medium, however, now no one believes they are not the kind of media.

From the point of view of social change and cultural development, changes in media technology bring the lifestyle changes, thereby affecting the cultural life of whole society. The post-80s live in the big era of change in the media, and also a multicultural society. In order to meet the needs of audience and attract the audience senses, each media created the space of a demand, desire, satisfaction and the liberation for the post-80s. In the digital age, all kinds of audio, animation, picture is symbols for all kinds of mass media dissemination, they are penetrating the life among the general population at the fast pace, occupy the space we live, they have become life content that we touch easily.

From an economic development perspective, after 30 years of reform and opening up, Chinese productivity level has been greatly improved, Chinese comprehensive national strength increased notably. The lives of ordinary people out of poverty into well-off gradually, family income, making the lives of 80 people do not like the previous generation constraints. With the "family planning" policy, a large part of the

generation after 80s is only one child in many families, they live in an era of material abundance, in the material needs, there is no memory of extreme poverty in young people's memory.

3.2 Advertising Trends in Audience Behavior

By the preceding analysis, it can be summarized the following three aspects of the change trend of advertising audience behavior under the background of media convergence, namely:

First, the media contact behavior goes from monotony to abundance. With the development and the innovation of the media tools, media types that audience can come into contact with increased. The audience may come into contact with the media everywhere, such as waiting for the elevator, taking a taxi, in the toilets and so on. Media Convergence greatly enriched the contact behavior of AD audience, single, monotonous media contact behavior of your audience becomes enriched.

Second, the information received behavior changed from passivity to activity. In the past, the information that ad audience came into contact with was received through the media spread, communicator was in active status, and the audience was in a passive position. The new media emerged and media convergence occurred, so that the original "push" information changes into "pull" information. In the dissemination process, the audience changed from the passivity to activity. They can search the products and advertising information that they need actively. Ad audience through subscription services can take the initiative to customize the advertising information they need, this unique personalized information services are very different from which all audiences receive exactly the same advertising content in the past.

Third, consumer behavior transactions transfer from the field to a virtual network. The emergence of the network, so that people have a huge change in the media contact, information received behavior. This change will eventually allow people to have a huge change in consumer behavior. Constrained by the conditions in the past, people could only compare goods and trade in the real store. The occurrence of media convergence on the network so that the audience can be traded, it provides a new way for the audience consumers. For people who surf the Internet every day, it is more convenient that "shop around" online directly than to go shopping "visiting the " street.

4 Advertising Marketing Communication Strategy under the Background of Media Convergence

4.1 Convergence of Communication Method

In the digital age, the new advertising communication mode will be more suitable. Product placement advertising is a representation of the fusion-style of communication, it is more and more popular by advertisers which spread business, brand, product placement information through the soft way. The early product placement advertising is mentioned in the film and television works or in some news or using some commodity. Now product placement advertising is increasingly

sophisticated, for example, the advertising in game must collocate with game perfectly, even users can not feel the existence of advertising ,experience a sense of the game better, in the game "Second Life", the advertisers in the game interface can be set up billboards on the main road, or you can allow users to play virtual real TV commercials, or set to in the real world to buy goods or retail store, click on the game's fast-food billboard that you can link to web pages that you can order in fast-food outlets has, or you can link to the ad product information, promotional offers information site.

4.2 Advertising Content Innovation

In the digital era of new media, only creativity advertising can attract the audience's attention. It can be said that the new media advertising itself is very innovative ideas. New media technology realized integrated forms for pictures, words and voices. Advertising under the media convergence offers more possibilities in the breadth, depth, accuracy and speed of ad creative information. In this context, the back of each ad should have a complete database support on products and services. The creativity is just an important point to mark to attract audiences to use the product database, it is the role of an index and navigation to guide people to search for information they need. The combination of smart mobile phone and two-dimensional code technology is representative. For example, when you see the poster of "Inception ", you can not wait to buy a ticket to go to see it, this time using mobile phone to take a look at posters on the two-dimensional code to log in directly to the booking movie ticket Web site, and you can watch the trailers.

4.3 Outstand Interactivity

The open nature of the new media has decided advertising audience to take advantage of new media to achieve human-computer interaction, personal interaction. Therefore, advertisers can enhance interaction with audience by other new media such as the internet and so on. First of all, they can produces a personal and one by one type of close interaction by e-mail, private letters, etc. Second, it can enhance interactive effect between the audience in the web search process and the products, such as the quick search to the desired information. Third, when the audience can visit the home page ad which allows the audience to participate to the home page. In addition, audience can also see other user's comments or the relevant comment link at this page. Therefore, advertisers can seize development trend of the media convergence, to achieve real-time interaction with your audience through digital marketing method, to seize the digital marketing market opportunities.

4.4 Cultivate the Audience Advertising Literacy

Generally, Advertising literacy contains two aspects: a general audience advertising literacy education and professional employees in the advertising industry of education. However, with further media technology and media integration, I think that advertising literacy capabilities also include the ability to effectively use new media and the capabilities to accept new media advertising. Advertiser has the responsibility and obligation to help your audience understand new media advertising, on one hand,

it has the advantages for the development of advertising mainstream itself, on the other hand, it can help your audience learn, understand the latest media trends and lifestyle better. Therefore, advertising literacy education for the advertising audience of the generation after 80s and even the citizens of the whole society has an important role that improves the audience advertising literacy. It can not only enhance the degree of social civilization of individual citizens, but can also promote the harmonious development of society as a whole.

5 Summary

With the deepening of media fusion process, behavior changes will be more apparent. Therefore, it is important to pay close attention to the media technology development and consumer behavior changes and then update the advertising strategy materials. That could be let the enterprise products and brands went further in the future.

References

1. Wang, F.: Advertising Pattern Transformation with Media Convergence. *Journal of International Communication*, 17–21 (2007)
2. Yang, H.: Ten Topics under Media Convergence Circumstance both in Theory and in Practice. *Journalists*, 146–148 (2007)
3. Liao, B.: A study of Media Transformation for Digital and Morphological Change of Advertising in China. *Journal of Advertising Study*, 54–57 (2009)
4. Han, H.: Characteristics of Consumer Behavior and ad strategy of the Generation after 80s. *China Advertising*, 125–129 (2009)

Building Smart Material Knowledge System Based on Ontology Bayesian Network and Grid Model

Jing Li and XiuYing Sun

Modern Education Technology Center, Huanghe science and technology college,
Zhengzhou, 450063, China
lilijingjing2011@sina.com,
sunxiuying2011@sina.com

Abstract. A smart material using piezoelectric ceramics to have the function of both the sensor and actuator is developed for such a vibration suppression system. This ontology is a guide, which provides a vocabulary for the visual description of domain classes. But traditional smart material system construction is time-consuming and costly procedure. This paper present a novel smart material system construction method based on ontology Bayesian network and grid model. The experimental results indicate that the Bayesian network building smart material algorithm achieves significant performance improvement.

Keywords: smart material, knowledge system, domain ontology, Bayesian Network.

1 Introduction

Magnetorheological fluids (MRF) are a kind of novel smart material, which are the suspension composed of based fluids, magnetic micro-particles and surfactants; it has significant magnetorheological effect in additional magnetic field. It has widely applied in mechanics, chemical engineering, and opto-electronics industry now. There has been much interest in developing new synthetic routes to prepare smart materials with novel compositions and topologies for various applications. As one of the most important issues in smart material theory, uncertainty of a set has been widely studied[1]. Mostly for performance reasons, retrieval systems nowadays still use rather simple thesaurus-based retrieval models (possibly based on statistical information). These measures include granulation measure, information entropy, smart material entropy, and knowledge granulation, and have become effective mechanisms for evaluating uncertainty in rough set theory. Applied Materials, Inc. reports that its flat panel display (FPD) and roll-to-roll coating systems are providing the advanced technology to enable more cost-efficient and scalable touch panel designs.

In this study, design of smart material made by piezoelectric ceramics, sensitivity and actuation evaluation of the smart material, optimal design of polarization and electrode layout by using ontology Bayesian Network and grid model. To support

study management and focused analyses, database queries must be written to extract subsets of data into specialized tools for those tasks. Rough set has been compared with other techniques. This includes comparison of performance of rough set and discriminates analysis. In the knowledge-based economy, where knowledge assets take central stage, whoever owns knowledge and can create knowledge from existing knowledge will enjoy absolute advantages over the business competition[2]. Specifically, we adopt directed graphs as our model for ontology schemas and use a generalized version of EM to arrive at a map between the nodes of the graphs. MR fluid is a kind of novel smart material, which was composed of based fluids, magnetic micro-particles and surfactants ,and it has significant magnetorheological effect in additional magnetic field.

By well-developed science and technology, smart buildings become a trend nowadays and more and more designers work with information technology to approach these smart ideas. The information is available over the Internet, published by various travel information providers. However, due to the heterogeneity of the information, it is difficult to automatically integrate the information. A travel plan consists of a number of smart material stages, such as choosing destinations, selecting tourist attractions, choosing accommodations, deciding routes, etc.

2 Smart Material System Based on Bayesian and Grid Model

The method of this thesis is case studies and data analysis, understanding the definitions, classifications and application of smart materials through literature review. Machine learning algorithms are known to degrade in performance when faced with many features (sometimes attributes) that are not necessary for rule discovery. Heterogeneity is here to stay for these very reasons and it is up to users and managers in terms of how and why to tackle the integration and distribution research issues.

2.1 Bayesian Networks and Smart Material Model

Most reactive materials design cases include two sections, detecting and motion which consist of reactive materials in architectural design. Such probabilities are not directly stored in the network; hence, it is necessary to calculate them[3]. The smart material X and Y are conditionally independent given the random variable Z if $P(x|y, z) = P(x|z)$. From the Bayesian rule, the global joint distribution function $P(x_1, x_2, \dots, x_n)$ of variables X_1, X_2, \dots, X_n can be represented as a product of local conditional distribution functions, for $x \in X$ and $m \in M$, denote $x|m$ to express that an object x is in a relation I with an attribute m . Given two sets $A \subseteq X, B \subseteq M$, we define Eq. 1.

$$P(x_1, x_2, \dots, x_n) = P(x_1)P(x_2) \dots P(x_n|x_1, \dots, x_{n-1}) \quad (1)$$

Let U denote a finite non-empty set, called the universe; the set $R_1 = \{X_1, X_2, \dots, X_n\}$ which satisfies Eq. (1) is called the classification or equivalence relation of U , and X_i is called an equivalence class of the equivalence relation R_1 . In the case of problems with many smart materials, the direct approach is often not practical. Nevertheless, at least when all the smart materials are discrete, we can expand the conditional independences encoded in the Bayesian Network to make the calculation more efficient.

Where $|X|$ is the cardinality of X and $c(X, Y)$ is the relative classification error of the set X with respect to set Y . An information table is a knowledge expressing system which can be used as an important tool to represent and process knowledge in machine learning, data mining and many other fields. It provides a convenient way to describe a finite set of objects called the universe by a finite set of attributes. The $BN_A(X)$ consists of objects that do not certainly belong to X on the basis of A . A set X is said to be *rough* (respectively *crisp*) if its $BN_A(X)$ is non-empty (respectively empty).

Constraint-based methods identify the dependencies between the two associated nodes by using smart material test. Smart material is one of the notable constraint-based algorithms. One of most advantages is that constraint-based algorithms are relatively fast and possess the ability to deal with latent variables.

$$h_{ij} = \begin{cases} H_i/H_j & \text{for the first time user} \\ HI_i/HI_j & \text{otherwise} \end{cases} \quad (2)$$

With the accuracy measure we can know the range of the boundary, but not its structure, on the other hand, the topological classification of the rough set gives us insight into the structure of the boundary, but nothing about its range. In the following, we first give the definitions of dispensable attribute and indispensable attribute in the concept lattices.

The dilemma says that the learning instability occurs because of the smart materials' adaptability (or plasticity), which causes prior learning to be eroded by more recent learning. Let $Y = \{Y_1, Y_2, \dots, Y_n\}$ be a classification (or partition) of U , and this classification is independent of attributes in Q . The main reason for such a definition of the generalized dominance principle is that the precipitations of data should not decrease lower approximations of decision classes which contain consistent knowledge for the considered decision table.

Let P and Q be equivalence relations of universe U , then the P -positive region of Q is defined by the union of all the objects of U which can be classified as the equivalence class of U/Q by the knowledge U/P . Hence, the similarity check plays a crucial role in the projected clustering of PART. In addition to the vigilance test, the PART adds a smart material test to increase the accuracy of clustering. The PART algorithm is presented below.

PART Algorithms:

0. Initialization: Initialize parameters $L, \rho, \sigma, \alpha, \theta_w, \theta_c$.

Input vectors: $D_j = (F_{1j}, F_{2j}, \dots, F_{ij}, \dots, F_{nj}), j=1, 2, \dots, m$. Output nodes: $Y_k, k=1, 2, \dots, m$.

Set Y_k does not learn any input pattern.

1. Input the pattern $D_1, D_2, \dots, D_j, \dots, D_m$.

2. Similarity Check: $h_{jk} = h(D_j, W_{jk}, W_{kj}) = h_\sigma(D_j, W_{kj})I(W_{jk})$

Where $h_\sigma(a, b) = \begin{cases} 1, & \text{if } d(a, b) \leq \sigma \\ 0, & \text{if } d(a, b) > \sigma \end{cases}$

$$I(W_{jk}) = \begin{cases} 1, & \text{if } w_{.j} > \theta \\ 0, & \text{if } w_{.j} \leq \theta \end{cases}$$

if $h_{jk}=1, D_j$ is similar to Y_k Else $h=0, D$ is not similar to Y_k

3. Selection of winner node: $T_k = \sum W_{jk} h_{jk} = \sum W_{jk} h(D_j, W_{jk}, W_{kj})$ Max $\{T_k\}$ is the winner node.

4. Vigilance and Reset: $R_k = \sum h_{jk} < \rho$

If the winner node succeeds in vigilance test, the input pattern will be clustered into the winner node. Otherwise, the input pattern will be clustered into a new node. Domain ontology can help users locate and learn related information more effectively. Hence, building the ontology rapidly and correctly has become an essential task for smart material based search on the Internet.

2.2 Grid and Smart Material Model

The thesis focuses on the use of materials and systems of the smart design cases. The method of this thesis is case studies and data analysis, understanding the definitions, classifications and application of smart materials through literature review. The architecture of ART is explained as follows[4]. The physical meaning of the loss functions can be interpreted based on more practical notions of costs and risks. Given an smart material system, rough sets can generate practical decision rules for objects of known classes, or predict classes to which new objects belong. The system designed in this paper provides an interactive and intuitive geographic interface for displaying the recommendation results and the complete itinerary, as well as for obtaining users feedback. Each is explained below. The itinerary contains the attraction names, transfer information, arrival time, and duration of the stay. Four variables (age, occupation, personalities, and tour motivation) are root nodes without parents. Three variables, age, occupation, and personalities, influence the traveler type that, subsequently combine with tour motivation to influence the preferred activities. In this section, the system uses PART neural network to cluster web pages. In order to obtain detailed information from the PART clustering, we add the notion of recursion to the PART architecture.

Step 1: The last stage updates the probability distribution of preferred activities given the evidence of other variables within the Bayesian network. The result with the highest probability is considered the preferred activities for the user.

Step 2: Choose the best attribute y , i.e. with the largest $V_y \times M_p$, let $Y = Y - y$, $R = R \cup y$, then using a rule reduction algorithm to reduce F_L .

3 Building Smart Material System Based on Ontology and Grid

The thesis focuses on the use of materials and systems of the smart design cases. Therefore, two similarity methods are proposed and focused on concept and instance respectively in the process of similarity calculation. If the ontology is additionally composed of properties, the corresponding similarity methods could be more. This problem has been a major focus of the research and practitioner communities alike. There is a large body of work in the database and smart material integration fields that ranges from matching database schemas to answering queries from multiple systems. For a formal ontology to be a good specification of a domain, both the

conceptualization of the domain itself and the formalization and specification of this conceptualization in a formal ontology must be good.

Most reactive materials design cases include two sections, detecting and motion which consist of reactive materials in architectural design. Ontology materials are increasingly considered a key technology for enabling smart material knowledge processing. Both knowledge representation and machine learning techniques are involved in the categorization process. The paper offers a methodology for building ontology for knowledge sharing and reusing based on smart material. Considering the cognizing, structure of knowledge and ontology, a method based on the smart material map is put forward here, which is extended to an ontology construction tool. Results of this study can facilitate exchange of knowledge and knowledge-related technologies between enterprises.

4 Using Ontology Bayesian Network and Grid Mode to Constructing Smart Material KD System

The purpose of this thesis is to design a smart material knowledge system by using ontology Bayesian Network and grid model for actuating the motion of the fingers. Applications of ontologies include knowledge description for intelligent reasoning, especially in the context of distributed applications like the semantic web, knowledge management. The primary content of this dissertation is to apply rough set technology to obtain all connotative concepts and hierarchy of them automatically from the designated data, which is not under the influence of developer.

In this paper, we apply the theory of smart material to automatically construct the concept hierarchy of ontology in knowledge management and to match up the binary relation matrix of documents and terms to express the independence, intersection and inheritance between different concepts to form the concept relationship of ontology. The goals of automatically constructing ontology in our research will help the information classification systems and ontology extraction for knowledge information.

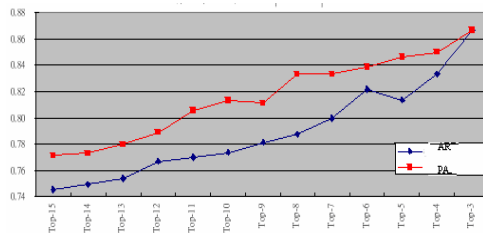


Fig. 1. The compared result of PA and AR

Smart structure is composed of smart elements (SMA) and matrix materials in physical or chemical product manufacturing process (casting, bound, extrusion etc.). The domain experts judged the node to be in the wrong location, showing that PART is superior to ART in clustering. Figure. 1 describes the method of comparison results

of AR and PA. By applying Bayesian network theory, we were able to generate a decision algorithm and hence helped to overcome the problems of the expert's knowledge by using the core part of the smart material.

5 Summary

The paper presents the method of constructions smart material knowledge system based on ontology Bayesian network and grid model in order to constructing the ontology model of knowledge management. After surveying the characteristics of different smart materials, shape memory alloy (SMA) is chosen for its large displacement.

References

1. Melnik, R.V.N.: Generalized solutions, discrete models and energy estimates for a 2D problem of coupled Field theory. *Applied Mathematics and Computation* 107, 27–55 (2000)
2. Kuo, R.J., Liao, J.L., Tu, C.: Integration of ART2 Neural Network and Genetic K-means Algorithm for Analyzing Web Browsing Paths in Electronic Commerce. *Decision Support Systems* 40(2), 355–374 (2005)
3. Cao, Y., Wu, J.: Dynamics of Projective Adaptive Resonance Theory Model: The Foundation of PART Algorithm. *IEEE Transactions on Neural Networks* 15(2), 245–260 (2004)
4. Zhang, S., Hsia, K.J.: Modeling the fracture of a sandwich structure due to cavitation in a ductile adhesive layer. *Journal of Applied Mechanics* 68, 93–100 (2001)

Research on Simulation of Electrostatic Discharge on Human Body Detonating the Gas

Shengman Liu^{*}, Ying Zhang, Tingtai Wang, and Jingchang Zhang

Zhongyuan University of Technology, Zhengzhou 450007, China
liusmlw@163.com

Abstract. Human body capacitance of miners decrease quickly to one tenth, body moving voltage increase up to a dozen at narrow exit in coal mine environment, which is a source easy to detonate the gas. The electrostatic half-life is relative with the material resistivity by study electrostatic leakage rules of human body. After a series of experiments of exploding the gas by human body electrostatic discharge simulation, the relationship between different human body capacitance, discharge gap and the gas concentration with exploding are obtained.

Keywords: simulation of electrostatic discharge on human body, human body capacitance, human body electrostatic potential.

1 Introduction

In recent years, many coal mine accidents happened, especially gas explosion accidents are common occurrences in the coal mine. Gas explosion caused by many reasons, as one of the natural hazard sources of society, electrostatic discharge caused a great loss and damage[1]. The gas explosion caused by electrostatic discharge, it is usually think that some insulating materials such as high-polymers produce static spark discharge in the coal, and the human body is ignored as an isolated conductor producing electrostatic discharge[2,3]. In fact, the human body electrostatic discharge is more harm than material's in coal mine. Therefore, it is necessary to research on human electrostatic discharge. In this paper, simulation of electrostatic discharges on human body and research on gas explosion under different conditions in coal mine environment.

2 Human Body Electrostatic Potential

JDY-3A electrostatic potential dynamic tester and TDS1001B oscilloscope is adopted to test the electrostatic potential of miners in the coal mine, as shown in figure 1(a). It is the peak waveform figure of human body electrostatic potential where miners take off rapidly, the peak value of the transient voltage is more than ten times, and the

^{*} Corresponding author.

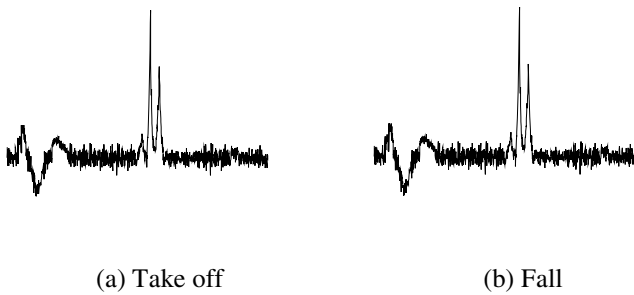


Fig. 1. Peak waveform figure of human electrostatic potential

figure 1(b) is the peak waveform figure of human body electrostatic potential where miners fallen suddenly, the peak value of the transient voltage is more than ten times. When the body voltage rise suddenly ten times such as 50V to 500V, the human body resistance is reduced to 1/10 the original or less, it affords the conditions for electrostatic rapid leakage.

3 Human Body Capacitance

The working place of miners is in underground mining, is in the narrow tunnel, the tunnel around the human body is coal wall, and the coal is conductor. We have designed a stainless steel cylinder of 1 meter in diameter, 3 meters high to simulate the narrow tunnel in mine. Men and women with different height and weight, in miners' clothes and dressed in different resistivity antistatic boots into the cylinder, and the human body capacitance in different locations is tested simulated in narrow tunnel. Table 1 is the human body capacitance's results simulated in the different locations of the tunnel. In the condition of temperature 19°C and relative humidity 35%, height range is 158-181cm, weight is 50-73kg. Outside is referred to the capacitance out of the cylinder of stainless steel is 145-175pF only. And inside, the capacitance was not much difference. Obviously, the human body capacitance has no direct relation with human's sex, height and weight. The results shown that the outside capacitance of the cylinder is lower obviously than inside, the human body capacitance increased ten times in tunnel more than it on common place. So when the miners are in the narrow tunnel exit, the capacitance reduce rapidly less than a tenth than it in the tunnel. When the human body static electricity did not change significantly, human body voltage will suddenly increase more than ten times. It's easy to become a source to ignite the gas. Therefore, the narrow tunnel exit is easy to become the source for accidents of human body electrostatic discharge.

Table 1. Results of human body capacitance in different locations of the narrow tunnel (Temperature : 19°C, Relative humidity : 35%)

Number	Sex	Height (cm)	Weight (kg)	capacitance (pF)				
				Outside	Front	Center	Back	Right
1	male	170	67	155	2610	2820	2620	2730
2	male	173	72	150	2400	2810	2800	2610
3	male	181	73	155	2710	3020	3000	2700
4	male	177	72	160	1700	1550	1520	1300
5	male	170	60	145	2900	3050	2910	2720
6	female	158	54	175	2800	3200	3150	2820
7	female	162	50	150	1800	2180	2100	2200
8	female	167	57	155	1610	1950	1520	1810
Average				156	2316	2573	2453	2361

4 Human Body Electrostatic Leakage Rules

Human body static electron leaks in two ways, one is the medium surface, the other is the medium inner, the former is related to surface resistivity, the latter is related to volume resistivity. The electrostatic leakage rules can be expressed by discharge half-life.

A gaussian face is taken from inner of the medium, the current through the closed surface between the current density vector $\vec{\delta}$ and medium electrical quantity Q meet:

$$I = \int_s \vec{\delta} \cdot d\vec{S} = -\frac{dQ}{dt}, \quad \text{and} \quad \vec{E} = \rho \vec{\delta}$$

$$\int_s \vec{E} \cdot d\vec{S} = \frac{Q}{\epsilon_0 \epsilon_r}, \quad \text{and} \quad \int_s \rho \vec{\delta} \cdot d\vec{S} = -\rho \frac{dQ}{dt}$$

or $-\rho \frac{dQ}{dt} = \frac{Q}{\epsilon_0 \epsilon_r}, \quad \frac{dQ}{Q} = -\frac{dt}{\epsilon_0 \epsilon_r \rho}, \quad \text{so} \quad Q' = Qe^{-\frac{t}{\epsilon_0 \epsilon_r \rho}}$

The time of electrical quantity leakage 1/2 is half-life,

$$Q' = \frac{1}{2} Q, \text{so}$$

$$\frac{1}{2} = e^{-\frac{\tau_{1/2}}{\epsilon_0 \epsilon_r \rho}} \quad \text{或} \quad \tau_{1/2} = 0.69 \epsilon_0 \epsilon_r \rho$$

$\tau_{1/2}$ is electrostatic half-life, ϵ_0 is vacuum dielectric constant, ϵ_r is relative dielectric constant, the value is from 3 to 9, electrostatic half-life is mainly relative with the medium resistivity. Therefore the index of the miners' clothes anti-static is vital whether it is qualified.

5 Human Body Electrostatic Discharge Model Detonated Gas Experiment

The apparatus is ‘‘Human body electrostatic discharge model detonated gas experiment system’’. The system is composed with gas mixture cavity, control unit, gas measuring unit, oxygen measuring unit, temperature measuring unit, body ESD model ignition devices, alarm display, PC and gas supply device. The system frame is shown in figure 2. The measurement accuracy of the gas concentration and the oxygen concentration for the system is 0.1%.

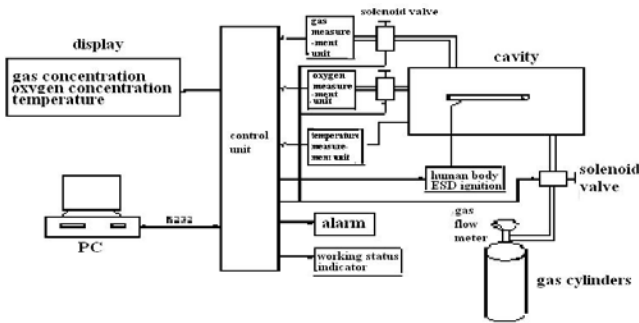


Fig. 2. System diagram

The experiment is carried out in the closed cavity, and the simulation system is controlled by computer, the cavity supply with the gas by gas supply device, and the environmental conditions oxygen content 20.9%, mixed gas temperature 22°C, and humidity 48%. The experiment began from gas concentration 5%; speed increased slowly 0.1% /s, until the gas concentration is up to 16%. In addition, the temperature and the concentration of oxygen and the gas by using sensors and infrared analyzer measuring in different time, and displayed by the display. Different body capacitances chosen to ignite by the human ESD model, simulation different human body capacitance in the coal, adjust the discharge gap, thus detonated the gas mixture in the tunnel. Detailed data is shown on table 2. It can be seen that the gas can be detonated, where the

Table 2. Results of the experiment system of detonated the gas by human ESD model (Oxygen content: 20.9%; Mixed gas temperature:22°C; Humidity: 48%)

Number	Gas concentration (%)	Human body capacitance (pF)	Human body resistance (Ω)	Discharge gap (mm)	Ruслut
1	8.8	1800	250	0.3	explosion
2	8.5	950	350	0.6	explosion
3	8.3	489	350	0.6	explosion
4	8.4	470	350	0.9	explosion
5	8.2	280	350	0.9	explosion
6	8.7	150	350	1.2	explosion
7	8.7	100	350	1.2	explosion

human capacitance range is change in 100-1800pF and the discharge gap is between 0.3-1.2 mm. And the most easy gas concentrations to explosive are in 8.5% or so.

6 Summary

In moving action, the human body electrostatic potential instantly improve more than ten times, when people get out of the narrow tunnel exit, because the human body capacitance reduced instantly and only a tenth of the original, so the voltage will instantly increase more than ten times, discharge energy greatly increased to become a source of ignition. Based on the analysis of the human body electrostatic leakage rules, electrostatic half-life is mainly relative with the medium resistivity. Therefore the index of the miners' clothes anti-static is very important. The results can be got from human body electrostatic discharge model detonated gas experiment, when the human body capacitance range is in 100-1800pF and the discharge gap is between 0.3-1.2 mm, it can detonated the gas, and the most explosive gas concentrations are in 8.5% or so.

Acknowledgements. This paper is supported by the National Natural Science Foundation of China (NSFC) with contact No. 50577068 and 50977093.

References

1. Liu, S.: Static Discharge and Danger Protect. Beijing University of Posts and Telecommunications Press, Beijing (2004) (in Chinese)
2. Nabours, R.E.: Static discharge hazard in explosive atmospheres. In: 2003 IEEE Technical Conference on Industrial and Commercial Power Systems, pp. 66–68 (2003)
3. Sam, M.M.: Avoiding Static Ignition Hazards in Chemical Operations. In: Chemical Process Safety, AIChE, pp. 105–106 (1999)

Delay-Dependent H_∞ Control for Uncertain Time-Delay Systems

Cheng Wang

College of Mathematics and Computer Science, Huanggang Normal University,
Huanggang 438000, China
awangc80@163.com

Abstract. This paper deals with the problem of delay-dependent robust H_∞ control for uncertain systems with time-varying delay and norm-bounded parameters. Sufficient conditions are proposed for the closed-loop stability with a guaranteed H_∞ performance index. The key features of the approach include the choice of an appropriate Lyapunov functional, the employment of free-weighting matrices and a method to estimate the upper bound of the derivative of Lyapunov functional without ignoring some useful terms. Sufficient condition is derived in terms of LMI that can be efficiently handled by using standard numerical algorithms.

Keywords: Robust H_∞ control, Time-delay system, delay-dependent criterion.

1 Introduction

Time-delays appear as an important source of instability or performance degradation in many practical systems. Therefore, the problem of H_∞ control for time-delay systems has received a lot of attention in the last decades. Depending on whether the existence condition of H_∞ controller includes the information of delay or not, the existing result can be classified into two types: delay-independent ones and delay-dependent ones. Generally, delay-dependent ones can usually provide less conservative results than delay-independent ones, especially when the time-delay is small. For recent years, researches have mainly focused on delay-dependent ones. In addition, in robust stability analysis of time-delay systems, early techniques for bounding cross terms were Park's inequality and Moon's inequality. Fridman and Shaked[1] proposed a descriptor model transformation of time-delay systems, and used the bounding techniques from both Park and Moon for H_∞ controller design. Gao and Wang[2] improved the results of [1]. Several other approaches have been developed to further reduce the conservativeness of delay-dependent conditions for robust control synthesis[1-7].

In this paper, the main contribution is to state LMI sufficient delay-dependent condition for the robust state feedback control stabilization design, which guarantees an H_∞ level of disturbance attenuation. The present result is derived by exploiting

an appropriate Lyapunov functional and free weighting matrices for time-delay systems that is less conservative, due to a method to estimate the upper bound of the derivative of Lyapunov functional, without ignoring some useful terms. Sufficient condition is derived in terms of LMI.

2 Problem Statement

Consider the following linear system with time-varying delay and parameter uncertainties

$$\begin{cases} \dot{x}(t) = (A + \Delta A)x(t) + (A_1 + \Delta A_1)x(t - h(t)) + (B + \Delta B)u(t) + B_1v(t) \\ Z(t) = Cx(t) + Du(t) \\ x(t) = \phi(t), \quad \forall t \in [-h, 0] \end{cases} \quad (1)$$

where $x(t) \in R^n$ is the state vector, $u(t) \in R^m$ is the control input, $v(t)$ is the disturbance input that belongs to $L_2[0, \infty)$, $z(t) \in R^q$ is the control output. $\phi(t)$ is the initial condition of the system. A, A_1, B, B_1, C and D are known parameter matrices of appropriate dimensions. $\Delta A, \Delta A_1, \Delta B_1$ denote the parameter uncertainties satisfying $[\Delta A(t) \Delta B(t) \Delta A_1(t)] = DF(t)[E_1 E_2 E_3]$, where D, E_1, E_2, E_3 are known real constant matrices, $F(t)$ is the time-varying uncertain matrix satisfying $F^T(t) \cdot F(t) \leq I \cdot h(t)$ is a time-varying function that satisfies $0 \leq h(t) \leq h$, $\dot{h}(t) \leq d$, where h and d are constants.

For control purposes, we consider the memoryless state feedback control law $u(t) = Kx(t)$.

Then, the closed-loop system of (1) is given by

$$\begin{cases} \dot{x}(t) = (A + B + \Delta A + \Delta BK)x(t) + (A_1 + \Delta A_1)x(t - h(t)) + B_1v(t) \\ x(t) = \phi(t), \quad \forall t \in [-h, 0] \end{cases} \quad (2)$$

The main control problem to be address in this section is stated below.

The robust H_∞ control problem: Given scalars h, d and $\gamma > 0$, determine a controller gain K such that the closed-loop system (2) is robustly stable and ensures a prescribed H_∞ disturbance attenuation, namely, under zero initial condition and for any nonzero $v(t) \in L_2[0, \infty)$, $\|z(t)\|_2 \leq \gamma \|v(t)\|_2$.

In this situation, the close-loop system is said to be robustly stable with disturbance attenuation level. The following lemma is introduced in order to handle the parameter uncertainties.

Lemma 1([7]). Given appropriately dimensioned matrices Ψ, H, G with $\Psi = \Psi^T$, Then $\Psi + HF(t)G + G^T F^T(t)H^T < 0$, holds for all $F(t)$ satisfying $F^T(t)F(t) \leq I$ if and only if for some $\varepsilon > 0$, $\Psi + \varepsilon HH^T + \varepsilon^{-1}G^T G < 0$.

2.1 Analysis and Synthesis for Uncertain Time-Delay System

In the following is presented the delay-dependent robust H_∞ performance analysis and control design for uncertain time-delay system(2).

Theorem 1. Given scalars h, d and $\gamma > 0$, the closed-loop system(2) is robustly stable with disturbance γ for time-varying delay if there exist symmetric positive definite matrices P, Q_1, Q_2, Z_1, Z_2 , positive scalars $\varepsilon > 0$, and appropriately dimensioned matrices $N_1, N_2, M_1, M_2, S_1, S_2$ satisfying

$$\begin{bmatrix} \psi_{11} & \psi_{12} & \psi_{13} & PB_1 & hN_1 & hM_1 & 0 & (C + DK)^T & \psi_{14} & \psi_{15} & E_1^T + K^T E_2^T \\ * & \psi_{22} & \psi_{23} & 0 & hN_2 & 0 & hS_1 & 0 & hA_1^T Z_1 & hA_1^T Z_2 & E_3^T \\ * & * & \psi_{33} & 0 & 0 & hM_2 & hS_2 & 0 & 0 & 0 & 0 \\ * & * & * & -\gamma^2 I & 0 & 0 & 0 & 0 & hB_1^T Z_1 & hB_1^T Z_2 & 0 \\ * & * & * & * & -hZ_2 & 0 & 0 & 0 & 0 & 0 & 0 \\ * & * & * & * & * & -hZ_1 & 0 & 0 & 0 & 0 & 0 \\ * & * & * & * & * & * & -hZ_2 & 0 & 0 & 0 & 0 \\ * & * & * & * & * & * & * & -I & 0 & 0 & 0 \\ * & * & * & * & * & * & * & * & \psi_{44} & \psi_{45} & 0 \\ * & * & * & * & * & * & * & * & * & \psi_{55} & 0 \\ * & * & * & * & * & * & * & * & * & * & -\varepsilon I \end{bmatrix} < 0 \tag{3}$$

where

$$\begin{aligned} \psi_{11} &= PA + A^T P + PBK + K^T B^T P + R_1 + R_2 + N_1 + N_1^T + M_1 + M_1^T + \varepsilon PDDP, \\ \psi_{12} &= PA_1 + N_2^T - N_1, \\ \psi_{13} &= M_2^T - M_1, & \psi_{14} &= h(A + BK)^T Z_1 + \varepsilon hPDDZ_1, \\ \psi_{15} &= h(A + BK)^T Z_1 + \varepsilon hPDDZ_2, \\ \psi_{22} &= -(1-d)R_1 - N_2 - N_2^T + S_1 + S_1^T, & \psi_{23} &= S_2^T - S_1, \\ \psi_{33} &= -R_2 - M_2 - M_2^T - S_2 - S_2^T, \\ \psi_{44} &= -hZ_1 + \varepsilon h^2 Z_1 DDZ_1, & \psi_{45} &= -hZ_1 + \varepsilon h^2 Z_1 DDZ_2, \\ \psi_{55} &= -hZ_2 + \varepsilon h^2 Z_2 DDZ_2. \end{aligned}$$

Proof: Choose a Lyapunov functional candidate as

$$V(t) = x^T(t)Px(t) + \int_{t-h(t)}^t x^T(s)R_1x(s)ds + \int_{t-h}^t x^T(s)R_2x(s)ds + \int_{-h}^0 \int_{\beta}^0 \dot{x}^T(t+\alpha)(Z_1 + Z_1)\dot{x}(t+\alpha)d\alpha ds$$

where P, R_1, R_2, Z_1, Z_2 , are symmetric positive definite matrices to be determined.

The time derivative of $V(t)$ is taken along the state trajectory (2), yielding

$$\begin{aligned} \dot{V}(t) \leq & 2x^T(t)P\dot{x}(t) + x^T(t)R_1x(t) + x^T(t)R_2x(t) - (1-d)x^T(t-h(t))R_1x(t-h(t)) + h\dot{x}^T(t)(Z_1 + Z_2)\dot{x}(t) \\ & - x^T(t-h)R_2x(t-h) - \int_{t-h}^t \dot{x}^T(\alpha)Z_1\dot{x}(\alpha)d\alpha - \int_{t-h(t)}^t \dot{x}^T(\alpha)Z_2\dot{x}(\alpha)d\alpha - \int_{t-h}^{t-h(t)} \dot{x}^T(\alpha)Z_2\dot{x}(\alpha)d\alpha \end{aligned} \quad (4)$$

From the Leibniz-Newton formula, the following equations hold for any appropriately dimensioned free-weighting matrices

$$2(x^T(t)N_1 + x^T(t-h(t))N_2)[x(t) - x(t-h(t))] - \int_{t-h(t)}^t \dot{x}(\alpha)d\alpha = 0. \quad (5)$$

$$2(x^T(t)M_1 + x^T(t-h)M_2)[x(t) - x(t-h)] - \int_{t-h}^t \dot{x}(\alpha)d\alpha = 0. \quad (6)$$

$$2(x^T(t-h(t))S_1 + x^T(t-h)S_2)[x(t-h(t)) - x(t-h)] - \int_{t-h}^{t-h(t)} \dot{x}(\alpha)d\alpha = 0. \quad (7)$$

Then , adding the left sides of (5)-(7)to (4), we have

$$\dot{V}(t) \leq \xi^T(t)(\Omega + h\tilde{N}Z_1^{-1}\tilde{N} + h\tilde{M}Z_2^{-1}\tilde{M} + h\tilde{S}Z_2^{-1}\tilde{S})\xi(t) + \Xi$$

where $\Omega = (\Omega_{ij})_{4 \times 4}$, $\Omega_{ij} = \Omega_{ji}$,

$$\begin{aligned} \Omega_{11} = & P(A+BK+\Delta A+\Delta BK) + (A+BK+\Delta A+\Delta BK)^T P + h(A+BK+\Delta A+\Delta BK)^T(Z_1+Z_2)(A+BK+\Delta A+\Delta BK) \\ & + R_1 + R_2 + N_1 + N_1^T + M_1 + M_1^T, \end{aligned}$$

$$\Omega_{14} = h(A+BK+\Delta A+\Delta BK)^T R(Z_1+Z_2) + PB_1, \quad \Omega_{24} = 0,$$

$$\Omega_{12} = N_2^T - N_1 + h(A+BK+\Delta A+\Delta BK)^T(Z_1+Z_2)(A_1+\Delta A_1) + P(A_1+\Delta A_1)$$

$$, \quad \Omega_{13} = M_2^T - M_1,$$

$$\Omega_{22} = -(1-d)R_1 - N_2 - N_2^T + S_1 + S_1^T + h(A_1+\Delta A_1)(Z_1+Z_2)(A_1+\Delta A_1),$$

$$\Omega_{23} = S_2^T - S_1,$$

$$\Omega_{33} = -R_2 - M_2 - M_2^T - S_2 - S_2^T, \quad \Omega_{34} = 0, \quad \Omega_{44} = hB_1^T(Z_1+Z_2)B_1,$$

$$\tilde{N} = [N_1^T, N_2^T, 0, 0]^T,$$

$$\Xi = \int_{t-h}^t (\xi^T(t)\tilde{M} + \dot{x}^T(\alpha)Z_1)Z_1^{-1}(\tilde{M}^T\xi(t) + Z_1\dot{x}(\alpha))d\alpha + \int_{t-h(t)}^t (\xi^T(t)\tilde{N} + \dot{x}^T(\alpha)Z_2)Z_2^{-1}(\tilde{N}^T\xi(t) + Z_2\dot{x}(\alpha))d\alpha$$

$$+ \int_{t-h}^{t-h(t)} (\xi^T(t)\tilde{S} + \dot{x}^T(\alpha)Z_2)Z_2^{-1}(\tilde{S}^T\xi(t) + Z_2\dot{x}(\alpha))d\alpha,$$

$$\tilde{M} = [M_1^T, 0, N_2^T, 0]^T, \quad \tilde{N} = [0, S_1^T, S_2^T, 0]^T.$$

Now, considering the H_∞ performance index

$$J = \int_0^\infty [z(t)^T z(t) - v(t)^T v(t)]dt.$$

Under the zero initial condition we have $V(0) = 0$ and $V(\infty) > 0$, the above index can be rewritten as

$$J \leq \int_0^\infty [z(t)^T z(t) - v(t)^T v(t) + \dot{V}(t)] dt \leq \int_0^\infty [\xi(t)^T \Gamma \xi(t) - \Xi] dt, \text{ where}$$

$$\Gamma = \Omega + h\tilde{N}Z_1^{-1}\tilde{N} + h\tilde{M}Z_2^{-1}\tilde{M} + h\tilde{S}Z_2^{-1}\tilde{S}$$

$$+ \begin{bmatrix} (C + DK)^T (C + DK) & 0 & 0 & 0 \\ * & 0 & 0 & 0 \\ * & * & 0 & 0 \\ * & * & * & -\gamma^2 I \end{bmatrix}$$

Since $\Xi \geq 0$, $\Gamma < 0$ implies that $J < 0$. After some manipulations using Lemma 1 and Schur complement, the equivalent to (3). Thus, system (2) is guaranteed to be robustly stable with H_∞ disturbance attenuation γ .

Based on the H_∞ stability analysis developed above the next theorem can be derived.

Theorem 2. Consider system (1) and let h, d and $\gamma > 0$ be given scalars. If there exist symmetric positive definite matrices X, Q_1, Q_2, T_1, T_2 , positive scalars $\epsilon > 0$, and appropriately dimensioned matrices $Y, \tilde{N}_1, \tilde{N}_2, \tilde{M}_1, \tilde{M}_2, \tilde{S}_1, \tilde{S}_2$ satisfying

$$\begin{bmatrix} \varphi_{11} & \varphi_{12} & \varphi_{13} & PB_1 & h\tilde{N}_1 & h\tilde{M}_1 & 0 & XC^T + Y^T D^T & \varphi_{14} & \varphi_{15} & XE_1^T + Y^T E_2^T \\ * & \varphi_{22} & \varphi_{23} & 0 & h\tilde{N}_2 & 0 & h\tilde{S}_1 & 0 & hQ_1 A_1^T & hQ_2 A_1^T & XE_3^T \\ * & * & \varphi_{33} & 0 & 0 & h\tilde{M}_2 & h\tilde{S}_2 & 0 & 0 & 0 & 0 \\ * & * & * & -\gamma^2 I & 0 & 0 & 0 & 0 & hQ_1 B_1^T & hQ_2 B_1^T & 0 \\ * & * & * & * & h(Q_2 - 2X) & 0 & 0 & 0 & 0 & 0 & 0 \\ * & * & * & * & * & h(Q_1 - 2X) & 0 & 0 & 0 & 0 & 0 \\ * & * & * & * & * & * & h(Q_2 - 2X) & 0 & 0 & 0 & 0 \\ * & * & * & * & * & * & * & -I & 0 & 0 & 0 \\ * & * & * & * & * & * & * & * & \varphi_{44} & \varphi_{45} & 0 \\ * & * & * & * & * & * & * & * & * & \varphi_{55} & 0 \\ * & * & * & * & * & * & * & * & * & * & -\epsilon I \end{bmatrix} < 0 \tag{8}$$

where

$$\varphi_{11} = AX + XA^T + BY + Y^T B^T + T_1 + T_2 + \tilde{N}_1 + \tilde{N}_1^T + \tilde{M}_1 + \tilde{M}_1^T + \epsilon DD,$$

$$\varphi_{12} = A_1 X + \tilde{N}_2^T - \tilde{N}_1,$$

$$\varphi_{13} = \tilde{M}_2^T - \tilde{M}_1, \quad \varphi_{14} = hXA^T + Y^T B^T + \varepsilon hDD,$$

$$\varphi_{15} = hXA^T + Y^T B^T + \varepsilon hDD,$$

$$\varphi_{22} = -(1-d)T_1 - \tilde{N}_2 - \tilde{N}_2^T + \tilde{S}_1 + \tilde{S}_1^T, \quad \varphi_{23} = \tilde{S}_2^T - \tilde{S}_1,$$

$$\varphi_{33} = -\tilde{R}_2 - \tilde{M}_2 - \tilde{M}_2^T - \tilde{S}_2 - \tilde{S}_2^T,$$

$$\varphi_{44} = -hQ_1 + \varepsilon h^2 DD, \quad \varphi_{45} = \varepsilon h^2 DD, \quad \varphi_{55} = -hQ_2 + \varepsilon h^2 DD.$$

Proof: By noting $Q_1 > 0, Q_2 > 0$, we have $(Q_2 - X)Q_2^{-1}(Q_2 - X) \geq 0$, $(Q_2 - X)Q_2^{-1}(Q_2 - X) \geq 0$, which are equivalent to

$$-XQ_1^{-1}X \leq Q_1 - 2X, \quad -XQ_2^{-1}X \leq Q_2 - 2X. \quad (9)$$

Pre-and post-multiplying (3) by

$$diag\{P^{-1}, P^{-1}, P^{-1}, I, P^{-1}, P^{-1}, P^{-1}, I, Z_1^T, Z_2^T, I\}$$

Setting

$$P^{-1} = X,$$

$$XM_i X = \tilde{M}_i, \quad XN_i X = \tilde{N}_i, \quad XS_i X = \tilde{S}_i, \quad XR_i X = T_i, \quad Z_i^{-1} = Q_i, \quad i = 1, 2,$$

$Y = KX^{-1}$, and using (9), we can obtain LMI (8). This complete the proof.

3 Conclusions

This paper has been concerned with the problem of robust H_∞ control for uncertain time-delay system. Based on the Lyapunov functional and free-weighting matrices, delay-dependent criterion has been formulated in terms of LMI that can be efficiently handled by using standard numerical algorithms.

Acknowledgments. This research is supported by the 2011 Excellent Youth Project of Hubei Provincial Department of Education to Cheng Wang, and the Project of Huanggang Normal University (No. 10CB146).

References

1. Fridman, E., Shaked, U.: IEEE Transactions on Automatic Control 47, 253–270 (2002)
2. Gao, H., Wang, C.: IEEE Transactions on Automatic Control 48, 520–525 (2003)
3. Fridman, E., Shaked, U.: International Journal of Control 76, 48–60 (2003)
4. Kim, J.H.: International Journal of System Science 32, 1345–1351 (2001)
5. Cao, Y.Y., Xu, S.Y., Lam, J.: IEE Proc. Control Theory Appl. 145, 338–344 (1998)
6. Palhares, R.M., Campos, C.D.: Computers and Mathematics with Applications 50, 13–32 (2005)
7. Yan, H.C., Zhang, H., Meng, X.Q.-H.: Neurocomputing 73, 1235–1243 (2010)

Statistical Analysis of Some Complex Censored Data

Huanbin Liu and Congjun Rao

College of Mathematics and Computer Science, Huanggang Normal University,
Huanggang 438000, China

lhb@hgnu.edu.cn, cjrao@foxmail.com

Abstract. Complex censored data, including right censored data, left-truncated and right censored data, multivariate failure time data and recurrent event data, etc., are a large class of important incomplete data existed in survival analysis, biological medicine research, reliability life test and other practical problems, and the statistical analysis for them has been valued all over the world, especially by developed countries, and the research results not only have important theoretical significance, but also have extensive application prospect. For the research on the four aspects, namely, regression analysis under left-truncated and right censored data, research on additive risk model under multivariate failure time data, parameter estimation for a general semiparametric ratio regression model under recurrent event data and the estimation of Cox model under the covariates with measurement errors and missing, this paper studies and reviews the development of those problems deeply, and points out the advantages and disadvantages of the existing studies, then puts forward some front issues.

Keywords: Right censored data, Left-truncated and right censored data, Multivariate failure time data, Recurrent event data.

1 Introduction

Complex censored data, including right censored data, left-truncated and right censored data, multivariate failure time data and recurrent event data, etc., are a large class of important incomplete data existed in survival analysis, biological medicine research, reliability life test and other practical problems, and the statistical analysis for them has been valued all over the world, especially by developed countries. Complex statistical analysis of censored data is focal point of research of modern statistics and the important part of the development of various disciplines. Analyzing complex data, establishing the corresponding statistical model, and revealing the internal laws of complex data are the important foundation of their relevant disciplines. Especially in the research on biology, medicine, ecology, demography, environmentology and economics and other disciplines, with the development of experimental techniques, testing methods and means of data analysis, the data obtained are more and more complex and precise in structure, and the information provided is more and more miscellaneous, which put forward higher requirements for the quantitative analysis of data. How to make statistical modeling and statistical

inference has become the frontier topic of biology, medicine, ecology, demography, environmentology and economics and other interdiscipline. In this research field, there still exist some problems to be solved by developing effective statistical methods. Statistical analysis and inference are made for left truncated and right censored data, multivariate failure time data, recurrent event data and the covariates with measurement errors and missing under the Cox model in this paper.

2 The Regression Method of Truncated and Censored Data

In reliability life test, biomedicine, astronomy, engineering, geological exploration and other practical issues, there often exists the situation that some interested random variables can not be observed, which mainly causes left truncated. But for those individuals which have entered in research, the general random right censorship might be caused, the data observed data are called left-truncated and right censored data, and the corresponding model is called left-truncated and right censored model. Research on this aspect can be seen Hyde [1], Tsai, etc. [2], Struchthers and Farewall [3], Uzunogullari and Wang [4] and He and Yang [5] and so on. Left truncated right censored model is a large class of important statistical model in survival analysis model, and plays its role in many areas of scientific research and industrial and agricultural production increasingly.

Consider the regression model $Y_i = x_i^T \beta + \varepsilon_i$, $i = 1, 2, \dots, n$, where x_1, x_2, \dots, x_n are the k dimensional nonrandom vector, x_i^T is the transpose of x_i , $\varepsilon_1, \varepsilon_2, \dots, \varepsilon_n$ are random variables which are independent and distributed identically with the distribution function F unknown, the response variable is left truncated right censored and can not be fully observed. It is assumed that (T_i, C_i) , $i = 1, 2, \dots, n$ are independent random vectors and independent from Y_i , let $Z_i = Y_i \wedge C_i = \min(Y_i, C_i)$, $\delta_i = I(Y_i \leq C_i)$. Because of censorship and truncation, (Z_i, δ_i) can be observed if and only if $Z_i \geq T_i$. Therefore, the observed data are $(Z_i, T_i, \delta_i, x_i)$, where $Z_i \geq T_i$, $i = 1, 2, \dots, n$. The discussion of the related models can be found in [6]-[7]. When $T_i = -\infty$, it is censored regression model; When $C_i = \infty$, it is truncated regression model; For the truncated and censored regression model, Lai and Ying [6,7] researched the rank estimation of β , and obtained the asymptotic normality of these estimations under certain conditions these. Here we put forward a kind of generalized product-limit estimates, and used it to define a kind of minimum L_2 distance of regression parameter estimates.

3 Additive Model under Multivariate Failure Time Data

Multivariate failure time data are data possessing several survival time, which are dependent with each other and has censored structure. Multivariate failure time data

often appear in the research fields such as biomedicine, economics and sociology and so on, for example, in the cohort studies in epidemiology (or cohort studies, cohort studies), when the disease broke out, the age data of a family member is multivariate failure time data or the treatment time received of littermate animals in animal experiments; in clinical trials, the presence of censorship, the complex dependency among multidimensional data, and covariates may be related to time.

Recently, most of the proposed marginal regression methods for the regression analysis of multivariate failure time data are supposed to be marginal risk Cox model. Liang et al. [8] proposed the marginal risk model for multivariate failure time data. Although the Cox risk model is considered to be the main tool in regression analysis of survival data, but the assumption of proportional hazards is not suitable for all data analysis. Therefore, it is necessary to find some new methods, and unite the risk function and risk factors of failure time together for statistical modeling. Additive hazard model can be used to describe different aspects of the links between the failure time and risk factors and fit the data fully. As Lin and Ying pointed out in [9], the estimate of regression coefficients of additive risk model has an explicit expression, contrasted with the Cox risk model; this expression will lead to more simple mathematical solution. In addition, for multivariate failure time data, the additive risk model is more credible than the Cox risk model in biology, and possesses a more intuitive interpretation for relative survival.

4 Recurrent Event Data

Recurrent event data are the data composed of recurring time of some interested events when several individuals are observed, which often appears in biology, medicine, society and economics and other research fields. For example, the multiple recurrence time of patient's certain disease, the repetitive infection time of AIDS and some infectious diseases, the repetitive recurrence time of anemia's certain tumor, each birth time of women in some countries, and the multiple recurrence time of mechanical defects and so on. The research on the kind of data is different from transversal data, because the recurring time of events is ordinal and has dependence, meanwhile, censored data exists and they might have dependence with the recurring time of events, making the analysis, modeling and statistical inference of recurrent event data become very difficult. However, due to the important features and a wide range of applications of recurrent event data's structure, the statistical analysis for it has been valued by countries all over the world, especially by developed countries, and the research results have not only of great theoretical significance, but also has broad application prospects.

In practical application, the individuals researched often possesses the effects of several covariates, some effects of the covariates are additive, some are multiplicative, and some are not only additive, but also multiplicative. In whole research process, when the data are recurrent event data, including at least three types of covariates: treatment factors; basic tumor number; most basic tumor size (measured in cm). The three covariates have different effects on the recurrence of the recurrent event obviously, some of which may be additive, and some might be a multiplicative.

5 Cox Model under the Measurement Errors and Missing of Covariates

In actual life, an ethnic group may mean a family, or the different observations corresponding to a single individual in the study. In general, the observations from the same ethnic group have the potential same characteristics, and there are correlations between them. The common method of fitting the correlation among life time data is to use a fragile model. The biggest problem of using fragile model is that the standard likelihood method can not directly be used to estimate parameters.

However, there has been some estimation methods under the assumption of given certain distribution. For example, On the assumption of log-normal distribution, McGilchrist and Aisbett [10] and McGilchrist [11] presented the estimation using the Cox partial likelihood method and the best linear unbiased prediction method; On the assumption of gamma distribution, Clayton and Cuzick [12], Klein [13], Klein, etc. [14] put forward an kind of EM-type algorithm, and required that the analytical form of conditional expectation of fragile variables existed under the observed data. On the same assumption of gamma distribution, Clayton [15], Aslanidou, Dey, and Sinha [16] proposed Monte Carlo method of Bayesian inference. For any fragile variable distribution with explicit laplace transform, Lam and Kuk [17] presented a marginal likelihood method to estimate the parameters, and realized it through Monte Carlo approximation method and re-sampling techniques.

In addition, covariates with measurement error are often encountered while analyzing the corresponding data. For independent survival data, some authors have researched measurement error. However, there are not many researches on the ethnicity censored data with measurement error. And Keiding, Andersen, and Klein [18] discussed the effects of rate risk models and accelerated failure time models when fragile variables and neglected covariates existed. Turnbull, Jiang and Clark [19], Jiang, Turnbull, and Clark [20] considered the effects of random individual heterogeneity and covariate measurement error on the parameter and semi-parametric regression of Poisson process respectively. Li and Lin [21] proposed a class of fragile measurement error model, when the fragile vector follows multivariate normal distribution and the measurement error is additive and normal. So far, there is no unified theory for the parameter estimation of the fragile model, especially when the covariates have measurement error, and there are no good estimate methods under general distribution assumption and covariate distribution assumption.

When no response can be neglected, there is a lot of work dedicated to research this parameter estimation of Cox model under such background. For example, when the data are missing at random completely (MCAR), Lin and Ying [22] proposed an asymptotic partial likelihood method, using full case estimation to replace part of conditional expectation. Paik [23] extended partial maximum likelihood method to the data missing at random through the interpolation method.

However, when the missing of covariates can not be ignored, for the Cox model, there is no satisfactory estimation method. Because the basic risk function is unknown, the previously mentioned methods can not be applied to such cases. Therefore, scientific and reasonable method has to be proposed to solve the parameter estimation problem of Cox model when the covariates are missing and the covariates can not be ignored, which is an important problem to be researched.

6 Conclusions

This paper summarizes some studies on complex censored data systematically and deeply, mainly including the regression analysis under left-truncated and right censored data, additive model under multivariate failure time data, statistical inference for a general semiparametric ratio regression model under recurrent event data, the estimation of Cox model under the covariates with measurement errors and missing. The study shows that simulation empirical analysis and the study on statistical properties for marginal partial likelihood method and the marginal likelihood methods and the marginal partial likelihood methods proposed by Cox model under the covariates with measurement errors and missing will be the hot issue which still need to be researched.

Acknowledgments. This work is supported by the Natural Science Foundation of Hubei Province, China (No. 2008CDB069), and Major Research Program of Hubei Provincial Department of Education, China (No. Z20092701), and the Innovative Group Project of Hubei Provincial Department of Education (No. 03BA85).

References

1. Hyde, J.: *Biometrika* 64, 225–230 (1977)
2. Tsai, W.Y., Jeweli, N.P., Wang, M.C.: *Biometrika* 74, 883–886 (1987)
3. Struthers, C.A., Faarewell, V.T.: *Biometrika* 76, 814–817 (1989)
4. Uzunogullari, U., Wang, J.L.: *Biometrika* 79, 297–310 (1992)
5. He, S., Yang, G.L.: *Ann. Statist.* 26, 992–1010 (1998)
6. Lai, T.L., Ying, Z.: *Ann. Statist.* 19, 531–556 (1991)
7. Lai, T.L., Ying, Z.: *Statistica Sinica* 2, 17–46 (1992)
8. Liang, K.Y., Self, S.G., Chang, Y.: *J. Roy. Statist. Soc. Ser. B* 55, 441–453 (1993)
9. Lin, Y.D., Ying, Z.: *Biometrika* 81, 61–71 (1994)
10. McGilchrist, C.A., Aisbett, C.W.: *Biometrics* 47, 461–466 (1991)
11. McGilchrist, C.A.: *Biometrics* 49, 221–225 (1993)
12. Clayton, D.G., Cuzick, J.: *J. R. Statist. Soc. A* 148, 82–117 (1985)
13. Klein, J.P.: *Biometrics* 48, 795–806 (1992)
14. Klein, J.P., Moeschberger, M.L., Li, Y.H., Wang, S.T.: *Estimating Random Effects in the Framingham Heart Study*. Kluwer, Dordrecht (1992)
15. Clayton, D.G.: *Biometrics* 47, 467–485 (1991)
16. Aslanidou, H., Dey, D.K., Sinha, D.: *Can. J. Statist.* 26, 33–48 (1998)
17. Lam, K.F., Kuk, A.Y.C.: *J. Amer. Statist. Assoc.* 92, 985–990 (1997)
18. Ha, I.D., Lee, Y., Song, J.K.: *Biometrika* 88, 233–243 (2001)
19. Turnbull, B.W., Jiang, W., Clark, L.C.: *Statist. Med.* 16, 853–864 (1997)
20. Jiang, W., Turnbull, B.W., Clark, L.C.: *J. Amer. Statist. Assoc.* 94, 111–124 (1999)
21. Li, Y., Lin, X.: *Biometrika* 87, 849–866 (2000)
22. Lin, D.Y., Ying, Z.: *J. Amer. Statist. Assoc.* 88, 1341–1349 (1993)
23. Paik, M.C., Tsai, W.Y.: *Biometrika* 84, 579–593 (1997)

Application Study on Detection of Pipeline Weld Defects Based on SVMs

Wu Xiao Meng, Gao Wei Xin, and Tang Nan

Xi'an Shiyou University, Xi'an, Shaanxi Province, China
xmwudz@xsyu.edu.cn, wxgao@xsyu.edu.cn,
ntang@xsyu.edu.cn

Abstract. A new method which is based on Support Vector Machines (SVMs) for the identification of pipeline weld defects is proposed. In order to enhance the quality of the image, a lot of actions, such as image enhancement, morphological processing and edge detection, have been dealt with. As a result, many problems, such as excessive noise, fuzzy edge and low contrast, have been solved and it's beneficial to extract the features of the image. Firstly, the results of the identification of the second category are given. Then combined with the characteristics of multiple classifications, three structures of clustering are presented and the structure of one against one has been adopted to identify the samples after analysis. The experimental results show that the proposed model has a lot of advantages, such as the identification accuracy, high speed, easy to implement, etc, and it's suitable for identification of pipeline weld defects.

Keywords: Support Vector Machine, Weld Defect, Image Segmentation, Feature Extraction, Identification.

1 Introduction

As a transmission device, the oil and gas pipeline is widely used in petroleum and petrochemical industries. The quality of welding has a direct impact on the safe operation of pipelines. It is very important for the security of oil and gas transportation to use testing technologies in different stages of the manufacture, installation of buried pipeline, by which the pipeline weld defect can be discovered timely.

There are many methods are included in non-destructive testing methods, such as radiation detection [1,2], ultrasonic testing method [3], magnetic detection method [4], eddy current testing method [5], and penetration testing method [6].The testing methods such as magnetic field, eddy current and penetration, are only suitable for surface or near surface defects, in which penetration testing method is limited to the surface breaking defect detection, and magnetic particle testing method is limited to ferromagnetic, and they have a higher sensitivity for linear defects such as cracks. Ultrasonic detection of internal defects is rapid and sensitive, but for quantitative or

qualitative analysis of defects certain difficulties are existed, and it is limited to the shape of the work pieces or grain size.

In recent years, with the rapid development of modern computer technology and digital imaging technology, some new detection method of weld defects based on machine learning and intelligent algorithms are developed quickly. In reference[7], the neural network quality monitoring model is used to predict solder joint shear strength, accuracy rate of 96.6%; In reference[8], the neural network model is used to predict the performance of body galvanized steel sheet spot welding; In literature [9], the neural network model is used to detect solder joint quality inspection and so on.

In order to solve a number of problems of the traditional detection of weld defects, and revise and improve some of the shortcomings of a number of intelligent algorithms, The Support Vector Machines (SVMs) is introduced in this paper, which is based on mathematical statistics theory. According to the limited sample information, the best compromise between the complexity of the model and learning ability (ie, error-free samples to identify any capacity) is found to obtain the best generalization ability to solve identification problem of the X negative weld defects.

2 Support Vector Machine

As a new universal learning method, Support vector machine was proposed by Vapnik, which is based on the VC dimension theory and structural risk minimization principle. The nonlinear based on small samples, high dimension and local minimum points and other practical problems can be solved better [10].

The basic idea of SVM is showed as Figure1, in the two-dimensional two types of linearly separable case, there are many possible linear classifiers to separate this set of data, but only one can get max margin interval of two categories, showing in graph H, the linear classifier is the optimal class hyperplane, and has better generalization by compared with other classifiers.

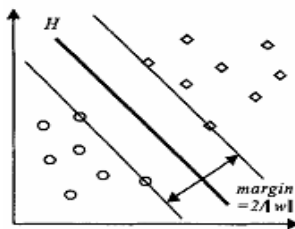


Fig. 1. The optimal class hyperplane

If the sample set $Q = \{(x_i, y_i) | i = 1, 2, \dots, n\}$ $x_i \in R^d, y_i \in [-1, +1]$, is linearly separable, then there exists a class hyperplane $\omega^T \cdot x + b = 0, x \in R^d$, for any (x_i, y_i) of sample set Q is met:

$$\begin{cases} w^T x_i + b \geq +1, \text{ 当 } y_i = +1 \text{ 时} \\ w^T x_i + b \leq -1, \text{ 当 } y_i = -1 \text{ 时} \end{cases} \quad (1)$$

R^d in the sample space $x = (x_1, \dots, x_d)^T$ to separating hyperplane, the distance $d = |w^T x + b| / \|w\|$, where:

$$\|\omega\| = \sqrt{\omega^T \cdot \omega} \quad (2)$$

When the presence of x makes $w^T x_i + b = \pm 1$, then classification of the interval of the super-plane in Figure 1:

$$margin = 2 / \|\omega\| \quad (3)$$

Maxing Classification interval margin, the hyperplane is the optimal class hyperplane. Finding the optimal class hyperplane will be translated into a quadratic programming problem as follows:

$$\min_{\Phi(\omega)} = \frac{1}{2} \|\omega\|^2 \quad (4)$$

Most samples α_i will therefore correspond to 0, a small part is not 0, which is a sample of the corresponding support vector. Finally, the classified discriminant function is:

$$g_{(x)} = \text{sgn}(f_{(x)}) = \text{sgn} \left(\sum_{\text{支持向量 } i} y_i \alpha_i^* (x_i, x) + b^* \right) \quad (5)$$

b^* is the classification threshold, which can take value from any pair of two kinds of support vector. According to the above easily knowing, for any sample $x = (x_1, x_2, \dots, x_d)^T$ of space R^d , when $|f_{(x)}| < 1$, then x is in the classification interval of hyperplane, the $|f_{(x)}|$ more tends to 0, the separating hyperplane for the discrimination between x is worse. When $|f_{(x)}| \geq 1$, x can be correctly classified. For linear inseparable problems, introducing slack variables can promote the concept of optimal separating hyperplane. More general approach is to meet the Mercer kernel function $K(x_i, x_j)$ which can be instead of type condition (5) in the inner product. It is through a non-linear mapping, in a high dimensional feature space, that an optimal separating hyperplane can be given.

3 The Application of SVMs in Detection of Pipeline Weld Defects

3.1 The Parameters Selection

According to GB6417-86 <metal fusion weld defect classification and description>, and with weld common situation, the weld defects roughly are divided into six

categories such as crack, incomplete penetration, incomplete fusion, porosity, slag, shape defect. As shape defects are recognized easily, so the other five defects about identification and classification are discussed in this paper.

Geometry of the image, the black level and black level distribution, and location of defects in the film are to identify defects on the three important aspects. By selecting the correct amount of extracted parameters, the correct weld defect will be identified and classified. Determining the characteristic parameters of defect categories includes the following six factors: aspect ratio $L1/L2$, round degree e , the equivalent area S / C , defects and the background gray level difference Δh , defect itself gray scale deviation δ and relative position of defects d .

3.2 Image Processing Technology

Before the weld images parameters were extracted, as the presence of noise in the picture, the picture must be pre-processing, to make the feature parameter extraction more accurate and easier. These image processing techniques mainly include:

Image enhancement: Usually people do not know the real reason for reduced image quality, but can take some measures to improve the picture quality. For example, the use of the enhance contrast method can make image more clearly, the use of filtering methods can reduce the noise to the image of the interference.

Edge detection: The extraction of target and background line, and then separating the target and background. Edge detection uses the difference between objects and background image features to achieve, these differences, including grayscale, color or texture and other features.

Morphological processing: Many morphological operations are based on dilation and erosion operations, for example, closed operation after the expansion operation and after the formation of a corrosive action is made, the result is the formation of the binary image the outline of a siege.

Binary: The performance difference between the background object is not the same gray value, the characteristics of this difference can be converted to grayscale difference, and then use threshold selection technique to split the image. Binaries image is a black and white picture, that is greater than the threshold value is set to be 255 gray, that is less than the threshold value is set to 0.

3.3 Characteristic Parameters Extraction

After weld image is preliminary processing, the next step is to extract the features of its six parameters. Length-width ratio $L1/L2$: In accordance with the mathematical definition, the aspect ratio is to be detected defect diameter and short diameter ratio.

Circular degrees: According to its mathematical definition: $e = 4\pi S^2 / C$. As long as the calculated area and perimeter of defects are obtained, circularity can be derived.

Equivalent area: According to the definition of style, that area and perimeter are known, equivalent area can be obtained. Gray scale difference Δh . Defined formula $\Delta h = \overline{Z_1} - \overline{Z_2}$. According to Function, the average gray background $\overline{Z_1}$ and

the defects of the average gray \bar{Z}_2 can be calculated, and then seek gray scale difference Δh .

Defect itself gray scale deviation δ . Defined as $\delta = \frac{\sum(Z_{\max} - Z)}{n}$, Z_{\max} is the maximum gray value for the defect, and Z is the gray value of any point defects. This parameter can also be achieved to strike through function. Parameters of weld pictures can be obtained by the above method.

4 Weld Image Identification Based on Support Vector Machine

4.1 Multi-classification Support Vector Machines Weld Image Recognition

It is not difficult to find that the general SVM is designed for two classifications, but not be directly used for many clustering problems. There are 5 types of weld defects, which is a multi-cluster problem, so SVMs can not be directly applied to solve real clustering of weld defects. Solve the clustering problems more commonly used in three ways: clustering method of one against rest, clustering method of & half against half, clustering method of one against one.

Clustering method of one to one is also called to ballot, which is in order for K class distinction between two training samples, during any two K categories, $[K*(K-1)] / 2$ SVM learning machines are constructed. That is any two samples to construct a learning model and the corresponding training samples will be divided into $[K*(K+1)] / 2$ samples, where each classifier is only in the corresponding subset to train and $[K*(K-1)] / 2$ SVM classifiers will be got. When tested by voting method, each testing sample is treated with $[K*(K+1)] / 2$ classifiers to identify, as it is the i -th class, then the i is added 1, otherwise the j -class is added 1 until the completion of all classifiers is over. That the class gets the most votes is the test sample category. Weld defects are in five categories, so it is necessary to establish the 10 SVM classifiers.

In this paper, using OAO strategy, first of all the training samples are divided into a sample subset; according to 10 samples, the corresponding SVM learning machine is established and then the corresponding subset of training samples are input to get the corresponding parameters W' and b' . According to 20 parameters W' and b' , 10 SVM classifiers are established to identify and test samples. That is the sign of the output value of y to determine the defect type.

5 Experimental Results

Classifier SVM-AB is by the A, B two types of training samples to get the classifier, SVM-AC, SVM-AD and... , SVM - meaning by analogy. In order to facilitate according to the output value judgment defect category, type of training sample subset of the letters on behalf of the front class is set to -1 class, the letter by the defect type is set to +1 after the class. If the sample includes A and B two types of samples, the A class sample is set to -1 class, and B class samples is set to +1 class, by analogy all samples can be centralized two i, j samples. (i separately defect category A, B, C, D, j

separately B, C, D, E, j represents category i after than by letters). So, when the classifier SVM- ij identification of a sample of the output is negative, it means that the classifier to determine the sample belongs to the i class; the result is positive, then the judge for the j class.

6 Conclusion

According to characteristics of the weld defect classification, three different multi-classification algorithms such as OAR, HAH and OAO are analyzed in this paper. OAO clustering method is selected, by which the defect of certain type of sample is voted used in SVM classifiers. The error caused by the individual classifiers is reduced. This is better for X-ray negative identification to get good recognition effect, with strong promotional.

Acknowledgment. This paper is Supported by the Science and Technology Project of Xi'an (YF07033), Specialized Research Plan Project of Shaanxi Provincial Education Department(09JK699), Natural Science Basic Research Plan Project of Shaanxi Province(2010JQ8033).

References

1. Dahai, R.: Automatic Analysis System of X-ray Real Time Imaging for Weld Line. Jointing Transaction 21(1), 61–63 (2000)
2. Zhang, X.: Exaction and Automatic Identification of jointing defect of radial detection. National Defense Publishing Company, Beijing (2004)
3. Chen, H.: Robot Used on Pipeline Detect by Ultrasonic. Robot Technique and Application (5), 28 (1995)
4. Chong, W.: Magnetism Dipole and Powder Detect. No Damage Check 12(3), 66–70 (1990)
5. Cao, X.: Whirlpool Detect of Welding Steel Tube on Product Line. South Steel (6), 33–35 (1997)
6. Gao, H., Sun, N.: Application of Metal Measure Method in Power Plant. Power Plant System Engineering 26(6), 55–58 (2010)
7. Zhang, P., Chen, J.: Spot Welding Inspection of Image Process Based on Welding Spot. Jointing Transaction 27(12), 57–60 (2006)
8. Zhao, X., Zhang, Y.: Performance Forecast of Spot Welding Based on Nerve Network Optimization. Jointing Transaction 27(12), 77–80 (2006)
9. Zhang, Z., Li, D., Zhao, H.: Function Selection of Nerve Network Detect Model. Jointing Transaction 23(3), 59–62 (2002)
10. Vapnik, V.: An overview of statistical learning theory. IEEE Transaction Neural Networks 10(5), 988–999 (1999)

Analysis and Evaluation of Operation Mode for 35kV Loop-Network of Oilfield Distribution

Wu Xiao Meng, Yan Su Li, and Gao Wei Xin

Xi'an Shiyou University, Xi'an, Shaanxi
Province, China
xmwudz@xsyu.edu.cn, yansl2002@163.com,
wxgao@xsyu.edu.cn

Abstract. Two operation mode of 35kV loop-network of oilfield are introduced in this paper. The power flow calculation and evaluation are also given for each mode. Comparing two modes from economy, reliability and sensitivity, results show that the closed loop mode is feasible.

Keywords: Loop-network, Operation Mode, Open Loop, Closed Loop, Oilfield.

1 Introduction

The 35kV system of certain oilfield distribution is the loop network operation. There are two mode of loop network: closed loop and open loop. There have different opinions about the losses of the main lines under different operation modes. Nowadays the operation mode of grid is closed loop operating, but which kind of operation is much better? For this, we need to make a detailed analysis from both economic and security aspect, and get the accurate conclusion which will act as a guiding help for the safety and economical operation in oilfield network.

Three basic requirements are needed for any grid operation mode, which are economy, reliability and sensitivity. Only considering comprehensively from these three aspects, at the same time combined with practical needs of oilfield network, the accurate conclusion can be got.

2 System Diagram and the Computation Basis Data

There are three lines: Kai-wen, Kai-sheng line and Sheng-wen line. The parameters are as following: $r_1 + jx_1 = (0.27 + j0.379)\Omega/\text{km}$, $b_1 = 2.76 \times 10^{-6} S/\text{km}$. The diagram of 35kV system is shown in Fig.1.

The parameters of line and equipment are show in table1, the variable ratio is 35kV/10.5kV.

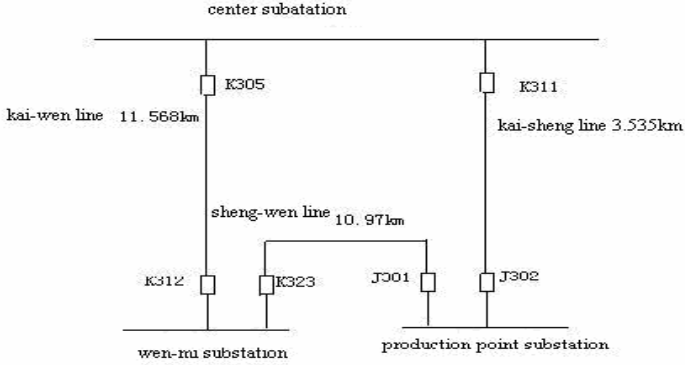


Fig. 1. 35kV system diagram

Table 1. The parameters of line and equipment

substation	transformer	load losses [kW]	unloaded losses [kW]	load of 10kV side[kVA]	
				1 #	2 #
Wen-mi	SF7-8000	46.671	9.7	3102.2+j639	3054.7+j497.3
production point	SF7-4000	32.5	5.65	2598.8+j1523.4	2603.2+j495.8

3 Calculation of Substation Load and the Losses of Line

3.1 The load of Wen-mi Substation and Production Point Substation

Wen-mi substation: The rated voltage for 10kV side of center transformer is 10.5kV.

1# main transformer:

$$U_2 = 10.5 \times 35 / 10.5 = 35kV \tag{1}$$

$$\Delta P_{\varepsilon T} = \frac{P^2 + Q^2}{U_2^2} R_T = 0.00728MW \tag{2}$$

$$\Delta Q_{\varepsilon T} = \frac{P^2 + Q^2}{U_2^2} X_T = 0.00097MVar \tag{3}$$

$$\Delta U_T = \frac{PR_T + QX_T}{U_2} = 0.00.0183kV \tag{4}$$

$$\delta U_T = \frac{PX_T - QR_T}{U_2} = -0.0055kV \tag{5}$$

$$U_1 = \sqrt{(U_2 + \Delta U_T)^2 + (\delta U_T)^2} = 35.08kV \tag{6}$$

$$\Delta P_{yT} = G_T U_1^2 = 0.00998MW \tag{7}$$

$$\Delta Q_{yT} = B_T U_1^2 = 0.000396MVar \tag{8}$$

$$\tilde{S}_1 = P_1 + jQ_1 = (P + \Delta P_{zT} + \Delta P_{yT}) + j(Q + \Delta Q_{zT} + \Delta Q_{yT}) = 3.12 + j0.641MVA \tag{9}$$

Similarly, the load for 2# main transformer of Wen-mi substation and center transformer of production point substation can be calculated, which showed in table2.

Table 2. The calculation result

substation	the load for 35kV side of 1 # [MVA]	the load for 35kV side of 2 # [MVA]	The voltage for 35kV side [kV]	The total load for 35kV side [MVA]
wen-mi	3.12+j0.641	3.07+j0.5	35.08	6.192+j1.139
production point	2.617+j1.526	2.623+j0.498	35.19	5.24+j2.019

3.2 Preliminary Power Distribution of 35kV Loop-Network

Assuming the whole network are all rated voltage $U_N=35kV$,it count to the corresponding load of the substation that generate reactive power which are on the Kai-wen line,Kai-sheng line,Sheng-wen line.

For, half of the Susceptance are $1.6 \cdot 10^{-5}S$, $4.878 \cdot 10^{-5}S$, $1.514 \cdot 10^{-5}S$ for Kai-wen line, Kai-sheng line and Sheng-wen line respectively. Then the reactive power are $-j0.0011MVA$ and $-j0.0007MVA$, which connect with the bus of Wen-mi substation and the bus of production point substation respectively.

The power load of production point and Wen-mi substation are $5.24+j2.023MVA$, $6.192+j1.138MVA$ respectively.The impedance of Kai-sheng line, Kai-wen line, Sheng-wen line are $0.954+j1.34 \Omega$, $3.123+j4.384 \Omega$, $2.962+j4.158 \Omega$ respectively.

The total line length is $l=l_{12}+l_{23}+l_{31}=26.073km$. Preliminary power distribution shown in Fig.2.

4 Power Flow Calculation and Evaluation of Closed Loop

4.1 Closed Loop Flow Calculation

It choose K323 switch which is wen side in the wen-sheng line as the ring network breaking point because of the reactive power points in wen-mi substation, the voltage of two main transformer regard as switching voltage on either side.

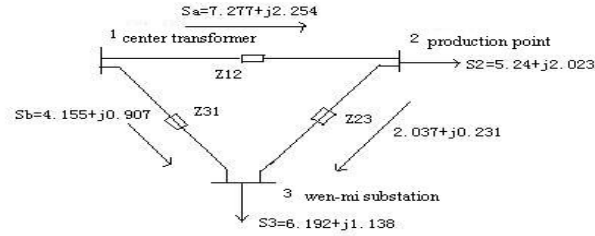


Fig. 2. Preliminary power distribution

The circular power is $0.183+j0.257$ MVA. The direction of cycle power is counterclockwise. According to the rated voltage of the network is 35kV, computing power loss is $3.972+j0.65$ MVA.

For Kai-wen line, the power on the Kai side is $4.013+j0.708$ MVA. For Sheng-wen line, the power on the Sheng side is $2.233+j0.506$ MVA. For Kai-sheng line, the power on the Sheng side is $7.473+j2.529$ MVA. For Kai-sheng line, the power on the Kai side is $7.522+j2.579$ MVA. The total output power of 35kV center transformer is $11.535+j3.305$ MVA. The total substation load is $11.432+j3.161$ MVA. The total loss power is $0.103-j0.147$ MVA. The transmission efficiency in closed loop mode is $1-0.103/11.535=99.11\%$. If considering the transformer loss, the transmission efficiency is $11.36/11.535=98.48\%$.

4.2 The Preliminary Evaluation of Closed Loop Operation

Under closed loop running modes, grid supplies electricity from both two sides which greatly improving the reliability of the grid operation. Although the relay protection way of closed loop operation mode is more complex compared with the open-loop operation, because we need to take directional property of the closed loop relay protection into consideration, but as long as we set the protect setting value well, and the oilfield network is relatively simple which will produce little influence on the reliability of grid operation. If we consider from the economical aspect, the meritorious loss of 35kV ring network lines covers as much as 0.89 percent of the whole output active power. The economy property of oilfield power grid is comparable good in close loop running modes.

5 Power Flow Calculation and Evaluation of Open Loop Operation Mode

5.1 The Power Flow Calculation of Open Loop Operation

Now will give the J301 switch of sheng side off on the sheng-wen line, as the breaking point for the open-loop operation. Let Kai-wen line carry the load of Wen-mi substation, let Kai-sheng line carry the load of substation which are production point substation.

Made power system flow calculation after giving the J301 switch off for the sheng side.

The power loss of kai-sheng line is $0.0243+j0.027$ MVA. The transmission efficiency of kai-sheng line is $5.24/5.2643=99.54\%$. Obviously, the transmission efficiency of kai-sheng line is very high.

Use the same method to calculate the trend of kai-wen line. So the power loss of Kai-wen line is $0.101+j0.12$ MVA. The transmission efficiency of Kai-wen line is: $6.192/6.293=98.4\%$. Obviously, the transmission efficiency of Kai-wen line is also very high.

The line loss of the whole loop network system with open operation is $0.125+j0.147$ MVA, it is $0.022+j0.003$ MVA more than closed loop operational mode which is $0.103+j0.144$ MVA.

The sum of the power which outflow of the center transmission is $11.557+j3.305$ MVA when the whole ring network system is open loop, it is increased 0.022 MW than in the closed loop operational modes which is $11.535+j3.305$ MVA;

The total transmission efficiency of line is $11.432/11.557=98.92\%$, it is reduced 0.19% than in the loop operational modes which is 99.11% .

5.2 The Evaluation of the Open Loop Operation Mode

From the reliable property, open-loop operation mode is less complex in some degree, but the reliable property of grid operation declined greatly when examining and repairing equipments. From the economy property, open-loop operation mode has no superiority. Compared with closed loop operation mode, the loss of open loop operation mode of the main grid road will increase: $22*24*365=192720$ kW·h. So the open loop operation mode is relatively Simpler compared with the relay protection ways of close loop operation mode. The reliability of supplying power in oilfield network will decline if we use Open-loop operation mode, this grid operation mode is not advisable.

6 The Comprehensive Evaluation of Operation Mode

Reliability

Bilateral power supply in closed loop running modes greatly improve the reliability of using electricity, compared with open-loop operation mode, the close loop operation mode has Incomparable advantages. Although closed loop operation mode is more complex in relay protection, because oilfield power system is relatively simpler, As long as we set the relay protection setting value well, this disadvantage does not influence reliability of grid operation.

Economy

Closed loop operation mode has a better economy property than open-loop operation mode because of the uniform loads of two substation, the features of circular power, structure characteristics of oilfield distribution etc. Of course, if Kai-sheng line can be a little bit longer, the economy property of open-loop operation mode will be obvious. Assumed that the open production line is three times longer, namely it has the same length with another two lines. Line loss of loop operation mode will reach above

200kW which is two times than that at present. Therefore, in order to maintain the current line loss and circular power level, the voltage drop of two 35kV substations must be remained at a lower level. The most important thing is to ensure the production point substation is consistent with Wen-mi substation. Even transfer it to 35/10, the line loss of main line also will reach 288kW.

Circular Current

There will be a circular current as strong as $5.23+j7.34$ A in loop net adopting closed loop mode which will bring certain hidden trouble for the safe operation of power grids. Analyzed the process and result of flow calculation, the reasons of circulation current production is that the production point substation does not balance 35kV side voltage. Therefore it is very important to maintain the two voltages balanced in close loop mode. First of all, the two substations change simultaneously. By calculating, the loop network voltage will drop to 1.64 kV, if the change reaches to 3.5/10, Circular current will be 14.91 times than that at present, namely $77.98+j109.44$ A, which is very dangerous.

Bus Voltage Drop of Center Substation

Bus voltage drop is caused by excessive circulating current increases, which will have cumulative effect on the main transformer by reducing their enduring Disconnecting the two bus will increase the unity of operating mode, the reliability of power grid will be further reduced. If the two 35kV buses of the center transformer associated, the bus pressure drop will be reached 0.37kV under the open loop mode, but in the closed loop mode, it will be 0.11kV, that is much smaller than open loop mode.

7 Conclusion

By considering the above four aspects, closed loop operation mode is better than open loop mode both the reliability and economical efficiency of grid operation with great superiority. Therefore close loop operation mode should be adopted in 35kV loop network system of oilfield, except the line maintenance and inevitable power outage.

Acknowledgment. This paper is Supported by CNPC Innovation Foundation (2010D-5006-0601).

An Improved Differential Evolution Algorithm for Optimization Problems

Libiao Zhang¹, Xiangli Xu¹, Chunguang Zhou¹, Ming Ma², and Zhezhou Yu^{1,*}

¹ College of Computer Science and Technology, Jilin University,
Changchun 130012, China
yuzz@jlu.edu.cn

² Information Management Center, Beihua University,
Jilin 132013, China
lbzhang@jlu.edu.cn

Abstract. There are many optimization problems in the intelligent material and adaptive material fields. Differential evolution (DE) is simple and effective and has been successfully applied to solve optimization problems. And it can be applied to intelligent material field. It is easy to understand and realized and has a strong spatial search capability compared to other evolutionary algorithms. In order to avoid the original versions of DE to remain trapped into local minima and accelerate the optimization process, several approaches have been proposed. The mutation of the classical DE is improved in this paper. It effectively guarantees the convergence of the algorithm and avoids the local minima. Testing and comparing results showed the effectiveness of the algorithm.

Keywords: Differential Evolution, Optimization Problems, Evolutionary Algorithms, Intelligent Materials.

1 Introduction

The many problems are the optimization problems in intelligent material field. Evolutionary Algorithms (EA) have been successfully applied to solve optimization problems [1, 2, 3, 4]. The most popular EA include: Genetic Algorithm (GA) [5], Particle Swarm Optimization (PSO) [6], and DE [7] and so on. Recently, many works have been proposed to improve the EA in order to accelerate its convergence speed and to prevent the algorithms from getting trapped into local minima of the objective function [8, 9].

DE is a new evolutionary algorithm was proposed by Storn and Price in 1997[7]. It is population-based, direct search algorithm, adopting real number coding, simple and effective and has been successfully applied in various fields [10, 11]. It is easy to understand and realized and has a strong spatial search capability compared to other evolutionary algorithms. As a new evolutionary algorithm, DE is similar to GA in the sense that it uses same evolutionary operators like mutation, crossover and selection

* Corresponding author.

for guiding the population towards the optimum solution. DE algorithm firstly generates initial population at random in the search space. DE algorithm creates new individuals by adding the vector difference between two randomly chosen individuals to a third individual in the population. If the new individual has a better value of the fitness function then it will replace old individual. In order to avoid the original versions of DE to remain trapped into local minima and accelerate the optimization process, several approaches have been proposed [12, 13]. The mutation of the classical DE is improved in this paper. It effectively guarantees the convergence of the algorithm and avoids the local minima.

2 Differential Evolution

DE algorithm is easy to understand and realized and is also very efficient computationally compared to other evolutionary algorithms. The main operators of DE are mutation, crossover and selection. The main operator in DE is rather different than in other evolutionary algorithms. Given the population size is NP and D is the dimensions of the vector then each individual is represented as a real parameter target vector $x_i = [x_{i1}, x_{i2}, \dots, x_{iD}]$ ($i = 1, \dots, NP$) in the population. For each a target vector, a so called mutant vector v_i is generated, as the follows formula:

$$v_i = x_{r_1} + F \times (x_{r_2} - x_{r_3}), \quad i = 1, \dots, NP \quad (1)$$

Where, $x_{r_1}, x_{r_2}, x_{r_3}$ are selected distinct vectors from the population at randomly, and $r_1 \neq r_2 \neq r_3 \neq i$. F is a real constant parameter that controls the effect of the differential vector $(x_{r_2} - x_{r_3})$. It is called scaling factor and lies in the range 0 to 2.

The crossover operator of DE algorithm increases the diversity of the mutated vector by means of the combination of mutant vector v_i and target vector x_i . The algorithm generates new vector $u_i = [u_{i1}, u_{i2}, \dots, u_{iD}]$ by as the follows formula:

$$u_{ji} = \begin{cases} v_{ji} & \text{if } randb \leq CR \text{ or } j = randr, \\ x_{ji} & \text{if } randb > CR \text{ or } j \neq randr, \end{cases} \quad (2)$$

$$i = 1, \dots, NP, \quad j = 1, \dots, D,$$

Where, $randb$ is a uniform random number from $[0,1]$. CR is a parameter in $[0,1]$, which specifies the crossover constant. $randr \in [1, 2, \dots, D]$ is a randomly chosen index which ensures that u_i gets at least one element from v_i , otherwise no new parent vector would be produced and the population would not alter.

The selection operation of DE uses a greedy selection scheme: If and only if the new vector u_i have a better fitness function value compared with the target vector x_i , the new vector u_i becomes a new parent vector at next generation, otherwise the old vector x_i is retained to serve as a parent vector for next generation once again.

Pseudo code for the original versions DE algorithm as follows:

- (1) Set the algorithm parameter: the population size NP , scale factor F , crossover rate CR ;
- (2) Generate the initialized population P in the constrained;
- (3) Evaluate objective function fitness for the initialized population P ;
- (4) For each individual x_i perform the mutation operator via by Equation (1), and generate mutant vector v_i ;
- (5) For each mutant vector v_i perform the crossover operator via by Equation (2), and generate the new vector u_i ;
- (6) For each the new vector u_i perform the selection operator, if $u_i > x_i$, then $x_{i+1} = u_i$, else $x_{i+1} = x_i$;
- (7) If the terminal conditions meet, otherwise for new generation individual x_{i+1} return to (4).

3 Improved Differential Evolutions

The analysis of DE algorithm can be seen that the mutation is relatively blind, thus convergence of the algorithm to be affected. Therefore, DE algorithm has been improved in this paper. The crossover and selection are same as original DE. In the mutation process, for the mutation vector v_i of any one target vector x_i , it is decided by three vectors that the global best $gBest$ and local best vector $lBest$ and target vector x_i . $gBest$ is the best vector of the population has experienced by far the group has experienced. $lBest$ is the best vector in current population. This mutation operation than a random selection of two vectors have a clearer direction. It is a better guarantee of convergence, and it guaranteed the diversity of solutions by the select mode of $gBest$ and $lBest$ and current vector, thus the search capabilities of the population is further strengthened. The formula of improved mutation is as follows:

$$v_i = lBest + (gBest - x_i), \quad i = 1, \dots, NP \quad (3)$$

4 Experimental Settings and Results

As to the parameters of DE, set the population size $NP = 20$, zoom factor $F = 0.6$, and cross constant $CR = 0.5$, maximum number of generations is 200. The four well-known benchmark problems of single objective optimization are used to assess performance of the proposed algorithm in this paper in the Table 1. For each benchmark function, twenty experiments were done. This paper algorithm has been compared to DE for the test functions.

Table 1. Test Functions

Test function	Dimensionality	Ranges of the variables	f_{\min}
$f_1(x) = \sum_{i=1}^N x_i^2$	30	$-100 \leq x_i \leq 100$	0
$f_2(x) = \sum_{i=1}^N (\lfloor x_i + 0.5 \rfloor)^2$	30	$-100 \leq x_i \leq 100$	0
$f_3(x) = \sum_{i=1}^N (x_i^2 - 10 \cos(2\pi x_i) + 10)$	30	$-5.12 \leq x_i \leq 5.12$	0
$f_4(x) = \sum_{i=1}^{N-1} ((1 - x_i)^2 + 100(x_{i+1} - x_i^2)^2)$	30	$-5 \leq x_i \leq 10$	0

Table 2. Test Results

Test function	DE		This paper	
	Mean	Best	Mean	Best
f_1	0	0	0	0
f_2	0.8956	0.3243	0.0231	0
f_3	192.4446	185.1046	16.3689	4.9945
f_4	781.1454	770.6392	28.4231	27.7710

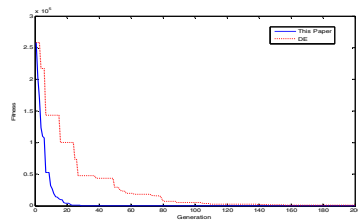
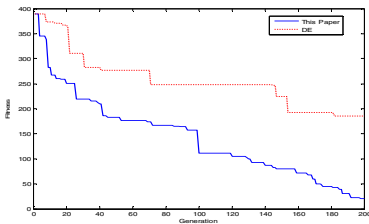


Fig. 1. Convergence Graph for f_3 **Fig. 2** Convergence Graph for f_4

According to test results in Table 2, it was observed that the results of the proposed algorithm are better than DE algorithm. It was observed that the proposed mutation can improve the DE performance and better convergence stability, too. Furthermore, it was observed from Fig 1 and Fig 2 that the proposed algorithms converged much faster than the DE.

5 Conclusions

In this paper, the Improved DE has been presented. It can be applied to intelligent material field. The mutation of the classical DE is improved, and this mutation operation than a random selection of two vectors have a clearer direction and a better guarantee of convergence. When compared this paper algorithm with DE, it is clear that it has better performance and better convergence. Therefore this paper algorithm is more effective than DE algorithm.

Acknowledgment. This paper is supported by (1) the National Natural Science Foundation of China under Grant No. 60873146、60973092、60903097, (3) project of science and technology innovation platform of computing and software science (985 engineering), (4) the Key Laboratory for Symbol Computation and Knowledge Engineering of the National Education Ministry of China, (5)the Science and Technology Development Planning Project of Jilin Province (No.20080168), (6)The Natural Science Foundation of Jilin Province (No.201115022).

References

1. Bäck, T., Schwefel, H.P.: An Overview of Evolutionary Algorithms for Parameter Optimization. *Evol. Comput.* 1, 1–23 (1993)
2. Deb, K., Pratap, A., Agarwal, S., Meyarivan, T.: A Fast and Elitist Multiobjective Genetic Algorithm: NSGA2 II. *IEEE Transactions on Evolutionary Computation* 6(2), 182–197 (2002)
3. Parsopoulos, K.E., Vrahatis, M.N.: Particle Swarm Optimizer In Noisy and Continuously Changing Environments. In: *Proceeding of the IASTED International Conference on Artificial Intelligence and Soft Computing*, pp. 2892–2894. I2ASTED/ ACTA Press, ICancun, Mexico (2001)
4. Michalewicz, Z., Shoenauer, M.: Evolutionary Algorithms for Constrained Parameter Optimization Problems. *Evolutionary Computation* 4(1), 1–32 (1996)
5. Goldberg, D.: *Genetic Algorithms in Search, Optimization, and Machine Learning*. Addison-Wesley, Reading (1989)
6. Kennedy, J., Eberhart, R.: Particle Swarm Optimization. In: *IEEE International Conference on Neural Networks*, Perth, Australia, pp. 1942–1948. IEEE Service Center, Piscataway (1995)
7. Storn, R., Price, K.: Differential Evolution-A Simple and Efficient Heuristic for Global Optimization Over Continuous Spaces. *Journal of Global Optimization* 11(4), 341–359 (1997)
8. Tsai, J.-T., Liu, T.-K., Chou, J.-H.: Hybrid Taguchi-Genetic Algorithm for Global Numerical Optimization. *IEEE Trans. Evolutionary Computation* 8(4), 365–377

9. Dorronsoro, B., Bouvry, P.: Improving Classical and Decentralized Differential Evolution with New Mutation Operator and Population Topologies. *IEEE Transactions on Evolutionary Computation* 15(1), 67–98
10. Mayer, D.G., Kinghorn, B.P., Archer, A.A.: Differential Evolution - an Easy and Efficient Evolutionary Algorithm for Model Optimization. *Agricultural Systems* 83(3), 315–328 (2005)
11. Rui, M., Arvind, M.: DynDE: A Differential Evolution for Dynamic Optimization Problems Mendes. In: *IEEE. Proceedings of the 2005 IEEE Congress on Evolutionary Computation (CEC 2005)*, pp. 2808–2815. IEEE Service Center, New York (2005)
12. Mezura-Montes, E., Velázquez-Reyes, J., Coello, C.A.C.: Modified Differential Evolution for Constrained Optimization. In: *2006 IEEE Congress on Evolutionary Computation, Vancouver, BC, Canada, July 16-21*, pp. 25–32 (2006)
13. Ali, M., Pant, M., Singh, V.P.: An Improved Differential Evolution Algorithm for Real Parameter Optimization Problems. *International Journal of Recent Trends in Engineering* 1(5), 63–65 (2009)

Case Study about City Brand Image Design Orientation of ZhangShu

Guobin Peng

Design and Art College GuiLin University of Electronic Technology
Guilin, P.R. China
pengguobin@guet.edu.cn

Abstract. City image design orientation not only need to conform to local conditions, but also need to consider long-term requirements which local government stress on the city's brand strategy, have to fully utilize and tap the city features and resources of the region, through the Investigation and analysis of urban image pinpoint to exactly locate city image, so as to make city image targeted, distinctive and feasible, provide adequate proof and reliable protection for the late promotion of city brand image.

Keywords: ZhangShu, City, Image Elements, Orientation.

Preface

With the accelerated process of urbanization in China and competition fierce, especially medium and small cities as the representative of the city must establish a good brand image of the city, so as to occupy its own place in future urban development, how to determine the city image position and what the problem should be paid attention to is an urgent problem facing the current city, this paper take ZhangShu which is a county-level city in China as a case study, to start research on medium and small cities image location, intended to provide some method of establishing the brand image for the other cities.

1 City Image Resources Investigation

1.1 Geographical Features and Traffic of Location

ZhangShu city is located in central Jiangxi Province, the climate is subtropical humid monsoon. Meanwhile, many rivers within ZhangShu, close to the Gan River, beautiful mountains scenery, fresh air, beautiful environment, no pollution, especially for people living, the natural style of southern breadbasket representatives a good image of urban ecological environment. Zhangshu City has convenient transportation facilities, Zhejiang-Jiangxi Railway, Beijing-Kowloon railway, sea and land extending in all directions, is common hinterland of developed areas in southeastern China, is also one of the industrial transfer major undertaking, which has become an important guarantee of economic development in ZhangShu, also represents a good traffic and location image of ZhangShu. (see table 1).

Table 1. Distance from main cities

ShangHai	GuangZhou	NanJing	FuZhou	WuHan	ChangSha	capital of NanChang
860 km	780 km	880 km	650 km	480 km	440 km	76 km

1.2 Industry and Economic Characteristics

- (1) ZhangShu City in recent years to create industry characteristic economy, to help companies build brands, the emergence of a large number of outstanding companies, become as "Sinopharm capital " recognized by medicine industry colleagues at home and abroad, the traditional annual exchange of the session of the National Conference of medicine attracted large number of people at home and abroad come here to trade, invest and negotiate.
- (2) form a diversification of economic structure salinization that "SiTe wine, " wine industry as the leading corporations, together with insurance equipment, machinery manufacturing and salt industry, constitute the city's economic image of ZhangShu.

1.3 Urban History and Humanities

ZhangShu springs from a long history, is a famous historical and cultural city. ZhangShu has ancient culture, taoism culture, drug culture, wine culture, salt, culture, tourism cultural resources are very rich, such as: Lomond Mountain Resort, Mountain House Soap, Jade Mountain and so on. to form historical ancient culture represented by Mountain House Soap, Shang Dynasty ruins of city Wu, built the acropolis, Camp, Fancheng heap.

1.4 Urban Amenity

Zhangshu City is typical of small and medium cities in China. Appearance of Zhangshu city greatly changed in recent years, gradually developed to a new city on the basis the old city, a park along the river has been completed, reconstruction of a drug park, one leisure square park and one promenade park, urban green area of 23 %, the city is clean and tidy, the city is a new look.

1.5 City People Image

People in Zhangshu formed the spirit of Zhangshu gang representated by Zhangshu medicine gang medicine gang as early as 1800 years ago, they are honest and trustworthy, faithful to goodness, hard-working. Since ancient in Zhangshu there are a lot of talents, famous generals, celebrities and scholars talent. People now in Zhangshu base on the succession of predecessors to understand life, love life, after fashion, full of vitality, hospitality, they are industrious and brave, daring to do, be couraged to struggle and forge ahead. This constitutes the quality and urban people image that modern Zhangshu men have.

1.6 The Image of the Government

Zhangshu city government proposed guiding ideology of city development identified by establishing the cultural city, making city stronger by economy, improving people's livelihood, harmonious development, the city government proposed to build a city brand of modern drug city, promote other economic industries by traditional

industries, form a diversified economic structure, promotion of urban development by economy, improving people's livelihood, build Zhangshu into a Star of the modern city of Jiangxi Province and the city business travel with economic prosperity, people are living happy, good environmental and ecological characteristics, the traditional industrial-based tourism, commerce and technology, diversified culture, which are important and decisive to constitute the strategic promotion of Zhangshu brand image.

1.7 Other Data Collection

Zhangshu education, radio and television, health, sports and other undertakings have developed greatly, and gradually improving with Zhangshu economic development, which provides a good life conditions and living environment for people living. Zhangshu city flower is the gardenia, white flowers, fragrant and pleasant to eat, the fruit produced can be used as medicine, is a locally produced valuable traditional Chinese medicine, City tree: camphor tree, camphor tree evergreen, tall and dense, disseminate faint smell, can also be used as medicine.

Survey summary: Zhangshu City has a good location advantages for development, superior geographical conditions, formation of water, land and air transportation network, transportation is convenient. Zhangshu has a thousand years of drug culture, has deep historical and cultural heritage, formation of the Chinese medicine city. In economy area the development of other industries driven by the pharmaceutical and wine industry, a diversified economic structure, modern Zhangshu people inherited the spirit of Zhang bang are confident and vigorous, the government is seizing the opportunity to comprehensively promote the development of social undertakings, in order to work hard for building up the city brand.

2 Positioning Analysis of the City Image of Zhangshu

Through real visits and trips to Zhangshu City and read a lot of local literature search to obtain a large amount of data and information, and to extract and analyze of the information, provide the basic proof for accurate positioning of brand image design for Zhangshu city, in the following we

Table 2. Analysis of city image position of Zhangshu

Image category	City advantage	Description of image position
Geographic location image	Jiangnan land of plenty, Gan River Sea, a beautiful scene	Beautiful ecological environment
Traffic image	Close to developed cities, convenient at sea, land, air transport	Development advantage
Economy image	Mainly of medicine, the development of wine making, salt, logistics, manufacturing, diversified economic structure	Medicine city, the development advantages
Historical culture image	Wu Shang City Site, Mountain House Soap, a deep history culture	A deep medicine culture
Appearance of the city image	Neat, clean, modern, bright and beautiful urban environment	Beautiful ecological environment
Public image	Love life, fashion, energy, enthusiasm, loyal	Dynamic
Investment and environmental image	The rise of urban development, rapid economic development policy is superior, honest and have faith human environment, and supporting facilities	Development advantages
Government Imag	Scientific development, brand position, improve people's livelihood, social services	Development advantages
Service environment image	Education, health, sports have been developed, supporting facilities,	Happy life
The image of tourism environment	Lomond Leisure Resort, star hotel, tourism constitutes a major commercial center of resort properties	Happy life
The image of the living environment	Rivers, lakes, numerous water resources, eco-green is good, fit for human habitation	Beautiful ecological environment

further analyze of constitution and positioning of Zhangshu city image resources based on the original investigation, in order to obtain more accurate basis on city image position, the following is the table analysis of city image position of Zhangshu (see table 2).

3 Brand Image Position of ZhangShu City

Brand Image position of ZhangShu City need to follow the following principles on the basis of fully tap and analyze the resources:

- (1) the principle of local cultural differences. This difference is evolved from the long-term development of local culture, is the soul of a city and culture carrier, ZhangShu, nearly two thousand years ancient of the pharmaceutical history, form Chinese medicine city, form its unique pharmaceutical culture and medicine bang spirit, only heritage of its inherent characteristics, and constantly enrich and develop their own, will have real charm, this diversity is also reflected in the regional culture of "people" on the subtle differences, the characteristics of human nature which constituted by this difference has a great impact on local economic development.
- (2) characteristic, distinctive principles. Characteristics and personality is the vitality and competitiveness of the host city, to achieve optimal development, we must avoid weaknesses, to develop competition and development strategies. Through the analysis of their own resources and the environment to determine the optimal functional position itself, to maximize the competitive edge to improve the city. Medicine city ZhangShu is close to the Gan River, abundant at materials, known as the land of plenty, is also Chinese medicine city, to fully tap its features and advantages.
- (3) forward-looking principle. the city brand positioning can not only look to the current situation, to neglect of the city future development, forward-looking principle is to focus on the premise of current situation, forecasting and advance planning of city future brand image, urban brand image continue to inheritly develop with the development of the city, European cities brand building at this point is that we can learn, not making a tremendous impact on urban brand building with the general government policy makers change, ZhangShu brand building also has to follow this principle.
- (4) people-oriented principle. City is the people's city, in the city planning and urban construction, we must adhere to people-oriented principle. The starting point is to respect people's needs, so as to provide a good spiritual impetus and intellectual support for urban brand construction and development. To create a good society and harmonious interpersonal relationships, thereby creating a cohesive and appealing human environment, promote on the construction of harmonious cities brand, ZhangShu city brand image is to respect people, service people.
- (5) the principle of accuracy. City image position must be accurate, consistent with the city image of their own position, commensurate with the city's identity, can not be divorced from the actual urban development. Otherwise, it must bring a lot of adverse effects for the design and promotion of city image.

According to the basic principles of city brand positioning, combined with the existing image resource conditions survey and analysis, the status of urban development and municipal government on urban development planning and city building thought of ZhangShu city, ZhangShu city brand positioning can be summarized as :

First, take advantage of ZhangShu local traditional industries advantage, to create "Chinese medicine city" brand. Second, the construction of ecological city that a harmonious development between man and nature, with beautiful environment, the city with rapid economic development, enthusiastic and vibrant city. Third, fit for investment and housing, social harmony and stability of the well-being city.

This city image position of ZhangShu city not only embodies the cultural characteristics of ZhangShu, but also reflects the beautiful urban environment, simply and clearly outlines the industry features and beautiful livable urban environment, pointing out the direction of future development of ZhangShu, also shows a better blueprint for ZhangShu urban development.

Summary

Through this case study of a typical small city to explore the basic theory and practices of city image positioning, further clarify "what the city is", "what resources it has", "what features it has", the city image orientation is highly summarized and refined on the basis of city of culture, history, industry, environment and other resources, fully demonstrate the character of the city, improve the city value, highlight urban charm, point out the direction for urban development.

Acknowledgement. Project Fund: 2010 scientific research established by Guangxi Education Department .Project number: 201010LX136.

References

1. Li, L.: Changsha city image (CI) Localization of shape. Hunan University 10(4), 61–64 (2003)
2. Cha, Z.: On the composition of city image. Urban Development 16(5), 90–93 (2009)

Maximum Power Point Tracking in Photovoltaic Grid-Connected Generation System by Using Fuzzy Control Algorithm

Jie Liu¹ and HaiZhu Yang²

¹ Department of Computer Science and Technology, Henan Polytechnic University,
Jiaozuo 454000, China
liujie@hpu.edu.cn

² Department of Electrical Engineering and Automation, Henan Polytechnic University,
Jiaozuo 454000, China
yanghaizhu@hpu.edu.cn

Abstract. According to solar battery's non-linear characteristics and disadvantages of high cost, low transfer efficiency, to improve the efficiency of photovoltaic grid-connected generation system, a novel modified fuzzy control method of MPPT is introduced. After analyzing the mechanism and disadvantages of traditional control methods of Maximum Power Point Tracking (MPPT), fuzzy control algorithm is studied and applied to photovoltaic grid-connected generation system. Simulation results show that this method can rapidly track MPP changes and operate in maximum power point steadily with smaller disturbance. The expected goal is achieved.

Keywords: Fuzzy Control, Photovoltaic, MPPT, Simulink.

1 Introduction

The system of photovoltaic grid-connected generation has some advantage. For example, no pollution, noise, inexhaustible and so on. the PV system attracts a great deal of attention with the trend of electric power deregulation and environmental preservation. However, there have some problems about developing photovoltaic system, initial investment cost and transfer efficiency. So we must improve photovoltaic array's transfer efficiency and make the output power maximization, It also says we come up with the problem about The maximum Power Point Tracking (MPPT) in theory and in practice. Because power grade of the PV array usually is big in photovoltaic grid-connected generation system, so making use of intelligent control method to control the non-linear PV system is a good choice.

2 Characteristic of the PV Array

Solar battery's equivalent circuit and temperature characteristic. Solar battery is a semiconductor device about photoelectric conversion, it produces voltage and

current that It is impacted by temperature and light intensity. When solar battery by light irradiation connects loads, light products current to flows through load and establish ends voltage in both ends in load (see Fig.1) [1].

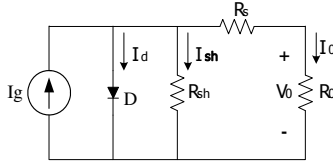


Fig. 1. Equal circuit of solar battery

When resistance R_0 changes from 0 to infinity, the road character curve of the solar battery can be obtained (Fig.2).

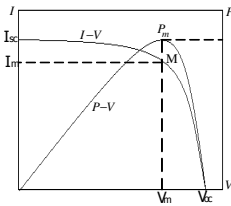


Fig. 2. The output character of solar battery

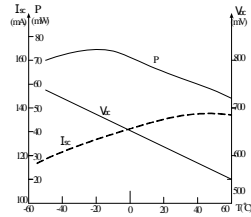


Fig. 3. Temperature character of solar battery

From Fig. 1 it can know that output power of PV depends on highly an insolation condition and a surface temperature of the PV array. Fig.3 is a temperature character of solar battery [2,3].

3 The Principle of MPPT and Control Algorithm

The principle of MPPT. MPPT utilize some type of control circuit or logic to search for this point. crossing to monitor the output voltage and current of PV system to make sure the current working point and the maximum Power Point, then moving the operating point to the vicinity of the real peak power point to avoid to converge to the local maximal power point. If the power increases, keep the next voltage change in the same direction as the previous change. Otherwise, change the voltage in the opposite direction as the previous one, finally the controlled voltage swings to the vicinity of the real peak power point.

MPPT control algorithm. Many papers have been reported in relation to the MPPT control technique. Those papers are based on, for example, so called the constant voltage tracking algorithm(CVT), the Perturb-and-observe (P&O) method, incremental conductance algorithm (IC) method and so on.

The CVT have some advantage, For example, simple control, high reliability, good stability, easy to implement and so on. however, maximal power point voltage of PV array will change with changing the temperature, in term of where the temperature between the day and night great, the method can't track maximal power point of PV array on current time. the P&O is that increasing or decreasing output voltage of PV array occasionally and observing power changing direction to make sure the next control signal. its simple implementation, high reliability, but When the irradiance decreases, the P&O method tracks the maximum power point well and the tracking error is nearly zero. However, when the irradiance increases, the P&O control does not track the maximum power point well [4].

The main task of the incremental conductance(IC)algorithm is to find the derivative of PV output power with respect to its output voltage, that is dP/dV . The maximum PV output.

Power can be achieved when its dP/dV approaches zero. The controller calculates dP/dV based on measured PV incremental output power and voltage. If dP/dV is not close zero, the controller will adjust the PV voltage step by step until dP/dV approaches zero, at which the PV array reaches its maximum output. The main advantage of this algorithm is its fast power tracking process. However, it has the disadvantage of possible output instability due to the use of derivative algorithm.

Since the PV array exhibits a non-linear current-voltage or power-voltage characteristic, its maximum power point varies with the insolation and temperature. Some algorithms such as fuzzy control with non-linear and adaptive in nature fit the PV control.

4 The Basic Principle of Fuzzy Control

Choosing the fuzzy controller inputs and outputs. According to the principle of the P&O confirm objective function is output power(P) and control variables is duty step(D). fuzzy controller inputs of the N moment are power error of the N moment and duty step of the N-1moment, the outputs of the N moment are duty step of the N moment [5,6].

Confirming fuzzy set theory of inputs and outputs. First making the power error $e_p(n)$ and duty step $e_d(n)$ quantify, then imaging them to fuzzy set theory E_d and E_p .

$$E_p = \{NB, NM, NS, NO, PO, PS, PM, PB\} :$$

$$E_d = \{NB, NM, NS, PS, PM, PB\}$$

Where NB is negative large in size , NM is negative middle in size , NS is negative small in size , NO is negative zero in size, PO is negative zero in size , PS is negative small in size , PM is negative middle in size , PB is negative larger in size.

fuzzy set number theory

$$E_p = \{-6, -5, -4, -3, -2, -1, -0, +0, 1, 2, 3, 4, 5, 6\} :$$

$$E_d = \{-6, -5, -4, -3, -2, -1, 0, 1, 2, 3, 4, 5, 6\}$$

The membership function. According to the PV system characteristics chooses the triangle as the membership function shape. It shows that the curve is far from origin

the more nearer the more steeper, in order to improve resolution. and the more farer the more slower, in order to track speed.

The membership function of power error(see Fig.4), the membership function of duty step(see Fig.5) .

Control rule of fuzzy control. According to the PV system output power (P) and duty step (D) can obtain the following rules:

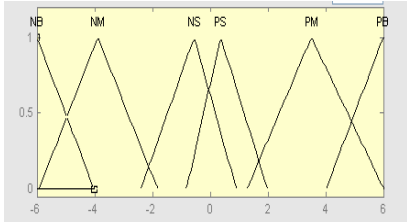


Fig. 4. The membership function of power error

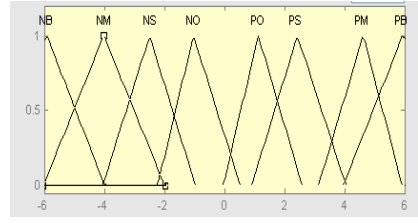


Fig. 5. The membership function of duty step

①Far from Maximum Power Point uses larger step to accelerate tracking speed, the ②Maximum Power Point neighborhood uses smaller step to decrease Searching loss.

If output power increases, keep the next voltage change in the same direction, Otherwise, change the voltage in the opposite direction.

③When output power takes place great changes with Sunshine intensity, temperature, the system has rapid reaction.

According to Matlab can get the overview of control rules (see Fig.6).

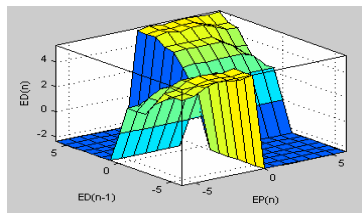


Fig. 6. The overview of control rules

5 Simulation Experiment

Simulation model of fuzzy control. According to the State Space Model of DC-DC converter, solar battery array model, the basic principle of Fuzzy control use MATLAB to MPPT control simulink(seeFig.7) [7].

Simulation results. Assuming PV battery parameters, the surface temperature is 25°C, trial-and-error, quantification factors are 0.01 and 0.1, using ode23tb algorithm

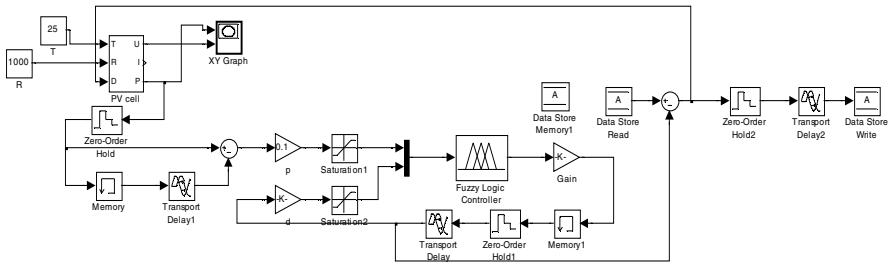


Fig. 7. Simulation model of fuzzy control

and simulink time is 10s, so the simulation results of the system of PV can be obtained (see Fig. 8, see Fig. 9).

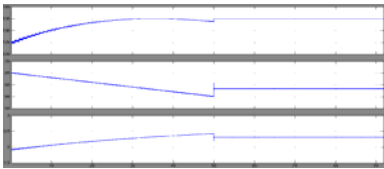


Fig. 8. The changing course of output voltage, current and power of PV array (Fuzzy Control)

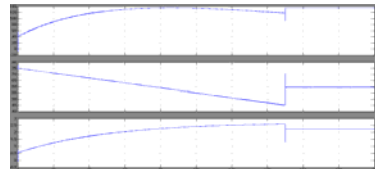


Fig. 9. The changing course of output voltage, current and power of PV array (P&O)

In Fig.8 using Fuzzy Control to get the changing course of output voltage, current and power of PV array, and in Fig.9 using P&O get it. The top is the power changing curve, in simulation PV array’s output power increase from 0 to the Maximum Power 135W, then down to 118W, output voltage changes from 75V to 45V, the current changes from 0.5A to 2.6A. Then crossing the MPPT algorithm to make the system operate in the optimum power point. Simulation results show the maximum Power output is 135W, its corresponding duty step is 0.708, at this time PV array output voltage is 59V and current is 2.3A. tracking speed about power changing Fig. 10 is faster than Fig 9, it also to say that it can track light intensity changing more faster that fluctuations of voltage and current increase obviously.

6 Conclusion

According to Solar battery characteristics that non-linear, environment temperature and sunshine sensitive this paper apply a novel modified fuzzy control method of MPPT, by using duty step as the control variables, making use of output power error to duty step self-adaptive control. Simulation results show that the system can operate in maximum power point steadily and rapidly track the MPPT.

References

1. Shen, H., Zeng, Z.: Photovoltaic generation technology. Chemical Industry Press, BeiJing (2005)
2. Simoes, M.G., Franceschetti, N., Friedhofer, M.: Fuzzy logic based photovoltaic peak power tracking control. In: Proc IEEE Conf. International Symposium on Industrial Electronics, Pretoria, pp. 300–305 (1998)
3. Mao, M., Yu, S., Su, J.: Versatile Matlab Simulation Model for Pholovoltaic Array with MPPT Function. *Journal of System Simulation* 17(5), 1248–1251 (2005)
4. Xiao, W., Dunford, W.G.: A modified adaptive hill climbing MPPT method for photovoltaic systems. In: 35th annual IEEE Power Electronic Specialists Conference, Germany, pp. 1957–1963 (2004)
5. Ye, Q.: A Study on the Photovoltaic Maximum Power Tracking System Using a Fuzzy Controller. Donghua University, ShangHai (2006)
6. Tafticht, T., Agbossou, K.: Development of a MPPT method for photovoltaic systems. In: *Electrical and Computer Engineering, 2004 Canadian Conference*, Canada, vol. 5(2), pp. 1123–1126 (2004)
7. Wang, H., Su, J., Ding, M.: Maximum Power Tracing Control for Photovoltaic Merged Grid Power Generation System. *Transactions of China Electrotechnical Society* (9), 4–6 (2004)

Research on the Power Marketing Technique Supporting System Based on Semantic Web Services

Jun Liu and ChaoJu Hu

School of Control and Computer Engineering,
North China Electric Power University, Baoding, Hebei, 071003, China
liujun2008514@sina.com.cn

Abstract. In the power marketing technique supporting system, the data can not be shared, processes can not communicate, there are a large number of information isolated islands. This paper analyzes the deficiency of Web Services and put forward an integration framework and platform of power marketing technique supporting system based on semantic web services, The platform of the application achieves the unified expression of system resources. the system connected through the application integration platform interacte In a unified way, without considering the difference, which enhances the independence, flexibility, and maintainability of the system.

Keywords: Semantic Web Services, power marketing, XML.

1 Introduction

Along with the power marketing technique supporting system, the electricity supply companies formed a technical support system, which relied on technology of distribution network, based on the power marketing management information system. the call center system and bank and power on behalf of the charging system is the extension of technical support system, Load management, automatic meter reading, line loss management provide the decision-making. However, due to development and application of the system have successively, the system of targeted relatively strong, the system architecture, the result can not share data, processes can not communicate, the software can not be reused, which makes the sharing of the system to the poor, especially for marketing management statistics business analysis and decision support applications is extremely limited. The use of web services can be adapt to this change by automatically re-locating and binding in the UDDI, Therefore, the dynamic of integration can be achieved, and meet the needs of EAI, making Web services can call each other to complete the business collaboration[1].

But, the traditional service lacks the semantics. it can only search the service through the key words, can not realize the semantic expression of the business relation, the agreement and the service rule by the way of computer understanding. At present, the development of semantic web provides a chance for web service. Using semantic web, all informations on the network have their semantics. Thereby, the machine can understand and deal with these informations. Combining the character of

loose couple of web services with the semantic informations provided by semantic web, we can match, find, invoke web services automatically, so as to build and execute business process dynamically. As a result, we can integrate the application systems from different enterprises better. So we combine semantic web with web services to form semantic web services[2].

This paper analyzes the deficiency of Web services and put forward an integration framework of power marketing technique supporting system based on semantic web services.

2 Semantic Web Services

Semantic Web services are a combination of Web services technology and Semantic Web, Package of semantic services can be easily automated service discovery, invocation, interoperation, composition, execution, monitoring and so on. Semantic Web services is the markup language (eg OWL-S) enhance the semantic description of Web services. the external agents and procedures can be found, combined and called semantic Web services by the Semantic description. The semantic Web service research's basic task is carries on the mark to the Web service, enable users to understand and becomes the entity which transparent and easy to process to the user. Figure 1 shows hierarchical structure of semantic Web.

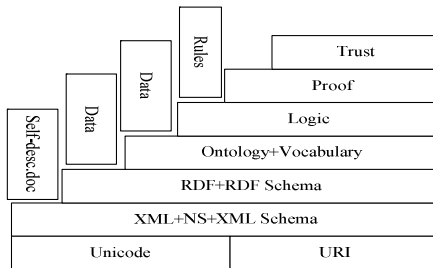


Fig. 1. Hierarchical Structure of semantic Web

In the hierarchy of semantic web, Unicode and URI is the basis of semantic of semantic web, Unicode provides the coding resources,The URI can be used to identify resources. In the second layer, XML+NS+XML Schema provides that the syntax of the data content and structure. The third to the fifth layer is the core of semantic web providing interactive support of semantic.RDF+RDFS provides data model and primitive type of web resources, which Expresses the judgment and defines the pattern. the Ontology level is the concept and the relational abstract description which defines in the RDFS foundation, can be used in describing the knowledge of application, Logical description of the original language was defined in the fifth layer,which provides support for higher-level semantic reasoning. The proof layer and the trust layer can make logical reasoning and proof, on the basis of support on the lower layer[4].

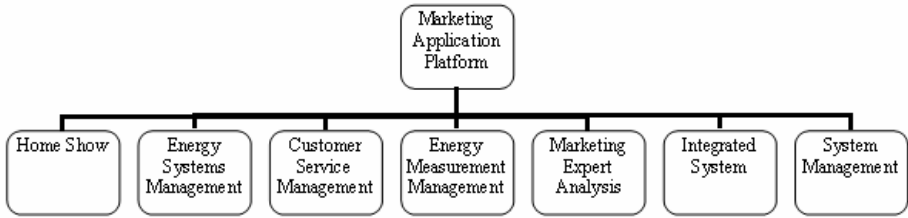


Fig. 2. Composite Application Platform Module Category

3 Power Marketing and Management System Structure

Integrated application platform marketing support system is built based on the marketing of various subsystems integrated analysis, statistics, query applications. To be completed by City Distribution Line Loss calculation, abnormal electrical analysis, integrated search function integrated query, etc.

Marketing support integrated application system as an integrated application of marketing analysis platform, is a system to integrate the data analysis to generate electricity to meet the business needs of marketing service data. Data sources currently include: Marketing Management Information System, call center systems, load management systems, distribution transformer monitoring system, people reading system, the six regional electric energy collection system, system wide data sources, while the data are distributed in different system, its information, standardization, network security and system scalability in the system need to be considered in the overall structural design, and overall system architecture to meet the advanced requirements to ensure that the system can be easily expanded. as shown in Figure 2.

4 Research on the Power Marketing Technique Supporting System Based on Semantic Web Services

This paper presents the framework of the power marketing technique supporting system based on semantic web services. as shown in Figure 3.

The system has the following features:

- 1) Through pre-planning, we can build the organization system of power enterprise information classification. Using the enterprise ontology library, we can realize the unified management of information resources.
- 2) Using the semantic web services, we can achieve the collection, conversion, integration of heterogeneous information resources of the power enterprise marketing system. In a uniform format for information resources services, shielding the distribution of information resources, types and complexity of structure.
- 3) Adopting a unified information processing and Management platforms, we can achieve on-demand process customization.

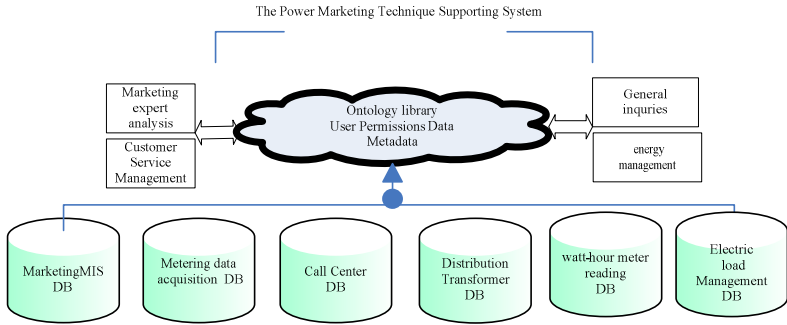


Fig. 3. The framework of the power marketing technique supporting system based on semantic web services

5 Platform

The platform includes the following major components of several modules: a central coordinating module, service registration mode, the service matching module, the module and the semantics of business process management module. shown in Figure 4.

- Central coordination module is the core of the platform, control and coordination of scheduling module is the external interface platform. Its main features include three parts:

Service Request agent: the equivalent of a message server role. It achieves the message's storage and management, is the entrance of the platform to receiving service, It receives service requests and resolve the service request, give the relevant information to the other modules for further processing platform.

Service call agent: The main form by the process execution engine, used to control the platform to run the generated executable process and returns the result to the service request broker.

Control and scheduling: schedule of the modules together to complete a service request process.

- Work service registry by a number of modules to achieve application service registration, query and semantic mapping work, and Compatible with the traditional UDDI operation, and supports semantic operations, including semantic service publishing, semantic service discovery, service updates, and service semantics semantic deleted.
- Service matching module

Match Engine: According to the service request content, services, registry services for semantic matching, and returns the best service.

Service quality assessment: According to the service matching and service operation to assess the situation, assess the results as part of an additional registration

information Registration information to the service, the service matching and selection for future reference factors.

● Business Process Module:

When a service request requires a complex business process to complete, the request of the service will be the decomposition as the basic service requests (tasks), each basic service requests must go through the service matching process, and finally, all matching service Defined by the business logic defined in the order of service composition, the formation of an executable process instance, and finally interpreted.

● Semantic Management Module:

Management and access of Domain ontology and service ontology should be through this module,the module is the semantic base of support is to study the semantic Web services-based framework.

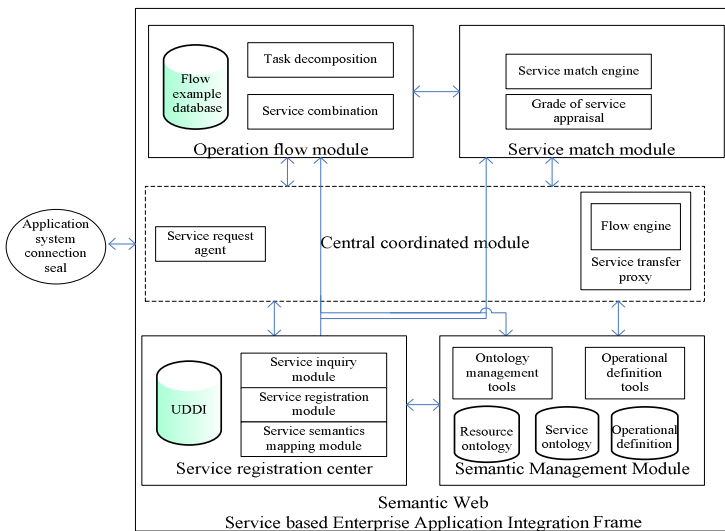


Fig. 4. The Platform of the Power Marketing Technique Supporting System based on Semantic Web Services

6 Conclusion

For the power marketing technique supporting system, the data can not be shared,processes can not communicate, there are a large number of ‘information isolated island’. This paper analyzes the deficiency of Web services and put forward an integration framework and platform of power marketing technique supporting system based on semantic web services, The platform of the application achieves the unified expression of system resources. the system connected through the application integration platform interact In a unified way, without considering the difference. Which enhances the independence, flexibility, and maintainability of the system.

Acknowledgement. This work is supported by the Teacher's Research Foundation of North China Electric Power University (200811019).

References

1. Zhang, H.: Research and Design on the Enterprise Application Integration Based on SOA. Northwestern University, 21–28 (2008)
2. Zheng, W.: Research on the power marketing technique supporting system. East China Normal University, 1–4 (2007)
3. Li, X., Yuan, J.: Research and Implementation of integration of information between power enterprises MIS Based on Web services. North China Electric Power University 32(4), 80–82 (2005)
4. Yan, s.: Research of EAI based on Semantic Web Services 29(14), 3642–3643 (2008)
5. Dong, T.: Research On Semant1C Webserv1Ce Framework 1N EAI 36, 22–25 (2008)

Design of Mechanics of Materials Study Monitor System Based on Distance Education Environment

Ai Xiao Yan

College of Information Engineering, Yulin University, Yulin, China
axy_9522@163.com

Abstract. Mechanics of Materials is the basis for other disciplines as civil engineering and mechanical engineering, which also has a strong engineering practice. Compared with classroom education and study, distance network education of Mechanics of Materials has problems of poor controllability, poor teaching effect and difficult to evaluate, main reason of which is that most distance teaching system based on Web lack of effective monitor and feedback of online study process of learners. To address the problem, the paper used study monitor mechanism that combines self-monitoring and outer-monitoring and presented design schema of monitor and feedback on study process of learners under distance network education environment. The schema divided system into study log module, information collection module, information statistics module and feedback module. Design of these modules in detail was also provided, which laid good foundation for system implementation.

Keywords: Mechanics of Materials, distance education, network environment, monitoring.

1 Introduction

Mechanics of Materials is the first basic technique courses contacted by engineering students, which plays important role in engineering education. It acts as a bridge to connect basic courses and specialized courses. Meanwhile, it is the basis for other disciplines as civil engineering and mechanical engineering, which also has a strong engineering practice. In modern education conditions, distance education has provided a platform for engineering students to better master the course. From the perspective of modern information science, monitoring aims at collecting various kinds of information activities of the objects with manners of inspection, assessment, tracking, screening, summary and other forms. It is a further operation and processing measure to eliminate bias between target implementation and intended target according to regulated targets and principles in the plan, so as to correct deviations and errors and make it develop in predetermined direction [1-3]. Among them, constantly changing information goes through the monitoring process, including information reception, transmission, accessing and processing. We can think that monitoring is essentially effective control by tracking and feedback.

Therefore, learning monitoring in the network education of *Mechanics of Materials* refers to plan, track, feedback and control on learning processing to ensure effectiveness and quality of networking learning. The information collection, accessing and processing is going through this process. Network learning is typical self-control learning and the learning activities are controlled by learners themselves [4]. The network environment is relatively free and loosely. In such external control environment, high self-control demanding is required to learners [5]. To ensure the learning effectiveness and quality, the best measure is to develop self-learning ability and self-control of learners. But in a relatively long period of transition, we need to develop monitoring mechanism that combines self-monitoring and external monitoring, and try to guide the learners gradually develop self-learning ability and self-control in the process. Based on the idea of combining self-monitoring and external monitoring, the paper conducted overall design on learning monitoring system in networking education environment and designed various functional sub-systems in detail. The paper is organized as follows. Section 2 implements overall design on learning monitoring system. Section 3 conducts detail design on functional sub-systems and section 4 concludes our work.

2 Overall Design of Learning Monitoring System

Design Ideas. The ideal learning monitoring is mainly self-study and self-monitoring of students [6]. But it is a long process cycle, or even an expectation of the ideal state. In this graduation process, we can select monitoring mechanism that combines self-monitoring and external monitoring and achieve functions of learning monitoring and management to some extent. Meanwhile, we can try to inspire learners cultivating capabilities of self-studying and self-control.

Therefore, the key of learning monitoring is supporting self-monitoring and self-adjustment on learning process [7]. The learners should developed learning objectives, monitor their own learning activities in a timely manner and accurately estimate the extent to achieve their learning goals, evaluate their own according to the standards of learning in the learning process, so as to discover their own shortcomings in the study and take appropriate strategies for improvement. The core of learning monitoring is self-monitoring. External monitoring is ultimately acting through self-regulation of the learners. The learners can be cultivated with self-study capabilities in this process. To better support self-monitoring of learners, the system used learning monitoring mechanism that combines self-monitoring and external monitoring and unified process monitoring and feedback control.

On this basis, the network learning monitoring system was consisted mainly by four functional functions, namely learning log module, information collection module, information statistic module and information feedback module. The overall system architecture was shown in Fig. 1.

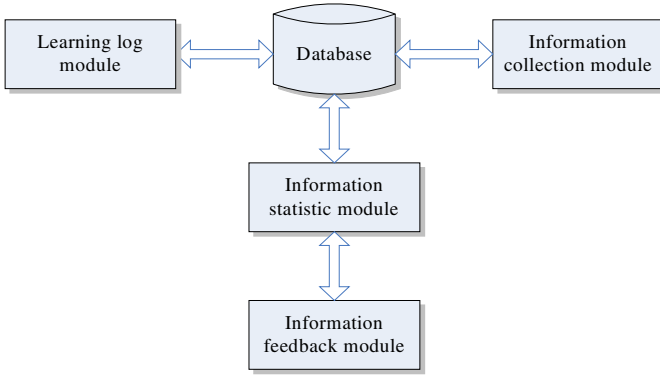


Fig. 1. Overall architecture of system.

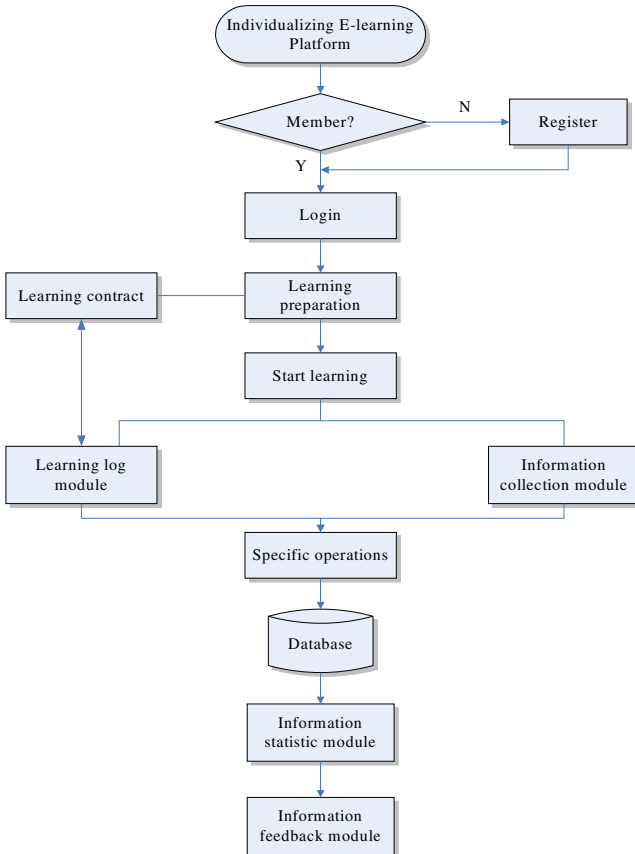


Fig. 2. System operation flow.

Overall Design. System is a Web-based distance learning system, which can not only provide for access at anytime and anywhere, but also provide an interactive learning environment. The system operation flow was shown in Fig. 2. After learners entered into built learning platform and completed login, learning preparation should be conducted. With learning contract, the learners can develop their own plan and start. In the process, learning log module enable learners constantly record their own learning status so that it can be consistent with learning contract signed previously. Meanwhile, information collection module accumulated data from specific distance learning actions from learners and stored in database. Then the information statistic module selected data from database. After statistical analysis, it will be shown to learners in the form of graphs and tables to convenient self-monitoring. Finally, information feedback module compared statistical analysis results and system settings to supervise and motivate learners.

3 Functional Module Design

Design of Learning Log Module. In the network learning process, *Mechanics of Materials* course learners can conduct self-reflective with learning log. As an effective self-monitoring tool, learning log provides learners with an output environment. The learner can use it to record a variety of learning experiences. Note that this is not mind running account, not just on the day of learning activities and learning content is simple or complex memories, but also highlight the reflective summary, so as to stimulate the learner's thinking, reflective learning process for learners and learning strategies used to detect learning deficiencies and take appropriate measures to be improved promptly. The focus of this paper is self-monitoring. In order to promote self-learning and self-monitoring, a contract will be signed before starting, so that learners can clear task and objectives to be achieved. Then record of learning log was conducted in the whole process, so that it is easy for learners to achieve self-control and adjustment. Record content can be analysis on the content or knowledge points or analysis on advantages as well as proposed higher objectives and measures, or conclusion of shortcoming and improvement on stage of learning tasks.

Design of Information Collection Module. Main functions of information collection module are to monitor and record online learning process and quantify the learning process. The session mechanism and DWR application framework were used to collect specific information of learning behaviors. Then these data was returned to be stored in learning monitoring database for processing by information statistic module. The timing and flow of information collection was shown in Fig. 3.

As seen from Fig. 3 we can know that online learning behaviors mainly include three aspects, namely online learning, questioning system and BBS discussion, where online learning can be divided into online web page learning, video-on-demand learning and browser development resources. From analysis on these learning behaviors, we need to focus on duration time of learning behavior as well as frequency of learning behavior.

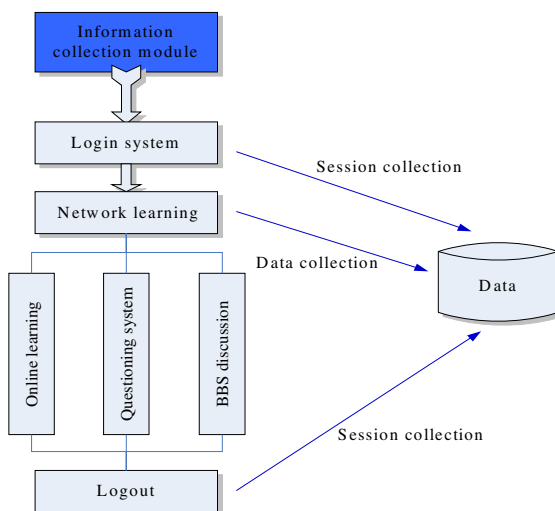


Fig. 3. Information collection.

Design of Information Statistics Module. The information statistics module mainly was responsible for collecting data and storing in database for processing. Then these data was shown in the form of graphs and tables to convenient real-time query, statistics and analysis, which helps learners and effective understanding and analysis of classroom the process of learning in all learners and provide reference for follow-up evaluation. The module has two main functions, namely data filtering and statistics analysis. Data filtering mainly carried out legitimacy verification on collected data and repair on uncompleted records. Statistics analysis pre-defined query manner of database and designed multiple query combination to comprehensively show online learning station of learners. In order to fully display, two angles of horizontal and vertical can be sued, namely individual learner and the curriculum itself as an object through the two points to cut the learner to be more understanding of the basic learning. The module is mainly implemented through open-source project BIRT reporting system as plug-in embedded systems.

(1) Data filtering

Data filtering refers to legitimacy verification on accessed data from database. In general, no matter how the initial information was obtained, there is noise and need to be performed some validation and filtering to ensure validity of the information. Data filtering mainly has three types, namely redundant information filtering, error messages filtering and invalid information filtering. The module firstly cleans up the data to remove some noise data and interference data, and then implement data integration and conversion.

(2) Statistics analysis

According to teaching experience, statistics analysis from two different aspects of vertical and horizontal can fully grasp the learning situation of learners. Vertical analysis means take individual learner as the object to describe the overall situation of

online learning and details. For example, describe the progress of individual learners and the total learning time as well as situation in BBS discussions. Vertical perspective analysis is conducive to the learner to grasp their own learning situation. Horizontal analysis means take course as object to describe situation of the course is to learn. For example, the chapters show a course was the visit of the visit and per capita number of learning time. From the horizontal angle will help understanding of each course learners are studying the overall situation in order to adjust the standard curriculum.

Design of Information Feedback Module. Information feedback module mainly strengthens behavior of learners in the form of feedback. It compared collected information in the learning process with pre-determined various requirements to provide early warning and encouragement. Two forms were used to strengthen learning. Firstly, notify learner to supervise learners. For example, when the learner does not meet the week online learning online learning requirement, the system will be based on their length of study time, combined with a pre-determined strategy within the system, or issued a warning on their tasks. Secondly, reward learners in form of integral grades. In order to better motivate learners, the system set points rewards. Learners each time you log into the learning interface can see their points, and the integral list. In addition, through the incentive mechanism, the currency integration into learning, and learning to learn currency exchange for the amount of prepaid card, learners achieve good topic for scholarships, ways to motivate these learners.

4 Conclusion

Learning monitoring in the network education of *Mechanics of Materials* refers to plan, track, feedback and control on learning processing to ensure effectiveness and quality of networking learning of *Mechanics of Materials* course. Compared with classroom education and study, distance network education has problems of poor controllability, poor teaching effect and difficult to evaluate, main reason of which is that most distance teaching system based on Web lack of effective monitor and feedback of online study process of material engineering learners. The paper used study monitor mechanism that combines self-monitoring and outer-monitoring and presented design schema of monitor and feedback on study process of *Mechanics of Materials* course learners under distance network education environment. The schema divided system into study log module, information collection module, information statistics module and feedback module. Design of these modules in detail was also provided, which laid good foundation for system implementation.

References

1. Xu, J.-p., Zhao, H.-q.: Explore on self-studying monitoring strategies based on network. *China Modern Educational Equipment* 3, 29–31 (2007)
2. Mazza, R., Dimitrova, V.: CourseVis: A graphical student monitoring tool for supporting instructors in web-based distance courses. *International Journal of Human-Computer Studies* 65, 125–139 (2007)

3. Liu, W.-q.: Status analysis and measures of modern distance education. *Journal of Jiangnan University (Social Sciences)* 22, 89–90 (2005)
4. Liang, G.-s., Guo, M.-z.: Design of learning process monitoring system in modern distance education. *Higher Education of Sciences* 3, 61–63 (2007)
5. Tang, Y.-x.: Real-time monitoring strategies in interaction of network education. *Journal of Jilin Radio and TV University* 3, 113–115 (2007)
6. Tao, M.-h., Wang, B.: Research on monitoring strategies and implementation method in network courses learning process. *Distance Education in China* 3, 60–63 (2010)
7. Wei, D.-s., Yang, X.: Design and implementation of automatically monitoring system of network learning behaviors. *China Education Info.* 1, 40–41 (2006)

An Improved Threshold Function for Wavelet De-noising

Zhong Li¹ and Dong-xue Zhang²

¹ School of Electrical and Electronic Engineering, North China Electric Power University,
Bao ding, 071003, China
ncepulz@126.com

² Hohhot Power Supply Bureau Inner Mongolia Power group, Hohhot, 010050, China
zhdx1234@126.com

Abstract. Wavelet de-noising is an important application of wavelet analysis in engineering. In this paper, an improved wavelet threshold function is proposed. Matlab simulation results on Blocks signal with additive white Gaussian noises show that this method is effective and can get the better de-noising effect than the traditional soft or hard threshold method.

Keywords: Wavelet transform, Wavelet de-noising, Threshold.

1 Introduction

In recent years, there has been abundant interest in wavelet methods for noise removal or de-noising in signals and images, a wide range of wavelet-based tools and ideas have been proposed and studied. The well-known soft thresholding analyzed by Donoho [1], due to its effectiveness and simplicity, is frequently used in the literature and it is one of the major methods of de-noising in the wavelet domain. The main idea is to subtract the threshold value from all coefficients larger than and to set all other coefficients to zero. The wavelet threshold de-noising consists of three steps [2].

- 1). Transform the noisy data into an orthogonal domain.
- 2). Apply soft or hard shareholding to the resulting coefficients, thereby suppressing those coefficients smaller than certain amplitude.
- 3). Transform back into the original domain.

Wavelet threshold value filtering is a kind of the simplest realization, the smallest calculation, and it has been widely applied. But its threshold value's selection is quite difficult, although Donoho has proved theoretically and has found the general threshold value, the results are unsatisfactory in the practical application. Much of the literature has focused on developing the best uniform threshold or best basis selection [3,4,5]. Generally, these methods use a threshold value that must be estimated correctly in order to obtain good performance.

The effectiveness of wavelet threshold de-noising is directly impacted by the threshold value. How to select the appropriate threshold function is one key issue of wavelet de-noising. This paper presents a new wavelet threshold function that could get better effectiveness of the de-noising.

2 Wavelet Threshold De-noising

De-noising by wavelet is quite different from traditional filtering approaches because it is nonlinear owing to a thresholding step. Suppose the clean signal $s(k)$ of length N is corrupted by white noise $e(k)$, with standard normal distribution $N(0, \sigma^2)$, and then the noisy signal $f(k)$ is shown as follows:

$$f(k) = s(k) + e(k) \quad 1 \leq k \leq N \tag{1}$$

Decomposition of the signal $f(k)$ is performed by levels J . If the noise energy is obviously less than signal energy, the corresponding noise wavelet coefficients will obviously smaller than the signal wavelet coefficients, select a suitable thresholding to set the wavelet coefficients which below the thresholding to zero and remain or shrink the wavelet coefficients which higher than the thresholding. If the thresholding is too low, noise will be remained and if the thresholding is too high, useful signal will be lost.

The most popular used threshold proposed by D. L. Donoho [6] can be expressed as follows:

$$\lambda = \sigma \sqrt{2 \log N} \quad \sigma = \text{mdeian}(|c|) / 0.6475$$

Where N is the signal length of noisy signal, σ is the hard deviation of zero-mean additive white Gaussian noise (WGN) estimated by Donoho and Johnston. c is the detail coefficients of wavelet transform.

The hard-threshold and soft-threshold function. The most used wavelet threshold functions are hard-threshold and soft-threshold function defined by (2) and (3) separately.

$$\hat{W}_{j,k} = \begin{cases} W_{j,k}, & |W_{j,k}| \geq \lambda \\ 0, & |W_{j,k}| < \lambda \end{cases} \tag{2}$$

$$\hat{W}_{j,k} = \begin{cases} W_{j,k} - \lambda, & W_{j,k} \geq \lambda \\ 0, & |W_{j,k}| < \lambda \\ W_{j,k} + \lambda, & W_{j,k} \leq -\lambda \end{cases} \tag{3}$$

Where $\hat{W}_{j,k}$ is the wavelet coefficient after threshold process, $W_{j,k}$ is the wavelet coefficient before threshold process, λ is the threshold.

Hard threshold method can successfully remain the local characteristics of the signal. But, the discontinuity of the shrinkage function may generates some artificial “noise points” in the restoration signal, and cause some vibration in the reconstruction signal. Soft threshold processing is good continuity and easy to be processed. But sometimes it will lose some useful high frequency information.

Improved threshold function. To overcome the disadvantages of hard and soft threshold function, a new threshold function was introduced here. The $\hat{W}_{j,k}$ is modified as:

$$\hat{W}_{j,k} = \begin{cases} W_{j,k} - t\lambda \log_2 \left(\left| \frac{\lambda}{W_{j,k}} \right| + 1 \right), & W_{j,k} \geq \lambda \\ 0, & |W_{j,k}| < \lambda \\ W_{j,k} + t\lambda \log_2 \left(\left| \frac{\lambda}{W_{j,k}} \right| + 1 \right), & W_{j,k} \leq -\lambda \end{cases} \quad (4)$$

Where $t = 0.618$, it is a regulatory factor.

If $|W_{j,k}| \geq \lambda, 0 < \frac{\lambda}{|W_{j,k}|} \leq 1$, then $0 < \log_2 \left(\left| \frac{\lambda}{W_{j,k}} \right| + 1 \right) \leq 1$. If the $|W_{j,k}|$ increases, then the $\left| \frac{\lambda}{W_{j,k}} \right|$ decreases, so the $\log_2 \left(\left| \frac{\lambda}{W_{j,k}} \right| + 1 \right)$ decreases continuously. This could effectively avoid the problems of the soft threshold method, which has fixed deviation and produces a constant attenuation. The attenuation of greater absolute value of wavelet coefficients decreases with the absolute value increases through $\hat{W}_{j,k}$ measuring the attenuation. It reduces attenuation dynamic and adaptive. It could avoid the loss of useful high frequency information and improve signal to noise ratio. The factor t decides signal to noise ratio after wavelet processing, the smaller the t is, the greater the signal to noise ratio is.

3 Experiments

In order to test the validity of the new wavelet threshold function, we test it in comparison with the traditional soft and hard thresholding. We select the Blocks signal with SNR=6 including Gaussian white noise signal. The db5 wavelet was chosen and the largest decomposition scale was $J = 4$. The de-noising effect is shown in Fig.1.

To illustrate the effectiveness of de-noising, signal to noise ratio (SNR), root mean square error (RMSE) and Peak error (PE) values were computed and listed in Table 1. It is clear that the use of the new method improves the results.

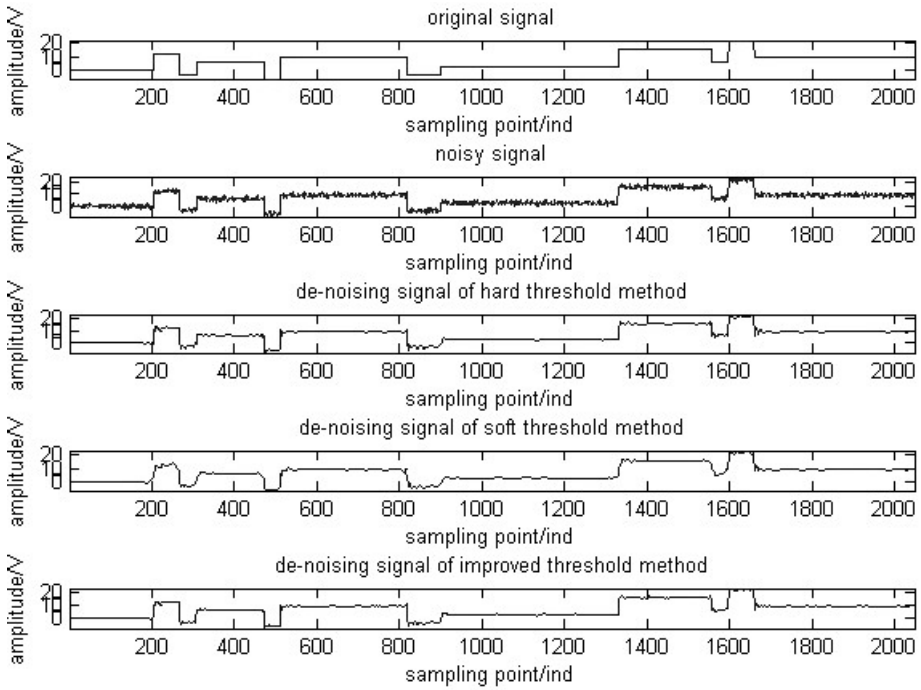


Fig. 1. Signal and de-noising results of different methods

Table 1. Comparative performance of different de-noising methods

De-noising method	Hard threshold method	Soft threshold method	New threshold
SNR(db)	27.7033	24.6919	28.8270
RMSE	0.1116	0.1297	0.1055
PE	4.6430	6.2062	3.3402

4 Conclusion

In this paper, a new threshold function for wavelet de-noising was proposed. Computer simulation results showed the new method gives better results than the hard and soft thresholding in signal de-noising, it can give a valuable reference for wavelet threshold de-noising.

Acknowledgments. This work was supported by the Fundamental Research Funds for the Central Universities, North China Electric Power University, No. 10QG04.

References

1. Donoho, D.L.: De-noising by soft-thresholding. *IEEE Trans. Inform. Theory* 41(5), 613–627 (1995)
2. Coifman, R.R., Donoho, D.L.: Translation-Invariant De-Noising. In: Antoniadis, A., Oppenheim, G. (eds.) *Wavelets and Statistics*. Springer, Berlin (1995)
3. Chang, S.G., Yu, B., Vetterli, M.: Spatially adaptive wavelet thresholding with context modeling for image denoising. *IEEE Trans. Image Processing* 9(9), 1522–1531 (2000)
4. Dong, Y.S., Yi, X.M.: Wavelet denosing based on four improved function for threshold estimation. *Journal of Math.* 26(5), 473–477 (2006)
5. Liu, Y.-x., Wang, X.: Optimal soft thresholding for signal denoising. *Acta Electronica Sinica* 43(1), 167–169 (2006) (in Chinese)
6. Donoho, D.L., Johnston, I.M.: Ideal spatial adaptive via wavelet shrinkage. *Biometrika* 81, 425–455 (1994)

A Modified MUSIC Algorithm Based on Eigen Space

Qian Zhao and WenJuan Liang

Xi'an University of Science and Technology, School of Communication and Information Engineering, Xi'an, China

qianzhaoza@sina.com, liangwenjuan36@163.com

Abstract. Among the algorithms of DOA estimation, MUSIC algorithm which has very high resolution and estimation precision. However, MUSIC, Improved MUSIC and Novel MUSIC can not estimate the signals when the signal intervals are very small in the case of the low SNR and existence of the signal correlation. To solve this problem, a Modified MUSIC is proposed in this paper which takes advantage of the signal subspace and the noise subspace, by making them orthogonal to each other through repeatedly reconstructing covariance matrix, we can obtain the two noise subspaces and signal subspaces. By averaging previous results and reconstructing covariance matrixes of signals and noise, DOA could be estimated through spectrum function. Computer simulation proves that among three methods only Modified MUSIC can accurately estimate the correlated signals with low SNR and its side beam is lower than the Novel MUSIC.

Keywords: Smart antenna, Direction of Arrival (DOA) estimation, MUSIC algorithm, Improved MUSIC algorithm, Novel MUSIC algorithm, Modified MUSIC algorithm.

1 Introduction

The smart antenna is always a hot research topic in communication technology and the direction of arrival(DOA) estimation is one of its important areas[1].

The current DOA estimation technology is focused on high resolution estimation algorithm. The MUSIC algorithm [2] is a very popular algorithm. However, MUSIC algorithm can only estimate relevant signals. the performance of the algorithm decreases and even becomes invalid[3]. Improved MUSIC Novel MUSIC Starts from the eigen value and makes full use of the signal subspace and noise subspace in the spatial spectrum estimation, the performance of Novel MUSIC, which has a lower side beam, is better than MUSIC and Improved MUSIC [4].

In this paper, a modified MUSIC is proposed which employs the signal subspace and the noise subspace, which are orthogonal to one another. Modified MUSIC can estimate the signals more accurately than the Improved MUSIC and Novel MUSIC, Moreover, its side beam is lower than the Novel MUSIC[5] when the signals interval are very small under the condition of the low SNR and occurrence of the correlation.

2 Algorithm

MUSIC Algorithm[6]. Calculation MUSIC spectrum, as shown in (1)

$$\hat{P}_{MUSIC}(\theta) = \frac{a^H(\theta)a(\theta)}{a^H(\theta)V_nV_n^H a(\theta)} \tag{1}$$

Make θ to change, find \hat{D} maximum peak of $\hat{P}_{MUSIC}(\theta)$ to estimate DOA.

Improved MUSIC Algorithm[7]. Improved MUSIC algorithm decomposes the signal covariance matrix, the signal for the rank of covariance back to $rank(R_X) = D$, So that it can effectively estimate the signal DOA. Calculation Improved MUSIC spectrum, as shown in (2)

$$\hat{P}_{IMUSIC}(\theta) = 1/[a^H(\theta)VUVU^H a(\theta)] \tag{2}$$

Novel MUSIC Algorithm[8]. Novel MUSIC algorithm based on eigenspace is proposed, it makes full use of the signal subspace and noise subspace in the spatial spectrum estimation. Calculation Improved MUSIC spectrum, as shown in (3)

$$\hat{P}_{NMUSIC}(\theta) = \frac{a^H(\theta)R_{ssa}(\theta)}{a^H(\theta)U_NU_N^H a(\theta)} \tag{3}$$

Modified MUSIC Algorithm. Modified MUSIC algorithm decomposes the signal covariance matrix, makes full use of the signals subspace and the noise subspace, on basis of the signals subspace obtained be orthogonal to the noise subspace.

Implement of the Modified MUSIC Algorithm procedures can be summarized as follows:

(1) Collect input samples $X(i), i = 1, \dots, N$, Estimate input covariance matrix, as shown in (4).

$$\hat{R}_X = \frac{1}{N} \sum_{i=1}^N X(i)X^H(i) \tag{4}$$

(2) Reconstruct a new covariance matrix RX , as shown in (5).

$$RX = \hat{R}_X + J\hat{R}_X^*J \tag{5}$$

(3) Eigen-decompose the reconstructed covariance matrix $RX = U\Lambda U^H$, according to the sequence from big arrive small, RX is divided into signal subspace and noise subspace, that is showed in (6)

$$RX = U_{S1}\Lambda_{S1}U_{S1}^H + U_{N1}\Lambda_{N1}U_{N1}^H \tag{6}$$

(4) Using low ranks matrix instead of full rank matrix RX , Reconstruct a new covariance matrix RXX , eigen-decompose the reconstructed covariance matrix RXX , repeat the above steps, reconstruct noise subspace and signal subspace. As show in (7):

$$RXX = U_{S2}\Lambda_{S2}U_{S2}^H + U_{N2}\Lambda_{N2}U_{N2}^H \tag{7}$$

(5) Make an average about signal subspace, signal eigenvalue, noise subspace and noise eigenvalue, as show in (8):

$$U_S = (U_{S1} + U_{S2})/2, U_N = (U_{N1} + U_{N2})/2, \Lambda_S = (\Lambda_{S1} + \Lambda_{S2})/2, \Lambda_N = (\Lambda_{N1} + \Lambda_{N2})/2 \tag{8}$$

(6) According to $Rs = U_S\Lambda_S U_S^H$, calculating $Rss = U_S\Lambda_S^{-1}U_S^H$, According to $R_N = U_N\Lambda_N U_N^H$, calculating $Rnn = U_N\Lambda_N^{-1}U_N^H$;

(7) Structure space spectrum function, as shown in(9)

$$\hat{P}_{FMUSIC}(\theta) = \frac{a^H(\theta)[(RssRss^H)/(MM)]a(\theta)}{a^H(\theta)Rnna(\theta)} \tag{9}$$

Seek optimal at θ for spectral peak of $\hat{P}_{FMUSIC}(\theta)$, spectrum peaks θ which is wanted θ is the estimate of the incident signal DOA .

3 Simulation Results

Experiment 1: Non-ideal circumstances, Simulation model is 8 array elements with uniform linear array,array element spacing is 1/2 of the wavelength of the carrier, or $d = \lambda/2$, Suppose three narrowband signals respectively incident to the antenna array with $-60^\circ, 30^\circ, 45^\circ$, for the strong correlation between the signals 30° and 45° , SNR is 10dB, number of snapshots is 1024, the simulation results about MUSIC algorithm and improved MUSIC algorithm is showed in Fig. 1, the simulation results about MUSIC algorithm and Novel MUSIC algorithm is showed in Fig. 2.

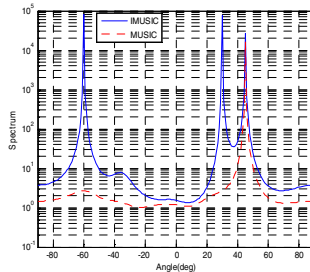


Fig. 1. Performance of MUSIC, Improved MUSIC when strong correlation

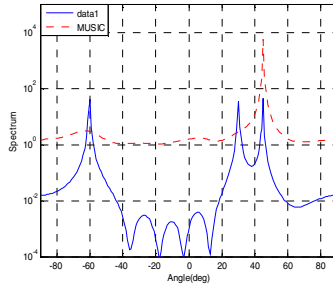


Fig. 2. Performance of MUSIC, Novel MUSIC when strong correlation

Experiment2: Non-ideal circumstances, Simulation model is 8 array elements with uniform linear array, array element spacing is $1/2$ of the wavelength of the carrier, or $d = \lambda/2$, Suppose three narrowband signals respectively incident to the antenna array with $-13^\circ, -10^\circ, 45^\circ$, Signal irrelevant, SNR is 5dB, number of snapshots is 1024, the simulation results about MUSIC algorithm and improved MUSIC algorithm is showed in Fig. 3, the simulation results about MUSIC algorithm and Novel MUSIC algorithm is showed in Fig. 4.

Experiment3: Non-ideal circumstances, Simulation model is 10 array elements with uniform linear array, array element spacing is $1/2$ of the wavelength of the carrier, or $d = \lambda/2$, Suppose three narrowband signals respectively incident to the antenna array with $45^\circ, 30^\circ, 60^\circ, 65^\circ$, for the strong correlation between the signals 30° and 60° , number of snapshots is 1024, the simulation results about Improved MUSIC algorithm, Novel MUSIC algorithm and Modified MUSIC algorithm under the SNR=5 and SNR=10 separately are showed in Fig. 5, 6.

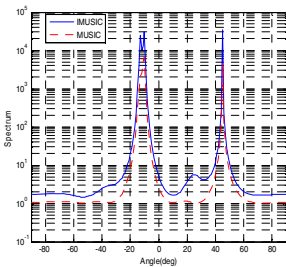


Fig. 3. Performance of MUSIC, Improved MUSIC when small snapshot

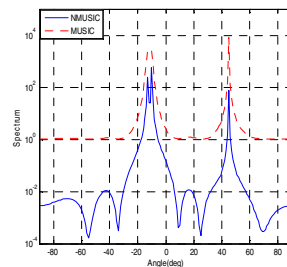


Fig. 4. Performance of MUSIC, Novel MUSIC when small snapshot

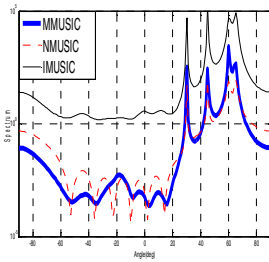


Fig. 5. Strong correlation and small snapshot when SNR=10

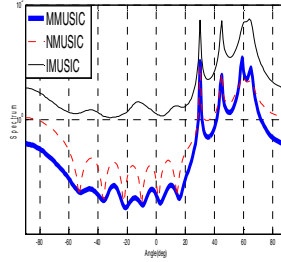


Fig. 6. Strong correlation and small snapshot when SNR=5

4 Simulation Results Analysis

From the Fig. 1, 2, 3, 4, we can find when incoming signals are correlated or the signals interval are very small under the condition of the lower SNR, the performance of the MUSIC algorithm sharply decreases, even becomes invalid, DOA can not distinguish the signal source. Improved MUSIC and Novel MUSIC can estimate the signals that MUSIC cannot, its performance is better than the MUSIC, Novel MUSIC have a lower side beam and it is very useful for the estimation of the DOA. However, when the signals interval are very small under the condition of the lower SNR and exist the correlated signals, Improved MUSIC and Novel MUSIC can not estimate the signals accurately. From the Fig. 5, we can find when SNR=15dB, Improved MUSIC, Novel MUSIC and Modified MUSIC can estimate the signals. However, when SNR=5dB, Improved MUSIC and Novel MUSIC cannot distinguish the 60° , 65° , Modified MUSIC can estimate the signals accurately and side beam is lower than the Novel MUSIC.

5 Summary

This paper mainly investigated the most classical MUSIC algorithm used for DOA estimation. In-depth study of its principles, reveals. Improved MUSIC and Novel MUSIC can estimate the signals that MUSIC cannot. Novel MUSIC have a lower side beam and is very useful for the estimation of the DOA. However, when the signal intervals are very small under the condition of the low SNR and existence of the correlated signals, Improved MUSIC and Novel MUSIC can not estimate the signals accurately.

To tackle this problem, a modified MUSIC is proposed which makes full use of the signal subspace and the noise subspace orthogonal to each other, through multiple reconstruction signal covariance matrix and noise covariance matrix, Modified MUSIC can estimate the signals accurately that Improved MUSIC or Novel MUSIC can not. In addition, its side beam is lower than the Novel MUSIC.

Acknowledgment. This work was supported by Industrial Science and Technology Department of Shaanxi Province PR project. NO: 2010K01-074 ; NO: 2010K06-03.

References

1. Mathews, C.P., Zoltowski, M.D.: Eigenstructure techniques for 2-D angle estimation with uniform circular arrays. *IEEE Trans. on SP* 42, 2395–2407 (1994)
2. Schmidt, R.: Multiple Emitter Location and Signal Parameter Estimation. *IEEE Transactions on Antennas and Propagation AP-34*(3), 276–280, 1–10 (1986)
3. Lie, S., Rahim Leyman, A., Chew, Y.H.: Fourth-Order and Weighted Mixed Order Direction-of-Arrival Estimators. *IEEE Signal Processing Letters* 13(11), 691–694 (2006)
4. Jian, X.H., Zhang, C.M., Zhao, B.C., et al.: The application of MUSIC algorithm in spectrum reconstruction and interferogram processing. *Optics Communication* 281(9), 2424–2428 (2008)
5. He, Z.-s., Huang, Z.-x., Xiang, J.-c.: The performance of DOA estimation for correlated signals by modified MUSIC algorithm. *Journal of China Institute of Communications* 21(10), 14–17 (2000)
6. Bihan, L., Mion, N., Mars, S., et al.: MUSIC algorithm for vector-sensors array using biquaternions. *IEEE. Transaction on signal processing* 55(9), 4523–4533 (2007)
7. Jian, X.H., Zhang, C.M., Zhao, B.C., et al.: The application of MUSIC algorithm in spectrum reconstruction and interferogram processing. *Optics Communication* 281(9), 2424–2428 (2008)
8. Zhang, X., Lv, W., Shi, Y., Zhao, R., Xu, D.: A Novel DOA estimation Algorithm Based on Eigen Space. In: *IEEE Internation Symposium on Microware, Antenna, Propagation, and EMC Technologies For Wireless Communcations*, pp. 551–554 (2007)

The Theoretical Study of Paper Screening System

Qingwen Qu, Chengjun Wang, Xiaodan Lou, and Bo Zheng

School of Mechanical Engineering, Shandong University of Technology,
Shandong Zibo, China

quqingwen@sdut.edu.cn, wchengjun58@sina.com.cn,
Lowxiaodan@163.com.cn, Zhengbo@163.com.cn

Abstract. According to the general domestic and international trends in the development of paper industry, the new requirements of screening system from the paper industry have been analyzed. And combining the new development in pulp screening at home and abroad, the analysis method in designing paper screening system has been studied. The latest design concepts of screening equipment are summarized. These provide theoretical guidance for design, innovation and improvement of the equipment. Besides, a few of scientific problems of screening system to be solved recently are predicted. And the methods are discussed.

Keywords: screening system, design concepts, theoretical guidance, analysis method.

1 Introduction

Paper consumption in China is the world's major powers. Annual consumption of paper and paper products is about eighty million tons. However, China is also paper resource-poor country. Don't be abundant in forest. And the straw pulp has more serious pollution for environment.

So recycling of waste paper is the general trend of the paper industry development [1~2]. The structure of papermaking raw materials is further optimized in fifth period. The proportion of waste paper pulp has rapid growth. It has increased from 41% to 54%. As a result, improving the processing of waste paper pulp will be of great significance for the development of the paper industry.

On one hand, as the rapid development of the chemical industry, printing industry and office automation, the types of waster paper are more and more, the composition become more complex. And waste paper processing will be increasingly difficult. On the other hand, the domestic from the early eighties began to gradually develop and design waste paper processing equipment. The start is late and the technology is backward. Comparing with international advanced equipment, there is a large gap in the variety, capacity, complete sets, equipment levels and other aspects of the waste treatment equipment. So new technologies, new processes and new equipments need to be constantly developed. And the level of waste treatment technology is improved [3].

The outlook of making paper of waste paper pulp is optimistic. According to the nature of waste paper pulp and the analysis results of the screening system process mathematical model, appropriate pulping equipments are chosen. The production process is allocated reasonably [4]. The various parameters of screening system are mastered for bringing into play character of the equipment fully. And using advanced process control methods, the product quality can be improved and better economic benefit may be obtained so as to enhance the overall level of the entire paper industry.

2 Research Status and Development Dynamic Analysis at Home and Abroad

The past 10 years, waste paper market, the price of waste paper, waste paper technology and equipments in entire world (including China) have undergone great changes. In TAPPI meeting, participants reviewed the development of waste treatment technology in the last 25 years. The experts looked to the future direction of waste treatment technologies. In which, simplifying screening system process, enhancing the performance of screening equipment and improving screening quality and reducing system energy consumption and improving the mathematical control model of system are the focus of development. The followings are the main researches which have been done by the domestic and international scholars in recent years.

Chen suping from industrial control technology Institute of Zhejiang University reviewed the course of development of beating process control and the characters, scope and results achieved of several typical control systems. And for the future development trends, a more comprehensive analysis and estimation are given [5]. He said the start of the study about beating control was late and unpopular.

In 2003, American Khanbaghi, Maryam and other people introduced a nonlinear dynamic model of pressure screens [6]. The model would be used to design a simple nonlinear multivariate control model, through which performance evaluation and plant experiments can be done.

In 2005, Mokamati, S V and so on proposed the idea that the computer fluid dynamics analysis was introduced into studying the effect of geometry on the stock flow. The factors of the forming of turbulence and vortex were discussed [7].

In 2006, Keinanen, Pasi and so on from Finland pointed that with the latest development in computer and camera technology, a new revolutionary method can be used to measure fiber properties and shiver content of the pulp [8]. These new measurements had been used in on-liner analyzer.

In 2010, Ferluc Alexandre, Lanouette Robert and Bousquet Jean-pierre, from Canada, analyzed the effect of refining consistency on modulation pulp quality. They pointed that when recombining the refined fractions together to recreate the initial pulp, the refining consistency affects the pulp quality greatly. In addition, they said the best fractionation process is a pressure screen cascade using baskets with very small apertures.

According to the recent study content about screening waste paper, screening process control is of great significance for improving the paper quality and productivity, reducing energy consumption. Thus creating a perfect control model and

doing analysis and research are the key technologies for the screening system. At the same time, the quantitative description of the processes of screening system and the specific application of the waste paper pulp screening remain to be further studied.

3 The Latest Design Ideas of the Screening Equipments

With the development of pulp screening industry and the requirement of paper for pulp quality, the paper industry has higher and higher requirement for screening efficiency, filter quality and energy consumption reducing. This spurs innovation of screening equipment to meet industry requirements. The latest international basic idea of the screening equipment design is to create the optimum hydraulic conditions throughout the screen from the feed to the accept area and no to the reject discharge. As a result, the highly effective and flexible combination of rotor and screen basket, allowing the screen to adapt quickly and easily to the various different raw materials, can develop its full potential. Thus, highest screening efficiency is achieved at low energy consumption and with good reliability.

3.1 The Rotor Design

The latest development of the rotor is the so-called P-Rotor which is as shown in fig.1. In design of the P-rotor, considerable emphasis was placed on achieving the maximum possible flexibility, in addition to observing the laws of hydraulics. The foils are bolted to the retaining arms. With a simple change to the vane geometry or by modifying the spacing between the vanes, additional means are available to optimize the screen. In addition to this, service work is simpler and costs are reduced because only the foils have to be changed instead of the entire rotor.



Fig. 1. P-rotor

For the P-rotor, the interval between blade and basket, peripheral speed of the rotor and the rotor types can be set according to the need. Because of the flexibility, P-rotor can be easily adapted to various applications and meet the clean filter requirements.

For another example, the evolution of the beating equipment rotor is entirely the application of hydraulics. At first the Vokes rotor is exerted to the beater. It is as shown in fig.2. In fig.3, the later rotor is the old FSR rotor. However, now the latest rotor is the new S rotor as shown in fig.4.



Fig. 2. Vokes rotor



Fig. 3. Old FSR rotor



Fig. 4. New S rotor

The new S rotor includes suction vane and cleaning vane. The suction vane generates strong vortex, making pulp inner loop. And the contact between pulp and rotor gets increased. Thus, the raw materials can be broken at utmost. The mechanical energy has an effective role on the fiber. So that moderate friction can be realized. The breaking effectiveness may be improved. On the other hand, the cleaning vane produces high pressure for increasing the throughput, ensuring the good pulp can be rapidly discharged and the equipment load can be reduced. Fig.5 is the result of the fluid dynamics analysis on S-rotor. It shows the flow characters of pulp in the region near the rotor.

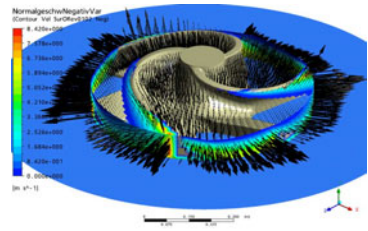


Fig. 5. Paper pulp fluid analysis

Advantages of the S-Rotor are as follows:

- 1 The rotor has good pulping capacity and the balance of pulping results. So it can reduce pulping time and increase productivity.
- 2 Low energy consumption and small fluctuations in the motor load. Under the same energy consumption, the production capacity is raised. Or with the same production capacity, the energy consumption is cut down. It is benefit for the life of the motor and drive mechanism.
- 3 High pulp consistency. It mainly depends on the friction between the fibers to achieve fiber dissociation, not simply relies on mechanical pulping.
- 4 The low investment can realize the growth of the production. Installation and maintenance are easy and ensure long-term efficient.
- 5 The surface of the rotor has special wear-resistant treatment. Maintenance is very few. The service life is long.

3.2 The Housing Design

For the housing design, as fig.6, twin-cone housing is adopted. In order to obtain a constant flow in the accept area, the shape must be adapted to suit the material flow. So the housing widens from the inlet side to the point where the accept branch is mounted. As from this sector, accept is taken from the accept area, thus reducing the volume flow. Thus, the cross-section of the accept area must also be reduced. Advantages of the twin-cone housing:



Fig. 6. Twin-cone housing

The inlet area is optimized. The inner cone on the cover is for even deflection of the flow in circumferential direction. Also the accept area is optimized. Twin cones can ensure constant flow speeds over the entire height of the screen basket. Besides in reject area, low volume brings higher speeds in order to prevent clogging.

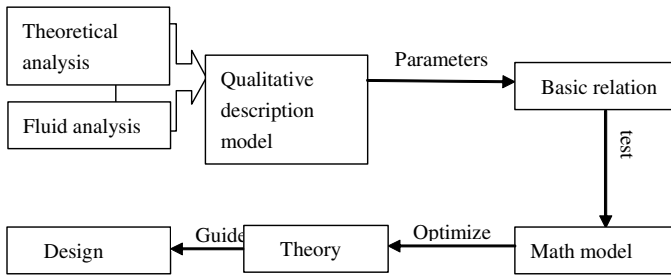
4 Predict Some Key Scientific Problems to Be Solved Recently in the Paper Industry

- (1) Pulp and pulp balance, pulp and water balance and water and water balance in screening system. The relationship between feed stocks, accepts and rejects is the problem of the balance of pulp and pulp. The feed and water, pulp flow and water cycles are shown in pulp and water balance problem. Dilution and concentration are two aspects of the water and water balance.
- (2) Flow field analysis of the whole screening system will be achieved. And the multiphase flow character which benefited for the separation between accepts and rejects and saving fibers will be obtained.
- (3) Accurate mathematical control model is established. Through the screening system simulation experiment, the performance of screening system may be effectively assessed. And the theory model of screening system is optimized. In addition, the mathematical model gets perfection.
- (4) For realizing better separation between stock and reject, a wide range of impurities in waste paper pulp are classed. And the suitable separation mechanisms are made respectively. The design theories of screening equipment are formed.

5 Discuss the Analysis Method

Based on fluid, motion and force (energy), according to the law of conservation of mass, momentum conservation law and the law of energy and three equilibrium theory, the flow balance, the law of mechanical movement and the interaction between fluid and basket, rotor and housing are researched. Using the Fluent software and the Euler-Lagrange method, the multiphase flow is studied. The fluid phase is looked as continuous phase. And the N-S equation is to be solved. However, the discrete phase flow field is obtained by calculating the movement of a large number of particles. There are momentum, mass and energy exchanges between the discrete phase and the fluid phase.

Starting from the balance between pulp and water in screening system and combining the separation of impurities and pulp and the fluid analysis, screening system theory model is established. That is qualitative description model. The basic relationship equations are built by specific energy, load and other stock flow parameters. Then the tests are done. And the factors that affect the screening and the mathematical relationship model of the parameters of the screening process. The screening effect can be optimized. In addition, it can guide the design and production of screening system. The basic technical line diagram can be expressed as follows:



Combining the existing mathematical model control theory and screening mechanism hypothesis, all aspects of the screening process are to be analyzed. Through the experiments, precise mathematical control models are established. In the literature, writer took into account many uncertain factors in beating process. For example, the consistency and the flow become change. The rotor is worn. The uncertain linear system model is given:

$$\dot{x}(t) = (A + \Delta A)x(t) + (B + \Delta B)u(t), x(0) = x_0.$$

ΔA 、 ΔB are uncertain norm-bounded uncertain parameters. Practice proves that the control model is more realistic and practical applications than the general linear model.

6 Conclusions

The development of paper industry and the complication of paper making raw material have higher requirements for the screening system and screening equipment. They not only ensure the quality of pulp, but also pay attention to the screening system efficiency and reduce energy consumption and wear to improve life in order to achieve better economic. The paper describes the developments in domestic and international screening system. The latest design concepts of the international screening equipment are pointed out. In addition, some key technologies to be solved recently are predicted. And the study methods are discussed. These provide direction and method for designing screening system. However, the specific works need further study and discussion.

References

1. Zhu, f., Qin, h.: The status of the use of waste paper in China and the proposals. Paper and making (4) (2002)
2. Blanco, M.A., Negro, C.: Paper Recycling, Stickies Problems in Recycling. China Pulp & Paper Industry 24(9) (September 2003)
3. Chen, s., Pi, d., Sun, y.: The status and trend of the beating course control. China paper (3), 51–56 (1994)

4. Pescantin, M., Edwards, L.: Screening technology: Industrial experience with compact, high performance, high consistency screens. In: 2000 TAPPI Recycling Symposium, vol. 2, pp. 645–651 (2000)
5. Olson, J.: Fibre length fractionation caused by pulp Screening, slotted screen plates. *Journal of Pulp and Paper Science* 27(8), 255–261 (2001)
6. Khanbaghi, M., Allison, B., Olson, J.: Modeling and control of an industrial pressure screen. *Control Engineering Practice* 11(5), 517–529 (2003)
7. Mokamati, S.V., Olson, J.: The effect of wire shape on the flow through narrow apertures in a pulp screen cylinder. In: Proceedings of the American Society of Mechanical Engineers Fluids Engineering Division Summer Conference, vol. 2, pp. 695–700 (2005)
8. Keinanen, P., Piirainen, E., Maatta, J., Riippa, T.: New ways to manage drainability fibre properties and shive content of the pulp. In: Appita Annual Conference. 60 th Appita Annual Conference and Exhibition –Proceedings, pp. 503–514 (2006)
9. Ferluc, A., Lanouette, R., Bousquet, J.-P., Bussiere, S.: Optimum refining of TMP pulp by fractionation after the first refining stage. *Appita Journal* 63(4), 308–314 (2010)

Solving Method of Dimension Chain Based on Interval Analysis

Jirong Yang, Weiyue Xiao, and Yuehua Cai

College of Mechanical Engineering, Hunan University of Arts and Science
Changde, 415000, P.R. China
yjrtt1028@sina.com

Abstract. For uncertainty of error and tolerance in mechanical parts, it is used to describe it by random uncertain theory. The advantage interval analysis is analyzed and interval arithmetic is described. INTLAB toolbox tutorial is also introduced. An numerical example was given. The result proved the correctness and validity of the proposed method.

Keywords: Interval Analysis, parts tolerance, dimension chain, INTLAB toolbox.

1 Introduction

Dimension chain analysis is the basis of mechanical manufacturing. For uncertainty of error and tolerance in mechanical parts, it is used to describe it by random uncertain theory. SPA analysis is a new method [1]. The concept of interval analysis is to compute with intervals of real numbers in place of real numbers. While floating point arithmetic is affected by rounding errors, and can produce inaccurate results, interval arithmetic has the advantage of giving rigorous bounds for the exact solution. An application is when some parameters are not known exactly but are known to lie within a certain interval; algorithms may be implemented using interval arithmetic with uncertain parameters as intervals to produce an interval that bounds all possible results. If the lower and upper bounds of the interval can be rounded down and rounded up respectively then finite precision calculations can be performed using intervals, to give an enclosure of the exact solution. Although it is not difficult to implement existing algorithms using intervals in place of real numbers, the result may be of no use if the interval obtained is too wide. If this is the case, other algorithms must be considered or new ones developed in order to make the interval result as narrow as possible. In this paper, parts tolerance is analyzed with Interval Analysis. An example proved that the proposed method is correct and effective.

2 Interval Arithmetic

A real interval x is a nonempty set of real numbers.

$$\mathbf{x} = [\underline{x}, \bar{x}] = \{x \in \mathbf{R} : \underline{x} \leq x \leq \bar{x}\}$$

where \underline{x} is called the infimum and \bar{x} is called the supremum. The set of all intervals over \mathbf{R} is denoted by \mathbf{IR} where

$$\mathbf{IR} = \{[\underline{x}, \bar{x}], \underline{x}, \bar{x} \in \mathbf{R} : \underline{x} \leq \bar{x}\}$$

The midpoint of \mathbf{x} , $mid(\mathbf{x}) = \tilde{x} = \frac{1}{2}(\underline{x} + \bar{x})$, and the radius of \mathbf{x} ,

$rad(\mathbf{x}) = \frac{1}{2}(\bar{x} - \underline{x})$, may also be used to define an interval $x \in \mathbf{IR}$. An interval

with midpoint a and radius r will be denoted by $\langle a, r \rangle$. If an interval has zero radius it is called a point interval or thin interval, and contains a single point represented by $[x, x] \equiv x$. A thick interval has a radius greater than zero.

The absolute value or the magnitude of an interval \mathbf{x} is defined as $|\mathbf{x}| = mag(\mathbf{x}) = \max\{|\tilde{x}| : \tilde{x} \in x\}$ and the mignitude of \mathbf{x} is defined as $mig(\mathbf{x}) = \min\{|\tilde{x}| : \tilde{x} \in x\}$. These can both be calculated using the end points of \mathbf{x} by

$$mag(\mathbf{x}) = \max\{|\underline{x}|, |\bar{x}|\}$$

$$mig(\mathbf{x}) = \begin{cases} \min\{|\underline{x}|, |\bar{x}|\} & \text{if } 0 \in x \\ 0 & \text{otherwise} \end{cases}$$

An interval \mathbf{x} is a subset of an interval \mathbf{y} , denoted by $\mathbf{x} \subseteq \mathbf{y}$, if and only if $\underline{y} \leq \underline{x}$ and $\bar{y} \geq \bar{x}$. The relation $\mathbf{x} < \mathbf{y}$ means that $\bar{x} < \underline{y}$, and other inequalities are defined in a similar way.

Interval arithmetic operations are defined on \mathbf{IR} such that the interval result encloses all possible real results. Given $\mathbf{x} = [\underline{x}, \bar{x}]$ and $\mathbf{y} = [\underline{y}, \bar{y}]$, the four elementary operations are defined by

$$\mathbf{x} \ op \ \mathbf{y} = \{x \ op \ y : x \in \mathbf{x}, y \in \mathbf{y}\} \quad \text{for } op \in \{+, -, \times, \div\} \tag{1}$$

Although (1) defines the elementary operations mathematically, they are implemented with

$$\mathbf{x} + \mathbf{y} = [\underline{x} + \underline{y}, \bar{x} + \bar{y}]$$

$$\mathbf{x} - \mathbf{y} = [\underline{x} - \bar{y}, \bar{x} - \underline{y}]$$

$$\mathbf{x} \times \mathbf{y} = [\min\{\underline{x}\underline{y}, \underline{x}\bar{y}, \bar{x}\underline{y}, \bar{x}\bar{y}\}, \max\{\underline{x}\underline{y}, \underline{x}\bar{y}, \bar{x}\underline{y}, \bar{x}\bar{y}\}] \tag{2}$$

$$1/\mathbf{x} = [1/\bar{x}, 1/\underline{x}] \quad \text{if } \underline{x} > 0 \text{ or } \bar{x} < 0$$

$$\mathbf{x} \div \mathbf{y} = \mathbf{x} \times 1/\mathbf{y}$$

For the elementary interval operations, division by an interval containing zero is not defined. It is often useful to remove this restriction to give what is called extended interval arithmetic, which will be used in later sections. Extended interval arithmetic

must satisfy (1), which leads to the following rules. If $\mathbf{x} = [\underline{x}, \overline{x}]$ and $\mathbf{y} = [\underline{y}, \overline{y}]$ with $\underline{y} \leq 0 \leq \overline{y}$ and $\underline{y} < \overline{y}$, then the rules for division are as follows:

$$\mathbf{x}/\mathbf{y} = \begin{cases} [\overline{x}/\underline{y}, \infty] & \text{if } \overline{x} \leq 0 \text{ and } \overline{y} = 0, \\ [-\infty, \overline{x}/\overline{y}] \cup [\overline{x}/\underline{y}, \infty] & \text{if } \overline{x} \leq 0 \text{ and } \underline{y} < 0 < \overline{y}, \\ [-\infty, \overline{x}/\overline{y}] & \text{if } \overline{x} \leq 0 \text{ and } \underline{y} = 0, \\ [-\infty, \infty] & \text{if } \underline{x} < 0 < \overline{x}, \\ [-\infty, \underline{x}/\underline{y}] & \text{if } \underline{x} \geq 0 \text{ and } \overline{y} = 0, \\ [-\infty, \underline{x}/\underline{y}] \cup [\underline{x}/\overline{y}, \infty] & \text{if } \underline{x} \geq 0 \text{ and } \underline{y} < 0 < \overline{y}, \\ [\underline{x}/\overline{y}, \infty] & \text{if } \underline{x} \geq 0 \text{ and } \underline{y} = 0. \end{cases} \quad (3)$$

The addition and subtraction of infinite or semi-infinite intervals are then defined by the following:

$$\begin{aligned} [\underline{x}, \overline{x}] + [-\infty, \overline{y}] &= [-\infty, \overline{x} + \overline{y}], \\ [\underline{x}, \overline{x}] + [\underline{y}, \infty] &= [\underline{x} + \underline{y}, \infty], \\ [\underline{x}, \overline{x}] + [-\infty, \infty] &= [-\infty, \infty], \\ [\underline{x}, \overline{x}] - [-\infty, \infty] &= [-\infty, \infty], \\ [\underline{x}, \overline{x}] - [-\infty, \overline{y}] &= [\underline{x} - \overline{y}, \infty], \\ [\underline{x}, \overline{x}] - [\underline{y}, \infty] &= [-\infty, \overline{x} - \underline{y}]. \end{aligned}$$

For further rules for extended interval arithmetic see [4].

3 INTLAB Toolbox Tutorial

INTLAB enables basic operations to be performed on real and complex interval scalars, vectors and matrices. These operations are entered similar to real and complex arithmetic in MATLAB. The user should work through this tutorial by typing what appears after the command prompt `>>`. It is assumed that the user is familiar with MATLAB and has INTLAB correctly installed. To start INTLAB type:

```
>> startintlab
```

This adds the INTLAB directories to the MATLAB search path and initialises the required global variables.

There are four ways to enter a real interval. The first is the function `intval` which allows the input of a floating point matrix.

```
>> A = intval('0.1 2 3 4');
```

Notice that A is a column vector. All output using a string argument produces a vector of this form. It may be changed to a 2×2 matrix by:

```
>> A = reshape(A,2,2);
```

The third alternative is to give an interval by its midpoint and radius.

```
>> B = midrad([1,0;0.5,3],1e-4);
```

Finally an interval may be input by its infimum and supremum.

```
>> C = infsup([-1,0;2,4],[-0.9,0;2.4,4.01]);
```

The default output is to display uncertainties by “_”. This means that an enclosure of the interval is given by the midpoint as the digits displayed and the radius as 1 unit of the last displayed figure. The midpoint, radius, infimum and supremum of an interval may be obtained.

The default output may be changed to display all intervals in one of these two notations.

To change to midpoint/radius:

```
>> intvlin('displaymidrad')
```

To change back to the original default:

```
>> intvlin('display_')
```

To change to infimum/supremum:

```
>> intvlin('displayinfsup')
```

All the standard arithmetic operations can be used on intervals. An arithmetic operation uses interval arithmetic if one of the operands is of interval type. Standard functions, such as sin; cos and log can be used with intervals. The default is to use rigorous standard functions which have been verified to give correct and narrow enclosures. The alternative is to use faster approximate functions which give a wider enclosure. More detailedly Tutorial, please see [5].

4 Application to Planar Dimension Chain

Planar dimension chain is shown as Figure 1. Given $A_1 = 30^{+0.02}_0$ mm, $A_2 = 20^{+0.05}_{-0.05}$ mm, $A_3 = 25^{+0.015}_{-0.015}$ mm, $A_4 = 25^{+0.06}_{-0.02}$ mm, find A_Σ ?

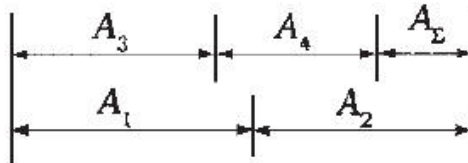


Fig. 1. Dimension chain diagramm

According to Figure 1, we obtain equation: $A_\Sigma = A_1 + A_2 - A_3 - A_4$. To find A_Σ , at first, transform dimension to interval number and start startintlab, then compile program with INTLAB toolbox as follows and run it.

```
intvlin('displayinfsup')
A1=infsup(30,30.02);A2=infsup(20-0.05,20+0.05);
A3=infsup(25-0.03,25); A4=infsup(25-0.02,25+0.06);
A=A1+A2-A3-A4
```

The result is intval A =[-0.110,0.120] and is the same as that of traditional extremum method.

5 Conclusions

While floating point arithmetic is affected by rounding errors, and can produce inaccurate results, interval arithmetic has the advantage of giving rigorous bounds for the exact solution. An application is when some parameters are not known exactly but are known to lie within a certain interval; algorithms may be implemented using interval arithmetic with uncertain parameters as intervals to produce an interval that bounds all possible results. Parts tolerance can be expressed as uncertain parameters and can be found with Interval Analysis toolbox INTLAB based on MATLAB. An example of planar dimension chain proved that the proposed method is correct and effective.

Acknowledgement. This research is supported by the grant of the 12th Five-Year Plan for the construct program of the key discipline (Mechanical Design and Theory) in Hunan Province and Hunan Province Scientific Research Program (2010FJ3031).

References

1. Yang, J.R., Cai, Y.H.: Modern Manufacturing Engineering (7), 112–114 (2006)
2. Neumaier, A.: Interval Methods for Systems of Equations. Cambridge University Press, Cambridge (1990)
3. Hansen, E.R.: Global Optimization Using Interval Analysis. Marcel Dekker, New York (1992)
4. Hansen, E.R.: Mathematics of Computation 22(102), 374–384 (1968)
5. <http://www.ti3.tu-harburg.de/~rump/intlab/index.html>

Solving Method of Dimension Chain Based on ScientificErrorAnalysis Package

Jirong Yang, Yuehua Cai, and Weiyue Xiao

College of Mechanical Engineering, Hunan University of Arts and Science
Changde, 415000, P.R. China
yjrtt1028@sina.com

Abstract. For uncertainty of error and tolerance in mechanical parts, it is used to describe it by random uncertain theory. The ScientificErrorAnalysis package provides representation and construction of numerical quantities that have a central value and associated uncertainty or error, which is some measure of the degree of precision to which the quantity's value is known. The ScientificErrorAnalysis package is introduced. The numerical example was given. The result proved the correctness and validity of the proposed method.

Keywords: parts tolerance, dimension chain, ScientificErrorAnalysis Package, uncertainty.

1 Introduction

Dimension chain analysis is the basis of mechanical manufacturing. For uncertainty of error and tolerance in mechanical parts, it is used to describe it by random uncertain theory. SPA analysis is a new method [1]. The ScientificErrorAnalysis package is used to calculate dimension chain. After introducing the overview ScientificErrorAnalysis Package, an example proved that the proposed method is correct and effective.

2 Overview of the ScientificErrorAnalysis Package

The **ScientificErrorAnalysis** package provides representation and construction of numerical quantities that have a *central value* and associated *uncertainty* or *error*, which is some measure of the degree of precision to which the quantity's value is known. Various first-order calculations of error analysis can be performed with these quantities. Each command in the **ScientificErrorAnalysis** package can be accessed by using either the long form or the short form of the command name in the command calling sequence [2-5]. The essential **ScientificErrorAnalysis** commands used for error assignment and computation are combine/errors (combine quantities-with-error in an expression), Covariance(return the covariance between two quantities-with-error), GetCorrelation(return the correlation between two quantities-with-error), GetError(return the uncertainty of a quantity-with-error), Quantity(construct a

quantity-with-error), SetCorrelation(set the value of the correlation between two quantities-with-error), Variance(return the variance of a quantity-with-error) .

In **ScientificErrorAnalysis**, a structure that has numerical quantities with associated *errors* is called a *quantity-with-error* structure. Instances of such structures, which have a particular quantity and error, are called *quantities-with-error*. There is a quantity-with-error structure native to **ScientificErrorAnalysis**, constructed using the Quantity constructor.

```
> with(ScientificErrorAnalysis):Quantity( 10., 1. );
```

In the above, the first argument is the central value and the second argument is the associated error, which can be specified in absolute, relative, or units in the least digit form. In the returned object, the error is in absolute form. The minimal interpretation placed on a quantity-with-error by **ScientificErrorAnalysis** is that of an unknown value with *central tendency*, where the *error* value is some statistical measure of the *spread* of the distribution of particular values (as obtained from an experiment or trial, for example). Nevertheless, many calculations of both error analysis and the **ScientificErrorAnalysis** package are only strictly valid for Gaussian distributions. However, in any particular application, this condition may not be strictly satisfied, and the interpretation of *error* values is the responsibility of the application. What the **ScientificErrorAnalysis** package *does not do* is perform what is called *interval arithmetic*. The *error* value of an object in the **ScientificErrorAnalysis** package *does not* represent an *interval* in which possible values must be contained. To extract the central value and error of a quantity-with-error, for example the above object, use evalf and GetError.

The **combine(expr, errors, opts)** command *combines* quantities-with-error in a mathematical expression, or in other words, *propagates* the errors through an expression, *expr* - expression containing quantities-with-error, *opts* - (optional) equation(s) of the form **option=value**, where **option** is one of 'rule' or 'correlations'; determine behavior. The **opts** argument can contain one or more of the following equations that determine the behavior.

```
> with(ScientificErrorAnalysis):
a := Quantity( 10., 1. ):
b := Quantity( 20., 1. ):
combine( a*b, errors );
```

Quantity(200., 22.36067977)

Although ScientificErrorAnalysis and ScientificConstants are separate packages, there are many connections between them.

The usual expressions for error propagation through simple functions are easily obtained.

```
> e1 := Quantity( x, delx );
```

e1 := Quantity(*x*, *delx*)

```
> e2 := Quantity( y, dely );
```

$$e2 := \text{Quantity}(y, \text{dely})$$

Error in a sum:

> **combine**(e1+e2, 'errors');

$$\text{Quantity}(x + y, \sqrt{\text{delx}^2 + \text{dely}^2})$$

Error in a product:

> **combine**(e1*e2, 'errors');

$$\text{Quantity}(x y, \sqrt{y^2 \text{delx}^2 + x^2 \text{dely}^2})$$

Relative error² in the product:

> **expand**(GetError(%)²/GetValue(%)²);

$$\frac{\text{delx}^2}{x^2} + \frac{\text{dely}^2}{y^2}$$

The initial default rounding rule is **digits**, for which no rounding is performed.

The general formula for the error σ_y in y , where y is a function of variables x_i is:

$$\sigma_y^2 = \sum_{i=1}^N \left(\frac{\partial}{\partial x_i} y \right)^2 \sigma_{x_i}^2$$

where σ_{x_i} is the error in x_i and the partials are evaluated at the central values of the x_i .

With covariances σ_{x_i, x_j} taken into account, the formula is:

$$\sigma_y^2 = \left(\sum_{i=1}^N \left(\frac{\partial}{\partial x_i} y \right)^2 \sigma_{x_i}^2 \right) + 2 \left(\sum_{i=1}^{N-1} \left(\sum_{j=i+1}^N \left(\frac{\partial}{\partial x_i} y \right) \left(\frac{\partial}{\partial x_j} y \right) \sigma_{x_i, x_j} \right) \right)$$

The covariance σ_{x_i, x_j} may be expressed in terms of the correlation r_{x_i, x_j} and errors σ_{x_i} , σ_{x_j} as follows:

$$\sigma_{x_i, x_j} = r_{x_i, x_j} \sigma_{x_i} \sigma_{x_j}$$

2.1 Numerical Example

Planar dimension chain is shown as Figure 1. Given $A_1 = 30_0^{+0.02}$ mm, $A_2 = 20_{-0.05}^{+0.05}$ mm, $A_3 = 25_{-0.015}^{+0.015}$ mm, $A_4 = 25_{-0.02}^{+0.06}$ mm, find A_Σ ?

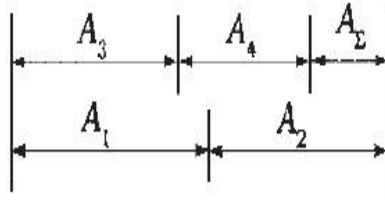


Fig. 1. Dimension chain diagramm

According to Figure 1, we obtain equation: $A_{\Sigma} = A_1 + A_2 - A_3 - A_4$. To find A_{Σ} , at first, transform dimension to construct a quantity-with-error Quantity and start Maple 13, then compile program with **ScientificErrorAnalysis** and **ScientificConstants** package as follows and run it.

```
> restart;
with(ScientificConstants);
with(ScientificErrorAnalysis);
A1:=Quantity(30.01,0.01);
A2:=Quantity(20.00,0.05);
A3:=Quantity(24.985,0.015);
A4:=Quantity(25.02,0.04);
A:=combine(A1+A2-A3-A4,'errors',rule=round[2]);
Smean:=GetValue(A);DetaS:=GetError(A);
LB:= Smean-2*DetaS;
UB:= Smean+2*DetaS;
```

After Running, we obtain results as follows and the $A_{\Sigma} = [-0.129, 0.139]$.

```
A1 := Quantity(30.01, 0.01)
A2 := Quantity(20.00, 0.05)
A3 := Quantity(24.985, 0.015)
A4 := Quantity(25.02, 0.04)
A := Quantity(0.005, 0.067)
Smean := 0.005
DetaS := 0.067
LB := -0.129
UB := 0.139
```

With extremum method, we can obtain $A_{\Sigma} = [-0.11, 0.12]$. The difference is very little.

3 Conclusions

The ScientificErrorAnalysis package provides representation and construction of numerical quantities that have a central value and associated uncertainty or error, which is some measure of the degree of precision to which the quantity's value is known. With ScientificErrorAnalysis and ScientificConstants package, we can use them to find dimension chain of mechanical parts. A example is given and it shows that the proposed method is correct and effective.

Acknowledgement. This research is supported by the grant of the 12th Five-Year Plan for the construct program of the key discipline (Mechanical Design and Theory) in Hunan Province and Hunan Province Scientific Research Program (2010FJ3031).

References

1. Yang, J.R., Cai, Y.H.: Modern Manufacturing Engineering (7), 112–114 (2006)
2. Bevington, P.R., Robinson, D.K.: Data Reduction and Error Analysis for the Physical Sciences, 2nd edn. McGraw-Hill, New York (1992)
3. Mohr, P.J., Taylor, B.N.: Rev. Mod. Phys. 72(2), 351–495 (2000)
4. <http://physics.nist.gov/cuu/index.html>
5. Taylor, J.R.: An Introduction to Error Analysis: The Study of Uncertainties in Physical Measurements. University Science Books (1982)

Feasibility Analysis on Tax Incentives Policy of Venture Capital

Rong Jiang

Department of Business and Trade, Changzhou Textile Garment Institute,
Changzhou, 213164, P.R. China
jrmhome@sina.com

Abstract. As the core of intellectual economy, high-tech industry is one of the most important economic powers of any advanced economy, has become a pillar of economic development gradually. In recent years the development of venture capital was also given adequate attention, and some tax policies were introduced to promote the development of venture capital companies, incentives for venture capital companies were further clear. Along with the rapid development of high-tech industry, venture capital need to be established a favorable macroeconomic environment, especially a favorable tax policy environment which is a significant content of the process of high-tech industrialization. Based on the problem of tax law on venture capital, this paper puts forward to some proposals for promoting the development of venture capital in china.

Keywords: venture capital, proposals, tax incentives, legal analysis.

1 Introduction

As the core of intellectual economy, high-tech industry is one of the most important economic powers of any advanced economy, has become a pillar of economic development gradually. In comparison with those traditional industries, high-tech industry is with the obvious characters of high input, high risk and high income. Thus venture capital as a kind of new financing mechanism has been founded. In recent years the development of venture capital was also given adequate attention, and some tax policies were introduced to promote the development of venture capital companies, incentives for venture capital companies were further clear. However, tax incentives police is not perfect and mature in our country, and have not a mature legal system as foreign to norm and incentive venture capital.

As the venture capital industry has a external positive effect, the government should increase its supply by tax incentives and other measures. At present the tax burden of China's venture capital industry is relatively heavy, so that the current tax system has hampered the development of China's venture capital industry. As some unsolved problems in venture capital development, the status quo of venture capital in china is not ideal. The imperfection of tax policy is one of the factors that restrict from the development of venture capital in china. Venture capital lacks of strong

support of tax policy. So along with the rapid development of high-tech industry, venture capital need to be established a favorable macroeconomic environment, especially a favorable tax policy environment which is a significant content of the process of high-tech industrialization. [1]

2 Characteristics of Venture Capital in China

Venture capital has the features of high risk, high input and the technological research and development has some externalities. The support from the good legal system, including finance, tax, government procurement, intellectual property protection, is essential to the prosperity of venture capital. To promote national venture capital activities, many developed countries formulated a series of tax allowance regulations. Tax allowance may decrease the risk of investments and increase the profit of investors. As an important factor in the whole process of venture capital activity, tax allowance was used to promote and guide the development of venture capital industry in recent years. [2]

Venture capital mainly involves in high-tech industries, and high-tech industry is an important force in promoting economic development, and is also one of important factors reflecting in innovation of the national economy in a country. The development of high-tech industry can overcome the constraints to high consumption of resources, so as to achieve sustainable and healthy economic development, and promote industrial upgrading, and then optimize the economic structure. This determines the behavior of venture capital firms pursuit for economic interests partly out of instinct to the; on the other hand, it also products some public goods, for example, upgrade their technological level. It is precisely because both the provision of public goods of venture investment properties, and the external positive effect in a market economy, that it need the government to give tax incentives to correct the "market failure", so as to achieve optimal allocation of resources. Therefore as a technology booster it has the external positive effect.

As venture capital gains except for investment income, but also takes great risk, to a large extent, so the success of investment can enhance the technological level of a country. Enhancing scientific and technological strength of a country is reflected in final upgrading of a country's national strength, and enhancement of national strength has the obvious attributes of public goods, so development of venture capital has a significant the external positive effect to upgrading the industrial structure and enhancing the strength of our country. [3]

3 Legal Analysis on Tax Incentives of Venture Capital

From the law view, in terms of the three basic principles of tax law, the thesis emphasized on the legislation of the tax allowance policy to provide a fair competition environment for venture capital. By analyzing the impact of the tax law and the "self-liquidating" effect of the taxation, this paper demonstrated the tax incentive measure is feasible. So our country should establish the tax allowance legal system as soon as possible.

Civil and Commercial Law corresponds with the private economy, and its adjustment can not solve the issues of market failure in provision of public goods and other, while the tax law, as the department of economic law, can make up for these shortcomings of civil and commercial law adjustment. The direct objective of tax law is to resolve the conflict between the individual profit and social welfare by gaining tax revenue and providing public goods; through the effective implementation of redistribution and configuration of resources, to achieve macro-regulation and promote social welfare and equality objectives in order to balance between efficiency and equity; through the protection of economic fairness and social justice, to promote steady economic growth and social welfare. [4]

Either from the statutory tax revenue, tax fairness or from a view point of efficiency tax, the tax law support on venture capital has both theoretical and practical necessity. As it not only help to eliminate the inferior position of venture capital compared with the traditional investment, so as to provide a relatively fair playing field for venture capital, but also improve resource allocation efficiency in the whole society by promoting the development of venture capital, so as to drive the growth of the entire national economy. Therefore, we should establish a sound legal system of tax incentives to support and guide the development of venture capital.

4 Feasibility Analysis on Tax Incentives to Venture Capital

In a purely free market economy without government intervention, the economic externalities makes the price depended on in making economic decisions not only accurately reflect the full marginal social benefits, but also accurately reflect the full marginal social cost. Therefore, the market transaction price in venture capital with positive external effects can not fully reflect its marginal social benefits. The investment decisions made by venture capital companies based on this distortion of price signals will make an error allocation of social resources without achieving the required Pareto optimal efficiency. The Government has often taken the measures of tax incentives to behavior has significantly external positive effect so as to compensate for external positive benefit, thus contribute to firm behavior so as to achieve optimal allocation of resources.

For an entrepreneurial act, if in the absence of government involvement in, the balance achieved in case of market forces alone, according to economic principles, can not achieve the optimal allocation of resources. Therefore, if only the Government through tax incentives compensate for external positive effect, thus make the venture capital achieve a new equilibrium, it could achieve the optimal allocation of social resources so as to achieve Pareto optimal state.

As shown in Fig.1 is the relationship model of positive external effect with the efficiency of resource allocation. In the figure, MC is the marginal cost curve of venture capital enterprises. The marginal cost of venture capital companies is the time value of invested capital, which is constant in a certain period, so it is horizontal. Demand curve D may measure the marginal private benefit (MPB) of venture capital investors. Investors will choose the intersect point q_1 of their demand curve and marginal cost curves as its optimal level of venture capital. The marginal social benefit (MSB) is the sum of the marginal private benefits and marginal external

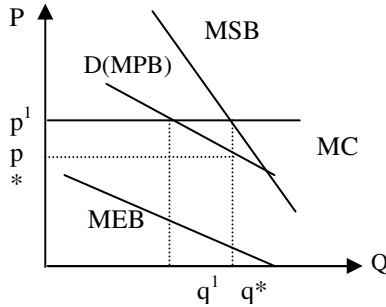


Fig. 1. Relationship model of positive external effect with efficiency of resource allocation

benefits at each venture capital level, that is $MSB = D + MEB$. Effective venture capital level q^* is the intersect point of MSB with MC curves, then the marginal social benefit of increasing venture capital is equal to the marginal cost of venture capital.

Because investors did not receive all the benefits of venture capital, there has been no efficiency, so the price $p1$ is too high, it can not encourage investment in venture capital investors to achieve social ideal levels. To encourage investors to provide an effective supply level, it will need to lower prices p^* . Therefore, from an economic perspective, the investment tax incentives given for venture capitalists by government can just make up outside income that venture capital can not get, so as to achieve the optimal allocation of social resources of venture capital. [5]

5 Proposals for Tax Incentives Policy of Venture Capital

In order to Legal system of tax incentives play a truly role, it must be combined with its own characteristics of venture capital then be adjusted accordingly, it is necessary to not only focus on attracting investment, but also form a risk compensation mechanism, so that the overall income level of venture capital is higher than of the general investment. Overall, in the tax incentives legislation to promote the venture capital industry, the following basic principles should be followed: (1) General principle. The legal system should focus on systemic and integrity of the whole venture capital industry. (2) Appropriate principle. Tax allowance has its own limitations, so we should just take it for appropriate control. (3) Combinative principle. We should pay attention to the coordination of the tax allowance and other basic legal system.

Establishing a sound legal system of venture capital tax. The development of various national venture capital shows that, if the tax laws deals with same venture capital as common investment behavioral, then the tax will erode much more risk premium, and the normal development of venture capital would be inhibited. Venture capital needs special support from tax law, this mainly promotes venture capital by tax incentives. Participants in venture capital, including venture inventors, venture capital organizations and enterprises, can share in various tax incentives provided by the state through law, so as to advance the development of whole venture capital industry. To achieve the purpose of promoting the development of venture capital by

China's tax laws, it is a priority to establish a sound venture capital tax laws system. It is urgent to draft our country's "Venture Capital Laws" as the basic law of venture capital, so as to define issues in the form of law, such as the venture capital subject, venture capital achievements, exit channels for venture capital etc., this is an important prerequisite of implementation of scientific and effective tax incentives.

Optimizing means of tax incentives of venture capital. The risk of venture capital is very great, if without interest it could not enjoy tax incentives, which is very unfair to venture capital. The risk is the greatest at R&D stage of product, and the costs of purchasing equipment and paying research personnel are very high, then tax law should focus on indirect incentives, such as accelerated depreciation of machinery and equipment, expenses net of research and development etc. Therefore, in the choice of means of tax incentives, the government should adhere that the indirect benefits is main, and direct benefits is supplement so that the venture investors can really benefit from there. This is not only a common trend of development of various national tax incentives legislation, but also a reality choice consistent with its own operational characteristics of venture capital.

Focusing on tax incentives to venture capital organization and resolving double taxation. Venture capital organization is the core of venture capital system, and is the financial intermediation that venture capital flow from investors to venture business. According to the different forms of organization, venture capital organizations in general can be classed into three types, including corporate, limited partnership and trust fund system. The double taxation to venture investment in China can be solved by reduction of the tax burden of venture capital firms and the formation of other types of venture capital enterprises. At present, there are still some difficulties in fully exempt from income tax of corporate venture capital companies, and the major occurrence of double taxation to the venture capital companies and venture investors is some of the transfer of equity investment gains and dividends from the start-ups, bonuses. So in the development stage of China's venture capital industry, the proceeds of venture capital companies may be implemented at lower rates or direct tax-free. At the same time the approach allowing the venture capital business to offset taxable income with investment and extract the risk reserves should be further improved. [6]

6 Conclusion

By studying on laws governing venture capital selects the legal systems on venture capital taxation and by analyzing the current situation and problems in china, some countermeasures on taxation law are put forward. Based on the problem of tax law on venture capital, this paper puts forward tax law promoting the development of venture capital in china. Venture capital in our country is still at primary stage, and it needs the great support of government. It is necessary for venture capital in our country to be offered good legal environment and clear policy guidance.

This paper analysis the concept and features of venture capital, notes the necessity and feasibility of the tax allowance legal system to promote the venture capital industry. By drawing advanced lessons from tax allowance regulations and by analyzing the current situation and problems in china, the perfect tax allowance legal

system of the venture capital industry is put forward to from the view of legislation and institution.

Acknowledgements. This study was supported by Philosophy and Social Science Foundation Project from Department of Education of Jiangsu Province (No. 09SJD790002).

References

1. Survey of the Economic and Social Impact of Venture Capital in Europe, http://www.evca.com/images/attachments/tmpl_9_art_37_att333.pdf
2. Keuslmigg, C., Nielsen, S.B.: Tax Policy, Venture Capital, and Entrepreneurship. NBER Working Paper No.7976, 10 (2000)
3. Gompers, P., Lerner, J.: An Analysis of Compensation in the U.S. Venture Capital Partnership. *Journal of Financial Economics* 3, 139–145 (2006)
4. Zhang, W.: Research on the Tax Policy Promoting the Development of China's Venture Capital Industry. *Transaction of Jilin University, Social Science* 1, 89–94 (2006)
5. Wang, S.: China Venture Investment Development Report 2005. Economic Management Press, Beijing (2005)
6. Huang, F.: The Taxation of Venture Capital Industry. *Tax research* 6, 156–161 (2004)

Design and Simulation of Caterpillar Drive System for Multifunction-Paver

Wu Guoyang

Material Engineering College of Panzhuhua University,
Panzhuhua, 617000, P.R. China
Guoyang_wu@163.com

Abstract. The walking drive system is the major component of the multifunction-paver, in which adaptive material and structure for multifunction-paver was presented. Fuzzy-PI dual-mode control had been set up, simulated and analyzed by Matlab in order to get a constant speed. The simulation results show that when the fuzzy-PI dual-mode control was used, the walking stability of paver will get a very good guarantee, not only fast response, but also no steady-state error.

Keywords: Multifunction-paver, Simulation, Walking drive system, Fuzzy-PI.

1 Introduction

Multifunction-paver[1] has very strict requirements of the constant speed in the pavement process. The flatness of the road, the initial density and the segregation level of paving are directly influenced by its driving performance. Therefore, control of paver walk can be achieved, the driving performance of paver can be improved. The quality of pavement mechanization construction can also be improved by controlling the paver driving system[2-4]. Currently, the full hydraulic-driven electro-controlled hydraulic pump-motor system was equipped in multifunction paver driving system to achieve continuously variable. With the development of electro-hydraulic control technology, and the realizing products technology upgrading of intelligent control technology began to be applied to the multifunction-paver driving system. In this paper, the multifunction-paver of the walking hydraulic system of the control was studied by bring in a fuzzy-PI dual-mode control theory to achieve the multifunction-paver drive system of the speed control [5].

This paper is organized as follows: Section 2 presents Mechanics calculation of the paver drive system[6-8]. Paver drive system dynamics simulation is analyzed in the section 3 by using Matlab, which includes the mathematical model of paver walking mechanism, and Simulation and analysis of paver walking mechanism. Section 4 contains a summary of the work.

2 Paver Drive System Mechanics Calculation

The efficiency of walk mechanism of the crawler type paver can be written as[9]:

$$\eta_x = \frac{N_{kp}}{N_k} = \eta_r \frac{F_{kp} V}{F_k V_t} = \eta_r \frac{(F_k - F_f)V}{F_k V_t} \tag{1}$$

In above equation: V_t -theory drive speed (m /min); V -actual drive speed (m/min); N_{kp} -effectively traction power of driving wheel tangent line (kW); N_k -traction power of driving wheel tangent line (kW); η_f -rolling efficiency, $\eta_f = \frac{\varphi_x - f}{\varphi_x}$; η_δ -slide efficiency; $\eta_\delta = 1 - \delta$; φ_x -attached to the weight of the utilization coefficient; f -rolling resistance coefficient; η_r -crawler machine efficiency.

Checking the maximum gradability: when paver works under the maximum gradability, its slope resistance can be written as:

$$F_\alpha = gm_y (f \cos \alpha_{\max} + \sin \alpha_{\max}) \tag{2}$$

In above equation: α_{\max} - the maximum gradability (rad); m_y - Total mass of paver (kg).

System pressure $P_{P\alpha}$ can be written as:

$$P_{P\alpha} = \frac{2\pi T_L + P_r + \sum \Delta P}{\eta_m q_m} = \frac{2\pi r_k F_{ks}}{\eta_m \eta_r \eta_L q_m i} + P_r + \sum \Delta P (F_{ks} = 0.6F_\alpha) \\ = \frac{1.2\pi r_k m_y g (f \cos \alpha_{\max} + \sin \alpha_{\max})}{\eta_m \eta_r \eta_L q_m i} + P_r + \sum \Delta P \tag{3}$$

$P_{P\max} > P_{P\alpha}$ That is to say the maximum pressure $P_{P\max}$ by setting of the system is greater than the system pressure determined by the maximum gradability.

3 Paver Drive System Dynamics Simulation

The multifunction-paver of the walking hydraulic system is a typical machine-electric-hydraulic coupling system with fast dynamic response, high precision and so on. But because of the electro-hydraulic servo system of nonlinearity (such as the servo valve flow-pressure nonlinearity, servo zero bias, gain nonlinearity, hysteresis nonlinearity) and the uncertainties of parameters and other factors, in this system, parameter time-varying, large external disturbance range and nonlinear problems exist generally, which causes the describing system of a mathematical model difficultly to be established. Therefore, applications of models and parameters to determine control

methods have significant limitations. The classic PID control performance is poor, because it is easy to produce overshoot, instability and can not be quickly and reliably track the input and other shortcomings in the operation process, which is difficult to meet the control performance requirements so that the multifunction-paver is difficult to adapt to modern high-quality grade highway pavement construction requirements. Because the fuzzy control does not rely on precise mathematical model of controlled object, and its fast response, strong robustness, disturbance and parameters on control effect of the impact is greatly reduced, especially for nonlinearity, time-varying and pure hysteresis system of the control. However, if there is no integral part of the fuzzy control, and the processing of input is a discrete and limited, that is to say the control surface is trapezoidal rather than smooth, so that the steady-state error will sure be produced, that the small amplitude of the limit ring oscillation phenomenon may be appear near the equilibrium point. This phenomenon is caused by the input fuzzification and the output defuzzification factors, so that the system has the multi-valued relay characteristic.

In order to improve the steady-state performance of fuzzy controller, the usual practice is to bring a fuzzy integral into controller. However, the introduction of integral control has different forms.

3.1 Paver Walking Mechanism Mathematical Model

In the crawler type paver traveling drive loop, the proportional control axial piston variable displacement pump is more used in hydraulic pump. To meet the power conditioning and automatic (intelligent) control requirements, the variable pump control method has been considerable development in recent years. The electrical - mechanical conversion elements and the control valve are used by the proportional control variable pump to manipulate the variables institution, not only the manipulation ways are different, more important is that electrical signals can be used to achieve the power regulation and adaptive control. This is of great significance for the high-voltage power system performance improvement and energy conservation. Proportional control type displacement adjust is divided in accordance with the feedback way between the variable piston and the control valve, there is a displacement direct feedback, a displacement-force feedback and a displacement-electric feedback. The displacement direct feedback is the equivalent of the regular variable pump servo variable way, the variable piston follows the tracks of the control valve displacement to fix position. The variable piston displacement is used by the displacement-force feedback which makes the control spool closing the valve port in the equilibrium condition through the spring feedback, so that the variable piston is fixed position.

The proportional valve used for the variable pump variable adjusting mechanism is the electro-hydraulic proportional direction flow valve, it is a kind of compound valve which has a flow direction control function and a flow rate control function. In the case of constant differential pressure, its flow in proportion with input electric signal, but its flow direction depends on the electric signal on-off and direction. This paper adopts the direct-acting proportional directional flow valves. Its transfer function can be written as:

$$x_v(s) = \frac{K_I I(s)}{(m_T + m_v)s^2 + (B_T + B_v)s + (K_y + K_v + K_{fv})} \tag{4}$$

In above equation: K_I -Proportional electromagnet current power gain (N/A); K_y - The sum of the proportional electromagnet displacement power gain and the zero spring stiffness (N/m); m_T - Armature assembly quality (kg); B_T - Damping coefficient (N·s/m); m_v - Valve core quality (kg); B_v - Valve core of viscous damping coefficient (N·s/m); K_v -Valve core of spring stiffness (N/m); K_{fv} - Acting on the valve core steady-state hydraulic dynamic stiffness coefficient (N/m).

In the pump control system, as a two-way variable pump displacement control mechanism of controlling hydraulic cylinder link (ie, a variable mechanism) is a four-way slide valve control for the symmetric double-acting hydraulic cylinder structure, which can guarantee as displacement adjusting mechanism of the pump inclined dish for positive and negative motion to make the suction and discharge oil reciprocity easily, but also ensure the two-way action of dynamic characteristic of consistency. However, the location system must use an assisted oil source, which is an external control variables institution to ensure the pump does not make the control and feedback losing efficacy in the emissions to zero situation. The transfer function is:

$$y(s) = \frac{AK_q x_v(s) - (K_c + C_{ic} + \frac{V}{4\beta_e} s) F_c(s)}{\frac{m_p V_t}{4\beta_e} s^3 + \frac{B_p V_t}{4\beta_e} + K_c m_c + C_{ic} m_c s^2 + (K_p B_c + C_{ic} B_c + \frac{K V_t}{4\beta_e} + A^2) s + K(K_c + C_{ic})} \tag{5}$$

In above equation: K_q -Slide valve in steady state set-point nearby flow gain (m²/s); K_c -Slide valve in steady state set-point nearby flow rate-pressure coefficient (m⁵/N·s); A-Hydraulic cylinder piston effectively end area (m²); C_{ic} - Total leakage coefficient of hydraulic cylinder (m⁵/N·s); m_c -the total mass of piston and load (kg); B_c -the piston and the load of viscous damping coefficient (N·s/m); K -the piston and the load spring stiffness (N / m); F_c -Load external force (N); V_t -Two oil chamber hydraulic cylinder total volume (m³); β_e -Oil effective volume elastic modulus (N/m²)

3.2 Paver Walking Mechanism Simulation and Analysis

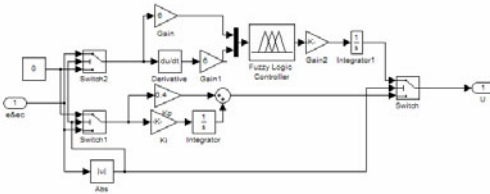


Fig. 1. Paver walking mechanism control system

In the MATLAB environment, a drive system of simulation model can be easily constructed by using the SIMULINK simulation language in the model window. The Subsystem in the diagram is paver walking mechanism of control model, the expansion shown in Fig.1.

When the paver driving speed is 6m/min and without a controller, the paver driving speed curve is shown in Fig.2. From Fig.2, it can be seen that under step signal excitation, the paver driving speed of peak time is 1 second, regulation time is 2 seconds, and has a larger overshoot.

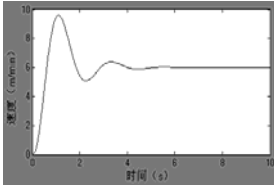


Fig. 2. The paver driving speed without the controller

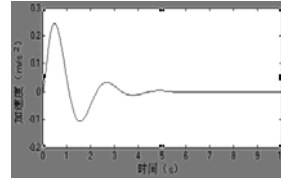


Fig. 3. paver driving acceleration with the fuzzy-PI control

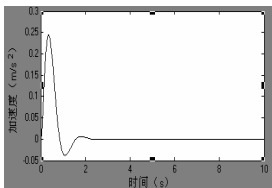


Fig. 4. Paver speed as acceleration

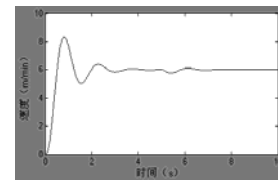


Fig. 5. Paver speed at impact

However, because the fuzzy control without the integral part, and the processing of input is a discrete and limited, that is to say the control curved surface is trapezoidal rather than smooth, so the small amplitude of the limit ring oscillation phenomenon appears near the equilibrium point, so that the paver can not drive steadily under the set speed.

When the paver driving speed is 6m/min and using the fuzzy-PI control, the paver driving acceleration curve shown in Fig.3, from Fig.3, it can be seen that under step signal excitation, the paver can quickly achieve the set acceleration and no overshoot, no steady state error, and has good features. Acceleration is shown in Fig.3.

The paver speed response curve is shown in Fig.4. From Fig.4 it can be seen that the paver can accelerate the set value in a relatively short period of time and no overshoot.

When the dump truck and the paver are rapidly separated, the dump truck of unloading process has been completed, reducing the dump truck loads only decreases their loads on the paver, at this time, the paver speed fluctuations as Fig.5. From Fig.5 it can be seen that when the dump truck and the paver are rapidly separated, the paver driving speed can quickly return the set value.

4 Conclusion

This paper introduces the principle, structure, and working process of walking drive system of multifunction-paver. By using AMESim software, we have established a

simulation model and performed a performance simulation. By using Matlab, the fuzzy-PI dual-mode control has been simulated and analyzed in order to get a constant speed, simulation results show that when using the fuzzy-PI dual-mode control, the walking stability of paver will get a very good guarantee. Control of paver walk can be achieved, the ride ability of paver can be improved, and the quality of pavement mechanization construction can also be improved by controlling the paver walking system.

References

1. Truong, D.Q., Ahn, K.K.: Force control for hydraulic load simulator using self-tuning grey predictor-fuzzy PID. *Mechatronics* 19(2), 233–246 (2009)
2. Ahn, K.K., Truong, D.Q.: Online tuning fuzzy PID controller using robust extended Kalman filter. *Journal of Process Control* 19(6), 1011–1023 (2009)
3. Avramov, K.V.: Analysis of forced vibrations by nonlinear modes[J]. *Nonlinear Dynamics* 53(1-2), 117–127 (2007)
4. Chen, D., David, B.B.: Six-DOF vibrations of partial contact sliders in hard disk drives. *Microsystem Technologies* 15(10-11), 1539–1546 (2009)
5. Koh, B.H., Nagarajaiah, S., Phan, M.Q.: Reconstructing structural changes in a dynamic system from experimentally identified state-space models. *Journal of Mechanical Science and Technology* 22(1), 103–112 (2008)
6. Alpay, D., Gohberg, I.: The State Space Method Generalizations and Applications. *Integral Equations and Operator Theory* 53(1), 145–148 (2005)
7. Yano, K., Yano, K.: A self-organizing state space model and simplex initial distribution search. *Computational Statistics* 23(2), 197–216 (2008)
8. Zhu, Q., Li, Z.-G.: Improvement on Paver Auger and Application. *Construction Machinery and Equipment* 38(9), 40–43 (2007)
9. Sun, Q.-F., Zhang, W., Zhang, Y.-f., et al.: Configuration Characteristic and Work Performance of Leveling Benchmark of Asphalt-pavers. *Journal of Wuhan University of Technology* 29(9), 141–143 (2007)

A Hybrid Biometric Personal Identification Method Based on Chinese Signature

Yongjian Zhao and Haining Jiang

Institute of Information Engineering, Shandong University at Weihai,
Weihai 264209, China
zhaoyj@sdu.edu.cn, jian123cn@sina.com

Abstract. This paper presents a hybrid method for online Chinese signature identification. Based on the better properties of B-spline function, we present a group of 4th order B-spline wavelet bases, which can be used to each stroke of the signature through wavelet decomposition. The Fisher distinction criterion function is a generalized Rayleigh quotient in essence. After effective signature characteristic is synthesized, the perfect properties of generalized Rayleigh quotient are analyzed and a novel method is developed so as to establish a stable and effective pattern library, which can be dynamically adapted in runtime to model the variation of signature.

Keywords: wavelet transform, pattern library, Fisher distinction criterion, threshold.

1 Introduction

Biometric personal identification is an active research item aiming at automatic identity and is receiving growing interest from academia and industry [1]. As Chinese signature is easy to obtain and different people have different signature characteristic, Chinese signature based biometric personal identification has a wide of applications in financial security, electronic commerce and national security. The principle of online Chinese signature identification is firstly to collect the reference signature provided by the specific person to computer and extract reliable signature characteristic so as to establish pattern library for the appointed person. After inputting the certain signature which needs to be identified, one can compare its characteristic with those in the pattern library so as to find out whether it is authentic or forged [1,2].

The kernel step of Chinese signature identification is to obtain stable signature characteristics so as to form an effective pattern library. As B-spline function has many natures, such as recursion, local positive supported, multi-scale and the smallest compact supported, B-spline wavelets constructed by B-spline function have both desirable properties. We develop a 4th order B-spline wavelet bases which are used for wavelet transform to each stroke of signatures, so the extracted characteristics are more suitable to the whole signature. From the aspect of optimum, the Fisher distinction criterion function is a generalized Rayleigh quotient in essence. The

extremum properties of generalized Rayleigh quotient are analyzed and a novel method of forming pattern library is proposed, which can be dynamically adapted in runtime to model the variation of signature. One can first work out the optimum classifying direction of signatures by the host and the imitators, and then project the feature vector to the classifying direction. After a proper threshold is selected to classify the signature samples, a more representative pattern library is formed. At last, a proper classifier is developed which can be more effective and robust than the traditional Euclid distance. The simulation results show that this method has better stability and reliability.

2 Stable Signature Extraction Based on Wavelet Transform

Due to the perfect property of adaptive feature and mathematical microscope feature, wavelet transform has becoming a focus issue in the field of signal processing [3,4]. The basic principle of wavelet transform is to seek for a series of orthogonal wavelet bases, on which primal signals can be decomposed and synthesized. The performance of wavelet bases plays an important role in the whole process of wavelet transform. It is more effective and accurate to construct wavelet bases in accordance with specific application occasion [1,2,3,4].

The 1th order B-spline function $N_1(x)$ is feature function in interval $[0,1]$. For $m \geq 2$, $N_m(x)$ is recursively defined as

$$N_m(x) = \int_{-\infty}^{+\infty} N_{m-1}(x-t)N_1(t)dt = \int_0^1 N_{m-1}(x-t)dt .$$

Based on the better properties of B-spline function [1,2,3], we construct a function

$$\phi_1(x) = N_m(x + m/2), \text{ whose Fourier transform is } \hat{\phi}_1(\omega) = \left[\frac{\sin(\omega/2)}{\omega/2} \right]^m .$$

If we set $e_n(\omega) = \sum_{k=-\infty}^{+\infty} \frac{1}{(\omega + 2k\pi)^{n+2}}$, we can deduce that

$$e_n^1(\omega) = -(n+2) \sum_{k=-\infty}^{+\infty} \frac{1}{(\omega + 2k\pi)^{n+2+1}} = -(n+2)e_{n+1}(\omega) \quad \text{and}$$

$$e_{n+1}(\omega) = -\frac{1}{n+2} e_n^1(\omega) .$$

Because $e_0(\omega) = \sum_{k=-\infty}^{+\infty} \frac{1}{(\omega + 2k\pi)^2} = \frac{1}{4 \sin^2(\omega/2)}$, we can find that

$$e_{n+1}(\omega) = -\frac{1}{n+2} e_n^1(\omega) \text{ and } \sum_{k=-\infty}^{+\infty} \left| \hat{\phi}(\omega + 2k\pi) \right|^2 = 2^{2m} \sin^{2m}\left(\frac{m}{2}\right) e_{2(m-1)}(\omega) .$$

$$\text{So } \hat{\phi}(\omega) = \left[\frac{\sin(\omega/2)}{\omega/2} \right]^m \cdot \frac{1}{\sin^m(\omega/2)} \cdot \frac{1}{\sqrt{\sum_{k=-\infty}^{+\infty} \frac{1}{(\omega + 2k\pi)^{2m}}}} = \frac{1}{\omega^m} \cdot \frac{1}{\sqrt{e_{2(m-1)}(\omega)}} ,$$

where function $\phi(x)$ satisfies the define of multi-scale: $\sum_{k=-\infty}^{+\infty} |\hat{\phi}(\omega + 2k\pi)|^2 = 1$.

As $\hat{\phi}(2\omega) = H(\omega)\hat{\phi}(\omega)$, we can obtain that $H(\omega) = 2^{-m} \sqrt{\frac{e_{2(m-1)}(\omega)}{e_{2(m-1)}(2\omega)}}$. When

we set $m=4$, we implement the construction of 4th order B-spline wavelet.

The discrete inverse Fourier transform of $H(\omega)$ is impulse response $\{h_l\}_{l=0 \dots 511}$ from scaling function $\psi(t)$, whose value can be calculated. Due to space, we do not give the value of h_l and g_l ($l=0 \dots 511$) where $g_k = (-1)^{k-1} h_{512-k}$, $k=1 \dots 511$, $g_0 = (-1)h_1$.

After wavelet decomposition and synthesis [1,2,3,4], we can obtain effective signature characteristics.

3 The Construction of Pattern Library

Although one's signatures are stable, they can vary with time and writing environment. Obviously, some signatures can not reflect the signature characteristics of the signer precisely, so the formation of effective pattern library is very difficult and its performance can decide the entire effect of the signature identification system to a great extent [2,3]. From the aspect of optimum, based on the fact that the Fisher distinction criterion function is a generalized Rayleigh quotient in essence and the extremum properties of generalized quotient, a novel method is proposed, which first works out the optimum classifying direction of signatures by the host and the imitators, and then project the feature vector to the classifying direction, through choosing a proper threshold to classify the signature samples, a more representative pattern library is formed. In this way, a proper classifier is developed which can adapt to the systemic characteristic and further enhance the identifying effect.

We can suppose all training samples are x_k ($k = 1, 2, \dots, n$) where n is the sample number. We also suppose n_1 come from class ω_1 and n_2 come from class ω_2 where $n = n_1 + n_2$. As x_k ($k = 1, 2, \dots, n$) may be multidimensional, it is difficult to estimate whether a specific sample is come from class ω_1 or ω_2 . We can make a transform as $y_k = \omega^T x_k$, $k = 1, 2, \dots, n$ where y_k is the one-dimensional scalar achieved from x_k through the transform of ω . In fact, for the given ω , y_k is the value of the decision function. Y_1 and Y_2 are the mapping sets of subsets X_1 and X_2 , respectively. Because we are only concerned with the direction of ω , we can make $\|\omega\| = 1$, then y_k is the projection of x_k in the direction of ω . The direction of ω , which can be easily used to distinguish subset Y_1 from subset Y_2 , is the normal direction that can be used to distinguish the hyperplane. We can set

$m_i = \frac{1}{n_i} \sum_{x_k \in X_i} x_k$, $i = 1, 2$ where m_i is the sample mean vector in the d dimensional

space from various classes. After projected to the one-dimensional space through the transform of ω , the mean value of the various classes is $M_i = \frac{1}{n_i} \sum_{y_k \in Y_i} y_k, i = 1, 2$.

After the projection, the discrete degree inside various sample classes can be defined as $S_i^2 = \sum_{y_k \in Y_i} (y_k - M_i)^2, i = 1, 2$. Obviously, we hope that the larger distance

between mean values of two classes after projection is the better, whereas the smaller discrete degree inside each class is the better. So the Fisher criterion function can be

defined as $J_F(\omega) = \frac{|M_1 - M_2|^2}{S_1^2 + S_2^2}$.

The analytic value ω^* that makes J_F maximum is the optimum solution vector, which also is Fisher linear discriminant. We can set

$$S_b = (m_1 - m_2)(m_1 - m_2)^T \text{ and } S_i = \sum_{x_k \in X_i} (x_k - m_i)(x_k - m_i)^T,$$

so $S_1^2 + S_2^2 = \omega^T (S_1 + S_2) \omega = \omega^T S_\omega \omega$ where $S_\omega = S_1 + S_2$, S_i is called the discrete degree matrix inside the pattern class of the original d multidimensional space and S_ω is the whole discrete degree matrix inside the pattern class [1,2]. Obviously, in order to be more easily classified, the smaller of the discrete degree inside the class is the better, which means the smaller S_ω is the better. According to the above analysis, the explicit function of $J_F(\omega)$ can be concluded as

$$J_F(\omega) = \frac{\omega^T S_b \omega}{\omega^T S_\omega \omega},$$

where $J_F(\omega)$ is the famous generalized Rayleigh quotient,

whose maximum value can be worked out through Lagrange multiplication as follows $\omega^* = S_\omega^{-1} (m_1 - m_2)$, where ω^* is the solution that makes the criterion function $J_F(\omega)$ maximum. ω^* is also the optimum projecting direction for the patterns projection from the d multidimensional space to the one-dimensional space.

With the help of ω^* and $y_k = \omega^T x_k, k = 1, 2, \dots, n$, the multidimensional space can be projected into one-dimensional space. If we choose a proper threshold T_0 and we can classify the samples by comparing the projecting point y_n with T_0 . The threshold T_0 is achieved from the following equation $T_0 = \frac{N_1 \tilde{m}_1 + N_2 \tilde{m}_2}{N_1 + N_2}$.

In above formula, N_1 and N_2 are the sample numbers from two classes whereas \tilde{m}_1 and \tilde{m}_2 respectively are the mean mapping values of the sample collections in the

Fisher optimum classifying direction. According to the Fisher distinction criterion in the first experiment, the signatures are stable and effective only if their projection points are larger than T_0 . We put the satisfying signature samples into the specific signature pattern library and desert the rest.

4 Matching Identification and Conclusions

Chinese signature identification is a complicated process, which is on the premise of the precise understanding of the details of differences between signatures to be identified with those in the pattern library, such differences are found through comparison of the corresponding characteristics between signature to be identified with those in the pattern library [1,2,6]. After a series of stable characteristics of the signature are extracted and an effective pattern library is established, what we must do is to identify the signature through distance match between characteristics of the signature to be identified with those in the pattern library. In our experiments, we use the famous Mahalanobis distance to process matching identification [1,3].

Provided that x and y are the samples taken from class π whose covariance matrix is Σ and the mean mean is μ , the Mahalanobis distance between x , y is defined as [1,3]

$$D(x, y) = [(x - y)' \Sigma^{-1} (x - y)]^{\frac{1}{2}}$$

The Mahalanobis distance between sample x and class π is defined as

$$D(x, \pi) = [(x - \mu)' \Sigma^{-1} (x - \mu)]^{\frac{1}{2}} .$$

We further provided that the mean vectors of class π_1 and class π_2 are μ_1 and μ_2 respectively, the covariance matrix are Σ_1 and Σ_2 respectively. Now given an individual x , we want to figure out from which parental class x comes. We can first calculate Mahalanobis distance from x to class π_1 and π_2 by the Mahalanobis distance between specific sample and class, and then compare the two distances $D(x, \pi_1)$ and $D(x, \pi_2)$. If $D(x, \pi_1) \leq D(x, \pi_2)$, we can decide that x belongs to class π_1 , otherwise x belongs to class π_2 .

In order to testify the reliability and validity of our method, we conduct a lot of experiments. After 50 independent trials, we find that the mean identification rate and the optimum identification of our method is 92.8% and 94.7% ,respectively. It must be worthwhile to mention that the method in [5] is 85.6% and 88.9%, respectively. We can draw a conclusion that the method proposed in this paper can achieve a better performance to Chinese signature identification. The theoretical framework being developed here should provide a strong foundation for future research and application.

References

1. Bian, Z.: Pattern Recognition. The Tsinghua University Press (1994)
2. Zhao, Y.: Chinese writing identification based on wavelet transform. *Computer Project* 8, 135–147 (2005)
3. Ripley, B.D.: Pattern Recognition and Neural Networks. Cambridge University Press, Cambridge (2006)
4. Chui, C.K.: Approximation Theory and Functional analysis. Academic Press, Boston (2001)
5. He, Z., Chen, Q.: A neural network expert system for Chinese handwriting-based writer identification. *Machine Learning and Cybernetics* (2002)
6. He, Z.Y., Tang, Y.Y.: Chinese handwriting-based writer identification by texture analysis. *Machine Learning and Cybernetics* (2004)

The Interference in Numerical Control Machine System and Response

Hengyu Wu, Ling He, and Minli Tang

Hainan software vocational and technical college, Hainan,
Qionghai, 571400, China
whytml@163.com, heling_2818@126.com,
gslstml@163.com

Abstract. This paper states the main source of the interference in numerical control machine, the response for the anti-interference and some effective anti-interference measures in the actual applications which can improve the competency of anti-interference and the stability of system operating.

Keywords: numerical control machine system, Interference, anti-interference.

1 Introduction

According to KPMG report, China has outstripped Germany and become the largest market of machine tools in the world. In 2010, the consumption of numerical control machine was over 6 thousand million dollars and the amount of machines was more than 100 thousand[1]. With the development and wide application of numerical control machines, the EMI of the system has become more and more serious, which leads to the increasing importance of the anti-interference technology (known as EMC). It demands both the improvement of the numerical control machine processability and the competency of anti-interference. Otherwise, there must be something unreliable on the application and processability of the numerical control machine. First and foremost, as the part always touched by operators and maintainers, the metal shell will get circuit leakage and lead to personal injury with a bad earth. Secondly, the metal parts with a bad earth are out of control and cannot absorb electromagnetic wave, which will lead to signal disturb to electrical elements and then, the elements will be in unmoral operating condition and have a unstable performance.

2 Source of the Interference in Numerical Control Machine System

The numerical control machine system is made up as chart 1. The system consists of heavy current installation with HV and high current, and control and signal processing equipment and sensor with low voltage and undercurrent, as called weak current installation. The strong EMI caused by heavy current installation threatens the weak

current installation heavily. What’s more, when the system is located in a workplace with a hostile electromagnetic environment where disturbs from line load, power-supply system and the atmosphere will have a serious influence on the weak current system inside. Because the weak current system is controlled by the heavy current installation, the whole system will finally be irregular and even paralysis following that the weak current system is disturbed[2].

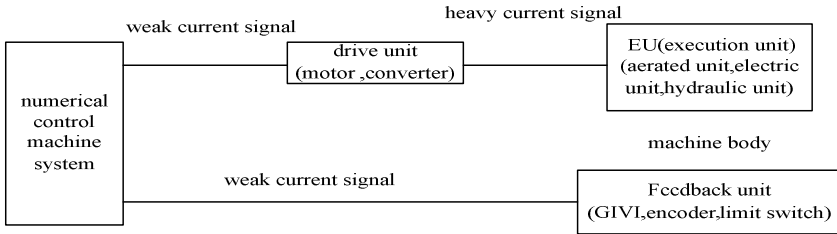


Chart 1. Numerical control machine system

Therefore, it’s the main route to make the system to reach the electromagnetic compatibility that we should try to suppress the undesired signal, cut off the transmission path of disturb and improve the anti-interference capability of victims. Three of the most frequently used measures are grounding, filter and shield.

3 Measures to Interference to Numerical Control Machine System

Grounding technology. Grounding technology is one of the effective measures to improve EMC of electronic equipments. Correct grounding can not only restrain electromagnetic interference, but also restrain the equipment itself sending interference out. The meaning of Grounding is to provide an equipotential point or potential which can be classified in terms of the proposes of grounding as safety ground, lightning protection ground and working ground[3].

Safety ground. Safety ground means the enclosure grounding. It can protect charge from accumulating on the enclosure, which leads to electrostatic discharge and threats the equipments and workers. On the other hand, when the insulation damages and the enclosure charges, it will arouse the protection mechanism to cut off in time so that the workers can be safe.

The enclosure grounding is a shielding layer provided for reliable operation against interference, which can segregate interior from the noise outside. The shield of each unit’s enclosure, mounting plate and interface cable should be connected together. The relatively general method at present is to connect each enclosure by wires so that it can be under cover. On the contrary, the enclosure will look like a cobweb and it will not only affect the appearance but also fail to ground. The enclosure grounding is always connected by two pieces of Pt, including hole-to-hole connection, hole -to-S CLS SP connection and hole-to-screw hole connection. Connection as Chart2 can make sure the safety grounding and make a perfect appearance.

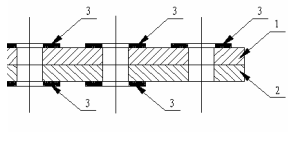
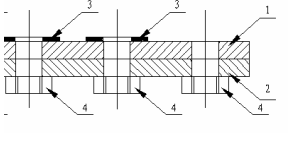
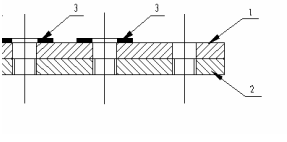
hole-to-hole connection	hole -to-S CLS SP connection	hole-to-screw hole connection
		
<p>Three parts of metal plate1 is weld with stainless steel plate3 and correspondingly three parts of metal plate2 is weld with the plates. All above make Plate1 weld with Plate2 by stainless steel nails to make sure to ground</p>	<p>Three parts of metal plate1 is weld with stainless steel plate3 and correspondingly three parts of metal plate2 is weld with the S CLS SP 4. All above make Plate1 weld with Plate2 by stainless steel nails to make sure to ground.</p>	<p>Stainless steel plate3 weld on Plate1 and the corresponding screw hole on Plate2 are connected by stainless steel link nails so that they can link Plate1 and Plate2 together to ground.</p>

Chart 2. Ways connected to the machine casing

lightening protection ground. When power electronic equipments are struck by lightning, whether directly or inductively, they will be damaged seriously. Setting a lightning conductor against lighting struck can protect workers and equipments from damage. The two methods mentioned above are both on the base of safety and connected to the earth directly.

working ground. Working ground provides a reference potential for the normal performance of circuits. The reference potential can be defined as a spot, a part or a piece of the circuit. When the reference potential is not connected with the ground, it will be regarded as the relative zero potential. The relative zero potential will change following the electromagnetic field outside, which leads to the instable performance of the circuit system. If it is connected to the ground, the reference potential will be regarded as the earth's zero potential and it cannot be influenced by field outside. But the wrong working ground can affect the performance more, for example the influences from shared earth wires or earth loop circuit. In order to prevent the interference as mentioned above, there are several methods to ground.

To prevent interference from different circuits so that they can be compatible, on the bases of nature, we classify the working ground into different terms: direct ground, AC ground, artificial circuit ground, signal ground, GQD ground and power ground. All methods of grounding above should be installed respectively.

signal ground. Signal ground is that sensors of various physical qualities and shared standard wires whose signal source has a zero potential, providing reference level for control signal (OV). The weak current holding wire must be shielded and the susceptible shielding layer must be grounded. The electricity cabinet should have earth plates. Shielding lines of each unit should ground through grounding copper

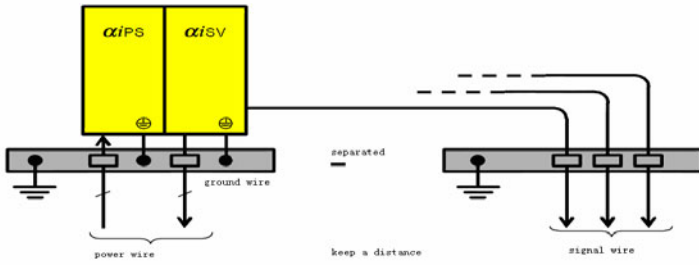


Chart 3. The strong and the weak current ground separately

lugs. As shown in chart3, the earth copper tape of strong current (power) and the one of weak current should be separated from each other a distance. It cannot share the same earth copper tape with other systems, such as PLC controller, material equipment and the external detection equipment.

artificial circuit ground. The artificial circuit ground is that its public benchmark circuit has an artificial circuit with zero potential. Since the circuit undertakes the amplification of both small signals and the large signal power, which contains LF and HF, the artificial circuit is easy to be disturbed and generate interference. For this reason, we should take sufficient consideration of the choice of earth point of artificial circuit and how to lay the earth wires.

signal ground. The signal ground is that its public benchmark circuit has a signal circuit with zero potential. The signal circuit is always in the pulse operation and both the front and back edges of the pulse are steep or it has a HF, which can lead to disturb to the signal circuit. For this reason, we should take sufficient consideration of the choice of earth point of signal circuit and how to lay the earth wires.

GQD ground. The GQD ground is that its public benchmark circuit has a source with zero potential. The source supply to each unit of the whole system at the same time and each unit has a different requirement for the character and parameter of the power-supply. So it's necessary to keep both the source and the other units have a stable operation.

power ground. Power ground is a public benchmark circuit of the zero potential of load circuit or GQD. The load circuit or GQD has a strong current and a HV, so it has a serious interference on the power grounding wire. As a consequence, the power ground should be installed separately with other weak current groundings.

Synthetically including the designs of artificial circuit ground, signal ground, GQD ground and power ground, chart4 is the typical design of cubicle ground: different kinds of methods of grounding operate respectively and finally get to the ground together. Single point grounding, multipoint grounding, mixed grounding and floating cooperate with each other well and form a fine grounding system which is for the purpose of numerical control machine system disturbing interference.

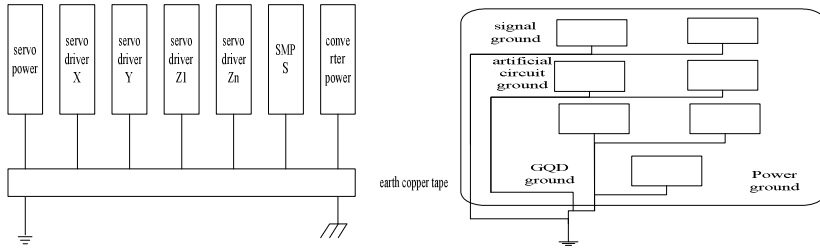


Chart 4. Typical control cabinet grounding

shielding technique. Shielding technique is used to forbid magnetic noise spreading through space, which means cut down the route of transmission of radiate electromagnetic noise[4]. This method usually take use of metal material or magnetic material to cover the area which should be shielded so that the fields inside and outside the shield can be segregated. In order to forbid the noise source generate interference to the field, we should shield the noise source, which is called active shielding. In order to forbid the victim being disturbed, we should shield the victim, which is called positive shielding.

The heavy current equipments can realize active shielding by metal case grounding.

The victim can realize positive shielding by grounding.

Keep the distance between control lines and power lines (L、N) and motor driving lines(U、V、W) as much as possible to avoid crossing. For example, when we locate two drivers in the same case of the multi-axial drive system, we should make one data plate ahead and the other back and try to make the leads as short as possible. If the heavy current wire cannot be segregated with the holding wire, we should use shielding line as the heavy current wire and the shielding layer should ground.

Filter technique. Filter technique is used for restraining conducted interference which transmit through the wire, especially for the restraining of power interference and holding wire interference. The filter is the frequency selective network which consists of the inductance, the capacity, the resistance or ferrite components. It can be inserted into the transmission line and restrain the unnecessary rate transmission[5].

As shown in Chart5, add the power filter to protect the alternating current power supply from interference.

The ferrite used for restraining electromagnetic noise is a kind of magnetic material which is mixed by oxide of Fe, Ni and Zn. The oxide is always made into a ducted body so that current can pass by when the LFC can get through without loss but the HFC will have a big loss transmitting to heat. So the oxide and the wire inside can be the absorption-type low pass filter, which can effectively restrain the interference of EFT[6]. Setting data line filter on the holding wire can effectively restrain high frequency common-mode interference. Data line filter is made up by ferrite bead or feedthru capacitor. For example, the best way to get the input cable into the ferrite bead on the rim is to use the connector with the filter directly. The socket of t his kind of connector has the filter made by ferrite bead and feedthru capacitor on each pin.

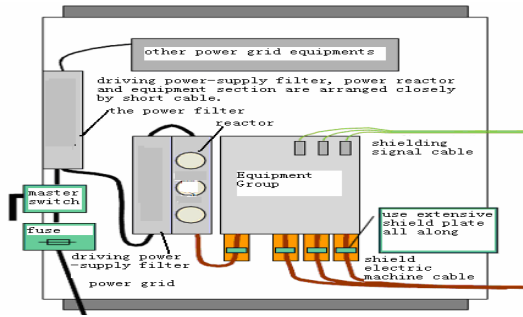


Chart 5. Design of adding the power filter control cabinet

4 Conclusion

Taking the measures above can reduce the wrong and abusing alarm so that we can improve the capacity of disturbance of the numerical control machine system and the safety and stability of the system, even the cost performance of the machine system.

Acknowledgment. This work is sponsored by the National Natural Science Foundation of Hainan(No.610230) and Hainan Provincial Educational Science, "Eleventh Five-Year Plan"2009 annual research topic(No. QJJ11506).

References

1. <http://www.chncnc.com>
2. Shepherd: Electromechanical integration system emc technology. China Electric Power Press, Beijing (1999)
3. Kaiser, B.E.: Emc principle. Electronic Industry Press, Beijing (1985)
4. cairengang: Emc design principles and prediction technology. Beijing aerospace university press, Beijing (1997)
5. zhangsongchun, zhuzifang, zhaoxiufen, jiangchunbao: The electronic control device anti-interference technology and its application. Machinery industry press, Beijing (1995)
6. zhubangtian: Electronic circuit practical anti-interference technology. People's wiley&sons press, Beijing (1996)

A Structure for the Model of Intelligent Plan Agent

Lei Wang

Department of Computing, The Chinese People's Armed Police Forces Academy,
China

wangLeiwjxy@qq.com

Abstract. This paper constructs a structure for the model of intelligent plan agent based on artificial intelligence. In this paper, through the method of simulation state graph and the formal description of the adversarial action, it realizes the decomposition process of intelligent plan. And by the effective analysis of adversarial action, it realizes the effectively recognition and reply of the intelligent plan.

Keywords: Intelligent plan agent, adversarial action, simulation state graph.

1 Introduction

With the fast development of network technology, information sharing and network connects with each other have been an inevitable trend in development. Information sharing enhances the information exchanging between individuals and also enhances the intercourse and information transmitting between nations. However, it is just like Pandora's Box; the development of network also brings hackers' recklessly attack and the renewals and wide spread of virus. In this way, computer system and agent system will face serious invasion, threat and destruction. Therefore, computer safety is increasingly becoming the focus that people has always been following with interest. Intelligent plan agent [1] comes into being, which is just from this point to solve the practical problems. However, there is not much research on intelligent plan agent at home and abroad [2]. This paper just points to such problems. This paper will be through simulation state graph and a formal description method of intelligent plan agent, building a model of the intelligent plan agent based on artificial intelligence, and through the application of the model, it implements of effective decomposition of intelligent plan. Finally, by the decomposition of the adversarial action, it realizes the effectively recognition and reply of the intelligent plan.

2 Definition

2.1 Adversarial Action

Adversarial action refers to some offensive and destructive operations of instantiation that are executed by agent [2].

2.2 Simulation State Graph

Simulation state graph consists of three basic actions nodes and two sides, that the attack nodes are the initial state process node (S) of the initial state and the behavior node (A) of aggressive behavior, and expressed by for the role of behavior node to achieve the ultimate objective of the possibility of the target state nodes (G); the two sides is a prerequisite side and motion effects side [3, 4].

2.3 A Graphic Description of the Adversarial Action

In a intact simulation state graph, usually including the initial state node, the attack process achieves the ultimate goal state nodes and the number of attack steps, and the resulting intermediate state and cause the prerequisite side which aggressive behavior occurs, and lead to the action effects side which possible target state set generated[4].

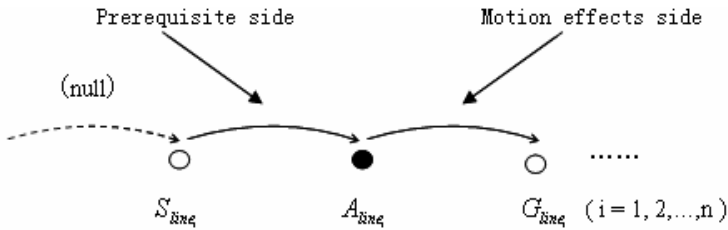


Fig. 1. The composition of simulation state graph

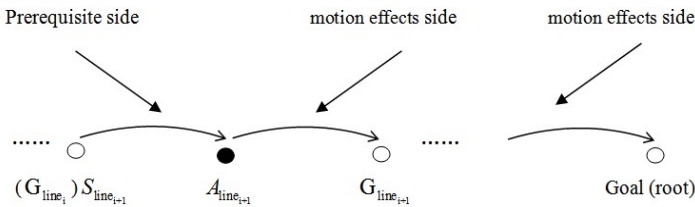


Fig. 2. Abstract representation of simulation state graph

2.4 The Simulation State Graph of the Attack Process

The solid line represents part of the process with the attacks, the initial state node, aggressive behavior and the final target state node which aggressive behavior node generated; the dashed line represents the part that's, the n nodes (n = 1,2, ..., m) relationship possibilities generated by the target state under attack. Through to each kind of possible analysis of the relative crisis of target state node, from which selected value with the greatest degree of relative crisis, the possibility that a target state node status as the ultimate goal of the final node [3].

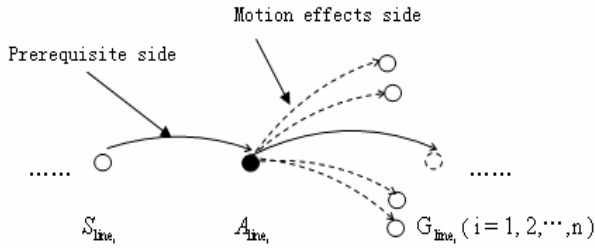


Fig. 3. The simulation state graph of the attack process

2.5 A Formal Description of Adversarial Action

In this paper, it first puts forward a 3-tuple formula, $P^a = \langle A^a, G^a, \lambda^a \rangle$ ($a \geq 1$), which is from the angle of opponent agent and indicates adversarial action to the attacked agent. In it, ‘a’ refers to the number of agents, who makes the intelligent plan; ‘A’ refers to a series of attacking destructive actions (actions set) which are executed by agents; ‘G’ refers to the goal to be attacked or to be destructed this time by agents (goal set); ‘λ’ is called crisis coefficient. It shows the threatening extent of the opponent agent action against the agent goal attacked in 3-tuple, $\lambda \in [0, 1]$ [2].

The maximum relative crisis degree of the ultimate goal state is calculated as [3]:

$$[P(\lambda_{G_{line_i}} / G)_{max}]_{max} = \left[1 - \frac{P(\lambda_{G_{line_i}})}{\sum_{x=1}^n P(\lambda_{G_{line_i}})} \right]_{max} \tag{1}$$

2.6 The Algorithm Description of the Attack Process

```

process({: preStat
      : action
      : time
      : effects{ ..... })
{: action name
      : preState      (S_{n-1})
      : preConds      (and (action))
      : effect         (S_n))
      : max(P(\lambda_{G_{line_i}} / G)_{max})
      : [P(\lambda_{G_{line_i}} / G)_{max}]_{max} \to G_n
      : G_n \to target}
    
```


2.7 The Components of the Intelligent Plan Agent

In view of the characteristics of planning recognition and reply, on this base we can realize the disposal of distributed and discontinuous intelligent plan by constructing a formal model of intelligent plan agent. The agent mainly consists of three parts [2].

2.8 Adversarial Planning Base

Adversarial planning base is the most basic adversarial action base in the intelligent plan agent. It stores records in the form of adversarial action mentioned above, and every adversarial goal item recording stored in adversarial planning base is the one that is most possible to be attacked by adversarial agent. It mainly realizes the matching between the current planning (action) leaf node and the records in adversarial planning base. When adversarial needle in adversarial planning base discovers the sub-node which decomposed from the current adversarial searching tree is matching with a basic action in the process of corresponding paragraph searching according to crisis grade, planning decomposing is over. And it gives goal item corresponding to the successful matching action return to intelligent plan agent. At the same time, it puts the successful matching value of ' λ ' into adversarial knowledge base to realize partial update of adversarial knowledge base [2].

2.9 Adversarial Knowledge Base

Adversarial knowledge base is one of the cores in intelligent plan agent. It mainly stores two kinds of knowledge. One is so called open adversarial knowledge in relevant domains of hardware and software, such as the disadvantages in software domain, IP address, hardware interface to be attacked and destructed, intrusion detection of network etc. a series of concerned conceptions, facts and theories; the other is about the goal to be attacked and destructed by intelligent plan. It is so called individual knowledge and experience by some knowledge engineers and experts in this domain. The experience is accumulated gradually by professional practice of experts in this domain and much experience is called heuristic information. By this kind of knowledge base, intelligent plan agent realizes the decomposition of fuzzy planning which is compounded by combinatorial factors to make the action decomposition planning continue to extend and to provide the possibilities for the ultimate adversarial recognition[2, 5].

2.10 Adversarial Reasoning Mechanism

In fact, adversarial reasoning mechanism is a group of reasoning knowledge modules in the whole intelligent plan agent. Its main function is to harmonize the actions in the Agent, decide how to choose the relevant knowledge in the knowledge base, decompose the concrete intelligent plan and reasoning correctly all kinds of intelligent plan which is executed by opponent agent to make the planning decomposition continue to execute. In this way, adversarial reasoning mechanism provides the powerful mechanism for searching the basic adversarial action and accomplishing the intelligent plan recognition [2].

3 The Recognition and Reply of the Intelligent Plan Based on Intelligent Plan Agent [4]

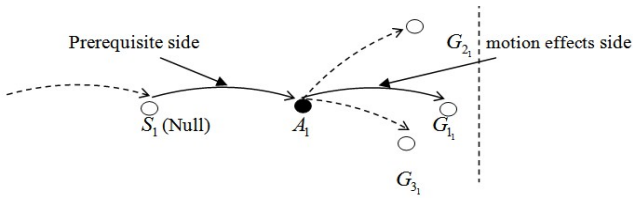


Fig. 4. The aggressive behavior on the simulation state graph

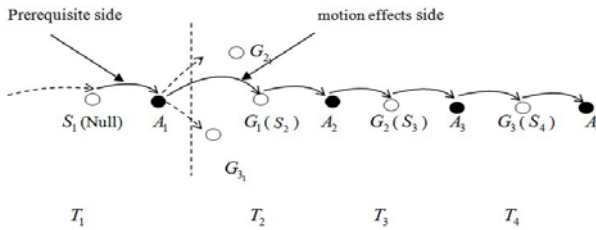


Fig. 5. The specific attack on the simulation state graph

4 Conclusions

In this paper, we have introduced a formal structure of the intelligent plan agent. And it realizes the effectively recognition and reply of the intelligent plan agent. It bases on the simulation state graph.

References

1. Willmott, S., Bundy, A., Levine, J., Richardson, J.: Adversarial Planning in Complex Domains. Submitted to ECAI 1998, January 20 (1998)
2. Gu, W.-X., Wang, L., Li, Y.-L.: Research for Adversarial Planning Recognition and Reply in the Complex Domains and the more Agents Conditions. In: Proceeding of 2005 International Conference on Machine Learning and Cybernetics, pp. 225–230 (2005)
3. Wang, L.: Research and Implementation of Plan Recognition Model Based on Action State Graph. Northeast Normal University (Master Paper) (2007)
4. Wang, L.: Recognition and Reply of Adversarial Planning Based on Simulation State Graph. In: 2011 International Conference on Teaching Materials, Education and Information Technology (August 2011)
5. Wang, L.: Research of Plan Recognition Model in Specifically Intrusion Detection Problem. Information Technology (2009)

Tele-education Technology Eliminating Chinese Knowledge Poverty Based on Information Technology

Lei Wang¹ and Dan Han²

¹ Department of Computing, The Chinese People's Armed Police Forces Academy, China
wangLeiwjxy@qq.com

² Department of computing, The Chinese People's Liberation Army Air Force Aviation University, China
87939060@qq.com

Abstract. This article expatiates the domestic knowledge poverty status and the comparison between China and others based on information technology, the relationship between Tele-education technology based on information technology and eliminating Chinese knowledge poverty and the rationality choice of Tele-education technology based on information technology eliminating our country's knowledge poverty. According to our country's national condition, this article elaborates the practical significance that Tele-education technology based on information technology solving our country's knowledge poverty under the information age background.

Keywords: Tele-education technology, Information technology, Knowledge, Knowledge poverty.

1 Introduction

In taking the knowledge innovation as the characteristic of modern society, the knowledge factor becomes the economic growth and the social progress key aspect. The 21st century's competition, the essence is the knowledge competition, the human resources competition. Therefore we will get rid of the knowledge to be impoverished, also has become various countries the magic weapon which defeats in the competition. But as a developing country, our country's knowledge poverty question obviously prominent, it has seriously restricted the progress and the development of society. This paper proposes that the use of Tele-education technology based on information technology slows down the knowledge poverty degree; it causes the general knowledge poverty to go out the impoverished condition as soon as possible, and joins to the information age ranks.

2 Situation Analysis which Knowledge Poverty of Our Country

2.1 Domestic Concrete Manifestation of Knowledge Poverty

The person concerned pointed out that the 21st century's China which the most population was at the knowledge poverty state, and it has carried on the detailed analysis, presently induces as follows:

- The people which the knowledge poverty is low or simply has not received the educational level, they does not have method gains and the exchange information and so on opportunity, and their ability is low which they use newspaper, books, telephone, Internet.
- The Chinese knowledge poverty condition existence serious regional disparity, the western area and the national minority area are the victimized persons of knowledge poverty, knowledge ability is serious insufficient.
- The Chinese knowledge poverty condition is existence serious differences between town and country, and the countryside area's knowledge impoverished condition is much more serious than the city. From the population matriculation rate, the education level as well as the telephone, the network popular rate look that the countryside also far is lower than the city. Quite many rural populations are at the condition of the education isolation, the information isolation. Its development and the modernization pace are back and forth in the boundary zone.
- The Chinese knowledge poverty also has the serious gender differences, compares with the male; the female is in more serious knowledge poverty.

3 China and Developed Country in Knowledge Poverty Related Dimension Contrast

Chinese knowledge poverty exists between various areas, between the city and countryside, exists between China and the world. The United Nations Secretariat announces an item of material demonstrated: it creates the value through the information technology and the new economy is the rich country phenomenon. Developed country in the centralized process of knowledge authority, through the innovation superiority, they capture the market share, and carry on the large-scale industrial reorganization to obtain the forerunner benefit, but the majority developing countries continue to occupy the information to be impoverished" [1]. The following some data may show this question.

- 20 century's ends, in the Chinese 460,000,000 countryside labor force, the illiterate person and the semiliterate have more than 100,000,000 people, accounts for 22.7%, the elementary school years of schooling more than 200,000,000 people, accounts for 45.5%. The dissemination of technology personnel which the countryside of developed country and ratio of the agricultural population is 1:100, China is 1:1200, average 10,000 acre cultivated land insufficient countryside technical personnel [2].
- According to "Chinese Information Newspaper" reported: An investigation which makes by the State Statistical Bureau international statistical information center indicated that China's information ability arranges at the world first floor, is only the US 8.6%, South Korea 15.3%, Brazil's 40.2%[3].
- A data demonstrated: China receives higher education's population only to account for the entire population proportion 5.7%, but the US is 60%, Japan,

South Korea are 30%, India is 16%[4]. China was still in the pool of labor power, but the powerful nation of the human resources also requires very long period of time diligently.

- Our country educational outlay accounted for the gross national product (GDP) the percentage still to be lower than the peripheral developing country. Human resources level's low, caused the traditional industry to reside in the dominant position directly in our country economic structure, the technical level, the production efficiency and the energy consumption is at relative backward condition [5].

4 Tele-Education Technology Based on Information Technology and Knowledge Poverty Elimination

A. Eliminating the Knowledge Poverty to Depend upon the Tele-education Technology Based on Information Technology

The educational level low degree is occupying the pivotal status one of as knowledge poverty weight targets. Because the develop economy must from improve worker's quality to obtain, but the knowledge production is improves the educational level of workers the important means.

The knowledge production stems from the education, if education backwardness and the knowledge poverty which causes by the education backwardness will be very fearful. The review history, many impoverished originate in the final analysis from the knowledge poverty. On the contrary, we will have the knowledge also to give a country to bring the infinite opportunity.

5 Tele-education Technology Based on Information Technology and Knowledge Poverty Elimination

In recognition of education in the total pattern of social and economic development of the role and status, the most countries first to universal education, promoting lifelong learning and create a learning society, in order to follow the development trend. But only rely on traditional teaching methods to meet various educational needs, even for the richest countries, the cost is also overwhelmed. Therefore, the cost be accepted to a variety of learning objectives and learning habits of the large and diverse population to provide education and training. This challenge requires a global education system on the center of the stage. Governments around the world to expand, strengthen and accelerate the development of Tele-education technology learning program based on information technology reflect the serious efforts of the world trend. Furthermore, modern information and communication technology also makes the rise of Tele-education technology based on information technology is more popular.

6 Tele-education Technology Based on Information Technology Is the Rational Choice which Eliminating the Knowledge Poverty in Our Country

A. Tele-education Technology Based on Information Technology Can Eliminate the Possibility of Knowledge Poverty

- Tele-education technology based on information technology has the popularity and the characteristics of wide coverage, breaking a learning space and learning time limit. It can be determined in accordance with the actual learning time, the choice of the nearest place to learn, and their commitment in social and family responsibilities to adapt the structure of learning. Thus it can realize the request which to the study society's transition and lifelong studies.
- Tele-education technology based on information technology has rich and varied teaching resources, but also sharing, so that teaching can reduce costs, enhance the timeliness of teaching; also can enhance the awareness and understanding of the outside world, the establishment of self and environment links.
- Tele-education technology based on information technology resources provide by the sound and picture. Reading books, reading newspapers and other traditional methods compared to the more persuasive, attractive and appealing; it also can be implemented, interactive teaching, autonomy, large flexibility, easy to learn communication and answer questions.
- The Tele-education technology based on information technology can save the massive teacher resources, but student's quantity actually greatly increases. In the human resources investment reduces in the situation, the human resources deliver actually obtain the big promotion.

B. Tele-education Technology Based on Information Technology Is the Rational Choice Which Eliminating the Knowledge Poverty in Our Country

Knowledge age, the world will be the development of re-education as to achieve prosperity and sustainable socio-economic development of major strategic decisions. China is also true. As a populous country, China has hundreds of millions of children under the age of 15 and hundreds of millions of adults under age 24 lack of formal education opportunities; the million adults over the age of 24 require continuing education opportunities. Moreover, there are millions of people eagerly look forward to receiving post-secondary education. However, full-time campus of the traditional education is difficult to adapt to and meet the great educational requirements. Because the unique characteristics of Tele-education technology based on information technology: teachers and students can communicate through electronic media, to overcome the barriers of distance space, the implementation of two-way interactive instruction to send and open learning to take responsibility for our distance learners to meet the education and training, to achieve life-long education, lifelong learning and learning society's mission.

At present, China Mainly distributes in the adult education higher education and secondary education, professional education, and non-academic education and training. Tele-education technology based on information technology has become our national education system is an important part [6]. Since the late nineties, the Chinese Tele-education technology based on information technology has entered a strategic innovation and the take-off period: the most colleges and universities in China have launched two-way interactive satellite TV and computer network for technology-based Tele-education technology based on information technology; radio and TV university in China in promoting openness and modernization , and joint educational colleges and universities have made significant progress; our government has decided to implement a modern Tele-education technology based on information technology, Tele-education technology network based on information technology, to promote higher education and lifelong education system and the formation of life-long learning society; our country are accelerating building the national information technology infrastructure and Tele-education technology network platform based on information technology, and the industry of our country and open society and Tele-education technology attention platform and investment growth.

C. It's Practical Significance That the Tele-education Technology Based on Information Technology to Eliminate Our Country Knowledge Poverty

- The Tele-education technology based on information technology to adjust and improves our country higher education and the specialized middle school professional education level proportion, the discipline specialized structure and the geography layout has displayed significant function [7].
- Tele-education technology based on information technology throughout the country, especially in remote, rural, grassroots and ethnic minority areas suitable for cultivation of various types of specialized personnel to local needs, especially economic, management, law, teacher training, science and engineering, agriculture, forestry and other professionals.
- The Tele-education technology based on information technology provides the academic education and the non- academic education improved the national quality, the development for all employed people and social other members lifelong to study have created the condition.

7 Conclusions

In the knowledge economy, knowledge out of poverty can be said that poverty must be free of all by the way, and we have knowledge of all is the same as with the power of "nuclear." In this age, the education is more than a profound impact on twentieth century economic and social development; and Tele-education technology based on information technology will be anti-intellectual poverty and the knowledge development to provide a broad platform, with irreplaceable role of value creation and far-reaching practical significance.

References

1. Chen, X.: Asian countries face the digital divide and digital opportunities. The international press (2001)
2. Liu, Y.: Rural poverty and higher education of rural areas (DB / OL),
<http://www.edu.cn/20030115/3075978.shtml>
3. Knowledge of poverty will profoundly affect the 21st century (DB / OL),
<http://www.green-web.org/ubb/Forum2/HTML/000551.html>
4. Status of knowledge of poverty in China (DB / OL),
http://weaso.com/Article/guanli/gggl/xzgl/200506/Article_21076.html
5. Ding, X.-f.: Tele-education. Beijing Normal University Press, Beijing (2001)

Grey Clustering Evaluation for Road Traffic Safety Condition

XiaoKun Miao and MingYang Li

College of Automobile and Transportation, Liaoning University of Technology,
Jinzhou, 121001, China
316770717@qq.com, limingyang.www@gmail.com

Abstract. Base on MATLAB software, a grey clustering analysis method was applied to evaluate road traffic safety condition in this paper. Road traffic safety condition was divided into four grey grades, such as excellent(A-level), good(B-level), average(C-level) and poor(D-level). According to the grey clustering method, the evaluation matrix, whiten weight functions of every grey grade and comprehensive decision weights were given. Evaluation results suggest that: the theory of grey clustering evaluation for road traffic safety condition is practicable and reliable.

Keywords: road, grey clustering evaluation, traffic safety.

1 Introduction

Road traffic safety condition can be evaluated through the objective and subjective safety feeling degree. Safety degree is used to reflect the objective of the traffic accident through various quantifications. It is an important index of traffic safety evaluation for improving road traffic safety condition [1]. The evaluation matrixes of traffic safety are established based on five road data in this paper. Grey clustering evaluation method is introduced. Four grades of grey clustering are classified for the traffic safety. Based on grey clustering evaluation method, the results are concluded. The results obtained are for improving road safety condition.

2 Evaluation Indices Selected

Based on “Urban Road Traffic Management Evaluation Indices System (the 2008 version)”[2], Combining with the actual situation, 10000 vehicles mortality, 100000 bikes mortality and 100000 population mortality are selected as evaluation indices in this paper.

3 Grey Clustering Evaluation Method

Grey clustering evaluation method is built upon the basic method of grey number's definite weighted functions, based on grey clustering to summarize whiten number of

the clustering objects, which different clustering indices owned, judging the type that clustering object owns.

3.1 Grey Clustering Evaluation Model

Aiming at the characteristic of incomplete information about road traffic safety condition, grey theory is used as the clustering evaluation method. Supposing that n is the number of evaluation items, m is referred as evaluation index items, there into, evaluation indices $j \in \{1,2,\dots,m\}$, $i \in \{1,2,\dots,n\}$, d_{ij} is represented as the evaluation specimen matrix [3-5]., therefore:

$$d_{ij} = \begin{bmatrix} d_{11} & d_{12} & \dots & d_{1m} \\ d_{21} & d_{22} & \dots & d_{2m} \\ \vdots & \vdots & \vdots & \vdots \\ d_{n1} & d_{n2} & \dots & d_{nm} \end{bmatrix} \tag{1}$$

3.2 Determination of Grey Clustering and Whiting Values

Adopting probability and statistical method, the actual data of evaluation index are dimensionless processed. Then accumulative frequency percentage is analyzed and the accumulative frequency curve is drawn as figure1. Using four grades of grey clustering to classify the traffic safety indices of road, that is excellent (A-level), good (B-level), average(C-level) and poor (D-level). The 15%, 40%, 60%, 85% accumulative frequency percentage corresponding points are selected to determine the excellent(A-level), good(B-level), average(C-level) and poor(D-level) [1]. λ_1 、 λ_2 、 λ_3 、 λ_4 corresponding 15%、40%、60%、85% points are separately referred as the whiting values of excellent, good, average and poor.

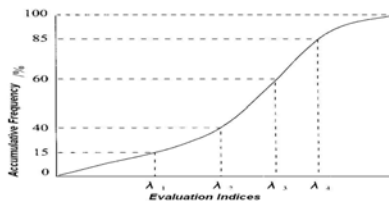


Fig. 1. Accumulative frequency percentage curve

3.3 Definite Whiten Weight Functions of Grey Clustering

The smaller the value of each index, the better they are. The below are four grey grades corresponding definite whiten weight functions, and then drawing definite whiten functions figures.

$$f_A(x) = \begin{cases} 1 & x < \lambda_1 \\ \frac{\lambda_2 - x}{\lambda_2 - \lambda_1} & \lambda_1 \leq x \leq \lambda_2 \\ 0 & x > \lambda_2 \end{cases} \quad (2)$$

$$f_B(x) = \begin{cases} 0 & x < \lambda_1 \\ \frac{x - \lambda_1}{\lambda_2 - \lambda_1} & \lambda_1 \leq x \leq \lambda_2 \\ \frac{\lambda_3 - x}{\lambda_3 - \lambda_2} & \lambda_2 < x \leq \lambda_3 \\ 0 & x > \lambda_3 \end{cases} \quad (3)$$

$$f_C(x) = \begin{cases} 0 & x < \lambda_2 \\ \frac{x - \lambda_2}{\lambda_3 - \lambda_2} & \lambda_2 \leq x \leq \lambda_3 \\ \frac{\lambda_4 - x}{\lambda_4 - \lambda_3} & \lambda_3 < x \leq \lambda_4 \\ 0 & x > \lambda_4 \end{cases} \quad (4)$$

$$f_D(x) = \begin{cases} 0 & x < \lambda_3 \\ \frac{x - \lambda_3}{\lambda_4 - \lambda_3} & \lambda_3 \leq x \leq \lambda_4 \\ 1 & x > \lambda_4 \end{cases} \quad (5)$$

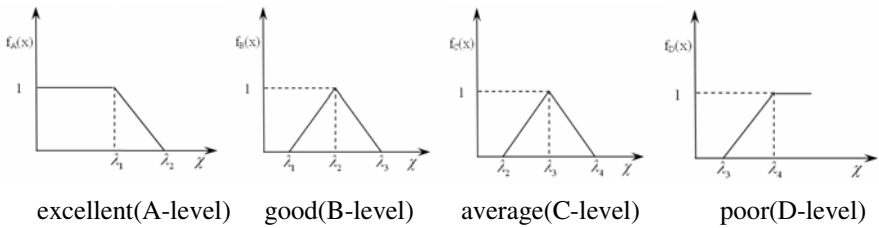


Fig. 2. Whiten weight functions figure of every grey grade

3.4 Determination of Clustering Weight and Evaluation Value of Grey Clustering

η_{jt} is referred as clustering weight, t is represented as evaluation grey clustering, and $t \in \{1, 2, \dots, k\}$, k is used as the number of evaluation grey clustering. η_{jt} is determined by the following formula.

$$\eta_{jt} = \lambda_{jt} / \sum_{j=1}^m \lambda_{jt} \quad (6)$$

In the formula:

η_{jt} — item j evaluation index is included in clustering weight of the t grey clustering grade.

λ_{jt} — item j evaluation index belongs to whiting value of the t grey clustering grade.

Based on the following formula to obtain the clustering evaluation value σ_{it} of item i evaluation object to item t grey clustering grade:

$$\sigma_{it} = \sum_{j=1}^m f_{it}(d_{ij}) * \eta_{jt} \tag{7}$$

Grey clustering evaluation sequence of evaluation object i $\sigma_i = (\sigma_{i1}, \sigma_{i2}, \dots, \sigma_{ik})$, evaluation object belongs to grey clustering k^* , fulfilling $\sigma_{ik}^* = \max\{\sigma_{i1}, \sigma_{i2}, \dots, \sigma_{ik}\}$, thus determining the road traffic safety condition of clustering object. In this paper, $K=4$, the level of road traffic safety condition is divided into excellent(A-level), good(B-level), average(C-level) and poor(D-level).

4 Application Example

Five roads in some region were taken as evaluation objects. The 10000 vehicles mortality, 100000 bikes mortality and 100000 population mortality were selected as evaluation indices. Accumulative frequency percentage curve was drawn by MATLAB program to determine whiting values of every grey grade [6]. The statistic data of five roads were as table1.

Table 1. The statistic data of five roads

Road number	10000 vehicles mortality	100000 bikes mortality	100000 population mortality
1	11.430	1.752	4.509
2	10.173	1.755	4.316
3	9.353	1.750	4.238
4	9.692	1.744	4.693
5	6.937	1.727	4.396

Based on MATLAB software, the accumulative frequency percentage curve was drawn. According to 15%, 40%, 60%, 85% points, the whiting values of every grey grade were confirmed as follows.

10000 vehicles mortality: λ_1 、 λ_2 、 λ_3 、 λ_4 for excellent(A-level), good (B-level), average(C-level) and poor(D-level) were 7.567,9.346,10.346 and 11.373.

100000 bikes mortality: λ_1 、 λ_2 、 λ_3 、 λ_4 for excellent(A-level), good (B-level), average(C-level) and poor(D-level) were 1.739,1.748,1.754 and 1.760.

100000 population mortality: λ_1 、 λ_2 、 λ_3 、 λ_4 for excellent(A-level), good (B-level), average(C-level) and poor(D-level) were 4.259,4.366,4.463 and 4.611.

Run the program based on the data, the 3 whiten functions matrixes for evaluation indices were as follows.

$$f_{it}(d_{i1}) = \begin{bmatrix} 0 & 0 & 0 & 1 \\ 0 & 0.1730 & 0.8270 & 0 \\ 0 & 0.9930 & 0.0070 & 0 \\ 0 & 0.6540 & 0.3460 & 0 \\ 1 & 0 & 0 & 0 \end{bmatrix} \quad f_{it}(d_{i2}) = \begin{bmatrix} 0 & 0 & 0.3333 & 0.6667 \\ 0 & 0 & 0.8333 & 0.1667 \\ 0 & 0 & 0.6667 & 0.3333 \\ 0.4444 & 0.5556 & 0 & 0 \\ 1 & 0 & 0 & 0 \end{bmatrix}$$

$$f_{it}(d_{i3}) = \begin{bmatrix} 0 & 0 & 0.6892 & 0.3108 \\ 0.4673 & 0.5327 & 0 & 0 \\ 1 & 0 & 0 & 0 \\ 0 & 0 & 0 & 1 \\ 0 & 0.6907 & 0.3093 & 0 \end{bmatrix} \quad \text{Based on}$$

$\eta_{jt} = \lambda_{jt}^* / \sum_{j=1}^m \lambda_{jt}^*$, η_{jt} was obtained.

$$\eta_{jt} = \begin{bmatrix} 0.5578 & 0.6045 & 0.6246 & 0.6409 \\ 0.1282 & 0.1131 & 0.1059 & 0.0992 \\ 0.3140 & 0.2824 & 0.2695 & 0.2599 \end{bmatrix} \quad \text{Based on}$$

$\sigma_{it} = \sum_{j=1}^m f_{it}(d_{ij}) * \eta_{jt}$, σ_{it} was obtained.

$$\sigma_{it} = \begin{bmatrix} 0 & 0 & 0.2210 & 0.7878 \\ 0.1467 & 0.2550 & 0.6048 & 0.0165 \\ 0.3140 & 0.6003 & 0.0750 & 0.0331 \\ 0.0570 & 0.4582 & 0.2161 & 0.2599 \\ 0.6860 & 0.1951 & 0.0833 & 0 \end{bmatrix} \quad \text{Based on}$$

$\sigma_{ik}^* = \max\{\sigma_{i1}, \sigma_{i2}, \dots, \sigma_{ik}\}$, the grey clustering evaluation results were as table2.

Table 2. The grey clustering evaluation results

Road number	1	2	3	4	5
Result	D	C	B	B	A

The evaluation result: No.1 road traffic safety condition is poor(D-level), which need to undertake rationalization improvement. No.2 is average(C-level). No.3 and No.4 are good(B-level). No.5 is excellent(A-level). Five road safety condition evaluation results basically comply with the actual situation.

5 Summary

Road traffic safety condition has no clear quantitative standard; causing traffic situation is not very good. Grey clustering evaluation has the characteristics to solve the problem of “part information known, and part information unknown” [7]. On the condition that evaluation indices have no clear quantitative standard, grey clustering method is used for evaluation objects, and evaluation results are basically reasonable.

References

1. Yulong, P.: Road safety, pp. 197–213. China communication press, Beijing (2009)
2. Urban Road Traffic Management Evaluation Indices System (the version 2008)
3. Lin, L.-W., Chen, C.-H., Chang, H.-C., Chen, T.-C.: Applying the grey assessment to the evaluation system of ecological green space on greening projects in Taiwan. *Environ Monit Assess* 136, 129–146 (2008)
4. Yuan, X., Li, B., Cui, G., Zhao, S., Zhou, M.: Grey Clustering Theory to Assess the Effect of Mineral Admixtures on the Cyclic Sulfate Resistance of Concrete. *Journal of Wuhan University of Technology-Mater. Sci. Ed.* 25(2), 316–318 (2010)
5. Marchand, E., Whitehead, J.: Statistical Evaluation of Compositional Differences between Upper Eocene Impact Ejecta Layers. *Mathematical Geology* 34(5), 555–572 (2002)
6. Su, J., Yuan, S.: MATLAB practical course, pp. 59–88. China publishing house of electronic industry, Beijing (2005)
7. Li, F.-y., Li, Q.-Y., Guan, X.: The impact of road traffic noise on the environment and the management of road traffic noise. *Journal of Hunan Agricultural University (Natural Sciences)* 35(1), 44–47 (2009)

Injection Material Selection Method Based on Optimizing Neural Network

ZengShou Dong, YueJun Hao, and RenWang Song

Taiyuan University of Science and Technology, Shanxi 030024
haoyuejun@126.com

Abstract. Injection molding materials selection based on neural network has broad application prospects in material selection problem. This paper puts forward a PSO-H-BP algorithm and applies to injection material selection on the basis of traditional BP algorithm. This method uses Hopfield network which optimized by particle swarm algorithm for original data pretreatment then selects material by BP network. The MATLAB simulation and result shows that: this method has higher classification accuracy and good expansibility compared with traditional BP neural network and H- BP neural network.

Keywords: Neural Network, Injection molded part, Material selection.

1 Introduction

Injection products function demands diversification, each demand is the result of comprehensive consideration by analyzing material's various physical characteristics. At present, the method of injection material selection mainly depends on artificial introduction, experience accumulation and the existing products analogy. Recent years, the computer assisted selection has become hot research, mainly focused on intelligent material selection (such as expert system, the fuzzy diagnosis and neural network). Expert system itself has the limitation of "knowledge acquisition bottleneck", "knowledge narrow steps" and weak numerical reasoning ability [1]; fuzzy reasoning has the weakness that calculation is too large and steady precision is not high [2], The BP neural network has some limitations such as slow convergence speed, need to structure the training sample sets, although is the most widely used and successful neural network model [3]. On the basis of BP neural network studying, this paper pretreats BP neural network's input data through PSO- Hopfield neural network, and then applies this optimized PSO - H - BP neural network to injection molding materials selection.

2 Neural Network Optimization

A. PSO-H Neural Network

Hopfield neural network was proposed by J.Hopfield in 1982 which can be used as a lenovo memory in the Internet, every neuron of Hopfield neural network is

interconnected with each other, that every neuron is mutually and two-way connected. It is a cyclic neural network which makes each neuron’s output feedback to other neurons’ input of the same layer. Although Hopfield network has achieved good effect on some fields such as pattern recognition, image processing and problems optimization, but it is easy to fall into local minimum when energy function drops and the stability is not very good.

Particle swarm algorithm is based on the group evolution and prey on bird behavior research [4]. This algorithm is succinct, easy to realize, less parameter adjustment and no need gradient information, it is the effective tool of nonlinear continuous optimization, combinatorial problems and mixed integer nonlinear optimization problems.

Particle swarm algorithm is to initialize problem’s solution to a group of particles. In each iteration, particles update themselves by tracking individual extremum (pbest) and global extreme value point (gbest). The particle updates its speed and position according to type (1) and type (2).The position of i particle labeled as

$$X_i = (x_{i1}, x_{i2}, \dots, x_{id}), \text{ Speed is tagged as } V_i = (v_{i1}, v_{i2}, \dots, v_{id}).$$

$$v_{id}^{k+1} = v_{id}^k + c_1 \times rand_{1,2}^k \times (pbest_{id}^k - x_{id}^k) + c_2 \times rand_{1,2}^k \times (gbest_{id}^k - x_{id}^k) \tag{1}$$

$$x_{id}^{k+1} = x_{id}^k + v_{id}^k \tag{2}$$

Above Types, v_{id}^k is particle i ’s d dimension speed in the k iteration; c_1, c_2 is learning factor, $rand_{1,2}$ is a random number between $[0, 1]$; x_{id}^k is particle i ’s d dimension current position in the k iteration; $pbest_{id}$ is particle i ’s individual pole position in the d dimension; $gbest_{id}$ is particle i ’s global pole position in the d dimension, basic flowcharts figure as:

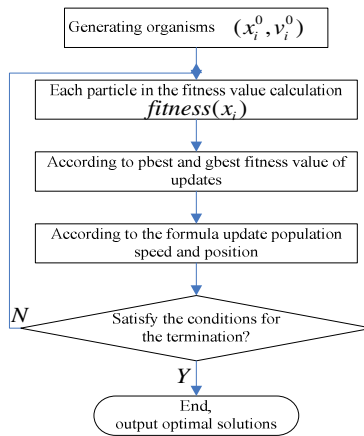


Fig. 1. Particle swarm algorithm basic flowcharts

Combining PSO algorithm with Hopfield neural network algorithm can improve global convergence property of the Hopfield neural network. Initializing weight matrix of Hopfield network to a group of random particles, particle position expresses weight matrix of Hopfield network, the dimension of each particle means the number of weight with connection role in Hopfield neural network. Selecting fitness function $fitness() = \text{sqrt}(f(WU) - U - I)$ (U is a stable state of Hopfield network, $\text{sqrt}()$ is the mean square error function), fitness value obtained is as a basis for judging whether the particles can get better performance. Take the pretrained weights matrix of Hopfield neural network as the current global optimal particles of particle swarm algorithm, run particle swarm optimization algorithm, then each particle will move inside the weights space and search the position with smaller fitness value, also change the speed of particle and update the position of particle, namely update weights matrix of network. During each iteration process, all particles update their position according to the new calculated rate and move to new orientation. Fitness function value is used for judging whether new position has got more optimized value, if fitness value decreased, record the current position that PSO algorithm mentioned *pbest*, or give up and find new positions. Compare the minimum fitness value particle produced in iteration process with the current global optimal particle namely PSO algorithm mentioned in the *gbest*, if the former is smaller, update the current global optimal particle position and take the former particle's position as the current global optimal particle position. In this way, the particle swarm optimization algorithm will obtain the particle position with smallest fitness value in certain iteration times, which is optimized weights matrix. In order to guarantee the optimized matrix is still available, PSO output data format is in accordance with the Hopfield network weights matrix.

B. PSO-H-BP Neural Network

PSO-H-BP neural network fault diagnosis model working principle is: preprocess fault diagnosis original sample data through PSO-H neural network optimization calculation, make the objective function correspond to energy function, determine network weights, make minimum power value through the PSO-H network operation, that is, attenuate noise of original data and redundant signals, realize the original data optimization also, take the optimized data as BP neural network's input and obtain the final judgment by the BP neural network.

3 Injection Material Properties and Selection

A. Injection Material Performance Parameters

The mechanical properties of injection product structure usually have six main performance elements: tensile resistance, flexural resistance, impact resistance, precision and heat resistance and abrasion resistance. Other aspects of injection products also have minor parameters requirements such as shrinkage rate, shrink volatility rate, bibulous rate and linear expansion coefficient and so on. Focusing on 6 main performance requirements of injection products, this paper proposes 10 indicators

as reference, namely tensile resistance, impact resistance, flexural resistance, high size precision, medium size precision, the general size precision, high heat resistance, heat resistance, high wear-resisting, general wear-resisting. When the node values is "1", which namely selects the feature, "0" says no selecting. Therefore, the BP neural network's input vector is described by 10 dimension vector which the value is 1 or 0.

The paper chooses 19 kinds of injection molding commonly used plastic material composition candidate set, respectively RPVC, PC (10% ~ 40% glass fiber reinforced), PS (ordinary), PS (resistant to blunt), SAN, PP (fiberglass enhancement), ABS (high heat-resistant), ABS (PA6 resistant blunt), (30% ~ 35% fiberglass enhancement), PPO, PC, PA6, PSU, PA66 (33% fiberglass enhancement), PP, PA66, POM (single polymerization), POM (copolymer), HDPE. The output of them as a neural network for $y_1 \sim y_{19}$ respectively.

B. Injection Selection Based on PSO-H-BP Neural Network

The BP neural network training parameters are chosen according to influence factors numerical of each material in engineering handbook candidate materials set [5], then decides selection degree by fuzzy subordinate relations according to the size of its numerical, taking (3) as an example:

$$\mu(x) = \begin{cases} 1, & x < \lambda_1 \\ \frac{\lambda_2 - x}{|\lambda_2 - \lambda_1|}, & \lambda_1 \leq x < \lambda_2 \\ 0, & x \geq \lambda_2 \end{cases} \quad (3)$$

Finally, calculating membership as the training input of BP neural network. In order to prevent partial neurons from achieving supersaturated and prevent some low numerical features from flooding, we need to normalize the sample data before establishing network [6]. Taking membership of selection material parameters $X = (x_1, x_2, \dots, x_{10})$ as the input of BP network and the Hopfield, using select material result $Y = (y_1, y_2, \dots, y_{19})$ for the output of BP network, establishes the nonlinear mapping relation between selection materials requirements and selection materials. Simulation in MATLAB 7.0, neural network parameters are set as follows: BP network with three layers, the number of input layer and output layer neurons are respectively 15, 10, Sigmoid function as activate function, training error is set for 0.0001, step is 2, 000; the weights of Hopfield network are from the training result of PSO, PSO network parameters are set as: inertia weight $\omega=0.15$, acceleration coefficient $c_1 = c_2 = 0.001$, particle count is 20, maximum iterating times $gen_{max} = 100$, accuracy is 10^{-6} .

C. The Simulation Results Analysis

By training established neural network with the capacity of 57 samples according to above mentioned rules, then tests samples with the capacity of 20, getting the average error of the output as 0.48.

Table 1 is a test material selection, its input for (1,1,0,1,0,0,1,0,0,1), namely that the injection products function requirement is "tensile, impact resistance, high dimension accuracy, high heat resistance, general wear-resisting", table 1 shows that network real output of 3 kinds of material with maximum and minimum selected degree are consistent with the expectations, illustrating that selection network maintains its stability and has enough resolution ability. We can select according to the case that the output values is close to 1.

Table 1. Selection network’s selecting results for a test sample

NO.	1	2	3	4	5	6	7	8	9	10	11	12	13	14	15	16	17	18	19
OUT	0.4015	0.9752	0.2744	0.3961	0.0194	0.3928	0.4482	0.5487	0.9234	0.0288	0.9307	0.5811	0.2475	0.7561	0.2785	0.5941	0.2576	0.2106	0.3653
EXP	0.3935	0.9999	0.3317	0.4001	0.0001	0.4126	0.4201	0.5589	0.8739	0.0742	0.9628	0.2643	0.3943	0.7221	0.2529	0.3885	0.2672	0.2645	0.2732

Diagnosing 20 groups test samples in a single BP, Hopfield - BP, and PSO-H-BP neural network respectively, and taking its maximum of selection degree for mapping 2.

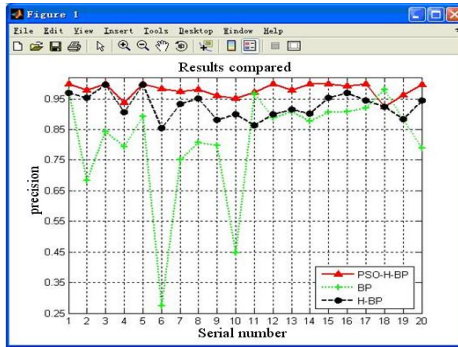


Fig. 2. Three kinds of material selection neural network precision contrast

Figure 2 shows that select material precision of this paper’s algorithm is obviously better than the single BP neural network and Hopfield - BP neural network. It explains this selection network has good generalization ability.

4 Summary

Injection material selection based on neural network is an important direction of artificial intelligence field. This paper studies the Hopfield neural network and the particle swarm optimization algorithm, combining the traditional BP neural network algorithm, a kind of PSO - H - BP neural network algorithm is put forward. Personnel experience requirement is low and can give the correct selection scheme in this injection material selection method; also, the network has the extendibility and is convenient to join new materials.

References

1. Gong, W., Li, X., Zhao, J.: Fault Diagnosis System Based on BP Neural Network and Expert System. *Computer Engineering* (8) (2007)
2. Chen, X., Bai, L.: Based on the MATLAB environment stylized method of fuzzy reasoning. *Application of Electronic Technique* (12) (2000)
3. Zhou, K., Kang, Y.: Neural network model and its MATLAB simulation program design. Tsinghua university press, Beijing (2005)
4. Ji, Z., Liao, H., Wu, Q.: Particle swarm algorithm and application. Science press, Beijing (2008)
5. Huang, R.: Plastic engineering manuals development (book1&book 2). Mechanical industry press, Beijing (2000)
6. Feng, L., Duan, Z., Teng, W.: The BP neural network in mining machinery hydraulic system failure diagnosis of application. *Popular Science & Technology* 5(129) (2010)

Collaborative Knowledge Management and Innovation Integration of Strategic Management Post Mergers and Acquisitions

Yu Gu¹ and Song Chen²

¹ School of Economics and Management, Tongji University, Shanghai 200092, China
1983guyu@tongji.edu.cn

² School of Economics and Management, Tongji University, Shanghai 200092, China
chens@tongji.edu.cn

Abstract. With the development of globalization and technology progress, firms are experiencing ever intense pressure to collaborate with their trading partners to compete with other competitors. Firms are seeking to collaborate with their partners at greater extent by the means of mergers and acquisitions in the areas such as knowledge management and innovation integration to exploit the potentials of an efficient and effective business operation. The theoretical implications of the research include providing understanding to the factors that facilitate knowledge collaboration in mergers process. The paper identified major components of the process of collaborative knowledge management, important antecedents, potential outcomes, and provided valid measurement instrument post mergers and acquisitions, so that practitioners can take it as a roadmap to guide them through the implementation process.

Keywords: Collaborative Knowledge Management, Innovation Integration, Strategic Management, Post Mergers and Acquisitions.

1 Introduction

Mergers and acquisitions is a complex process of organizations extending both on the upstream side into tiers of suppliers and on the downstream side into a network of customer companies, retailers and final consumers (Desouza, Chattaraj and Kraft, 2003). Mergers and Acquisitions management has been a common process in today's business world. As pointed out by numerous researchers, current competition is no longer between organizations, but between mergers processes. Organizations must integrate their operations with trading partners, rather than work against them in order to maintain competitive advantages for the entire mergers process. In today's business environments, it is no longer an option, but a must to better manage and integrate the mergers process (Spekman et al., 1998; O'Connell, 1999).

Through Collaborative Knowledge Management, firms achieve integration by tightly coupling processes at the interfaces between stages of the value chain (Lin et al, 2002). Sakkas et al. (1999) believe that the introduction of Collaborative Knowledge Management triggers the formation of new organizational entities to

resume the role of the information broker and in effect re-shape the traditional mergers process. Thus, Collaborative Knowledge Management is believed to enhance the competitive advantage of the mergers process as a whole.

This paper is organized as follows: Section 2 discusses the literature review of organizational knowledge, organizational knowledge management system, mergers process knowledge, and Collaborative Knowledge Management. There we summarize the theoretical background of the research. Section 3 we put forward the analytical framework of Collaborative Knowledge Management with mergers process integration and performance. Section 4 concludes.

2 Literature Review and Theoretical Background

A. Organizational Knowledge

Choo and Bontis (2002) view organizations as bundles of knowledge assets. The organizational capability to learn, create and maintain knowledge, as well as the conditions under which such capabilities are developed, has been deemed critical to the operational and strategic health of organizations. This is simply because from the resources based view, knowledge is a strategic resource that is hard to imitate and provides its possessor a unique and inherently protected advantage. Thus, any techniques and approaches that facilitate knowledge growth and application are considered as critical to today's business success. However, it is until relatively recent that the importance of organizational knowledge is emphasized (Stewart, 1997).

Organizational knowledge is commonly understood as intellectual capital encompassing both knowledge of individuals employed by the organization and group knowledge that is embedded in the organizational policies, procedures and protocols. Both the individual and group knowledge have two basic forms: those that can be easily codified and transmitted in formal, systematic language and shared asynchronously are called explicit knowledge. Vasconcelos et al (2000) presented an ontological diagram illustrated the classification of knowledge as well as the relationships of various kinds of knowledge within an organizational domain.

B. Organizational Knowledge Management System

The emergent trend of recognizing the growing importance of organizational knowledge surely brings about increasing concerns over how to create, store, access, transfer and make full use of such super abundance of organizational knowledge. A knowledge management system is often introduced to facilitate the organizational functions of identifying and mapping intellectual assets, generating new knowledge, and systemizing knowledge storage, retrieval and sharing.

Organizational knowledge management is a broad and multi-faceted topic involving social-cultural, organizational, behavioral, and technical dimensions (Alavi and Tiwana, 2003). King (2001) defined knowledge management as a mechanism involves the acquisition, explicating and communicating of mission specific professional expertise in a manner that is focused and relevant to an organizational participants who receive the communications. Marshall (1997) considered that KM refers to the harnessing of intellectual capital within an organization.

Globalization, advancement in technology and the increasingly intense competition in post-industrial business world have made cross-functional and inter-organization collaboration a very popular System (e.g. integrated product development).

C. Theoretical Background Summary

The theoretical base for our study is based on Rogers's diffusion of innovations theory (1983), Tornatzky and Fleisher's (1990) TOE model and the organizational technology adoption model by Iacovou et al. (1995).

The literature has rich discussions on technology adoption (e.g. Agarwal and Prasad 1999, Pick and Roberts 2005, Verhoef and Langerak 2001, and Venkatesh and Davis 2000). Many of these studies were based on Rogers's (1995) diffusion of innovation theory (DOI) to investigate how organizations absorb new technologies. Tornatzky and Fleisher's (1990) TOE model extended Rogers's framework to explain a firm's technological innovation decision making behavior.

- Perceived benefits: expectations of advantages or opportunities reflected by operational and performance improvements related to the adoption of the technology system, such as improved knowledge management operational efficiency, innovation, integrated mergers process relationships.
- Organizational characteristics: we approach this issue from two perspectives: technological Infrastructure looks at the technological preparation of the firm for Collaborative Knowledge Management implementation; organizational infrastructure studies the whether the firm is structurally and culturally ready for its adopting and implementation.

3 Theoretical Framework

To better understand the antecedents and consequences of Collaborative Knowledge Management, a framework is established to describe the causal relationships between facilitating factors, CKMS, and its impact. This study has 2 objectives: 1) to identify the most important factors that drive organizations to implement CKMS such as organizational, technological infrastructures, and external facilitators; 2) to explore the potential favorable organizational outcome of CKMS implementation such as higher knowledge quality, closer relationship with business partners, and superior mergers process performance.

There are 3 CKMS implementation antecedent constructs and 3 impact construct following section would do a through literature review and operationalize these constructs as well as their sub-constructs.

A. Organizational Characteristics

Organizational characteristics refer to the structural and infrastructural features of the organization related to its readiness to implement CKMS. There are 2 sub-dimensions for this construct: (1) technological infrastructures, the tools and systems that are instrumental to the operation of cross-organizational knowledge communication and management; and (2) organizational infrastructural, the factors that prepare the collaboration ready and knowledge smart. firm to be collaboration ready and knowledge smart.

1) Technological Infrastructure

Technological infrastructure has been emphasized as an important antecedent for knowledge management Systems by many researchers.

Knowledge generation, storage, access, dissemination and application are the five essential processes that new knowledge is created, transferred and utilized in the business context. Five sub-constructs of technological infrastructure including communication support system, knowledge database management system, enterprise information portal, collaborative system, and decision support system, which support the above knowledge processes.

The collaborative system is the one where multiple users or agents engage in a shared activity, usually from remote locations.

Decision support system is defined as computer based systems that support unstructured decision-making in organizations through direct interactions with data and analytical models (Sprague and McNurlin, 2001).

2) Organizational Infrastructure

The second dimension to measure organizational characteristics is organizational infrastructure. An organization can be viewed as a social system of interactions among entities constrained by shared norms and expectations (Bertrand, 1972). Organizational Infrastructure thus can be defined as firm's internal configurations and arrangements involving organizational structure, business process and work design etc.

B. Perceived Benefits

Perceived benefits refer to the level of recognition of the relative advantage that CKMS can provide to the organization. Many practitioners and researchers have attempted to identify the potential advantages that knowledge management system has to offer. Firms must be able to identify substantial benefits from adopting knowledge to motivate and justify their commitment.

Therefore, our understanding to firm's perceived knowledge management capability improvement is based on the five activities of the generic knowledge management process identified by Cormican and O'Sullivan (2003), i.e. firm's capabilities improvement is based on the five activities of the generic knowledge management process identified by Cormican and O'Sullivan (2003), i.e. firm's capabilities on mergers process knowledge generation, storage, access, dissemination and application are all expected to be facilitated by Collaborative Knowledge Management.

C. Collaborative Knowledge Management Impact

The impact of Collaborative Knowledge Management implementation refers to the real benefits adopters believe they have received from utilizing CKMS (Iacovou et al, 1995). We assume these impacts are closely associated with the perceived Collaborative Knowledge Management benefits. All of the expected benefits should be reflected as an outcome from Collaborative Knowledge Management, providing the implementation is successful.

Thus there are two general dimensions of impacts: the first is the improve knowledge capabilities as represented by high mergers process knowledge quality, and the second dimension is the organizational performance advancement, as reflected by mergers process integration as well as mergers process performance.

4 Conclusion

There were direct and positive relationship between internal/external drivers, collaborative knowledge management Systems, and the organizational performance impacts.

Knowledge management has been gaining increasing attention from both practitioners and academia. However, the existing studies on managing knowledge across organizational boundaries are sparse in quantity and limited in scope.

The study could stimulate more research to be done on how trading partners collaborate to leverage knowledge assets for mergers process competitiveness.

The paper prints out a roadmap for organizations to collaborate with trading partners for knowledge management and improve performance. All three hypotheses for Collaborative Knowledge Management outcomes were confirmed with high effect sizes. It suggested that investment in Collaborative Knowledge Management would undoubtedly reward organizations with direct and sizable positive results. Organizations must be serious with Collaborative Knowledge Management attempts; they must invest in infrastructural technology, substantially change organizational culture, and establish knowledge collaboration with selected trading partners whose knowledge is perceived complementary.

Acknowledgement. The research was supported by Science and Technology Commission of Shanghai Municipality under Grant 200906020 (Ph.D. Candidate Dissertation Programme) and German Studies Exchange Promotion Fund of German Studies Centre of Tongji University.

References

1. Desouza, K., Chattaraj, A., Kraft, G.: Mergers process perspective to knowledge management: Research propositions. *Journal of Knowledge Management* 7(3), 129–138 (2003)
2. Spekman, R.E., Kamauff Jr., J.W., Myhr, N.: An empirical investigation into mergers process management: A perspective on partnerships. *Mergers process Management* 3(2), 53–67 (1998)
3. O'Connell, J.: Streamlining Mergers process Management Processes. *Document World* 41(1), 40–42 (1999)
4. Pfeiffer, H.: *The Diffusion of Electronics Data Interchange*. Springer, New York (1992)
5. Pick, J., Roberts, K.: Corporate adoption of mobile cell phones: business opportunities for 3G and beyond. In: Pagani, M. (ed.) *Mobile and Wireless System Beyond 3G: Managing New Business Opportunities*, pp. 24–50. IRM Press, Hershey (2005)
6. Crawford, A.: Reform at work: Workplace change and the new industrial order. *New Zealand Journal of Industrial Relations* 21(2), 199–200 (1996)
7. Song, X.M., Moytona-Weiss, M.M., Schmidt, B.: Antecedents and consequences of cross functional cooperation: a comparison of R&D, manufacturing and marketing perspectives. *Journal of Product Innovation Management* 15, 35–47 (1997)
8. Lin, C., Hung, H.C., Wu, J.Y., Lin, B.: A knowledge management architecture in collaborative mergers process. *Journal of Computer Information System* 42(5), 83–95 (2002)

Dispatch of Many Kinds of Fast Consumable Goods in Large-Scale Emergency

Wei Qin Tang

School of Information and Safety engineering Science,
Zhongnan University of Economics and Law, Wuhan 430073, P.R. China

Abstract. In the later-stage large-scale emergency, the demand quantity of each demand point can be basically determined with the gradual transparency of information, the dispatch way of emergency commodities is transformed from the way pushed by supply in the early-stage emergency to way drawn by demand, the main goal of emergency is the minimum cost under the constraint of emergency time and the type of emergency commodities is mainly the fast consumable goods with sufficient supply. On the basis of these characteristics, this paper transforms the dispatch of many kinds of fast consumable goods in the late large-scale emergency to be the definite combination optimization of mobilization points, establishes 0-1 mixed integer-programming model and gives pseudo algorithm of multinomial time.

Keywords: the later-stage large-scale emergency, many kinds of fast consumable goods, depositing center of emergency commodity, 0-1 mixed integer-programming model.

1 Introduction

In the past few years, China has undergone quite a few large-scale emergencies such as the snow disaster of the South, the wenchuan earthquake, H1N1 Flu. A large-scale emergency has a long duration, so there are different dispatch tasks, emergency commodities of different kinds and different scheduling ways of commodities in its different stages. In the later period of a large-scale emergency, the basic task of emergency transforms from rescuing lives and property of the affected population to settle down their living; The type of emergency commodities transforms from the initial durable goods such as tents, medical instruments, rescuing aids to the fast consumable goods such as instant noodles, bread, tap water and so on. With more and more transparent information such as disaster areas, affected population, the demand quantities of every demand point of emergency can be counted accurately in a certain time. At the same time, the source of emergency commodities gradually broadens when the emergency time lapses and the supply quantities are sufficient. The scheduling way of emergency commodities also transfers from the way pushed by supply in the initial emergency period to the way pulled by demand. However, fast consumable goods of emergency are different from the durable goods of emergency in that their value can vanish along with their uses. Their demand quantities are closely related to the length time of emergency besides the disaster degree, disaster

area and disaster population. The longer the duration is, the more the demand quantities of this kind of emergency commodities are. The demand quantities of entire process are difficult to be forecasted at a certain time point, which decides that the scheduling of this kind of commodities should be carried on according to every stage, and the commodities should be supplemented at intervals. Therefore, the scheduling of large-scale emergency at the later stage can be transformed to be the dynamic combination optimization problem of the emergency service point, that is, a few rescuing points are selected from the available rescuing points to participate in emergency activities of this stage and their corresponding supply quantities are determined in order to maximize the emergency efficiency.

The existing literatures about the scheduling of emergency commodity concentrate mostly on the research on static or disposable scheduling and establish the models of simple target model, two-level optimization models, and as well as multi-objective model. The single-objective model mainly takes the earliest starting time of emergency as the goal.[1] Two-level optimization model usually takes the smallest number of rescuing points or the minimum emergency cost into account under the premise of the shortest time of emergency. For example, Li Lian-hong et al.[2] established a two-level mathematical optimization model by taking the smallest rescuing points of emergency as the upper-level optimization goal. But it only solved the scheduling problem of emergency commodities of single demand point, and are not suitable for the situation of coexisting multi-demand points when a large-scale emergency occurs. There are many literatures about multi-objective model. For example, Lin Hao et al.[3] established a multi-objective mathematical model of the shortest time and the minimum cost, transformed it to a single-objective model by using the method of ideal points and carried out a solution by citing the algorithm of particle swarm.

Above literatures considered the dispatch of emergency commodities is static and one-off. However, fast consumable goods such as convenient noodles, breads, mineral water and so on must be supplemented at intervals and be scheduled dynamically according to the demand quantities of various demand points in each time section. Therefore, the traditional combination optimization method of multi rescuing spots can't be used to solve the scheduling problem of fast consumable goods in large-scale emergencies. Some literatures studied the dynamic scheduling problem of emergency commodities. For example, Fiedrich[4] studied the scheduling of resources under the different rescuing tasks by establishing dynamic programming models. Fiorucci et al.[5] studied the allocation and scheduling of emergency resources before or after the fire by establishing dynamic models. Barbarosoglu[6] proposed a two-stage model of multi-transportation mode and multi-type network flows of cargo to simulate transportation plan of relief goods. But these literatures didn't consider that the scheduling of fast consumable goods was different from that of durable goods when a large-scale emergency occurred. Tang Weiqin, Chen Rongqiu[8] discussed how to dynamically select supply points from the available supply spots of commodities to take part in emergency and their respective quantities according to the demand of some kind of emergency commodities in each time section in the later-stage large-scale emergency. Based on their research, this paper expands the scheduling of fast consumable goods of emergency from a single kind of commodity to many kinds of commodities.

2 Problem Discription

Let A_1, A_2, \dots, A_n be n supply points of emergenc. y_{jk} ($j = 1, 2, \dots, h; k = 1, 2, \dots, K$) in time T_j ($j = 1, 2, \dots, h$) be the needing quantities of depositing center of emergency in a disaster scene to commodities k ($k = 1, 2, \dots, K$). y_{jk} equals the sum of demand quantities of various demand points in time section $[T_j, T_{j+1}]$, and it can be counted out by injured population and their average consumption quantity and the stock-out isn't permitted in any time. Commodities k ($k = 1, 2, \dots, K$) can be supplied in time t_i (t_i is called admitted time of A_i) by supply point A_i ($i = 1, 2, \dots, n$). d_i ($d_i > 0, i = 1, 2, \dots, n$) denotes the distance from supply point A_i to the depositing center and q_{ik} ($q_{ik} > 0, i = 1, 2, \dots, n; k = 1, 2, \dots, K$) denotes unit transportation cost of commodities k ($k = 1, 2, \dots, K$) from supply point A_i to the depositing center. If x_{ik}, x'_{ik} denote retaining quantities and actual supply quantities of supply point S_i to commodities k respectively, then $0 < x'_{i_r} \leq x_{i_r}$, where, $r = 1, 2, \dots, m$, i_1, i_2, \dots, i_m is an entire arrangement to the subrow of 1, 2, ..., n . Suppose $T_1 < T_2 < \dots < T_h$ and $t_1 < t_2 < \dots < t_n$,
 If $\phi = \{(A_1 : x'_{11}, x'_{12}, \dots, x'_{1K}), (A_2 : x'_{21}, x'_{22}, \dots, x'_{2K}), \dots, (A_n : x'_{n1}, x'_{n2}, \dots, x'_{nK})\}$, where $0 \leq x'_{ik} \leq x_{ik}$, ($k = 1, 2, \dots, K$) denotes any scheme by which commodity k is dispatched from supply point of emergency to the depositing center, then selected scheme ϕ of supply point of emergency commodities must satisfy the following conditions:

$$\forall j \in \{1, 2, \dots, h\}, \quad \sum_{i=1}^{T_j} x'_{ik} \geq \sum_{m=1}^j y_{mk}, \quad (k = 1, 2, \dots, K) \tag{1}$$

The left of odds (1) denotes the whole arrival commodities of the selected scheme ϕ and the right denotes the demand quantities of commodities supply centers before time T_j .

3 Model Formulation

According to the above description, the mathematical model which minimizes the total cost for the choice question of supply points may be established as follows:

$$\begin{aligned} \min TC &= \sum_{k=1}^K \sum_{i=1}^n q_{ik} d_i x'_{ik} + \sum_{k=1}^K \sum_{i=1}^n p_{ik} x'_{ik} \tag{2} \\ \text{s.t.} \quad \sum_{i=1}^n x'_{ik} &= \sum_{j=1}^h y_{T_j, k} \quad (k = 1, 2, \dots, K) \tag{3} \end{aligned}$$

$$\forall j \in \{1, 2, \dots, h\}, \sum_{i=1}^{T_j} x'_{ik} \geq \sum_{m=1}^j y_{T_m k}, \quad (k = 1, 2, \dots, K) \tag{4}$$

$$a_{ik} = \{0, 1\} \tag{5}$$

$$0 \leq x'_{ik} \leq x_{ik}, \quad (k = 1, 2, \dots, K) \tag{6}$$

In the above model, formula (2) is the objective function. Because quantities and time of emergency commodities in the depositing center are strictly limited, emergency commodities will be put into use after they are dispatched into the depositing center, so the stocking cost may be ignored. because the stockout isn't permitted, the cost of stockout does not exist, Therefore, the total emergency cost

should be composed of two parts: the first part $\sum_{k=1}^K \sum_{i=1}^n q_{ik} d_i x'_{ik}$ is the total transportation cost of various kinds of emergency commodities; the second part $\sum_{k=1}^K \sum_{i=1}^n p_{ik} x'_{ik}$ is the purchased cost of emergency commodities, formula (3) denotes

the actual supply quantities of various kinds of emergency commodities are equal to the total demand quantities. Formula (4) means all the commodities of emergency arriving at the depositing center should be larger than or equal the demand of the depositing center at time T_j . In Formula (5), a_{ik} is a binary variable. When a_{ik} is zero, it means that the supply point of A_i does not participat the supply of commodity k ; and when a_{ik} is one, it means that the supply point of A_i does participating the supply of commodity k . Formula (6) assures that the actual supply quantities of each supply point should be larger than or equal zero but should not exceed the available supply quantities.

4 Model Algorithm

Obviously, the model is 0-1 mixed integer- programming model. it may be solved by the algorithm of branching delimitation, but this paper cites pseudo algorithm of multinomial time[9] which will make the operation simpler.

- 1) Definition of related concepts in the algorithm

Definition 1. The supply set of commodities k : Suppose the set of supply points whose promising time is not greater than time T_i is $\{A_{i_1}, A_{i_2}, \dots, A_{i_m}\}$, then set $\Theta = \{(A_{i_1}, x_{i_1 k}), (A_{i_2}, x_{i_2 k}), \dots, (A_{i_m}, x_{i_m k})\}$ is supply set in time T_i .

Definition 2. The effective supply set of commodities k : Suppose the set of supply points whose promising time is not greater than time T_j is $\{A_{i_1}, A_{i_2}, \dots, A_{i_m}\}$, then set $\Theta_k = \{(A_{i_1} : x'_{i_1k}), (A_{i_2} : x'_{i_2k}), \dots, (A_{i_m} : x'_{i_mk})\}$, ($k = 1, 2, \dots, K$) is call effective supply set of commodity k in time T_j , where x'_{vk} ($v = 1, 2, \dots, u; k = 1, 2, \dots, K$) is the effective supply of surplus after various supply quantity of commodities are determined in time $T_1 \sim T_{j-1}$.

2) Algorithm steps

Step1 $s = 1, \varphi_k^* = \phi, k = 1$;

Step2 (1) The supply set $\Theta_k = \{(A_{i_1} : x'_{i_1k}), (A_{i_2} : x'_{i_2k}), \dots, (A_{i_u} : x'_{i_uk})\}$ of supply points to commodity k in time T_s is determined;

(2) The effective supply set

$\Phi_k = \{(A_{i_1}, x'_{i_1k}), (A_{i_2}, x'_{i_2k}), \dots, (A_{i_u}, x'_{i_uk})\}$ ($\Phi = \Theta - \phi^*$) of supply points to commodity k in time T_s is determined, then $N_{i,k} = q_{i,k}d_{i,k}x'_{i,k} + p_{i,k}x'_{i,k}$ is counted. If the least is $N_{i,k}$, namely $N_{i,k} = \min\{N_{i,k}\}$, then supply point A_{i_i} is selected out, $a_{i,k} = 1$;

If $x'_{i,k} < y_{sk}$, then $x'_{i,k}$ is supply quantity of supply point A_{i_i} , $\varphi_k^* = \varphi_k^* \cup \{(A_{i_i}, x'_{i,k})\}$, $y_{sk} = y_{sk} - x'_{i,k}$, go to step (2).

If $x'_{i,k} \geq y_{sk}$, then y_{sk} is supply quantity of supply point A_{i_i} , $\varphi_k^* = \varphi_k^* \cup \{(A_{i_i}, y_{sk})\}$, $s = s + 1$, go to step 3.

Step3 If $s > h$, then go to step 4, or else, go to step 2.

Step4 The supply quantity of the same supply points in scheme φ_k^* is merged, the choice scheme φ_k^* ($k = 1, 2, \dots, K$) of supply point to commodity k , $k = k + 1$, if $k > K$, go to Step 5; if not, then $s=1$, $\varphi_k^* = \phi$, go to step 2.

5 Conclusions

This paper discusses how to dynamically determine the supply points of commodities participating in emergency and their respective quantities according to the demand of the kind of emergency commodities in each period under the premise that there are many candidate emergency supply points in the later-stage large-scale emergency. But this paper only studies the dispatch of many kinds of fast consumable goods. In fact, the dispatch of durable goods such as tents, medical instruments, rescue aids is extremely important, which will be the next emphasis of research.

Acknowledgement. This paper is supported by the Fundamental Business Foundation of Zhongnan University of Economics and Law under Grant No2009097 and Natural Science Foundation of China under Contract No. 91024004.

References

1. List, G.F.: Routing and Emergency-Respond-Team Sitting for high-level radio Active Waste Shipments. *IEEE Transaction on Engineering Management* 45(2) (1998)
2. Li, L.-h., Wang, Y.-j., Li, J.-f., Chen, J.: Study on Optimization Model for Emergency Dispatch Problem with Multi-Resource and Nonconstant Material Consumption. *Journal of Beijing Institute of Technology* 26, 157–160 (2006)
3. Lin, H., Xu, W.-s.: Research of Emergency Materials Scheduling Solved by Binary PSO. *Computer Knowledge and Technology* 3(7), 1503–1505 (2008)
4. Fiedrich, F., Gehbauer, F., Rickers, U.: Optimized Resource Allocation for emergency response after earthquake disaster. *Safety Science* (25), 41–57 (2000)
5. Fiorucci, P., Gaetanti, F., Minciardi, R., et al.: Real time optimal resource allocation in national hazard management. In: *Proceeding of IEMSS 2004-complexity and integrated resource management* Osnabreuck, Germany (2004)
6. Barbarosoglu, Y.A.: A Two - stage Stochastic Programming Framework for Transportation Planning in Disaster Response. *Journal of the Operational Research Society* 55, 43–53 (2004)
7. Tang, W.Q., Chen, R.-q., Zhao, m., et al.: Dispatch of fast consumption goods in large-scale emergency. *Science Research Management* (2), 121–125 (2010)
8. Liu, C.: The network optimization of supply chain-the design of the model and algorithm. Doctoral dissertation of Zhongnan University (12), 46-51 (2006)

A Conformist Mechanism to Promote Collaboration Emergence

Yi He¹ and Jia-zhi He²

¹ School Office, Yantai University, Yantai, Shandong, China
ytuheyi@sina.com

² School of Electromechanical Automobile Engineering, Yantai University,
Yantai, Shandong, China
cad@ytu.edu.cn

Abstract. As for the impact of the characters of nodes in complex network on collaborate level, this paper puts forward an iterated game model based on conformist mechanism. In this new model, the nodes update strategies not only accord to their payoffs but also to their group, which ensures that nodes in the same group adopt the same strategies based on intelligent materials. Simulation results reveal that the collaborated level of the networks based on conformist mechanism is higher than the networks based on normal mechanism. The collaboration level is related to the group number. The collaboration level is higher when the group number is few. In addition, the average payoffs increase linearly with the penalty gene increasing instead of rising alternatively. As a result, the new model enhances the collaboration level and the average payoffs in complex network.

Keywords: Conformist Mechanism, Iterated Game, Collaboration Emergence, Complex Network, Intelligent Materials.

1 Introduction

It is considered that natural selection inclines to selfish and strong individual according to the traditional evolutionary game theory. But more comprehensive collaboration exists in the nature. More kinetic mechanism was considered in order to study collaboration strategies emergence. The possibility of fleeing betrays each other was provided by iterated game. Because by means of some retaliatory measures or mechanisms, the individual can avoid the opposite side adopt betrayal strategies when iterated gaming. So it is beneficial to the mergence and maintenance of collaboration strategies. Santos and Pacheco found that the scale-free networks are benefit to the mergence and maintenance of collaboration strategies [1]. In addition, they also discussed the snow model game based on scale-free networks [2]. It was found by Vainstein and Arenzon that the potential disruption under the sparse grids can enforce the density of collaboration [3]. A game model without reciprocity mechanism was studied by Riolo.etc. The game individual decides to cooperate or not according to the similarity of opponent and itself. Collaboration can be found in this model, but a harsh condition was supposed. In this condition, the game individual usually

cooperates with its similarity. The game would degrade to prisoner difficulty game model once the condition was loosed.

The conformist mechanism, which takes into account the influence of gaming result involving majority psychology, was presented. While the nodes update their strategies, the self payoffs were considered as well as the strategies that were adopted by most nodes of group in networks. The conception of conformist mechanism was introduced in the beginning of this paper. And a game model which was favorable to promote collaboration emergence was proposed. And then the discussion of simulation result was conducted. It was shown in the result that new model can effectively promote the collaboration emergence of nodes in networks. Beside, compare to the other models, conformist mechanism can avoid the average payoffs rise alternatively. It is also can be found that there are proportional relation between average payoffs and penalty gene.

2 Conformist Mechanism

When game model adopted update strategies, instead of the affect of group the self payoffs or characteristics of networks were usually considered. But the formation of networks group was determined by characteristics of nodes. When most of nodes in group adopt one kind of strategy, a node which belongs to the group will adopt strategy that most nodes do, though the opposite one benefits it. This is the conformist mechanism theory.

The Zachry network was chosen to study. The number of club member did not increase in a period of time [6]. But subtle changes would occur among relationship of club members, as the interest confliction exists between two clubs which centered on schoolmaster and club. So we can classify the networks by beneficial characteristics of members. The differences between networks groups mentioned above and society with flexible networks can be found according to analyzing by clustering algorithm. In previous studies some characteristics of nodes were ignored and only an individual was taken into accounted. In this paper some characteristics, such as the economic interest of nodes, were considered when the networks were set up. And cluster analyses to nodes in networks were conducted according to these characteristics. Then nodes in networks were divided into different groups.

The game model was set up according to conformist mechanism:

(1) Set up the payoff matrix. In order to simplify the number of parameters in payoff matrix, the matrix used by Nowak and May was adopted $A = \begin{bmatrix} 1 & 0 \\ b & 0 \end{bmatrix}$.

Meanwhile $1 < b < 2$; strategies of nodes initiation is give each node strategy randomly.

(2) Node i games with its neighbor j in turn. If strategy C was adopted by individual i in the last round, the payoff matrix was not modified and the gaming continued. Otherwise the payoff matrix was modified before next round. Make $b = b - Q$, where Q is called the penalty factor. The payoff $S(l_{ji})$ of each l_{ji} which is the neighbor of individual i was recorded. Among neighbors the one l_{jmax} with maximal payoff $\max(S(l_{ji}))$ was selected (If there are neighbors with equal payoff, choose anyone randomly), after the gaming among individual i and its neighbors. Then the strategy of individual i was replaced by the neighbor l_{jmax} .

(3) The round of next. Nodes in networks were divided into different groups according to clustering algorithm. The same strategy was adopted by nodes in the same group. And different ones were adopted by nodes in different groups.

Repeat step (2) and (3) until the game finished.

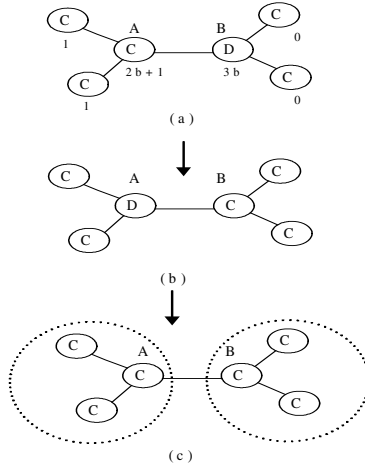


Fig. 1. Process of conformist mechanism

The process of gaming about new model was described in figure 1. The initial strategies were given randomly. And the initial strategies and the payoffs in networks are shown in figure 1(a). Strategy of node B was adopted by node A after a round of gaming, because the payoff of node B is the maximal one among neighbors of node A. For the same reason, as shown in figure 1(b), strategy of node A was adopted by node B. But according to conformist mechanism, strategy of node A should be in accord with most nodes being in the same species. So strategy C was adopted by node A. As shown in figure 1(c), broken lines indicate two groups in networks which divided according to cluster analysis. The evolutionary process was expressed in figure 1. As shown in the figure, because of the effect of conformist mechanism, the collaborated level of networks was improved by new model.

3 Simulation Result and Discussion

By means of clustering algorithm, networks were divided into three groups according to the characteristics of nodes. The gaming was conducted 100 times repeatedly. Strategies were updated according to conformist mechanism in each gaming. The effect on collaborated level of networks after evolution was presented in figure 2. As shown in figure, in each round of gaming, collaboration strategies are higher than betrayal strategies. And strategies in Tomochi and Kono model rise alternatively. It proves that conformist mechanism promotes the emergence of collaboration strategies.

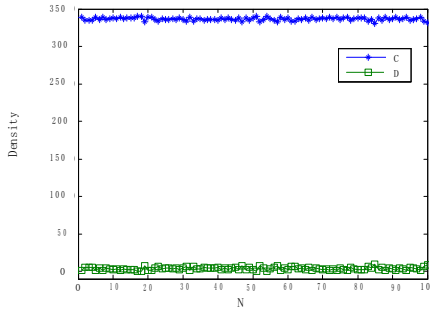


Fig. 2. The strategies density in networks (3 groups)

In order to study the effect on collaboration emergence involving the number of groups, ten groups were discussed. The strategies density of nodes in networks is shown in figure 3.

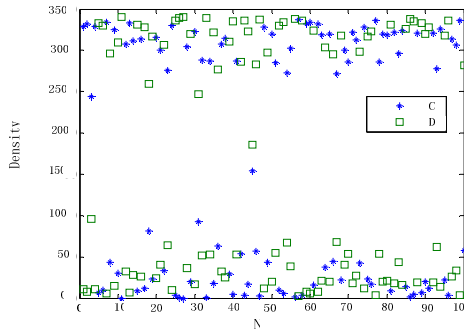


Fig. 3. The strategies density in networks (10 groups)

As interpreted in figure 3, collaboration strategies and betrayal strategies rise alternatively, with no clear limit. It shows that when the number of groups becomes large, effect on conformist mechanism is less visible than small number ones. The reason is that the networks were divided into many small interest groups when the number of groups is large. And the attraction within groups becomes weak, so that selfish occurs. But collaboration strategies predominate as a whole.

The relationship between number of groups and the collaborated level of networks is shown in figure 4. Because full collaboration or full betrayal can be realized by one step of evolution, there is little contribution to study on the collaborated level of networks. So the situations which divide networks into 1group and 34 groups are not taken into account. As indicated in figure 4, the collaborated level was separated into 3 stages. When group number is less than 4, the collaborated level of networks is very high; with almost all the individuals adopt collaboration strategies. When group number is larger than 4 and less than 10, the collaborated level of networks is at the same level; with 2/3 of individuals adopt collaboration strategies.

When group number is larger than 10, 1/2 of individuals adopt collaboration strategies. Generally, the collaboration level is highest when the number reaches 3.

Analysis above shows that the larger number of groups, the lower collaborated level of networks. When the number of groups is large, the number of individuals in the same group becomes small, the majority psychology becomes weak, so the little effect on individuals in groups. And large-scale collaboration emergence is difficult to form. When then number of groups and the number of individuals in group is large, the effect on individuals in groups is strong. Large-scale collaboration emergence is easy to form.

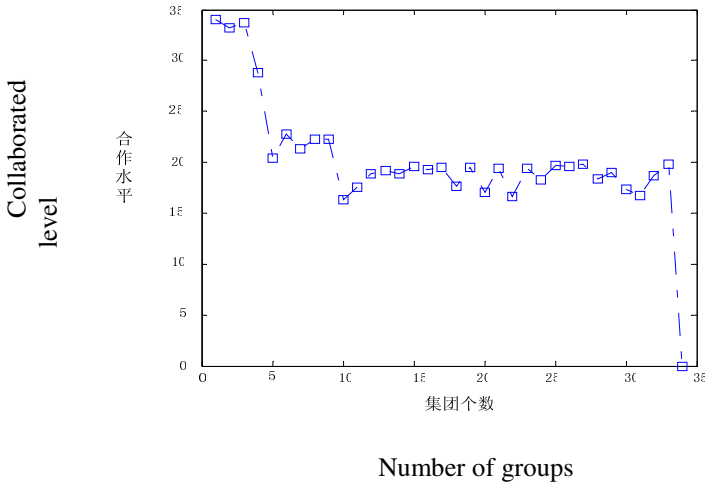


Fig. 4. Number of groups and collaborated level

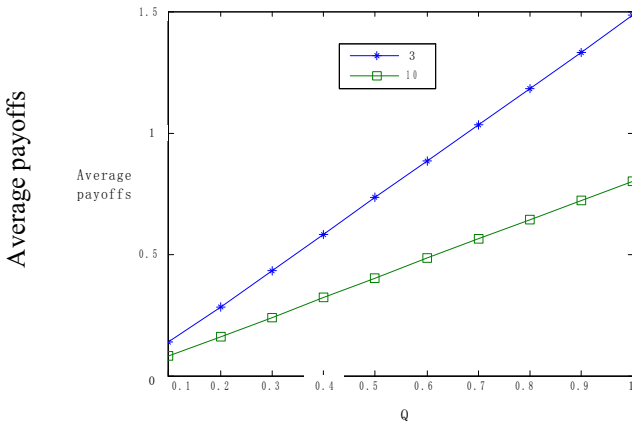


Fig. 5. The average payoffs of networks

In addition, the average payoffs of the whole networks can be improved by conformist mechanism. The average payoffs of networks rise alternatively by using model in reference [7]. But by means of the conformist mechanism, there is a linear relationship between average payoffs of networks and penalty factor Q . The average payoffs of networks with 3 and 10 groups respectively are shown in figure 5. It reveals that the larger number of network types the lower average payoffs. The reason is that the collaboration strategies are not always dominant when the number of network types is not large. So it leads to lower average payoffs of networks.

4 Summary

In this paper basing on the practical networks, a kind of conformist mechanism based on intelligent materials that is favorable to collaboration strategies emergence was presented. Each node adopted the node strategy with maximal payoff among its neighbors in the process of repeated gaming. If the strategy is not in accord with strategies of other nodes in group, the strategy of this node was updated according to its group. Collaboration strategies were promoted through repeated gaming. And the same strategy was selected effectively by nodes in the same group through conformist mechanism. So with this model, strategies of nodes in one group were quickly consistent. And the collaboration emergence was effectively promoted.

References

1. Santos, F.C., Pacheco, J.M.: Scale-Free Networks Provide a Unifying Framework for the Emergence of Cooperation. *Physical Review Letters* 95, 101–104 (2005)
2. Santos, F.C., Pacheco, J.M., Lenaerts, T.: Evolutionary dynamics of social dilemmas in structured heterogeneous populations. *Proc. Natl. Acad. Sci. U.S.A.* 103, 3490–3494 (2006)
3. Vainstein, M.H., Arenzon, J.J.: Disordered environments in spatial games. *Phys. Rev. E* 64(5), 1–6 (2001)
4. Riolo, R.L., Cohen, M.D., Axelrod, R.: Evolution of Cooperation without Reciprocity. *Nature*, 441–443 (2001)
5. Nowak, M.A., Sigmund, K.: Five Rules for the Evolution. *Science* 314(5805), 1560–1563 (2006)
6. Zachary, W.W.: An Information Flow Model for Conflict and Fission in Small Groups. *Journal of Anthropological Research* 33, 452–473 (1977)
7. Tomochi, M., Kono, M.: Spatial Prisoner's Dilemma Games with Dynamic Payoff Matrices. *Phys. Rev. E.* 65(2), 1–6 (2002)

Indefinite LQ Optimal Control for Systems with Multiplicative Noises: The Incomplete Information Case

Guojing Xing, Chenghui Zhang, Peng Cui, and Huihong Zhao

Shandong University, 17923# of jingshi Road, Jinan, Shandong, China
xgjsdu@mail.sdu.edu.cn, zchui@sdu.edu.cn, cuipeng@sdu.edu.cn,
huihong1980@mail.sdu.edu.cn

Abstract. The finite horizon indefinite LQ optimal output feedback control based on anti-noise materials for discrete time stochastic systems with state and control dependent multiplicative noises is considered. In the case of no standard Separation Theorem, a separation property in suboptimal sense holds as long as a generalized difference Riccati equation (GDRE) admits a solution. Then, the optimal output feedback control can be computed iteratively via a state feedback control problem and an estimation problem optimal with respect to each other. A completion of squares technique was used to derive the linear output feedback control, and an equivalent system transformation approach and the Kalman filter design method were used to obtain the recursive linear optimal state estimation algorithm.

Keywords: Indefinite LQ control, multiplicative noise, anti-noise materials, incomplete information.

1 Introduction

The linear quadratic (LQ) optimal control problem has received much attention in control theory due to its wide area of applications in practice. Many excellent results have appeared in early research since 1960's [1][2]. In classical stochastic LQ optimal control problems, it is assumed that the disturbances are additive Gaussian noises, and the assumption that the state weighting matrix is positive semi-definite and control weighting matrix must be positive definite is necessary for the problem to be well-posed.

However, linear stochastic systems with multiplicative noises, which are dependent on state/control or both of them, are general in practice. This kind of system can also be called bilinear stochastic system (BLSS). Many diffusion model in finance and economy, aerospace engineering, communication, biology and chemistry can be described by the BLSS[3]. One important benefit of considering multiplicative noise is that the resulting controller appears robust[4]. Research about LQ optimal control with multiplicative noises early appeared in late of 1960's [5][6][7]. Dynamic programming and maximum principle were used there leading to some theories completely parallel to the deterministic LQ problem. For partially observable systems with signal dependent noises, a coordinate descent algorithm guaranteed to converge to a feedback control law and a linear estimator optimal with respect to each other

was derived in [8]. However, the positive definiteness of the control weighting matrices were still assumed for the aforementioned results. But, an interesting phenomenon was that a positive definite control weighting matrix was not necessary for the LQ problem to be well-posed in the presence of multiplicative noises[9]. This reveals one of the significant differences between deterministic and stochastic LQ problems[10].

An LQ problem is called indefinite when the cost weighting matrix for the state and the control can be indefinite. This problem is of interest since it subsumes, as special cases, the problem of H_2 , H_∞ , game-theoretic and risk-sensitive control [11]. To our knowledge, Kleinman firstly considered the indefinite LQ problem[6]. Up to now, the indefinite stochastic LQ theory has been extensively developed, especially by X.Y.Zhou's recent work[9][12][13][14]. In [9], the deep nature of the stochastic indefinite LQ Problems was discussed in detail. A kind of linear matrix inequality(LMI) condition was introduced in [14], and it was proved that the feasibility of the LMI, the solvability of the associated generalized difference Riccati equation(GDRE), and the well-posedness of the indefinite LQ problem are all equivalent.

Hitherto, most results about indefinite stochastic LQ problem are derived in state feedback form in complete information case. The problem to construct an optimal indefinite output feedback control for the aforementioned BLSS remains up to now unsolved for general disturbed measurements. We emphasize here that the Separation Theorem proposed by Potter and improved by Wonham was an excellent result for incomplete information output feedback control[15][16]. Making use of the Separation Theorem, the stochastic LQ problem can be divided into two independent state feedback control and the related state estimation problems. However, the Separation Theorem does not hold in the presence of multiplicative disturbances because the strict Gaussian assumption for the Separation Theorem to hold can not be satisfied. It brings us an immediate difficulty because the observable process depends on the control, and the control and the estimation problem must be solved simultaneously[12]. A kind of Separation Theorem in suboptimal sense was constructed via heuristic reasoning for continuous time stochastic systems with state and control dependent noises in the incomplete information case[17]. But, the state weighting matrix was still assumed to be positive semi-definite and the control weighting matrix positive definite there.

Moreover, the optimal filtering problem for the system considered in our paper is very complicate, and the optimal estimation in sense of conditional expectation has not been solved until now. For classic filtering problem, we refer to [18]. In linear Gaussian case, Kalman filter can give the optimal linear estimation, which coincides with the minimum variance estimation. But in general, including the system in this paper, the state and control signal are non-Gaussian even if the initial condition and noise signals are all Gaussian[19]. In contrary to standard Kalman filter, the gain of the linear minimum square error filter do depend on the past control. Therefore, the minimum mean variance error estimator will be nonlinear and infinite dimensional. Although nonlinear filtering theory has had many results, but it's difficult to obtain a compute effectively recursive algorithm like the Kalman filter. Some suboptimal approximation approach has been used. In [19], a kind of linear minimum square error filter which had the structure of Kalman filter was proposed. In [12], an

approximation filter was derived by linearizing the Kalman gain via Taylor expansion and neglecting the quadratic and high-order terms in state estimation and control. A kind of polynomial filter is proposed for discrete time non-Gaussian system in presence of state dependent multiplicative noises[20]. However, the problem with the approximation methods is that the resulting algorithm is not always stable.

The aim of this paper is to find a suboptimal output feedback controller for the indefinite LQ optimal control problem of the system with multiplicative noises in discrete time case. The problem is divided into two folds via a kind of non-standard separation technique called enforced separation theorem. First, provided a GDRE considered in [14] admits a solution, a kind of separation property holds. Then, a kind of state estimation feedback control law is derived by completion of square. Second, find the optimal linear estimation of the states with respect to the optimal feedback control law. For this purpose, a kind of system transformation approach is adopted to obtain a linear system, which is equivalent to the original BLSS, with a Wide Sense Wiener process(WSW) diffusion defined in [21]. Then, a Kalman filter design methodology is used to design a linear optimal filter for the transformed linear system. It's worthy noticing that this filter reserves a Kalman-like filter structure. Replacing the real state by its optimal estimate, the LQ problem can be solved by a linear control law and a linear filter optimal with respect to each other whenever the separation property holds.

The paper is organized as follows. In section 2, the statement of the considered problem is given. In section 3, the solution of the suboptimal linear output feedback control problem is obtained. In section 4, the solution of the associated filtering problem is presented.

2 Problem Statement

Consider the LQ optimal control problem of linear discrete-time stochastic system with state and control dependent noises:

$$x(k+1) = A(k)x(k) + B(k)u(k) + \sum_{i=1}^q A_i(k)x(k)W^i(k) + \sum_{i=1}^d B_i(k)u(k)N^i(k) \quad x(0) = x_0 \quad (1)$$

$$y(k) = C(k)x(k) + V(k) \quad y(0) = 0 \quad (2)$$

$$J(x_0, u(0), \dots, u(N-1)) = E \left[\sum_{k=0}^{N-1} x_k^T Q_k x_k + u_k^T R_k u_k + x_N^T Q_N x_N \right] \quad (3)$$

$x_k \in R^n, u_k \in R^r, y_k \in R^p$ are, respectively, the states, inputs and output measurements. The coefficients matrices $A(k), B(k), A_i(k), B_i(k)$ and $C(k)$ are all deterministic. W, N and V are, respectively, standard q, d and p dimensional Brownian motion, and are uncorrelated with each other. $W^i(k), N^i(k)$ denote the i_{th} component of $W(k)$ and $N(k)$, respectively. $Q_0, \dots, Q_N, R_0, \dots, R_N$ are symmetric matrices with appropriate dimensions. E denotes the expectation.

The optimization problem we need to deal with is to find a control sequence $u^*(0), \dots, u^*(N-1)$, which belongs to the admissible control set, to minimize the quadratic cost, ie,

$$J(x(0), u^*(0), \dots, u^*(N-1)) = \inf_{u \in U_{ad}} J(x(0), u(0), \dots, u(N-1)) \tag{4}$$

We only assume that Q_0, \dots, Q_N and R_0, \dots, R_N are symmetric matrices. So, the optimization problem is called an indefinite LQ problem when $Q_0, \dots, Q_N, R_0, \dots, R_N$ are indefinite. The indefinite LQ problem may be ill-posed in general case. Some examples were given in detail in [21].

3 Solution of the Linear Feedback Problem

For continuous time case, the linear state feedback control law had been given in [6] by converting the stochastic optimization problem into a deterministic optimal control problem and invoking the Matrix Maximum Principle. For discrete time problem(1)-(3), we can get similar results via completion of square directly. First, let's give some useful definitions and lemma.

Definition 1: The LQ problem (1)-(3) is called well-posed if

$$V(x_0) = \inf_{u(0), \dots, u(N-1)} J(x_0, u(0), \dots, u(N-1)) > -\infty \tag{5}$$

Moreover, The LQ problem is called attainable if there exists an admissible control sequence $u^*(0), \dots, u^*(N-1)$ such that $V(x_0) = J(x_0, u^*(0), \dots, u^*(N-1))$ for any random variables x_0 , and $u^*(0), \dots, u^*(N-1)$ is called an optimal control.

Definition 2: The following Riccati equation (6) associated with the system (1)(2) is called a generalized difference Riccati equation(GDRE). G_k is called an effective control weighting matrix.

$$\left\{ \begin{aligned} S_k &= A^T(k)S_{k+1}A(k) + Q_k + \sum_{i=1}^q A_i^T(k)S_{k+1}A_i(k) + H_k^T G_k^{-1} H_k \quad S_N = Q_N \\ G_k &= R_k + B^T(k)S_{k+1}B(k) + \sum_{i=1}^d B_i^T(k)S_{k+1}B_i(k) > 0 \\ H_k &= B^T(k)S_{k+1}A(k) \end{aligned} \right. \tag{6}$$

Lemma 1: In the complete information(fully observed states) cases, the LQ problem (1)-(3) has solutions $u_k = K_k x_k$ if and only if the GDRE (6) is solvable. The optimal feedback gain is uniquely given by $K_k = -G_k^{-1} H_k$. For detailed discussion and proof, please refer to theorem 4.1 and corollary 5.1 in [11].

However, in the incomplete information case, we can't get the exact states of the system. What can we derived is just the state estimate based on the disturbed measurements. One nature thought inspired by the well-known Separation Theorem is to firstly design the optimal state feedback control law, then use the state estimate to achieve the control law instead of the real state.

Theorem 1: Suppose a solution exists for the GDRE (6), and define \hat{x}_k as the estimate of x at time k . Then the unique solution of the optimal control problem (1)-(3) is given by

$$u_k^o = K_k \hat{x}_k = -G_k^{-1} H_k \hat{x}_k \tag{7}$$

Proof: First, let S_1, \dots, S_N solve the GDRE (6), we have the equality that

$$E \sum_{k=0}^{N-1} (x_{k+1}^T S_{k+1} x_{k+1} - x_k^T S_k x_k) = E(x_N^T S_N x_N - x_0^T S_0 x_0) \tag{8}$$

By adding equation (8) to the cost function and using the system equation (1), we have

$$\begin{aligned} & J(x_0, u(0), L, u(N-1)) \\ &= E[\sum_{k=0}^{N-1} x_k^T Q_k x_k + u_k^T R_k u_k + x_{k+1}^T S_{k+1} x_{k+1} - x_k^T S_k x_k] + E[x_N^T (Q_N - S_N) x_N + x_0^T S_0 x_0] \\ &= E[\sum_{k=0}^{N-1} x_k^T (Q_k - S_k + A^T(k) S_{k+1} A(k) + \sum_{i=1}^q A_i^T(k) S_{k+1} A_i(k)) x_k + 2x_k^T A^T(k) S_{k+1} B(k) u_k \\ &\quad + u_k^T (R_k + B^T(k) S_{k+1} B(k) + \sum_{i=1}^q B_i^T(k) S_{k+1} B_i(k)) u_k] + E[x_0^T S_0 x_0] \end{aligned} \tag{9}$$

By completing the square, we have

$$J(x_0, u(0), L, u(N-1)) = E[\sum_{k=0}^{N-1} (u_k + G_k^{-1} H_k x_k)^T G_k (u_k + G_k^{-1} H_k x_k)] + E[x_0^T S_0 x_0] \tag{10}$$

From the above expression of J , we know that to minimize J is equivalent to minimize the quantity $\|u_k - K_k x_k\|$ for $k = 0, \dots, N-1$. By projection principle, the minimum is achieved by the control sequence $u_k^o = \Pi [K_k x_k / \ell(Y_k)]$, where $\ell(Y_k)$ is the σ -field generated by the measurements y_0, \dots, y_k , and Π denotes the projection operator. Because of the linearity of the feedback gain K_k , the optimal control can be expressed as $u_k^o = K_k \Pi [x_k / \ell(Y_k)] = K_k \hat{x}_k$. The optimal control (8) has been expressed in terms of the solution to GDRE (6) with one degree of freedom. So, the uniqueness of the optimal control follows the uniqueness of S .

It is assumed that S is a solution of (6). Suppose \tilde{S} is another solution, and set $\hat{S} = S - \tilde{S}$. Then, \hat{S} satisfies

$$\left\{ \begin{aligned} \hat{S}_k &= A_k^T \hat{S}_{k+1} A_k + \sum_{i=1}^q A_i^T(k) \hat{S}_{k+1} A_i(k) - A_k^T \hat{S}_{k+1} B_k \tilde{G}_k^{-1} B_k^T \tilde{S}_{k+1} A_k - A_k^T S_{k+1} B_k G_k^{-1} B_k^T \hat{S}_{k+1} A_k \\ &\quad + A_k^T S_{k+1} B_k G_k^{-1} [B_k^T \hat{S}_{k+1} B_k + \sum_{i=1}^d B_i^T(k) \hat{S}_{k+1} B_i(k)] \tilde{G}_k^{-1} B_k^T \tilde{S}_{k+1} A_k \quad \hat{S}_N = 0 \\ G_k &= R_k + B_k^T S_{k+1} B_k + \sum_{i=1}^d B_i^T(k) S_{k+1} B_i(k) > 0 \\ \tilde{G}_k &= R_k + B_k^T \tilde{S}_{k+1} B_k + \sum_{i=1}^d B_i^T(k) \tilde{S}_{k+1} B_i(k) > 0 \end{aligned} \right. \quad (11)$$

Because the coefficients of system (1)(2) are all deterministic, it is obvious that $\hat{S} \equiv 0$. The uniqueness of the optimal control is proven.

The solution is similar to the one obtained by the classical LQG method. However, The GDRE (6) differs from the classical Riccati difference equation(RDE) for the presence of extra term in G_k . Such terms can be interpreted as a further weighting on the control. This means that the control-dependent noise calls for more conservative control. Our result extends the results proven in [6][11][15] to the indefinite control weighting matrix, discrete time and incomplete information case. The next problem needs to be dealt with is to design a linear optimal filter.

4 The Associated Filtering Problem

The original system was first transformed into an equivalent linear system with WSW diffusion. Then, the linear optimal filter was derived through the Kalman-Bucy scheme.

Let ξ be a random vector, we will denote $\Psi_\xi = E[(\xi - E(\xi))(\xi - E(\xi))^T]$ the unconditional covariance of ξ , and $m_\xi = E(\xi)$ the expectation. Let symmetric matrix $M \in R^{\alpha \times \alpha}$ be semi-positive definite, such that $Rank(M) = \rho \leq \alpha$. It is well known that there exists a full column rank matrix N such that $NN^T = M(M^{1/2} = N)$. It is noted that the matrix $(M^{1/2})^T M^{1/2}$ is nonsingular. I denotes the identity matrix. $P_{k+1|k}, P_{k|k}$ denote the one-step prediction error variance and the filtering error variance, respectively.

Theorem 2: For system (1)(2) with $u_k = K_k \hat{x}_k$, \hat{x}_k satisfies the following equations.

$$\left\{ \begin{aligned} \hat{x}_{k+1} &= [A_k + B_k K_k] \hat{x}_k + F_k [y_{k+1} - C_{k+1} (A_k + B_k K_k) \hat{x}_k] \quad \hat{x}_0 = E(x_0) \\ F_k &= P_{k+1|k} C_{k+1}^T (C_{k+1} P_{k+1|k} C_{k+1}^T + I) \\ P_{k+1|k} &= A_k P_{k|k} A_k^T + \sum_{i=1}^q A_i(k) (\Psi_{x(k)} + m_{x(k)} m_{x(k)}^T) A_i^T(k) + \sum_{i=1}^d B_i(k) K_k (\Psi_{\hat{x}(k)} + m_{\hat{x}(k)} m_{\hat{x}(k)}^T) K_k^T B_i^T(k) \end{aligned} \right. \quad (12)$$

Proof: Let

$$\tilde{A}_i(k) = \begin{cases} [A_i(k) \Psi_{x(k)} A_i^T(k)]^{1/2} & i = 1, \dots, q \\ A_{i-q}(k) m_{x(k)} & i = q + 1, \dots, 2q \end{cases}$$

$$\tilde{B}_i(k) = \begin{cases} [B_i(k) K_k \Psi_{\hat{x}(k)} K_k^T B_i^T(k)]^{1/2} & i = 1, \dots, d \\ B_{i-d}(k) K_k m_{\hat{x}(k)} & i = d + 1, \dots, 2d \end{cases}$$

$$\tilde{W}^i(k) = \begin{cases} [\tilde{A}_i^T(k)\tilde{A}_i(k)]^{-1}\tilde{A}_i^T(k)A_i(k)[x(k) - m_x(k)]W^i(k) & i = 1, \dots, q \\ W^{i-q}(k) & i = q+1, \dots, 2q \end{cases}$$

$$\tilde{N}^i(k) = \begin{cases} [\tilde{B}_i^T(k)\tilde{B}_i(k)]^{-1}\tilde{B}_i^T(k)B_i(k)[\hat{x}(k) - m_{\hat{x}}(k)]N^i(k) & i = 1, \dots, d \\ N^{i-q}(k) & i = d+1, \dots, 2d \end{cases}$$

Then, system (1) can be transformed into an equivalent linear system with WSW processes below.

$$x(k+1) = A(k)x(k) + B(k)K_k\hat{x}(k) + \sum_{i=1}^{2q}\tilde{A}_i(k)\tilde{W}^i(k) + \sum_{i=1}^{2d}\tilde{B}_i(k)\tilde{N}^i(k) \quad (13)$$

\tilde{W}, \tilde{N} are mutually uncorrelated WSW. Using the following notations, we can rewrite (13) in a compact form (14).

$$\begin{cases} \tilde{A}(k) = [\tilde{A}_1(k), \dots, \tilde{A}_{2q}(k)] & \tilde{W}^T(k) = [\tilde{W}^1(k), \dots, \tilde{W}^q(k), W^T(k)] \\ \tilde{B}(k) = [\tilde{B}_1(k), \dots, \tilde{B}_{2q}(k)] & \tilde{N}^T(k) = [\tilde{N}^1(k), \dots, \tilde{N}^q(k), N^T(k)] \end{cases}$$

$$x(k+1) = A(k)x(k) + B(k)K_k\hat{x}(k) + \tilde{A}(k)\tilde{W}(k) + \tilde{B}(k)\tilde{N}(k) \quad (14)$$

Let $Y(k)$ denote the linear space spanned by the measurement $\{ \{y(s)\}_{s=0}^k \}$, by projection principle

$$\hat{x}_{k+1} = E[x_{k+1} | Y_{k+1}] = E[x_{k+1} | Y_k, \tilde{y}_{k+1|k}] = \hat{x}_{k+1|k} + R_{x_{k+1}\tilde{y}_{k+1|k}} R_{\tilde{y}_{k+1|k}}^{-1} \tilde{y}_{k+1|k} \quad (15),$$

where $\tilde{y}_{k+1|k} = y_{k+1} - \hat{y}_{k+1|k}$ is called the innovation process.

$$R_{x_{k+1}\tilde{y}_{k+1|k}} = E[(x_{k+1} - \hat{x}_{k+1|k})(C_{k+1}(x_{k+1} - \hat{x}_{k+1|k}) + V_{k+1})^T] = P_{k+1|k} C_{k+1}^T \quad (16)$$

$$R_{\tilde{y}_{k+1|k}} = E[(C_{k+1}(x_{k+1} - \hat{x}_{k+1|k}) + V_{k+1})(C_{k+1}(x_{k+1} - \hat{x}_{k+1|k}) + V_{k+1})^T] = C_{k+1} P_{k+1|k} C_{k+1}^T + I \quad (17)$$

From the time update equation $\hat{x}_{k+1|k} = [A(k) + B(k)K_k]\hat{x}_k$ and (15)-(17), the first two equations of (12) can be obtained. The one-step prediction error variance used can be calculated by

$$\begin{aligned} P_{k+1|k} &= E[(x_{k+1} - \hat{x}_{k+1|k})(x_{k+1} - \hat{x}_{k+1|k})^T] = E\{[A(k)(x_k - \hat{x}_k) + \tilde{A}(k)\tilde{W}(k) + \tilde{B}(k)\tilde{N}(k)]\tilde{W}^T(k) + \tilde{B}(k)\tilde{N}^T(k)\} \\ &= A_k P_{k|k} A_k^T + \sum_{i=1}^q A_i(k)(\Psi_{x(\delta)} + m_{x(\delta)} m_{x(\delta)}^T) A_i^T(k) + \sum_{i=1}^d B_i(k)K_k(\Psi_{x(\delta)} + m_{x(\delta)} m_{x(\delta)}^T) K_k^T B_i^T(k) \end{aligned} \quad (18)$$

Summary: A kind of separation in suboptimal sense, which is useful from the practice view of point, was derived in this paper. It is shown that the suboptimal output feedback control law is a linear function of the linear optimal state estimation, and the optimal control law can be computed iteratively. The results obtained are natural extension of the complete information case. However, what kind of extent should we made to find the optimal separation theorem? How to deal with the dependence of the filter gains on the control, which is called the dual effect of the control? These are all open problems, which will be discussed in our subsequent works.

Acknowledgement. This work is supported by the National Nature Science Foundation of China(No.61034007, No.60774004), and the National Nature Science Foundation of Shandong Province(No.Z2007G01).

References

1. Kalman, R.E.: Contribution to the theory of optimal control. Bol. Soc. Mat. Mexicana (1960)
2. Anderson, B.D.O., Moore, J.B.: Optimal control: linear quadratic method. Prentice-Hall, Englewood Cliffs (1989)
3. Gerson, E., Shaked, U., Yaesh, I.: H^∞ control and estimation of state-multiplicative linear system. LNCIS. Springer, London (2005)
4. El Ghaoui, L.: State-feedback control of systems with multiplicative noise via Linear Matrix Inequalities, System and Control Letters. Elsevier, Amsterdam (2008)
5. Wonham, W.M.: Optimal stationary control of a linear system with state dependent noise. SIAM J. Control 5(3), 486–500 (1967)
6. Kleinman, D.L.: Optimal stationary control of a linear system with control dependent noise. IEEE Transaction on Automatic Control 14(6), 673–677 (1969)
7. MacLane, P.J.: Optimal stochastic control of linear systems with state and control dependent noises. IEEE Transaction on Automatic Control 16(6), 793–798 (1971)
8. Todorov, E.: Stochastic optimal control and estimation methods adapted to the noise characteristics of the sensorimotor system. Neural computation (2005)
9. Chen, S., Li, X., Zhou, X.: Stochastic linear quadratic regulators with indefinite control weight costs. SIAM J. Control Optim. 36(5), 1685–1702 (1998)
10. Chen, S., Yong, J.: Stochastic linear quadratic optimal control problems. In: Applied Mathematics & Optimization, vol. 43, pp. 21–45. Springer, Heidelberg (2001)
11. Hassibi, B., Sayed, A.H., Kailath, T.: Indefinite-quadratic estimation and control: a unified approach to H_2 and H^∞ theories. SIAM, Philadelphia (1999)
12. Moore, J.B., Zhou, X.Y., Lim, A.E.B.: Discrete Time LQG Controls with Control Dependent Noise. System & Control Letters, 199–206 (1999)
13. Rami, M.A., Zhou, X.Y.: Linear matrix inequalities, Riccati equations, and indefinite stochastic linear quadratic controls. IEEE Transaction on Automatic Control 45(6), 1131–1143 (2000)
14. Rami, M.A., Chen, X., Zhou, X.Y.: Discrete-time indefinite LQ control with state and control dependent noises. Journal of Global Optimization 23, 245–265 (2002)
15. Wonham, W.M.: On the separation theorem of stochastic control. SIAM J Control 6(2), 312–326 (1968)
16. Davis, M.H.: Linear estimation and stochastic control. Chapman & Hall, London (1977)
17. Carravetta, F., Mavelli, G.: Suboptimal stochastic linear feedback control of linear systems with state-and control-dependent noise-the: incomplete information case. Automatica 43, 751–757 (2007)
18. Anderson, B., Moore, J.B., Eslami, M.: Optimal filtering. Prentice-Hall, Englewood Cliffs (1979)
19. Joshi, S.M.: On optimal control of linear systems in the presence of multiplicative noise. IEEE Transaction on Aerospace and Electronic Systems, 80–85 (1976)
20. Carravetta, F., Germani, A., Raimondi, M.: Polynomial Filtering for Linear Discrete Time Non-Gaussian Systems. SIAM Journal on Control and Optimization 34(5), 1666–1690 (1996)
21. Carravetta, F., Germani, A., Shuakayev, M.K.: A new suboptimal approach to the filtering problem for bilinear stochastic differential systems. SIAM J. Control Optim. 28, 966–979 (1990)

Chaos Memory Less Information Material Analysis and Modeling

Feng Shan Pu, Ping chuan Zhang, and Hangsen Zhang

Luohe vocational Technology College, Luohe China, 462002
pufengshan0001@163.com, redmoon123456@126.com,
zhanghangsen@126.com

Abstract. This paper discussed the modeling method of chaos material. And did a profound research on the chaos memory less material, and analyzed the Gaussian property, derived the autocorrelation function. The work is very valuable for the related applications such as information material and property estimation.

Keywords: Chaos material property, Information material, Jacobin transformation, Gaussian modeling.

1 Introduction

Chaos property is an important mathematics characteristics in majority information material [1]. A chaos material, also called a random property material, this is a very simple generalization of the concept of a random structure variable (RV.). A chaos property is an RV that changes with time. There are four types of chaos property [2, 3]: continuous random property; discrete random material; continuous random sequence; discrete random sequence. For the high temperature each day can be considered a chaos property [4]. However, this propperty is not stationary. The property may change with the temperature, the high temperature on a day in summer might be an RV with a mean of 30 degrees, but the high temperature on a day in winter might have a mean of -30 degrees. This is a chaos property whose statistics change with time, so the property is not stationary [5,6]. This paper aims at the chaos basic algorithm analysis; derive math function description. This work is valuable for all similar chaos materials analysis, design and applications.

2 Basic Chaos Material Property Description

Let ξ denote the random outcome of an experiment. To every such outcome suppose a property waveform is got. The collection of such waveforms form a chaos property is shown as in figure 1. The set of and the time index t can be continuous or discrete (countable infinite or finite) as well. For fixed $\xi_i \in \mathcal{S}$ (the set of all experimental outcomes), $X(t, \xi)$ is a specific time function. For fixed t , $X_1 = X(t_1, \xi_i)$ is a random variable. The ensemble of all such realizations over time represents the chaos. For a property $X(t)$ of Fig.1, the input signal is

$$X(t) = a \cos(\omega_0 t + \varphi). \tag{1}$$

Where φ a uniformly distributed random variable in is $(0, 2\pi)$, represents a chaos property. Chaos processes are everywhere: Brownian motion, stock market fluctuations, various queuing systems all represent chaos phenomena.

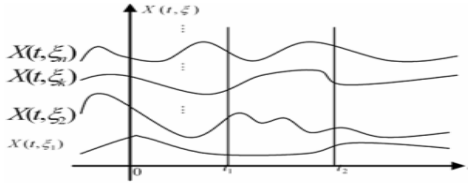


Fig. 1. Waveforms form of a chaos property

3 Memory Less Chaos Materials

A deterministic property transforms [7,8] each input waveform $X(t, \xi_i)$ into an output waveform $Y(t, \xi_i) = T[X(t, \xi_i)]$ by operating only on the time variable t . Now we discuss the typical deterministic system -memory less material property. The general memory less systems is shown as in Fig 2. The output $Y(t)$ in this case depends only on the present value of the input $X(t)$.

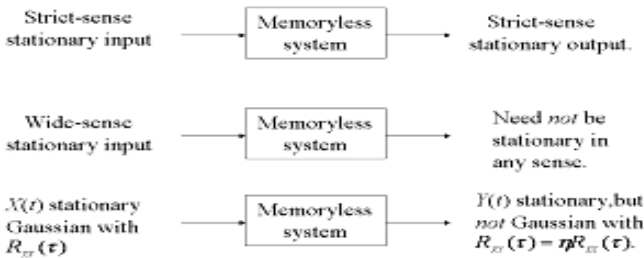


Fig. 2. Memory less systems

Theorem: If $X(t)$ is a zero mean stationary Gaussian property, and $Y(t) = g[X(t)]$, where $g(\cdot)$ represents a nonlinear memory less device. Then

$$R_{xy}(\tau) = \eta R_{xx}(\tau), \quad \eta = E\{g'(X)\}. \tag{2}$$

Proof:

$$R_{xy}(\tau) = E\{X(t)Y(t-\tau)\} = E\{X(t)g\{X(t-\tau)\}\} = \iint x_1 g(x_2) f_{x_1 x_2}(x_1, x_2) dx_1 dx_2 \tag{3}$$

Where $X_1 = X(t)$, $X_2 = X(t-\tau)$ are jointly Gaussian random variables, and hence

$$\begin{aligned}
 f_{x_1, x_2}(x_1, x_2) &= \frac{1}{2\pi\sqrt{|A|}} e^{-\underline{x}^* A^{-1} \underline{x} / 2} \\
 \underline{X} &= (X_1, X_2)^T, \quad \underline{x} = (x_1, x_2)^T \\
 A &= E\{\underline{X}\underline{X}^*\} = \begin{pmatrix} R_{xx}(0) & R_{xx}(\tau) \\ R_{xx}(\tau) & R_{xx}(0) \end{pmatrix} = LL^*
 \end{aligned}
 \tag{4}$$

Where L is an upper triangular factor matrix with positive diagonal entries. i.e.

$$L = \begin{pmatrix} l_{11} & l_{12} \\ 0 & l_{22} \end{pmatrix}
 \tag{5}$$

Consider the transformation

$$\underline{Z} \stackrel{\Delta}{=} L^{-1} \underline{X} = (Z_1, Z_2)^T, \quad \underline{z} \stackrel{\Delta}{=} L^{-1} \underline{x} = (z_1, z_2)^T
 \tag{6}$$

So that

$$E\{\underline{Z}\underline{Z}^*\} = L^{-1} E\{\underline{X}\underline{X}^*\} L^{*-1} = L^{-1} A L^{*-1} = I
 \tag{7}$$

And hence Z_1, Z_2 are zero mean independent Gaussian random material variables. Also

$$\underline{x} = L\underline{z} \Rightarrow x_1 = l_{11}z_1 + l_{12}z_2, \quad x_2 = l_{22}z_2$$

And hence

$$\underline{x}^* A^{-1} \underline{x} = \underline{z}^* L^* A^{-1} L \underline{z} = \underline{z}^* \underline{z} = z_1^2 + z_2^2.
 \tag{8}$$

The Jacobin of the transformation is given by

$$|J| = |L^{-1}| = |A|^{-1/2}.
 \tag{9}$$

Hence substituting these into Eq. (3), we obtain

$$\begin{aligned}
 R_{xx}(\tau) &= \int_{-\infty}^{+\infty} \int_{-\infty}^{+\infty} (l_{11}z_1 + l_{12}z_2)g(l_{12}z_2) \frac{1}{|l_{11}|} \frac{1}{2\pi l_{22}^{1/2}} e^{-z_1^2/2} e^{-z_2^2/2} \\
 &= l_{11} \int_{-\infty}^{+\infty} \int_{-\infty}^{+\infty} z_1 g(l_{12}z_2) f_{z_1}(z_1) f_{z_2}(z_2) dz_1 dz_2 + l_{12} \int_{-\infty}^{+\infty} \int_{-\infty}^{+\infty} z_2 g(l_{12}z_2) f_{z_1}(z_1) f_{z_2}(z_2) dz_1 dz_2 \\
 &= l_{11} \int_{-\infty}^{+\infty} z_1 f_{z_1}(z_1) dz_1 \int_{-\infty}^{+\infty} g(l_{12}z_2) f_{z_2}(z_2) dz_2 + l_{12} \int_{-\infty}^{+\infty} z_2 g(l_{12}z_2) \underbrace{f_{z_2}(z_2)}_{\frac{1}{\sqrt{2\pi}} e^{-z_2^2/2}} dz_2 \\
 &= \frac{l_{11}}{E} \int_{-\infty}^{+\infty} u g(u) \frac{1}{\sqrt{2\pi}} e^{-u^2/2} du,
 \end{aligned}
 \tag{10}$$

Where $u = l_{22}z_2$. This gives

$$\begin{aligned}
 R_{xx}(\tau) &= l_{12} l_{22} \int_{-\infty}^{+\infty} g(u) \underbrace{\frac{u}{l_{22}} \frac{1}{\sqrt{2\pi} l_{22}} e^{-u^2/2 l_{22}^2}}_{-\frac{df_u(u)}{du} = -f'_u(u)} du \\
 &= -R_{xx}(\tau) \int_{-\infty}^{+\infty} g(u) f'_u(u) du,
 \end{aligned}
 \tag{11}$$

Since $A = LL^*$, gives $l_{12}l_{22} = R_{xx}(\tau)$. Hence

$$R_{xy}(\tau) = R_{xx}(\tau) \{-g(u) f_u(u)\}_{-\infty}^{+\infty} + \int_{-\infty}^{+\infty} g'(u) f_u(u) du = R_{xx}(\tau) E\{g'(X)\} = \eta R_{xx}(\tau).
 \tag{12}$$

The desired result, where $\eta = E[g'(X)]$. Thus if the input to a memory less device is stationary Gaussian, the cross correlation function between the input and the output is proportional to the input autocorrelation function. In that case the autocorrelation function is given by

$$\begin{aligned} R_{xx}(t_1, t_2) &\triangleq E\{X(t_1)X^*(t_2)\} \\ &= \int \int x_1 x_2^* f_x(x_1, x_2, \tau = t_1 - t_2) dx_1 dx_2 \\ &= R_{xx}(t_1 - t_2) \triangleq R_{xx}(\tau) = R_{xx}^*(-\tau). \end{aligned} \quad (13)$$

i.e., the autocorrelation function of a second order strict-sense stationary property depends only on the difference of the time indices $\tau = t_1 - t_2$. The basic conditions for the first and second order stationary – Eq. (10) and (12) – are usually difficult to verify. In that case, we often resort to a looser definition of stationary, known as Wide-Sense Stationary (W.S.S), by making use of (11) and (13) as the necessary conditions. Thus, a property $X(t)$ is said to be Wide-Sense Stationary if

$$(i) \quad E\{X(t)\} = \mu. \quad (14)$$

And

$$(ii) \quad E\{X(t_1)X^*(t_2)\} = R_{xx}(t_1 - t_2). \quad (15)$$

4 Conclusion

The basic chaos material model is discussed and on emphasis, analyzed on the memory less chaos information material in detail, and derived its basic algorithm. The results are valuable for all similar chaos material property analysis, system design and application developments.

References

1. Fang, A., Koschny, T., Wegener, M., Soukoulis, C.M.: Self-consistent calculation of metamaterials with gain. *Physical Review, B* 79, 241104 R 2009 *Rapid Communications* 1098-0121/2009/79 24 /241104 4 (2009)
2. Simon, D.: *Optimal State Estimation: Kalman, H and Nonlinear Approaches*. A John Wiley & Sons, Inc., Publication, Chichester (2006)
3. Farmer, J.D., Sidorowich, J.J.: Predicting chaotic time series. *Phys. Rev. Lett.* 59(8), 845–848 (1987)
4. Sugihara, G., May, R.M.: Nonlinear forecasting as a way of distinguishing chaos from measurement error in time series [J]. *Nature* 344, 734–741 (1990)
5. Peebles, P.: *Probability, Random Variables, and Random Signal Principles*. McGraw Hill, New York (2001)
6. Moon, T., Stirling, W.: *Mathematical Methods and Algorithms for Signal Processing*. Prentice Hall, Upper Saddle River, New Jersey (2000)
7. Maybeck, P.: *Chaos Models, Estimation, and Control*, vol. 3. Academic Press, New York (1984)
8. Jake, Z., Kiss, G.: Application of noise reduction to chaotic communications: a case study. *IEEE Transactions on Circuits and Systems-Fundamental Theory and Applications* 47(12), 1720–1725 (2000)

An Approximate Retrieval of Uncertain Data in Data Sources

Taorong Qiu, Haiquan Huang, Yuyuan Lin, and Xiaokun Yao

Department of Computer, Nanchang University, Nanchang 330031, China
taorongqiu@163.com

Abstract. It is a very important issue to build an approximate retrieval model of material data sources with uncertain contents. Based on the rough relational database theory, the approximate retrieval model of material data sources with incomplete internal structure was studied. The adjacency list was used to store equivalence classes. According to the hamming distance, the index of uncertain data in incomplete material data sources was constructed. Based on the equivalence classes, an approach to calculating the similarity between two sets was introduced. In accordance with the similarity, an algorithm for retrieving uncertain data in the material data sources was presented. Finally, a real world example was illustrated and it is shown that the proposed algorithm is useful and effective.

Keywords: Rough Sets, Rough Relation Database, Approximate Retrieval, Uncertain Data.

1 Introduction

With the development of material science research, there are an increasing number of material data source with substantial information. This kind of data source is semi-structured, which has characteristics of incomplete internal structure, incomplete, imprecise or uncertain contents. Approaches to implementing approximate retrieval from this kind of data source have become much more important now. Based on the rough set theory [1,2], T.Beaubouef proposed the Rough Relational Database Model (RRDM) in 1993. RRDM is an extension of the traditional relational database model, which drops the restriction of satisfying first normal form in the traditional relational database theory. RRDM is used mainly in dealing with uncertain knowledge. RRDM becomes a hot research area. Many scholars have done a lot of work in the study of RRDM theory and achieved some results such as the rough entropy theory of rough relational database [3], relational operators theory [4,5], and the rough data query theory [6] and functional dependency theory [7].

How to build an effective retrieval model of material data sources has a direct impact on the querying precision and efficiency. So, in this paper, a query approach for retrieving uncertain data from material data sources based on the rough relational database theory is studied.

2 The Storage of Data in an Incomplete Material Data Source

2.1 The Data Structures of the Rough Relationship

The description of relation is called relational model. A 3-tuple $R=(U,A,D_j)$ is defined as a RRDM[8], where $U=\{u_1,u_2,\dots,u_i,\dots,u_n\}(U\neq\phi)$ is a non-empty finite set of tuples, and $A=\{A_1,A_2,\dots,A_i,\dots,A_m\}(A\neq\phi)$ is a non-empty finite set of attributes and $D_j(1\leq j\leq m)$ is the value range of attribute A_j . For any tuple u_i , supposing the value of attribute A_j is denoted by d_{ij} , then the distinction is that in RRDM d_{ij} is a subset of D_j ($d_{ij}\subseteq D_j,d_{ij}\neq\phi$) while in traditional DB d_{ij} is an element of D_j ($d_{ij}\in D_j$). This is because the fact that RRDB is the set of attribute values constituted by non-atomic ones. (As shown in table 1)

2.2 Storage of Equivalence Class

Adjacency list, a chain storage structure of graph, is used as a way to store equivalence class in this paper. Adjacency list consists of head nodes and list nodes. Each head node has two fields. One is information field (Info) storing the number of elements in the same equivalence class. The other is chain field (Firstarc) storing the element address of equivalence class. Each list node has two fields as well. One is adjacent field (Adjvex) storing elements of equivalence classes. The other is chain field (Nextarc) pointing the next element in the same equivalence class. Furthermore, in order to facilitate the indexing comparison, elements in the same equivalence class are stored by English alphabetical order

2.3 Hamming Distance

Let two strings be $x=(x_1,x_2,\dots,x_n),y=(y_1,y_2,\dots,y_n)$, a Hamming distance is defined:

$$DIS = 1 - \frac{D(x, y)}{n}, \text{ Where } D(x, y) = \sum_{k=1}^n x_k \oplus y_k, \text{ and } \oplus \text{ is modulo 2 addition,}$$

$x_k, y_k \in \{0, 1\}$. It objectively reflects the similarity of two strings.

3 Similarity Degree and Approximate Retrieval Algorithm

3.1 Similarity Degree

The similarity degree means the degree of similarity of two objects. In RRDB, it means the degree of similarity of two objects on the same attribute. For convenience, considering the data to be queried with respect to attribute p in RRDB, which is denoted $A = \{x_1, x_2, \dots, x_n\}$, where the element $x_i, 1 \leq i \leq n$ may belongs to V_p which is the value range of attribute p , or not belongs to V_p , let A_1 be the set of the elements which belong to V_p , and A_2 be the set of the elements which don't belong

to V_p , then $A = A_1 \cup A_2$. Let $B = \{y_1, y_2, \dots, y_m\}$ be the value set of attribute p with respect to tuple t in RRDB, where the element $y_j, 1 \leq j \leq m$ must belong to the value range V_p of attribute p . We compute the similarity degree between A and B by computing the following four data values according to the method proposed in [9].

$$count = Card[(\cup[x_i] | \forall x_i \in A_1) \cap (\cup[y_j] | \forall y_j \in B)] ;$$

$$num_1 = Card(\cup[x_i] | \forall x_i \in A_1) + Card(A_2) ;$$

$num_2 = Card(\cup[y_j] | \forall y_j \in B); num_3 = Card(A - V_p)$. Where $[x]$ is the equivalence class of x , $card(A)$ denotes the cardinal number of A . So the similarity degree is defined as follows:

$$Similarity(A, B) = \frac{2 * count * num_1}{(num_1 + num_2) * \sqrt{num_2 * (num_1 + num_3)}}$$

3.2 An Approximate Retrieving Algorithm Based on the Similarity Degree

Input: equality_data.text;table_data.text;index.text;U_Data[MAX_Equ], δ ;
 //equality_data.text stores the equivalence classes; table_data.text stores the data of simple table in RRDB; index.text stores the index file of RRDB; U_Data stores the data to be retrieved; δ is the similarity degree threshold.

Output: A retrieval result set of the U_Data.

Algorithm Description:

Step1: Create the adjacency list and orthogonal list from the text file equality_data.text and table_data.text;

Step2: Input the data to be queried and store it to U_Data;

Step3: Retrieve the data $t_i[A_j]$ of a tuple t_i in the index.file

Step4: Computing the Similarity degree $Similarity(t_i[A_j], U - Data)$;

If $(Similarity(t_i[A_j], U - Data) > \delta)$ then display the tuple, and store it to the sets of the retrieval result set;

Step 5: Repeat the above two steps, until all tuples in RRDB is retrieved

Step 6: Algorithm end.

Obviously the time complexity of the algorithm is $O(n)$.

4 A Real Example

By taking the attribute QUALITY in table 1 as example, the whole process of the index and search of the data from the index.file or a single table in RRDB is illustrated as follows.

- (1) Store equivalence classes with respect to attribute Quality in adjacency list;
- (2) Index the values of attribute Quality in tuples;

Firstly, the value of attribute Quality of all tuples is described by using a binary string. Secondly, compute DIS to obtain the following distance matrix in fig. 1 as follows.

1									
$\frac{3}{4}$	1								
$\frac{1}{2}$	$\frac{1}{4}$	1							
$\frac{1}{2}$	$\frac{1}{4}$	1	1						
$\frac{3}{4}$	1	$\frac{1}{4}$	$\frac{1}{4}$	1					
1	$\frac{3}{4}$	$\frac{1}{2}$	$\frac{1}{2}$	$\frac{3}{4}$	1				
$\frac{3}{4}$	1	$\frac{1}{4}$	$\frac{1}{4}$	1	$\frac{3}{4}$	1			
$\frac{1}{2}$	$\frac{3}{4}$	0	0	$\frac{3}{4}$	$\frac{1}{2}$	$\frac{3}{4}$	1		

Fig. 1. Approximate matrix

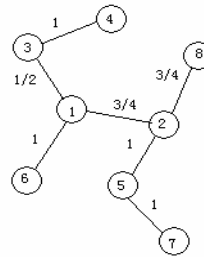


Fig. 2. Maximum tree

Table 1. Soil information table of RRDB

No.	Color	Size	Quality
1	Brown	Medium	Normal
2	Black, tan	Large	Normal, fertile
3	Gray	Medium,small	Poor
4	Black	Tiny	Poor
5	Gray, brown	Large	Normal, productive
6	Gray, white	Medium	Normal
7	Gray, black	Big	Normal, fertile
8	Tan, gray, White,	Enormous, big	Good, normal productive,

Thirdly, using the Maximum Tree Algorithm[10] to create a special tree in Fig. 2, and then grouping them. According to the above maximum tree, tuple 1 and 6 is a group, tuple 2 and 5 and 7 is a group, tuple 3 and 4 is a group, tuple 8 is a group, and save them to an index file index.text.

(3) Retrieve the approximate tuples

Assuming that the similarity degree threshold is $\delta = 0.8$, and given a querying data $U_data = \{good, Normal\}$. In the index file, the data of the value of attribute Quality denoted by A_3 is $\{Normal\}$ in $t_1[A_3]$, and we can obtain Similarity degree $2\sqrt{2}/3$. For $t_2[A_3] = \{Normal, Fertile\}$, $t_3[A_3] = \{Poor\}$ and $t_8[A_3] = \{Good, Productive, Normal\}$, we can compute Similarity degree $2\sqrt{6}/15$, 0 and $\sqrt{2}/3$, respectively. According to the results, the data in tuple 1 and 6 is similar to the data U_data , so the set of retrieving results is tuple 1 and 6. Although, $U_Data = \{Good, Normal\}$ is more similar to $t_8[A_3] = \{Good, Productive, Normal\}$, if taking the equivalence class of the element into consideration, $t_8[A_3]$ is transformed into $t_8[A_3] = \{Good, Productive, Fertile, Normal\}$, the similarity degree between two sets is changed.

5 Summary

We study the method of querying an uncertain data from an incomplete material data sources based on the rough relation database theory. By using the adjacency list and orthogonal list to store the equivalence classes and the material data source, we propose an algorithm of approximate retrieval of uncertain data from the incomplete material data sources. The algorithm has been proven effective by a given real material data source. Future work includes improving the algorithm and making test on big material data sources.

Acknowledgements. Supported by National Natural Science Foundation of China (#61070139) and the Science and Technology Planning Project of the Education Department of Jiangxi Province in China (GJJ11286, S00945).

References

1. Miao, D.Q., Wang, G.Y., Liu, Q.: Granular computing: past, present and prospect. Science Press, Beijing (2007)
2. Zhang, W.X., Wu, W.Z., Liang, J.Y.: Rough set theory and methods. Science Press, Beijing (2001)
3. Beaubouef, T., Petry, F., Arora, G.: Information-theoretic Measures of Uncertainty for Rough Sets and Rough Relational Databases. *Information Science* 109, 185–195 (1998)
4. Beaubouef, T., Petry, F.: Fuzzy Set Quantification of Roughness in a Rough Relational Database Model. In: *IEEE International Conference on Fuzzy Systems*, Orlando, pp. 172–177. IEEE, Los Alamitos (1994)
5. An, Q.S., Xu, J.C., Shen, J.Y.: Rough Relational Database Model and its Relational Operations. *Computer Science* 29(7), 72–89 (2002)
6. An, Q.S., Xu, J.C., Wang, G.Y.: Rough Data Querying of Rough Relation Database Based on Rough Set. *Journal of Xi'an Jiaotong University* 36(8), 859–862 (2002)
7. Nakata, M., Murai, T.: Data Dependencies over Rough Relational Expressions. In: *IEEE International Conference on Fuzzy Systems*, pp. 1543–1546. Institute of Electrical and Electronics Engineers Inc, Melbourne (2001)
8. Wang, D., Wu, M.D., Liu, Y.S.: The Spatial Structure and Rough Sets Model of Rough Relational Database. *Computer Engineering and Design* 41(34), 163–167 (2005)
9. Huang, X.Z., Lo, R.H., Lu, Z.D.: A RDF-Based Query Algorithm of Multi-Valued Systems. *Computer Engineering and Science* 29(8), 68–70 (2007)
10. He, Z.X.: Fuzzy mathematics and its application. TianJing Academic Press, TianJing (1985)

Moving Object Detection through Efficient Detection and Clustering of Reliable Singular Points

Jianzhu Cui, Ping Wang, Zhipeng Li, Jing Li, and Yan Li

The Key Laboratory of Embedded System and Service Computing supported by Ministry of Education, Tongji University, Cao'an Highway 4800, Shanghai, China
tongjiyizhu@hotmail.com, pwang@mail.tongji.edu.cn,
lizhipeng@mail.tongji.edu.cn, ljactive@163.com, yanli@163.com

Abstract. This paper presents a method to detect vehicles from a moving camera. The detection component involves a cascade of modules. First, motion estimation of singular points in video sequences is used to detect moving vehicle. Finding the image points is the selection of singular points. We impose restrictions about the gradient magnitude and the cornerness. A sparse motion vector field outlines the image motion. We obtain excellent results in real sequences in China. At last, vehicles are detected by clustering of singular points.

Keywords: Aerial video, vehicle Detection, singular points detection, Motion Estimation, Singular Point, Point Matching.

1 Introduction

Research in the use of aerial imagery for transportation has been conducted for many years [1]. One of the aspects where technology has helped is on minimizing the amount of manual work. During the past two decades a substantial amount of work has been done to automate image processing for traffic management applications. In [7], the author presents a framework and details of the key components for automatic exploitation of aerial video for surveillance applications, involving separating an aerial video into the natural components corresponding to the scene. In [6], the altitude and position of the helicopter were recorded using a Global Positioning System (GPS) receiver. The author uses an inertial measurement unit (IMU) to collect data on the roll, pitch and yaw of the helicopter. High-precision GPS and IMU data are then used to automatically register the imagery, providing an accurate means of geo-referencing. The main difficult of moving vehicle detection in dynamic background is that the motion of both the vehicle and the platform. Image registration is always used to resolve this question. Image registration algorithms can be classified into intensity-based and feature-based [2]. One of the images is referred to as the reference and the second image is referred to as the target [3]. The contribution of this paper is that we propose a novel moving vehicle detection system in dynamic background.

The major difference between our system and others is our singular points detection, matching and clustering algorithm. The singular points detection, matching algorithm is used for computing the motion vector. Calculating the motion vector from two consecutive input frames is the main step of image registration. Our image registration algorithm follows feature-based paradigm. The organization of the paper is as follows: Section 2 is the overview of the system. Section 3 describes the strategy to select reliable singular points for motion estimation. Section 4 describes the identification of moving vehicle based on singular points clustering.

2 System Overview

The complete system overview is shown in Fig 1. The input to the system is a sequence of images captured by the camera installed inside the UAV (Unmanned aerial vehicle). A SONY DCR-DVD805 camera has been used to acquire the video sequences. The input interface records the images delivered by the camera, and performs the necessary operations to accommodate them to the format expected by the video processing module, i.e., decompresses, rotates and de-interlaces the image, and rescales it to a 760x320 format.

The proposed algorithm is divided into three major steps as shown in fig. 1. First, the selection of singular points is carried out by imposing three different restrictions. Then Singular points of consecutive images are matched using the Euclidean distance between the corresponding descriptor as similarity measure. Erroneous correspondences are discarded comparing its similarity measure with the one related to the second best correspondence. At step three moving vehicles is detected by singular points clustering.

3 Selection of Singular Points

A chain of restrictions is imposed to the image points to select the best ones in order to compute the image motion. The first restriction selects the points whose gradient magnitude value is above a noise-adaptive threshold. Fig 3 shows the points, resulting of thresholding the gradient magnitude image.

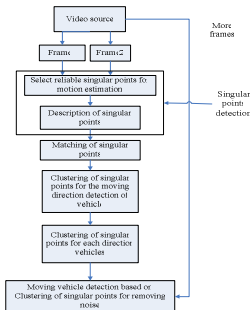


Fig. 1. Moving vehicle detection systems in dynamic background (a)First frame (b)Second frame

Fig. 2. Two original intensity images are as shown.

Fig. 3. Singular points (in white), for the original image presented in Fig 2(a).

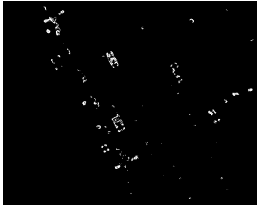


Fig. 4. shows the singular points belonging to corners



Fig. 5. shows the singular points belonging to the last result

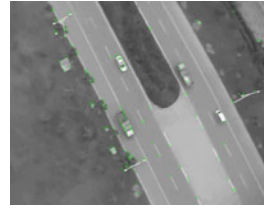


Fig. 6. shows the matching of singular points between two images

These points are characterized by a low cornerness response, what means that they have a large principal curvature along the edge. We adopt the approach of Harris and Stephen[4]. A non-maximal suppression is applied to obtain the final selection of singular points. Figure 4 and Figure 5 respectively show the points in cornerness and the last result from the singular points. This restriction improves the matching accuracy, as shown in Fig 6.

4 Identification of Moving Vehicle Based on Singular Points Clustering

In this stage, we detect the moving vehicle based on singular points clustering for three times. We use kmeans clustering [5] algorithm.

First clustering: The singular points are clustering for three parts: the vehicle whose direction is opposite with the plane, the background, and the vehicle whose direction is same with the plane. The motion vector $Dis(P_i)$ of each singular points P_i is:

$$Dis(P_i) = Coordinate(\bar{P}_i) - Coordinate(\bar{P}_j) \tag{1}$$

\bar{P}_i, \bar{P}_j are the matched points in consecutive images. The motion vector $Dis(P_i)$ of singular points in the vehicle whose direction is opposite with the plane is larger than the background, which is larger than the vehicle whose direction is same with the plane. So the result of clustering is well, as shown in Fig7, just with a little false clustering.

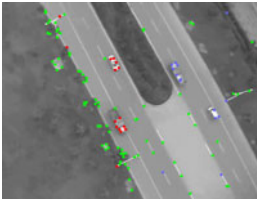


Fig. 7. At first clustering, the singular points are clustering for three parts: the vehicle whose direction is opposite with the plane, the background, and the vehicle whose direction is same with the plane.



Fig. 8. At second clustering: The singular points are clustering for two vehicles with few noise.



Fig. 9. At third clustering: The singular points are clustering for two clusters: vehicle and the noise.

Second clustering:

The number of clustering can be calculated as: $No_{cluster} = sub(\frac{Number_{points}}{Number_{vehicle}})$ (2)

$Number_{points}$ is the number of all the singular points, $Number_{vehicle}$ is the number of each vehicle, here $Number_{vehicle} = 6$ (because each vehicle nearly have six singular points); $No_{cluster}$ is number of clusters, sub means $No_{cluster}$ is the nearest integer with $\frac{Number_{points}}{Number_{vehicle}}$, less than $\frac{Number_{points}}{Number_{vehicle}}$. The singular points are

clustering for two vehicles with few noise. The vector $Dis(P_m)$ of each singular points P_m is :

$$Dis(P_m) = Coordinate(\vec{P}_m) - Coordinate(\vec{P}_j) \tag{3}$$

\vec{P}_i, \vec{P}_j are different points in the same image. The motion vector $Dis(P_i)$ of singular points in the vehicle whose direction is opposite with the plane is larger than the background, which is larger than the vehicle whose direction is same with the plane. So the result of clustering is well, as shown in Fig8, just with a little false noise.

Third clustering: The singular points are clustering for two clusters: vehicle and the noise. And in two clusters, the distance between singular points is different. The vehicle is the cluster that has less distance. The noise is the cluster that has larger distance, as shown in Fig9.

The algorithm proposed in this paper is performed with a sequence of images extracted from a camera attached to a UAV (Unmanned aerial vehicle). The experimental results are showed below. Figure 10 depicts the detection result.

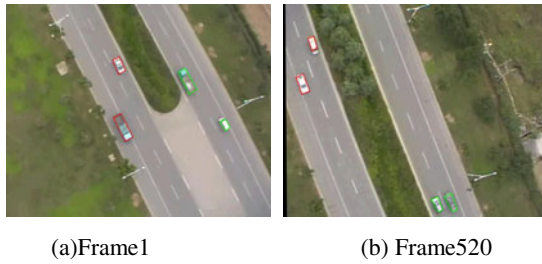


Fig. 10. Experimental results of moving vehicle detection

Figure 10(a) is the first frame of the test image sequence. Figure 10 (b) is the 520th frame of the test image sequence.

This paper presents Moving vehicle detection systems in dynamic environment including experimental results. The robustness of the moving vehicle detection technique to noise, illumination changes and small variations yields sparse motion vector fields of high quality. In addition, the matching process evaluates the reliability of each correspondence, being able to discard erroneous motion vectors. Our method is better than KLT[6] and kmedios.

Acknowledgments. This work has been partially supported by the 863 Project from Science and Technology Department (2009AA11Z220), china. The program is air-ground network traffic monitoring and early warning systems based on the sparse information technology, 2009.1-2011.12.

References

1. Angel, A., et al.: Methods of analyzing traffic imagery collected from aerial platforms. *IEEE Trans. Intelligent Transportation Systems* 4(2), 99–107 (2003)
2. Dagan, E., Mano, O., Stein, G.P., Shashua, A.: Forward Collision Warning with a Single Camera. In: *IEEE Intelligent Vehicles Symposium (IV 2004)*, Parma, Italy (June 2004)
3. Salgado, L., Nieto, M., Jaureguizar, F.: Real-time vehicle detection and tracking based on perspective and non-perspective space cooperation. In: Arróspide, J. (ed.) *Proceedings of the SPIE*, vol. 7244, pp. 72440H–72440H-12 (2009)
4. Harris, C., Stephens, M.: A combined corner and edge detector (PDF). In: *Proceedings of the 4th Alvey Vision Conference*, pp. 147–151 (1988)
5. Ding, C., He, X.: K-means Clustering via Principal Component Analysis. In: *Proc. of Intel. Conf. Machine Learning (ICML 2004)*, July 2004, pp. 225–232 (2004)
6. Shi, J., Tomasi, C.: Good Features to Track. In: *IEEE Conference on Computer Vision and machine learning*, pp. 593–600 (1994)
7. Okada, R., et al.: Obstacle detection using projective invariant and vanishing lines. In: *Proceedings of the 9th ICCV* (2003)

Study on Packaging Technology of Small-Type FED Panel with Cold Field Emitter

Dong Yan¹, Li Qiang², Zhao Feng², and Han Lifeng²

¹ School of electronic information, Zhongyuan Institute of Technology, Zhengzhou, China
dongyan1209@yahoo.com.cn

² Jiyuan power supply company, Jiyuan, China

Abstract. With flat soda-lime glass was adopted as glass plate, the small-type triode field emission display (FED) panel was fabricated, which the carbon nanotube was used as the cold field emitter. The blank glass plate, the base glass plate and the glass spacer would combine to a panel chamber, and the panel image would be formed on the anode glass plate, which would be included in the vacuum environment of panel chamber. A gap would be reserved between the blank and anode glass plate for the fabricated FED panel. The high effective screen-printing process was utilized in the panel fabrication course, and the sealed FED panel demonstrated good field emission performance and high luminance brightness.

Keywords: packaging, glass plate, field emission, sintering.

1 Introduction

Field emission display (FED) was a new vacuum panel, which possessed many excellent features including the high image quality, low power consumption, fast response time and wide work temperature region [1-2]. For the cathode part of FED panel, carbon nanotube (CNT) could be used as attractive cold field emitters because of its unique characteristics, such as high aspect ratio, high chemical stability and small radii of curvature, etc. Only with proper electric-field on the cathode surface, CNTs could emit lots of electrons by the field emission form [3-5]. However, without the vacuum environment, not only the electrons should not be emitted from CNT emitters, but also the electric beam also could not fly in the panel chamber. So, in the fabrication course of FED panel, the vacuum packaging with transparent and flat-panel structure was necessary [6-8]. For triode FED panel with CNT as field emitter, the anode glass plate was a key element because the panel image would be formed on its inner surface. For achieving the high performance displayed image, the structure of anode glass plate should be designed and considered carefully. The screen-printing method was a high effective and low manufacture cost process, and would be adopted for fabricating the anode glass plate of FED panel [9]. In this paper, the small-type triode FED panel was developed, and the fabrication process was also presented in detail. The panel vacuum chamber would be formed by the blank glass plate, the base glass plate and glass spacer. The anode glass plate only was used to display panel

image. The field emission properties of sealed FED panel were studied, and the displayed image was also demonstrated.

2 Experimental Details

A structure schematic diagram for the whole FED panel was shown in Fig.1. The triode FED panel mainly consisted of four parts, which were the blank glass plate, the anode glass plate, the glass spacer and the base glass plate, respectively. Considering the sintering process compatibility with low melting glass frit in the packaging process, all the four parts of whole FED panel were made of the common soda-lime glass. The blank glass plate, the glass spacer and the base glass plate would combine to a panel chamber, in which the anode glass plate would be included. The FED panel had three sets of electrodes, which would be fabricated on the panel glass surface. Thereinto, the cold-cathode parts and the gate parts were fabricated on the base glass plate surface, respectively. And the anode parts would be formed on the anode glass plate surface.

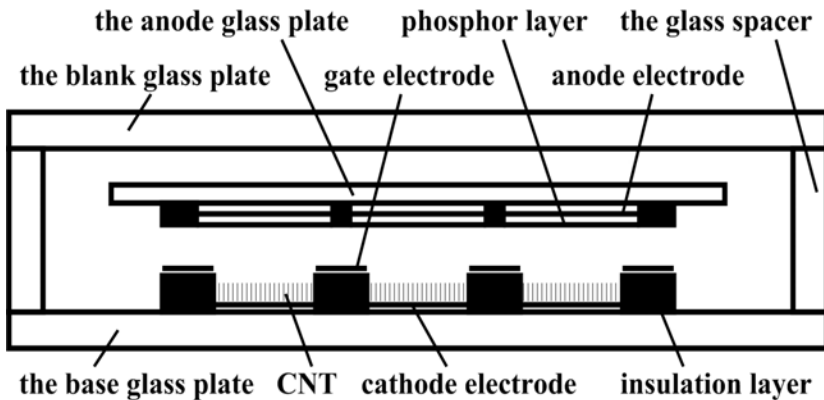


Fig. 1. The schematic of fabricated small-type triode FED panel

For the blank glass plate, the insulation slurry was prepared with the simple screen-printing process. After the conventional sintering process, the printed insulation slurry would be solidified to form the covering layer. Of course, the void existed in the covering layer for exposing the displayed image on the anode glass plate in the vacuum chamber. For the anode glass plate, the indium tin oxide (ITO) thin film covered on the glass plate surface would be divided into many bar anode electrodes with precise photolithography process. And the phosphor powder was prepared on the anode electrodes surface to form the phosphor layer. For the base glass plate, the cathode electrodes and the gate electrodes were all fabricated with printed silver slurry, and were separated by the insulation layer with better insulation performance. The CNT prepared on the cathode electrodes surface would be used as the cold field emitters. In the course of panel packaging, the glass supporting block would be inserted first between the anode and base glass plate, so the distance between them

would be determined by the thickness of glass supporting block. Moreover, the anode glass plate would also be fixed by the glass supporting block on the base glass plate. It was certain that the precise alignment was essential for forming the image. Second, the other subsidiary element including the getters and exhaust tube would be assembled on the base plate. Third, the glass spacer and the blank glass plate were combined with the base glass plate, and the low melting glass frit was used to seal the whole FED panel. The gas in the panel chamber would be evacuated out through the exhaust tube with the high vacuum exhausting system.

3 Results and Discussion

The soda-lime flat glass was adopted as the panel fabrication material. Not only the used glass plate possessed better physical stability and smoothness, but also the manufacture cost was low. Because of its good transparency, the visible light could penetrate through glass plate to form a displayed image. Meanwhile, because of its better hardness, the atmosphere pressure difference between the interior and exterior of panel chamber could be bore by the glass plate to a certain extent. Of course, if the atmosphere pressure difference was too large, the glass plate combined to the panel chamber would also be cracked. For the fabricated small-type triode FED panel, the electrons would be emitted from the CNT cold field emitters with proper gate voltage applying between the gate electrodes and the cathode electrodes on the base glass plate, and the anode voltage applying between the anode electrodes on the anode glass plate and the cathode electrodes was fixed. The panel image would be formed after the phosphor layer was bombarded by the high speed electric beam. So the main performance of the blank glass plate was to form a panel vacuum chamber, and the anode glass plate only was used to display image. On the one hand, the image deformation phenomenon would be avoided because all the anode glass plate resided in the vacuum environment. Without the atmosphere pressure difference, the anode glass plate would not be deformed naturally. Furthermore, the anode and blank glass plate of FED panel was separated. Under the circumstance, although the minor glass deformation for the blank glass plate occurred, the panel image on the anode glass plate would not be affected at all. On the other hand, the thickness of anode glass plate could also be reduced for achieving better glass surface smoothness. For the fabricated FED panel, the thickness of the blank glass plate was about 3mm. As we know, the thick glass plate was a precondition for forming a large vacuum chamber. Certainly, with the supporting action of inner insulation spacer and thick packaging flat glass, the more large area FED panel could be realized. And it was also quite clear that the thin anode glass plate could not bear large atmosphere pressure.

The high quality image displayed by the FED panel always was the goal in pursuit by many researchers. In the panel fabrication course, the fixing and installation of anode glass plate used to display image was completed usually with low melting glass frit. However, the position shifting phenomenon of anode glass plate also usually existed in the sintering course of glass frit, which was disadvantageous for forming the better panel image. So, two measures were adopted for the fabricated triode FED panel. One was that the precise alignment process was carried out in the anode glass plate assemblage course. The anode glass plate would be fixed firstly with the glass

supporting block on the base glass plate, and the packaging process of blank glass plate was conducted subsequently. The other was that the gap was reserved between the blank and anode glass plate. Because the fabricated FED panel was small-type, the thick blank glass plate could resist alone the atmosphere pressure difference. If the blank glass plate would shift in the sealing course, the situation of anode glass plate should not change. On the blank glass plate inner surface, the covering layer was fabricated. The formed panel image on the anode glass plate could be seen from the void existed in the covering layer, and other panel element would become invisible because of the shelter action with the covering layer.



Fig. 2. The emission image of fabricated small-type triode FED panel

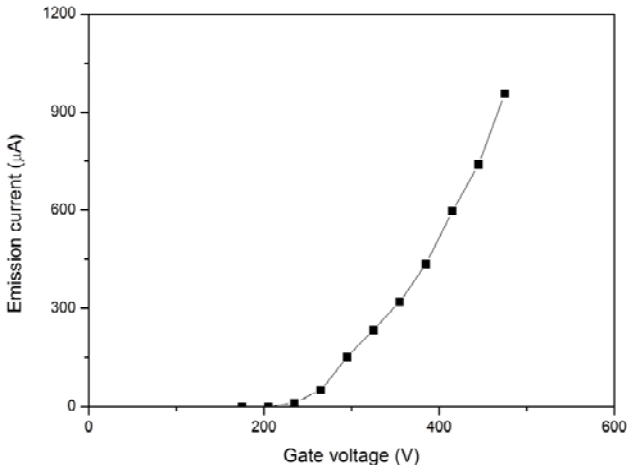


Fig. 3. The typical emission curve of FED panel

In Fig.2, the emission image of sealed FED panel with cold field emitters was presented. The green phosphor layer prepared on the anode glass plate inner surface was used to form the panel image. Because the blank glass plate was transparent, the displayed panel image could be seen from the panel exterior. With the simple fabrication structure, the formed panel image possessed better brightness uniformity

and high luminance brightness. The typical field emission curve was illustrated in Fig.3 for the fabricated small-type FED panel. The action of applied gate voltage was mainly to make that the CNT field emitters could emit plenty of electrons. Seen from the given curve, with the fixed high anode voltage, the field emission current would enhance as the increasing gradually gate voltage, which showed a good field emission characteristic.

4 Conclusion

The flat soda-lime glass was adopted as the fabrication material, and the low-melting glass frit was used to seal the whole chamber. So the small-type triode FED panel was fabricated, which the printed CNT was used as cold field emitters. The panel image would be formed on the anode glass plate, which was included in the panel chamber and was fixed on the base glass plate by the supporting block. The main performance of the blank glass plate was to form a panel vacuum environment. The thickness of the blank glass plate was large, which was helpful for resisting the existed atmosphere pressure difference. The panel image was also given, which showed high luminance brightness and better brightness uniformity.

References

1. Kim, T., Kwon, S., Yoon, H., et al.: Colloids and surface A: physicochemical and engineering aspects 313-314, 448 (2008)
2. Guo, P.S., Chen, T., Chen, Y.W., et al.: Solid-state electronics 52, 877 (2008)
3. Kao, C.-c., Liu, Y.-c.: Materials chemistry and physics 115, 463 (2009)
4. Kuznetsov, A.A., Lee, S.B., Zhang, M., et al.: Carbon 48, 41 (2010)
5. Liu, C.-K., Hu, C.-T., Yang, Y.-H., et al.: Diamond and related materials 18, 345 (2009)
6. Li, Y., Zhu, C., Liu, X.: Diamond and related materials 11, 1845 (2002)
7. Khan, G.G., Mukherjee, N., Mondal, A., et al.: Materials chemistry and physics 122, 60 (2010)
8. Li, Y., Li, C.: Key engineering materials 428-429, 436 (2010)
9. Zeng, F.-g., Zhu, C.-c., Liu, W., et al.: Microelectronics Journal 37, 495 (2006)

Combining Stock Market Volatility Forecasts with Analysis of Stock Materials under Regime Switching

Dong Jing-rong, Chen Yu-Ke, and Zou Yan

School of Economics and Management, Chongqing Normal University,
Chongqing, P.R. China
cqdjrr@vip.sina.com, cqchenyk@126.com,
congzhshu@hotmail.com

Abstract. Forecasting stock market volatility is an important and challenging task for both academic researchers and business practitioners. The recent trend to improve the prediction accuracy is to combine individual forecasts using a simple average or weighted average where the weight reflects the inverse of the prediction error. However, a problem in the existing forecast combination methods is that the weights remain fixed over time. This may prove inadequate, especially in economics data, where changes in policy regimes may induce structural change in the pattern of forecast errors of the different models, thereby altering the relative effectiveness of each model over time. In this paper, we present a new forecast combination approach where the forecasting results of the Generalized Autoregressive Conditional Heteroskedastic (GARCH), the Exponential GARCH (EGARCH), stochastic volatility(SV), and Moving average(MAV) models are combined based on time-varying weights that can be driven by regime switching in a latent state variable. The results of an empirical study indicate that the proposed method has a better accuracy than the GARCH, EGARCH, SV and MAV models, and also combining forecast methods with constant weights.

Keywords: Combining forecasts, GARCH, Stochastic volatility, Regime switching, Stock market volatility.

1 Introduction

While traditional financial economics research has tended to focus upon the mean of stock market returns, in recent times the emphasis has shifted to focus upon the volatility of these returns. Moreover, the international stock market crash of 1987 has increased the focus of regulators, practitioners and researchers upon volatility. These concerns have led researchers to examine the level and stationarity of volatility over time. Specifically, research has been directed toward examining the accuracy of volatility forecasts obtained from various econometric models.

There is a large literature on forecasting volatility. Many econometric models have been used. However, no single model is superior. Using US stock data, for example, Brooks (1998) finds the GARCH models outperform most competitors [1]. Brailsford and Faff (1996) (hereafter BF) find that the GARCH models are slightly superior to

most simple models for forecasting Australian monthly stock index volatility [2]. Using data sets from Japanese and Singaporean markets respectively, however, Tse (1991) and Tse and Tung (1992) find that the exponentially weighted moving average models provide more accurate forecasts than the GARCH model [3,4]. Dimson and Marsh (1990) find in the UK equity market more parsimonious models such as the smoothing and simple regression models perform better than less parsimonious models, although the GARCH models are not among the set of competing models considered [5].

The weakness of most previous studies is their dependence on a single model that is expected to capture all aspects of the volatility formation process. An alternative solution to overcome the limitation is to combine individual forecasts based on models of different specifications and/or information sets [6]. Armstrong (2001) reported that an equally weighted combination of forecasts reduced the average forecasting error by 12.5% [7]. Bates and Granger (1969) advocated the use of a weighted average when combining forecasts with the weight being calculated from the variance and covariance of the different forecasting errors [8]. Similarly Russell and Adam (1987), Schwaerzel and Rosen (1997) combined individual forecasts using weights that were obtained from the mean squared error, mean absolute error, or MAPE (Mean Absolute Percentage Error) of the individual models [9,10]. Menezes et al. (2000) presented a detailed review on combining models and covered the simple average method, regression-based methods, and the switching method [11]. Chan et al. (2004) used quality control techniques to decide when one needs to recalculate the combining weights [12]. Their approach is relatively new. However, a problem in the existing forecast combination methods is that the weights remain fixed over time. This may prove inadequate, especially in economics data, where changes in policy regimes may induce structural change in the pattern of forecast errors of the different models, thereby altering the relative effectiveness of each model over time.

In this paper, we present a new approach where the forecasting results of the Generalized Autoregressive Conditional Heteroskedastic (GARCH), the Exponential GARCH (EGARCH), stochastic volatility(SV), and Moving average(MAV) models are combined based on time-varying weights that can be depended on regime switching process driven by a latent variable. The results of an empirical study indicate that the proposed method has a better accuracy than the GARCH, EGARCH, SV and MAV models, and also combining forecast methods with constant weights. The remainder of this paper is organized as follows. Section 2 presents the individual prediction models along with combining algorithms. In Section 3, a comparison study based on Shanghai stock market data is performed and the results are summarized. Conclusions are drawn in Section 4.

2 Forecasting Model

In this section we describe five different models applicable to stock market volatility prediction: (i) GARCH; (ii) EGARCH; (iii) SV; (iv) MAV; and (v) Combining forecasts using a nonparametric kernel regression.

2.1 Individual Forecasting Models

GARCH Model

The generalized autoregressive conditional heteroscedastic (GARCH) model was developed by Bollerslev and is an extension of the autoregressive conditional heteroscedastic (ARCH) model introduced by Engle (1982) to allow for a more flexible lag structure [13,14]. The GARCH model involves the joint estimation of a conditional mean and a conditional variance equation. Usually, a GARCH (1,1) is found to be sufficient to adequately model volatility. The GARCH (1,1) model employed in this study can be described as follows:

$$\begin{cases} r_t = \mu + \varepsilon_t, & \text{where } \varepsilon_t | \Omega_{t-1} \sim N(0, h_t) \\ h_t = \omega + \alpha \varepsilon_{t-1}^2 + \beta h_{t-1} & \omega > 0, \alpha > 0, \beta > 0 \end{cases} \quad (1)$$

Where r_t is the return on the stock index measured as the logarithm of relative price change and h_t is the conditional volatility. Ω_{t-1} is the information set available at time t .

EGARCH Model

A limitation of the GARCH model described above is that the conditional variance responds to positive and negative innovations in the same manner. However, there is a body of evidence that suggest that the restriction is not empirically valid, in other words, it has been noted that often negative shocks to the conditional mean equation have a larger effect upon volatility than positive shock. One model which remove the assumption of symmetric responses of volatility to shocks of different sign are the exponential GARCH (EGARCH) model proposed by Nelson(1991) [15].The EGARCH(1,1) model used in this study can be described as follows:

$$\begin{cases} r_t = \mu + \varepsilon_t & \text{where } \varepsilon_t | \Omega_{t-1} \sim N(0, h_t) \\ \ln(h_t) = w + \beta \ln(h_{t-1}) + \gamma \left(\frac{\varepsilon_{t-1}}{\sqrt{h_{t-1}}} \right) + \alpha \left[\frac{|\varepsilon_{t-1}|}{\sqrt{h_{t-1}}} - \sqrt{\frac{2}{\pi}} \right] \end{cases} \quad (2)$$

In the EGARCH model, the asymmetry arises from the direct inclusion of the term in ε_{t-1} , normalized by the standard deviation of the data. There are no nonnegativity restrictions on these parameters in the EGARCH model. This is a particularly useful property which significantly simplifies the estimation of parameters and avoids a number of possible difficulties in a negative estimation of GARCH model.

SV Model

The SV model used in this study is defined by

$$\begin{cases} r_t = \sigma_t \varepsilon_t = \exp(0.5h_t) \varepsilon_t \\ h_t = \lambda + \alpha h_{t-1} + v_t \end{cases} \quad (3)$$

Where $\varepsilon_t \sim iidN(0,1)$, $v_t \sim iidN(0, \sigma_v^2)$, and $corr(\varepsilon_t, v_t) = 0$. Like the ARCH-type models, the SV model also models conditional mean and conditional variance by two different equations. As an alternative setup to the ARCH-type models, however, the SV model is supposed to describe financial time series better than the AECH-type models, since it essentially involves two noise processes (ε_t and v_t). This added dimension makes the model more flexible (for further discussion, see Ghysels et al., 1996)[16]. Unfortunately, the density function for the SV model has no closed form and hence neither does the likelihood function. This is true even simplest version of the SV model such as the one defined by Equation 3. It is a consequence of this that direct maximum-likelihood estimation is infeasible. Probably due to this reason, despite its intuitive appeal, the SV model has received little attention in the literature on forecasting volatility.

Recently several methods have been proposed to estimate the SV model. Such methods include quasi-maximum likelihood (QML) proposed by Ruiz (1994)[17], and Markov Chain Monte Carlo (MCMC) by Jacquier *et al.* (1994)[18]. Some of these methods, such as QML and MCMC, not only obtain the estimates of the model, but also produce forecasts of volatility as by-products. In this study, QML is used to estimate parameters in the SV model and obtain volatility forecasts.

MAV Model

An additional model we used to produce individual volatility forecasts is the MAV model (Pagan and Schwert, 1990)[19] which defines the forecast of future a simple average of the lagged volatility observations:

$$ht = \frac{1}{N} \sum_{n=1}^N \sigma_{t-n} \tag{4}$$

Where σ_t is the daily volatility measure. The number of lags (N) was set equal to the number of observations over the estimation period.

2.2 Optimal Forecast Combination under Regime Switching

There are often good reasons to expect that the optimal forecast combination weights change over time. Individual forecasting models can be viewed as local approximations to the true underlying data generating process and their ability to approximate can be expected to change in the presence of structural breaks and as a function of the state of the economy.

Assume that a decision maker is interested in predicting some univariate series, y_{t+1} , conditional on information at time t, Z_t , which comprises a set of individual forecasts, $\hat{y}_{t+1} = (\hat{y}_{1t+1}, \dots, \hat{y}_{mt+1})'$ in addition to current and past values of y, i.e.

$Z_t = \left\{ \hat{y}_{\tau+1}, y_{\tau} \right\}_{\tau=1}^t$. Optimal time-varying forecast combination used in this study can

be described as follows:

$$y_{\tau+1} = \omega_{0t} + \overline{\omega}_t' \hat{y}_{\tau+1} + \varepsilon_{t+1} \tag{5}$$

where $(\omega_{0t}, \overline{\omega}_t)$ are the optimal combination weights.

Here we propose a simple regime switching scheme that captures the optimal combination weights. Suppose that the joint distribution of the target variable and the vector of forecasts is driven by a latent state variable, S_{t+1} , which assumes one of k possible values, i.e. $S_{t+1} \in (1, \dots, k)$. S_{t+1} is not assumed to be known, so $S_{t+1} \notin Z_t$. However, conditional on Z_t and the underlying state, $S_{t+1} = s_{t+1}$, we assume that the joint distribution of y_{t+1} and \hat{y}_{t+1} is Gaussian

$$\begin{pmatrix} y_{t+1} \\ \hat{y}_{t+1} \end{pmatrix} \sim N \left(\begin{pmatrix} \mu_{y^{s_{t+1}}} \\ \mu_{\hat{y}^{s_{t+1}}} \end{pmatrix}, \begin{pmatrix} \sigma_{y^{s_{t+1}}}^2 & \sigma'_{y\hat{y}^{s_{t+1}}} \\ \sigma_{\hat{y}^{s_{t+1}}} & \Sigma_{\hat{y}^{s_{t+1}}}^2 \end{pmatrix} \right) \tag{6}$$

Following Hamilton (1989)[19], we further assume that the states are generated by a first-order Markov chain with transition probability matrix

$$P(s_{t+1} | s_t) = \begin{pmatrix} p_{11} & p_{12} & \dots & p_{1k} \\ p_{21} & p_{22} & \dots & \vdots \\ \vdots & \vdots & \dots & p_{k-1k} \\ pk-1 & \dots & p_{kk-1} & p_{kk} \end{pmatrix} \tag{7}$$

Conditional on $S_{t+1} = s_{t+1}$, the expectation of y_{t+1} is linear in the prediction signals and thus takes the form of state-dependent intercept and combination weights:

$$E[y_{t+1} | Z_t, s_{t+1}] = \mu_{y^{s_{t+1}}} + \sigma'_{y\hat{y}^{s_{t+1}}} \Sigma_{\hat{y}^{s_{t+1}}}^{-1} (\hat{y}_{t+1} - \mu_{\hat{y}^{s_{t+1}}}) \tag{8}$$

where we recall that $\hat{y}_{t+1} \in Z_t$. Hence, if the future value of the state variable, S_{t+1} , was known, the population value of the optimal combination weights under mean squared forecast error (MSFE) loss would be

$$\omega_{0s_{t+1}} = \mu_{y^{s_{t+1}}} - \sigma'_{y\hat{y}^{s_{t+1}}} \Sigma_{\hat{y}^{s_{t+1}}}^{-1} \mu_{\hat{y}^{s_{t+1}}} \tag{9}$$

$$\bar{\omega}_{s_{t+1}} = \sum_{y_{s_{t+1}}}^{-1} \sigma_{y_{s_{t+1}}} \hat{y}_{s_{t+1}}$$

In practice, the underlying state is likely to be unobservable, so the decision maker is interested in minimizing the MSFE conditional only on the current information, Z_t

$$E[e_{t+1}^2 | Z_t] = \sum_{s_{t+1}=1}^k \pi_{s_{t+1,t}} \left\{ \mu_{es_{t+1}}^2 + \sigma_{es_{t+1}}^2 \right\} \tag{10}$$

Where $e_{t+1} = y_{t+1} - \hat{y}_{t+1}$ is the scalar forecast error from the combination $(\hat{y}_{t+1} = \hat{\omega}_{0t} + \bar{\omega}'_t \hat{y}_{t+1})$,

$\pi_{s_{t+1,t}} = \Pr(S_{t+1} = s_{t+1} | Z_t)$ is the (filtered) probability of being in state s_{t+1} in period $t + 1$ conditional on current information, Z_t , and, assuming a linear forecast combination in the general class (5),

$$\mu_{es_{t+1}} = E[e_{t+1} | Z_t, s_{t+1}] = \mu_{y_{s_{t+1}}} - \omega_{0t} - \bar{\omega}'_t \mu_{y_{s_{t+1}}} \tag{11}$$

$$\sigma_{es_{t+1}}^2 = Var(e_{t+1} | Z_t, s_{t+1}) = \sigma_{y_{s_{t+1}}}^2 + \bar{\omega}'_t \Sigma_{y_{s_{t+1}}} \bar{\omega}_t - 2\bar{\omega}'_t \sigma_{y_{s_{t+1}}}$$

Differentiating (10) with respect to ω_{0t} and $\bar{\omega}_t$ and solving the first-order conditions, we get the following combination weights,

$$\omega_{0t} = \sum_{s_{t+1}=1}^k \pi_{s_{t+1,t}} \mu_{y_{s_{t+1}}} - \left(\sum_{s_{t+1}=1}^k \pi_{s_{t+1,t}} \mu'_{\hat{y}_{s_{t+1}}} \right) \bar{\omega}_t \equiv \bar{\mu}_{y_t} + \bar{\mu}'_{\hat{y}_t} \bar{\omega}_t \tag{12}$$

$$\bar{\omega}_t = \left(\sum_{s_{t+1}=1}^k \pi_{s_{t+1,t}} \left(\mu_{y_{s_{t+1}}} \mu'_{y_{s_{t+1}}} + \Sigma_{y_{s_{t+1}}} \right) - \bar{\mu}_{\hat{y}_t} \bar{\mu}'_{\hat{y}_t} \right)^{-1} \times \left(\sum_{s_{t+1}=1}^k \pi_{s_{t+1,t}} \left(\mu_{y_{s_{t+1}}} \mu_{y_{s_{t+1}}} + \sigma_{y_{s_{t+1}}} \right) - \bar{\mu}_{y_t} \bar{\mu}_{y_t} \right)$$

where $\bar{\mu}_{y_t} = \sum_{s_{t+1}=1}^k \pi_{s_{t+1,t}} \mu_{y_{s_{t+1}}}$ and $\bar{\mu}'_{\hat{y}_t} = \sum_{s_{t+1}=1}^k \pi_{s_{t+1,t}} \mu'_{\hat{y}_{s_{t+1}}}$. It is clear from (12) that the

optimal combination weights will, in general, be state dependent in this setting with weights that vary over time as the state probabilities are updated. Consistent estimates of the combination weights for each state can readily be computed by estimating the model

$$y_\tau = \omega_{0s_\tau} + \widehat{\omega}_{s_\tau}^i \hat{y}_\tau + \varepsilon_\tau, \varepsilon_\tau \sim N(0, \sigma_{\varepsilon s_\tau}^2), \tau = 1, \dots, t \tag{13}$$

to get parameter estimates $(\widehat{\omega}_{0t}, \widehat{\omega}_{s_t})$ and state probabilities, $\pi_{s_t,t} = \Pr(S_t = s_t | Z_t)$. One-step-ahead state probabilities $\pi_{s_{t+1},t} = \Pr(S_{t+1} = s_{t+1} | Z_t)$ can be computed from the filtered state probabilities $\pi_{s_t,t} = \Pr(S_t = s_t | Z_t)$ using the transition probabilities $p_{s_t, s_{t+1}}$. The (conditionally) optimal forecast of y_{t+1} is then obtained as

$$E[y_{t+1} | Z_t] = \sum_{s_{t+1}=1}^k \pi_{s_{t+1},t} E[y_{t+1} | Z_{t,s_{t+1}}] \tag{14}$$

3 Empirical Study

3.1 Data Description and Research Method

The data analysed in this paper are the daily Shanghai Stock Exchange (SSE) closing composite stock price index for the period 2 January 2004 to 30 July 2009. The Shanghai Stock Exchange publishes a daily composite index that is based on the weighted market capitalization of all listed companies. The data was obtained from Datastream. Daily returns are identified as the difference in the natural logarithm of the closing index value for two consecutive trading days.

Table 1. Sample statistics for daily returns (January, 2, 2004-July, 30, 2009)

NO.of obs	Mean (%)	Standard deviation (%)	Skewness coefficient	Kurtosis	LB(12) return	LB ² (12) squared return
1449	-0.0943	3.376	1.3542	12.1247	23.312	126.32

Table 1 contains the number of return observations for the stock index and statistics testing the null hypothesis of independence and identically distributed normal variates. The descriptive statistics for the return series are mean, standard deviation, skewness, kurtosis and Ljung-Box statistics LB(12) and LB²(12) for the return series and the squared return series. Under the assumption of normality, skewness and kurtosis have asymptotic distributions $N(0,6/T)$ and $N(3,24/T)$, respectively, where T is the number of return observations. The return distribution is positively skewed, indicating that the distribution is non-symmetric. Furthermore, the relatively large value of kurtosis statistics suggests that the underlying data are leptokurtic, or fattedailed and sharply peaked about the mean when compared with the normal distribution.

The Ljung-Box LB(12) statistics for the cumulative effect of up to the twelfth order autocorrelation in the return exceeds 21.026 (5% critical value from a chisquared distribution with 12 degrees of freedom). It indicates that there is some evidence for serial correlation in the stock return series that should be accounted for in the mean equation.

Even if there was a lack of serial correlation, evidence would imply only that the series was uncorrelated, and no conclusion could be drawn on independence. The Ljung-Box LB²(12) statistics for the squared return provides us with a test of intertemporal dependence in the variance. The LB²(12) statistical value 126.32, which exceeds 26.217 (1% critical value from a chi-squared distribution with 12 degrees of freedom), rejects significantly the zero correlation null hypothesis. In other words, the distribution of the next squared return depends not only on the current squared return but also on several previous squared returns, which will result in volatility clustering. These results clearly reject the independence assumption for the time series of daily stock returns. In sum, there are dependence, non-normality, thick tails and volatility clustering in the time series data of Shanghai daily stock returns.

The approach taken in this paper is one-step-ahead forecasts. One-step-ahead prediction is useful in evaluating the adaptability of a forecasting model. Since our main goal is to evaluate the volatility forecasting performance of eight models, we wish to consider a reasonably large hold-out sample. Therefore, the sample data set of daily Shanghai composite index prices is divided into two parts. The first part is from 2 January 2004 to 31 December 2009. The second part is from 2 January 2009 to 30 July 2009. The second part of the data set serves as the test or comparison period in which the out of sample forecasts from the models are compared. The first part of the data set is reserved for estimating the initial parameters of the models. Furthermore, since it is not a priori assumed that one model necessarily dominates other models over the whole sample, we repeat our modelling and forecasting exercise for different subsamples. We thus fit the models to a sample of five years, generate a one-step-ahead forecast, delete the first observation from the sample and add the next one, and generate again a one-step-ahead-forecast. This process continues until we get a volatility forecasts for each day from 2 January 2009 to 30 July 2009.

3.2 Out-of-Sample Model Forecast Results

Two commonly used loss functions or error statistics: the root mean squared error (RMSE) and the mean absolute percentage error (MAPE) are employed to measure the performance of out-of-sample model forecast results. They are defined as follows:

$$RMSE = \sqrt{\frac{1}{n} \sum_{t=1}^n (\sigma_t - \hat{\sigma}_t)^2}$$

$$MAPE = \frac{1}{n} \sum_{t=1}^n |\sigma_t - \hat{\sigma}_t| / \sigma_t$$

where σ_t and $\hat{\sigma}_t$ denote the actual volatility and the forecasted volatility forecast in time t , respectively.

Table 2. Out-of-sample forecasting performance of competing models for the volatility of stock index (January 2, 2009-July 30, 2009)

Error statistics Model	RMSE	MAPE
GARCH(1,1)	0.00880	2.8615
EGARCH(1,1)	0.00872	2.8452
SV	0.00853	2.84513
MAV	0.00932	2.9356
OLS combining	0.00823	2.84204
NRLS combining	0.00837	2.84207
ERLS combining	0.00824	2.84102
RS combining	0.00612	2.8223

Table 2 reports the root mean squared forecast error (RMSE) and the mean absolute percentage error (MAPE) for each of the individual models and each of the combining methods for the out-of-sample period 2 January 2009 to 30 July 2009. In terms of RMSE and MAPE, the Combining methods are better than the individual forecasting methods. Within the Combining methods, the RS outperforms the alternative combining method (e.g. OLS, NRLS, ERLS) based on RMSE and MAPE. Within the individual forecasting models, the SV model performed better than other individual models (e.g. GARCH, EGARCH, MAV), and the EGARCH model has almost the same accuracy as the GARCH model with both these models being more accurate than the MAV model using either measure of performance.

4 Conclusion

Stock market volatility forecasting is a widely researched area in finance literature. The performance of forecasting models of varying complexity has been investigated according to a range of measures and generally mixed results have been recorded. On the one hand some argue that relatively simple forecasting techniques are superior, while others suggest that the relative complexity of ARCH-type models is worthwhile. The weakness of most previous studies is their dependence on a single approach that is expected to capture all aspects of the volatility formation process. In this paper we seek to extend previous studies by combining individual forecasts based on models of different specifications and/ or information sets to produce improved volatility forecasts.

In an effort to improve the accuracy of forecasting stock market volatility, This article proposed a new approach to forecast combination that lets the combination weights depend on a regime switching process driven by a latent variable. This approach is theoretically appealing in the presence of instability of unknown form in the forecasting performance of individual models. Indeed, several mechanisms could give rise to time variations in the combination weights, such as changes between recession and expansion periods, institutional shifts, or even differences in the learning speed of individual forecasting models representing varying degrees of complexity. Under any of these scenarios, a forecasting strategy of keeping the combination weights constant through time is unlikely to be the best available option to a decision maker. The performance of the proposed method and seven other

forecasting models in predicting Shanghai Stock market volatility have been investigated. The results of our empirical study indicate that the proposed method outperforms the individual prediction models and the alternative combining method.

Acknowledgement. This research was supported by 08XJY007, CSTC2010CE0056, CSTC2010BB6388.

References

1. Brooks, C.: Predicting stock index volatility: Can market volume help? *Journal of Forecasting* 17, 59–80 (1998)
2. *Banking and Finance* 20, 419–438 (1996)
3. Tse, Y.K.: Stock return volatility in the Tokyo stock market. *Japan and the World Economy* 3, 285–298 (1991)
4. Tse, Y.K., Tung, S.H.: Forecasting volatility in the Singapore stock market. *Asia Pacific Journal of Management* 9, 1–13 (1992)
5. Dimson, E., Marsh, P.: Volatility forecasting without data-snooping. *Journal of Banking and Finance* 14, 399–421 (1990)
6. Clemen, R.: Combining forecasts: a review and annotated bibliography. *International Journal of Forecasting* 5, 559–583 (1989)
7. Armstrong, J.S.: Combining Forecasts in *Principles of Forecasting: A Handbook for Researchers and Practitioners*, 417–439 (2001)
8. Bates, J.M., Granger, C.: The combination of forecasts. *Operational Research Quarterly* 20, 451–468 (1969)
9. Russell, T.D., Adam, E.E.: An empirical evaluation of alternative forecasting combinations. *Management Science* 33, 1267–1376 (1987)
10. Schwaerzel, R., Rosen, B.: Improving the accuracy of financial time series prediction using ensemble networks and high order statistics. In: *Proceedings of the International Conference on Neural Networks*, Houston, TX, vol. 4, pp. 2045–2050 (1997)
11. Menezes, L.M., Bunn, D.W., Taylor, J.W.: Review of guidelines for the use of combined forecasts. *European Journal of Operational Research* 120, 190–204 (2000)
12. Chan, C.K., Kingsman, B.G., Wong, H.: Determining when to update the weights in combined forecasts for product demand—an application of the C-USUM technique. *European Journal of Operational Research* 153, 757–768 (2004)
13. Bollerslev, T.: Generalized autoregressive conditional heteroscedasticity. *Journal of Econometrics* 31, 307–327 (1986)
14. Engle, R.F.: Autoregressive conditional heteroscedasticity with estimates of the variance of United Kingdom inflation. *Econometrica* 50, 987–1007 (1982)
15. Nelson, D.B.: Conditional heteroskedasticity in asset return: A new approach. *Econometrica* 59, 347–370 (1991)
16. Lainiotis, D.G.: Adaptive estimation and structure identification. *IEEE Trans. Automat. Control* 16, 160–170 (1971)
17. Petridis, V., Kehagias, A.: Modular neural networks for Bayesian classification of time series and the partition algorithm. *IEEE Trans. Neural Networks* 7, 73–86 (1996)
18. Petridis, V., Kehagias, A.: *Predictive Modular Neural Networks: Time series Applications*. Kluwer Academic, Dordrecht (1998)
19. Hamilton, J.D.: A New Approach to the Economic Analysis of Nonstationary Time Series and the Business Cycle. *Econometrica* 57, 357–386 (1989)

Impulsive Consensus of the Leader-Following Multi-agent Systems

Wanli Guo and Guoqing Wang

Department of Mathematics and Physics, China University of Geosciences,
Wuhan, P.R. China.
guowanliff@163.com, gqwug@163.com

Abstract. This paper is mainly concerned with the consensus problem of the leader-following multi-agent system. In terms of the impulsive communication from the leader, a consensus protocol which can well describe practical architectures of more realistic systems is proposed. And some simple but not conservative criterions for the consensus are derived. Finally, a simple example is provided to demonstrate the effectiveness of the theory.

Keywords: Consensus problem, Leader-following multi-agent systems, Impulsive communication.

1 Introduction

As one type of critical problems for cooperative control of multi-agent systems, consensus problems have been found to possess broad applications [1-10] in animal groups, computer science, vehicle teams, and so on. The main objective in consensus problems is to design appropriate protocols and algorithms such that a group of agents converges to some consistent value under exchanged information between each other. For example, in Ref. [1], the authors proposed a simple neighbor based rule that makes all agents eventually move in the same direction. Ref. [2] provided a theoretical explanation for the consensus behavior of the Vicsek model using the graph theory. Ref. [7] designed a set of coordination control laws that enable the group to generate stable flocking motion. The authors in Ref. [8, 9] proposed a different neighbor-based "observer" to estimate the unmeasurable state of an active leader. In [10], the authors introduce second-order consensus protocols distributed in the sense that each agent only needs information from its local neighbors.

As is known, since the control input is implemented by the "sudden jumps" of some state variables at some instants, impulsive control is very effective and robust, and with a low cost. This control method dramatically reduces the cost needed, which makes impulsive control more efficient and applicable than continuous control, thus having received considerable attention. In practice, there exist a lot of instantaneous breakdown phenomena, such as population-growth models [11], maneuvers of spacecraft[12], and so on. In the past few years, impulsive control has been widely studied in stabilization and synchronization of chaotic systems [13-15].

From the practical point of view, we try to use impulsive control method to solve the consensus problem of the multi-agent system. Therefore, in this paper, we mainly concern the issue of consensus problem of the leader-following multi-agent system. In terms of the impulsive communication from the leader, a consensus protocol which can well describe practical architectures of more realistic multi-agent systems is proposed. Based on the stability theory for impulsive differential equations, some simple but not conservative criterions are derived for the consensus of such multi-agent system. Furthermore, simulated examples indicate the effectiveness of the criterion.

2 Problem Formulation

In this paper, the state vector of all the considered agents can be described as:

$$\dot{x}_i(t) = u_i, \quad x_i, u_i \in R^m, \quad i = 1, 2, \dots, n \tag{1}$$

where $x_i(t)$ is the position vectors of the i^{th} agent, u_i is the control input. The problem is to let all the follower-agents keep the same pace of the leader. The leader of this considered multi-agent system is active; that is, its state variables keep changing. Its underlying dynamics can be expressed as

$$\dot{x}_0 = v_0 \tag{2}$$

where $x_0, v_0 \in R^m$ are the position and velocity vectors of the leader, respectively.

Our aim here is to propose a decentralized control scheme for each agent to follow the leader, that is $x_i(t) \rightarrow x_0$ for all $i = 1, 2, \dots, n$, which implies that the leader-following multi-agent system obtain consensus.

Considering the impulsive communication from the leader, for each agent, we give the local control scheme -- a neighbor-based feedback law as:

$$u_i = v_0(t) + h_i(x_i(t), x_2(t), \dots, x_n(t)) - b_{ik} \delta(x_i(t) - x_0(t)), \quad i = 1, \dots, n, k = 1, \dots \tag{3}$$

where b_{ik} are positive constants, $h_i : R^{nm} \rightarrow R^m$ are uncertain linear or nonlinear coupling function that reflect the coupling influence between agent i and its neighbors, and $\delta(t_k)$ satisfies

$$\delta(t_k) = \begin{cases} 1, & t = t_k, \\ 0, & t \neq t_k, \end{cases}$$

where the impulsive instant sequence $\{t_k\}_{k=1}^\infty$ satisfies that

$$t_1 < t_2 < \dots < t_k < \dots, \lim_{k \rightarrow \infty} t_k = \infty.$$

So we have the impulsive leader-following multi-agent system described by following impulsive differential equations:

$$\begin{cases} \dot{x}_0(t) = v_0(t), \\ \dot{x}_i = v_0 + h_i(x_1(t), x_2(t), \dots, x_n(t)), t \neq t_k, \\ \Delta x_i(t_k) = -b_{ik} \mathcal{D}(x_i(t_k) - x_0(t_k)), t = t_k, k = 1, 2, \dots \end{cases} \quad (4)$$

where $\Delta x_i(t_k) = x_i(t_k^+) - x_0(t_k^+)$ is the ‘‘jump’’ in the state variable at the time instant t_k , where $x_i(t_k^+) = \lim_{t \rightarrow t_k^+} x(t)$, $x_i(t_k^-) = \lim_{t \rightarrow t_k^-} x(t)$. In general, for simplicity, it is assumed that $x_i(t_k) = x_i(t_k^-)$, which means $x_i(t)$ is continuous from the left.

If we defines the tracking error between the agent i and the leader as $e_i(t) = x_i(t) - x_0(t)$, then the tracking error of the multi-agent systems can be rewritten as follows:

$$\begin{cases} \dot{e}_i(t) = \dot{x}_i(t) - \dot{x}_0(t) = h_i(x_1(t), x_2(t), \dots, x_n(t)) - h_i(x_0(t), x_0(t), \dots, x_0(t)), t \neq t_k, \\ \{e_i(t_k^+) = x_i(t_k^+) - x_0(t_k) = x_i(t_k) + b_i(x_i(t_k) - x_0(t_k)) - \dot{x}_0(t_k) = (1 + b_i)e_i(t_k). k = 1, 2, \dots. \end{cases} \quad (5)$$

Assumption 1. Assume that there exist positive Scalars $c_j > 0, j = 1, \dots, n$, such

$$\text{that for } i = 1, 2, \dots, n, \|h_i(x_1(t), x_2(t), \dots, x_n(t))\| \leq \sum_{j=1}^n c_j \|x_j(t) - x_i(t)\|.$$

The stability of the trivial solution of (5) implies that the multi-agent system 4) achieve consensus.

Theorem 1. If there exists a constant $\xi > 1$ such that $\ln \xi \lambda_k + 2Ln(t_k - t_{k-1}) \leq 0, k = 1, 2, \dots$, then, the trivial solutions of the tracking error systems (5) are asymptotical stable, which implies that the multi-agent system (4) achieves consensus.

Proof. Choose a Lyapunov function as $V(t) = \frac{1}{2} \sum_{i=1}^n e_i^T(t) e_i(t)$. When

$$\begin{aligned} t \in (t_{k-1}, t_k] \text{ the time derivative of } V(t) \text{ with respect to (5) is} \\ \dot{V}(t) = \sum_{i=1}^n e_i^T(t) (h_i(x_1(t), x_2(t), \dots, x_n(t)) - h_i(x_0(t), x_0(t), \dots, x_0(t))) \leq \sum_{i=1}^n \|e_i^T(t)\| (\sum_{j=1}^n c_j \|e_j(t)\|) \\ \leq \frac{1}{2} \sum_{i=1}^n (\sum_{j=1}^n c_j (e_i^T(t) e_i(t) + e_j^T(t) e_j(t))) = \frac{L}{2} \sum_{i=1}^n (n e_i^T(t) e_i(t) + \sum_{j=1}^n e_j^T(t) e_j(t)) = 2LnV(t) \end{aligned}$$

where $L \geq \max\{c_1, \dots, c_n\}$. Thus, when $t \in (t_{k-1}, t_k]$,

$$V(t) \leq V(t_1^+) \exp[2Ln(t - t_1)].$$

On the other hand, it follows from (5) that when $t = t_k^+$,

$$V(t_k^+) = \frac{1}{2} \sum_{i=1}^n e_i^T(t_k^+) e_i(t_k^+) = \frac{1}{2} \sum_{i=1}^n (1 - b_{ik})^2 e_i^T(t_k) e_i(t_k) \leq \frac{1}{2} \max_{i=1}^n \{(1 - b_{ik})^2\} V(t_k) = \lambda_k V(t_k),$$

where $\lambda_k = \max_{i=1}^n \{(1 - b_{ik})^2\}$.

So for $t \in (t_0, t_1], V(t) \leq V(t_0^+) \exp[2Ln(t - t_0)]$, which leads to $V(t) \leq V(t_0^+) \exp[2Ln(t_1 - t_0)]$ and $V(t_1^+) \leq \lambda_1 V(t_1) \exp[2Ln(t_1 - t_0)]$.

Therefore, for $t \in (t_1, t_2]$, we have

$$V(t) \leq V(t_1^+) \exp[2Ln(t - t_1)] \leq \lambda_1 V(t_0^+) \exp[2Ln(t_1 - t_0)] \exp[2Ln(t - t_1)] = \lambda_1 V(t_0^+) \exp[2Ln(t_2 - t_0)]$$

In general, for $t \in (t_{k-1}, t_k]$, $V(t) \leq \lambda_1 \lambda_2 \cdots \lambda_{k-1} V(t_0^+) \exp[2Ln(t - t_0)]$. From the (2.6), we obtain that there exists a constant such that $\lambda_k \leq \exp(2Ln(t_k - t_{k-1})) / \xi$, then, for $t \in (t_{k-1}, t_k]$,

$$V(t) \leq V(t_0^+) \exp[2Ln(t - t_{k-1})] / \xi^{k-1} \leq V(t_0^+) \exp[2Ln(t_k - t_{k-1})] / \xi^{k-1}$$

Thus, the trivial solutions of the tracking error systems (5) are asymptotical stable, which implies that the multi-agent system (4) achieves consensus.

Particularly, if the impulsive interval $\Delta_k = t_k - t_{k-1} = \Delta$ is a positive constant, and $b_{ik} = b_i$, then the following corollary is immediate.

Corollary 1. Assume the impulsive interval $\Delta_k = t_k - t_{k-1} = \Delta$ is a positive constant, and $b_{ik} = b_i$. Then, the trivial solutions of the tracking error systems (5) are asymptotical stable, if there exists $\xi > 1$, such that $\ln \xi \lambda + 2\Delta \leq 0, k = 1, 2, \dots$ where $\lambda = \max_{i=1}^n \{(1 - b_i)^2\}$.

2.1 Numerical Simulation

Simulations are performed with 6 agents moving in a 3-dimensional space and a leader satisfying the Chua's circuit system. The Chua's circuit is the differential equations system

$$\begin{cases} \dot{x}_{01} = 10(x_{02} - x_{01} - m_0 x + 0.5(m_1 - m_0)(|x_{01} + 1| - |x_{01} - 1|)), \\ \dot{x}_{02} = x_{01} - x_{02} + x_{03}, \\ \dot{x}_{03} = -14.97 x_{02}. \end{cases}$$

It has a chaotic attractor when $m_0 = -0.68, m_1 = -1.27$.

The coupled multi-agent system is given as

$$\begin{cases} \dot{x}_i = x_0 + \sum_{j=1}^6 a_{ij}x_j, \\ \Delta x_i = b_{ik} \delta(t_k)(x_i(t_k) - x_0(t_k)), t = t_k, \end{cases} \quad \text{where}$$

$$A = (a_{ij})_{6 \times 6} = \begin{pmatrix} -6 & 1 & 2 & 1 & 1 & 1 \\ 2 & -6 & 2 & 1 & 0 & 1 \\ 1 & 3 & -7 & 0 & 1 & 2 \\ 2 & 1 & 1 & -9 & 2 & 3 \\ 1 & 2 & 1 & 2 & -7 & 1 \\ 2 & 1 & 2 & 1 & 1 & -7 \end{pmatrix},$$

$b_{1k} = 0.5, b_{2k} = 0.5, b_{3k} = 0.5, b_{4k} = 0.6, b_{5k} = 0.8, b_{6k} = 0.5$ and $\Delta = 0.02$, for all $k = 1, 2, \dots$.

Then, we can obtain the tracking error from 3 different points. From the figure 1, we can see that the tracking error between each agent and the leader node damps out with the evolution of time. This implies that the linear coupled leader-following multi-agent system obtains consensus.

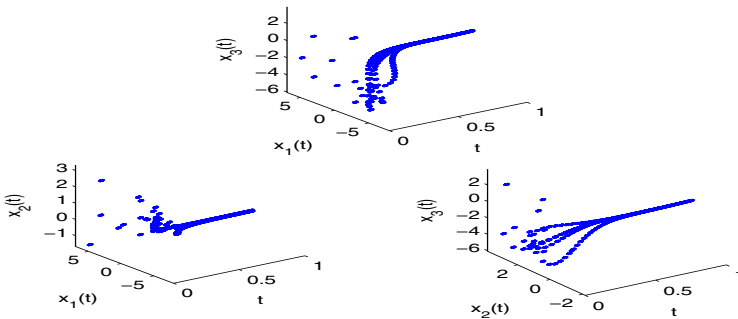


Fig. 1. The tracking error between each agent and the leader node

Acknowledgements. The work is supported by the National Basic Research Program of China (973 program NO.2011CB710605) and the Fundamental Research Funds for the Central Universities, China University of Geosciences (Wuhan) (NO. CUG100310).

References

1. Jadbabaie, A., Lin, J., Morse, A.S.: IEEE Trans. on Auto. Contr. 48, 998 (2003)
2. Olfati-Saber, R., Murray, R.M.: IEEE Trans. on Auto. Contr. 49, 1520 (2004)
3. Ren, W., Beard, R.W.: IEEE Trans. on Auto. Contr. 50, 655 (2005)
4. Earl, M.G., Strogatz, S.H.: Phys. Rev. E 67, 036204 (2003)
5. Hu, J., Hong, Y.: Phys. A 374, 853 (2007)

6. Barahona, M., Peoora, L.M.: *Phys. Rev. Let.* 89, 054101 (2002)
7. Moreau, L.: *IEEE Trans. on Auto. Contr.* 50, 169 (2005)
8. Hong, Y., Hu, J., Gao, L.: *Automatica* 42, 1177 (2006)
9. Hong, Y., Chen, G., Bushnell, L.: *Automatica* 44, 846 (2008)
10. Ren, W., Ella, A.: *Int. J. Robust Nonlinear Control* 17, 1002 (2007)
11. Liu, X.: *Dyn. Stab. Syst.* 9, 163 (1994)
12. Liu, X., Willms, A.R.: *Math. Probl. Eng.* 2, 277 (1996)
13. Stojanovski, T., Kovcarev, L., Parlitz, U.: *Phys. Rev. E* 54, 2128 (1996)
14. Yang, T., Chua, L.O.: *IEEE Trans. Circuits Syst. I* 44, 976 (1997)
15. Zhang, G., Liu, Z., Ma, Z.: *Chaos* 17, 043126 (2007)

Application of Computer Aided Instruction Technology on Hydromechanics Experiment Teaching

Bing Wang

School of Mechanical Engineering, Huaihai Institute of Technology,
Lianyungang, China
hrbwb2001@163.com

Abstract. Hydromechanics mainly studies fluid status and interaction between fluid and solid wall and between fluid and fluid and other status. Application on Computer Aided Instruction has been taken into account more and more, a strategy is propounded for actualizing individualized education by creating computer-aided instruction (CAI) software, based on characteristic of hydromechanics experiment in classroom teaching of university curriculum which means to cultivate students' interest and make sure the result's precise and form religious manner, and use computer network to check results of actualizing idiomatical education. This strategy provides an effective method in solving problem of education for development and innovative education.

Keywords: CAI, hydromechanics experiment, idiomatical education, hydromechanics materials.

1 Introduction

Hydromechanics is an important branch of mechanics which mainly studies fluid status and interaction between fluid and solid wall and between fluid and fluid and other status. Experiment is a very important link in teaching process on hydromechanics. Through experiment, abstract theory image at class may reappearance and deepen basic theory and strength excellent capacity and question analysis and solution and train synthesized ability and basic essence. To match the experiment result and theory, many experimental data must to be modified and so the experiment doesn't receive expected results and so lack strong scientific foundation. Currently human have entered the information era, and the application of computer has entered the information era, and the application of computer technology is an important sign. CAI has characteristics of achieving individual teaching, so it was widely used and developed. Since knowledge of basic mechanics has closely related with many industries, in the curriculum setting of higher engineering college, it has become basic professional courses in science and technology specialties. It is an indispensable diathesis for science and technology college students to grip knowledge of basic mechanics and apply it to various engineering fields creatively. In present, individualized education is one of the themes that education reform concerns, and it is the needs for the development of the times[1]. Combined with theoretical mechanics

teaching by CAI, this paper makes researches on problems of individualized education in higher college curriculum teaching.

2 Connection of Idiomatical Education

The current educational research shows that characteristic is the basis of creativity. And creativity is one or more psychological process based on full development of individuality [2]. Human individuality exists objectively. It is growing, developing, and changing in positive way or negative way. As a result, actualizing individualized education is objective, necessary and possible.

2.1 Main Idea of Idiomatical Education

1) Respect Human and Human Personality: This is determined by the value and status of human, as well as determined by the characteristics of education itself. It is the radical idea of idiomatical education.

2) Dig Potential Advantages of Human Personality: It is not an average development of digging potential of students. What individualized education emphasizes is developing advantages of the student's personality potential and finding spark of personality in every student.

3) Cultivate Human of Good Character Qualities and Comprehensive Harmonious Development: This is the aim of individualized education.

4) Feature of Education: The feature of education is to stimulate students' creativity.

2.2 Education for All-Around Development, Innovative Education and Individualized Education

At present, in Chinese education sector, there are three kinds of opinions in exploring direction of education development [3]: education for all-around development, innovative education and individualized education. It should be recognized that the three kinds of opinions are essentially uniform. Implementation of education for all-around development redounds to develop student's personality. It is helpful to improve diathesis of student by strengthening individualized education. The process of improving individual quality by individualized education is also a process of establishing individual creativity. Thus, the three kinds of opinions are unified. Since we do not pay attention to individual development of students, the process of pushing education for all-around development has once been in a difficult "bottleneck" [4].

3 Strategy of Using CAI in Hydromechanics Teaching Experiment to Go along Idiomatical Education

3.1 Update Educational Ideas, Constitute Scientific Syllabus1

The precondition of going along individualized education in classroom teaching is update of educational ideas and thought: Education decision-maker, education

governor, majority of teachers and students should thoroughly change the concept, which is called 'cut it even at one stroke'. The concept of diathesis and talent should be taken into consideration and it should be established by focusing on the personality and creativity in fostering the talents with the coordinated development of intelligent and non-intelligent. The drawbacks of traditional education should be overcome, which includes paying attention to common and ignoring the individuality, paying attention to knowledge indoctrination and ignoring of intelligent, paying attention to rational training and ignoring harmonious development. It should profoundly be convinced that the purpose of education is to bring up people and promote the comprehensive and harmonious development of human. Education should focus on the development of the human personality needs. It is the requirement of the times to promote active, diverse and individualized learning approach. Building up lifelong learning concepts and bringing up good character in whole life is the requirement of human survival and social life in new era.

3.2 The Foundation of Talent Training Is Syllabus, and It Is also a Foundation in Determining Contents of Individualized Education in Teaching Process

American scholar H.A.Pasowu advanced that the syllabus fitting for cultivation of personalized talent should be guided by the following principles: developing student's effective ideation, cultivating student's interest and desire of acquiring knowledge constantly, cultivating student's ability of using necessary documentation consciously, encouraging student's creativity and independence in learning, promoting student to develop unattached consciousness and to comprehend nature syllabus should be a compendium. It should define and enrich the basic knowledge and skills in order to expand the scope of choice. Syllabus of hydromechanics experiment should make sure in requirements of cultivating ability, such as model capabilities, thinking capabilities, calculating skills and independent learning capabilities.

3.3 Popularize Individualized Education Combined with Curriculum Feature

1) Cultivate interest: modern teaching method may cultivate interest to experiment and come alive the class mood. The experimental teaching experiences make clear that experiment not only deepen perceptual knowledge to abstract conception but also enlighten student's thought and enlarge scope of knowledge. Hydromechanics has many experiments which must measure ten groups' data and handle and draw up curves to illustrate principle of fluid. But in past the experimental time are short and workload is large. Though doing experiments, the results can't be done. Now applying CAI, after experiments the results can be inputted to computer and data can be handled and curves can be drawn up soon. Through the results, teacher link experimental phenomenon and propose question. The method can make student class concentration and the atmosphere active.

2) Make sure that the result is precise and form religious manner: veracity of the experimental data decides the experimental success. In past teacher get across all of links which make students depend on. Now applying CAI software, during experiment process, academic adviser may speak purpose and requisition and new

instruments' usage. And students may arrange experiment independently and computer can handle with measure data. And analyze reasons to false result which not upright attitude but cultivate religious scientific attitude.

3) **Examine by computer network:** in order to test outcome of students' individualized education in class, using various and pluralistic assessment method is an effective avenue. In the process of curriculum teaching, it reacts on stimulating effect for promoting individualized education. The current method of exam is relative simple and the method is usually a closed book examination. This method is propitious to check mastery of basic mechanics theory and basic mechanics laws, but it is difficult to check student's ability [5]. Using the method of computer networks for exam can test ability. The design of questions should be multiform and flexible for selecting questions randomly in exam nets. For example, we can give some engineering background problems, let students analyze, build model, and solve problem, at last, students submit their answers online. It can check the circumstances that students enhance their ability in learning process.

4 Application of CAI Software Promotes Reform and Development of Hydraulics Lab's Experimental Teaching

With the application of CAI software, the experimental reform has been developed, first, add the experiment preparation system. And then require signature and save on student's experimental result which not upright attitude to experiment but raise teacher's responsibility. Application of CAI software not only raises students' interest and broadens scope of knowledge and strengthens skill train but also improves experimental teaching method and guide student to experiment scientifically and pay attention to experimental result arrangement and change attitude to experiment and establish precise scientific attitude. Application of the modernization teaching method like a staff which examines student and teacher and improve teaching quality and strengthen cultivation to students' synthetic ability and diathesis cultivation.

5 Summary

Hydromechanics is a subject which studies mechanics characteristics of motion and application on fluid. The in-depth reform of higher education, it is imperative to actualize individualized education in curriculum teaching. The aim of education should look forward and the object of education training is builders of future community. By individualized education, student's abilities in cognition, discovery, learning, self-education and creativity are cultivated. Students learn correct method of study, and they also enhance abilities in lifelong learning and handling information. With these abilities, students can adapt the needs of future social development. Popularizing individualized education by CAI is an effective method. However, dealing relationship between CAI and blackboard forms of traditional teaching methods well and organic combining both are important. In the process of advancing CAI, it requires us to confirm assignment and aim of CAI, organize contents of CAI effectively, pay attention to interact in 'teaching' and 'learning' during teaching

process. In addition, in order to promote teacher's enthusiasm of promoting individualized education in class, examination of teaching results should include: whether exert spirit of student's voluntary learning and whether exert a leading role in cultivating student's personality development, etc.

References

1. Liu, B.-C.: Review on individuation trend of World Higher Education. *Tsinghua Journal of Education* (4), 102–107 (2002)
2. Liu, W.-X. (ed.): *Individuality education theory*. Normal University Press, Beijing (1997)
3. Meng, X.L.: The essence of individualized education and China's strategy of choice. *Journal of Guangdong Radio & Television University* 14(1), 92–97 (2005)
4. Yang, M.H.: Make college education in favor of individualized talent growth. *Hubei Education* (2004)
5. Wei, M.-X.: Theoretical Mechanics teaching and quality education. *Journal of Guangxi university for nationalities (natural science edition) (suppl.)*, 97–99 (2004)

Image Segmentation Technology of the Ostu Method for Image Materials Based on Binary PSO Algorithm

Shuo Liu

Department of Mathematics and Physics, Wuhan Polytechnic University,
Wuhan 430023 China
ls22115@yahoo.com.cn

Abstract. The threshold segmentation technology is an important significance in image analysis and image recognition. The Ostu Method is widely used for calculating effective, simple and stable. But it has disadvantage of more complexity and time-consuming. In order to overcome the problem, the paper presents a new automatic threshold segmentation algorithm after studying the Ostu method and the BPSO algorithm. Firstly the Ostu method is extended to multi-threshold segmentation. Secondly taking the advantage of PSO algorithm and taking the maximal variance of gray image as the fitness, the algorithm can obtain the optimal thresholds. Finally the experiments show that compared with the traditional method, the algorithm is not only of better segmentation quality but also of faster computational speed.

Keywords: Image Segmentation, Particle Swarm Optimization Algorithm, Ostu Method.

1 Introduction

Image segmentation is the key techniques from image processing to image analysis. Some segmentation algorithms can be directly used for variety type of images, and some algorithms can only apply to specific type of image. Segmentation result is good or bad depend on the specific requirements of the occasion. So there is no single standard for segmentation method.

In many algorithms, the Ostu method became one of the most important methods for its simple thinking, stable and efficient. But it also has its weaknesses: the computational complexity and need large amount of time, even for complex image segmentation effect is poorer. Therefore, in this paper the Ostu method is extended to multiple thresholds. Then, in order to overcome the great amount of calculation, intelligent algorithm-the binary particle swarm optimization algorithm will be used.

Particle swarm algorithm for solving optimization problems is a common way, many domestic scholars have done work in this area. In the process of solving, the significant advantage of particle swarm optimization algorithm is fast. but it also has its shortcomings, easy to fall into local optimum. In this paper, the adaptive selection of weighting factor and overload operations are used to improve the algorithm performance.

2 Image Segmentation of the Otsu Method

2.1 Problems Description

The Otsu method is put forward by Otsu in 1978, and has been widely used for its simple thought and stability calculation. From the perspective of pattern recognition, the optimal threshold value should be the goal to produce the best separation performance of object class and background class, this performance is characterized by type of variance, for the introduction of the variance within the class, between-class variance and total variance.

The variance is the Statistics, and characterized of the unbalanced distribution of data. The greater the variance, the differences bigger between the two parts of an image. If some targets are wrong to part of the background, the differences between the two parts will smaller, so make the largest variance means that minimum the probability of mistake segmentation, optimum threshold will make the variance largest between target and background.

In consideration of computation, usually get the threshold by optimizing the third criterion. This method has its flaws, as kittler and Illingworth experiments revealed: when the ratio of the image of target and background is very small , method is failure.

In the image f , the number of pixels is n and it's gray value is i .The total number of pixels is $N = \sum_{i=1}^L n_i$.for each pixel the probability of appears is $p_i = \frac{n_i}{N}$. Use gray value T as threshold images can be divided into two areas (target and background), 1 to T and T + 1 to L respectively to belongs to A (target area) and B (background area).

In practice, use the simplified formula: $\sigma^2 = \omega_A (\mu_A - \mu)^2 + \omega_B (\mu_B - \mu)^2$

The probability of class A is $\omega_A = \sum_{i=1}^t p_i$, the average gray of class A is

$$\mu_A = \frac{1}{\omega_A} * \sum_{i=1}^t p_i i$$

The probability of class B is $\omega_B = 1 - \omega_A$, the average gray of class B is

$$\mu_B = \frac{1}{\omega_B} * \sum_{i=t+1}^n p_i i$$

The total average gray is $\mu = \sum_{i=1}^n p_i i$, the between-cluster variance is σ^2 .

Use the threshold T, image segment into two parts A and B, the best single threshold is the one that making the between-cluster variance maximum.

2.2 Double Threshold Segmentation

For relatively simple images, the method has achieved good segmentation results. For some complex images, such as its histogram showe multiple peaks, the effect of

single-threshold segmentation method will drop, even result in errors. In order to make the method to apply for complex image, the Otsu method can be extended to two-or multi-threshold algorithm. $\sigma^2 = \omega_1(\mu_1 - \mu)^2 + \omega_2(\mu_2 - \mu)^2 + \omega_3(\mu_3 - \mu)^2$.

Through multi-threshold segmentation algorithm, the effect of image segmentation can be improved. The way to get the optimal threshold, in generally, ergodic all possible gray levels, so computation is great, especially when extended to multi-threshold, the increase in computation is enormous. Traditional optimization means is often difficult to meet the requirements. Therefore an intelligent algorithm introduced: an improved particle swarm optimization.

3 Binary Particle Swarm Optimization

Particle Swarm Optimization is a new evolutionary algorithm by Dr. Eberhart and Dr. Kennedy who through simulating the foraging behavior of birds developed random search algorithms based on collaborative group. PSO algorithm is a kind of evolutionary algorithms, and genetic algorithms similar, it is starting from a random solution, to find the optimal solution through iteration, it is through the fitness to evaluate solution quality. But it is much simpler than the rules of the genetic algorithm, genetic algorithm it does not "cross" (Crossover) and "variability" (Mutation) operation, it by following the optimal value of the current search to find the global optimum.

Binary PSO is similar with the basic particle swarm, but in generating new particles, improved the formulae. The particle position x_i , speed v_i , the best position each particle p_{ibest} , the best position of all particles G_{best} .

3.1 The Basic Operation of Binary PSO Algorithm

For each generation of particles, use the following formula to update the speed and position of particles:

$$v_{i,d}^{n+1} = \omega v_{i,d}^n + c_1 r_1^n (P_{ibest} - x_{i,d}^n) + c_2 r_2^n (G_{best} - x_{i,d}^n)$$

$$S(v_{i,d}^{n+1}) = 1 / (1 + \exp(-v_{i,d}^{n+1}))$$

$$\begin{cases} x_{i,d}^{n+1} = 0, r < S(v_{i,d}^{n+1}) \\ x_{i,d}^{n+1} = 1, \dots \dots \dots \text{其它} \end{cases}$$

r is random on $[0, 1]$. In order to prevent saturation, speed is restricted in $[-4, 4]$.

3.2 Improved Particle Swarm Optimization Algorithm

The algorithm in view of the cooperation and competition to iterative particle, once discovered the optimal location, the other particles close it quickly, so that the entire community is stagnant. After Particle into the local optimal neighborhood, it is hard to search other region, this is the so-called precocious phenomena.

(1). Dynamic inertial weights strategy

When the two iterations of the mean change of fitness value larger particles is that during the global search at this time, given the larger weight; conversely, weights to smaller. So PSO is better adapted to practical environment.

(2). Overloading operation based on Gaussian distribution

In order to prevent premature phenomena, in the traditional PSO added overloaded operation. Its thought comes from pigeons to feed. In the park, the pigeons will return to pigeonhole from time to time, and then come out to feed. In fact this increased the random search space, so it can be used to avoid premature. In the actual operation, utilize the fitness value adapt to control the time of overloading. Set a threshold, if the fitness value of particle number exceeds the value, it means particle is too concentrated, easy to fall into local optimum, the reload operation. Current optimal particle retention, and other particles randomly initialized, then the iteration.

After the independent operation of particles, the distribution of the particle's fitness similar to the characteristics of a Gaussian distribution. In every generation, about $2/3$ of the particle is located near the center of particle swarm. Assume that in a generation the average fitness value is μ , the fitness value is $F(i)$. If $-\sigma < F(i) - \mu < \sigma$, the number of particles greater than $2/3$, and more than a given threshold, it means particles were over-concentrated. If the number of over-concentrated appear more than a given threshold, we can say particle swarm into local optimum.

4 Design of Algorithms

Based on the dual-threshold Ostu Method, use an improved binary particle swarm algorithm, the algorithm flow is as follows:

- (1) The encoding and fitness function: in this paper we use the most common binary coding scheme. Since the image gray value between 0-255, it can be use a eight binary code express a segmentation threshold. For the case of multi-threshold can used several 8-bit binary code, every particle express the appropriate number of thresholds. Fitness function is usually determined based on the objective function, in this paper, two-dimensional maximum between-cluster variance function is the objective function.
- (2) Generation initial particle swarm: set the initial particles size M , the length of each particle is 16, express two thresholds. The maximum number of iterations is I . Initial particles velocity set to 0.
- (3) The particle's iterative: when $I = 1$, randomly generated solution, calculate the fitness of each particle, determine whether the current iteration number reaches the maximum number of iterations I or each particles are all optimal solution. if so, terminate the program. Or update the number of iterations $I = I + 1$. Record the group best location and the each particle optimal location.

Utilize the improved binary particle swarm optimization algorithm updates the velocity and position of each particle, calculate the fitness of each particle.

For a typical image, based on traditional algorithm and the particle swarm optimization algorithm, through MATLAB, the results as follows:



Fig. 1. Example of a figure segmentation

The traditional algorithm can put target from the background, but for the ground segment is not very obvious. Using the improved algorithm, the ground is basically disappeared from the target, it can conclude that the improved effect is indeed to be excellent. Single threshold algorithm is extended to multi-threshold algorithm, and utilize intelligent algorithm-binary particle swarm optimization to calculate multiple threshold. Through adaptive selection of weighting factor and add overloaded operators to overcome the premature of the algorithm and improve the performance of the algorithm, the example shows the superiority of the algorithm.

References

1. Haralick, R.M., Shapiro, L.G.: Image segmentation techniques. *CVGIP* 29, 100–132 (1985)
2. Xu, L., Ln, L., Liu, J.: Modified particle swarm optimization for reconfiguration of distribution network. *Automation of Electric Power Systems* 30(7), 27–30 (2006)
3. Feng, B., Wang, Z., Sun, J.: Image threshold segmentation with Ostu base on quantum-behaved particle swarm algorithm. *Computer Engineering and Design* 29(13), 3429–3434 (2008)
4. Lienhart, R., Effelsberg, W.: Automatic text segmentation and text recognition for video indexing. *Multimedia System* (1), 69–81 (2000)
5. Li, H., Doermann, D., Kia, O.: Automatic text detection and tracking in digital video. *IEEE Transactions on Image Processing* 9(1), 147–156 (2000)
6. Lienhart, R., Wernicke, A.: Localizing and segmenting text in images and videos. *IEEE Transactions on Circuits and System for Video Technology* 12(4), 256–268 (2002)
7. Shi, R., Li, Z., Jiang, T.: Several algorithms and applications of image segmentation. *Modern Electronics Technique* 30(12), 111–114 (2007)
8. Kennedy, J., Eberhart, R.: Particle swarm optimization. In: *Proc. of Int. Conf. on Neural Networks*, Perth, Australia, pp. 1942–1948 (1995)
9. Feng, B., Wang, Z., Sun, J.: Image threshold segmen-tation with Ostu based on quantum-behaved particle swarm algorithm. *Computer Engineering and Design* 29(13) (2008)

Collection and Processing of the Point Clouds of Telephone Receiver by Reverse Engineering

Dongsheng Wang, Yanru Zhao, and Xiucai Chen

The College of Mechanical and Power Engineering, Henan Polytechnic University,
Jiaozuo 454000, P.R. China
xhwds@163.com, yanruzhaoh@163.com,
cxc@hpu.edu.cn

Abstract. With the development of science and technology, the information manufacturing based on the information material has been used widely. The digital measurements of the telephone receiver were carried out by a three dimensional measuring machine and the data point clouds of the contours of telephone receiver were got. Using reverse engineering software, Imageware, the data point clouds of the telephone receiver were processed, including of data smoothing, data reducing, data point clouds resample and feature lines extracting. Based on the shape features of the telephone receiver, the 3-dimensional models of the telephone receiver were reconstructed with the boundary curves and the scanning data point groups successfully.

Keywords: Reverse engineering, Telephone receiver, 3D geometrical model reconstruction, Information material.

1 Introduction

With the development of science and technology, the information manufacturing based on the information material has been used widely. In reverse engineering, the coordinate values of contours of existing workpieces (specimens or models) can be measured accurately and rapidly with 3D digital measuring instrument and then their surfaces can be reconstructed. After edited and amended, the surfaces are transferred to a normal CAD/CAM system and then are sent to CNC for processing manufacturing by NC processing route of the cutting tool brought by CAM or rapid prototyping machine to make the models [1,2]. The prototype of workpiece can be modified and redesigned with the CAD model reconstructed in reverse engineering.

Taking a telephone receiver as the research object, the application of reverse engineering in 3D geometrical model reconstruction was described through the process of model reconstruction of the research object in the paper.

2 Materials and Methods

Research Object. The telephone receiver is the key part of a telephone which decides whether the sound quality is good or not and the connection directly. The telephone

receiver gathers sound play and reception together, so the design of which would influence the applied effect. It is obvious that the telephone receiver is with lots of complicated curves and surfaces and only the material object of the telephone receiver, in many cases, can be got. It is very difficult to describe the complicated curves and surfaces of the the telephone receiver with mathematical model. It is impossible to plot the technical drawings of the telephone receiver with common methods and then to process according to the drawings. It is of great difficulty for manual surveying and drawing, so does the describe of the complicated curves and surfaces, even impossible.

It is of large trouble for the measurement that the material object of the telephone receiver has been with some wear for a period of time and with some holes itself. The surface of the telephone receiver was disposed with plaster, which was required to be smooth to fill the measurement requirement.

Measuring Equipment. The digital measurements of the telephone receiver were carried out by a three dimensional measuring machine FARO Gage (the portable measurement system). The complicated contours of the cusp and pit of an object surface to be measured can be got with the portable measurement system which is with high accuracy and fast speed. The exact data point groups of an object surface can be obtained by selecting and setting up proper parameters. The digital point groups is the basis of model reconstruction, processing manufacturing, imitation simulation and characteristic analysis.

3 Results and Discussion

Telephone Receiver Surface Digitizing. The telephone receiver is symmetrical so the accuracy of half of the data point groups at least should be ensured in the measurement. The contours of telephone receiver was measured with the three dimensional measuring machine FARO Gage and the data point groups with high density were got, as shown in Fig. 1(a). The quality of the data point groups may degrade due to the interference of various of noise during the course of generation. The data point groups should be smoothed in order to eliminate or cut down the effect of noise, that is, only the data with low frequency can pass and high frequency cannot. The quality of 3D model reconstructed can be improved with data smoothing [3].

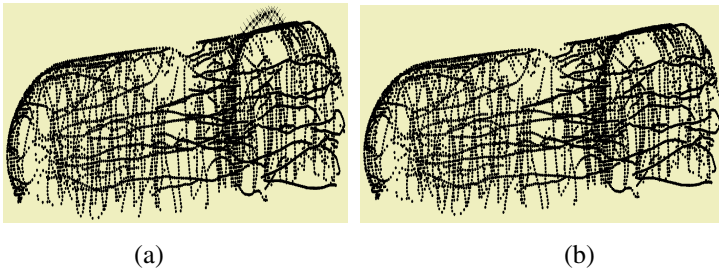


Fig. 1. The data point clouds of the telephone receiver obtained by the three coordinates measuring machine. (a) Before noise elimination; (b) After noise elimination

The information offered by parameters with unknown values should keep invariable in smoothing method. If the smoothing of the value in a position of infinite nodes was considered, the value $\{P_n\}$ smoothed can be obtained by applying linear superposition principle to the value $\{P_v\}$, which can be expressed as follows.

$$\{P_v\} \quad (v = \dots, -1, 0, 1, \dots). \quad (1)$$

$$P_n = \sum_{v=-\infty}^{+\infty} P_v L_{n-v}. \quad (2)$$

Where, $\{P_v\}$ is the value in a position of infinite nodes, $\{P_n\}$ is the value smoothed and $\{L_v\}$ is the weight factor, respectively.

The value $\{P_n\}$ is smoother than $\{P_v\}$, that is, the fluctuation of the value smoothed does not exceed that of the original value and the deviation between the two values can not be too large.

The mean value of distances from a point to points in the neighborhood was calculated, if the mean distance exceeds a set value and the point can be regarded as noise which should be eliminated. The data point groups after noise elimination of the telephone receiver is shown in Fig. 1(b).

Data Point Clouds Resample. The telephone receiver was scanning with the three coordinates measuring machine and a lot of data points can be obtained. There were a plentiful of redundant data existing in the data point clouds with high density, if the model is to reconstruct with the data point clouds directly that would cost a great deal time for data storage, processing and model reconstruction and the whole process can not be controlled. The data point clouds should be cut down before model reconstruction [4].

The resample was made to the data point clouds of the outer surface with the method of changing the distances among the points and the data point clouds reduce from 5036 to 2809 after resample, so does the inter surface. Fig. 2 shows the point clouds after resample.

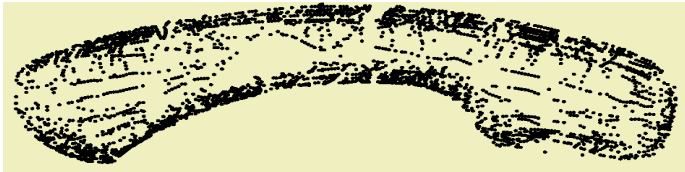


Fig. 2. The data point clouds after resample

Telephone Receiver 3D Model Reconstruction. The process of model reconstruction is to reconstruct the geometrical topological information and reproduce characters of the material object according to its data point clouds. In reverse engineering, a common method of model reconstruction is to fit the data point clouds into spline curves with interpolation or approximation and then the surfaces are completed with molding tools such as sweep, blend, lofting and boundary, at last, the whole model can be got with extending cutting and transiting [5].

In CAD/CAM system, the models of Bezier, B-Spline and NURBS are used widely. For complex curves, Bezier and B-Spline are fitted to deal with flat data point clouds and NURBS uneven [6,7].

The equations of NURBS can be expressed as follows.

$$C(u) = \frac{\sum_{i=0}^n N_{i,p}(u)\omega_i P_i}{\sum_{i=0}^n N_{i,p}(u)\omega_i} = \sum_{i=0}^n R_{i,p}(u)P_i \tag{3}$$

$$R_{i,p}(u) = \frac{N_{i,p}(u)\omega_i}{\sum_{j=0}^n N_{i,p}(u)\omega_j} \tag{4}$$

Where, P_i is the control point, $N_{i,p}(u)$ is B-Spline basic function of order p , ω_i is the weight factor and u is the parameter, respectively.

NURBS surface can be got by extending parameters from 1D to 2D and shown as follows.

$$S(u,v) = \frac{\sum_{i=0}^m \sum_{j=0}^n N_{i,p}(u)N_{j,q}(v)\omega_{ij} P_{ij}}{\sum_{r=0}^m \sum_{k=0}^n N_{r,p}(u)N_{k,q}(v)\omega_{rk}} = \sum_{i=0}^m \sum_{j=0}^n R_{i,p;j,q}(u,v)P_{ij} \tag{5}$$

$$R_{i,p;j,q}(u,v) = \frac{N_{i,p}(u)N_{j,q}(v)\omega_{ij}}{\sum_{r=0}^m \sum_{k=0}^n N_{r,p}(u)N_{k,q}(v)\omega_{rk}} \tag{6}$$

Where, P_{ij} is the control point, $R_{i,p;j,q}(u,v)$ is NURBS basic function.

Using reverse engineering software, Imageware, the curvature change from the point and its adjacent points can be found out according to that of the point clouds and then the sharp boundaries of the model can be obtained. The feature lines extracted from the telephone receiver is shown in Fig. 3.

The best method of surface construction is to extract the boundary curves of point clouds and then the surface is constructed with the boundary curves. The curves within the tolerance limits were established according to the point clouds and then the reparametrization of curves was made, at last, the curves with adjacent control points and uniform parameters were got.

Based on the shape features of the telephone receiver, the 3D models of the telephone receiver were reconstructed with the boundary curves and scanning data point groups. The 3D geometrical models of the top surface and bottom surface of the telephone receiver are shown in Fig. 4.

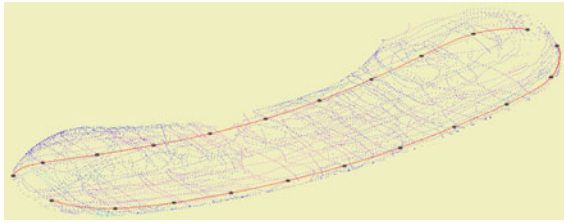
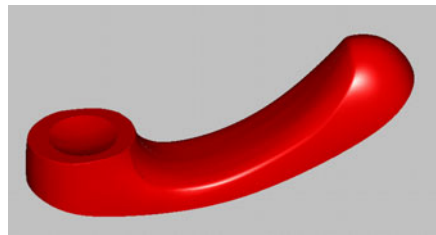


Fig. 3. The feature lines extracted



(a)



(b)

Fig. 4. 3D geometrical models of the telephone receiver. (a) The top surface; (b) The bottom surface

4 Summary

The digital measurements of the telephone receiver were carried out by a three dimensional measuring machine and the data point clouds of the contours of telephone receiver were got. The data point groups should be smoothed in order to eliminate the effect of noise. The data point clouds should be cut down for the convenience of data storage, processing and model reconstruction. The boundary curves of point clouds were extracted. Based on the shape features of the telephone receiver, the 3-dimensional models of the telephone receiver were reconstructed with the boundary curves and the scanning data point groups.

The wide application of reverse engineering based on information material in the design of modern machine parts, which may shorten the production cycle, reduce the production cost, ensure the machining quality, improve the utilization rate of NC equipment and realize the rapid manufacturing.

Acknowledgment. This work was supported by Doctor Foundation of Henan Polytechnic University (grant no. B2008-74) and by the 7th key subject of Henan province.

References

1. Wu, N., Tong, J., Chen, D.H., Zhang, S.J., Chen, B.C.: Submitted to Transactions of the Chinese Society for Agricultural Machinery (2006)
2. Tong, J., Wu, N.: Submitted to Transactions of the Chinese Society for Agricultural Machinery (2006)
3. Li, S.W., Tong, J., Zhang, S.J., Chen, B.C.: Submitted to Transactions of the Chinese Society for Agricultural Machinery (2004)
4. Motavalli, S., Bidanda, B.: Submitted to Journal of Manufacturing Systems (1991)
5. Li, J.X., Ke, Y.L.: Submitted to Chinese Journal of Mechanical Engineering (2000)
6. Hoppe, H., Derose, T., Duchamp, T., Stuetzle, W.: Submitted to Computer Graphics (1992)
7. Cheng, R., Xie, X.B.: Submitted to Journal of Harbin Institute of Technology (2002)

Characteristic Extraction of Chinese Signature Identification Based on B-Spline Function and Wavelet Transform

Yongjian Zhao and Haining Jiang

Institute of Information Engineering, Shandong University at Weihai,
Weihai 264209, China

zhaoyj@sdu.edu.cn, jian123cn@sina.com

Abstract. This paper presents a hybrid method to extract stable signature characteristic. We first develop a group of 4th order B-spline wavelet based on the better properties of B-spline function. After applying the novel B-spline wavelet to each stroke of the signature through wavelet decomposition, we design a set of formulas to synthesize characteristic value of each stroke so as to obtain signature characteristic values which have many good performances such as rotation invariance, translation invariance and scale invariance. Furthermore, a proper classifier is developed which can be more effective than the traditional Euclidean distance. The simulation results show that this method has better stability and reliability.

Keywords: spline wavelet, wavelet transform, signature, characteristic value, stroke.

1 Introduction

Chinese handwriting signature has long been legally established and widely accepted as a useful biological feature for reliable identity verification. The basic principle of online Chinese signature identification is to compare one's signature characteristic value with those in the appointed pattern library's so that the signature to be identified is classified as either authentic or forged[1,2,3]. Characteristic extraction is the key step in the whole Chinese signature identification process, which determines the performance of whole system to a large extent[1,2]. At present, a few extraction methods have been developed based on Fourier transform and neural networks[1,3,4,5,6]. But these methods have some shortcomings such as the difficulty to perform, the low identification rate and the tendency to lose geometric qualities of the signature.

Due to the perfect property of adaptive feature and mathematical microscope feature, wavelet transform has becoming a focus issue in the field of signal processing[1,2,3,7]. This paper proposes a hybrid approach to extract stable signature characteristic through wavelet transform. The proposed method in this paper dealing with wavelet decomposing and synthesis is based on the application of wavelet transform to each stroke of Chinese signature. It is worthwhile to mention that 4th

order B-spline function has many good properties to deal with curve and surface in computer graphics[1,3]. Chinese signature is composed of a few strokes and each stroke can be regarded as a curve, so we first design a group of novel 4th order B-spline wavelet based on B-spline function. Then we apply wavelet transform based on the novel 4th order B-spline wavelet to each stroke according to wavelet decomposition formulas of multi-resolution analysis. Furthermore, we synthesize signature characteristic values of strokes through a series of new formulas proposed in this paper so as to extract signature characteristics which are rotation invariant, translation invariant and scale invariant. These extracted values can furthermore reflect the total signature characteristics so as to improve the identification performance.

2 The Construction of 4th Order B-Spline Wavelet

The basic principle of wavelet transform is to seek for a series of orthogonal wavelet bases, on which primal signals can be decomposed and synthesized. The performance of wavelet bases plays an important role in the whole process of wavelet transform. It is more effective and accurate to construct wavelet bases according to specific application occasion[1,2,7]. As B-spline function has many excellent natures, such as recursion, local positive supported, multi-scale and the smallest compact supported, B-spline wavelets constructed by B-spline function have both desirable properties.

The 1th order B-spline function $N_1(x)$ is feature function in interval $[0,1]$. For $m \geq 2$, N_m is recursively defined

$$\text{as } N_m(x) = \int_{-\infty}^{+\infty} N_{m-1}(x-t)N_1(t)dt = \int_0^1 N_{m-1}(x-t)dt .$$

The m th order B-spline N_m satisfies the following properties[1,2,7]:

$$(1) N_m(x) = \frac{1}{(m-1)!} \Delta^m x_+^{m-1} = \frac{1}{(m-1)!} \sum_{k=0}^m (-1)^k \binom{m}{k} (x-k)_+^{m-1}$$

where $\Delta f(x) = f(x) - f(x-1)$, $x_+ = x (x \geq 0)$, $x_+ = 0 (x < 0)$.

$$(2) N_m(x) = \frac{x}{m-1} N_{m-1}(x) - \frac{m-x}{m-1} N_{m-1}(x-1).$$

$$(3) \text{ The Fourier transform of } N_1(x) \text{ is } \hat{N}_1(\omega) = \frac{1-e^{i\omega}}{i\omega} = e^{-\frac{i\omega}{2}} \left[\frac{\sin(\omega/2)}{\omega/2} \right].$$

(4) The Fourier transform of $N_m(x)$ is

$$\hat{N}_m(\omega) = \left(\frac{1-e^{i\omega}}{i\omega} \right)^m = e^{-\frac{im\omega}{2}} \left[\frac{\sin(\omega/2)}{\omega/2} \right]^m .$$

Based on the better properties of B-spline function, we construct a function $\phi_1(x) = N_m(x + m/2)$, whose Fourier transform

$$\text{is } \hat{\phi}_1(\omega) = \left[\frac{\sin(\omega/2)}{\omega/2} \right]^m.$$

If we set $e_n(\omega) = \sum_{k=-\infty}^{+\infty} \frac{1}{(\omega + 2k\pi)^{n+2}}$, we can deduce that

$$e_n^1(\omega) = -(n+2) \sum_{k=-\infty}^{+\infty} \frac{1}{(\omega + 2k\pi)^{n+2+1}} = -(n+2)e_{n+1}(\omega) \quad \text{and}$$

$$e_{n+1}(\omega) = -\frac{1}{n+2} e_n^1(\omega).$$

Because $e_0(\omega) = \sum_{k=-\infty}^{+\infty} \frac{1}{(\omega + 2k\pi)^2} = \frac{1}{4\sin^2(\omega/2)}$, we can find that

$$e_{n+1}(\omega) = -\frac{1}{n+2} e_n^1(\omega) \text{ and}$$

$$\sum_{k=-\infty}^{+\infty} \left| \hat{\phi}(\omega + 2k\pi) \right|^2 = 2^{2m} \sin^{2m}\left(\frac{m}{2}\right) e_{2(m-1)}(\omega).$$

$$\text{So } \hat{\phi}(\omega) = \left[\frac{\sin(\omega/2)}{\omega/2} \right]^m \cdot \frac{1}{\sin^m(\omega/2)} \cdot \frac{1}{\sqrt{\sum_{k=-\infty}^{+\infty} \frac{1}{(\omega + 2k\pi)^{2m}}}} = \frac{1}{\omega^m} \cdot \frac{1}{\sqrt{e_{2(m-1)}(\omega)}},$$

where function $\phi(x)$ satisfies the define of multi-scale:

$$\sum_{k=-\infty}^{+\infty} \left| \hat{\phi}(\omega + 2k\pi) \right|^2 = 1.$$

Because $\hat{\phi}(2\omega) = H(\omega)\hat{\phi}(\omega)$, we can get

$$H(\omega) = 2^{-m} \sqrt{\frac{e_{2(m-1)}(\omega)}{e_{2(m-1)}(2\omega)}}. \text{ When we set } m=4, \text{ we implement the construction of}$$

4th order B-spline wavelet.

The discrete inverse Fourier transform of $H(\omega)$ is impulse response $\{h_l\}_{l=0...511}$ from scaling function $\psi(t)$, whose value can be calculated. Due to space, we do not give the value of h_l and $g_l(l=0, \dots, 511)$ where $g_k = (-1)^{k-1} h_{512-k}$, $k=1, \dots, 511$, $g_0 = (-1)h_1$.

3 The Wavelet Presentation of Strokes from a Signature

After preprocessing, each stroke from specific signature can be expressed by 512 discrete complex number[1,2,7]. Supposed that the signature have M strokes, the m th stroke can be described as

$$\{ f_m(k)=x_m(k)+iy_m(k) \quad k=0,1,\dots,N-1,N=512,m=0\dots M-1 \}.$$

Above stroke signals are finite, whose multi-resolution can be expressed as

$$A_j^d f_m(n) = \sum_{k=0}^{2^{j+1}N-1} h(l)A_{j+1}^d f_m(k) = \sum_{k=0}^{2^{j+1}N-1} h(l)A_{j+1}^d x_m(k) + i \sum_{k=0}^{2^{j+1}N-1} h(l)A_{j+1}^d y_m(k)$$

and

$$D_j^d f_m(n) = \sum_{k=0}^{2^{j+1}N-1} g(l)A_{j+1}^d f_m(k) = \sum_{k=0}^{2^{j+1}N-1} g(l)A_{j+1}^d x_m(k) + i \sum_{k=0}^{2^{j+1}N-1} g(l)A_{j+1}^d y_m(k),$$

where $l=[k-2(2n+1)] \bmod (2^{j+1}N), n=0, \dots, 2^jN-1, j=-1, -2, \dots, -J, J>0, A_0^d f_m(K)=f_m(K)=x_m(K)+iy_m(k), k=0 \dots N-1.$

When decomposed to the j th order layer, the sample number of $A_j^d f_m(k)$ and $D_j^d f_m(k)$ is 2^jN respectively, where $j<0$ and $k=0, \dots, 2^jN$. If the stroke is decomposed to J th layer, wavelet representation of this stroke can be described as

$$\{ \{ A_{-j}^d f_m(k) \text{ where } k=0 \dots 2^jN \} \text{ and } \{ D_j^d f_m(k) \text{ where } j=-J, -J+1, \dots, -1, k= 0 \dots 2^jN \} \}.$$

4 The Characteristic Synthesis of a Signature

Based on these properties of discrete complex wavelet transform, we construct a series of wavelet formulas to synthesis characteristic of a signature[1,2,7].

For $A_{-j}^d f_m(k)$, we set

$$A_{-j}^d \bar{x}_m = \frac{1}{2^{-j}N} \sum_{K=0}^{2^{-j}N-1} A_{-j}^d x_m(k) \text{ and } A_{-j}^d \bar{y}_m = \frac{1}{2^{-j}N} \sum_{K=0}^{2^{-j}N-1} A_{-j}^d y_m(k),$$

$$j=-J, -J+1, \dots, -1, m=0, \dots, M-1.$$

For $D_j^d f_m(k)$, we set

$$D_j^d \bar{x}_m = \frac{1}{2^{-j}N} \sum_{K=0}^{2^{-j}N-1} D_j^d x_m(k) \text{ and } D_j^d \bar{y}_m = \frac{1}{2^{-j}N} \sum_{K=0}^{2^{-j}N-1} D_j^d y_m(k), j=-J, -$$

$J+1, \dots, -1, m=0, \dots, M-1.$

For $FA_{-j}^d f_m$, we set

$$FA_{-j}^d f_m = \frac{\sqrt{\sum_{K=0}^{2^{-j}N-1} ((A_{-j}^d x_m(k) - A_{-j}^d \bar{x}_m)^2 + (A_{-j}^d y_m(k) - A_{-j}^d \bar{y}_m)^2)}}{\sum_{m=0}^{M-1} \sqrt{\sum_{K=1}^{2^{-j}N-1} ((A_{-j}^d x_m(k) - A_{-j}^d x_m(k-1))^2 + (A_{-j}^d y_m(k) - A_{-j}^d y_m(k-1))^2}}$$

$$j=-J, -J+1, \dots, -1, m=0, \dots, M-1.$$

For $FD_j^d f_m$, we set

$$FD_j^d f_m = \frac{\sqrt{\sum_{k=0}^{2^j N-1} ((D_j^d x_m(k) - D_j^d \overline{x_m})^2 + (D_j^d y_m(k) - D_j^d \overline{y_m})^2)}}{\sum_{m=0}^{M-1} \sqrt{\sum_{k=1}^{2^j N-1} ((D_j^d x_m(k) - D_j^d x_m(k-1))^2 + (D_j^d y_m(k) - D_j^d y_m(k-1))^2)}} ,$$

$j=-J,-J+1,\dots,-1,m=0,\dots,M-1$.

Above synthesis formulas have excellent performances such as rotation invariance, transformation invariance and scale invariance. The characteristics of the m th stroke are $\{FA_{-j}^d f_m, FD_j^d f_m, j=-J,-J+1,\dots,-1\}$, whose layer characteristic number is $J+1$. In our experiment, we set $J=5$ and demonstrate by experiments that $\{FA_{-5}^d f_m, FD_j^d f_m, j=-5,-4,-3\}$ are robust and reliable. If we select $\{FA_{-5}^d f_m, FD_j^d f_m, j=-5,-4,-3\}$ as characteristic of the m th stroke, the whole signature characteristic can be described as $\{FA_{-5}^d f_m, FD_j^d f_m, j=-5,-4,-3, m=0,1,\dots,M-1\}$.

5 Matching Identification

Chinese signature identification is a complicated process, which is on the premise of the precise understanding of the details of differences between signatures to be identified with those in the pattern library, such differences are found through comparison of the corresponding characteristics between signature to be identified with those in the pattern library[1,3]. Now what we must do is to identify the signature through distance match between characteristic values of the signature to be identified with those in the pattern library[1,2]. The method we used for measuring the distance is Mahalanobis distance.

The Mahalanobis distance between point x and the class π is defined as[1,3]

$$D(x, \pi) = [(x - \mu)' \Sigma^{-1} (x - \mu)]^{\frac{1}{2}}$$

where μ is the mean value of π and Σ is the covariance matrix. Suppose the mean vectors of class π_1 and class π_2 are μ_1 and μ_2 respectively, the covariance matrix is Σ_1 and Σ_2 , respectively. Now given an individual x , we want to figure out from which parental class x comes. First we can calculate Mahalanobis distance from x to class π_1 and π_2 , and then compare the two distances $D(x, \pi_1)$ and $D(x, \pi_2)$. If $D(x, \pi_1) \leq D(x, \pi_2)$, we can decide that x belongs to class π_1 , otherwise x belongs to class π_2 .

In our experiments, 20 signatures from a genuine writer are collected on a computer connected a digitizer. The method proposed in this paper is used to extract signature characteristic so as to construct a pattern library. The other 2 signatures from genuine writer and forgery writer are also collected and applied characteristic extraction respectively.

Table 1. Comparisons of the identification results

method	mean distinction rate(%)	optimum distinction rate(%)
Method in this paper	89.6	95.0
Method in [6]	85.6	88.9

From Table 1, one can find the method in this paper is more effective and stable than the traditional method. The characteristic extraction is applied to each stroke of signature so that it can better reflect the signer's characteristic. Moreover, after stable feature extraction, the samples' distribution is more reasonable than before and the samples are more likely to assemble to the mean value, that is to say, the samples tend to be act as normal distribution.

6 Conclusions

Based on wavelet transform, a novel signature identification method is proposed in this paper. Because this method develops the 4th B-spline wavelet and applies wavelet transform to each stroke of a signature, the extracted signature characteristic is more effective and reliable, thus enhancing the effects of identification. The appropriate classifier is developed and further improves the identification performance. The theoretical framework being developed here should provide a strong foundation for future research and application.

References

1. Bian, Z.: Pattern Recognition. The Tsinghua University Press, Beijing (1994)
2. Zhao, Y.: Chinese writing identification based on wavelet transform. *Computer Project* 8, 135–147 (2005)
3. Ripley, B.D.: Pattern Recognition and Neural Networks. Cambridge University Press, Cambridge (2006)
4. Bovik, A.C., Gopal, N., Emmoth, T.: Localized measurement of emergent image frequencies by Gabor wavelets. *IEEE Trans. Inf. Theory* 56(2), 691–712 (2004)
5. He, Z., Chen, Q.: A neural network expert system for Chinese handwriting-based writer identification. *Machine Learning and Cybernetics* (2002)
6. He, Z.Y., Tang, Y.Y.: Chinese handwriting-based writer identification by texture analysis, *Machine Learning and Cybernetics* (2004)
7. Chui, C.K.: Approximation Theory and Functional analysis. Academic Press, Boston (2001)

Classification of Rice According to the Geographic Origin Based on Inductively Coupled Plasma Atomic Emission Spectrometry and Chemometrics

Xiaoying Niu, Liya Xia, and Xiao-yu Zhang

College of Quality and Technical Supervision, Hebei University, Baoding,
Hebei 071002, China

xiaoyingniu@126.com, xialiya@126.com, rainzhang85@yahoo.com.cn

Abstract. Rice is the important foodstuff for human. And the classification of the geographic origin of rice is significant for protecting the interests of consumers and producers, to enhancing quality of rice and developing rice exportation. In this paper, nineteen Xiangshui rice samples and ten non-Xiangshui rice samples were analyzed by Inductively Coupled Plasma Atomic Emission Spectrometry (ICP-AES), to obtain content value of P, B, Zn, Fe, Cu, Mn, Na, K, Mg and Ca in rice samples, and then classified using chemometrics methods of principal component analysis and discriminant analysis. The result of the former was not satisfactory, while the latter was optimal, the accuracy 100% and 93.1% for calibration and leave-one-out cross validation respectively. A new classification method and technique of rice was provided for producers, sellers and departments of quality and technical supervision in this paper.

Keywords: Rice; Classification, ICP-AES, chemometrics.

1 Introduction

Rice is one of the most important foodstuffs for human. The chemical compositions of affecting rice quality are starch, protein, moisture content and all kinds of trace metals. Among them, the more content of the trace metal of Zn, Fe, Cu, Mn, Se and I, the higher nutrition value of the rice [1]. The chemical compositions are root in the growth environment of rice in a large degree. In our country, there are many rice producing regions. The rice of northeast region was favoured by Japan, Korea and other countries, because of the excellent quality. Thus, there is great export potential for this area [2]. Now, it is the market condition of fixing prices according to quality of products. In order to make exorbitant profits, many illegal businessmen often sell seconds at best quality prices. Therefore, it harmed the interest of the consumers and the company of the rice production. For avoiding the happening of more such things, we must study efficient methods for the discrimination of the rice geographic origins. Besides protecting the benefits of the consumers and the companies, it has much important practical significance for enhancing the rice quality and driving the development of rice export of our country. ICP-AES has many virtues, such as low detection limit, high precision, wide linearity range, and could determine all kinds of

trace metals at the same time. Based on the above reasons, it was applied for the determination for the trace metals of all kinds of samples of foodstuff and farm products. In 1997, Shindoh K et al. [3] (come from Japan) have determined the trace metals K, Mg, Ca, Zn, Mn and Fe, using the method of ICP-AES. In 2000, they [4] determined the trace metals content for the discrimination of the brown rice (produced in Japan), using ICP-AES, chemometrics of principal components analysis and cluster analysis. In 2005, Jung MC [5] determined the trace metals of Mg, Ca, Si, Zn, Na, Al in polished rice from South Korea by the way of ICP-AES. At the same year, Xiaoning Tan [6] determined the 11 trace elements in rice by ICP-AES, the recoveries for the 11 elements are in the range of 96%-109%. In 2008, Manjusha R [7] determined the trace elements in Indian rice by ETAAS and ICP-AES; including beneficial trace metals Fe, K, Cu, Zn, Mn, and harmful trace metals Pb, Cr, Cd.

Xiangshui rice is the best of northeast rice; it contains abundant nutritive elements, such as trace metals, due to its growing environment. In this work, in order to study the different quality of different regions, some Xiangshui rice samples and some non-Xiangshui rice samples were selected, and the trace metals were determined through the Inductively Coupled Plasma Atomic Emission Spectrometry Instrument. The geographic origin of the rice was discriminated according to the content of the trace metals and by the method of chemometrics.

2 Material and Methods

Instrument and reagent. VISTA-MPX machine (Varian, USA), HCL and ultrapure water.

Instrument working parameters. Power 1.2kW, observation height 10mm, integration time 10s, cooling gas flow 12.5L/min, carrier gas pressure 200kPa, auxiliary gas 1.25L/Min; Temperature 20□, humidity 50%; Quartz torches, burgener and peristaltic pump sapling.

Sampling and sampling treatment. Nineteen Xiangshui rice samples of this work were provided by Ning'an City Bureau of Quality and Technical Supervision, Heilongjiang Province, and the other ten non-Xiangshui rice samples were purchased from local supermarkets. The different batches rice samples were pulverized by agate mortar, and vacuum drying 24 hours at 20°C. The 0.5 g of samples were in porcelain crucible, which was placed in muffle furnaces and the temperature rised into 500°C, the time of ashing was 4 h. When the time is over, it was withdrawn. After cooling, the 5 ml 1+1 HCL was extracted and constant value was 25 ml, and then determined.

3 Conclusions and Discussions

ICP-AES.The determined results, using the methods of ICP-AES, for the content of trace metals of the Xiangshui and non-Xiangshui rice, including P, B, Zn, Fe, Cu, Mn, Na, K, Mg, Ca, were listed in Table 1. From the table, it can be seen that: the difference of the trace metals' concentration range and the average value is not much

in Xiangshui and non-Xiangshui rice samples. But the change of the standard deviation of the non-Xiangshui rice is common bigger. In other words, the trace metal difference of the non-Xiangshui rice is bigger. This maybe caused by the reason that the non-Xiangshui rice samples were come from different regions. Because of the overlap of the trace metal range of Xiangshui and non-Xiangshui rice samples, it could not directly use the content of one or some trace metals for the discriminating the rice origin regions. From the point of the trace metals, it could find the different characters of the different regions, and then discriminated them.

Table 1. Trace metals content in rice samples detected by ICP-AES

Index	Sample type	Concentration [μg/g]	Average [μg/g]	Standard Deviation [μg/g]
P	Xiangshui	798-1066	939.856	74.374
	Non-Xiangshui	768-1025	904.166	91.826
B	Xiangshui	0.71-2.77	1.142	0.491
	Non-Xiangshui	0.72-2.74	1.399	0.632
Zn	Xiangshui	12.5-19.3	15.369	1.756
	Non-Xiangshui	13.1-21.3	17.864	2.825
Fe	Xiangshui	5.15-10.4	7.076	1.238
	Non-Xiangshui	6-10.9	7.870	1.658
Cu	Xiangshui	2.97-6.33	4.432	0.943
	Non-Xiangshui	3.77-7.74	5.742	1.451
Mn	Xiangshui	8.66-16.9	12.909	2.376
	Non-Xiangshui	7.37-13.6	10.000	2.476
Na%	Xiangshui	0.003-0.008	0.0053	0.0014
	Non-Xiangshui	0.002-0.007	0.0051	0.0017
K%	Xiangshui	0.062-0.087	0.0751	0.0079
	Non-Xiangshui	0.069-0.099	0.0836	0.0102
Mg%	Xiangshui	0.02-0.03	0.0266	0.0025
	Non-Xiangshui	0.018-0.033	0.0251	0.0049
Ca %	Xiangshui	0.009-0.016	0.0109	0.0016
	Non-Xiangshui	0.01-0.014	0.0116	0.0013

Principal component analysis. Through extracting the principal component of the trace metal content data of the samples, the contribution rate of the first three principal components is 71.812%. Among them, the contribution rate of the first is 37.919%, the second is 24.199%, and the third is 9.649%. The first three principal components include most data message of the samples. So a three-dimensional image using the scores of the first three principal components for classification of rice samples was illustrated in Figure 1. It shows the clustering result of the Xiangshui rice samples and non-Xiangshui rice samples. From the result, it can be seen that, the two kinds of samples both have clustering tendency. Non-Xiangshui rice samples were clustered two groups, and the character of the two groups was relatively far, and the result was similar to the above two kinds of methods. It means that the selected non-Xiangshui rice samples had different characters of the trace metals. On the other hand,

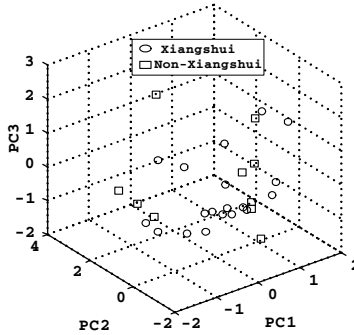


Fig. 1. Scores of the first three principal components for classification of rice samples

Xiangshui rice samples had distinct clustering tendency, and their characters are relatively near, which indicate that they have same character.

Discriminant analysis. In this method, the original variables of ten trace metals were all put in Fisher linear discriminant functions. Table 2 lists the classification function coefficient of Fisher’s linear discriminant functions for Xiangshui and non-Xiangshui rice samples. To the non-Xiangshui rice samples, the coefficient absolute value of element Mg is the biggest in the ten trace metals. From the table, it could be seen that, during the determination of whether one sample was non-Xiangshui rice, the effect of the content deviation of element Mg is bigger than others. As well, to Xiangshui rice samples, the criterion of judgement is according to the content of the element Ca.

Table 2. Classification function coefficients of Fisher’s linear discriminant functions

Index name	Coefficient of discriminat functions	
	R1 (Xiangshui)	R2(non-Xiangshui)
P	0.659	0.665
B	-14.008	-9.034
Zn	-0.28	-1.263
Fe	-10.803	-8.005
Cu	27.904	28.191
Mn	1.354	3.574
Na	1092	854.852
K	945.485	-112.86
Mg	-8615	-5900
Ca	-4790	-7671
Constant item	-237.436	-233.059

The back substitution was carried on the above discriminant function equations, which could get the result of Table 3. Because the number of the sample is smaller, validation set was not allocated, and the discriminative result was validated by Leave-one-out cross-validation method. Table 3 shows that the calibration sets of the two kinds of samples were both 100%, so the total accurate rate was 100%. To Leave-one-out cross-validation, the discriminating accurate rate of the Xiangshui rice samples was 100%, and the non-Xiangshui rice was 80%, so the total rate was 93.1%. Generally speaking, the discriminating result of the calibration set and the cross-validation method is very closer. It indicates that the model is steady.

Table 3. Classification results of rice samples using discriminant analysis

Sample type		Sample discriminant		Accurate rate [%]	Wrong sample number
		non-Xiangshui	Xiang-shui		
Calibration set	Non-Xiangshui	10	0	100	0
	Xiangshui	0	19	100	0
Cross-validation	Non-Xiangshui	8	2	80	2
	Xiangshui	0	19	100	0

Conclusion. In this work, nineteen Xiangshui rice samples and ten non-Xiangshui rice samples were analyzed by ICP-AES to obtain the content value of P, B, Zn, Fe, Cu, Mn, Na, K, Mg and Ca in rice samples, and then classified using chemometrics methods of principal component analysis and discriminant analysis. The result of principal component analysis was not very satisfactory, while the discriminant analysis could get the optimal result, the accuracy 100% and 93.1% for calibration and leave-one-out cross validation respectively.

In the following studies, it should increase the number of the samples, especially for non-Xiangshui rice. On the other hand, it should select the non-Xiangshui rice samples from neighbouring regions and do some primary studies. After making intensive studies, it could expand the samples production regions in order to make the model having higher extensibility. From the aspect of clustering method, it should attempt and experiment more supervision clustering methods, and compare the clustering result and find the optimal clustering method.

Acknowledgements. This paper is supported by the Natural Science Foundation of Hebei Province (C2011201096), the Project of the Education Department (2010107) and the Special Project of Welfare Industries of General Administration of Quality Supervision, Inspection and Quarantine of the People's Republic of China (200810345).

References

1. Gao, Y., Fan, B.: Estimation of Rice Quality and Its Main Affected Factors. *Guangdong Trace Elements Science* (12), 12–16 (2005)
2. Liu, W.: Brief Analysis on the Condition of Rice Export Trade in China. *Tianjin Agricultural Science* 15(2), 17–19 (2009)

3. Shindoh, K., Yasui, A.: Determination of mineral contents in a single grain of rice by ICP-AES. *Bunseki Kagaku* 46, 813–818 (1997)
4. Yasui, A., Shindoh, K.: Determination of the geographic origin of brown-rice with trace-element composition. *Bunseki Kagaku* 49, 405–410 (2000)
5. Jung, M.C., Yun, S.T., Lee, J.S., et al.: Baseline study on essential and trace elements in polished rice from South Korea. *Environmental Geochemistry and Health* 27, 455–464 (2005)
6. Tan, X.: Determination on Multiple Trace Elements in Rice by ICP-AES. *Chinese Journal of Spectroscopy Laboratory* 22, 1079–1082 (2005)
7. Manjusha, R., Dash, K., Karunasagar, D., et al.: Determination of trace elements in Indian rice by ETAAS and ICP-AES. *Atomic Spectroscopy* 29, 51–55 (2008)

A Code Dissemination Protocol of Intelligent Wireless Sensor Network Based LEACH Algorithm

HaiYan Li¹, KaiGuo Qian^{2,*}, and ZuCheng Dai³

¹ Institute of Information Technology, Kunming University, China
hayali88@sina.com

² Department of Physics Science and Technology, Kunming University, China
qiankaiguo@qq.com

³ Department of Physics Science and Technology, Kunming University, China
dzcheng88@126.com

Abstract. We present an new Code Dissemination Protocol using clustering hierachical topological control structure based on LEACH algorithm after discussion of the problem for code Dissemination protocol to support remote code update technology for wireless sensor network, which called CDP_LEACH. The new protocol utilize the advantages of clustering hierachical to meet requirement of decrease energy dissipation and prolong the network life. Performance analysis and Simulation results show that the new protocol can make full use of limited energy of nodes and has the better performance of data distribution then Delude.

Keywords: Code Dissemination Protocol, LEACH, CDP_LEACH, energy efficiency.

1 Introduction

Wireless sensor networks(WSN) [1] is self-organization network system through wireless communication for real-time monitoring, perception, acquisition and processing various information of monitoring objects, which constructed of cheap and miniature nodes deployed in testing area. WSN is widely used environmental monitoring, medical care, urban traffic management, warehouse management, military reconnaissance etc and become the most hot research field.

Once deployed, there are several deployment scenarios for which physically reaching all nodes is either impractical such as Battlefield monitoring,or hard to take out all nodes which is embedded into the surrounding environment(e.g., nodes inside buildings). On the other hand, it is impossible to design all application software system once on nodes before deployed because of limited resource constraints. For these reasons, there is a real need to add or upgrade the software running on those nodes and need remote programmability in order to add new functionality to the nodes especially when the knowledge of the environment is not complete or when

* Corresponding author: KaiGuo Qian (1979.9-), male, Kunming University, Yunnan, China, Lecturer, Research area:Wireless Sensor Networks(WSN).

monitoring task changed. The new application code image is distributed to all nodes over wireless communication among wireless sensor networks during the Upgrade process. Wireless sensor network node usually carry limited battery power and the node become invalid once the batteries run out, which cause requirement of reducing energy consumption and prolong the lifecycle of the system when design code distribution protocol. The existing code distribution protocol more proposed plane flooding, in which form, all nodes maintain active state and turn on the radio no matter whether there is new code data transmission or not, meanwhile, it produce more redundant data and collisions. This paper introduce a new Code Dissemination Protocol based LEACH[2] called CDP-LEACH, which propose clustering hierarchy topological control structure, Base station trigger code distribution process and cluster head control the code distribution within local cluster.

2 Related Work

There are several code distributed protocol and data routing protocol research facing the wireless sensor network application upgrade. In-Network Programming [3] is support by TinyOS 1.0[4], The mechanism is single-hop only: the basestation (source) transmits code capsules to all nodes within a broadcast domain. After the entire image has been transmitted, the basestation polls each node for missing capsules. MOAP[5] is multiple hops code distribution agreement which adopted ripple dissemination protocol, unicast retransmission policy and sliding window for segment management. MNP[6] propagates new program code in a hop-by-hop fashion. In each neighborhood, a source node sends program code to multiple receivers. When the receivers get the full program image, they can become source nodes, and send the code in their neighborhood. Deluge[7] is an epidemic protocol and operates as a statemachine where each node follows a set of strictly local rules to achieve a desired global behavior: the quick, reliable dissemination of large data objects to many nodes. Deluge shares many ideas with MOAP, including the use of NACKs, unicast requests, broadcast data transmission, and windowing to efficiently manage which segments are required. LEACH[8] is a clustering-based protocol that minimizes energy dissipation in sensor networks for data routing and gathering from wireless sensor network nodes to base station(end-user). PEGASIS[9] is a near optimal chain-based protocol that is an improvement over LEACH. In PEGASIS, each node communicates only with a close neighbor and takes turns transmitting to the base station, thus reducing the amount of energy spent.

The existing implementation method that currently used in wireless sensor network application upgrade generally adopted plane flooding transmission, this mechanism produce more redundant information, cause the problems of “information overlap”, implosion and Information collisions, all nodes maintain active state and turn on the radio, Those all cause unnecessary energy consumption. Cluster-based control structure mechanism improve the defects of plane flooding through cluster head complete code distribution within the local cluster.

3 System Model and Problem Describe

To meet the requirements of lower energy consumption and prolong the system lifetime for code distribution protocol, we assume the following system model of wireless sensor network and the radio energy model.

Network Model. We assume that $M \times M$ square area A random is distributed N sensor nodes and this sensor network has the following features:

- each sensor node is stationary after completion of wireless sensor network deployment.
- The base station is fixed and located far from the sensors.
- All nodes in the network are homogeneous and energy constrained.
- Sensor nodes can communicate with base stations directly, but communication between the sensor nodes and the base station is expensive.
- The RF power can be adjusted according to the distance of nodes.
- the radio channel is symmetric such that the energy required to transmit a message from node A to node B is the same as the energy required to transmit a message from node B to node A.

The above all feature confine boundary that the CDP-LEACH applicable sensor network.

Radio Energy Model. We take the same Radio Energy Model that stated in paper [2], assume a simple model for the radio hardware energy dissipation where the transmitter dissipates energy to run the radio electronics and the power amplifier, and the receiver dissipates energy to run the radio electronics, as shown in Fig 1.

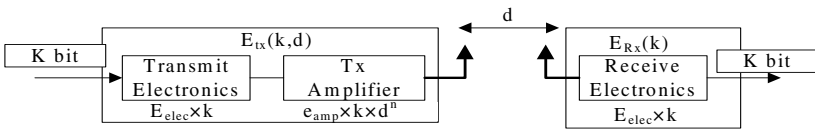


Fig. 1. Radio Energy model

There are two power loss models according to distance(d) between the transmit and receive,.if the distance(d) is less than a threshold(d_0), the free space (fs: d^2 power loss) model is used; otherwise, the multipath (mp: d^4 power loss)) model is used. Thus, to transmit k -bit message distance d using this radio model, the energy dissipation as shown equation 1.

$$E_{Tx}(k,d)=\begin{cases} kE_{elec} + k\epsilon_{fs}d^2 : d < d_0 \\ kE_{elec} + k\epsilon_{mp}d^4 : d > d_0 \end{cases} \tag{1}$$

equation 1 Energy Dissipation Equation for k -bit message and receive k -bit message the energy dissipation as shown equation 2.

$$E_{Rx}(k) = kE_{elec} \tag{2}$$

In above model, Eelec is the radio dissipates to run the transmitter or receiver circuitry, Thus, the protocols for the code distribute should try to minimize the transmit distances in order to Save energy.

Problem Describe. There are two design goals of the code distribution protocol for saving energy: one is minimize the loss of energy of the system, the other is allowing the energy requirements of the system to be distributed among all the sensors. To meet this goals, the code distribution protocol based clustering topological structure should follow requirements.

- The protocol itself should be distributed algorithm, the nodes organize themselves into local clusters,with one node acting as the cluster head decided by local cluster nodes information such as energy and numbers of cluster-heads.
- The distance between the nodes should try to meet free space model($d < d_0$),
- Cluster head in network area relatively evenly distributed.
- One node choiced as the cluster head decided by itself information(Energy and Communication cost between node to base station),This strategy can better ensure energy costs be evenly distributed to each node so as to avoid the individual nodes premature death.

4 CDP_LEACH, The Code Distribution Protocol Based LEACH Algorithm

This paper introduces a new code data distribution mechanism based clustering structure used LEACH[2] [8]algorithm called CDP_LEACH, which improve energy efficiency to make up the disadvantages of generic code flooding.

The Principle of CDP_LEACH. CDP-LEACH is a self-organizing, adaptive clustering protocol which the nodes build themselves into local clusters Triggered by the base station node when When a new task for code distribution. CDP_LEACH operated by the rounds separate into three Cluster Head Selection, Cluster Set-Up and code distributed phase. In Cluster Head Selection phase, a node chose a priori to act as a cluster head, then broadcasts an advertisement message to the rest of the nodes use a CSMA MAC protocol. Each non-cluster-head node decides the cluster to which it will belong for this round and it must inform the cluster-head node that it will be a member of the cluster. This decision is based on the received signal strength of the advertisement. The cluster-head node creates a TDMA schedule for each node and broadcast it to all nodes in the cluster, the cluster-head transmits the new code to each node in its time slot and the other nodes sleep.

Cluster Head Selection Algorithm. LEACH forms clusters by using a distributed algorithm, where nodes make autonomous decisions without any centralized control, which cause uneven distribution of the cluster head at the Network area and the distance More farther than threshold d_0 . We improve Cluster Head Selection Algorithms in CDP-LEACH.

We assume the size of cluster is fixed and the radius $r_c < d_0/2$, The distance between two adjacent cluster-heads $d > r_c$. For above two conditions, the least number

K of cluster head nodes [10] required by the Sensor network monitoring area meet the equation 3

$$\frac{n\pi r_c^2}{A} = \frac{2\pi}{27} \quad (3)$$

So, we can set the $P_{init}(i)$ (probability for each node S_i) as shown equation 4

$$P_{init}(i) = \frac{2\pi}{\sqrt{27}Nr_c^2} \quad (4)$$

N is the num Initial energy of the sensor nodes, each node decides whether or not to become a cluster-head for the current round by the probability $P_{CH}=P_{init}(i)*W$.

$$W = C_1 \times \frac{E_{cur}}{E_{init}} + C_2 \times \frac{1}{D_{CH} + 1} \quad (5)$$

E_{cur} is the current surplus energy of the node, E_{init} is initial energy of the node, D_{CH} is the number of node already acted as cluster-head. When each round begins, each node choosing a random number between 0 and 1. If the number is less than P_{CH} , the node becomes a cluster-head for the current round.

Cluster Formation. Once a cluster-head has elected for the current round, it broadcasts an advertisement message (include node ID and cluster distinguish information) to the rest of the nodes. each non-cluster-head node decides the cluster to which it will belong for this round According to Signal strength of receive cluster-head advertisement message. After each node has decided to which cluster it belongs, it must inform the cluster head node that it will be a member of the cluster. Each node transmits a join-request message (Join-REQ) back to the chosen cluster head This message is again a short message, consisting of the node's ID and the cluster head's ID. With this way, the random clustering topological control structure for the code distribution formed.

Code Distributed Phase. The cluster-head node creates a TDMA schedule telling each node when it can transmit. This schedule is broadcast back to the nodes in the cluster. To reduce energy dissipation, The cluster-head transmits code to the rest nodes and the radio of each non-cluster head node is turned off until its allocated receive code time.

5 The Performance Simulation

An experiment is designed in NS-2.27 to simulate the simple_Deluge and CDP-LEACH to estimate the performance. The experimental parameters Setted as follows: d_0 is 87m, cluster radius is 30m, E_{elec} is 50nJ/bit, C_1 is 0.8, C_2 is 0.2, ϵ_{fs} is 10pJ/bit/m², ϵ_{mp} is 500Byte.

Lifetime of system. The node is regarded as death when the remaining energy consume to zero in the experiment for the lifetime. The total number of nodes that remain alive over the simulation time is shown by Fig 2. The nodes are all death in 60

seconds with the Simple Deluge protocol, while in CDP-LEACH, the nodes begin to die after 130 seconds and none of nodes remain active state until 300s of the simulation time.

Energy consumption. In order to facilitate comparison of Energy consumption, we set the init energy 10J for each node in Simple Deluge and 2J in CDP-LEACH. The total Energy consumption over the simulation time is shown as Fig 3, The energy consumption of the CDP-LEACH much less than which of the simple Deluge over the simulation time.

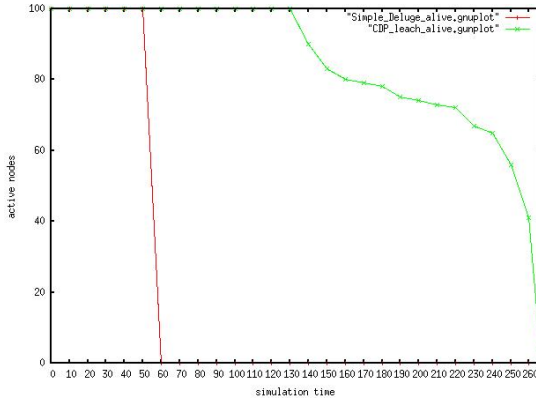


Fig. 2. The number of the active sensors nodes over the time

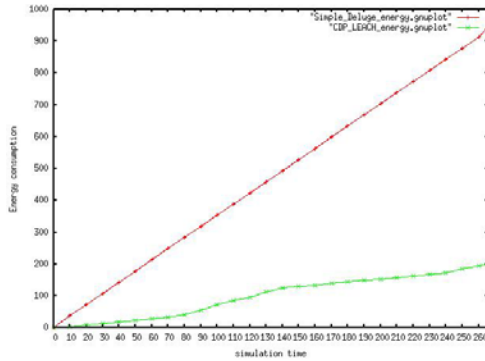


Fig. 3. The Energy consumption over the time

6 Conclusion

This paper propose a Code Dissemination Protocol Applied in wireless sensor network remote upgrades based LEACH, which adopt clustering topology control structure to avoid to produce more redundant information and collisions that is the

shortcoming of the plane flooding form. In the meantime, it shorten the distance between the nodes and base station and introduce node sleep scheduling mechanism. For those reason, it improve energy efficiency and prolong the network system lifetime.

Acknowledgement. This research was supported by Foundation of Yunnan Educational Committee(2010Y503), China. The authors thank the anonymous reviewers whose comments have significantly improved the quality of this article.

References

1. Akyildiz, L.F., Su, W.L., Sankarasubramaniam, Y., Cayirci, E.: A survey on sensor networks. *IEEE Communications Magazine* 40(8), 102–114 (2002)
2. Heinzelman, W.R., Chandrakasan, A., Balakrishnan, H.: Energy-Efficient Communication Protocol for Wireless Microsensor Networks. In: *IEEE Proceedings of the Hawaii International Conference on System Sciences*, Maui, Hawaii, January 4-7, pp. 3005–3014 (2000)
3. Jeong, J., Kim, S., Broad, A.: *Network Reprogramming*. University of California at Berkeley, Berkeley (2003)
4. Levis, P., Madden, S., Polastre, J., Szewczyk, R., Whitehouse, K., Woo, A., Gay, D., Hill, J., Welsh, M., Brewer, E., Culler, D.: TinyOS: An operating system for wireless sensor networks. In: *Ambient Intelligence*, Springer, New York
5. Stathopoulos, T., Heidemann, J., Estrin, D.: A remote code update mechanism for wireless sensor networks. Technical Report CENS-TR-30, University of California, Los Angeles, Center for Embedded Networked Computing (November 2003)
6. Kulkarni, S.S., Wang, L.: Mnp: Multihop network reprogramming service for sensor networks. In: *25th International Conference on Distributed Computing Systems (ICDCS)*, Columbus, OH (2005)
7. Hui, J.W., Culler, D.: The dynamic behavior of a data dissemination protocol for network programming at scale. In: *Proceedings of the 2nd international conference on Embedded networked sensor systems*, pp. 81–94 (2004)
8. Heinzelman, W.B., Chandrakasan, A.P., Balakrishnan, H.: An Application-Specific Protocol Architecture for Wireless Microsensor Networks. *IEEE Transactions on Wireless Communications* 1(4), 660–669 (2002)
9. Lindsey, S., Raghavendra, C.S.: PEGASIS: Power-Efficient GATHERing in Sensor Information Systems. *IEEE aerospace and Electronic System Society*, 1125–1130 (2002)
10. Slijepcevic, S., Potkonjak, M.: Power efficient organization of wireless sensor networks. In: *Proc. IEEE International Conference on Communications*, pp. 472–476. IEEE Computer Society, Helsinki (2001)

Study on Photoelectrocatalytic Technology of Three-Dimensional Electrode

Ying Liu and Honglei Du

School of Environmental and Chemical Engineering, Shenyang Ligong University,
Shenyang 110159

liuyingsy@sina.cn, qingqing567@163.com

Abstract. Titanium oxide film (TiO₂/Ti) were formed on the titanium surface by micro-arc oxidation(MAO) in Na₃PO₄ solution. And using the TiO₂/Ti as anod electrode, the titanium as counter electrode in the system of three-dimensional electrode.coated γ -Al₂O₃(TiO₂/ γ -Al₂O₃) that prepared by sol-gel dipcoating method, and scrap iron mixture as particle electrode, combining with the UV lamp and regulated power supply make up the three-dimensional electrode photoelectrocatalytic technology system.The photoelectrocatalytic ability were evaluated by degradation of methylthionine chloride aqueous solution.The influence of some factors was studied, including cell voltage, electrolyte concentration and some other factors.When the methylthionine chloride concentration of 5mg/L, cell voltage of 7V, Na₂SO₄ aqueous solution concentration of 0.02M. The photoelectrocatalytic technology of three-dimensional electrode degradation of methylene blue compare to traditional two-dimensional plate electrodes which without particle electrode increase 43.35% after 3 hours photoelectrocatalysis.

Keywords: Photoelectrocatalytic technology, three-dimensional electrode, micro-arc oxidation.

1 Introduction

Semiconductor TiO₂ photocatalysis as the characteristic of high activity, good stability, non-toxic and low cost, which was used to treat organism in wastewater has become a hot topic in the field.Photoelectrocatalytic technology of three-dimensional electrode is a kind of effective method for removing organic pollutants, because the three-dimensional electrode technology was characterized with the large specific surface areas and high performance in comparison to conventional two-dimensional plate electrodes [1,2]. Micro-arc oxidation (MAO) can change metal basal body into oxide ceramics directly which exhibit firmness of integration between film and basal body. However, compound center of photoelectron-hole is formed which reduces the efficiency of light quantum at TiO₂ film surface for electrolyte solution contains sodium generally [3]. TiO₂ film formed on the titanium net (Ti-net) by MAO according to our experiment was the anode, combining plus power source and UV limgt consist of the three-dimensional electrode photoelectrocatalytic technology system in methylene blue simulative dye waste water.

2 Experiment

Preparation of γ -Al₂O₃-supported TiO₂. The γ -Al₂O₃-supported TiO₂ particle electrode prepared by sol-gel dipcoating method as follows: Put γ -Al₂O₃ (after pretreatment) into the petri dish, then dip-coated with sol-gel solution[4] and left to congeal at room temperature. The coated particle electrode was heated at 120°C for 2 hours, then heat-treated at 450 °C for 2 hours by muffle roaster with Model SXL-1208. After these procedures, the one layer TiO₂ film particle electrode was prepared completely. This step was repeated several times we can obtain more layers TiO₂ film particle electrode.

Three-dimensional Electrode Photoelectrocatalysis Experiment. Three-dimensional electrode photoelectrocatalysis experiment was reacted in tall form beaker (150ml). Put 5mg L⁻¹ methylene blue simulative dye waste water into the 150ml beaker, then put TiO₂/Ti films[4] and partiel electrode into it, after that carry out experiment under 20W ultraviolet lamp (main wavelength 254nm) which was 10cm above liquid surface. The power supply of three-dimensional electrode photoelectrocatalysis reactor was three-way stabilized voltage supply with Model SG1732SC3A, and using Na₂SO₄ aqueous solution as supporting electrolyte. Examine absorbency (A) every few minutes at 664nm by visible spectrophotometer with Model 721E and calculate the rate of photocatalytic degradation using $\eta = (A_0 - A_t / A_0)$ (A₀, A_t mean the absorbency before and after reaction).

3 Results and Discussion

Characterization of TiO₂ Coated activated aluminium oxide (TiO₂/ γ -Al₂O₃). Object-phase analysis is carried out on Philips analytical X-ray Service Hot Line. Condition Copper butt (wavelength 0.154178nm) Voltage (35KV) the rate of Scanning(0.1°/s), scope (2 θ) 10-70°. The particle size of supported TiO₂ photoelectrocatalysts from 103 nm to 140 nm according to formula Scherer [5].

Properties of Three-dimensional Electrode Photoelectrocatalytic Technology. The photoelectrocatalysis behaviour of the system was characterized in 5mg L⁻¹ methylene blue solutions. The dye solution was added with 0.02M Na₂SO₄ as the supporting electrolyte. Put the mixture of TiO₂/ γ -Al₂O₃ 0.5g and scrap iron 1.5g, and 10mL Na₂SO₄ (0.04M) aqueous solution into the beaker respectively, and supply the voltage of 7V. The three-dimensional electrode photoelectrocatalytic degradation of methylene blue compare to traditional two-dimensional plate electrodes which without particle electrode and only adsorption is shown in Fig.1. From which we can draw the conclusion that the efficiency of three-dimensional electrode photoelectrocatalysis increase much more than other processes. There are some reasons as follow for the efficient of three-dimensional electrode photoelectrocatalysis synergistic effect. TiO₂/ γ -Al₂O₃ not only has the properties of electrochemistry but also photocatalysis, The interpretation from the theory of semiconductor: TiO₂/ γ -Al₂O₃ which prepared by sol-gel dipcoating method after roasting under 450°C, generate Titanium dioxide (TiO₂) which is a semiconductor, and its conductivity

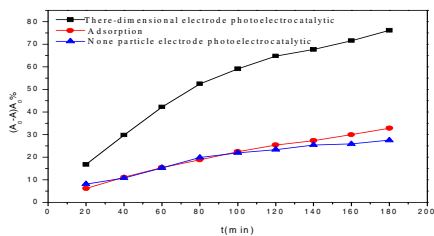


Fig. 1. The efficiency of the photoelectrocatalytic degradation by Three-dimensional electrode

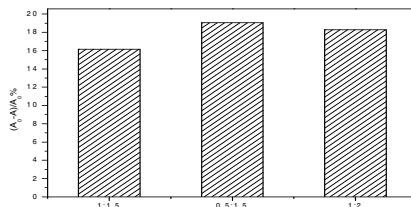


Fig. 2. Photoelectrocatalytic efficiency of different particle ratio group

between metal and insulators. When $\text{TiO}_2/\gamma\text{-Al}_2\text{O}_3$ and scrap iron mixed gently, the electronic transfer reaction can be accelerated. Filling them in between main electrodes, the particle electrode ends in potential difference for the reasons of electrostatic induction. Each particle and the surrounding water formed a micro cell, and countless micro cell in series. So as to that the degradation efficiency was improved obvious because of $\cdot\text{OH}$, which was generated in the electrolysis of water on the surface of particle electrode. Meanwhile, photogenerated electron/hole pairs were excited when TiO_2 was lighted under UV light, when the electric field were added, which could reduce combination of electron and hole, and increased efficiency of photogenerated electron/hole. A series of reaction generate $\cdot\text{OH}$, $\cdot\text{O}^{2-}$ and $\cdot\text{HO}_2$, which were strong oxidizing agents that could degrade organic contaminant gradually into small molecular compound like CO_2 and H_2O . Therefore, the efficiency of the photoelectrocatalytic degradation by Three-dimensional electrode was enhanced evidently.

Effect of Different Particle Ratio of $\text{TiO}_2/\gamma\text{-Al}_2\text{O}_3$ and scrap iron on Photoelectrocatalytic Technology. Change the particle ratio of $\text{TiO}_2/\gamma\text{-Al}_2\text{O}_3$ and scrap iron at 1:1.5, 0.5:1.5 and 1:2, then carry out photoelectrocatalysis experiment on methylene blue dye wastewater according to the process of Three-dimensional Electrode Photoelectrocatalysis Experiment. The reactor last one hour. The results were shown on Fig.2. It is thus clear that the effects of different particle ratio of $\text{TiO}_2/\gamma\text{-Al}_2\text{O}_3$ and scrap iron is very different. Because $\text{TiO}_2/\gamma\text{-Al}_2\text{O}_3$ conducts electricity poorly, which is put into the electric scrap iron particle. That particle system could block short-circuit current, and the repolarization of charged particles make the three-dimensional electrode system stabilized. If the loading particles less, due to the polarization properties of particles weaken, the system generate short-circuit current and will cause bad effect of electrocatalytic. In addition, the photocatalytic degradation of the particles will reduce. But if the loading particles more, mean conductive particles decreases, leading to the effect of electrocatalytic feeble directly. So the reasonable particle ratio is essential for the system. It is noteworthy that $\text{TiO}_2/\gamma\text{-Al}_2\text{O}_3$ and scrap iron with much adsorption may result in different degradation efficiency of the different particles. So the final degradation efficiency was total decolorization deduct adsorption of particles. Form the Fig.4 we

can conclude that the best particle ratio of $\text{TiO}_2/\gamma\text{-Al}_2\text{O}_3$ and scrap iron is 0.5:1.5 (0.5g $\text{TiO}_2/\gamma\text{-Al}_2\text{O}_3$ and 1.5g scrap iron).

Effect of Different Electrolyte Concentration on Photoelectrocatalytic Technology. Put electrolyte of different concentration (0.01M, 0.02M, 0.03M,

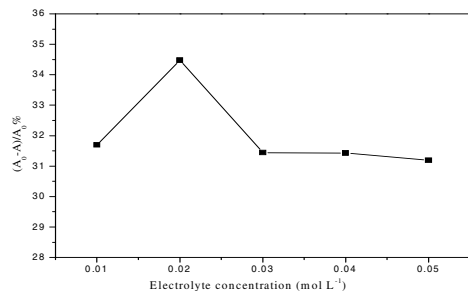


Fig. 3. Photoelectrocatalytic efficiency of different electrolyte concentration

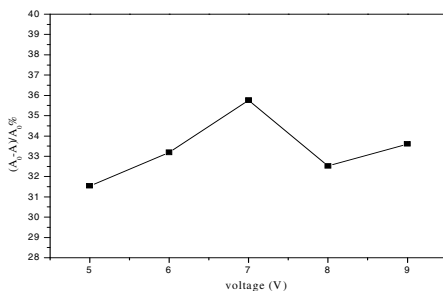


Fig. 4. Photoelectrocatalytic efficiency of different cell voltage

0.04M, 0.05M) into different beaker, which is equipped according to the process of *Three-dimensional Electrode Photoelectrocatalysis Experiment*, and carry out photoelectrocatalysis experiment on methylene blue dye wastewater for 1 hour. The results were shown on Fig.3, which indicated that the efficient degradation is at the concentration of 0.02M. It can be found that the degradation decreased with the increase of electrolyte concentration (operation period 60 min) in all process. Adding electrolyte solution can increase conductivity ability, and increase catalytic efficiency, but some researcher[6] considered, SO_4^{2-} can trapped h^+ and $\cdot\text{OH}$, which were generated under UV light. The oxidizability of SO_4^{2-} is weak generally. That means there exist inhibiting effect result from SO_4^{2-} , and degradation of dyes decreased with the increase of concentration of SO_4^{2-} at a certain range.

Effect of Different Cell Voltage on Photoelectrocatalytic Technology. According to previous publications [7,8], the cell voltage plays an important role in photoelectrocatalytic degradation of organic pollutants. Applied different cell voltage (5V、6V、7V、8V、9V) to the simulative reactor, and went along photoelectrocatalysis experiment according to the process of Three-dimensional electrode for 1 hour. The degradation efficiencies of dyes at various cell voltages are calculated, and values are plotted in Fig.4, from which it was found that the degradation efficiencies increased from 31.54% to 35.76% with the increase of the cell voltage. But the degradation decreased with the increase of cell voltage after 7V. The apparent enhancement effect on photoelectrocatalytic process at a certain cell voltage may be attributed to factors below. External electric field, especially for three-dimensional electrode with expanded specific areas, can efficiently capture photogenerated electrons, reducing the recombination of these electrons and holes, and resulting in the improvement of degradation efficiency in the photoelectrocatalytic process. As the increased of the applying cell voltage, the complex system of three-dimensional electrode polarization degree increased, and the

motive power of electrochemistry reaction of organic contaminant increased. The degradation rised while the potential difference of electrochemical oxidation and reduction reaction amplified, but with further increases, there would emerge side reaction on surface of particles easily. Amount of bubbles affected adsorption of contaminant around charged particle. And also increased the short-circuit current strongly and energy consumption. So the suitable voltage exist efficient result and also the reactor can greatly decrease the manufacturing cost.

4 Conclusions

The study has found that, with filling TiO₂ coated particles, methylene blue could be more efficiently removed by three-dimensional electrode photoelectrocatalytic process than by individual discoloration of either of the other two processes—adsorption or electrochemical process. The experimental results showed that the methylene blue removal efficiencies increased swiftly with the certain cell voltages. When the methylthionine chloride concentration of 5mg/L, cell voltage of 7V, supporting electrolyte Na₂SO₄ aqueous solution concentration of 0.02M. The three-dimensional electrode photoelectrocatalytic technology degradation of methylene blue compare to traditional two-dimensional plate electrodes which without particle electrode increase 43.35% after 3 hours.

References

1. Bockris, J.O., Kim, J.: *J. Appl. Electrochem.* 27, 890 (1997)
2. An, T.C., et al.: *Applied Catalysis A: General* 279, 247–256 (2005)
3. Cui, Y., Du, H.: *Environ. Chem. Lett.* 7, 321–324 (2009) (in Chinese)
4. Su, H.D., Du, H.L.: *Advanced Materials Research* 156-15, 344–349 (2010)
5. Beruhisa, O., Dsisuke, H., Kan, F., et al.: *Chem. B* 101, 6415–6419 (1977)
6. Hu, C., Yu, J.C., Hao, Z., Wong, P.K.: *Appl. Catal. B: Environ.* 40, 35 (2003)
7. An, T.C., Xiong, Y., Li, G.Y., Zha, C.H., Zhu, X.H.: *Photochem. Photobiol. A: Chem.* 152, 155 (2002)
8. Vinodgopal, K., Kamat, P.V.: *Chemtech.* 26, 18 (1996)

Research on Process-Oriented Design Method and Technology

Songbo Huang¹, Guangrong Yan¹, and Sijia Yu²

¹ School of Mechanical Engineering & Automation, Beihang University, Beijing
power_bo@sohu.com

² School of Mechatronics Engineering,
University of Electronic Science and Technology of China, Chengdu
ygr@caxa.com

Abstract. In order to organize and standardize the operation in the design system effectively, and to get the correct design product with the most optimized sequence, least steps and most resource assignment according to previous design experience, the concept of process-oriented design method is introduced and a rapid design technology platform in CAD system is built up. The key techniques of this design method such as model construction, part and assembly design, knowledge base, and design process template are presented in this paper. The design method has been approved in a reducer design.

Keywords: Process-oriented design method, Part modeling, Assembly design, Process template.

1 Introduction

The technology of 3D CAD is evolving since the wireframe 3D system developed in 1960's. With the development of 40 years, it has experienced several phases, such as wireframe modeling, surface modeling, solid modeling, feature design, parametric and variational design, 3D CAD technology is maturing, and widely used in many industries, for example manufacturing industry. All important improvements of 3D CAD are based on the enhancement of geometric modeling technologies. Product modeling becomes more and more convenient and intuitive, but with strong universality and weak specialty, that is, the modeling ignores the product specialized features, which causes low design efficiency and impacts innovation of engineers. Though more design information, such as precision, material, assembly, analysis is added to geometric model, the major product model in CAD system, which extends the aided design range of CAD systems, there still exists a large gap to the practical design requirement. High Efficiency design system should be knowledge based and professional. While the design method oriented to product design process is one of the ideal strategies to integrate various resource and knowledge. Designers can get the development experience in the product design process, and build up the entire product design process model which includes both geometric model and non-geometric pivotal logical rules [1]. This paper presents a process-oriented design method which

package mature geometric modeling methods including feature modeling, parametric and variational design methods, achieves the fusion of design intent, experience and knowledge, and is an exploration and attempt to evolve the universality 3D CAD technology to specialty CAD technology.

2 The Conception of Process-Oriented Design

In this paper, feature modeling, parametric design, variational design and knowledge design technologies are reconstructed based on the product design process in 3D CAD system to build up a rapid design technology platform, and then a professional 3D CAD system is constructed based on the industry product design process, consequently a new design method for rapid product innovation is established. This method is called process-oriented design method or technology in the paper.

Process-oriented design method is combined with case-based design [2, 3], process-based design [4, 5], knowledge-based design [6-10] and several innovative design ideas, but is different from them. It is based on the knowledge accumulated over the years by the enterprise and designers, makes use of variable and modular design, and use successful design cases as resources. It can configure resources and function modules effectively within CAD system, standardizes design planning, decision making, evaluation, feedback and optimizing processes, makes design activities move on smoothly with the help of smart wizard, so that efficiency and success rate of innovation can be improved significantly.

It actually is a special case-based design, not only reuses previous design instance directly, but also reuses the process information, design experience and design knowledge contained in the instance. Such entire reuse of exiting design resource will need to improve existing mechanisms to preserve and show the successful design experiences, and to use the mechanisms to drive new design.

Process-oriented design method includes the following key techniques: mathematical model technology, part modeling and assembly design technology, integrated knowledge base technology and the implementation technology.

3 The Key Technologies of Process-Oriented Design

Mathematical model of process-oriented design. A design can be treated as a task which can be achieved by a process. The process is consisted of several steps, if one step is considered as a sub-task, then the task will be broken to several sub-tasks. To accomplish the sub-task, the designer must implement specific design operation such as calculation, reasoning or inquiring behaviors, additionally, design-related resources, for example, function modules, product library or database in CAD system are also needed. The end stage of the sub-task is a milestone design result which evolves, deepens or refines the previous staged result, so there are sequential constraint relations between the tasks. The last stage result is the final design result. Figure 1 presents this process.

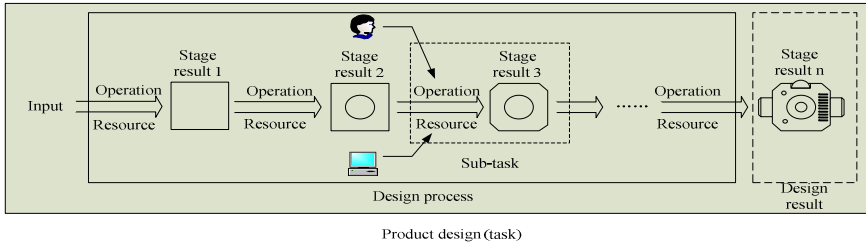


Fig. 1. Design process

After the mathematical model of design process is established, the process presented above can be visualized into the structure shown in Figure 2.

$$X_I(Q_0) \Rightarrow Q_1 \rightarrow \dots \xrightarrow[\boxed{K}]{\boxed{C_{i-1}}} Q_i \rightarrow \dots \Rightarrow Q_n(X_o)$$

Fig. 2. The meaning of design process

The dynamic process model which is established by using graph theory and matrix theory can be used for initially planning of the design sequence and the design navigation process [11].

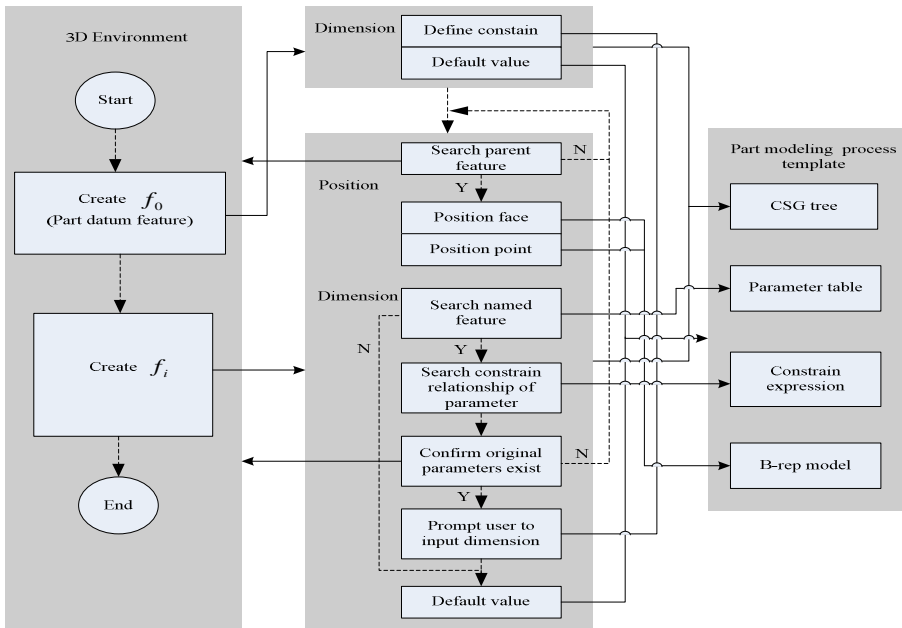


Fig. 3. Part modeling process in process-oriented design

Part modeling and assembly design in process-oriented design. The object manipulated by part modeling is the basic non-divided shape features in 3D environment, and the link between them is mainly the association of the shape sizes. Product design expert defines the associated dimension information in the completed design instance to reflect design intent, and the information accompanies part CSG/B-rep mode to form a modeling constrains network. When template is called in system, CSG tree of the part is regenerated in background, and the engineer interacts with the system and makes design decision with the help of the information defined by the experts to realize the customized design. Figure 3 illuminates the steps of process-oriented part modeling design.

The unit feature, such as the part composed by shape feature or the assembly composed by parts, operated in assembly design task is more complex. The process to define design steps by expert is a bottom-up process, which is to design the individual part first, and then assemble the parts into a component, finally assemble the components into a comprehensive product. But the design process of the designer who uses the design template defined by expert is top-down, because the complete assembly framework has been built up in the template. Figure 4 illuminates the steps of process-oriented assembly design.

Design knowledge base in process-oriented design. In process-oriented design, the abundant design experience is saved in process template which is considered as a container. However, a specific process is only a combination and sequencing of a part of knowledge, which itself is also a kind of design knowledge. So it is necessary to build a broader content of knowledge to manage all the design experience of experts, design knowledge accumulated in the enterprise over years, common design method

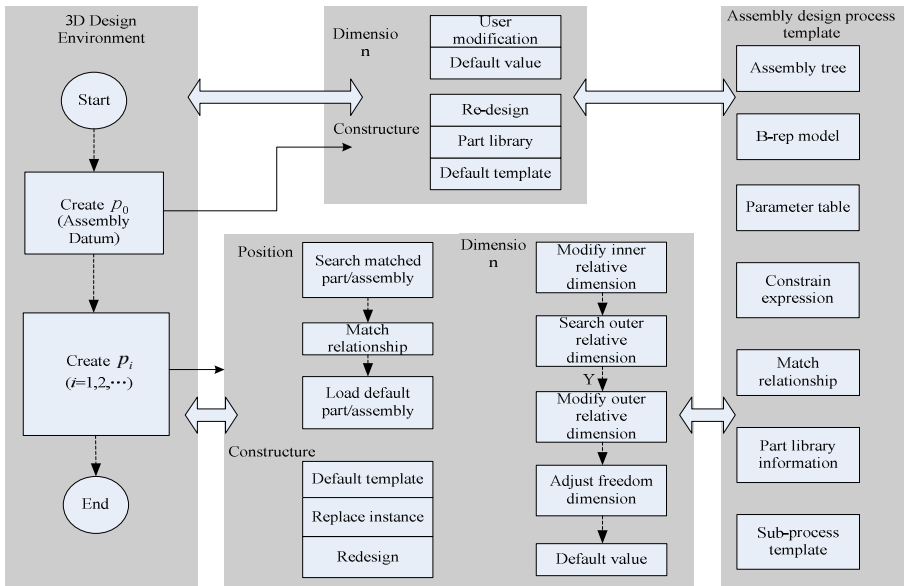


Fig. 4. Assembly design process in process-oriented design

and successful design cases, so that all kinds of resources can be utilized when process template is used in design phase and the knowledge reuse can be realized.

The knowledge base in 3D system is a set of database, text files and design cases, which is illuminated in figure 5. Access Database is the core of knowledge base presented in this paper, while there are various kinds of other carriers to store design knowledge.

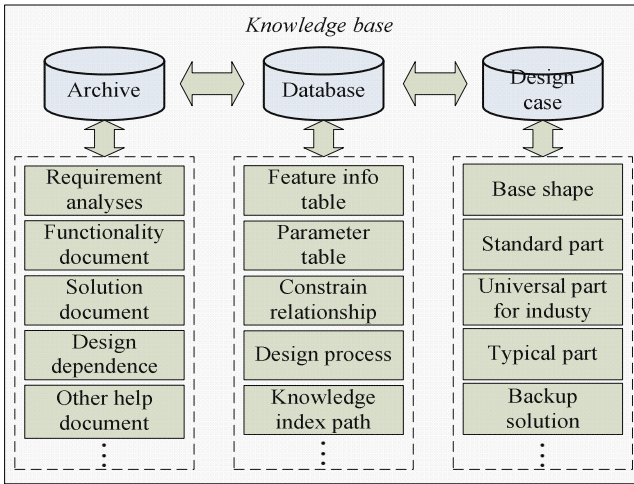


Fig. 5. Knowledge base

Implementation technology of process-oriented design. Product design process is an unstructured business process, that is, the sequence of process activities cannot be determined in advance, so the process must be defined first before it is used to guide the design. A defined process is called process template, the persons who can design the process template are often experienced, professional and knowledgeable, they are called design expert. Thus, the implementation of process-oriented design is clearly divided into two stages - template definition and template utilization, which are implemented by two roles separately - design expert and the designer. However, in order not to bring more difficulties to definition of process template for design expert, it is generally not recommended to add another process modeling environment, instead, a corresponding tools should be provided in the familiar 3D CAD to integrate the design experience with the information from 3D modeling and to build up process template. Figure 6 vividly represents the implementation of process-oriented design.

Implementation of process-oriented design is to improve the design standardization and efficiency, and to integrate design resources and knowledge. So the process should be improved continuously according to the requirement change, and thus the implementation of the process-oriented design is a continuous and cyclized improvement process. The process template definition process in CAD environment is subjected to a specific product design process, that is, when design expert finishes a product design, a process template is also defined at the same time. Similarly, when designer uses process template defined by expert to design a product, a new process

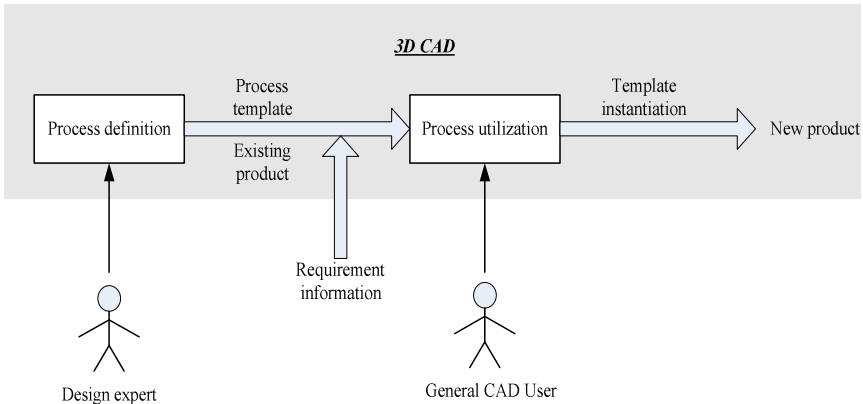


Fig. 6. Implementation of process-oriented design

template is created, or that template is improved and perfected. So both implementation stages can have double properties, and also the designer can be a double-role in the process-oriented design as shown in figure 7.

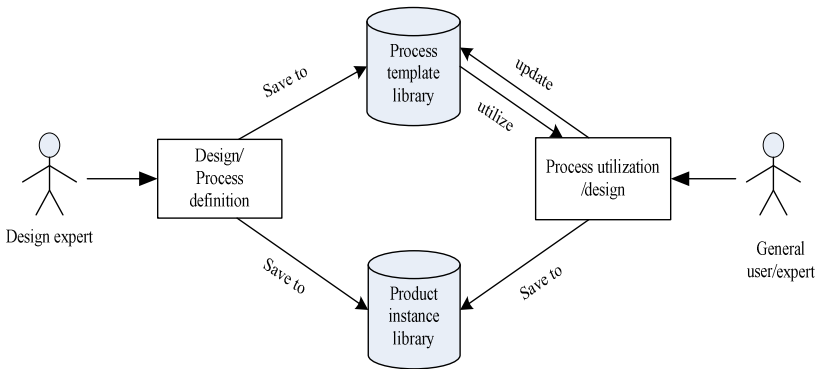


Fig. 7. The cycle of design implementation

4 Summary

The innovations of this paper are as following:

The process-oriented design method is presented in this paper. Current design method does not cover the guidance of design process, which makes the 3D CAD system operation complex. This paper presents the concept of process-oriented design and build up process-oriented design method further. The purpose is to organize and standardize the operation in the design system effectively, and to get the correct design product with the most optimized sequence, least steps and most resource assignment according to previous design experience.

Different types and different resource of design knowledge are integrated with 3D CAD system, which make the process-oriented design more intelligent and more humanized. The design constraint is enhanced from geometric constraint and engineering constraint to knowledge constraint. All kinds of design knowledge in computer are unified to 'knowledge item'; the relationship between the knowledge item, knowledge constraint and knowledge variable is build up and the multimedia design knowledge database for knowledge integration is constructed.

The method in this paper has been realized in 3D CAD software platform developed by research group, and the high efficiency of process-oriented design method has been approved in the sample of reducer design.

Acknowledgment. The author thanks China's 863 program--"Key Technologies of i-Plane for Large Aircraft Development" for the sponsorship of this paper. The project number is 2009AA043302.

References

1. Lou, M., Cicognani, M.A., Simoff, S.: An Experimental of Computer Mediated Collaborative Design. *International Journal of Design Computing* (1), 106–114 (1998)
2. Hou, J., Mo, R., He, Y.: Research on Case-based Design Fixture CAD System. *Computer Engineering and Applications* (6), 43–44 (2002)
3. Watson, I., Perera, S.: Case-based Design: A Review and Analysis of Building Design application. *Artificial Intelligence for Engineering Design, Analysis and Manufacturing* (11), 59–87 (1997)
4. Yu, J.: CAD Method and Model for Product Creative Design. Zhejiang University, Hangzhou (1999)
5. Yu, J., Geng, W., Pan, Y.: A Survey of Computer Aided Product Creation Design Method. *Journal of Computer-Aided Design & Computer Graphics* 11(2), 185–188 (1999)
6. Jiang, P.: Research on Knowledge based Rapid Innovation Design of Mechanical Product. Shandong University, Jinan (2005)
7. Yoashikawa, H.: General Design Theory and a CAD System. In: Proceedings of the IFIP working group working conference on Man-machine communication in CAD/CAM, pp. 35–53. North-Holland, Amsterdam (1982)
8. Lu, H.: Research on Support Technology of Product Design Based Knowledge Engineering. Zhejiang University of Technology, HangZhou (2004)
9. Zhang, J., Tang, H., Gong, J.: Research on the Theoretic Architecture of Design Reuse Technology. *Computer Engineering and Applications* (2), 68–72 (2002)
10. Lian, Y.: Research and Practice on Product Knowledge Management for Reusable Design. University of science and technology, Wuhan (2004)
11. Yu, S., Shan, Q., Lei, Y.: Process Navigation Model of Product Design in 3D Development Environment. *Modular Machine Tool & Automatic Manufacturing Technique* (12), 103–105 (2005)

OPC Server Technology Development in the System Software Integration

Yucheng Liu¹ and Yubin Liu²

¹ School of Electrical & Information Engineering,
Chongqing University of Science & Technology, Chongqing, China
lych68782763@163.com

² Computer Science School, Panzhihua University, Panzhihua, China
lybwxy1zh@163.com

Abstract. The information system of comprehensive automation in enterprise is a complex system. The computer integrated plant automation is based on the realization of integration between control and management in the system. Therefore, the data access mechanism has to be established among devices, databases and application software in high efficiency and universal manner. Because of the variety of the devices and the non-compatibility of the drive programs, it is difficult to realize seamless integration among different systems. This paper made a brief discussion for information interconnection between field devices of control system and supervisory control systems and for key technique of the OPC in openness.

Keywords: System Integration, component object model, distributed component object model.

1 Introduction

Enterprise information is the inevitable trend of the future competition, and the serious gap between the production process control and information management decision-making level has become the bottleneck of the development of enterprises, so the information integration of the control layer and management layer has become imperative for enterprise development. The control system integration has usually several ways, for example, the use of the special interface or transmission of information through a database as a background interface. The cost of the implementation of these methods is expensive, so the difficulty of system integration is greater. The use of the OPC technology can solve these problems well. Information in the industrial automation systems has two types according to different levels, that is, control information reflecting the state of the control system operation, which is located on the ground control network; management information reflecting system upper management and decision support, which is located on the senior management information network. The basic technologies achieving integration of the control network and information network [1] are dynamic data exchange technology, Internet technology, telecommunications technology and database access technology. To enable users to be liberated from the underlying communication module development

to focus on the software function development, for the integration of the heterogeneous industrial control systems group software features, the article roughly discussed the OPC-based automation system integration technology.

2 OPC Overview

The OPC (Object Linking Embedding (OLE) for Process Control) specification was an industry standard developed by the world's leading automation vendors (such as Fisher, Rosemount, Rockwell and Software.) in collaboration with Microsoft, It has the Component Object Model (COM) and Distributed Component Object Model (DCOM) technology as its base, using client/server model to define a set of COM objects and their interface specification. The OPC has established a set of the communication interface specification for meeting the requirements of industrial control so that control software can achieve efficient and stable data access operation of hardware equipment, the information can be flexibly exchanged between system applications, greatly improving the control system interoperability and adaptability. It has become a viable solution of control system integration.

3 OPC-Based System Integration

OPC Advantage. The OPC (OLE for process control) is the object linking and embedding technology used for process control field, is the key technologies of achieving interconnection between control system field devices and process monitoring level and achieving the control of open control system [2]. The OPC technology can solve the communication between applications and various equipment drivers. It is a development approach to simplify the system I/O-driven. Before the OPC technology was not used, a system which had M types of applications and N kinds of equipment required to develop $M \times N$ drivers. While the client / server system of using OPC provides a unified, standard interface specification for the link between server and client, only need to develop $M + N$ drivers and OPC interfaces, as shown in Fig. 1. It is that such data access features of the OPC make use of OPC technology have great technical and economic advantages. It is generally summed up the advantages of the following three areas: Openness, high productivity and the "plug and play" connectivity. OPC can be said: OPC = Openness + Productivity + Connectivity.

OPC Technology and Application. The OPC technology is now beyond the original intention to replace the driver and become Microsoft's core of Distributed internet Application Architecture for Manufacturing (DNA-M), as shown in Fig. 2. As the core, the OPC is the equivalent to the software "board". It can connect directly to the PLC of the field, industrial control network, data acquisition and Windows CE devices. It can obtain real-time data from the field through rapid and effective way. A variety of monitoring applications, control applications and management applications inside the PC, such as plugged into the software "chip" on the OPC motherboard, The communication between chips is in accordance with the OPC agreement, they can access the real-time data of the field through the OPC and can also exchange information with each other through the OPC.

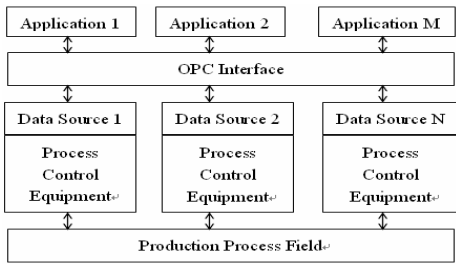


Fig. 1. The OPC Interface between application and data source

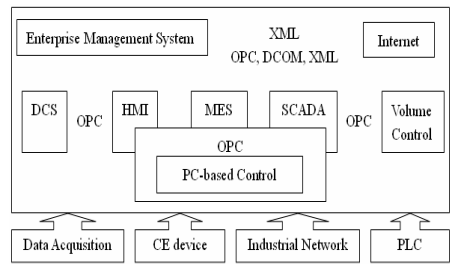


Fig. 2. Microsoft's DNA-M system

In the field bus applications, the OPC technology is a key technology to open control system. Using the OPC as a universal interface can easily connect the field signal to the SCADA host monitoring Software, Human-Machine Interface (HMI) software. The OPC can also easily connect the field signal to some of the PC universal development platform and application software platform, such as VB, VC, C++, Excel and Access. Signal transmission relationship between these parts had been shown in Fig. 3. The purpose of the OPC development is to establish the interface standard for the communication between industrial control system applications, to establish the unified data access specification between the industrial control equipment and control software. The interface specification can be used not only within a single computer, and can support the network communication between distributed applications, as well as communication between applications on different platforms. The role of the OPC Server in the enterprise information system is that the OPC server uses uniform standards in the underlying control system to achieve the effective connection between applications and the field devices. It plays a bridge role in promoting the integration of business field control layer and process monitoring layer, production management and business decision-making layer. The role of the OPC server in the enterprise information system had been shown in Fig.4.

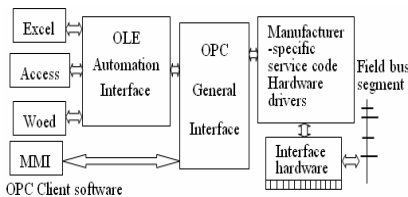


Fig. 3. OPC mode Connection Example

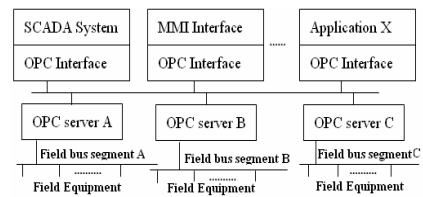


Fig. 4. OPC server's role in enterprise information system

OPC Technical Nature. With the development of the computer software science, application system functions are becoming more complex, the program even is more substantial and the difficulty of software development is greater. To do this, the application is divided into functionally independent modules. These modules synergistically completed the actual task. They are called components. They can be

individually designed, edited and debugged, so they have Open, easy-liter and easy maintenance [3].

The Component Object Model (COM) is a programming model proposed by Microsoft. The COM is designed to improve interoperability between software configurations and to improve the reusable ability of the code. The COM standard includes two parts: specification and implementation. The specification part defines the mechanism of communication between components. These specifications do not depend on any particular language and operating system, with language-independent. The implementation part is the COM library. The COM library provides some core services for the concrete implementation of the COM specification. Based on the client/server model, the COM has good stability and strong expansion capabilities. In the COM model, the software functionality is broken down into several components. Under certain conditions, these components are connected each other to achieve the corresponding functions by means of the COM protocol. In general, the COM objects can be divided into two types of client and server, the client achieves access to the server through the COM interface.

Distributed Component Object Model (DCOM) is a specification and service built on top of the COM. It provides a transparent network protocols for the COM component to join the network environment and achieves the communication and collaboration between different processes under the distributed computing environment. Physical interaction between Client programs and the COM components is the COM object. Clients must be through the interface to get services of the COM objects.

OPC Interface Method. The OPC specification provides two sets of interface programs, that is, the custom interface and automation interface. The custom interface is a set of the COM interfaces. It can be accessed through the C/C++ development programs. Automation Interface is a further package of the custom interface. Actually, it shielded the virtual function table of the custom interface and made a custom COM interface to be converted the automation OLE interface. Generally speaking, the custom interface has more powerful features but needs to master the COM technology, while automation interface is easier in the development but is vulnerable to interface itself functional limitations.

The OPC server object is divided into 3-layer structure: sever, group and item. The server is the group's container, while the group is the item's container. The OPC specification defines the COM interface and provides the standard for the interaction between server program and client program through interfaces, but it does not specify the method to achieve. The OPC service providers must implement the member functions of these interfaces according to their hardware features. Both custom interface and automation interface can be divided into required interface and optional interface. The required interface includes the most basic functions of the exchange between the client and the server, while the optional interface provides a number of additional advanced features. Client should use the query interface method to determine whether server program implemented the optional interface function.

4 Conclusions

With the rapid development of automation technology, types of automation hardware and software equipment are more and more, their update cycles are getting shorter. The product of using the OPC technical specifications can achieve interoperability and seamless integration between industrial automation systems and the “plug and play” of the field process control equipment. It brought the direct and significant economic benefits to software and hardware manufacturers and end users in this area. Therefore, we should strengthen the application of the OPC technology, actively promote the use of hardware and software with the OPC interface standard products and keep up with the trend of the world’s advanced automation technology.

Acknowledgment. This research is funded by Chongqing Natural Science Foundation (NO.CSTC, 2010BB2285) and science & technology project of Chongqing municipal education committee (No. KJ111417).

References

1. Li, P., Ying, L., Yi, Y.: Research on related techniques in the complex system control. *Southwest Norm University Journal* 29(6), 1066–1068 (2004)
2. Hwang, S., Lim, E., Lee, C.: Dynamic Web service selection for reliable Web service composition. *IEEE Trans. on Services Computing* 1(2), 104–116 (2008)
3. Chun, X., Ping, W.: Industrial control software interoperability standards for OPC and DDE review. *Industrial Computer* (12), 31–34 (2001)

Reliability Analysis for the Pareto Model Based on the Progressive Type II Censored Sample

Feng Li

Department of Mathematics, Wei Nan normal University, Wei Nan, 714000, Shaanxi, China
lifeng5849@163.com

Abstract. In this article, maximum likelihood and Bayesian estimators for the shape parameter, reliability, and failure rate functions of the Pareto distribution are derived based on progressive Type II censored samples. We obtained Bayesian estimators under the quadratic and LINEX loss function, when choosing the conjugate prior distribution for the unknown parameter. In order to investigate the accuracy of estimations, an illustrative example is examined numerically by means of Monte-Carlo simulation.

Keywords: Pareto distribution, reliability analysis, progressive type II censored, Bayesian estimation, Monte-Carlo simulation.

1 Introduction

Suppose that a random variable X has two-parameter Pareto distribution, then its probability density function (PDF) and cumulative distribution function (CDF) is respectively as follows:

$$\begin{aligned} f(x; \alpha, \theta) &= \alpha \theta^\alpha x^{-(\alpha+1)} \quad x \geq \theta, \alpha > 0, \theta > 0 \quad \text{and} \\ F(x; \alpha, \theta) &= 1 - (\theta/x)^\alpha \quad x \geq \theta, \alpha > 0, \theta > 0 \end{aligned} \quad (1)$$

The reliability and failure rate functions for a mission time t are, respectively

$$\begin{aligned} S(t; \alpha, \theta) &= (\theta/t)^\alpha \quad t \geq \theta, \alpha > 0, \theta > 0 \quad \text{and} \\ H(t; \alpha, \theta) &= \alpha/t \quad t \geq \theta, \alpha > 0, \theta > 0 \end{aligned} \quad (2)$$

The Pareto distribution provides has a wide variety of applications in many fields. Concretely, applications are seen in insurance risk studies, properly values, income, stock fluctuations, migration, size of cities and firms, service time in queuing systems. As mentioned by [1], the Pareto distribution is to one's benefit to have a wider choice of distributional results when modeling lifetime data. There are some results documented in the literature on the inference of Pareto distribution. Some related works [2-7] can be found.

The model of progressive Type II censoring is importance in the field of reliability and life testing. Suppose n identical units are placed in a life test. At the time of i th failure, R_i surviving unites are randomly withdrawn from the experiment,

$1 \leq i \leq m$. Thus, if m failures are observed, then $R_1 + R_2 + \dots + R_{n-1} + R_m$ units are progressively censored; hence $n = R_1 + R_2 + \dots + R_{n-1} + R_m + m$.

$X_{1:m:n} \leq X_{2:m:n} \leq \dots \leq X_{m:m:n}$ describe the progressively censored failure times where $R = (R_1, \dots, R_m)$ denotes the censoring scheme. As a special case, if $R = (0, \dots, 0)$ where no withdrawals are made we obtain the ordinary order statistics [8]. Many authors have been discussed inference under progressive censored using different lifetime distributions [9-12]. Further details and extensive references on progressive censoring may be obtained from the book [13].

In this study, we consider progressive Type II censored sample from Pareto distribution. In Sec 2, the likelihood function and Maximum likelihood estimates are derived. In Sec 3, Bayes estimates for the shape parameter, reliability and failure rate functions are obtained using both the squared error function and the LINEX loss function; this is done based on conjugate prior for the shape parameter when the scale parameter is known. In Sec 4, in order to compare MLE with Bayes estimators, we compute these via a Monte Carlo simulation study.

2 Maximum Likelihood Estimation

Let $X_{1:m:n} \leq X_{2:m:n} \leq \dots \leq X_{m:m:n}$ denote a progressive Type-II right censored order statistics from Pareto distribution, with (R_1, R_2, \dots, R_m) being the progressive censoring scheme. For simplicity of notation, we will use X_i instead $X_{i:m:n}$ and then $X = (X_1, X_2, \dots, X_m)$ is the observed progressive censored sample. The likelihood function (see [13]) for the parameters α and θ is then

$$L(X; \alpha, \beta) = C \prod_{i=1}^m f(X_i) [1 - F(X_i)]^{R_i} = C \alpha^{-m} \beta^m \prod_{i=1}^m X_i^{\beta-1} \exp[-\sum_{i=1}^m (1 + R_i) X_i^\beta \alpha^{-1}] \tag{3}$$

where $C = n(n-1-R_1)(n-2-R_1-R_2) \dots (n-m-R_1-R_2 \dots R_m + 1)$ and the natural logarithm of the likelihood function is given by

$$l = \ln L \propto m \ln \alpha + \sum_{i=1}^m \alpha(1 + R_i) \ln \theta - [\alpha(1 + R_i) + 1] \sum_{i=1}^m \ln X_i \tag{4}$$

Assuming a case in which θ is known, the maximum likelihood estimator (MLE), of α , denoted by $\hat{\alpha}_M$, is given

$$\hat{\alpha}_M = \frac{m}{\sum_{i=1}^m (1 + R_i) (\ln X_i - \ln \theta)} \tag{5}$$

the MLE of $S(t)$ and $H(t)$ may be obtained by replacing α by $\hat{\alpha}_M$, respectively

$$\hat{S}_M(t) = (\theta/t)^{\hat{\alpha}_M} \quad \hat{H}_M(t) = \hat{\alpha}_M / t \tag{6}$$

3 Bayesian Estimation

If β is known, the natural family of conjugate prior for α is a gamma with density function

$$\pi(\alpha) = \frac{\alpha^{\gamma-1} \delta^{\gamma-1} e^{-\delta\gamma}}{\Gamma(\gamma)}, \quad \alpha, \gamma, \delta > 0 \tag{7}$$

Applying Bayesian theorem, combining the likelihood function (3) and prior density (7), we obtain the posterior density of α in the form:

$$\pi(\alpha | X, \theta) = \frac{\alpha^{m+\gamma-1} e^{-\alpha(\delta+q-p)}}{\int_0^{+\infty} \alpha^{m+\gamma-1} e^{-\alpha(\delta+q-p)} d\alpha} = \frac{(\delta+q-p)^{m+\gamma} \alpha^{m+\gamma-1} e^{-\alpha(\delta+q-p)}}{\Gamma(m+\gamma)} \tag{8}$$

The LINEX loss function may be expressed as

$$L(\delta) \propto \exp(c\delta) - c\delta - 1 \quad c \neq 0, \delta = \hat{\alpha} - \alpha \tag{9}$$

The sign and magnitude of c reflects the direction and degrees of asymmetry, respectively (if $c > 0$, the overestimation is more serious than underestimation, and vice versa). For c closed to zero, the LINEX loss is approximately squared error loss and therefore almost symmetric. The posterior expectation of the LINEX loss function (9) is

$$E_\alpha[L(\delta)] \propto \exp(c\hat{\alpha}) E_\alpha[\exp(-c\alpha)] - c(\hat{\alpha} - E_\alpha[\alpha]) - 1 \tag{10}$$

where $E_\alpha(\bullet)$ denoting posterior expectation with respect to the posterior density of α . The Bayes estimator for α relative to LINEX loss function denoted by $\hat{\alpha}_{BL}$ is the value $\hat{\alpha}$ which minimizes (10), it is

$$\hat{\alpha}_{BL} = -c^{-1} \ln\{E_\alpha[\exp(-c\alpha)]\} \tag{11}$$

Provided that $E_\alpha[\exp(-c\alpha)]$ exists and is finite.

4 Bayes Estimation under Quadratic Loss Function

The Bayes estimators $\hat{\alpha}_{BS}$, \hat{S}_{BS} , \hat{H}_{BS} of the shape parameter, reliability and failure rate functions, are obtained by using the posterior PDF'S (8). The Bayes estimator for α is

$$\hat{\alpha}_{BS} = \int_0^{+\infty} \alpha \pi(\alpha | X, \theta) d\alpha = \frac{m + \gamma + 1}{(\delta + q - p)} \tag{12}$$

The Bayes estimator for the reliability function S is

$$\hat{S}_{BS} = E(S(t) | X) = \int_0^{+\infty} S(t) \pi(\alpha | X, \theta) d\alpha = \left(\frac{\delta + q - p}{\delta + q - p - w}\right)^{m+\gamma} \tag{13}$$

The Bayes estimator for the failure rate function H is

$$\hat{H}_{BS} = \int_0^{+\infty} H(t)\pi(\alpha | X, \theta)d\alpha = \frac{m + \gamma + 1}{t(\delta + q - p)} \tag{14}$$

5 Bayes Estimation under LINEX Loss Function

Under LINEX loss function (9), where $\delta = \hat{\alpha} - \alpha$, the Bayes estimator $\hat{\alpha}_{BL}$ of α using Equation (11) can be shown to be

$$\hat{\alpha}_{BL} = -c^{-1} \ln\{E_{\alpha}[\exp(-c\alpha)]\} = -c^{-1}(m + \gamma) \ln\left(\frac{\delta + q - p}{\delta + q - p + c}\right) \tag{15}$$

Similarly, the Bayes estimator of the reliability function S follows as:

$$\begin{aligned} \hat{S}_{BL} &= -c^{-1} \ln\{E_S[\exp(-cS)]\} \\ &= -c^{-1} \ln\left\{\int_0^{+\infty} e^{-ce^{c\alpha}} \frac{(\delta + q - p)^{m+\gamma} \alpha^{m+\gamma-1} e^{-\alpha(\delta+q-p)}}{\Gamma(m + \gamma)} d\alpha\right\} \\ &= -c^{-1} \ln\left\{\sum_{i=0}^{+\infty} \frac{(-c)^i}{i!} \left(\frac{\delta + q - p}{\delta + q - p - wi}\right)^{m+\gamma}\right\} \end{aligned} \tag{16}$$

The Bayes estimator of the failure rate function H is

$$\hat{H}_{BL} = c^{-1} \ln\{E_H[\exp(-cH)]\} = -t^{-1}c^{-1}(m + \gamma) \ln\left(\frac{\delta + q - p}{\delta + q - p + c}\right) \tag{17}$$

6 Simulation Study and Comparisons

Applying the algorithms [14], the following steps are used to generate a progressive Type II censored samples from the Pareto distribution.

1. Generate m independent $U(0,1)$ random variables z_1, z_2, \dots, z_m .
2. For given values of the progressive censoring scheme R_1, R_2, \dots, R_m , set

$$N_i = z_i^{1/(1+R_m+R_{m-1}+\dots+R_{m-i+1})} \quad i = 1, 2, \dots, m$$

3. Set $u_i = 1 - (N_m N_{m-1} \dots N_{m-i+1})$, $i = 1, 2, \dots, m$; then u_1, u_2, \dots, u_m is a progressive Type II censored sample of size m from $U(0,1)$
4. Thus, for given values of parameters α, θ , $X_i = \theta(1 - u_i)^{-1/\alpha}$, $i = 1, 2, \dots, m$, is the required progressive Type II censored sample of size m from $Pareto(\theta, \alpha)$ distribution.
5. The MLE of α, R and H , are computed as described in Sec 2.

6. The Bayesian estimates $((\bullet)_{BS}, (\bullet)_{BL})$ of α, S and H , are computed using results in Sec3.

We repeated the previous steps 1000 times, and computed the RMSE are computed for different sample sizes m and censoring schemes. The criteria for determining which estimate formulate performed best were based on the resulting root-mean(RMSE) calculating for each case using 1000 replications for each sample size. This computational results for the RMSE are displayed in Tables1 for the case of known parameter $\theta(\theta=3)$ and the prior parameters $\gamma=2, \delta=4 t=t_0=0.5$. For simplicity in notation, we will denote these schemes by $[(m-1)^*0, n-m]$ and $[n-m, (m-1)^*0]$, $c=0.01$.

Table 1. The RMSE's for $\alpha, S(t)$ and $H(t)$ for different samples size

n	m	R	$\hat{\alpha}_M$	$\hat{\alpha}_{BS}$	$\hat{\alpha}_{BL}$	\hat{S}_M	\hat{S}_{BS}	\hat{S}_{BL}	\hat{H}_M	\hat{H}_{BS}	\hat{H}_{BL}
20	3	[3*4]	0.8784	0.7781	0.05	3.890	2.443	1.756	6.187	1.367	1.243
					50	0	9	8	9	1	2
20	5	[5*3]	0.5150	0.9590	0.04	2.212	1.878	1.642	2.459	1.391	0.904
					28	7	1	3	5	7	9
30	5	[5*4]	0.7893	0.4484	0.02	3.941	2.059	2.021	6.529	1.245	0.524
					95	0	0	4	9	4	4
30	10	[5*4, 5*0]	0.7259	0.0977	0.00	2.193	1.983	1.830	2.162	0.851	0.485
					84	5	3	0	8	6	0
50	5	[4*5]	0.1744	0.1178	0.05	2.235	1.888	1.651	2.024	0.590	0.375
					59	5	3	3	8	6	0
50	10	[0, 4*5, 3*0, 2*3]	0.2989	0.0472	0.02	2.117	1.301	0.992	2.000	0.448	0.229
					53	0	7	2	4	7	2
50	15	[5*3, 5*0, 5*2]	0.2367	0.1160	0.05	2.107	1.230	0.901	1.978	1.169	0.596
					37	4	5	2	5	9	7

7 Conclusions

Our observations about the results are stated in the following points:

1. Table1, show that for both large and small samples the Bayesian estimates under LINEX loss function are better than the quadratic Bayesian estimates or MLEs in the sense of comparing the RMSE of the estimates.
2. Table1, show that the Bayesian estimates under LINEX loss function have the smallest RMSE as compared with quadratic Bayesian estimates or MLEs, by increasing n, R .
3. From the above results and discussion we observe that in most situations involving reliability and failure rate functions estimates, asymmetric loss function are more appropriate than quadratic loss functions. Finally, all results obtained in this paper can be extended to progressively Type I censoring model.

Acknowledgments. This work was supported partly by the Natural Science Foundation of the Education Department of Shaanxi Province (NO. 11JK0076).

References

1. Wu, S.J.: Estimation for the two-parameter Pareto distribution under progressive censoring with uniform removals. *J. Statist. Comput. Simulat.* 3(2), 125–134 (2003)
2. Geisser, S.: Predicting Pareto and exponential observables. *Canad. J. Statist.* 12, 143–152 (1984)
3. Hossain, A.M., Zimmer, W.J.: Comparisons of methods of estimation for a Pareto distribution of the first kind. *Commun. Statist. Theory. Meth.* 29(4), 859–878 (2000)
4. Howlader, H.A., Hossain, A.: Bayesian survival estimation of Pareto distribution of the second kind based on failure-censored data. *Computat. Statist. Data Anal.* 38, 301–314 (2002)
5. Wu, S.J., Chang, C.-T.: Inference in the Pareto distribution based on progressive type II censoring with random removals. *J. Appl. Statist.* 30(2), 163–172 (2003)
6. Kus, C., Kaya, M.F.: Estimation for the parameters of the Pareto distribution under progressive censoring. *Commun. Statist. Theory. Meth.* 36, 1359–1365 (2007)
7. Jose, A.V., Elizabeth, G.E.: A bootstrap goodness of fit test for the generalized Pareto distribution. *Computat. Statist. Data Anal.* 53, 3835–3841 (2009)
8. Baianmov, I., Eryilmaz, S.: Spacing exceedances and concomitants in progressive type II censoring scheme. *J. Statist. Plann. Infer.* 136, 527–536 (2006)
9. Balakrishnan, N., Sandhu, R.A.: Best Linear Unbiased and Maximum Likelihood Estimation for Exponential Distribution Under General Progressive Type II Censored Samples. *Sankya ser B* 58, 1–9 (1996)
10. Balakrishnan, N., Kannan, N., Liin, C.T.: Point and Interval Estimation for Gaussian distribution Based on Progressively Type II Censored Samples. *IEEE Trans. Reliab.* 152(1), 90–95 (2003)
11. Fernandez, A.J.: On Estimating Exponential Parameters with General Type II Progressive Censoring. *J. Statist. Plan. Inference* 121, 135–147 (2004)
12. Soliman, A.A.: Estimation of Parameters of Life from Progressively Censored Data Using Burr-XII Model. *IEEE Trans. Reliab.* 154(1), 34–42 (2005)
13. Balakrishnan, N., Aggarwala, R.: *Progressive Censoring and Applications*. Birkhäuser, Basel (2000)
14. Balakrishnan, N., Aggarwala, R.: Some Properties of Progressive Censored Order Statistics Form Arbitrary and Uniform Distributions with Applications to Inference and Simulation. *J. Statist. Plan. Inference* 70, 35–49 (1998)

Study on the Technology of the Secure Computation in the Different Adversarial Models

Xiaolan Zhang^{1,2}, Hongxiang Sun², Qiaoyan Wen¹, and Shi Sha¹

¹ State Key Laboratory of Networking and Switching Technology,
zhangxiaolan1994@bupt.edu.cn,
wqy@bupt.edu.cn, shisha1980@126.com

² School of Science Beijing University of Posts and Telecommunications
Beijing, 100876, China
shx@bupt.edu.cn

Abstract. This paper analyzes secure computation protocol efficiency in different (semi-honest and malicious and covert adversary) models. The semi-honest model is suitable for these high efficiency protocols that security requirements are not high. Secure and efficient protocols are designed in malicious model which one-sided simulatability, smartcards, cut-and-choose and black-box reduction technology are adopted, for highly sensitive data in practice. To achieve further improvement, The security definitions are relaxed in different requirements, such as privacy, correctness and so on, to create the special efficient protocols with different technology.

Keywords: smartcards, cut-and-choose technology, black-box reduction, adversaries.

1 Introduction

In the setting of secure computation, a set of parties wish to run some protocol for computing a function of their inputs while preserving security properties such as privacy, correctness, input independence, etc. This setting encompasses simple tasks such as coin-tossing and broadcast, alongside more complex tasks like electronic voting, electronic auctions, electronic cash schemes, contract signing, anonymous transactions and private information retrieval schemes. Consider for example the problem of electronic voting [3]. The privacy requirement states that no party should learn anything beyond the result of the election and in particular, no parties' individual vote can be learned. Furthermore the correctness requirement states that no party should be able to influence the results of the election beyond its legitimate vote. Due to its generality, the setting of secure multi-party computation can model every cryptographic problem.

General secure computation has been an early success of modern cryptography through works such as [2]. The early secure computation protocols used very generic techniques and were inefficient. Hence, now that most of the questions regarding the feasibility of secure computation have been addressed, many of the recent works have focused on improving the efficiency of these protocols [10, 12, 13, 14].

2 Preliminaries

The standard definition today [4, 5] generalizes all formalizes security in the following way. Consider an “ideal world” where there exists an external trusted party that helps the parties to carry out their computation. Every party sends its input to the trusted party, who then computes the desired function and sends back the appropriate output to every party. Several definitions of security for multi-party protocols have been suggested. These definitions aim to ensure some important security properties. The most central ones are privacy, correctness and independence of inputs.

A protocol is said to be secure if no adversary can do more harm in a real world execution than in an ideal world execution. To be more exact we require that for every adversary carrying out a successful attack in the real world, there exists an adversary succeeding in the same attack in the ideal world. Note that since successful attacks cannot be carried out in the ideal model, every attack in the real world is doomed to fail. This section describes the three main types of adversaries that have been considered in the literature:

1. Semi-honest adversaries: In this model, even corrupted parties follow the protocol steps. However, the adversary keeps an internal state of all the corrupted parties, including the received messages, and attempts to use this to learn private information.
2. Malicious adversaries: In this model, the corrupted parties follow the adversary's instructions and may arbitrarily deviate from the protocol specification. This model is stronger than the above one, since it allows arbitrary behavior.
3. Covert Adversaries: In this model, a malicious adversary may be able to cheat (e.g., learn the other party's private input). However, if it follows such a strategy, it is guaranteed to be caught with probability at least ϵ , where ϵ is called the “deterrence factor”.

3 The Semi-honest Model

Secure computation in the semi-honest adversary model can be carried out very efficiently, but, as mentioned, provides weak security guarantees. Yao's protocol [1] is the typical portocol in semi-honest model. Yao presented a constant-round protocol for securely computing any functionality in the presence of semi-honest adversaries. Loosely speaking, Yao's protocol works by having one of the parties (say party P_1) first generate a “garbled” (or encrypted) circuit computing $f(x, y)$ and then send it to P_2 . The circuit is such that it reveals nothing in its encrypted form and therefore P_2 learns nothing from this stage. However, the party P_2 can obtain the output $f(x, y)$ by “decrypting” the circuit. In order to ensure that P_2 learns nothing more than the output itself, this decryption must be “partial” and must reveal $f(x, y)$ only.

Yao's protocol is remarkably efficient in that it has only a constant number of rounds and uses one oblivious transfer per input bit only. An actual implementation of

the protocol was presented in [6], authors constructed a secure two-party computation system with very reasonable performance. The semi-honest adversaries have access to a fraction of the deployed keys of the network, but do not cause nodes to deviate from the specified protocol. Authors showed a concrete key establishment protocol that guarantees security in the presence of a semi-honest adversary [7].

With the acceleration of global information propagation speed, privacy-preserving computation has become a hot spot, in [8] authors presented new algorithms for privacy-preserving computation of all pairs shortest distance and single source shortest distance, as well as two new algorithms for privacy-preserving set union. The algorithms are significantly more efficient than generic constructions. And it guarantees security to against semi-honest adversary.

In a word, some of protocols which solve problems in practice don't need too high security, but need good availability, namely efficiency must be high. For example, key distribution, fairplay, privacy-preserving and sort problems could design efficient special protocols in semi-honest model respectively.

4 The Malicious Model

Regarding malicious adversaries, it has been shown that, under suitable cryptographic assumptions, any multiparty probabilistic polynomial-time functionality can be securely computed for any number of malicious corrupted parties [5]. However, this comes at a price. These feasibility results of secure computation typically do not yield protocols that are efficient enough to actually be implemented and used in practice.

In this section, some protocols are analyzed from three aspects in order to insure security requirements and the highest efficiency.

- One-Sided Simulatability

According to this notion of security, full simulation is provided for one of the corruption cases, while only privacy (via computational indistinguishability) is guaranteed for the other corruption case. This notion of security is useful when considering functionalities for which only one party receives output. Two of our protocols achieve a level of security that we call one-sided simulation. In these protocols, P_2 receives its specified output while P_1 should learn nothing. In one-sided simulation, full simulation is possible when P_2 is corrupted. However, when P_1 is corrupted, we only privacy is guaranteed, meaning that it learns nothing whatever about P_2 's input (this is straightforward to formalize because P_1 receives no output). This is a relaxed level of security and does not achieve everything we want; For example, independence of inputs and correctness are not guaranteed. Nevertheless, for this level of security we are able to construct highly efficient protocols that are secure in the presence of malicious adversaries.

[9] presented a constant-round efficient protocol for secure coin-tossing of polynomially many coins (in parallel), only one party received output. In this case, privacy is guaranteed when the party not receiving output is corrupted. Oblivious Transfer protocols allow one party, the sender, to transmit part of its inputs to another

party, the chooser, in a manner that protects both of them: the sender is assured that the chooser does not receive more information than it is entitled, while the chooser is assured that the sender does not learn which part of the inputs it received. In [10] authors took advantage of the one-sided simulatability technology to construct an efficient OT protocol. OT is used as a key component in many applications of cryptography. Its computational requirements are quite demanding and they are likely to be the bottleneck in many applications that invoke it. So, efficient OT protocol is the key factor of secure computation protocol. In [11] authors solved a new connection between keyword search and the oblivious evaluation of pseudorandom functions, and provided efficient solutions for various settings of keyword search, based either on specific assumptions or on one-sided simulatability technology.

The first approach is still strong enough to capture meaningful notion of security but enable us to construct protocols that is much more efficient than anything known that achieves full security in the presence of malicious adversaries.

- Smartcards

The second approach for achieving efficient protocols considers the assumptions regarding the resources that the parties have at their disposal while carrying out their computations.

In [3] authors present secure protocols that use smartcards in addition to standard network communication. Specifically, in addition to sending messages over a network, the participating parties may initialize smartcards in some way and send them to each other. Of course, such a modus operandi is only reasonable if this is not over-used. However, it is suitable whenever parties with non-transient relationships need to run secure protocols. Thus, this model is suitable for the purpose of privacy-preserving data mining between commercial, governmental and security agencies.

- Cut-and-Choose Technology and Black-Box Reduction

The third approach for achieving efficient protocols considers applying cut-and-choose techniques to the original circuit and inputs. Security is proved according to the ideal/real simulation paradigm, and the proof is in the standard model with no random oracle model or common reference string assumptions.

In [12] authors showed efficient secure two-party protocol, based on Yao's construction, which provided security against malicious adversaries. The protocol combined the cut-and-choose technique for efficiently proving consistency of inputs. And the protocol [12] can also be interpreted as a constant-round black-box reduction of secure two-party computation to oblivious transfer and perfectly-hiding commitments, or a black-box reduction of secure two-party computation to oblivious transfer alone, with a number of rounds which is linear in a statistical security parameter. Most of constructions use general zero-knowledge proofs to compile honest-but-curious secure computation protocols into fully malicious protocols. These zero-knowledge compilers are of great theoretical importance but lead to rather inefficient constructions. These compilers make a non-black-box use of the underlying cryptographic primitives.

In the malicious model, scholars usually utilize one-sided simulatability, smartcards, cut-and-choose and black-box reduction technology to construct efficient secure computation protocols respectively, for different special needs.

5 The Covert Model

An adversary model that accurately models adversarial behavior in the real world, on the one hand, but for which efficient, secure protocols can be obtained, on the other. The covert adversaries, which we believe faithfully models the adversarial behavior in many commercial, political, and social settings. Under the definition of security for covert adversaries and show that it is possible to obtain highly efficient protocols that are secure against such adversaries.

Aumann and Lindell [13] presented an efficient two party computation protocol secure against covert adversaries. They were able to utilize cut and choose techniques rather than relying on expensive zero knowledge proofs. In a protocol secure against covert adversaries, any attempts to cheat by an adversary is detected by honest parties with probability at least $1 - 1/t$, where $1 - 1/t$ is the deterrence probability. The rounds of the protocol are constant, and the communication complexity of the protocol is $O(t|c| + tsm)$, where $|c|$ is the circuit size, m is the input size, and s is the statistical security parameter.

To achieve further improvement in communication complexity, in [14] authors took a different approach to constructing the garbled circuit. In order to compute a garbled circuit (and the commitments for input keys), party P_1 generates a short random seed and feeds it to a pseudorandom generator in order to generate the necessary randomness. He then uses the randomness to construct the garbled circuit and the necessary commitments. When the protocol starts, party P_1 sends to P_2 only a hash of each garbled circuit using a collision-resistant hash function. Later in the protocol, in order to expose the secrets of each circuit, party P_1 can simply send the seeds corresponding to that circuit to P_2 , and not the whole opened circuit. In this protocol secure against covert adversaries, any attempts to cheat by an adversary is detected by honest parties with probability at least $1 - 1/t$, where $1 - 1/t$ is the deterrence probability. The rounds of the protocol are still constant, and the communication complexity of the protocol is $O(|c| + sm + t)$.

In summary, these covert adversary notions are not necessarily sufficient for all applications. In particular, security in the presence of covert adversaries would not suffice when the computation relates to highly sensitive data or when there are no repercussions to a party being caught cheating. Also, the guarantee of privacy alone is sometimes not sufficient. For example, the properties of independence of inputs and correctness are not achieved and they are sometimes needed. Consider secure protocols for elections and auctions. Correctness is clearly crucial in elections to ensure that the candidate with the most votes is elected, and independence of inputs is needed in auctions in order to prevent an adversary from always winning by giving a bid that is only \$1 higher than the other bids. Indeed, every criticism should always be taken within context, especially when efficiency is a crucial consideration when designing a protocol.

6 Summary

This paper presents the efficiency of the secure computation in the different adversarial models. The semi-honest model is suitable for these high efficiency protocols that security requirements are not high. In malicious model, security of protocols is high that the efficiency could be improved by adopting some technology, such as one-sided simulatability, smartcards, cut-and-choose, black-box reduction and so on. According to the special needs, we can relax the security definitions to create the special efficient protocols in covert model.

Acknowledgement. This work is supported by NSFC (Grant Nos. 60873191, 60903152, 61003286, 60821001), the Fundamental Research Funds for the Central Universities (Grant Nos. BUPT2011YB01, BUPT2011RC0505).

References

1. Yao, A.C.: How to generate and exchange secrets. In: Proceedings of the 27th IEEE symposium on Foundations of Computer Science, pp. 162–167 (1986)
2. Goldreich, O., Micali, S., Wigderson, A.: How to play any mental game or a completeness theorem for protocols with honest majority. In: Proceedings of 19th Annual ACM Symposium on Theory of Computing, pp. 218–229 (1987)
3. Information on, <https://users-cs.au.dk/carmit/PhDthesis.pdf>
4. Goldreich, O.: Foundations of Cryptography: Basic Applications, vol. 2. Cambridge University Press, Cambridge (2004)
5. Canetti, R.: Security and Composition of Multiparty Cryptographic Protocols. *Journal of Cryptology* 13(1), 143–202 (2000)
6. Malkhi, D., Nisan, N., Pinkas, B., Sella, Y.: Fairplay – A Secure Two-Party Computation System. In: The 13th USENIX Security Symposium, pp. 287–302 (2004)
7. Burmester, M., Safavi-Naini, R., Taban, G.: Secure Random Key Pre-Distribution against Semi-Honest Adversaries, <http://eprint.iacr.org/2008/446>
8. Brickell, J.: Privacy-preserving graph algorithms in the semi-honest model. In: Roy, B. (ed.) ASIACRYPT 2005. LNCS, vol. 3788, pp. 236–252. Springer, Heidelberg (2005)
9. Lindell, Y.: Parallel Coin-Tossing and Constant-Round Secure Two-Party Computation. *Journal of Cryptology* 16, 143–184 (2005)
10. Naor, M., Pinkas, B.: Efficient Oblivious Transfer Protocols. In: 12th SODA, pp. 448–457 (2001)
11. Freedman, M.J., Ishai, Y., Pinkas, B., Reingold, O.: Keyword Search and Oblivious Pseudorandom Functions. In: Kilian, J. (ed.) TCC 2005. LNCS, vol. 3378, pp. 303–324. Springer, Heidelberg (2005)
12. Lindell, Y., Pinkas, B.: An efficient protocol for secure two-party computation in the presence of malicious adversaries. In: Naor, M. (ed.) EUROCRYPT 2007. LNCS, vol. 4515, pp. 52–78. Springer, Heidelberg (2007)
13. Aumann, Y., Lindell, Y.: Security against Covert Adversaries: Efficient protocols for realistic adversaries. In: Vadhan, S.P. (ed.) TCC (2007)
14. Goyal, V., Mohassel, P., Smith, A.: Efficient two party and multi party computation against covert adversaries. In: Smart, N.P. (ed.) EUROCRYPT 2008. LNCS, vol. 4965, pp. 289–306. Springer, Heidelberg (2008)

The Research of Simulation and Optimization of Multimodal Transport System Based on Intelligent Materials on Container Terminal Job Scheduling

Qing Yu¹, Changhui Zhang², and Jinlin Wang³

¹ Tianjin Key Laboratory of Intelligence Computing and Novel Software Technology, Tianjin University of Technology, 300191, Tianjin, China

² Tianjin University of Technology, 300191, Tianjin, China

³ Tianjin Zhonghuan Electronic Computer Corporation
fengzhiyunyu@163.com

Abstract. Multimodal transport system on container terminal is a complex stochastic system, so it is difficult to solve accurately by mathematical model. This paper presents a simulation-based optimization method for scheduling optimization of container terminal. First, from the aspect of whole operation process, based on Hybrid Flow Shop Scheduling problem a mathematical model is developed to optimize the operation sequence of quay cranes, yard trailers and yard cranes simultaneously. Second, a simulation optimization method of combining with the GA and simulation for operation scheduling in container terminals is proposed. Finally, case studies show that this method is applicable and effective to the problem of coordinating job sequence optimization.

Keywords: Container terminal, multimodal, simulation optimization.

1 Introduction

International multi-modal transport of goods emerges and develops from transport by container, generally takes container as medium, which is a combined transportation and new transportation organization method of using container. It combine marine transport, cargo by rail, highway transportation and air transportation and so on which are traditional single transport mode of traditional single together to accomplish international cargo transportation.

This research attempts to answer the following the whole of working procedure of container terminal, through analyzing the operation procedure of unship. Based on the *Hybrid Flow Shop Scheduling* (HFSS) problem unship job scheduling model is found. Combine the simulation and optimization algorithm, job scheduling optimization problem is found the solution, propose the method of simulation and optimization of multimodal transport system on container terminal job scheduling, drew the optimum result of various device operation sequence in the unship work[1].

2 The Whole Operation Procedure of Multimodal Transport System on Container Terminal

For import container, ships loaded with import container fetch up at the wharf, is assigned to container berths which have lifting equipment for loading and unloading container operation, vehicle to container is waiting above the drawbridge, import container does loading and unloading operation from crane internal card, and import container will be sent to yard, with the operation of the yard mobile and portal crane, place the import box to the yard's specified position[2].Not until the final import container is placed on yard can discharge be considered over. The import containers are shipped to midland by rural highway or railway wharf export box working procedure is counter to the import box.

3 Multimodal Transport System on Container Terminal Job Scheduling Integration Model

Container dock loading and unloading operation can be broken down(can break down) under four stages, take import container for instance, quayside starts unloading the ship, horizontal transport vehicles ship containers to assigned heap region, import box could be sent across wildcard to midland(or across train a fleet of vehicles of train to train dump and station ,in the upshot, to the midland). In this chapter, discharge operation is taken as an example, from the point of view of the HFSS problem ,discharge operation order optimize operation model is created, quay cranes, yard trailers and yard cranes are optimized, and the optimal solution of optimization algorithm design solution model is added.

According to the description of HFSS's problem, now suppose there are n containers, which are processed in proper order according to the machining path of agreed direction in the 3 working procedures ,perhaps every process may have $M_r \geq 1$ ($r=1, 2, 3$) the same parallel machines, the k working procedures of each container may be processed in this working procedures' any Parallel Machine[3,4]. To convert working procedure of dock import box into scheduling problem of the import box , as shown in *Figure 1*.

Suppose discharge container job task aggregation is represented by n, $j=1, 2, 3, 4$ indicate quayside container crane, inside card, field bridge, outside card respectively; t_{ij} shows the machining time of the jth process of container; L is a large enough number; X_{i1} is a variable from 0 to 1 (it will return 1 if container(i) is positioned in the first position, otherwise it returns 0) ; K is a variable from 0 to 1, too(it will return 1 if the jth of container(i) is positioned in the kth equipment , otherwise it returns 0) ; S_{ij} shows the processing time of beginning of the jth process of the ith container; S_{ij} shows the completion times of the jth process of the ith container. Multimodal transport system on container terminal job scheduling can be represented:

$$\min \max_{\substack{i=1, \dots, n \\ m=1, 2, 3, 4}} \{e_{im}\} \tag{3-1}$$

$$\sum_{k=1}^{M_j} y_{ijk} = 1, \quad i = 1, \dots, n; \quad j = 1, 2, 3, 4. \tag{3-2}$$

$$e_{ij} = s_{ij} + t_{ij}, \quad i = 1, \dots, n; \quad j = 1, 2, 3, 4. \tag{3-3}$$

$$e_{ij} \leq s_{i(j+1)}, \quad i = 1, \dots, n; \quad j = 1, 2, 3, 4. \tag{3-4}$$

$$\sum_{i=1}^n x_{il} s_{ij} \leq \sum_{i=1}^n x_{i(l+1)} s_{ij}, \quad i, l = 1, \dots, n; \quad j = 1, 2, 3, 4. \tag{3-5}$$

$$\sum_{i=1}^n x_{i l_1} y_{ijk} e_{ij} \leq \sum_{i=1}^n x_{i l_2} y_{ijk} s_{ij} + (1 - \sum_{i=1}^n x_{i l_2} y_{ijk} s_{ij}) \times L. \tag{3-6}$$

$l_1, l_2 = 1, \dots, n; \quad l_1 \leq l_2; \quad j = 1, 2, 3, 4; \quad k = 1, \dots, M_j.$

When $j = 1, 2, 3, 4$ $\rho_{j \min} \leq \frac{\sum_{i=1}^n y_{ik}}{n} \leq \rho_{j \max}, \quad k = 1, \dots, M_j.$

$\rho_{j \min} \rho_{j \max}$ indicate the permitted minimum and maximum utilization rate respectively. (3-7)

Target Function: (3-1) indicates container maximum finish time to be minimized.

Restrained Condition: (3-2) indicates each container be only completed by one equipment in any one step; (3-3) indicates relation between container completion service time and starting time on the same step; (3-4) indicates the current step must be finished before the next step for the same container; (3-5) Indicates the time begin to process of container is performed based on sort order in the scheduling permutation; (3-6) presents that the same process allots the container on the same machine, the low-ranking containers can be operated only after the containers in front have been operated, however choose a number large enough can make expression (3-6) true when different ranking containers are not in the same device.

4 Implementation of Model of the Simulation and Optimization

In this paper, simulation optimization technique are employed to find the solution for optimization problem of multimodal transport system on container terminal [5], Genetic Algorithm is adopted for the optimum method.

1) The basic principle of genetic algorithm

Crossover operation produces two new offspring through reproduce selected location from two parents string, the i th location of some parents is reproduced to produce the i th location of its each offspring. Variations operated from a single parents, which can produce a series of random and small change, whose approach is to select a place and take the opposite [6].

2) Coding Design scheme

In the Container Dock scheduling, 5 chromosomes are first constructed, the integer coding is adopted, the length of each chromosome is defined by the number of container waiting to be processed. The same gene holder of five chromosomes corresponds to the operation information of the same container, that is to say, operation sequence of container is determined.

3) Set the adaptive value

The concept of virtual simulation is came up ,that is to say, before simulation, we should decide whether this solution is in compliance with the simulated condition, if the solution meet the simulated condition, simulation should be implemented, otherwise simulation would be abbreviated ,consequently, decrease simulation application times will be decreased, model evaluation calculation amount will be decreased. This paper considers the practical reality, before simulation application, initial solution is acquired through choice intersection variation of genetic algorithm, judge container proportion of every transportation facility in these initial solution, define a scope of proportion, the simulation will not be performed if proportion goes beyond this proportion, simulation is implemented to draw adaptive value, the solution which is not simulated whose adaptive value is set the minimum value.

5 Analysis of a Case

Take multimodal transport on container terminal in Tianjin for example, in accordance with alternative specimen contrast the following algorithm's efficiency.

- (a) Using Genetic Algorithm for searching solution space.
- (b) Using Genetic Algorithm for searching solution space, filter the solution which is not Optimal Solution in the simulation application.

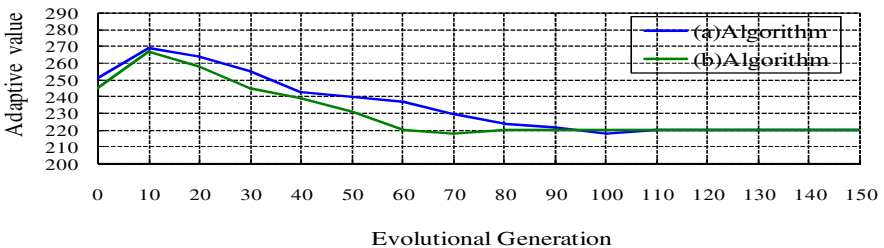


Fig. 1. (a) and (b) the result of a calculation of algorithm

From *Figure 1*, we find that the algorithm (a) and (b) can be convergent, on the rate of convergence, (b) is faster than (a), (b) is up to convergence after 80 circulation, however,(a) is up to convergence after 110 circulation. Join in virtual simulation in the SA algorithm can improve the convergence speed of algorithm. Further, according to different container、yard cranes、quay cranes、the quantity of container truck, 20 specimen are selected for calculating, different algorithm computation efficiency is contrasted. It can be concluded from *Table 1* that (b) has a flagrant advantage over

(a) in calculating time respect, computation time decreases by 71 percent, and simulation number and the iteration times of Genetic Algorithm for (b) is obviously fewer than (a) after using virtual simulation method, for those solution which is not good is not simulated ,so gobs of time is saved, judging from final container completion times, enhance virtual simulation method does not decrease algorithm’s searching excellent performance.

Table 1. Comparison of algorithm Performance

Computational Method	(a)	(b)
Computational time[h]	302	87
Iteration times	110	80
Simulation times	58721	5643
完成时间(s)	4561	4662

6 Conclusions

This paper deals with the optimization of *multimodal transport system on container terminal* job scheduling which is based on simulation optimization, establish multimodal transport system on container terminal job scheduling model which can optimize various device operation array in discharge operation, which can be applied in shipment job scheduling and discharge job scheduling, then combine merits of simulation and genetic algorithm to find the solution, case studies show that this method is applicable and effective to the problem of coordinating job sequence optimization.

Acknowledgments. This work was supported by the Science and Technology Support Project of Tianjin under Grant No.11ZCKFGX00500 and the Science and Technology Innovation Foundation of The Ministry of Science and Technology under Grant No. 09C26211200221.

References

1. Jin, C., Zhao, L., Gao, P.: Study on allocation of resources coordination and optimization of multimodal transport system on container port. *Journal of system simulation* (2009)
2. Guo, X.: Research on Simulation and Optimization of container port loading and unloading technology system. Dalian Maritime University, Dalian (2006)
3. Zeng, Q.: Model and method for Container Dock loading and unloading Integrated dispatch. Dalian Maritime University, Dalian (2008)
4. Wang, L.: In job-shop scheduling and genetic algorithm. Tsinghua University press, Beijing (2003)
5. Pan, Y., Zhou, H., Feng, C.: A genetic reinforcement learning algorithm of the same order F1ow-shop question. *System Engineering Theory and Practice* (2007)
6. Wang, X., Cao, L.: Genetic algorithm - theory application and software design. Xi’an Jiaotong University, Xi’an (2002)

Design of Program-Controlled Micro-flow Feeding System Based on Single Stepping Motor

Qing Song¹, Cunwei Zou², and Yuan Luo³

¹ Beijing University of Post and Telecommunications, Automation School,
Beijing100876, China
Songqing512@126.com

² Beijing University of Post and Telecommunications, Automation School,
Beijing100876, China
coby_yuan@126.com

³ Beijing University of Post and Telecommunications, Automation School,
Beijing100876, China
lyabby1007@yahoo.com.cn

Abstract. This paper describes the requirements of droplet analysis system for feeding liquid stability, trace and controllable, devised a system for liquid pump. In the mechanical structure design process, two functions of driving the actuating device and the switching mechanism was considered, so the system can be driven by a single stepping motor. The circuit design corresponding to machine operation, and microcomputer and motor drive design for pump control system were given. Using LabVIEW serial communication functions, finished the PC program. Experiments show that the system improves the stability of for liquid feeding effectively.

Keywords: Drop analysis, Feeding pump, Mechanical, Microcomputer, LabVIEW, Stepping motor.

1 Introduction

Droplet analysis technology refers to the technology that under certain test system circumstances, in droplets form process, measured liquid by various means to obtain physical and chemical characteristic parameters of measured liquid, to identification liquid qualitative and quantitative [1]. In the actual experiment condition, droplets are always in a continuous growth process. In order to make the droplet in some particular moment as close to "ideal balance", need liquid feeding system to provide trace, stable and facilitate the droplet, make droplets can meet the requirement of experiment of "almost balance". So put forward high requirements for fluid system[2].

Combined with the technical requirements, the overall for fluid system design is divided into three sections: the mechanical structure design, stepping motor control design and PC program design.

2 Structure Design of Micro-flow Feeding System

Liquid system uses "piston pump" basic principle, mainly including five parts: stepping motor and its driver, a transmission mechanism, liquid feeding piston, switching valves and control software. In general piston pump, transmission parts and switch valve parts are driven respectively by two stepping motor, for to design fluid feeding system, need to consider both piston pumps movement and control of the conversion of liquid feed function and liquid pump function. Mechanical structure designed in this paper combined switching valves and piston movement function, as shown in Fig. 1 below. Stepping motor 1 drive motor gears 2 which is meshing with gear 18. Two functions of Pistons movements up and down and valve switch will be accomplished by gear 18 of which both sides designed a pin.

The right of gear 18 is tie rod pin 15, through which gear 18 drive valve 14. After the movement of switch plate 13 and Axis 12, finish the switch of fluid pumping function and liquid feeding function.

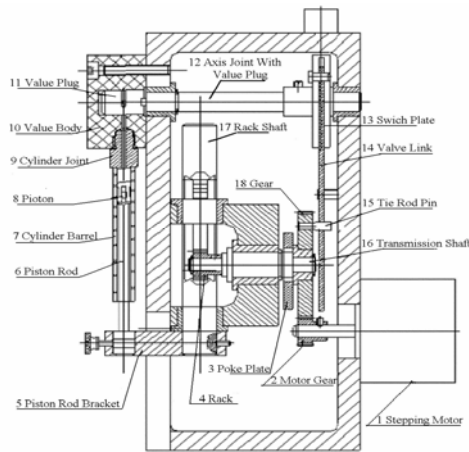


Fig. 1. Machine assembly drawings

There is a pin on the left of gear 18 (Not visible in Fig. 1, can be seen in Fig. 2), which is used to drive the rotation poke plate 3, through axis 16. Rack wheel 4 rotate with axis 16, makes rack shaft 17 meshes with it, drive the rack move up and down and finally through piston rod bracket 5, driving the piston rod 6 and piston 8 move. Figure 1 (b) is gear transmission relations schemes. When gear 18 roll with motor gears 2, in the first half circle, due to the special shape of poke plate 3, poke plate 3 and rack wheel 4 and piston rod 6 are all keep static, at this moment, gear 18 is driving tie rod pin 15 work for the switch function. Until gear 18 rotating 180°, the pin on the left of gear 18 can touch plate 3 and drive it rotate, meanwhile, tie rod pin 15 leave the trough of valve link 14, switching function finished, then piston began to pump liquid. After a circle rotating of gear 18, the piston runs a trip to down point. Later, motor rotate reversal, ready to move up to feed fluid. Similarly, in the first half circle gear 18 switch the valve, turn pump hole to feed hole. After rotation of 180°,

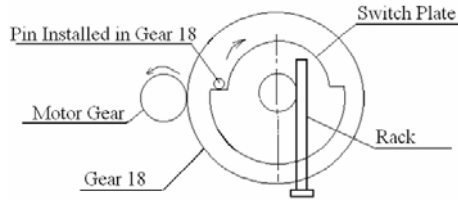


Fig. 2. Gear transmission relations sketch map

gear 18 drive poke plate 3 rotate a circle, the piston runs a trip from down point to up point. In order to ensure accurate rotation of gear 18, add the photoelectric sensor in structure, as Fig. 2 shows[3].

At the edge of the poke plate 3 a light pole was installed, work with photoelectric sensor made of led and photoelectric diode. The position can be judged According to the photoelectric signal. When gear 18 work as switching function, light pole keep static in the covering area of photoelectric sensor, make the light signal(Called "key") is 0; When gear 18 drive plate 3 move, light pole leave covered area, photoelectric sensor receive light signal of led, right now key = 1; Until poke plate 3 rotate a circle, light pole move into the covering area of photoelectric sensor, key = 0 again, then the position of gears 18 can be judged by the photoelectric signal changes, so as to control the moment of the motor reversal.

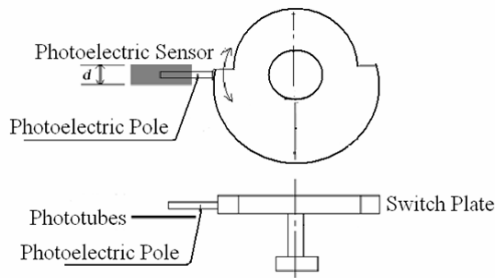


Fig. 3. Schematic of using photoelectric sensor control transposition

3 Control System Design

Fig. 4 is wiring diagram of feeding system control part. This instrument select stepping motor model for "17HS101", two phase, step distance angle of 1.8° [4]; Stepping motor drive models for "SH - 2H042Mb", 40 subdivision; The I/O card type "PCI - 8408 ", the input signal for 16 road in Common cathode mode, the output signal of source for 16 road Altogether anode way. Choose AT89C2051 SCM, It compatible with command and pin of MCS251 series microcontroller of industrial standard. SCM communicate with computer through standard RS2232C serial

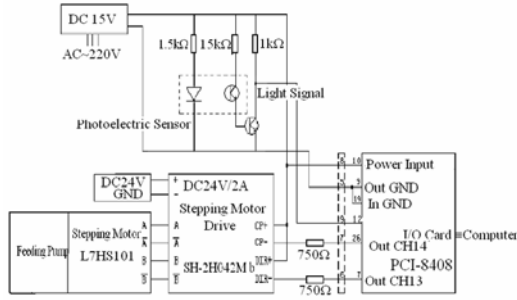


Fig. 4. Wiring diagram of feeding system control part

interface. In the application, choose the most common MAX232 chip to realize signal transition of SCM level (TTL level) and RS2232C level.

Interrupt signal can be obtained by Key specific signal to control motor reversing. Whenever Key specific is jump from high level to low level, should make motor stop, put DIR pulse reverse.

4 The Design of LabVIEW PC Program

The design of PC communication program is shown in Fig.5, the front panel of the program is shown in Fig.5. At first initialization of serial port should be finished, set baud rate for 9600b/s, 8 bits of data bits, stop bits 1, and no parity checking. Select com ports of computer of itself, put VISA Write and VISA Read in Conditions framework in while circulate, in conditions of control of reading and writing process. Send confirmation button was set at data sender. Use Bytes at port in receiver, make SCM read the Bytes returns at port, judge, if it not equal to zero, then read operation goes[5].

After PC send commands to lower machine, SCM began to carry out the instructions, and microcontroller return corresponding string to PC. Setting the rules of reading this string, analytical and read to indicate to corresponding instrument, lights in front, which represent work condition of the different parts of liquid system, such as Key specific, the discretion of the motor[6].

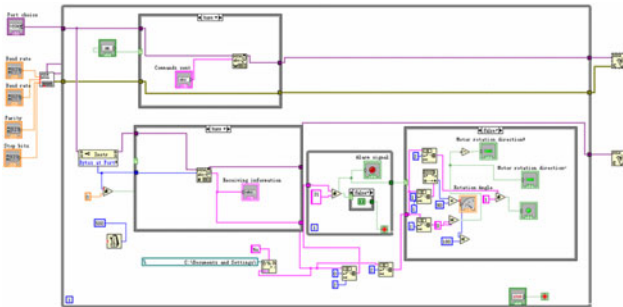


Fig. 5. PC program modules

5 Summary

Commonly two stepper motor were used to control the switching function of liquid feed and liquid pump and control of piston motion, then there are some problems happened, such as two motor frequent movements is not harmonious. The design of mechanical structure solved those problems, Using the labVIEW serial communication function design PC and communicate with SCM , can increase the stability of the system operation, easy to design various required function, and is convenient for monitoring and observation the system, actual use prove that the system greatly improved the stability of liquid feeding systems.

Acknowledgment. The project is supported by the Natural Science Foundation of China (NSFC) and the Fundamental Research Funds for the Central Universities (FRFCU).

References

1. McMillan, N.D., Finlayson, O., Fortune, F., et al.: The fibre drop analyser: a new multi analyser analytic instrument with applications in sugar processing and for the analysis of pure liquids. *Measurement Science and Technology*, 746–764 (1992)
2. Qiu, Z.: Research of droplet analysis technology. Tianjin university (2000)
3. Song, Q., Zhang, G., Qiu, Z.: Capacitance droplet analyzer principle and experimental. *Instruments Journal*, 348–351
4. SH series stepping motor drives use manual, Beijing mechanical and electronic technology development Co.,LTD (2002)
5. Liu, J.: LabVIEW virtual instrument design. Electronic industry press (2003)
6. Yang, L., Li, H., Xiao, X.: LabVIEW program design and application (2001)

Static Hedging for the Prices of Raw Materials to Hedge Based on Poisson Jump-Diffusion Model

YongMing Jiang^{1,2} and HangSheng Tan¹

¹ School of Mathematical Sciences and Computing Techniques, Central South University, Changsha 410004, China

² Fortune Securities, Changsha 410005, China
jiangym@cfzq.com

Abstract. This paper investigates the static hedging strategies of American binary warrants to hedge the prices of raw materials based on the Poisson jump-diffusion model. We extend the model in Peter Carr (1999) by taking jumps of stock price into account. The main idea is replicating the American binary warrants by exotic warrants, replicating the exotic warrants by path-independent warrants, and then replicating the path-independent warrants with vanilla warrants. Since vanilla warrants are free of timing risk, therefore, using hedging strategies above, investors can hedge the time risk of American binary warrants in the jump-diffusion model. Finally, we provide methods to construct the hedging strategies.

Keywords: jump-diffusion model, static hedge, binary warrants, the prices of raw materials to hedge.

1 Introduction

Theoretical hedging strategies fall into two groups, dynamic hedging strategies and the static hedging strategies. The pioneer model of dynamic hedging strategy is the BS model [2] and Leland model [3]. BS model assumes that there are no transaction costs and tax in the market and the hedging securities can be traded continuously. Investors must continuously adjust the position in underlying asset and the riskless asset, and hence adjust the hedge ratio, to eliminate the market risk. However, in practice, due to the presence of transaction costs, investors who employ such a dynamic hedging strategies suffer from the continuous accumulation of transaction costs which tends to be infinitely high. Hence investors can only take intermittent discrete hedging strategies. On the other hand, although the intermittent hedging reduces transaction costs, it increases the hedging error, and making the risk-free investment portfolio impossible. Therefore, the discrete hedging strategy for the prices of raw materials to hedge is not optimal strategy.

Leland (1985) proposed a model with modified volatility to solve the hedging error problem caused by transaction costs. The basic idea is: Assuming hedging adjustments in given time interval is allowed under the framework of Black Scholes model, through adding item with transaction cost factors to volatility expression

which lead to the increasing volatility and the warrant price, this exactly offsets the impact from the transaction costs. Thereby the Black Scholes formula is amended to make it can still be used in hedging with transaction costs. His model assumes that the underlying asset price follows a standard lognormal distribution, and investors can update the portfolios in fixed time intervals with transaction costs which are proportional to the trading volume in a fixed ratio.

Davis and Zariphopoulou (1993) [4], Hodges and Neuberger (1998) [5] and other stochastic control methods price the warrants by maximizing the investors utility. However, due to the complexity of the algorithm, their method is not practical. Whalley and Wilmott (1997) [6] propose a hedging algorithm which is relatively easier to be implemented by providing an asymptotic analysis of the model of Hodges and Neuberger (1989) assuming that transaction costs are small. They offer a decision rule for monitoring the stock price at each time and determining whether change to hedge positions to avoid the huge accumulation of transaction costs. The basic idea of their model is that the Delta hedging strategy is determined by the market movement. If the difference between the actual assets holding and Delta is greater than a decision function value, then the portfolio will need to be re-adjusted to match the Delta. The value of warrants is still function of the expected rate of return and the risk-free interest rate.

The literatures mentioned above are all about dynamic hedging. An important characteristic of dynamic hedging strategy is the need of frequently adjusting the position, moreover, the transaction cost is not known in advance. In this respect, regarding the prices of raw materials to hedge, the static hedging strategy has a comparative advantage, that is, investors can use the buy and hold trading strategy. This reduces considerable management costs, save time, and the most importantly, avoids huge amount of transaction costs. Moreover, since the transaction costs when using static hedging strategy is predictable in advance, hence investors can make the investment budget much easier. This is one of the reasons why we are interested in static hedging strategy.

A static hedging strategy for hedging time risk is provided in this article. Many exotic warrants involve a payoff that occurs at the first time the stock price crosses a constant barrier. Although the amount to be paid is known, the time at which it is paid is not. We refer this kind of risk as timing risk. Peter Carr (1999) [1] have shown how to establish static hedges of American binary warrants with timing risk. This paper studies static hedging strategies which hedge the timing risk for American Binary warrants in the Poisson jump-diffusion model.

Binary warrant is a new type of warrant with discrete gains functions. Generally, the two main types of binary warrants are the cash-or-nothing binary warrant and the asset-or-nothing binary warrant. The cash-or-nothing binary warrant pays some fixed amount of cash if the warrant expires in-the-money while the asset-or-nothing pays the value of the underlying security. This paper derives the static hedging strategies for cash-or-nothing binary warrants. Specifically, the hedging approach including using other exotic warrant replicates the value of American binary calls, then using path-independent warrants replicates the value of exotic warrant, using vanilla warrants replicates the value of path-Independent warrants. Since the vanilla warrants is independent of timing risk. Hence, by the above methods, we can hedge the timing risk in American binary calls based on a jump diffusion model, and hedge prices of raw materials.

2 Poisson Jump-Diffusion Model and the Stationary Solutions the Value Equation

In the jump diffusion model, the stock price follows the following stochastic differential equation

$$\frac{dS}{S} = (\mu - \lambda\kappa)dt + \sigma dz + dq \tag{1}$$

where, μ is the expected return rate, λ is the annual frequency of the jumps and, $q(t)$ is Poisson process, and the expected relative jump size is $\kappa = E(\eta - 1)$, $\eta - 1$ is the random variable percentage change in stock price if the Poisson event occurs.

We first derive differential Partial Integral-Differential Equation (PIDE) which we will use in the following warrant pricing based on the jump diffusion model.

Kushner and Dupris (1992) [7] provides Ito formula take the Poisson jump into account. Let F is the twice differentiable function with respect to S , and

$$dF = (F_t + (\mu - \lambda\kappa)SF_S + \frac{1}{2}\sigma^2 S^2 F_{SS})dt + \sigma SF_S dz + dQ_F \tag{2}$$

where $dQ_F = F(S(t)) - F(S(t^-))$.

Let $F = \ln S$, we have

$$d \ln S = (\mu - \lambda\kappa - \frac{1}{2}\sigma^2)dt + \sigma dz + \ln S(t) - \ln(S(t^-))$$

Assuming all parameters are constant, integral both sides of the above equation, we obtain

$$S(t) = S \cdot \exp((\mu - \lambda\kappa - \frac{1}{2}\sigma^2)t + \sigma \cdot z) \prod_{i=1}^{n(t)} \eta_i$$

where $n(t)$ is the Poisson random variable with mean $\lambda\kappa$. By Eq. (2) are

$$\frac{dF}{F} = (\mu_F - \lambda\kappa_F)dt + \sigma_F \cdot dz + dq_F \tag{3}$$

where $\kappa_F = E(\frac{F(S\eta, t) - F(S, t)}{F(S, t)}) = \frac{E(F(S\eta, t))}{F(S, t)} - 1$ is the warrants return random process, i.e., if and only if when the Poisson event of the stock price occurs, Poisson event of warrants return occurs.

Compare Eq. (2) and Eq. (3) we can obtain,

$$\mu_F = \frac{F_t + (\mu - \lambda\kappa)SF_S + \frac{1}{2}\sigma^2 S^2 F_{SS} + \lambda\kappa_F F}{F} \tag{4}$$

$$\sigma_F = \frac{\sigma S F_S}{F} \tag{5}$$

To obtain the warrants pricing equation, we consider a portfolio which is made up with an underlying asset, warrants and risk-free assets. The weights of the underlying assets, warrants and non-risk assets is W_S , W_F , and $1 - W_S - W_F$ respectively.

In the Black-Scholes model, we can construct the following risk-free portfolios

$$\begin{cases} W_S \sigma + W_F \sigma_F = 0 \\ W_S (\mu - r) + W_F (\mu_F - r) + r = r \end{cases}$$

Hence $\frac{\mu - r}{\sigma} = \frac{\mu_F - r}{\sigma_F}$ (6)

Substitute Eq. (4) and Eq. (5) into Eq. (6) and let $\lambda = 0$, we can achieve the Black-Scholes equation

$$F_t + \frac{\sigma^2 S^2}{2} F_{SS} + r S F_S - r F = 0$$

substitute Eq. (4) and Eq. (5) into Eq. (6), we have

$$F_t + \frac{\sigma^2 S^2}{2} F_{SS} + (r - \lambda \kappa) S F_S - r F + \lambda \kappa_F F = 0$$

Substitute κ_F into above equation, we have

$$F_t + \frac{\sigma^2 S^2}{2} F_{SS} + (r - \lambda \kappa) S F_S - r F + \lambda (E(F(S\eta, t)) - F(S, t)) = 0$$

Assume $\eta - 1$ follow the log-normal distribution, thus the above equation changes to the following equation, moreover, we can obtain the price of European warrants by solving the following equation.

$$F + (R - \lambda \kappa) S F + \frac{1}{2} \sigma S F - (r + \lambda) F + \lambda \int_0^\infty F(S\eta, t) G(\eta) d\eta = 0$$

where $G(\eta) = \frac{\exp(\frac{1}{2}(\frac{\ln(\eta) - m}{\delta})^2)}{\sqrt{2\pi} \delta \eta}$.

where, m is the mean of $\ln(\eta)$, δ^2 is the variance of $\ln(\eta)$, and δ is the standard variance of $\ln(\eta)$.

Because there is integral expression in above stochastic differential equations, therefore, it is called Partial Integro-Differential Equation.

The above equation has analytical solutions which can be expressed as

$$c = \sum_{n=0}^{\infty} \frac{e^{-\lambda T} (\lambda T)^n}{n!} f_n \tag{7}$$

where $\lambda' = \lambda(1 + \kappa)$, and $\kappa = E(\eta - 1) = \exp(m + \frac{1}{2}\sigma^2) - 1$, T is the expired date. Variable f_n is the price of European warrants in the Black-Scholes model, however, f_n in the corresponding Black-Scholes model, he expected return change to $\sigma^2 + \frac{n\delta^2}{T}$, the risk free rate is $r - \lambda\kappa + \frac{n\gamma}{T}$, where $\gamma = \ln(1 + \kappa)$.

Hence we obtain the warrant pricing formula in the jump diffusion model. Below we discussed the stationary solutions of the pricing equation, and stationary payoffs. To hedge the time risk, we first derive the stationary payoffs function. It is so-called static payoff function (see Peter Carr (1999)), since the payoffs function is independent of time, and is a function of underlying asset prices. For example, omitting the variable with describe the time in the Black-Scholes model, we have

$$\frac{\sigma^2 S^2}{2} \frac{\partial^2}{\partial S^2} V(S, t) + rS \frac{\partial}{\partial S} V(S, t) - rV(S, t) = 0$$

Let $V(S, t) = S^p$, we can obtain an equation of the power p ,

$$\frac{\sigma^2}{2} p(p - 1) + rp - r = 0$$

Solving the above equation, we have two solutions as

$$p = \gamma + \varepsilon, \quad p = \gamma - \varepsilon$$

where, $\gamma \equiv \frac{1}{2} - \frac{r}{\sigma^2}$, $\varepsilon \equiv \sqrt{\gamma^2 + \frac{2r}{\sigma^2}}$,

hence, $S_T^{\gamma+\varepsilon}$ and $S_T^{\gamma-\varepsilon}$ is the stationary solution of the Black-Scholes model. Furthermore, we can express $S_T^{\gamma+\varepsilon}$ and $S_T^{\gamma-\varepsilon}$ as integral of payment function of the European warrant with the same expired date, we have

$$S_T^{\gamma+\varepsilon} = \int_0^{\infty} (\gamma + \varepsilon)(\gamma + \varepsilon - 1) K^{\gamma+\varepsilon-2} (S_T - K)^+ dK$$

$$S_T^{\gamma-\varepsilon} = \int_0^{\infty} (\gamma - \varepsilon)(\gamma - \varepsilon - 1) K^{\gamma-\varepsilon-2} (K - S_T)^+ dK$$

Similarly, by Eq. (7), in the jump diffusion model, we have the stationary solution of the pricing equation as

$$c^{\gamma+\varepsilon} = \sum_{n=0}^{\infty} \frac{e^{-\lambda'T} (\lambda'T)^n}{n!} (S_T^{\gamma+\varepsilon})_n$$

and

$$c^{\gamma-\varepsilon} = \sum_{n=0}^{\infty} \frac{e^{-\lambda'T} (\lambda'T)^n}{n!} (S_T^{\gamma-\varepsilon})_n$$

where, $(S_T^{\gamma+\varepsilon})_n$ and $(S_T^{\gamma-\varepsilon})_n$ have the expected return as $\sigma^2 + \frac{n\delta^2}{T}$, and the riskless rate is $r - \lambda\kappa + \frac{n\gamma}{T}$, where, $\gamma = \ln(1 + \kappa)$.

Hence, we express the stationary solution of the pricing equations in the jump diffusion model as a function of the payoff of the standard warrant, and it is a convergence of infinite series.

3 Replicate the Value of American Binary Warrants

Here call warrants are considered only. First assume that the initial stock price is S_0 which is lower than the price barrier H . Furthermore, throughout this paper, we employ the other basic warrant with expired date T to replicate the value of American binary warrants, and their payment function is stationary function which is independent of timing risk.

T maturity warrants to the other basic values to copy American-style two warrants, which warrants the payment function is static payoff function, that is no time to risk. Here, the hedging mechanism is that since the stationary payoff function of the warrant which we want to replicate can be replicate by the payoff function of simple warrant, thus the American Binary warrants can be replicate by the simple warrants.

In this paper, we only illustrate how to use exotic warrant to replicate the value of American Binary warrants in jump diffusion model. We omit the part of replicating the value of an UIPSNP, replicating an ABC with path-independent warrants, replicating path-independent warrants with vanilla warrants and replicating American binary warrants with vanilla warrants, since the mechanism is similar to that when we use exotic warrant to replicate the value of American binary warrants in jump diffusion model. Moreover, reasoning methods are similar to Peter Carr (1999).

We define American binary warrants as below, where letter J indicate it is the warrant in the jump diffusion model.

In the jump diffusion model, Jump-American binary call ($J - ABC$) pays

$$c = \sum_{n=0}^{\infty} \frac{e^{-\lambda'T} (\lambda'T)^n}{n!}$$

at the hitting time if this occurs before maturity.

We also need the below payoff functions of warrants

Jump-Pseudo-share ($J - PS$):

Pays $c^{\gamma+\varepsilon}$ at maturity

Jump-Pseudo-bond ($J - PB$):

Pays $c^{\gamma-\varepsilon}$ at maturity

Jump-Pseudo-share-or-nothing call ($J - PS \vee NC$):

Pays $c^{\gamma+\varepsilon} \times 1(S > H)$ at maturity

Jump-Pseudo-bond-or-nothing call ($J - PB \vee NC$):

Pays $c^{\gamma-\varepsilon} \times 1(S > H)$ at maturity

Jump-up-and-in-pseudo-share-or-nothing call ($J - UIPS \vee NC$):

Pays $c^{\gamma+\varepsilon} \times 1(S > H)$ at maturity if the barrier has been hit

Jump-up-and-in-pseudo-share-or-nothing put ($J - UIPS \vee NP$):

Pays $c^{\gamma+\varepsilon} \times 1(S > H)$ at maturity if the barrier has been hit

where function $1(S > H)$ and $1(S < H)$ are defined as

$$1(S > H) \equiv \begin{cases} 1, & \text{if } S > H \\ 0, & \text{if } S \leq H \end{cases} \quad \text{and} \quad 1(S < H) \equiv \begin{cases} 1, & \text{if } S < H \\ 0, & \text{if } S \geq H \end{cases}$$

We first consider the case of replicating value of American binary warrants using exotic warrant based on the Black-Scholes model without jumps.

In the Black-Scholes model, the payment function of warrant to be used in the replication process is defined as follows (also see Peter Carr (1999))

ABC	Pays \$1 at the hitting time if this occurs before maturity
PS	Pays $c^{\gamma+\varepsilon}$ at maturity
PB	Pays $c^{\gamma-\varepsilon}$ at maturity
$PS \vee NC$	Pays $c^{\gamma+\varepsilon} \times 1(S > H)$ at maturity
$PB \vee NC$	Pays $c^{\gamma-\varepsilon} \times 1(S > H)$ at maturity
$UIPS \vee NC$	Pays $c^{\gamma+\varepsilon} \times 1(S > H)$ at maturity if the barrier has been hit
$UIPS \vee NP$	Pays $c^{\gamma+\varepsilon} \times 1(S > H)$ at maturity if the barrier has been hit

Hence, the following relationship established.

$$ABC_t = \frac{1}{H^{\gamma+\varepsilon}} (PS \vee NC_t + UIPS \vee NP_t) \tag{8}$$

Since the right hand side of the equation is $\frac{1}{H^{\gamma+\varepsilon}}$ share of $PS \vee NC_t$ and $\frac{1}{H^{\gamma+\varepsilon}}$ share of $UIPS \vee NP_t$, if the stock price do not hit the barrier H, the value of ABC_t , $PS \vee NC_t$ and $UIPS \vee NP_t$ are all zero. Hence, ABC can be replicated by $PS \vee NC$ and $UIPS \vee NP$. If the stock price hit the barrier H, ABC pays \$1 at the hitting time if this occurs before maturity. And the value of the portfolio of $PS \vee NC$ and $UIPS \vee NP$ equals to $\frac{1}{H^{\gamma+\varepsilon}}$ paid at the hitting time. Since at the hitting time $S = H$, and they are both stationary payment function, hence, at the hitting time, the value of the portfolio on the right hand side is equal to 1\$. Therefore, no

matter what kind of the stock price path, the exotic warrant $PS \vee NC$ and $UIPS \vee NP$ can replicate the value of ABC via the portfolio in Eq. (8).

Note in the jump diffusion model, we have

$$c^{\gamma+\varepsilon} = \sum_{n=0}^{\infty} \frac{e^{-\lambda T} (\lambda T)^n}{n!} (S_T^{\gamma+\varepsilon})_n \left(\frac{1}{H^{\gamma+\varepsilon}}\right)_n \text{ and } c^{\gamma-\varepsilon} = \sum_{n=0}^{\infty} \frac{e^{-\lambda T} (\lambda T)^n}{n!} (S_T^{\gamma-\varepsilon})_n \left(\frac{1}{H^{\gamma+\varepsilon}}\right)_n$$

where, $(S_T^{\gamma+\varepsilon})_n$ and $(S_T^{\gamma-\varepsilon})_n$ have expected return as $\sigma^2 + \frac{n\delta^2}{T}$, and the riskless rate

is $r - \lambda\kappa + \frac{n\gamma}{T}$, where $\gamma = \ln(1 + \kappa)$. Therefore, by Eq. (8), we have the payment

of ABC At the hitting time if this occurs before maturity is

$$\begin{aligned} c &= \sum_{n=0}^{\infty} \frac{e^{-\lambda T} (\lambda T)^n}{n!} \\ &= \sum_{n=0}^{\infty} \frac{e^{-\lambda T} (\lambda T)^n}{n!} (S_T^{\gamma+\varepsilon})_n \left(\frac{1}{H^{\gamma+\varepsilon}}\right)_n + \sum_{n=0}^{\infty} \frac{e^{-\lambda T} (\lambda T)^n}{n!} (S_T^{\gamma-\varepsilon})_n \left(\frac{1}{H^{\gamma+\varepsilon}}\right)_n \end{aligned}$$

Define $f(H) \otimes c^{\gamma+\varepsilon} = \sum_{n=0}^{\infty} \frac{e^{-\lambda T} (\lambda T)^n}{n!} (S_T^{\gamma+\varepsilon})_n (f(H))_n$

and

$$f(H) \otimes c^{\gamma-\varepsilon} = \sum_{n=0}^{\infty} \frac{e^{-\lambda T} (\lambda T)^n}{n!} (S_T^{\gamma-\varepsilon})_n (f(H))_n$$

hence, by the definition of $J - ABC$, $J - PS \vee NC$ and $J - UIPN \vee NP$, we have

$$J - ABC_t = \frac{1}{H^{\gamma+\varepsilon}} \otimes (J - PS \vee NC_t + J - UIPN \vee NP_t)$$

Thus, in jump diffusion model, $J - ABC$ can be replicated by a portfolio of $J - PS \vee NC$ and $J - UIPN \vee NP$ under the operator \otimes , hence hedge the timing risk.

4 Conclusion

In the real world, continuous hedging for the prices of raw materials to hedge is not feasible. Taking transaction costs into account, the dynamic hedging strategies based on Black-Scholes model encounter huge difficulties in practice, especially when the stock price volatility is high. The paper tends to propose a method to overcome the high transaction cost in the dynamic hedging. After establishing the static hedging strategy for the prices of raw materials to hedge, no further trading is needed, hence, investors can avoid the high transition cost.

Specifically, compare to other standard warrants, American Binary warrants distinguish itself by the discrete payoff function and carrying timing risk. The paper offer a static hedging strategy to hedge the timing risk in a Poisson jump diffusion model and extend Peter Carr (1999) [1] to a case which considers stock price jumps. Basic mechanism is demonstrated with comparison to the model in Peter Carr (1999) [1].

Static hedging implies concept stationary replication. It can be widely applied to asset pricing and new financial product design, and play role in the internationalization of China's financial markets and process of liberalization.

References

1. Carr, P., Picon, J.-F.: Static Hedging of Timing Risk. *The Journal of Derivatives* 6(3), 57–70 (1999)
2. Black, F., Scholes, M.: The Pricing of Warrants and Corporate Liabilities. *Journal of Political Economy* 81, 637–659 (1973)
3. Leland, H.: Warrant pricing and replication with transaction costs. *Journal of Finance* 40, 1283–1301 (1985)
4. Davis, M.H., Panas, V.G., Zariphopoulou, T.: European warrant pricing with transaction costs. *SIAM J. Control and Optimization* 31, 470–493 (1993)
5. Hodges, S.D., Neuberger, A.: Warrant replication of contingent claims under transaction costs. *Rev. Fut. Mkts.* 8, 222–239 (1989)
6. Whalley, A.E., Wilmott, P.: An asymptotic analysis of an optimal hedging model for warrant pricing with transaction costs. *Mathematical Finance* 7, 307–324 (1997)
7. Kushner, H.J., Dupuis, P.: *Numerical Methods for Stochastic Control Problems in Continuous Time*. Springer, New York (1992)

Speech Material Recognition Technology on an Objective Evaluation System for the Rhythm of English Sentences

Jing Zhang and Min Zhang

School of computer science and technology, Guangdong University of foreign studies,
Guangzhou Guangdong 510006, China
ha_go@163.com, hebzm@163.com

Abstract. With the progress of speech material recognition technology, Computer-assisted Language Learning (CALL) technology, the auxiliary pronunciation learning became a hot research. But for today's education system and the existing computer-aided instruction systems, the rhythm, which is emphasis in communication with English in reality was often neglected, the pronunciation would seem unnatural for the rhythm of the sentence can not be grasped. To solve this problem, the paper explored how to improve the level of pronunciation and intonation of learners and an objective evaluation system of English sentences was established, the English sentences was redrawn by extracting the energy characteristics of speech, and in order to improve the assurance of speaker to the rhythm of English sentence, the improved algorithm of pairwise variability index (PVI) as the core of Sentence evaluation was used. According to the identification of speech experts, the evaluation results gotten by the achieved objective evaluation of system speech quality is objective.

Keywords: Speech Intonation, CALL, Speech Material Recognition Technology, Energy Characteristics, PVI, Rhythm.

1 Introduction

In China, the overall level of English learners in terms of speech has been greatly exceeded in recent years, particularly in the tone (vowel consonant) aspects. This is largely attributing to the focus of education and teaching resources from the State and the enthusiasm for learning English language learners. Therefore, for most English learners, they can better grasp the pronunciation of English word. But, in the reality, for the natural and fluent communication with English, the emphasis is rhythm. Many learners suffered a bottleneck after better grasping the pronunciation of tone, because they found themselves able to pronounce for each sound more standard, but the expression in English but still with a strong Chinese style. This group includes not only the beginner and many intermediate learners and students of English majors and even some people use English for long-term. Rhythm of speech is a very important factor in the sentence of speech material, each language has its own characteristics in terms of rhythm, and the sentence without the grasped rhythm of the language seems unnatural. With the progress of speech material recognition technology, CALL

technology, the auxiliary pronunciation learning became a hot research, while the objective and automatic evaluation for the speech quality is the core technology in computer-assisted language learning (CALL) system. The objective evaluation of English speech sentence mainly refers to the extent that the speaker grasped the rhythm and the main information of sentence, that is, the rhythm and stress of sentence. As described in paper, through the deep study of English pronunciation and intonation, and combined with computer programming, a system of objective evaluation for English sentences was designed; it was expected to improve the students grasping the rhythm and stress of English language and to increase student’s capability of communication with spoken English.

2 Objective Evaluation System of Speech Quality

The evaluation process of speech proposed in the paper was shown in Fig. 1. First, a series of preprocessing was applied to the collected speech signal, including pre-emphasis unit, and sub-frame processing unit, and window function unit, and endpoint detection unit as well. For the evaluation part of rhythm, the stress dividing of standard sentence and testing sentence was carried by the dual threshold comparison method; and for the divided sentences, the comparison of stress number executed, if certain conditions are met, then according to the length differences of English pronunciation unit, the operation of pairwise variability index (PVI) algorithm was carried out, then and gotten the score. Else, entered the scoring directly and got the evaluation score.

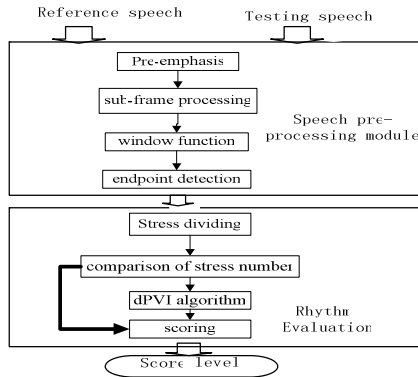


Fig. 1. The Evaluation Process of Speech

2.1 The Division of Stress Unit

The distribution of stress is one of features of rhythm, and it plays an important role in the statement organization and semantics expression. Therefore, in order to observe the rhythm characteristic of English sentences, the division of English sentences stress must be carried firstly. Fig. 2 shows the division processes of sentence stress unit:

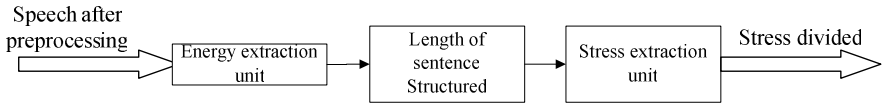


Fig. 2. Division of Stress Unit

The division of stress discussed in the paper was mainly based the three characteristics of stress, i.e. (1) sonority (2) the longer pronunciation (3) clear and easy to be distinguished. The division process of stress is as follows:

(1) The preprocessing include a series of processing of speech signal, and the last step is to wipe off the silence at the beginning and the end of sentence, then to eliminate the component that could influence the objective evaluation.

(2) The characteristic that the stress syllable of sentence is sonorous would be reflected to energy intensity in time domain, that the stress syllable represented great energy intensity. According to $E_n = \sum_{m=-\infty}^{\infty} [s(n)\omega(n-m)]^2$, the definition of short term energy of speech signal $s(n)$ to extract the energy value from the sentence.

(3) Because there is difference in speech speed between different people, so the difference of duration of same sentence pronounced by different people would form, but the pronunciation follows the rule that the duration of stress unit has certain proportion in the whole sentence. So, when the tested sentence was evaluated, the duration of sentence should be adjusted to closed extent with the standard sentence in proportion.

(4) The dual-threshold comparison was adopted in the paper to end detection of stress, according to a large number of experimentation; two thresholds were set as follows:

$$\text{Stress threshold } T_u = (\max(\text{sig_in}) + \min(\text{sig_in}))/2.5$$

$$\text{Non-stress threshold } T_l = (\max(\text{sig_in}) + \min(\text{sig_in}))/10$$

For the dual-threshold comparison, according to the energy value of sentence, the maximum speech signal S_{\max} with stress energy larger than T_u was searched one by one, then to search the speech signal S_l and S_r with stress energy equal to the non-stress threshold T_l on the left and right of signal S_{\max} . And then set the signal S_l and S_r as the stress signal of sentence and the value of signal energy between S_l and S_r should be set to zero in order to prevent the repeated search. The effect shown as Fig. 3.

(5) Because the pronunciation of stress syllable in sentence owns the characteristic of partial length, and the searched units of stress syllable in first step may be encountered by the problems of large energy, that the hearing represented as clangorous pronunciation but short duration, these units may be short vowel, or the interference of signal peak, the units of stress syllable could be farther selected according to the characteristic that the pronunciation of stress syllable owns the characteristic of partial length. The minimum unit of stress syllable was set a rough

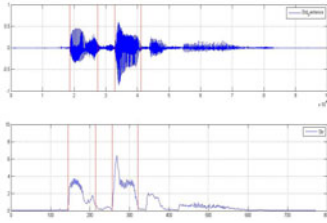


Fig. 3. The division of stress unit

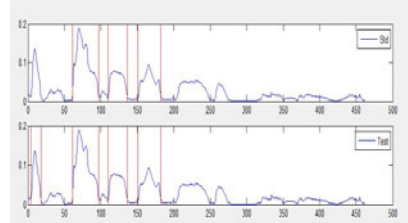


Fig. 4. The sentence after selection of duration threshold

unit [L1](Stressed vowel durations) , which is 100ms. The cross-comparison about the set of minimum duration of stress syllable as shown in figure 4 (std is the effect after set, test is before set). Through the steps hereinbefore, the unit division of stress syllable was done.

2.2 PVI Evaluation Algorithm and Its Improvement

The PVI (Pairwise Variability Index) is used to calculate the variability of duration between the adjacent units; smaller variability means the unit owns isochrony. LOW, who worked for Nanyang Technological University, Singapore, promoted PVI formula firstly in his study about the rhythm of Singapore English, and the formula was used to calculate the difference between the continuous and fore-and-aft syllables of stress and non-stress then got the pertinence. In the document [2], Grabe, who worked for Cambridge University didn't accept the prominent influence to the consonant interval by the speech speed. So Grabe proposed to calculate the difference of interval between the consonants by the using of original rPVI(The raw Pairwise Variability Index)parameter as Eq. 1.

$$rPVI = \left(\sum_{k=1}^{m-1} |d_k - d_{k-1}| / (m-1) \right) \tag{1}$$

Where, m means the summation of speech intervals, and d_k means the duration of speech unit of No. k, it including the duration of vowel and consonant(barring the length of pause), and the standardization of speech speed was neglected.

Because the characteristic that in English the duration is easy to be influenced by the speed when exist vowel in the sentence, the distance between the continuous and fore-and-aft syllables of stress and non-stress is obvious, which is considered a special character in the stress-timed language. In order to explore the obvious distance between the and fore-and-aft syllables and to get a natural ratio of serials and rhythm, LOW and Grabe promoted nPVI(Normalized Pairwise Variability Index) in documents[3], the character that PVI parameter tends to be influenced by the speech speed was improved, and through dividing by a mean duration of two adjacent serials as Eq. 2.

$$nPVI = 100 \times \left(\sum_{k=1}^{m-1} \left| \frac{d_k - d_{k+1}}{(d_k + d_{k+1}) / 2} \right| / (m-1) \right) \tag{2}$$

in documents[4], by different method, LOW and Grabe used the duration of conterminous syllable instead of vowel and non-vowel to calculate PVI parameter and obtain the distance of duration, and based which, the distance of stress-timed and syllable-timed and mora-timed speech was scaled.

The paper promoted the improved PVI parameter calculation formula, according to the characteristics of durational variability of English speech unit, the comparison of syllable unit between the standard and the tested speech was calculated, the transformed parameter (Eq. 3) would be used to the evaluation basis of system.

$$dPVI = 100 \times \left(\sum_{k=1}^{m-1} |d1_k - d2_k| + |d1_t - d2_t| \right) / Len \quad (3)$$

Where, d is divided speech unit, $m = \min(\text{Std stress num}, \text{Test stress num})$, Len is duration of standard speech, because the duration of test speech has been already regulated to that of standard speech, only Len could be used when calculated.

2.3 The Method and Basis of Evaluation

(1) According to the division described hereinbefore, the speech was structured as rhythm of binary alternation, that is *high* \cap *low*. It can be seen from the study about rhythm of English speech that English is a kind of language with rhythm emphasized. After being divided to binary alternation structure, the system carried evaluation and comparison for the rhythm, which is helpful to the learner to master the rhythm of speech.

(2) By the use of improved calculation formula of PVI parameter, the syllable duration of standard and test speech was compared and calculated, and the transformed parameter was used as evaluation basis of system.

(3) During the evaluation, the number of stress would be judged firstly, if the difference is large then the sentence be evaluated directly and corresponding hint would be promoted, else if the difference is equivalent, then the discrepant calculation of stress in standard and test speech would be neglected, but the neglect would due to the score be deducted in some extent.

3 System Evaluation

In the experiment, 10 sentences were recorded by authoritative English teachers in the as the standard sentences, and 10 sentences recorded by 10 English learners as the test sentence.

In the observation of speech data, it was found that there were obvious difference between the Standard sentence of teachers and Test sentences of students and as follows:(1) Most sentence of the students had intense sound in the end and had no contrast with the first half of the sentence, while the sentences of teachers featured that the intensity of sound was slow down in the tail;(2) After the Stress division, the number of syllable stress of students' sentence were more than that of teachers in general, when the sentence is longer, this feature became more obvious.

The following examples explained the achieved evaluation effect by the system: In Fig.5, the intensity of standard sentence featured slow down in the tail of sentence, which formed the contrast with that the intensity of first half of the sentence, while for the test sentences the intensity represent more strong at the tail of the sentence, and the stress is too much, then the system gave hints and the evaluation Level gotten.

In Fig.6, it was found after stress division that the number of stress syllable of test sentence is larger than that of the standard sentence, that is the students stressed syllable unit of sentence too much, and didn't grasp the rhythm of the sentence well.

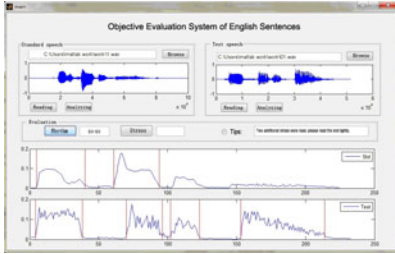


Fig. 5. Evaluation diagram of case 1

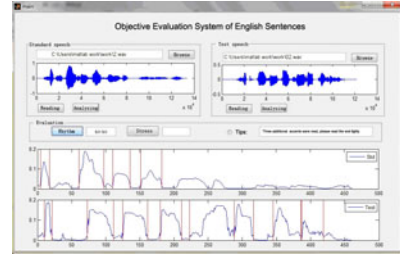


Fig. 6. Evaluation diagram of case 2

4 Summary

Speech material recognition technology for English Sentences described in the paper was mainly for the speaker to grasp the rhythm information of sentence, and to raise the skill of students to master the stress rhythm of English and to achieve the ability to improve their English communication. The research results can be applied to the aspects of interactive language learning and automatic oral testing and so on.

Acknowledgements. This work is partially supported by The ministry of education of humanities and social science project #10YJCZH220.

References

1. Wang, G.: English Pronunciation Intonation Tutorial. High Education Publications, Beijing (1996)
2. Grabe, E., Low, E.L.: Durational variability in speech and the rhythm class hypothesis. In: Papers in Laboratory Phonology 7. Cambridge University Press, Cambridge (2002)
3. Grabe, E., Low, E.L.: Durational Variability in Speech and the Rhythm Class Hypothesis. In: Laboratory Phonology VII. Mouton de Gruyter, Berlin (2002)
4. Low, E.L., Grabe, E., Nolan, F.: Quantitative Characterizations of Speech Rhythm: 'Syllable-timing' in Singapore English. *Language and speech* 43, 377–401 (2003)
5. Piankova, T.: Manual of English pronunciation. Language and Culture University press, BeiJing (2009)
6. Mok, P.: Using durational measures with non-native speech rhythm. In: Workshop on Empirical Approaches to Speech Rhythm. UCL, London (2008)

7. Rix, A.W.: Perceptual speech quality assessment a review. In: IEEE International Conference on Acoustics, Speech and Signal Processing, vol. 3, pp. 1056–1059 (2004)
8. Kim, D.-S.: Perceptual model for non-intrusive speech quality assessment. In: IEEE International Conference on Acoustic, Speech, and Signal Processing (ICASSP 2004), vol. 3, pp. 17–21 (2004)
9. Kim, D.-S.: Enhanced Perceptual Model for Non-Intrusive Speech Quality Assessment. In: IEEE International Conference on Acoustics, Speech and Signal Processing (ICASSP 2006), vol. 1, pp. 829–832 (2006)

Research on the Equipment Maintenance Support Quality Index System

Xiang Zhao, Bing Feng, and Qiangbin Yue

Dept. of Management in Shijiazhuang Mechanical Engineering College
Shijiazhuang, Hebei Province, China
zxcg2001@sina.com, fengbing@gmail.com,
yueqb@sina.cn

Abstract. Recently, more and more intelligent materials express in the equipment maintenance area. They bring much convenience to the repair. More and more new problems appeared. The equipment maintenance support quality is hardly under control. This paper took systematical research on the maintenance support process, combined with the practical quality evaluation work. It standardized the construction of the equipment maintenance support quality index system. Through analyzing the influence factors of maintenance support quality based on the intelligent materials, the paper put forward an index system of the quality evaluation in equipment maintenance support process. The paper defined the selecting criterions of the quality evaluation indexes. The quality evaluation index system that this paper brings forward is propitious to improve the level of the equipment maintenance support level and avoid the waste in the manpower, material and finance.

Keywords: Equipment maintenance support, Engineering, Quality evaluation, Index system, Intelligent Materials.

1 Introduction

Intelligent material means the material that can perceive the environment, including the internal and external environment. The intelligent materials can analysis, process, judge and make corresponding measures to the environment changes. The Equipment Maintenance Support Quality (EMSQ) is a quality control method for Equipment Maintenance Support. The aim of EMSQ is to ensure the reasonable quality of equipment that will be hand over to the army. How to evaluate EMSQ scientifically is doubtless a very important question we should solve now when constructing the Equipment Maintenance Support System. At present, the work of EMSQ evaluation still has some problems remained, such as defective evaluation indexes; the content of indexes are not perfect; the target of evaluation is not comprehensive and so forth. These problems generally result in low efficiency and lack availability. This article tries to solve these problems though the engineering research on EMSQ and apply the systematization and normalization methods to the analysis, filtration, validation and management process of EMSQ evaluation indexes. Based on the main line of

procedural control, this research builds the evaluation index system of EMSQ. It will improve the efficiency of EMSQ evaluation and fulfill the prescriptive requirements of EMSQ.

2 Definitions of EMSQ and Intelligent Materials

The EMSQ is the quality of equipment maintenance support process. In general terms, it is a set of system activities that integrated a quality management evaluation system and some methods by equipment maintenance department to ensure and improve the quality of the equipment maintenance products. The evaluation index system of EMSQ is an index system that can do systemic evaluation for the quality in the overall process of equipment maintenance support. It include organizing and dispatching maintenance staff, in the all phases of forming the EMSQ, synthetic research on various influence index of support quality, to achieve the purpose of the highest quality, lowest consumption and best service. So it can provide quickly and high quality maintenance service for the army.

The intelligent materials here should have these contents: Firstly, they have perceiving function. They can detect and recognized the inner and external stimulation, such as electric, optics, chemical and heat etc. Secondly, they have driving function. They can react to the external changes. Thirdly, they can choose and control the reacting action with the settings. The reacting action is sensitive, timely, and appropriate. Finally, the materials can recover the original state after the changes disappear.

The evaluation of EMSQ is a procedure that takes the EMSQ organizer as its subject, EMSQ working unit as its object. The purpose of it is to evaluate the EMSQ process and to estimate the EMSQ level.

3 Establishment of the Equipment Maintenance Support Quality Index System

Equipment maintenance support workflow. To construct a reasonable and adaptive EMSQ Evaluation indexes system, we must according to the demand of engineering and scientism, through the analysis of whole processes, to find out each index that influence the EMSQ in the process and validate its weight, then go on with final evaluation to ensure the EMSQ. The source of index is the systemic analysis of equipment maintenance support process. The equipment maintenance support is a work of comprehensive system engineering, its organizing sectors is inter-connected and check and inter-restricted. In the organizing and implementing process, a strict quality management must be put into practice. According to the proper order of maintaining process, the organizing work procedure includes define the level and plan of maintenance based on malfunction type, organization and divide the work, technique and material preparation, maintenance implementation and supervision and so on. Then organizing stuff to do the maintaining work, and carry on a quality examination for the equipment after maintaining. Finally the consumer unit checks and accepts, then hand over the equipment and track record the information.

Process of constructing EMSQ evaluation indexes system. According to the engineering theories, the construction of a system includes the arrangement of system structure and the configuration of system elements. Therefore, the construction of EMSQ Evaluation indexes system includes the distribution of the evaluation indexes system structure and the design of evaluation index. According to the complexity of equipment maintenance support process, its evaluation index system will be a tree type structure. Using the top-down method of systems analysis, the authors built up an EMSQ Evaluation index system. That is, from high to low, from abstract to concrete, from top to down, distributed the evaluation index system. Then defined layers, and designed evaluation indexes of each layer design according to its operational characteristics. The main steps are showed in Fig. 1.

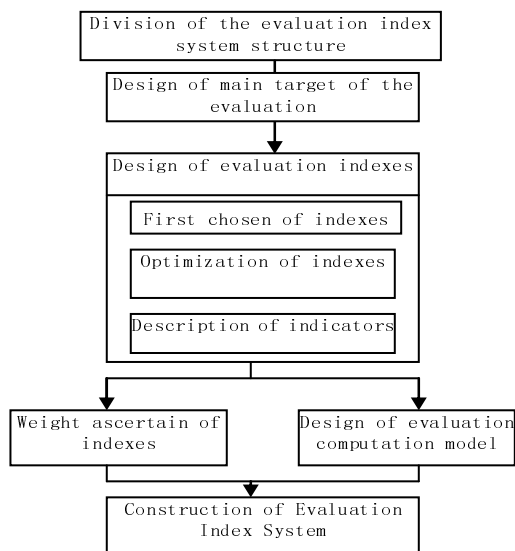


Fig. 1. Process of Constructing EMSQ Evaluation Index System

The main target of the evaluation is to get the quality grade of the maintenance support. It means to initialize the quality grades and the scores radius.

Design of evaluation indexes is a procedure of obtaining the concrete indexes step by step according to the system idea. It will make concrete of each evaluation index layer from top to bottom one by one until to the end layer. It is a cycle of understand, concrete, and optimize the indexes. The first chosen of index means to find out the affecting factors after analysis the maintenance support implement process. Then we design the primary indexes. The optimization of index means to screen out, emerge and delete, replace the indexes in the evaluation index system. Description of the index means to give expression to the index by a measurable language. Design of evaluation indexes is a repeating and advance process stage by stage. Through getting a cognition thoroughly, we can optimize the index system till obtain the evaluation target.

The weight ascertaining of indexes is to calculate the weight of the index according its importance. Design of evaluation computation model is the model to synthesize the

evaluation score of the maintenance support quality. There are many practicable models at present. Here we adopted the fuzzy comprehensive evaluation model.

Principles of designing EMSQ evaluation indexes. To realize the supervision for whole process of equipment maintenance support, it is particularly important to set up a set of perfect, feasible index system. According to the difference on the angle or depth of choosing indexes, sometimes this will affect the evaluation conclusion when the organizer constructing the index system. Therefore, in the process of constructing evaluation index system, these principles should be followed:

The Systematic Principle: That is the index system should reflect every aspects of equipment maintenance support features and rules in a comprehensive, systematic and integrated way. Because the equipment maintenance support system is very complex and is the comprehensive reactions of command, management and support activities, it determines that EMSQ evaluation index system must be a certain systemic, integrality and comprehensive system.

The Completeness principle: Including both the necessary and sufficient. When selecting indexes, one should make sure that any index's child index, can not only full description of the characteristics of the index, and give up any lower index will affect this characterization.

The Independency Principle: Various indexes cannot compatible with each other. That is, they neither been involved nor be replaced by each other. Some related index's contents may appear overlapping, but this relationship do not equal to compatible. The index system allows related index exist, but not allow compatible index exist. Namely, index must be "Independent", the same problem cannot be repeatedly multi-accessed.

In addition, there are some other principles still should be followed. Just as the scientific principle, dynamic principle, operational principle, comparability principle and so on. They help us to filter the proper EMSQ evaluation index from a great deal of quality impaction factors, and help us establish more suitable evaluation index system.

4 Contents of EMSQ Evaluation Index System

From the point of view of system engineering, the goal determines the index. The goal of EMSQ evaluation is to quantifying evaluates the whole process of equipment maintenance support, and then evaluating the EMSQ to improve the equipment maintenance support level. According to the basic principle of index design, through the analysis of equipment maintenance support activities, in general, the stages of EMSQ evaluation can be divided into four support essential factors. They are the staff support, material support, funds support and management support.

Staff support. That is the maintenance support system, executed at equipment maintenance tasks prepare, implement and acceptance stage, maintenance staff maintenance skills, stuff dispatch ability, remote maintenance ability quality evaluation. The maintenance staff support quality can be evaluated from several aspects as maintenance support stuff post rate, maintenance support staff assessment pass rate, spare parts production classification of quantity and quality, equipment repair rate, equipment maintenance support capacity, rework rate, support object

monitoring ability, support resources dispatching ability, remote maintenance support capacity assessment and so on.

Material support. That is the maintenance support system, executed at equipment maintenance tasks prepare, implement and acceptance stage, evaluating the needs of tools, equipment, facilities, equipment and other material support quality. Material support mainly includes equipment, tools supporting, calibration, inspection, the equipment the type, quantity or quality of preparation. The maintenance material support of quality can be evaluated from several aspects as repair support tools matching rate, maintenance support data fulfill rate, equipment calibration rate, facilities, equipment availability, facilities pass rate, qualified rate, equipment quantity fulfill rate, emergency equipment support ability an so on.

Funds support. That is the maintenance support system, executed at equipment maintenance tasks prepare, implement and acceptance stage, evaluating the maintenance funds support quality. The maintenance funds support can be evaluated from several aspects as the maintenance funds consuming, funds utilization, funding support in time or not etc.

Management support. That is the maintenance support system, executed when equipment maintenance tasks, evaluating the whole process of management. The maintenance management support can be evaluated from several aspects as the maintenance system implementation, support regulations, implement information support efficiency, task quantity balance degree, key job qualification rate, identification accuracy, maintenance technology documents matching rate, technical data fulfill rate and so on.

5 The Assurance of EMSQ Index Weights

As for a certain evaluation target, the relative importance of the evaluation indexes is different. The synthesize result of evaluation is rely on the index weight coefficient. Whether the weight coefficient is reasonable or not, relate to the creditability of the evaluation result directly. Therefore, the assurance of the index weight should be very carefully and precisely. AHP layer analysis is a kind of mature and effective evaluation method. The paper applied AHP layer analysis method to make sure the quality evaluating index weight. The calculating process includes the following five steps:

Making sure the important degree judge matrix of each index. We adopt an expert mark method while building each index's important degree judgment matrix. Suppose the index system contain n layer, one of the index layer has m evaluation indexes. In order to avoid single expert evaluating subjectively, the Satty list method was introduced [1].This method asks p experts to mark the importance degree of 1~9 scores that one index relative to the other. Thus formed p pieces of Satty judgment matrixes $A_k = (a_{ij}^k)_{m \times m}$ ($k=1,2,3 \dots p$). The a_{ij}^k means the score that the k_{th} expert gives the important degree of index i to index j . Then we calculated the average value of the p judge matrixes A .

The index sorting in the same layer. We adopted the characteristic vector method to the index in the same layer [2]. That is to say the index weight value $W_i(i=1,m)$ in the layer is gotten from the matrix average A .

The consistency examining intra-layer sorting. Firstly, the consistency indexes in each layer are calculated, viz. $C.I. = \frac{\lambda_{\max} - n}{n - 1}$. n in the equation is the rank of judge matrix. Then, consistency comparison is counted $C.R. = \frac{C.I.}{R.I.}$. The R.I. in the equation can be checked from table I, which is the average random consistency index table.

Table 1. The average random consistency index

Rank n	1	2	3	4	5	6	7	8
R.I.	0	0	0.52	0.89	1.12	1.26	1.36	1.41

When C.R. is less than or equal to 0.1, we generally think that the judges matrix consistency can be accepted. If the consistency examine in the layer is dissatisfied and then it's needed to adjust the judging matrix.

The layers overall sorting. The layers overall sorting is means sorting the indexes' importance weights that the index in the layer toward its superior index. This process is on the foundation of the layer intra-layer sorting and is done from above to bottom[3]. Suppose there are three layers in index system, that are A, B and C. Then the weight vectors of B and C layers to the A layer are $W_B = (W_{B1}, W_{B2}, W_{B3}, \dots, W_{Bm})^T$ and $W_C = (W_{C1}, W_{C2}, W_{C3}, \dots, W_{Cn})^T$. They

should all satisfy the equations $\sum_{i=1}^m W_{Bi} = 1$ and $\sum_{j=1}^n W_{Cj} = 1$.

The consistency examining of the overall sorting. The result of the overall sorting is also needed to be examined which is similar to the examination of the intra-layer sorting. Their expressions respectively are as follows.

$$C.I. = \sum_{i=1}^n a_i C.I._i, \quad R.I. = \sum_{i=1}^n a_i R.I._i, \quad C.R. = \frac{C.I.}{R.I.}$$

Among them, a_i is the n_{th} layer sorted weight after the overall sorting. We also hope C.R. is less than or equal to 0.10. If it doesn't satisfy, we also need to adjustment the judging matrix.

After the index weight is been made certain, the evaluation organizer can make use of evaluation index system to carry out the equality evaluation. Here we make use of the fuzzy comprehensive evaluation method to calculate the maintenance support quality level using the index weight. The comprehensive evaluating result C_k is

divided into five grades (excellent, good, general, pass, disqualified). The maintenance support quality level can be gotten by comparing the C_k value.

6 Summary

This paper discussed the definition and contents of the intelligent materials. It standardized the process of the EMSQ evaluation and built up the quality index system of the equipment maintenance support based on intelligent materials. It can provide evidence to the evaluation of the perform quality in equipment maintenance support mission. It also can research different indexes that influencing the EMSQ. Consequently, it can control more strictly the quality of the equipment maintenance support and increase the quality level of the equipment maintenance support based on intelligent materials. The more benefits will be achieved in the equipment maintenance based on intelligent materials.

References

1. Satty, T.L.: The analytic hierarchy process: planning, priority setting, pp. 55–62. McGraw-Hill, New York (1998)
2. Bai, X.S.: The hierarchy analysis theory——decision-making method, pp. 41–75. Tianjin Publishing Company (1988)
3. Osmundson, J.S., Huynh, T.V.: A Systems Engineering Methodology for Analyzing Systems of Systems. Naval Postgraduate School, March 2005, pp. 21–38 (2005)
4. Shaohua, Y.: The fuzzy comprehensive evaluation of the aerial defense command automatic system efficiency. *Journal of System theory and practice*, 114–118 (2002)
5. Bin, S.: Research on comprehensive evaluation of equipment support quality of equipment scientific examination. The Shijiazhuang Mechanic Engineering College Academic thesis, March 2007, pp. 13–17 (2007)

Modal Analysis and Optimization of Some Internal Rotor Radar Stabilized Platform

Shan Xue¹, GuoHua Cao², and YuLong Song³

¹ Changchun university of science and technology, Changchun, China
xueshan@cust.edu.cn

² Changchun university of science and technology, Changchun, China
caoguohua@cust.edu.cn

³ Changchun institute of optics, fine mechanics and physics,
Chinese academy of sciences, Changchun, China
lzy@cust.edu.cn

Abstract. The radar stabilized platform is the key part of radar supporting. It is used to isolate the loader movement and keep the radar relatively stable. The 3D model is built by Pro-E to aid the design of some internal rotor radar stabilized platform. The finite element model is built by Ansys after the 3D model is simplified. The modal of platform is analyzed through finite element theory and Ansys software. And the natural frequency and vibration catalog of the eighth modal for stabilized platform is acquired. The modal of different mesh and different materials are compared. It provides references for like analysis. And it also provides proof for optimization of stabilized platform. The program is designed to improve dynamic performance of stabilized platform.

Keywords: Internal rotor, Stabilized platform, Modal analysis.

1 Introduction

The radar is difficult to be stabilized due to the naval swing interference. Emergence of stabilized platform could keep the radar stationary isolating naval motion. Study on the structure, material and transfer method of stabilized platform is becoming more and more important. The development trend is light weight, small volume, high accuracy, large rigidity, and good dynamic performance and manufacture ability.

As the modern method to study the dynamic character of structure, the modal analysis is the most basic and important part of structure design, which provides one powerful tool to design and evaluate structure of product[1].

The body model of some internal rotor radar stabilized platform is built in Pro-E4.0 it is input Ansys12.1 after simplification. The modal is analyzed through finite theory and Ansys software. The eighth modal of nature frequency and vibration catalog is acquired. And the different modals and weights from different meshes and materials are compared. It provides reliable proof for the optimization of platform.

2 Digital Model Building of Some Internal Rotor Radar Stabilized Platform

The designed some internal rotor radar stabilized platform is composed of radar load stage, stator of pitch axis internal rotor moment electric engine, rotor of pitch axis internal rotor moment electric engine, pitch axis shell, azimuth axis shell, rotor of azimuth axis internal rotor moment electric engine, stator of azimuth axis internal rotor moment electric engine, base, shaft bearing, encoder, load stage, radar antenna, screw fastener and optical fiber gyro[2].

The digital model for structure of external rotor stabilized platform is built by PRO-E4.0. The model is shown as Fig.1.

3 The Finite Element Model Building of Some Internal Rotor Radar Stabilized Platform

The body model of some internal rotor radar stabilized platform in Pro-E4.0 is input Ansys12.1 after it is simplified. The shell and body are both applied in the finite model.

3.1 Simplification of Model

The components number of stabilized platform is large and the connecting relationship is complicated. So when the stabilized platform modal is analyzed, some components in structure should be simplified appropriately to improve computing speed with precondition of meeting computing accuracy. The simplification of structure is the key factor of finite model building.

A. Simplification of screw connecting

According to system character, the screw connecting rigidity is judged from modal analysis of components. The flexible or rigid connection is chosen. Through analysis, there is good rigidity in dense screw connection.

The rigid component is rigid connected in ansys operate environment. If there is less screw connection between two components, the connection will own bigger flexible effect. The connection parts are equivalent as dynamic model with many springs. The equivalent spring rigidity could be calculated by integration[1].

B. Simplification of bearing

Simplification of bearing is mainly for the bearing ball. The radial bearing ball could be simulated by 3D spherical body, 3D spatial bar and 3D spaces according practical conditions in engineering analysis. The bearing ball is simulated by 3D spatial bar in finite element model building. The internal and external parts of bearing are classified with body element. The internal and external parts are cemented. The external cage is cemented with the frame. And the longitudinal location of bearing is assured[3].

C. Other simplification

The aperture, beveling and rounding smaller than 2mm are omitted. The shaft is simulated by girder element. The bar is simulated by bar element.

3.2 Mesh Division of Model

The mesh division is very key in finite element analysis. According to the structure of stabilized platform, the meshes are divided in Ansys. The division method of all tetrahedron and combination of scanner and tetrahedron are both applied as shown in Fig.2 and Fig.3.

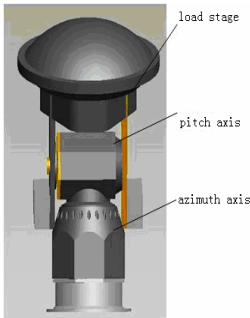


Fig. 1. Sketch of internal rotor stabilized platform structure

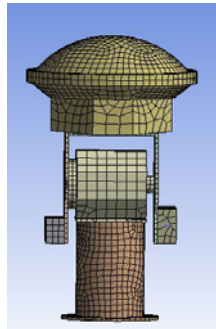


Fig. 2. Combination of scanner and tetrahedron method

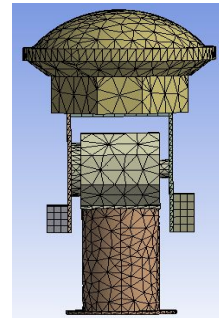


Fig. 3. All tetrahedron method

The division speed of all tetrahedron is fast with less error. But the division quality of meshes is not good. The demand for structure is higher in hexahedron division with good quality of meshes.

The meshes distortion of two methods is 0.45 and 0.86 respectively. The division method of combination of scanner and tetrahedron is preferred than all tetrahedron method.

3.3 Material of Stabilized Platform

The modal of stabilized platform with different material is analyzed.

It is for design and optimization of stabilized platform. The stabilized platform is designed with all parts steel. And it is also designed with part duralumin and combination of bearing and steel. The structure material is shown as Table 1.

Table 1. Parameters of structure material

No.	Material	E/MP	μ	$\rho(10^{-3}g/mm^3)$
1	2A12	72000	0.33	2.80
2	GCr15	207000	0.29	7.81
3	Q236	196000	0.3	7.85

4 Modal Analysis

The modal analysis is the most basic and important part of analysis of dynamic character. It is the modern method to study the dynamic character of structure. And it is the powerful tool to design and evaluate structure of product. The natural frequency and deformation amplitude of system could be acquired by modal analysis. The rigidity could be analyzed and the resonance vibration could be avoided[4].

From the variation principle of elastic mechanics, the dynamic balance equation of stabilized platform is as following.

$$[M]\{\ddot{u}\} + [C]\{\dot{u}\} + [K]\{u\} = \{P(t)\} + \{N\} + \{Q\} \tag{1}$$

In the expression, $[M]$ is the mass matrix, $[C]$ is the amortization matrix, $[K]$ is rigidity matrix, $\{P(t)\}$ is the external force function vector, $\{N\}$ is the nonlinear external force vector related with $\{\dot{u}\}$ and $\{u\}$, $\{Q\}$ is the boundary constrain counterforce vector, $\{u\}$ is the shifting vector, $\{\dot{u}\}$ is the speed vector, $\{\ddot{u}\}$ is the acceleration vector.

To solve the natural frequency and vibration catalog of stabilized platform, the external force and amortization is zero. The right side of the equation is equal to zero,

$$[M]\{\ddot{u}\} + [K]\{u\} = \{0\} \tag{2}$$

And the corresponding characteristic matrix equation is,

$$([K] - \omega^2 [M])\{u\} = \{0\} \tag{3}$$

In the expression, ω is the natural frequency.

Because the amplitude of free vibration is not zero, i.e. $\{u\} \neq 0$, the deformation of Eq.(3) will be as Eq.(4).

$$[K] - \omega^2 [M] = 0 \tag{4}$$

Then $\omega_1^2, \omega_2^2 \dots \omega_n^2$ and $\{\Phi_1\}, \{\Phi_2\} \dots \{\Phi_n\}$ could be solved. ω_i and Φ_i is the natural frequency and vibration catalog of the i th modal. The natural frequency and vibration catalog represent for the dynamic characters.

The above equations are solved by Ansys[5]. The modal of stabilized platform with different material is analyzed with Ansys. The comparison of the natural frequency of the 8th modal is shown as Table2. The first and second natural modal is shown I Fig.4, Fig.5, Fig.6 and Fig.7. Stabilized platform with part duralumin and bearing steel is analyzed. The natural frequency and vibration catalog of modal is described as Table.3. The weight of stabilized platform with part duralumin and bearing steel is 153kg. but the weight of Stabilized platform with all steel is 193kg.

Table 2. 8th natural frequency of modal comparison for stabilized platform with different material

	Stabilized platform with part duralumin and bearing steel (HZ)	Stabilized platform with all steel (HZ)
1st natural frequency	98.22	88.56
2nd natural frequency	145.37	95.56
3rd natural frequency	150.73	102.56
4th natural frequency	260.57	245.97
5th natural frequency	314.18	299.90
6th natural frequency	372.88	314.23
7th natural frequency	389.39	357.99
8th natural frequency	469.68	484.31

Table 3. Modal of stabilized platform with Stabilized platform with part duralumin and bearing steel

Order of modal	natural frequency(HZ)	Vibration description
1	98.22	Rotate around pitch axis
2	145.37	Partial swing with right balance weight
3	150.73	Swing around azimuth axis
4	260.57	Rotate around azimuth axis
5	314.18	Rotate around pitch axis +partial bending
6	372.88	Partial swing with right balance weight
7	389.39	Bending perpendicular to pitch axis plane
8	469.68	Up-and-down movement

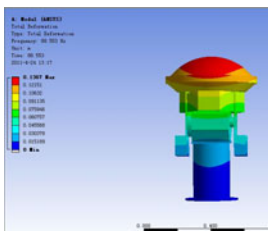


Fig. 4. The 1st modal of Stabilized platform with all steel

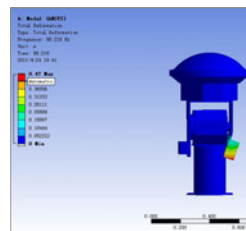


Fig. 5. The 1st modal of stabilized platform with part duralumin and bearing steel

The weight of stabilized platform with part duralumin and bearing steel is lightened by 20.7%. And the natural frequency is enlarged from 88.56 to 98.22. The rigidity is also intensified with the natural frequency enlargement.

It is shown in the modal analysis that in some internal rotor stabilized platform, material of the minor part could be duralumin, and the precise part should be bearing steel. The weight could be lightened and the rigidity could be intensified.

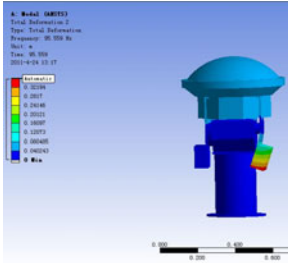


Fig. 6. The 2nd modal of Stabilized platform with all steel

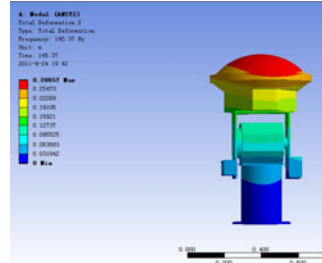


Fig. 7. The 2nd modal of stabilized platform with part duralumin and bearing steel

5 Summary

(1) A kind of some internal rotor stabilized platform is designed and the 3D body is built by Pro-E.

(2) The body model is input Ansys software for finite element model building after simplification. The connections are simplified correspondingly.

(3) The modal is analyzed with finite element theory and Ansys software. The natural frequency and vibration catalog of 8th modal is acquired. Modal and weight with different meshes and material are compared.

(4) The division method of combination of scanner and tetrahedron is preferred than all tetrahedron method. Material of the minor part could be duralumin, and the precise part should be bearing steel. The weight could be lightened and the rigidity could be intensified.

The design of radar stabilized platform is optimized through modal analysis. And the dynamic character is improved in large amount. It provides good references for design of like device.

References

1. Duan, Y., Gu, J., Ping, L.: Modal analysis and experimental study on radar antenna stage. *Mechanical Design and Fabrication* 2(2), 214–216 (2010)
2. Russell, J.C.: A Control System and Application Program Interface (API) for an Elevation Over Azimuth Tracking Pedestal. A dissertation submitted to the Department of Electrical Engineering, University of Cape Town, in partial fulfilment of the requirements for the degree of Bachelor of Science in Electrical and Computer Engineering (October 20, 2008)

3. Yang, X., Jia, H., Feng, C.: Finite Element Modal Analysis of the Gyroscope-Stabilized Platform. *Computer simulation* 25(9), 70–73 (2008)
4. Chen, G., Han, X., Liu, G.: Dynamic character analysis and optimization of some heavy duty commercial vehicle operator cabin. *Chinese Mechanical Engineering* 10(20), 2509–2513 (2010)
5. Zhang, c.: *Engineering application examples of Ansys structure analysis*. Mechanical industry press (2010)

Research on the Methods of Constructing Perfect Binary Array Pairs to Explore New Material Uses

Yuexia Qian and Guozheng Tao

Changzhou Institute of Mechatronic Technology, Changzhou,
Jiangsu, P.R. China
gwjczmec@163.com, 1589@czmec.cn

Abstract. Perfect binary array pairs have good autocorrelation properties and can meet two conditions required by the processing of perfect signal in communications. By analyzing the properties of perfect binary array pairs and differences set pairs, the differences set pairs method for constructing perfect binary array pairs is presented. Polynomial is a common method for designing the perfect discrete signal. This paper presents characteristic polynomial method for constructing perfect binary array pairs. A lot of perfect binary array pairs can be constructed by using these two methods, and more choices are provided for communication engineering.

Keywords: Perfect signal, Different set pairs, Array pairs.

1 Introduction

Cyclic correlation is the criterion of perfect signal with the most extensive application and the most in-depth study. The perfect binary array [1] with good correlation properties has important applications in various areas of engineering. Whereas, the existing space of perfect binary array, which is very limited and only exists in $4t^2$ (t be Integer), brings a lot of inconveniences in application of the project. Therefore, many types of perfect signal theories were presented including perfect binary array pairs [2] and perfect ternary array pairs [3-4] etc.

Perfect binary array pairs with good autocorrelation properties is a sort of perfect signal and meets the two conditions required by the processing of perfect signal in communications. The two conditions are described as follows: (1) Every signal can be distinguished easily from its translates in signals set. (2) Every signal can be distinguished easily from other signals and their translates in signals set. Therefore, the research on the methods of constructing perfect binary array pairs is an important subject.

At present, the methods of constructing perfect binary array pairs mainly focus on complete sampling, folding method and composite method. We put forward differences set pairs method and characteristic polynomial method for constructing perfect binary array pairs. We can construct many perfect binary array pairs by using these two methods, and which is realized easily with computer. So it is of great value for expanding the option ranges of applications in engineering.

2 Definitions

Definition 1. If the autocorrelation function of binary array pairs (X, Y) , $R_{XY}(u_1, u_2, \dots, u_n)$ satisfying

$$R_{XY}(u_1, u_2, \dots, u_n) = \begin{cases} E \neq 0 & (u_1, u_2, \dots, u_n) = (0, 0, \dots, 0) \\ 0 & (u_1, u_2, \dots, u_n) \neq (0, 0, \dots, 0) \end{cases} \quad (1)$$

then, the binary array pairs (X, Y) is perfect binary array pairs, E is called its peak.

Definition 2. [5] Suppose that U, V are two subset of the finite group $Z_{t_1} \times \dots \times Z_{t_n}$, k and k' are the numbers of element in U and V , that is $k = |U|$, $k' = |V|$. If the list of differences $\{(u_1, \dots, u_n) - (v_1, \dots, v_n) \mid (u_1, \dots, u_n) \in U, (v_1, \dots, v_n) \in V\}$ contains each element $(g_1, g_2, \dots, g_n) \neq (0, 0, \dots, 0)$ of $Z_{t_1} \times Z_{t_2} \dots \times Z_{t_n}$ exactly λ times, then (U, V) is called (E, k, k', λ) -differences set pairs of $Z_{t_1} \times Z_{t_2} \dots \times Z_{t_n}$. Where $Z_{t_1} \times Z_{t_2} \dots \times Z_{t_n}$ denote Cartesian product of $Z_{t_1}, Z_{t_2}, \dots, Z_{t_n}$, $E = \prod_{i=1}^n t_i$.

Definition 3. The characteristic polynomial of binary array $X = [x(s_1, s_2, \dots, s_n)]$ is defined as

$$F_X(x_1, x_2, \dots, x_n) = \sum_{s_1=0}^{N_1-1} \dots \sum_{s_n=0}^{N_n-1} x(s_1, s_2, \dots, s_n) x_1^{s_1} \dots x_n^{s_n} \quad (2)$$

Definition 4. Suppose that (U, V) is (E, k, k', λ) -differences set pairs of finite group $Z_{t_1} \times Z_{t_2} \dots \times Z_{t_n}$, let

$$p(s_1, s_2, \dots, s_n) = \begin{cases} 1 & (s_1, s_2, \dots, s_n) \in U \\ 0 & (s_1, s_2, \dots, s_n) \notin U \end{cases} \quad (3)$$

$$q(s_1, s_2, \dots, s_n) = \begin{cases} 1 & (s_1, s_2, \dots, s_n) \in V \\ 0 & (s_1, s_2, \dots, s_n) \notin V \end{cases} \quad (4)$$

Then, the array pairs (X, Y) consists of array $X = x(s_1, s_2, \dots, s_n) = 1 - 2p(s_1, s_2, \dots, s_n)$ and array $Y = y(s_1, s_2, \dots, s_n) = 1 - 2q(s_1, s_2, \dots, s_n)$ is called generated binary array pairs of differences set pairs (U, V) , this method for constructing array pairs is called differences set pairs method.

3 Differences Set Pairs Method

Theorem 1. (U, V) is (E, k, k', λ) -differences set pairs in finite group $Z_{t_1} \times Z_{t_2} \dots \times Z_{t_n}$, if parameters of (U, V) satisfying $E - 2(k + k') + 4\lambda = 0$, $\lambda \neq |U \cap V|$, then, the binary

array pairs (X, Y) constructed by differences set pairs (U, V) is the perfect binary array pairs.

Proof. The autocorrelation function of perfect binary array pairs (X, Y) is

$$\begin{aligned} R_{XY}(u_1, u_2, \dots, u_n) &= \sum_{s_1, s_2, \dots, s_n} x(s_1, s_2, \dots, s_n) y(s_1 + u_1, s_2 + u_2, \dots, s_n + u_n) \\ &= \sum_{s_1, s_2, \dots, s_n} (1 - 2p(s_1, s_2, \dots, s_n))(1 - 2q(s_1 + u_1, s_2 + u_2, \dots, s_n + u_n)) \\ &= \sum_{s_1, s_2, \dots, s_n} (1 - 2p(s_1, s_2, \mathbb{L}, s_n) - 2q(s_1 + u_1, s_2 + u_2, \mathbb{L}, s_n + u_n) \\ &\quad + 4p(s_1, s_2, \mathbb{L}, s_n)q(s_1 + u_1, s_2 + u_2, \mathbb{L}, s_n + u_n)) \\ &= E - 2k - 2k' + 4 \sum_{\substack{(s_1, s_2, \mathbb{L}, s_n) \in U \\ (s_1 + u_1, s_2 + u_2, \mathbb{L}, s_n + u_n) \in V}} 1 \end{aligned}$$

Let $e = |U \cap V|$ then $e \neq \lambda$,

$$\sum_{\substack{(s_1, s_2, \dots, s_n) \in U \\ (s_1 + u_1, s_2 + u_2, \dots, s_n + u_n) \in V}} 1 = \begin{cases} e & (u_1, u_2, \dots, u_n) = (0, 0, \dots, 0) \\ \lambda & (u_1, u_2, \dots, u_n) \neq (0, 0, \dots, 0) \end{cases}$$

From the definition of perfect binary array pairs, we can see that the binary array pairs (X, Y) constructed by differences set pairs (U, V) is the perfect binary array pairs.

Example 1. (U, V) is $(12, 7, 7, 4)$ – differences set pairs in finite group $Z_3 \times Z_4$, then the binary array pairs (X, Y) constructed by differences set pairs (U, V) is the perfect binary array pairs, where

$$\begin{aligned} U &= \{(0,1), (0,2), (1,0), (1,1), (2,0), (2,2), (2,3)\} \\ V &= \{(0,0), (0,1), (1,1), (1,2), (2,0), (2,2), (2,3)\}, \end{aligned}$$

$$\left[\begin{array}{c} X = \begin{bmatrix} + & - & - & + \\ - & - & + & + \\ - & + & - & - \end{bmatrix} \quad Y = \begin{bmatrix} - & - & + & + \\ + & - & - & + \\ - & + & - & - \end{bmatrix} \right].$$

4 Characteristic Polynomial Method

Theorem 2. The binary array pairs (X, Y) is the perfect binary array pairs if and only if

$$\begin{cases} F_X(x_1, x_2, \dots, x_n) F_Y(x_1^{-1}, x_2^{-1}, \dots, x_n^{-1}) = E \\ \text{mod } x_1^{N_1} - 1, \dots, x_n^{N_n} - 1 \end{cases} \tag{5}$$

Proof. In the conditions of $(\text{mod } x_1^{N_1} - 1, \dots, x_n^{N_n} - 1)$,

$$\begin{aligned}
 &F_X(x_1, x_2, \dots, x_n)F_Y(x_1^{-1}, x_2^{-1}, \dots, x_n^{-1}) \\
 &= \sum_{s_1=0}^{N_1-1} \dots \sum_{s_n=0}^{N_n-1} x(s_1, s_2, \dots, s_n)x_1^{s_1} \dots x_n^{s_n} \times \sum_{r_1=0}^{N_1-1} \dots \sum_{r_n=0}^{N_n-1} y(r_1, r_2, \dots, r_n)x_1^{-r_1} \dots x_n^{-r_n} \\
 &= \sum_{s_1=0}^{N_1-1} \dots \sum_{s_n=0}^{N_n-1} \sum_{r_1=0}^{N_1-1} \dots \sum_{r_n=0}^{N_n-1} x(s_1, s_2, \dots, s_n)(x_1^{s_1} \dots x_n^{s_n})y(r_1, r_2, \dots, r_n)x_1^{-r_1} \dots x_n^{-r_n} \\
 &= \sum_{s_1=0}^{N_1-1} \dots \sum_{s_n=0}^{N_n-1} \sum_{u_1=0}^{N_1-1} \dots \sum_{u_n=0}^{N_n-1} x(s_1, s_2, \dots, s_n)y(s_1 + u_1, s_2 + u_2, \dots, s_n + u_n)x_1^{-u_1} \dots x_n^{-u_n} \\
 &= \sum_{s_1=0}^{N_1-1} \dots \sum_{s_n=0}^{N_n-1} x(s_1, s_2, \dots, s_n)y(s_1, s_2, \dots, s_n) \\
 &\quad + \sum_{s_1=0}^{N_1-1} \dots \sum_{s_n=0}^{N_n-1} \sum_{u_1=1}^{N_1-1} \dots \sum_{u_n=1}^{N_n-1} x(s_1, s_2, \dots, s_n)y(s_1 + u_1, s_2 + u_2, \dots, s_n + u_n)x_1^{-u_1} \dots x_n^{-u_n} \\
 &= R_{XY}(0, 0, \dots, 0) + \sum_{s_1=0}^{N_1-1} \dots \sum_{s_n=0}^{N_n-1} \sum_{u_1=1}^{N_1-1} \dots \sum_{u_n=1}^{N_n-1} x(s_1, \dots, s_n)y(s_1 + u_1, \dots, s_n + u_n)x_1^{-u_1} \dots x_n^{-u_n}
 \end{aligned}$$

From the definition of perfect binary array pairs, we can see that the binary array pairs (X, Y) is perfect binary array pairs if and only if

$$F_X(x_1, x_2, \dots, x_n)F_Y(x_1^{-1}, x_2^{-1}, \dots, x_n^{-1}) = E$$

Theorem 3. Suppose that binary array pairs (X_1, Y_1) and (X_2, Y_2) with the sizes of $N_1 \times N_2 \times \dots \times N_n$ were perfect binary array pairs, and they have the same peak E , then there exists a perfect binary array pairs (X, Y) with the size of $N_1 \times N_2 \times \dots \times 2N_k \times \dots \times 2N_l \times \dots \times N_n$, where $1 \leq k \leq l \leq n$.

Proof. Suppose that characteristic polynomials of binary arrays X_1, Y_1, X_2 and Y_2 are $F_{X_1}(x_1, x_2, \dots, x_n)$, $F_{Y_1}(x_1, x_2, \dots, x_n)$, $F_{X_2}(x_1, x_2, \dots, x_n)$ and $F_{Y_2}(x_1, x_2, \dots, x_n)$, then $F_{X_1}(x_1, x_2, \dots, x_n)F_{Y_1}(x_1^{-1}, x_2^{-1}, \dots, x_n^{-1}) = E$, and $F_{X_2}(x_1, x_2, \dots, x_n)F_{Y_2}(x_1^{-1}, x_2^{-1}, \dots, x_n^{-1}) = E$, for binary array pairs (X_1, Y_1) and (X_2, Y_2) having the same peak E .

In the conditions of $(\text{mod } x_1^{N_1} - 1, \dots, x_k^{2N_k} - 1, \dots, x_l^{2N_l} - 1, \dots, x_n^{N_n} - 1)$, let

$$\begin{aligned}
 &P_X(x_1, x_2, \dots, x_n) \\
 &= (1 + x_k^{s_k})F_{X_1}(x_1, \dots, x_k, \dots, x_l^2, \dots, x_n) + x_l(1 - x_k^{s_k})F_{X_2}(x_1, \dots, x_k, \dots, x_l^2, \dots, x_n) \\
 &P_Y(x_1, x_2, \dots, x_n) \\
 &= (1 + x_k^{s_k})F_{Y_1}(x_1, \dots, x_k, \dots, x_l^2, \dots, x_n) + x_l(1 - x_k^{s_k})F_{Y_2}(x_1, \dots, x_k, \dots, x_l^2, \dots, x_n)
 \end{aligned}$$

then the coefficient of polynomials $P_X(x_1, x_2, \dots, x_n)$ and $P_Y(x_1, x_2, \dots, x_n)$ is ± 1 ,

$$\begin{aligned}
 &P_X(x_1, x_2, \dots, x_n)P_Y(x_1^{-1}, x_2^{-1}, \dots, x_n^{-1}) \\
 &= [(1+x_k^{s_k})F_{X_1}(x_1, \dots, x_k, \dots, x_l^2, \dots, x_n) + x_l(1-x_k^{s_k})F_{X_2}(x_1, \dots, x_k, \dots, x_l^2, \dots, x_n)] \\
 &\quad \times [(1+x_k^{-s_k})F_{Y_1}(x_1^{-1}, \dots, x_k^{-1}, \dots, x_l^{-2}, \dots, x_n^{-1}) + x_l^{-1}(1-x_k^{-s_k})F_{Y_2}(x_1^{-1}, \dots, x_k^{-1}, \dots, x_l^{-2}, \\
 &\quad \dots, x_n^{-1})] \\
 &= 2(1+x_k^{s_k})F_{X_1}(x_1, \dots, x_k, \dots, x_l^2, \dots, x_n)F_{Y_1}(x_1^{-1}, \dots, x_k^{-1}, \dots, x_l^{-2}, \dots, x_n^{-1}) \\
 &\quad + 2(1-x_k^{s_k})F_{X_2}(x_1, \dots, x_k, \dots, x_l^2, \dots, x_n)F_{Y_2}(x_1^{-1}, \dots, x_k^{-1}, \dots, x_l^{-2}, \dots, x_n^{-1}) \\
 &\quad + x_l^{-1}(1+x_k^{s_k})(1-x_k^{-s_k})F_{X_1}(x_1, \dots, x_k, \dots, x_l^2, \dots, x_n)F_{Y_2}(x_1^{-1}, \dots, x_k^{-1}, \dots, x_l^{-2}, \dots, x_n^{-1}) \\
 &\quad + x_l(1-x_k^{s_k})(1+x_k^{-s_k})F_{X_2}(x_1, \dots, x_k, \dots, x_l^2, \dots, x_n)F_{Y_1}(x_1^{-1}, \dots, x_k^{-1}, \dots, x_l^{-2}, \dots, x_n^{-1}) \\
 &= 4E
 \end{aligned}$$

From the theorem 2, we can see that the binary array pairs (X, Y) corresponding to polynomials $P_X(x_1, x_2, \dots, x_n)$ and $P_Y(x_1, x_2, \dots, x_n)$ is the perfect binary array pairs with the sizes of $N_1 \times N_2 \times \dots \times 2N_k \times \dots \times 2N_l \dots \times N_n$.

Theorem 4. Suppose that binary array pairs (X_1, Y_1) and (X_2, Y_2) with the sizes of $N_1 \times N_2 \times \dots \times N_n$ are perfect binary array pairs, and they have the same peak E , then there exists a perfect binary array pairs (X, Y) with the size of $N_1 \times N_2 \times \dots \times 4N_k \times \dots \times N_n$, where $1 \leq k \leq n$.

Proof. Suppose that characteristic polynomials of binary arrays X_1, Y_1, X_2 and Y_2 are $F_{X_1}(x_1, x_2, \dots, x_n)$, $F_{Y_1}(x_1, x_2, \dots, x_n)$, $F_{X_2}(x_1, x_2, \dots, x_n)$ and $F_{Y_2}(x_1, x_2, \dots, x_n)$, then

$$\begin{aligned}
 &F_{X_1}(x_1, x_2, \dots, x_n)F_{Y_1}(x_1^{-1}, x_2^{-1}, \dots, x_n^{-1}) = E \\
 &F_{X_2}(x_1, x_2, \dots, x_n)F_{Y_2}(x_1^{-1}, x_2^{-1}, \dots, x_n^{-1}) = E
 \end{aligned}$$

on account of (X_1, Y_1) and (X_2, Y_2) having the same peak E .

In the conditions of $(\text{mod } x_1^{N_1} - 1, \dots, x_k^{4N_k} - 1, \dots, x_n^{N_n} - 1)$, let

$$\begin{aligned}
 &P_X(x_1, x_2, \dots, x_n) \\
 &= (1-x_k^{2s_k})F_{X_1}(x_1, \dots, x_k^2, \dots, x_n) + x_k(1+x_k^{2s_k})F_{X_2}(x_1, \dots, x_k^2, \dots, x_n)
 \end{aligned}$$

$$\begin{aligned}
 &P_Y(x_1, x_2, \dots, x_n) \\
 &= (1-x_k^{2s_k})F_{Y_1}(x_1, \dots, x_k^2, \dots, x_n) + x_k(1+x_k^{2s_k})F_{Y_2}(x_1, \dots, x_k^2, \dots, x_n)
 \end{aligned}$$

Then, the coefficient of polynomials $P_X(x_1, x_2, \dots, x_n)$ and $P_Y(x_1, x_2, \dots, x_n)$ is ± 1 ,

$$\begin{aligned}
 &P_X(x_1, x_2, \dots, x_n)P_Y(x_1^{-1}, x_2^{-1}, \dots, x_n^{-1}) \\
 &= [(1-x_k^{2s_k})F_{X_1}(x_1, \dots, x_k^2, \dots, x_n) + x_k(1+x_k^{2s_k})F_{X_2}(x_1, \dots, x_k^2, \dots, x_n)]
 \end{aligned}$$

$$\begin{aligned}
 & \times [(1 - x_k^{-2s_k})F_{Y_1}(x_1^{-1}, L, x_k^{-2}, L, x_n^{-1}) + x_k^{-1}(1 + x_k^{-2s_k})F_{Y_2}(x_1^{-1}, L, x_k^{-2}, L, x_n^{-1})] \\
 = & 2(1 - x_k^{2s_k})F_{X_1}(x_1, L, x_k^2, L, x_n)F_{Y_1}(x_1^{-1}, L, x_k^{-2}, L, x_n^{-1}) \\
 & + 2(1 + x_k^{2s_k})F_{X_2}(x_1, L, x_k^2, L, x_n)F_{Y_2}(x_1^{-1}, L, x_k^{-2}, L, x_n^{-1}) \\
 & + x_k^{-1}(1 - x_k^{2s_k})(1 + x_k^{-2s_k})F_{X_1}(x_1, L, x_k^2, L, x_n)F_{Y_2}(x_1^{-1}, L, x_k^{-2}, L, x_n^{-1}) \\
 & + x_k(1 + x_k^{2s_k})(1 - x_k^{-2s_k})F_{X_2}(x_1, L, x_k^2, L, x_n)F_{Y_1}(x_1^{-1}, L, x_k^{-2}, L, x_n^{-1}) \\
 = & 4E
 \end{aligned}$$

From the theorem 2, we can see that the binary array pairs (X, Y) corresponding to polynomials $P_X(x_1, x_2, \dots, x_n)$ and $P_Y(x_1, x_2, \dots, x_n)$ is the perfect binary array pairs with the sizes of $N_1 \times N_2 \times \dots \times 4N_k \times \dots \times N_n$.

Example 2. Binary array pairs (X_3, Y_3) and (X_4, Y_4) are perfect binary array pairs, which are constructed from perfect binary array pairs (X_1, Y_1) and (X_2, Y_2) by using constructing methods of theorem 3 and theorem 4, where (X_1, Y_1) and (X_2, Y_2) have the same peak $E = 4$,

$$\begin{aligned}
 & [X_1 = [+ \ + \ + \ -] \quad Y_1 = [+ \ + \ + \ -]] \\
 & [X_2 = [+ \ - \ + \ +] \quad Y_2 = [+ \ - \ + \ +]] \\
 & \left[X_3 = \begin{bmatrix} + & + & + & - & + & - & + \\ + & - & + & + & + & - & - \end{bmatrix} \quad Y_3 = \begin{bmatrix} + & + & + & - & + & + & - & + \\ + & - & + & + & + & - & - & - \end{bmatrix} \right] \\
 & \left[X_4 = \begin{bmatrix} + & + & + & - \\ + & - & + & + \\ - & - & - & + \\ + & - & + & + \end{bmatrix} \quad Y_4 = \begin{bmatrix} + & + & + & - \\ + & - & + & + \\ - & - & - & + \\ + & - & + & + \end{bmatrix} \right].
 \end{aligned}$$

5 Conclusions

The perfect signal and its design method play an important role in the optimizing design in the area of modernistic communication, radar, sonar, navigation, space ranging and controlling and electronically antagonism system as well as new material uses. To study the properties and constructing methods of all kinds of sequence (array) in depth is important both in theory and application. The method of differences set pairs for constructing perfect binary array pairs is presented based on analyzing the theory of perfect binary array, perfect binary array pairs and differences set pairs. We define the method of constructing binary array from differences set, and proofs in a certain conditions that binary array pairs, which constructed from differences, is perfect binary array pairs. From the study of the design method of

polynomial, the characteristic polynomial method for constructing perfect binary array pairs is proposed.

References

1. Calabro, D., Wolf, J.K.: On the synthesis of two-dimensional arrays with desirable correlation properties. In: Proc. IEEE Information And Control, pp. 530–560 (1968)
2. Zhao, X.-q., He, W.-c., Wang, Z.-w., et al.: The Theory of Perfect Binary Array Pairs. *Acta Elecctonica Sinica* 27, 34–37 (1999)
3. Jia, Y.-g., Guo, J.-s.: Study on Perfect Ternary Array Paris. In: National Youth Communication Conference of China, pp. 268–275 (2006)
4. Jia, Y.-g., Guo, J.-s., Cui, L., et al.: The Study of Methods for Constructing Perfect Ternary Array Pairs. *Journal of Electronics & Information Technology* 30(4), 814–816 (2008)
5. Xu, C.-q.: Differences Set Pairs and Approach for the Study of Perfect Binary Array Pairs. *Acta Elecctonica Sinica* 29(1), 87–89 (2001)

Case-Based Reasoning for Data Verification with Data Structure in M&S

Guozhen Xu, Peng Jiao, and Yabing Zha

College of Mechatronics Engineering and Automation, National University of Defense
Technology, Changsha, 410073, China
xuguozen1234@163.com

Abstract. Data verification is an important approach to improve simulation data quality, data verification criteria and measurement are needed before verifying data. A novel method using CBR for data verification is proposed in this paper. Firstly, a template for data verification case representation based on frame is established, and then a case retrieving strategy and similarity measurement are proposed, finally, construction and maintenance principle of data verification case warehouse are presented.

Keywords: data quality, data verification, case-based reasoning, case representation, similarity.

1 Introduction

Models and simulations (M&S) require data to define the scenario, environment, doctrine, weapon system performance, and other factors [1]. Simulation system relies on data, the function of simulation system and credibility of simulation result depend on data quality. Data verification, validation and certification (VV&C) is an important approach to improve data quality for data producer and user. Data verification is checking the internal consistency and correctness of data, many database management systems provide facilities for performing some check, including checking allowed values range and data types. But, different verification methods and criteria may apply to a given database under different conditions or for different datasets, so it is difficult to establish measurement and criteria for data verification.

Case-based reasoning (CBR) is successfully applied in many areas as a knowledge reuse technology; we can find a solution for current problem by accessing the similar problem in case warehouse. A method based on CBR for data verification is proposed in this paper, when a new simulation data is needed to verify, by matching this data to datasets in a constructed data verification case warehouse, verification measurement and criteria for this data can be established.

2 Concept and Solution

2.1 Data Verification

The established DoD definition for data verification is presented here [2]:

Data Verification: The assessment of data with the intent to ensure that they satisfy specified constraints and relationships, conform to specified data standards, and are transformed and formatted properly for their intended use. Data user verification performs this assessment using specifications derived from the intended use of data in a particular model for a particular purpose. Data producer verification performs this assessment using standards and specifications derived from the producer's mission statement or the requirements of a specific data user or community.

2.2 Case-Based Reasoning

CBR is an important method for problem resolving and learning in artificial intelligence. The theory of CBR is solving the new problem with using previous experience. The cycle of reasoning constitute 4R process, naming them 4R cycle: *retrieve* the most similar case(s); *reuse* the case(s) to attempt to solve the problem; *revise* the proposed solution if necessary; *retain* the new solution as a part of a new case. A new problem is matched against cases in the case base and one or more similar cases are retrieved, a solution suggested by the matching cases is then reused and tested for success, unless the retrieved case is a close match the solution will probably have to be revised producing a new case that can be retained.

2.3 Case Based Reasoning for Data Verification

When verifying new simulation data, existing verification measurement and criteria are very important to the new data, how to make use of this knowledge effectively? The data verification cases can be organized and stored with CBR. The theory of CBR for data verification is presented in figure 1, when new simulation data need to verify, the characters of this data are extracted and matched with the characters of existing case, a existing case or more can be found after retrieving; then proposal verification methods and criteria can be obtained by reusing; also confirmed verification methods and criteria can be fixed after revising; finally, the data can be verified with this verification measurement and criteria. Also this new data verification case can be retained if needed.

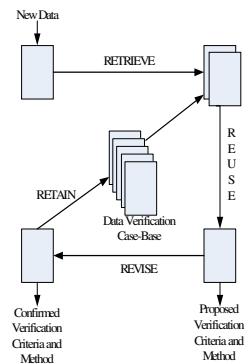


Fig. 1. CBR for data verification

3 Issues of CBR for Data Verification

During the process of data verification which based on CBR, some issues included: data verification case representation, characters extracting of new data, data

verification case retrieving strategy and method, and data verification case warehouse constructing and maintenance.

3.1 Data Verification Case Representation

Case representation includes: first order predicate logic representation, frame representation, semantic network representation, and object oriented representation. First order predicate logic representation can only describe simple problem, if the relation and reciprocity are complicated, knowledge representations like frame, semantic network and object oriented are needed. Frame representation is adopted here to describe the data verification cases.

A frame consists of a frame name and some “slots”, and each slot may include some side values, slot values and side values can be numbers, strings, Boolean values, some actions or processes under some condition, and even another frame name. A case representation template for simulation data verification is presented in table 1.

Table 1. Case representation template for simulation data verification

Case of Simulation Data Verification NO.X
Slot 1 simulation data representation
Side 1 base information of simulation data
Slot 2 character representation of simulation data
Side 1: source of simulation data
Side values: approach of getting data , authority of data source , credibility of data
Side 2: character of data amplitude and frequency
Side values: character of amplitude , character of time domain , character of frequency of frequency domain
Side 3: transform process
Side values: transform process undergone , transform method, unit transform
Side 4: purpose of data
Side values: purpose for using, constraints for using
.....
Side n :
Slot 3 Criteria and method for simulation data verification
Side 1: criteria for data verification
Side values: consistency criteria , integrity criteria , correctness criteria, accuracy criteria
Side 2: method for data verification
Side values: subjective verification method , objective verification method , qualitative verification method , quantitative verification method

3.2 Characters Extracting of New Data

Characters extracting of new data is a process including analyzing the data and extracting the characters for case retrieving. Firstly, the purpose of data should be

extracted for dividing, and then the source of data, time and frequency of data and other characters should be extracted. There is not a universal method for characters extracting, so a standard for characters is needed to be established before characters extracting, with referring to the standard, characters of new data can be extracted manually.

3.3 Data Verification Cases Retrieving Strategy and Method

Cases retrieving strategy

A two steps retrieving strategy for data verification is proposed here:

Step 1: dividing data case by approximate selection which bases on purpose of data;

Step 2: retrieving data case by precise selection with the method for computing similarity.

We divide the cases in case warehouse into l case volumes. A vector $Z_i = [z_{1i}, z_{2i}, \dots, z_{ni}]$ is built to describe the purpose of data, and $i = 1, 2 \dots l$, if the purpose exists, then set $z_{1i} = 1$, or else $z_{1i} = 0$.

The vector of current data is $Z_k = [z_1, z_2, \dots, z_n]$, we can put current data into some case volume by matching. An example is given in table 2, it shows that current case is matching with case volume 3, because only in case volume 3, the third purpose of data exists. After doing this work, we can go to step 2.

Table 2. Matching of approximate selection

Name	Values of z
Case volume 1	0 1 0 1 0 0 0
Case volume 2	0 0 0 1 0 1 0
Case volume 3	1 0 1 0 1 0 0
Current case	0 0 1 0 0 0 0

Case retrieving method

Precise selection is implemented with a new similarity method, and strings and numerical values are all considered in this method.

First we consider the similarity value of strings: Now two strings are given, we define the ratio of the same strings to the longer strings as similarity value of strings, the expression is as followed:

$$p = \frac{C(S_l, S_s)}{S_l} \tag{1}$$

$C(S_l, S_s)$ is the same strings of S_l and S_s , S_l is the longer strings.

Then similarity of numerical values is considered here: two values are given as $X(n) = (x^{(1)}, x^{(2)}, \dots, x^{(n)})$, $Y(m) = (y^{(1)}, y^{(2)}, \dots, y^{(m)})$, and $n > m$, similarity is computed by three steps:

Step1: $Y(m)$ is extended as the same dimension as $X(n)$,
 set $Y(n) = [Y(m), 0_{n-m,1}]$;

Step2: compute similarity value in each point

$$q^{(k)} = \frac{|x^{(k)} - |x^{(k)} - y^{(k)}|}{x^{(k)}}, (k = 1, 2, \dots, n) \tag{2}$$

Step3: integrate similarity of each point, q which represents similarity of $X(n)$ and $Y(m)$ is gained:

$$q = \sum_{k=1}^n \beta_k q^{(k)} \tag{3}$$

Often $\beta_k = \frac{1}{n}$.

At last, the whole similarity which include string and numerical value is computed as

$$sim(D_I, D_R) = \frac{\sum_{i=1}^N w_i \cdot q_i + \sum_{j=1}^M v_j \cdot p_j}{\sum_{i=1}^N w_i + \sum_{j=1}^M v_j} \tag{4}$$

D_I is the case in data verification case warehouse, D_R is the current case needed to solve, N is the characters number of numerical values, M is the characters number of strings, w_i is character weight of numerical value which order is i , v_j is character weight of string which order is j .

3.4 Data Verification Case Warehouse Constructing and Maintenance

Case warehouse constructing

The data verification cases can not be used to construct the case warehouse immediately, all the cases should be analyzed and characters should be extracted before constructing the case warehouse, the cases can only be represented by the characters. When frame is adopted to represent cases, these characters are expressed as slots. The main frame and slots correspond to table and item in database, and if the slot is a child frame, the child frame correspond to another table in database, all these tables constitute relationships in database. With the technology in database, each case can be built in database. By this way, cases are stored in the case warehouse with a table structure, and characters of case are represented by the items in the table. Cases can be stored by filling the items of data table.

Case warehouse maintenance

Three principles should be complied when case is added into case warehouse:

1. Case can be added when the case comes from the self-learning system in CBR;
2. Case can be added if the user need;
3. Case can be added if it is emphasized by subject matter experts, or new case can not be solved if the case is not added.

Case should be deleted when the case is useless, or there is a new case which is better than this case. Case can but only be deleted by person who maintains the system.

4 Conclusion

All simulation data can only be used after data VV&C, it is an important issue to establish measurement and criteria for data verification. Data verification based on CBR is introduced in this paper, case warehouse can be constructed under previous data verification cases, and it is used to establish the measurement and criteria for succeeding new data. Case representation, case retrieving and case maintenance is studied in this paper. Research in this paper provide a new approach for data verification, however, considering the special features of simulation data application, a lot of work is required.

References

1. Xue, Q.: Basis of Simulation for Combat equipment. National Defense Industry Press (2010)
2. Modeling and Simulation (M&S) Master Plan, DoDD 5000.59-P. Edited by Secretary of Defense for Acquisition and Technology (1995)
3. DeLong, B.B., Miller, M.O.: Verification and Validation Ensuring Data Credibility. In: European Simulation Interoperability Workshop 2001 SIW, pp. 206–214 (2001)
4. Rothenberg, J.: A Discussion of Data Quality for Verification, Validation and Certification (VV&C) of Data to be used in Modeling. Edited by Rand Project Memorandum PM-709-DMSO, pp. 24–61 (1997)
5. Chen, T.: Chinese characters matching arithmetic. Edited by Computer Engineering 29(13), 118–124 (2003)
6. Waston, I., Marir, F.: Case-Based Reasoning: A Review. Edited by Knowledge Engineering (2007)
7. Liu, J.-n., Liu, T., He, X.: Research on case retrieval strategy in fault diagnosis system based on case-based reasoning. Edited by J. Huazhong Univ. of Sci. & Tech (2008)
8. Tang, W.-y., Li, L.-j.: Case Representation and Case Warehouse Creating in CBR. Edited by Journal of Xi'an Univ. of Post and Telecommunications (2006)

Discussion on Prioritization Method of Make-to-Order Corporation for Sales Products

Hongyan Shi, Mei Chu, Man Liu, and Tao Wang

Xuzhou Air Force College Basic department Xuzhou, China
shy7823@163.com

Abstract. The final products of make-to-order corporation don't finalize the design. According to the different customer requirement the orders are different. So the product mix and product process may be different. Therefore, it can't make a product plan as the industry that manufactures standard products, it should focus on the customer's order, all of the work should keep order as the central task. The system of program management is an order-driven market management, whose aim is to make sure of order delivery. For example, Xuzhou weighing technology Company, LTD, ERP production management system. How to work out sorting order optimization is the key to solve the problem of ERP based on making to order.

Keywords: Ranking Model, Prior rank, Date of delivery.

1 Introduction

Sorting, according to the distribution time and different time in order, refers to use the limited manpower material resources to achieve the optimal or approximate optimal target. Generally speaking, sorting involves work pieces, the machine collections and work piece processing routes. And the goal involves some indexes, such as the job processing time, work piece delay degree and total resources occupation. It takes an important role in improving work efficiency and economic benefit on condition of existing conditions.

The primary task for sorting is to establish a ranking model and then according to the sorting model, adopt corresponding solving algorithm to get the optimal or approximate optimal solution of sorting. But ranking model is not fixed, different industries and different enterprises have different ranking model and different solving algorithm. Therefore it should establish corresponding sorting model theory according to concrete characteristics and sorting theory in order to look for solving algorithm.

2 Priority Sort Overview

Prioritization orders plays two important roles in Xuzhou Sanyuan management enquiry module. One is that due to 001 products in short supply and productivity insufficient, not only the date of delivery but also the order priority need to be

considered when determining on scheduling the first row in single simulation scheduling orders inquiry. There might be a lot of orders in approximate date of delivery, it must be chosen by limited ability. The other one is that in a single, in order to carry all the first priority calculating the choice to be inserted in the highest priority order, choose to insert already row in the lowest priority order, and to compare out first single, these are worth inserted through comparison to draw priority.

3 Means of Order Sorting

Arrange production orders are many index weight decisions. It doesn't only depend on the date of delivery, but also on other influences, such as cost, order amount, profit, product complexity, quality, material satisfaction and etc, which weight differently. The Analytic Hierarchy Process (AHP) can solve this kind of problems. Therefore, this paper is based on the index weight decision-making more solution – Analytic Hierarchy Progress (AHP) [2] [3] [4] to realize order priority sorting.

It provides a comprehensive and rational framework for structuring a decision problem, for representing and quantifying its elements, for relating those elements to overall goals, and for evaluating alternative solutions. It is used around the world in a wide variety of decision situations, in fields such as economic planning and management, energy policy and distribution, etc. Analytic hierarchy progress is a kind of common decision-making method. It expresses decisions through establishing multi-layer decision index system and makes alternative priority based on policymakers' judgment. Systematic analyzing on problems of social, economic and scientific management field, people usually have to face the system that is constituted with many interconnected and interacted elements and lack of quantitative data. Analytic Hierarchy Process provide a new simple and practical method for this kind of problems of decision and sorting.

Order priority sorting can be divided into the following several steps:

(1) Definition of evaluating indexes

To confirm the order priority, the first thing is to confirm the index and weight of order sorting. According to their own profit, every department of Sanyuan Co. Ltd. has different points of view. The sales department takes customer demand as index, the financial department takes order revenue as index and the production department takes production costs as index. From a strategic point of view, it doesn't only need consider elements such as delivery date, cost, quality and etc, but also needs consider its own production capacity and resources constraints, etc.

According to the constraint theory, there are three indexes measuring order sorting for production, output, inventory and production cost, and three for marketing, customer importance, delivery reliability, service and etc.

Combined with the specific conditions of extraterrestrial company, they choose the following elements as index to evaluate order priority: delivery date, profit, customer importance, order amount, cost, quality requirement, order materials satisfaction and etc. Enterprise can choose one among these indexes. They can also choose their own special indexes.

- Delivery time: the main index. The urgency of order delivery is the most important element of agility. The urgency of order delivery refers to the length between current date and delivery date. The great urgency is important, otherwise, less important.
- profit: the influences of profit. The high profit order has a high order sorting, otherwise, low.
- customer importance: refers to the current customers importance. The more important customer can get higher order sorting, otherwise, lower.
- order amount: The high order amount has the first priority, otherwise, later.
- cost: refers to the amount of production costs. The high production cost gets a low priority, otherwise, high.
- quality requirement: this index refers to the quality of the current order production and the difficulty of processing. The order of high quality demanding and difficult processing can't get low priority, otherwise, high.

Indexes are interconnected and also conflicted with each other. For example, high order amount means that it will occupy high cost and a important customer take a low profit order. So it needs more comprehensive indexes, and the above is only a hypothesis on the evaluation of a single order.

(2) Definition of evalusting indexes weighing

Weight is decided by business operators themselves according to the actual conditions and their strategies, such as customers importance degree, which can generally be divided into very important, important, more important, general, not important. Each level, in the right range, gives certain weights, importance weights of high grade is big.

- delivery time: according to the urgent delivery, generally can be divided into: degree of emergency, emergency and comparison is very urgent, and the general, extension and so on several levels. Value for: 1, respectively, 0.4, 0.6 to 0.8. 0.2.
- profit: according to the size of the profit, can generally be divided into: great, big, bigger, general, profits rarely five etc, are connects is: 1, 0.8, 0.6, 0.4, 0.2.
- customer importance: according to customer's important extent points: very important (strategic customers), important (gold customers), more important (profit), general customer important (ordinary customers), not important (scattered clients, small customer) five etc. Value for: 1, respectively, 0.6 to 0.8, 0.4, 0.2.
- order according to the amount the size of the order amount, are generally divided into: great, big, bigger, general, infantile a level. Value: 1, respectively, 0.6 to 0.8 0.4, 0.20 .
- cost: according to take fund calculate, generally divided into: high, high, high, general, low five etc. Value: 0.2, respectively, 0.6 to 0.8, 0.4, 1.
- the quality requirements for the quality of the products: press, generally divided into: request points high, high, high, and the general, low five etc. Value: 0. 2 respectively, 0. 4, 0. 6, 0. 8, 1.

(3) Order Priority Calculation

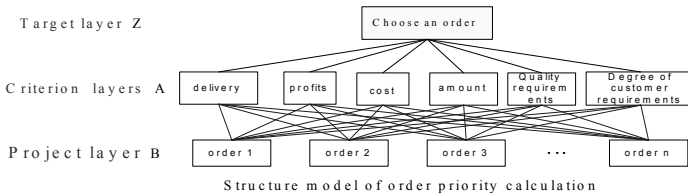
Extrattrestrial production management system uses analytic hierarchy process (AHP) to calculate the order priority main steps below:

4 Hierarchical Structure Building

Establish three layers: target strata, criterion layer, scheme layer.

According to the actual situation of extratrestrial company to level the levels, build choice as follows:

- Target layer: choose one order;
- Criterion layers A : the order priority each index;
- Project layer B : all your orders;



In make-to-order corporation, in order to meet the date of delivery, places the priority of customer orders to traversal compare and sort the production order in planning period(that is to assign the order that has been made and wait before device group to specific equipment by priority values assigned). The result of sorting the production work order is not only to arrange the order of the production line operations, but also to make the producing plan for each device. The plan identifies the processing time and objects in the device of each working procedure, and the relationship between process and equipment distribution will be subsequently identified.

References

1. Zhao, Z., Zhou, J.: Sorting and search theory and algorithm, vol. 6. Science press, Beijing (1993)
2. Lu, Y.: About the method of AHP theory and applied research. Master Thesis, Nanjing University of Aeronautics and Astronautics (3) (2002)
3. Wang, Y., Li, J.: Ahp evaluation index weight coefficients in the application. The First Military Medical University Journal 19, 2289–2379 (1999)
4. Han, Z.: Using the AHP method determining target preferences. Engineering mathematics 17(4), 74–76 (2001)

Adaptive Pinning Synchronization of Delayed Complex Dynamical Networks

Haiyi Sun¹, Ning Li², and Yang Li¹

¹ College of Science, Shenyang JianZhu University, Shenyang, 110168, China
shy_xx@163.com, li_yang810@163.com

² Institute of Systems Science, Northeastern University, Shenyang, 110819, China
lining80@163.com

Abstract. In this paper, we study the adaptive pinning synchronization of complex dynamical networks based on intelligent materials with coupling delays and delays in the dynamical nodes. Via the theory of Lyapunov stability and adaptive pinning control technique, we design adaptive pinning feedback synchronization controller. The numerical example of the adaptive pinning synchronization problem has been also provided to demonstrate the effectiveness of the theory.

Keywords: complex networks, delays, intelligent materials, pinning control, synchronization.

1 Introduction

Recently, the study of various complex networks has attracted increasing attentions from researchers in various fields of physics, mathematics, engineering, and sociology [1]. There have been a rich body of literature on analyzing complex networks, and one of the most significant dynamical behaviors of complex networks that have been widely investigated is the synchronization motion of its dynamical elements [2]. Some synchronization phenomena are very useful, such as the synchronization with environmental changes, self-repair of damages in intelligent materials [3].

In practice, the information transmission within complex networks is in general not instantaneous since the signal traveling speed is limited. This fact gives rise to the time delays that may cause undesirable dynamic network behaviors such as oscillation and instability. Therefore, time delays should be modeled in order to simulating more realistic networks. The time delay of the complex networks divides into two parts, one is in the couplings [4], and the other is in the dynamical nodes [5]. The synchronization of complex dynamical networks, which is considered both coupling delays and delays in the dynamical nodes, has only been lightly covered [6]. As a matter of fact, we can find a lot of examples in the real world which are characterized by complex dynamical networks with coupling delays and delays in the dynamical nodes. Therefore, it is imperative to further investigate complex dynamical networks with coupling delays and delays in the dynamical nodes.

2 Model Description and Preliminaries

The complex networks with coupling delays and delays in nodes can be described as follows:

$$\dot{x}_i(t) = f(x_i(t), x_i(t - \tau_1)) + \sum_{j=1}^N a_{ij} \Gamma_1 x_j(t) + \sum_{j=1}^N b_{ij} \Gamma_2 x_j(t - \tau_2) + u_i(t),$$

$$i = 1, 2, \dots, N \tag{1}$$

where $x_i(t) = (x_{i1}, x_{i2}, \dots, x_{in})^T \in R^n$ and $u_i(t)$ is the state and input variable of node i at time t , respectively. $f : R^n \times R^n \rightarrow R^n$ is a continuous and differentiable nonlinear vector function, individual intelligent materials dynamics is $\dot{x}_i(t) = f(x_i(t), x_i(t - \tau_1))$, τ_1 and τ_2 are the time delay of coupling delays and delays in the dynamical nodes, respectively, which are arbitrary but bounded, i.e., $\tau_1, \tau_2 \in (0, h]$, where h is a positive constant. $A = (a_{ij}) \in R^{N \times N}$ and $B = (b_{ij}) \in R^{N \times N}$ are the coupling matrices with zero-sum rows, which represent the coupling strength and the underlying topology for non-delayed configuration and delayed one τ_2 at time t , respectively, and $\Gamma_1, \Gamma_2 \in R^{n \times n}$ are positive diagonal matrices which describe the individual couplings between node i and j for non-delayed configuration and delayed one τ_2 at time t , respectively.

Definition 1. Let $x_i(t; t_0; \phi), i = 1, 2, \dots, N$ be a solution of delayed dynamical network (1), where $\phi = (\phi_1^T, \phi_2^T, \dots, \phi_N^T)^T$, $\phi_i = \phi_i(\theta) \in C([- \tau_m, 0], R^n)$ are initial conditions. If there is a nonempty subset $\Lambda \subseteq R^n$, such that ϕ_i take values in Λ and $x_i(t; t_0; \phi) \in R^n$ for all $t \geq t_0$ and

$$\lim_{t \rightarrow \infty} \|x_i(t; t_0; \phi) - s(t; t_0; s_0)\| = 0, \quad i = 1, 2, \dots, N \tag{2}$$

where $s(t; t_0; s_0) \in R^n$ is a solution of an isolate node, i.e.

$$s(t) = f(s(t), s(t - \tau_1)). \tag{3}$$

then the delayed dynamical network (1) is said to realize synchronization, and $\Lambda \times \Lambda \times \dots \times \Lambda$ is called the region of synchrony of the delayed dynamical network (1).

Define the error vector by

$$e_i(t) = x_i(t) - s(t), \quad i = 1, 2, \dots, N \tag{4}$$

Then the error system can be described by

$$\dot{e}_i(t) = f(x_i(t), x_i(t - \tau_1)) - f(s(t), s(t - \tau_1)) + \sum_{j=1}^N a_{ij} \Gamma_1 e_j(t) + \sum_{j=1}^N b_{ij} \Gamma_2 e_j(t - \tau_2) + u_i(t), \tag{5}$$

Then the synchronization problem of the complex network (1) is equivalent to the problem of stabilization of the error dynamical system (5).

Assumption 1. we always assume that $f(x_i(t), x_i(t - \tau_1))$ satisfied the uniform lipschiz condition with respect to the time t , i.e., for any $x(t) = (x_1(t), x_2(t), \dots, x_n(t))^T, y(t) = (y_1(t), y_2(t), \dots, y_n(t))^T \in R^n$, there exist constants $k_{ij} > 0, 1 \leq i \leq n$ satisfying

$$|f_i(x(t), x(t - \tau_1)) - f_i(y(t), y(t - \tau_1))| \leq \sum_{j=1}^n k_{ij} (|x_j(t) - y_j(t)| + |x_j(t - \tau_1) - y_j(t - \tau_1)|). \tag{6}$$

3 Adaptive Pinning Synchronization Control of the Delayed Complex Dynamical Networks

In the following, assume that $\|A\|_2 = \alpha$ and denote by ρ_{\min} the minimum eigenvalue of the matrix $(\bar{A} + \bar{A}^T)/2$. Let $\bar{A}^S = (\bar{A} + \bar{A}^T)/2$, where \bar{A} is a modified matrix of A via replacing the diagonal elements a_{ii} by $(\rho_{\min}/\alpha)a_{ii}$. \bar{B} has the same meaning of \bar{A} .

$$p_i = \frac{1}{2} \sum_{s=1}^m (2k_{is}^{2\epsilon} + k_{si}^{2(1-\epsilon)}), \quad q_i = \sum_{s=1}^m k_{si}^{2(1-\epsilon)}, \quad p = \max_{1 \leq i \leq m} p_i, \\ q = \max_{1 \leq i \leq m} q_i, \|\Gamma_i\| = \gamma_i.$$

Theorem 1. Suppose Assumption 1 holds. Then the pinning controlled delayed complex network (1) is globally synchronized with adaptive pinning controllers and updating laws

$$u_i(t) = \begin{cases} -\alpha_i(t)(x_i(t) - s(t)), & 1 \leq i \leq h; \\ 0, & h+1 \leq i \leq N; \end{cases} \tag{7} \\ \dot{\alpha}_i(t) = \begin{cases} \beta_i(t) \|x_i(t) - s(t)\|^2, & 1 \leq i \leq h; \\ 0, & h+1 \leq i \leq N; \end{cases}$$

provided that

$$\lambda_m \left(\gamma_1 \bar{A}^S + \frac{\gamma_2}{4\mu} \bar{B}^S \right) < -(p + \mu + \frac{q}{2}), \tag{8}$$

where μ can be any positive constant, $\beta_i > 0 (i = 1, 2, \dots, h)$.

Proof: Selecting a Lyapunov-Krasovskii function of the form

$$V(t) = \frac{1}{2} \sum_{i=1}^N e_i^T(t) e_i(t) + \sum_{i=1}^N \frac{q}{2} \int_{t-\tau_1}^t e_i^T(s) e_i(s) ds + \sum_{i=1}^N \mu \int_{t-\tau_2}^t e_i^T(s) e_i(s) ds + \sum_{i=1}^N \frac{1}{2\beta} (\alpha_i(t) - \alpha)^2. \quad (9)$$

Combining the Assumption 1, the time derivative of each $V(t)$ along the trajectories of the error complex dynamical networks (5) can be processed as

$$\begin{aligned} \dot{V}(t) &\leq \sum_{i=1}^N \sum_{r=1}^m \left[\frac{1}{2} \sum_{s=1}^m (2k_{rs}^{2\varepsilon} + k_{sr}^{2(1-\varepsilon)}) e_{ir}^2(t) + \frac{1}{2} \sum_{s=1}^m k_{sr}^{2(1-\varepsilon)} e_{ir}^2(t - \tau_1) \right] \\ &+ \sum_{i=1}^N a_{ii} \gamma_{1(\min)} \|e_i(t)\|^2 + \sum_{i=1}^N \sum_{j=1, j \neq i}^N a_{ij} \gamma_1 \|e_i(t)\| \|e_j(t)\| \\ &+ \sum_{i=1}^N \sum_{j=1, j \neq i}^N b_{ij} \gamma_2 \|e_i(t)\| \|e_j(t - \tau_2)\| + \sum_{i=1}^N b_{ii} \gamma_{2(\min)} \|e_i(t)\| \|e_i(t - \tau_2)\| \\ &+ \sum_{i=1}^N \frac{q}{2} \|e_i(t)\|^2 - \sum_{i=1}^N \frac{q}{2} \|e_i(t - \tau_1)\|^2 + \sum_{i=1}^N \mu \|e_i(t)\|^2 - \sum_{i=1}^N \mu \|e_i(t - \tau_2)\|^2 - \sum_{i=1}^h \alpha \|e_i(t)\|^2 \\ &= p \bar{e}^T(t) \bar{e}(t) + \bar{e}^T(t) \gamma_1 \bar{A}^S \bar{e}(t) + \bar{e}^T(t) \gamma_2 \bar{B}^S \bar{e}(t - \tau_2) + \mu \bar{e}^T(t) \bar{e}(t) \\ &+ \frac{1}{2} q \bar{e}^T(t) \bar{e}(t) \\ &\quad - \mu \bar{e}^T(t - \tau_2) \bar{e}(t - \tau_2) - \bar{e}^T(t) D \bar{e}(t) \\ &= \bar{\bar{e}}^T(t, t - \tau_1, \dots, t - \tau_l) \Phi \bar{\bar{e}}(t, t - \tau_1, \dots, t - \tau_l), \end{aligned} \quad (10)$$

where

$$\begin{aligned} \bar{\bar{e}}(t, t - \tau_1, \dots, t - \tau_l) &= (\bar{e}^T(t), \bar{e}^T(t - \tau_1), \dots, \bar{e}^T(t - \tau_l))^T, \\ \Phi &= \begin{bmatrix} (p + \mu + \frac{q}{2}) I_N + \gamma_1 \bar{A}^S - D & \frac{\gamma_2}{2} \bar{B}^S \\ * & -\mu I_N \end{bmatrix}, \end{aligned}$$

Due to the fact that (8), one has $(p + \mu + \frac{q}{2}) I_N + \gamma_1 \bar{A}^S - D + \frac{\gamma_2}{4\mu} \bar{B}^{S^2} < 0$ when

$\beta_i (i = 1, 2, \dots, h)$ are large enough according to Lemma 2 in [7], i.e., Φ is negative definite. We have $\dot{V}(t) < 0$. Then the delayed complex network (1) is globally synchronized. Theorem 1 is proved.

4 Simulation

Here, consider the delayed complex dynamical network (1) with $\tau_1 = 0.5$, $\tau_2 = 1$ that consists of 10 identical Lorenz systems with a single controller. In the simulation, the asymmetric coupling matrices as A and are random and satisfied with the coupling condition. And from [8], we know the Lorenz system satisfies Assumption 1. In this section, the parameters are set as $\alpha_4(0) = 1$, $\beta_4 = 1$, $\beta_i = 0$, else. According to Theorem 1, it is found the (8) is satisfied. The time series of the delayed complex network (1) with adaptive pinning controllers are numerically demonstrated as the figure 1. Clear, all errors are rapidly achieving synchronization. For this simulation, the initial values of states $x_i(0)$ and $s(0)$ are random.

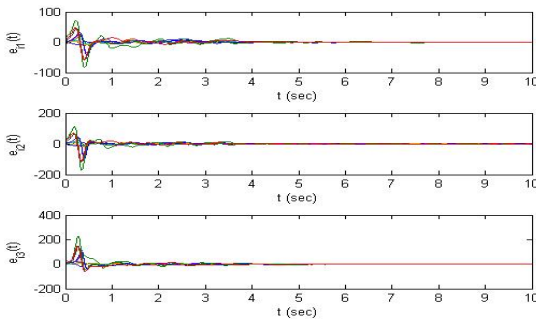


Fig. 1. Synchronization errors of network (1) under the adaptive pinning controller (7)

5 Conclusion

A general delayed complex dynamical network based on intelligent materials which represents a realistic form of networks has been studied in this paper. We design the adaptive pinning synchronization controllers via the theory of Lyapunov stability, adaptive technique and pinning control theory. The resulting adaptive pinning feedback controllers for achieving network synchronization are expressed in simple form that can be readily applied in practical situations. Finally, the effectiveness of these synchronization controllers is verified by numerical simulations.

References

1. Albert, R., Barabási, A.L.: Rev. Mod. Phys. 74, 47 (2002)
2. Sun, H.Y., Zhang, Q.L., Li, N.: Int. J. Innovative Computing, Information and Control 7, 927 (2011)
3. Cao, W.W., Cudney, H.H., Waser, R.: Intelligent Material Systems and Structures 19, 1029 (2008)

4. Li, C.G., Chen, G.R., Shi, P.: Phys. A 343, 263 (2004)
5. Xia, W.G., Cao, J.D.: Chaos 19, 013120 (2009)
6. Sun, H.Y., Li, N., Sun, H., Niu, H.: ICIC Express Letters 5, 3605 (2011)
7. Zhou, J., Wu, X.Q., Yu, W.W., Small, M., Lu, J.A.: Chaos 18, 043111 (2008)
8. Sun, W., Chen, S.H., Guo, W.L.: Phys. Lett. A 372, 6340 (2008)

Travel Path Guidance Method for Motor Vehicle

Ande Chang¹, Guiyan Jiang^{1,2}, and Shifeng Niu¹

¹ College of Transportation, Jilin University, Changchun, China
changad09@mails.jlu.edu.cn, nsf530@163.com

² State Key Laboratory of Automotive Dynamic Simulation, Jilin University,
Changchun, China
jianggy@jlu.edu.cn

Abstract. Along with the fast rise in number of motor vehicles, traffic congestions are more and more serious. Traffic congestions cause travel time wasting, traffic accident, environmental pollution, vehicles damage and so on. In order to alleviate traffic congestions deteriorating, a travel path guidance method for motor vehicle based on intelligent materials was designed using traffic simulation technologies, considering two common traffic information release systems, whose names are variable message sign and in vehicle navigation system, which will help doing better to make full use of basic traffic information. Then, the method was verified using VISSIM simulation software. The results show that the traffic congestions of experimental network are relieved obviously by the travel path guidance method in this paper.

Keywords: path guidance, motor vehicle, intelligent materials.

1 Introduction

Along with the fast rise in number of motor vehicles, traffic congestion is more and more serious. Traffic congestion will cause travel time wasting, traffic accident, environmental pollution, vehicles damage and so on, which will bring huge economic losses [1].

In recent years, the rapid development of ITS (Intelligent Transportation System) has brought a new thought for solving the problem of traffic congestion based on intelligent materials, in which the DTGS (Dynamic Traffic Guidance System) is considered as one of the most effective ways. DTGS can guide motor vehicles to avoid traffic congestion through releasing traffic information about the occurrence time and occurrence position of traffic congestion [2].

So far, VMS (Variable Message Sign) and IVNS (In Vehicle Navigation System) are two most commonly used traffic information release systems. After long-term accumulation, a lot of research achievements of travel path guidance methods for VMS or IVNS have been reported all over the world. Peeta S [3], Srinivasan K K [4] Lee D M [5] etc. have researched the travel path guidance methods for VMS, and Zuurbier F S [6], Hu J [7], Jeon Y W [8] etc. have researched the travel path guidance methods for IVNS. However, the travel path guidance methods involving VMS and

IVNS together are very rare, which might bring about conflicts of path guidance strategies between VMS and IVNS.

In this paper, a travel path guidance method for motor vehicle will be designed based on the traffic simulation technology considering VMS and IVNS together. Then, the method will be verified using VISSIM traffic simulation software.

2 Drivers Classification

Information acquisition conditions and reaction of information always are not same for different drivers; therefore, it is necessary to divide drivers into some groups whose characteristics are similar, so that more reasonable travel path guidance strategies can be developed.

Considering drivers whether can acquire IVNS guidance information, they are divided into two groups. The groups can acquire IVNS guidance information are called DWII (Drivers within IVNS Information); the groups can not acquire IVNS guidance information are called DBII (Drivers beyond IVNS Information).

Considering DBII whether can acquire VMS guidance information, they are divided into two groups. The groups can acquire VMS guidance information are called DWVI (Drivers within VMS Information); the groups can not acquire VMS guidance information are called DBVI (Drivers beyond VMS Information).

Considering DWVI whether obey VMS guidance information, they are divided into two groups. The groups obey VMS guidance information are called DOVI (Drivers Obey VMS Information); the groups not obey VMS guidance information are called DVVI (Drivers Violate VMS Information).

The research emphasis of this paper is the coordination problem of path guidance strategies between VMS and IVNS, so DBVI groups will not be considered. Then, the path guidance target groups are DWII, DOVI and DVVI.

3 Path Guidance Model

Because IVNS is a personalized traffic guidance system, it can be supposed that drivers choose to obey IVNS guidance information when IVNS guidance information can be obtained. According to the advantages of traffic simulation technologies, a travel path guidance simulation model is designed. In addition, considering the characteristics of different driver groups, the simulation model adopts a three-level traffic flow loading modes.

1) DVVI flow loading mode

DVVI choose travel paths based on their experiences, so a logit model is selected to calculate the probabilities for selecting travel paths by DVVI. The calculation formula is as follows:

$$p(k) = \frac{\exp(-gT_k)}{\sum_{k \in K} \exp(-gT_k)} \quad (1)$$

Where $p(k)$ is the selecting probability for path k by DVVI, K is the travel path set, T_k is link travel time of path k , and g is the feeling error to travel time of DVVI, $g=0.01$ in this paper.

2) DOVI flow loading mode

In order to make drivers comprehend VMS guidance information more clearly, a single path should be recommended at a time. The path with the smallest $C \times E$ should be recommended for DOVI. Where C is traffic capacity and E is traffic condition index (“3” represents no congestion, “2” represents mild congestion, and “1” represents very congestion).

3) DWII flow loading mode

IVNS is a personalized traffic guidance system, so every DWII can receive a specific recommended path. The formula for calculating quantity of DWII distributed to each path is as follows:

$$q(k) = \frac{E_k C_k}{\sum_{k \in K} E_k C_k} Q_{DWII} \quad (2)$$

Where $q(k)$ is quantity of DWII distributed to path k , C_k is traffic capacity of path k , E_k is traffic condition index of path k , and Q_{DWII} is the total quantity of DWII.

4 Simulation Validation

VISSIM traffic simulation software is used to verify the travel path guidance method for motor vehicle designed above. It is supposed that a small road network including two travel paths, in which the upper one is called L_1 and the lower one is called L_2 . L_1 has two lanes of unidirection, whose total length is 381m, and the length between two data collecting points is 338m; L_2 has three lanes of unidirection, whose total length is 385m, and the length between two data collecting points is 342m.

Figure 1 shows the simulation road network, in which vehicles run from right to left.

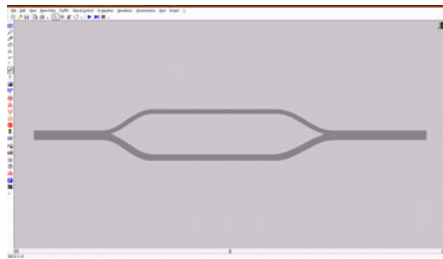


Fig. 1. Simulation road network

The propagation of traffic wave has time continuity, therefore, in order to reflect the variation of traffic condition, the time cycle for loading traffic flow should not be too small. In this paper, 10min is chose as the time cycle for loading traffic flow.

Traffic congestion is made on L_2 , then three-level flow loading modes are implemented successively. Table 1 shows the original scheme for flow loading.

Table 1. Original scheme for flow loading

Input items	Path	Path average speed	DVVI flow	DOVI flow	DWII flow
values	L_1	52km/h	500veh	300 veh	500 veh
	L_2	19km/h			

Figure 2 shows road network traffic condition without travel path guidance. Figure 3 shows road network traffic condition with travel path guidance. Table 2 shows the contrast results whether with travel path guidance.

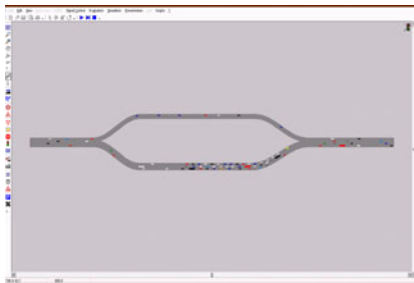


Fig. 2. Road network traffic condition without travel path guidance

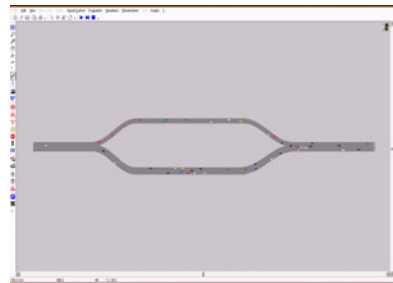


Fig. 3. Road network traffic condition with travel path guidance

Table 2. Contrast results whether with travel path guidance

Comparative items	Path L_1 average speed	Path L_2 average speed	Network average speed
without travel path guidance	52km/h	17km/h	34.5km/h
with travel path guidance	51km/h	25km/h	38.0km/h

According to Figure 2, Figure 3 and Table 2, it is observed that the road network traffic condition with travel path guidance is much better than the road network traffic condition without travel path guidance.

5 Summary

Here we may draw the following conclusions from experiments above.

The travel path guidance method for motor vehicle based on intelligent materials can alleviate traffic congestions obviously, which will make people travel more

conveniently from one place to another through making the road network traffic condition be more harmonious.

Acknowledgment. This paper is supported by Graduate Innovation Fund of Jilin University, Changchun, China (20101025).

References

1. Dong, J.: Anticipatory Traveler Information and Pricing for Real-time Traffic Management. Northwestern University, Evanston (2008)
2. Chiu, Y.C.: Generalized real-time route guidance strategies in urban networks. Texas University, Austin (2008)
3. Peeta, S., Gedela, S.: Real-time Variable Message Sign-based Route Guidance Consistent with Driver Behavior. *Transportation Research Record* (1752), 117–125 (2001)
4. Srinivasan, K.K., Krishnamurthy, A.: Roles of Spatial and Temporal Factors in Variable Message Sign Effectiveness Under Nonrecurrent Congestion. *Transportation Research Record* (1854), 24–134 (2003)
5. Lee, D.M., Pietrucha, M.T., Sinha, S.K.: Use of Fuzzy Sets to Evaluate Driver Perception of Variable Message Signs. *Transportation Research Record* (1937), 96–104 (2005)
6. Zuurbier, F.S., Van, Z., Henk, J.: Generating Optimal Controlled Prescriptive Route Guidance in Realistic Traffic Networks: A Generic Approach. *Transportation Research Record* (1944), 58–66 (2006)
7. Hu, J., Kaparias, I., Bell, G.H.: Spatial Econometrics Models for Congestion Prediction with In-vehicle Route Guidance. *Intelligent Transport Systems* 3(2), 159–167 (2009)
8. Jeon, Y.W., Daimon, T.: Study of In-vehicle Route Guidance Systems for Improvement of Right-side Drivers in the Japanese Traffic System. *International Journal of Automotive Technology* 11(3), 417–427 (2010)

Research and Realization of Real-Time Ultrasonic TOFD Scan Imaging System

Di Tang, Xingqun Zhao*, and Ling Xia

Department of Biomedical Engineering; Southeast University;
Nanjing Jiangsu 210096; China
ndt@seu.edu.cn

Abstract. This paper introduced the design of ultrasonic TOFD scan imaging system, explained the principle of TOFD, and illustrated the hardware, drivers and application software that are based on embedded system. With high-speed AD conversion and data acquisition driver, the system realized multi-channel ultrasound emission, high-speed data acquisition, real-time TOFD imaging and display. The TOFD image may reflect the defect location of the material clearly.

1 Introduction

As an essential effective tool of industrial development, the Non-destructive testing (NDT), whose significance has been widely recognized, can reflect a country's industrial development level. The advantages of the ultrasonic non-destructive testing technology include big detecting range, accurately localization, high precision, low cost, easy to operate, and harmless to the human body etc. Because of these characteristics, it is widely applied.

Time of Flight Diffraction (TOFD) is considered as the most effective method for examination of heavy wall Pressure Vessels welds. It was first advanced in 1977 by Silk and Lidington in Harwell lab [1]. Before applied into practice, as early as 10 years ago, many experiments had been done about it in Europe. Different from conventional pulse echo methods, which use the reflected wave produces in the flaw surface to detect, TOFD method relies on the diffraction of ultrasonic energies from 'tips' of internal structures (primarily defects) in a component under test. It can be used to scan, store and evaluate indication in terms of size, location, and orientation, with a degree of accuracy never achieved by other ultrasonic techniques [2-4].

2 Principle of TOFD

2.1 TOFD

TOFD is the abbreviation of the Time of Flight Diffraction Technique. In original intention, it is the common name of methods to quantitative defects, making

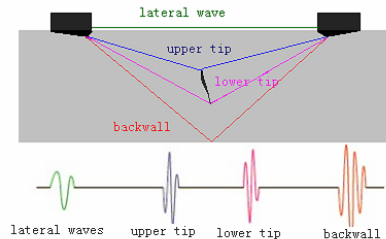


Fig. 1. Principle of TOFD

* Corresponding author.

use of diffracted wave propagating time at the tips of defects which are directly related to the true position and size of the defect. The principle of TOFD is explained in figure 1. On both sides of the weld, a pair of longitudinal wave probes with the same frequency, size and angle are placed symmetrically and oppositely. The distance between two probes depends on the board thickness, beam angle and detection frequency. One of the probes emits an ultrasonic pulse that is picked up by the probe on the other side. In the materials with no defect, one wave travels along the surface will be received by the probe, and another will reflect off the far wall. In the materials which defect exists, between the two waves, scattered wave from the upper tip of the defect and diffracted wave from the lower tip will be received by the probe, and two waves will have different propagating time and different paths [5,6].

To measure the difference of time t_D between lateral wave propagating on the surface of specimen and scattered wave or diffracted wave propagating at the tips of defect, we only need to know the sound speed C of longitudinal wave in the specimen and the distance $2Y$ between two probes. According to geometry, the burial depth of the defect tips will be obtained, as is shown in the formula below:

$$d = \frac{1}{2}(t_D^2 C^2 + 4t_D CY)^{\frac{1}{2}} \quad (1)$$

2.2 TOFD Imaging

TOFD image composed of a series of data of A scanning. When the probe is scanning and displaying waves in some place, we will get a gray line if A scanning data is mapped to gray data. As the position of probe moves smoothly, A scanning display changes into numerous gray lines, forming TOFD image [5].

3 Hardware Design

The system utilizes S3C2440 processor of family ARM9 by Samsung, which is of high-performance, low power consumption and portable. The hardware consists of six parts: ultrasonic emission/ receiving circuit module, data collection and processing module, display module, control module, memory module and communication module.

As the core of the hardware, development board of ARM9 manages the six parts above. The hardware framework is illustrated in Figure 2. The data acquisition card is mounted on the expansion bus. The control part assigns a unified address space for it.

The data acquisition card contains a CPLD chip, a high-speed A/D converter and a memory unit. The CPLD chip can implement a variety of control functions and combine logic signals. The driver of the data acquisition card gets the information of the channel and the gain, and then writes them into the memory. According to the data read from the memory, CPLD chooses right channel, controls the emission circuit which will emit the ultrasound to the objects. The echo will be collected, adjusted and enlarged by ultrasonic receiving circuit. The A/D converter converts the adjusted echo signal into digital signal, which will be saved in the memory at last.

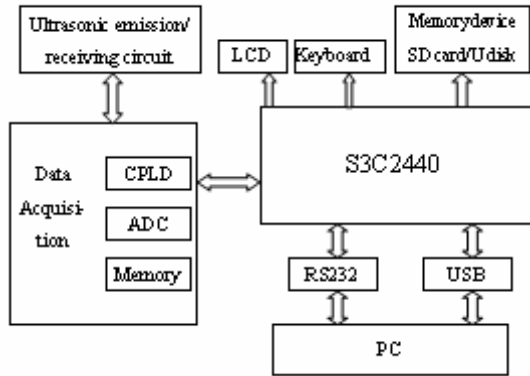


Fig. 2. Block diagram of hardware

The TFT screen (of the development board) will display the wave, the parameters and the menu. A 4*4 keyboard is configured to set the parameters and operate the system. By using SD card and U disk as the memory, a large number of data will be saved for reusing and analyzing.

4 Software Design

The entire software system is composed of three parts (operating system, device drivers and application program). Linux system is chosen as the operating system [7,8]. Drivers are added in the operating system as part of the kernel, which implement data transmission between the kernel mode and user mode [9]. The application program visits hardware devices through interfaces provided by drivers.

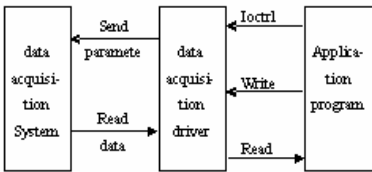


Fig. 3. Data acquisition driver

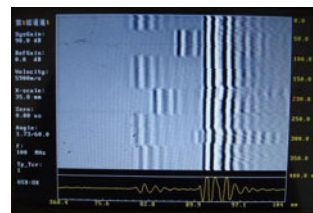


Fig. 4. The display surface

4.1 Driver Design

In this system, we have mainly completed the data acquisition driver and the keyboard driver, while application program visits equipment through standard

interface functions (Open, Write, Read, Io-control) [10,11]. The keyboard driver initializes keyboard equipment, gets key value through interrupt response.

Data acquisition driver is shown in Figure 3. Application program initializes data acquisition relates hardware through the Io-control functions; the write function transfers sampling frequency, parameters such as the gain value to homologous devices which A/D transforms; data is copied from ram to the application program in the read function. Data acquisition driver also send control parameters set by users to corresponding register to control the ultrasonic emission/ receiving circuit.

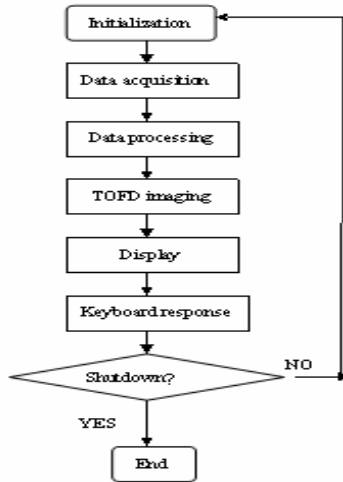


Fig. 5. Flow chart of the main loop

4.2 Application Program

The application program mainly includes the following modules:

- (1) Main loop, as is shown in Figure 5. The main loop controls all operations of the system, including parameters and devices initialization of all kinds of devices, data acquisition function and display function call, and buttons response, etc.
- (2) Data acquisition. The data acquisition system obtains data from its driver, and undertakes data handling and conversion into gray information which the TOFD image needs. Meanwhile the system also transfers the sample frequency and the amplifier parameters to hardware.
- (3) Demonstrating. Demonstrate the TOFD image, A-mode profile, the system parameters and the menu. The display surface is shown in Figure 4.
- (4) Keyboard response. It includes menu display, gain control, zero adjustment, channel selection, mode switching, etc.

5 Conclusions

Based on the arm9 S3C2440 platform, the ultrasonic TOFD scan imaging system has been embedded, which could transmit and receive four channel ultrasonic signals. The signal which probe receives has been filtered and magnified by hardware, then transformed into digital signal by high-speed ADC. The system which has realized high-speed digital acquisition, real-time TOFD imaging and demonstrate, could display the TOFD image as fast as the probe can move. Figure 6 shows two TOFD images. The left one (a) is achieved by detecting the material without defect while the right one with defects on the surface. The picture proves that the TOFD image may reflect the defect location of the weld clearly.

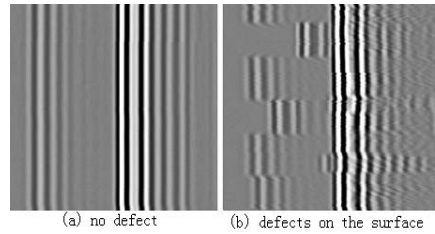


Fig. 6. TOFD images

References

1. Silk, M.G.: Sizing crack-like defects by ultrasonic means. In: Sharpe, R.S. (ed.) *Research Techniques in Non-destructive Testing*, vol. III. Academic Press, London (1977)
2. Shyamal, M., Sattar, T.: An overview TOFD method and its mathematical model. *NDT 5*, 83–87 (2000)
3. Lawson, S.: Ultrasonic testing and image processing for in progress weld inspection. *Ultrasonic testing online Journal* (April 1996)
4. Zahran, O., Shihab, S., Al-Nuaimy, W., et al.: Comparison between Surface Impulse Ground Penetrating Radar Signals and Ultrasonic Time-of-flight-diffraction Signals. In: *High Frequency Postgraduate Student Colloquium*. IEEE, Los Alamitos (2002)
5. Li, Y.: The principle and standard introduction of Ultrasound TOFD. *Non-destructive Testing 6* (2003)
6. Liang, Y., Wang, L., Wang, Y.: The Principle Analysis of Ultrasonic TOFD. *Non-destructive Testing 32(7)* (2010)
7. Kamal, R.: *Embedded Systems Architecture, Programming and Design*. The McGraw2Hill Companies, New York (2006)
8. Bi, C.-y., Liu, Y.-p., Wang, R.-f.: Research of Key Technologies for Embedded Linux Based on ARM. In: *2010 International Conference on Computer Application and System Modeling (ICCA SM 2010)*. IEEE, Los Alamitos (2010)
9. Sun, Q.: *Embedded Linux application development solutions*. People post and telecommunications publishing company, Beijing (2006)
10. Corbet, J., Rubini, A., Kroah-Hartman, G.: *Linux Device Drivers*, 3rd edn. O'Reilly Media, Inc., Sebastopol (2005)
11. Feng, J.: *Linux drivers design from approaches to master*. QingHua university publishing company, Beijing (2008)

Study of Integrated Design Processing Methods of Surge Links in Loose Logistics Transportation System

Xiaoping Bai and Yu Zhao

School of Management, Xi'an University of Architecture & Technology,
Xi'an, China, 710055
xp9981@sohu.com, Tonggd@vip.sina.com

Abstract. The logistics transportation system with surge links is widely used in mines, power plants, material yards; and etc. Bin capacity size in surge links has great influence on reliability and production efficiency of whole logistics transportation system. By utilizing some existing outcomes, this paper selects three-parameter Weibull distribution which can reflect general case and has wide application as the tool to present a new integrated design processing methods. Compared with existed references, presented method fully considers different influences of surge bin capacity on reliability and production efficiency of whole system and can realize cost and benefit overall optimization. The presented method can offer the reference for capacity optimization design of surge bin in loose material logistics transportation system.

Keywords: logistics, transportation, loose material, surge links, optimization, bin capacity.

1 Introduction

In some loose material logistics transportation system, surge bins are often set. By surge bin, links behind bin can continue transporting material of bin when links ahead of bin are in failure; on the other hand, links ahead of bin can continue transporting material to bin when links behind bin are in failure. Therefore setting surge bin can reduce the interacting of links ahead and behind bin to improve reliability of whole logistics transportation system. Theoretically surge bin have many virtues, such as buffering the interacting of links ahead and behind bin, buffering different transporting flows, adjusting and processing materials, and etc. But in practice because the whole transportation system will become very complex after setting surge bin, these theoretic virtues often can't be adequately reflected. In practical application, bin capacity size has great influence on reliability and production efficiency of whole logistics transportation system. So studying optimum design of surge bin capacity to fully realize its beneficial functions are very significance.

2 Some Relevant Studying References

Until now there have been many references studying surge system. In 1950's, the transportation system with surge bin was named as soft or flexibility connecting system by professor J.kerp that comes from Poland. He discussed the influencing function of surge bin for the transportation system, but lacked quantificational analyzing. In [1], a model to simulate the existing conveyor belt haulage system at an underground coal mine in Southern Utah, USA was presented, comparison of results for the belt system with and without a surge bin showed that the addition of a surge bin to the system increased production 13.2% [1]. In [2], computer simulation method was used to analyze how surge bin improve the validity of system [2]; In [3], stochastic process and linear extension methods were used to modeling and analyzing reliability of surge bin system [3]; In [4], authors made use of the theory of queuing system with surge bin to analyze the rational capacity of surge bin [4], and etc[5][6][7][8][9]. Compared with some existed references, this presented method fully considers different influences of surge bin capacity on reliability and production efficiency of whole logistics transportation system and realizes cost and benefit overall optimization design.

2.1 Some Influence of Designed Surge Bin Capacity on Reliability and Production Efficiency of Whole Logistics Transportation System

The block diagram of the logistics transportation system with surge bin is shown as Fig.1.



Fig. 1. The block diagram of the logistics transportation system with surge bin.

The influence of designed surge bin capacity on reliability and production efficiency of whole logistics transportation system can be discussed from following two aspects.

- (1) When links ahead of bin 1 are in failure, links behind bin 2 can continue transporting materials of bin, The maximum value of materials of bin is also designed bin capacity, supposed as Q tons. After a certain time if links ahead of bin 1 are still in failure, empty bin will occur, and then whole logistics transportation system will stop working.
- (2) When links behind bin 2 are in failure, links ahead of bin 1 can continue transporting materials to bin by rest capacity of surge bin. The maximum value of rest capacity of surge bin is designed bin capacity Q tons. After a certain time if links behind bin 2 are still in failure, full bin will occur, and then whole logistics transportation system will stop working.

2.2 Determining Probability Distribution of Some Random Variables in This System

For reflecting general case, this paper supposes fluctuation pattern of inputting materials quantity and outputting materials quantity, failure rule of links ahead of bin, links behind bin all being three-parameter Weibull distribution. Compare to general supposed negative exponential distributions and normal distribution, three-parameter Weibull distribution has wider application ranges, because negative exponential distributions and normal distribution can all be regarded as special phase cases of three-parameter Weibull distribution. The reliability function of three-parameter Weibull distribution is

$$R(t) = P(T \geq t) = 1 - F(t) = e^{-\left(\frac{t-\gamma}{\eta}\right)^m} \quad (t > \gamma) \tag{1}$$

Where m, γ, η are its shape parameter, initial position parameter, and scale parameter, which determine basic shape, initial position and divergent-convergent transformation of probability density curve. These parameters can be gotten by hypothesis testing and parameter estimation methods based on a large amount of practical statistical data.

3 The Presented New Method about Surge Bin Capacity Optimization

According to above assumption, Steps of presented method are as follows.

(1) When links ahead of bin 1 are in failure, links behind bin 2 can continue transporting materials of bin, The maximum value of materials of bin is designed bin capacity Q tons. Here only considering a kind of having influence case of designed surge bin capacity and maximum possible case of outputting materials quantity (tons/minutes) of links behind bin 2, when the duration time t_1 (minutes) of that links ahead of bin 1 are in failure satisfied following formula, empty bin will occur, and then whole logistics transportation system will stop working.

$$t_1 \geq t_{01} = \frac{Q}{E_2} \tag{2}$$

Where t_1 (minutes) is the duration time of that links ahead of bin 1 are in failure, Q (tons) is designed surge bin capacity, t_{01} (minutes) is the duration limit time of that links ahead of bin 1 are in failure, and E_2 (tons/minutes) is mathematical expectation of outputting materials quantity of links behind bin 2.

The occurring number of above empty bin in a year is

$$P_1 = n_1 R(t_{01}) = n_1 P(T \geq t_{01}) = n_1 \cdot e^{-\left(\frac{t_{01}-\gamma_1}{\eta_1}\right)^{m_1}} = n_1 \cdot e^{-\left(\frac{\frac{Q}{E_2}-\gamma_1}{\eta_1}\right)^{m_1}} \tag{3}$$

Where n_1 (numbers) is failure number of links ahead of bin 1 in a year, m_1, γ_1, η_1 are parameters of three-parameter Weibull distribution of failure time in links ahead of bin 1. Definitions of Q (tons), t_{01} (minutes), E_2 (minutes), and are as above.

The loss profit caused by one-time above empty bin s_1 (dollars) is

$$s_1 = \mu_1 \cdot E_2 (h_1 - h_2) \tag{4}$$

Where h_1 (dollars/tons) is the selling price of per ton material, h_2 (dollars/tons) is per ton material cost, definitions of E_2 (tons/minutes) are as above. μ_1 (minutes/numbers) is mean value of failure time of links ahead of bin 1, which can be calculated by

$$\mu_1 = \gamma_1 + \eta_1 \Gamma \left(1 + \frac{1}{m_1} \right) \tag{5}$$

The Gamma function in formula (5) is

$$\Gamma(x) = \int_0^\infty t^{x-1} e^{-t} dt \tag{6}$$

The loss profit l_1 (dollars/year) caused by above empty bin in a year is

$$l_1 = P_1 \cdot s_1 = \mu_1 \cdot E_2 \cdot n_1 \cdot e^{-\left(\frac{Q}{E_2} - \gamma_1\right) \frac{m_1}{\eta_1}} (h_1 - h_2) \tag{7}$$

(2) When links behind bin 2 are in failure, links ahead of bin 1 can continue transporting materials to bin by rest capacity of surge bin. The maximum value of rest capacity of surge bin is designed bin capacity Q tons. Here also only considering a kind of having influence case of designed surge bin capacity and maximum possible case of inputting materials quantity (tons/minutes) of links ahead of bin 1, when the duration time t_2 (minutes) of that links behind bin 2 are in failure satisfied following formula, full bin will occur, and then whole logistics transportation system will stop working.

$$t_2 \geq t_{02} = \frac{Q}{E_1} \tag{8}$$

Where t_2 (minutes) is the duration time of that links behind bin 2 are in failure, Q (tons) is designed surge bin capacity, t_{02} (minutes) is the duration limit time of that links behind bin 2 are in failure, and E_1 (tons/minutes) is mathematical expectation of inputting materials quantity of links ahead of bin 1.

Likewise, the occurring number of above full bin in a year is

$$P_2 = n_2 \cdot R(t_{02}) = n_2 \cdot P(T \geq t_{02}) = n_2 \cdot e^{-\left(\frac{t_{02} - \gamma_2}{\eta_2}\right)^{m_2}} = n_2 \cdot e^{-\left(\frac{E_1 - \gamma_2}{\eta_2}\right)^{m_2}} \tag{9}$$

Where n_2 (numbers) is failure number of links behind bin 2 in a year, m_2 , γ_2 , η_2 are parameters of three-parameter Weibull distribution of failure time in links behind bin 2. Definitions of Q (tons), t_{02} (minutes), E_1 (tons/minutes) are as above.

The loss profit caused by one-time above full bin s_2 (dollars) is

$$s_2 = \mu_2 \cdot E_1 (h_1 - h_2) \tag{10}$$

Where definitions of h_1 (dollars/tons), h_2 (dollars/tons), μ_2 (minutes/numbers), E_1 (tons/minutes) are as above. μ_2 (minutes/numbers) is mean value of failure time of

links behind bin 2. μ_2 (minutes/numbers) is mean value of failure time of links behind bin 2, which can be calculated by

$$\mu_2 = \gamma_2 + \eta_2 \Gamma \left(1 + \frac{1}{m_2} \right) \tag{11}$$

The loss profit l_2 (dollars/year) caused by above full bin in a year is

$$l_2 = P_2 \cdot s_2 = \mu_2 \cdot E_1 \cdot n_2 \cdot e^{-\left(\frac{\gamma_1 - \gamma_2}{E_1}\right)^{m_2}} (h_1 - h_2) \tag{12}$$

(3) Building surge bin need certain expenses, allocate these expenses to a year, then per year cost l_3 (dollars/year) is

$$l_3 = (b_1 / T + b_2) Q \tag{13}$$

Where b_1 (dollars/tons) is the building cost of per ton surge bin capacity, T (years) is service life of surge bin, b_2 (dollars/tons) is maintenance cost of per ton surge bin capacity.

(4) For getting the optimization value l of designed surge bin capacity, the following programming model can be established.

$$\text{MIN } l = l_1 + l_2 + l_3 = \mu_1 \cdot E_2 \cdot n_1 \cdot e^{-\left(\frac{\gamma_2 - \gamma_1}{E_2}\right)^{m_1}} (h_1 - h_2) + \mu_2 \cdot E_1 \cdot n_2 \cdot e^{-\left(\frac{\gamma_1 - \gamma_2}{E_1}\right)^{m_2}} (h_1 - h_2) + (b_1 / T + b_2) Q \tag{14}$$

According to extreme value principle, the necessary condition of that l achieve its extreme value is

$$\frac{dl}{dQ} = 0 \Rightarrow -\mu_1 \cdot n_1 \cdot e^{-\left(\frac{\gamma_2 - \gamma_1}{E_2}\right)^{m_1}} (h_1 - h_2) m_1 \left(\frac{\gamma_2 - \gamma_1}{E_2}\right)^{m_1 - 1} - \mu_2 \cdot n_2 \cdot e^{-\left(\frac{\gamma_1 - \gamma_2}{E_1}\right)^{m_2}} (h_1 - h_2) m_2 \left(\frac{\gamma_1 - \gamma_2}{E_1}\right)^{m_2 - 1} + (b_1 / T + b_2) = 0 \tag{15}$$

The equation (15) only has an unknown number Q, so designed surge bin capacity Q (tons) can be gotten by above equation (15). In practical application, the equation (15) can be solved by Newton Iteration Method and computer programs.

4 Conclusions

It can be seen from the equation (15) that fluctuation rules of inputting materials quantity and outputting materials quantity (such as parameters E_1, E_2), failure rules of links ahead of bin 1 and links behind bin 2 (such as parameters $n_1, n_2, \mu_1, \mu_2, m_1, \gamma_1, \eta_1, m_2, \gamma_2, \eta_2$), the building cost and maintenance cost of per ton surge bin capacity (such as parameters b_1, b_2), service life of surge bin (such as the parameter T), selling price and cost of per ton material (such as parameters h_1, h_2) should be all considered on designing surge bin capacity. In practical application, bin capacity size has great influence on reliability and production efficiency of whole logistics transportation system. This paper presents a new optimum method for designing surge bin capacity in logistics transportation system. This presented method fully considers different

influences of surge bin capacity on reliability and production efficiency of whole loose material logistics transportation system and realizes cost and benefit overall optimization design.

Acknowledgment. This research work was supported by grants from the national science foundation of china (59874019), Shanxi Province Natural Science Basic Foundation(2010JM7004) and Shanxi Province Key Discipline Construction Special Fund subsidized project in china.

References

1. McNearny, R., Nie, z.: Simulation of a conveyor belt network at an underground coal mine. *Mineral Resources Engineering* 9(3), 343–355 (2000)
2. Tang, Z.: The reliability of soft connection Transportation system under mine well. *Journal of China Coal Society* 18(1), 27–32 (1993)
3. Wang, Y., Wang, R.: The exact solution of the basic reliability model about soft connection mine well production line. *Journal of China Coal Society* 20(4), 17–20 (1995)
4. Lu, M., Zhang, D., Cai, Q.: Rational Capacity Setting of the Surge bin at Open pit Crushing Station. *Metal Mine* 30(9), 5–7 (2001)
5. Tang, Z.: A method calculating validity of soft connection Transportation system under mine well. In: *Proceedings of the 5th china conference of mine system engineering*, pp. 25–28 (1990)
6. Yu, S.: *Reliability Engineering Introduction in Coal Mines*, pp. 183–190. Coal Industrial Press (1988)
7. Liu, C., Jiao, Y., Liu, D.: Reliability simulation of mining haulage system with soft link. *The Chinese Journal of Nonferrous Metals* 7(2), 24–33 (1997)
8. Cai, Q., Peng, S., Zhang, D.: Reliability design and analysis of Transportation system with a surge bin in mines. *Journal of Liaoning university of engineer & technology* 26(1), 20–23 (1997)

Collection System Implementation for Four TCM Diagnostic Methods Information of Hyperlipemia and Research on Intelligent Symptom Classification Algorithm

YongQiu Tu¹, GuoHua Chen¹, ShengHua Piao^{3,4}, and Jiao Guo^{2,3,4,*}

¹ Department of Medical Information Engineering in Guangdong Pharmaceutical University, Guangzhou, 510006, China

tu.yongqiu@mail.scut.edu.cn, ghchen2007@yahoo.com.cn

² Guangzhou University of Chinese Medicine

guojiao@gzhtcm.edu.cn

³ Key Unit of Modulating Liver to Treat Hyperlipemia SATCM, 510006, China

⁴ Level 3 Laboratory of Lippid Metabolism SATCM, Guangzhou, 510006, China

Abstract. Establishment of collection system for collecting data derived from four diagnostic techniques is the precondition on TCM syndrome standardization of Hyperlipidemia. A collection system is implemented, which is consisted of tongue images acquisition, facial image acquisition, inquiry diagnosis, pulse diagnosis, and auscultation diagnosis information. Through this platform, 316 cases of hyperlipidemia clinical information have been gathered. Hyperlipidemia syndrome classification standardizing research is the hotspot in Chinese Medicine Domain. An intelligent classification algorithm is realized to analyze these 316 cases of hyperlipidemia clinical symptoms data, get statistically significant classification results, and find the corresponding relationship between these results and syndromes. Compare disease characteristics of samples in every category with syndromes category and find out the relationships between them, by which the hyperlipidemia syndrome differentiation standardization will be founded.

Keywords: four diagnostic methods, collection system, hyperlipemia, symptom classification algorithm.

1 Introduction

Hyperlipidemia is one of the main base lesions of vascular and viscera disease. Hyperlipidemia prevention and treatment by Traditional Chinese Medicine (TCM) has obvious advantages in less toxicity and better treatment, which makes TCM has received wide attention in the hyperlipidemia medical community. However, due to the disease and syndrome scattering and clinical lesions complexity of hyperlipidemia traditional Chinese medicine domain, standardization of TCM syndrome

* Corresponding author.

differentiation standard have not been found[1,2], but the result is still not fully satisfied. There are two main reasons for it: firstly, hyperlipidemia TCM syndrome differentiations mainly based on the theory of ancient documents, Lacking of applying statistical analysis method in large clinical samples which makes the result exists unilateralism; Secondly, the differences in dialectical systems make syndrome classification divided and restraints hyperlipidemia TCM syndrome classification standardization [3].

Using computer technology to solve TCM’s problems is receiving more concern and attention[4,5]. A hyperlipidemia TCM four methods of diagnosis information collection system needs to be established. By establishing this platform can remedy one-sidedness defects in classification research and help doctors record patient clinical manifestations during therapeutic process to summarize treatment experience and improve therapeutic effect. The collection platform and 316 cases of hyperlipidemia clinical information gathered by it will be described in detail below.

Hyperlipidemia syndrome classification standardizing research is the hotspot in Chinese Medicine Domain[6,7,8]. An intelligent classification algorithm is realized to analyze these 316 cases of hyperlipidemia clinical symptoms data. Statistical classification results are obtained. After that, the corresponding relationship between these results and syndromes are acquired. Clustering algorithm is programmed to classify syndromes and setting similarity threshold interface is available, which make it is possible to classify a large number of samples more adaptively. Compare disease characteristics of samples in every category with syndromes category and find out the relationships between them, by which the hyperlipidemia syndrome differentiation standardization will be founded.

2 Four TCM Diagnostic Methods Collection System

System Modules. The system consists of two modules: administrator module and four diagnostic method collection module. Administrator module includes four modules: doctor records management, patient records management, records management, and symptom management. Four diagnostic method module also contains four modules: looking, smelling, asking and cutting information collection. The collection module is illustrated as Fig. 1. Through the clinical four diagnostic information collection platform, hyperlipidemia TCM four diagnostic samples can be collected in extraordinary numbers and thus promote the standardization of Hyperlipidemia TCM syndrome classification.



Fig. 1. Collection module of the Hyperlipidemia four TCM Diagnostic methods collection platform

Clinical Information Collected by the System. 316 cases clinical data derived from hyperlipidemia four diagnostic methods were collected by collection system. Each sample record total 54 features, including the basic information of patients, blood identification information, and clinical data of Chinese medicine-related symptoms such as face-looking diagnosis, Inquiry information, and pulse diagnosis. Part of the information collected by the system is shown in Figure 2.

no	name	sex	age	waist	SBP	DBP	FBS	TC	TG	LDL-C	HDL-C	fat	palp	chest	tight	headache	sleepless	dream	pale	red	tough	white	fur
A1	Q. Feng	f	70	97	170	82	6	6.67	1.6	4.71	1.18	1	0	0	0	1	1	1	0	0	0	0	
A14	L. L. Gui	f	76	80	165	86	8.3	5.73	1.55	3.59	1.59	0	1	0	0	0	0	0	0	0	0	0	
A15	X. D. Hong	m	40	101	150	90	4.6	6.19	2.67	4.36	1.13	1	0	0	1	1	0	0	0	0	0	0	
A17	F. C. Chen	m	75	103	130	80	4.4	5.16	3.53	3.03	0.9	0	0	0	1	1	0	0	0	0	0	1	
A21	B. Z. Li	m	62	102	162	98	6.2	4.98	2.94	3.25	1.04	1	0	0	0	1	1	0	0	0	1	0	
A29	N. G. Xu	m	53	99	160	95	6.1	6.52	1.75	3.98	2.04	1	0	0	0	1	1	1	0	0	1	0	
A31	M. Y. Chen	m	42	90	134	100	6.4	6.44	2.86	5.3	0.82	1	0	0	0	1	0	0	0	0	1	0	
B62	J. P. Li	f	57	83	154	85	5.1	5.93	1.98	3.33	1.5	1	1	1	1	0	0	0	0	0	0	0	
B65	Y. M. Yuan	f	46	80	120	65	4.2	6	2.95	4.47	0.89	0	0	0	0	0	1	1	1	0	0	1	
B66	C. J. Zhou	f	55	90	185	80	5.5	5.11	2.14	3.09	1	0	1	1	1	0	0	0	1	0	0	0	
B82	J. Wang	m	52	95	150	80	7.2	8.95	4.21	6.75	0.52	1	1	1	1	1	1	1	0	0	1	0	
C11	Y. Liu	f	52	80	135	68	13.7	4.25	2.75	2.22	1.05	0	1	1	1	1	1	1	1	0	0	0	
D135	H. L. Ma	f	36	89	120	80	5.7	6.21	2.33	4.84	0.39	1	0	1	1	1	0	0	0	0	0	0	
D136	W. W. Lan	f	67	80	100	60	5.2	5.71	2.71	4.21	0.71	1	0	0	0	0	1	0	0	0	0	1	
D149	Y. Gao	m	42	93	132	80	5	6.95	3.71	4.91	0.53	1	1	1	1	1	1	0	0	1	0	0	
D155	W. W. Li	m	44	69	130	80	7.2	7.51	3.25	5.91	0.75	1	1	1	1	1	1	0	0	0	0	0	
D156	X. P. Guo	f	60	83	160	78	7.38	8.15	3.15	6.93	0.98	1	1	0	0	1	1	1	0	0	0	0	
D165	Q. N. Wang	m	72	90	140	100	8.08	6.75	3.67	3.85	0.73	1	0	0	0	1	0	1	0	0	0	0	
D167	L. Wang	m	51	90	120	80	16.8	6.16	2.63	4.49	1.08	1	0	0	0	1	1	0	0	0	1	0	
D173	S. Z. Zhong	f	61	82	140	80	13.1	6.86	1.18	4.5	1.76	1	0	0	0	1	1	1	0	0	1	0	

Fig. 2. Screenshot of 316 clinical cases information collected by the collection system

3 Intelligent Classification Algorithm

Clustering analysis is a kind of intelligent classification algorithm. Automatic clustering algorithm is implemented to classify the 316 cases, so that the hyperlipidemia syndrome differentiation standardization can be founded. At first, statistic data derived from 316 original samples is preprocessed as follow, then intelligent classification algorithm is introduced in detail, and finally classification result is illustrated and analysis.

Category Statics. Similar statistic is computed based on data derived from 316 original cases and is used to be classified by clustering algorithm. Distance coefficient, cosine value, and correlation coefficient are used as similar statistics. The corresponding computational formulas are shown below.

Distance Coefficient. The distance between the coefficient samples is computed in Eq. 1.

$$d_{ij} = \left(\sum_{k=1}^m (x_{ik} - x_{jk})^2 \right)^{\frac{1}{2}} \quad (1)$$

Cosine value. The cosine value of vector angle is used to record similar degree of samples, which is computed in Eq. 2.

$$\cos \theta_{ij} = \sum_{k=1}^m x_{ik} x_{jk} / \sqrt{\sum_{k=1}^m x_{ik}^2 \sum_{k=1}^m x_{jk}^2} \quad (2)$$

Correlation Coefficient. The correlation coefficient is computed by Eq. 3.

$$r_{ij} = \frac{\sum_{k=1}^m (x_{ik} - x_{ia})(x_{jk} - x_{ja})}{\sqrt{\sum_{k=1}^m (x_{ik} - x_{ia})^2 \sum_{k=1}^m (x_{jk} - x_{ja})^2}} \quad (3)$$

In these three equations, i and j signify sample number, m is the number of sample component, x_{ia} and x_{ja} denote the average of sample i and sample j respectively.

Cluster Algorithm. Categories are merged during clustering process. The algorithm is introduced in detail as follows.

- (0) Set the similarity condition P: $0 \leq P \leq 1$
- (1) Start: All samples are in the same group
- (2) Compute: Hypothetically, there are n groups C_1, C_2, \dots, C_n
 - ① Compute similar statistics, such as Distance coefficient, cosine value, and correlation coefficient.
 - ② Compute classification statistics: $S_m = \frac{\sum \cos(\theta_{i,j})}{k(k-1)}$
 - ③ Compute average similarity between classes: $S = \frac{(S_1 + \dots + S_n)}{n}$
- (3) Discriminate: If $S \geq P$, jump to (5), else go to (4)
- (4) Decompose: To every sample I in the class C_m whose $S_m < P$, do
 - ① Create a new class C_{n+1} for I
 - ② Classify I to $C_1, \dots, C_{m-1}, C_{m+1}, \dots, C_n$ and select the class whose S is increased largest.
 - ③ Go to (3)
- (5) Terminate

Experiment Result and Analysis. Collected hyperlipemia 316 cases clinical symptoms material are classified by the intelligent clustering program with the similarity threshold is set by 75%, just like Fig.3 shows.

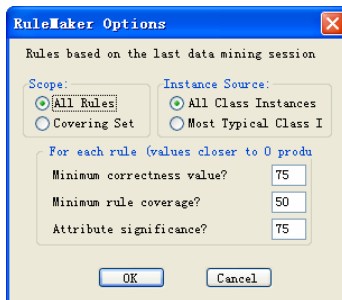


Fig. 3. Interface of setting threshold value

Samples are classified to five categories just like Fig. 4 shows. It is found by comparison that over 80% of the samples belongs to each five category correspond to “phlegm resistance type”, “liver gloomy and gas sluggish type”, “gas sluggish and blood stasis type”, “liver positive phlegm fire type”, and “spleen and kidney positive type” respectively.

CLASS RESEMBLANCE STATISTICS						
	Class 1	Class 2	Class 3	Class 4	Class 5	Domain
Res. Score:	0.715	0.725	0.727	0.726	0.79	0.69
No. of Inst.	73	109	113	12	9	316
Cluster Quality:	0.03	0.05	0.05	0.05	0.14	
DOMAIN STATISTICS FOR CATEGORICAL ATTRIBUTES						
Number of Classes:	5					
Domain Res. Score:	0.69					

Fig. 4. Clustering analysis results of 316 samples

4 Summary

Clinical information of four TCM diagnostic methods is collected by the collection system. 316 clinical cases are collected. Clustering algorithm is used to classify these samples and obtain five classes. The experience gained from traditional Chinese medicine is compared with the samples belongs to the five classes separately. Relationship between hyperlipidemia TCM syndrome categories and the classes achieved by clustering algorithm is obtained which is an objective classification based on the results of statistical analysis. System of standard hyperlipidemia syndrome classification can be build based on the research result introduced above.

Although the similarity of the five classes obtained by clustering algorithm attain to 70%, but the instance numbers of the fourth and fifth classes are significantly lower than the first three groups. Therefore, the hyperlipidemia clinical data collection need to be further expanded so that the clustering results can be more scientific and objective. In addition, the next step is to focus on introducing the theory of fuzzy rules to clustering algorithm to solve the complex syndromes classification problem. Associate miscellaneous syndromes with related single syndromes, rather than a completely independent type.

References

1. Huang, B.F.: Research Development in Hyperlipidemia TCM Treatment. Journal of Guangxi Traditional Chinese Medical University 11(4), 102–104 (2008)
2. Tang, S.L.: Research Development in TCM Hyperlipidemia Domain. Internal Medicine of China 3(1), 129–131 (2008)
3. Qian, X.Q., Chen, H., Tian, X.H., et al.: Exploration for Hyperlipidemia TCM Syndromes Classification Inconsistent Analysis. Shenzhen Journal of Integrated Traditional Chinese and Western Medicine 17(2), 25–26 (2007)

4. Wang, J., Li, H.X., Zhan, Z.Q., et al.: Study on syndrome manifestations of Chinese medicine based on complicated algorithm. *Journal of Beijing University of Traditional Chinese Medicine* 29(9), 581–585 (2006)
5. Bai, Y.J., Shen, H.B., Meng, Q.G., et al.: Study of syndromes nonlinear modeling Based on artificial neural network. *Chinese Journal of Information on Traditional Chinese Medicine* 14(7), 3–6 (2007)
6. Xu, R., Wunsch, D.: Survey of Clustering Algorithms. *IEEE Transaction on Neural Networks* 16(3), 645–678 (2005)
7. Wang, S.T., Jiang, H.F., Lu, H.J.: A New Integrated Clustering Algorithm GFC and Switching Regressions. *International Journal of Pattern Recognition and Artificial Intelligence* 16(4), 433–446 (2002)
8. Jiang, S.Y., Li, X.: A Hybrid Clustering Algorithm: *Fuzzy Systems and Knowledge Discovery*, vol. (1), p. 366 (2009)

Experience of Nurbas Modeling Design Process

Guobin Peng

Design and Art College GuiLin University of Electronic Technology Guilin, P.R. China
pengguobin@guet.edu.cn

Abstract. Nurbas curve modeling is one of a very important function of three-dimensional software, it provides another excellent way of modeling for three-dimensional object shape by its unique model features, which fully demonstrates functional advantages of its three-dimensional forming from the line to a surface, is a functional module which the other three-dimensional software must be integrated into. This paper based on the examples experience to study the Nurbas modeling characteristics and laws in 3DS MAX, to further enhance the ability of Nurbas modeling design, to enhance the understanding and grasp of the function.

Keywords: Nurbas modeling, modeling, Experience Design.

Preface

In the current number of three-dimensional design software, 3DS MAX software-based three-dimensional software is widely used in China, and our application process during the three-dimensional design, three-dimensional modeling is often the first priority must be completed, 3DS MAX software provides a variety of modeling methods, many of which were against nature objects both regular and irregular, which provides an alternative way of modeling, this is Nurbas modeling, this modeling approach is widely used in many three-dimensional software, this paper through design experience of Nurbs modeling in 3DS MAX software to do some discussion and study.

1 NURBS Modeling Concepts

3DS MAX software Nurbs modeling is one of the advanced modeling way of surface modeling, the principle is through control the curves to create surface models, NURBS of NURBS modeling is the abbreviation of English Non-Uniform Rational B-Splines, Non-Uniform is the influence of a control vertex can change the scope that it affects and controls, when you create an irregular surface that is very useful, through its change the points to control the impact of the surface modeling; Rational (reasonable) - refers to each NURBS objects can be defined by mathematical expressions, can also be turned into a kind of visual modeling; B-Spline can place series of anchor points to indicate the direction of the path to be followed, to generate B-spline path, B-spline anchor points for each path can be a curve or a corner control

point. We can simply understand NURB modeling is specifically a visual model of a modeling method of curved objects through control of point, line and surface. People can use it to make a variety of complex surface modeling and performance of special effects, such as human animals, people or streamlined sports car and so on.

2 The Basic Principles of Surface Modeling

3DS MAX software Nurbs modeling is the surface formed by Nurbs curve, again composed of three-dimensional model by surface, curve has its control points to control the curvature of curve, direction, length, which is its one of the major modeling methods at present. Nurbs surfaces can also be surrounded into a three-dimensional model, by control the points on the surface to change the model shape. But Nurbs surface modeling is different from the solid modeling, it is not fully parameterized, in the use of Nurbs modeling we need to be aware about the following common problems during the modeling process, master and control some of the basic principles of modeling.

(1) the boundary curves should be as simple as possible when create surfaces, to avoid causing too complex when we operate editing point, or the model structure is too complex in the later phase, under normal circumstances, the order is not more than 3 curves.

(2) the curve should maintain smooth and continuous when create surfaces boundary, to avoid sharp corners, cross and overlap. In addition, during creating surfaces, the radius should be as large as possible to avoid model processing difficult and complex shape, thus not conducive to model change.

(3) the surface should be as concise as possible, surface should be as big as possible. We need to cut the part unnecessary. The number of sheets of surface should be as little as possible.

(4) according to the shape characteristics of different components, to create a reasonable method of using a variety of surface features. Nurbs modeling in general are starting from the curve. You can create curve line by creating points, then creating surfaces by creating lines, can also extract or use the characteristics edge lines that existed in view toolbar to create surface. Its general creation is as follows.

a) First create a curve, create curves can be divided into points controlled curves and CV controlled curves, these curves were created according to model object structure analysis, to determine the shape of the curve and different linear constitution ways, which directly determine the model results generated behind, Nurbs provides eighteen command including the creation of lines and lines modify command, as shown in Figure 1.



Fig. 1. curve create and modify command

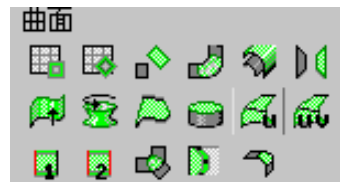


Fig. 2. surface generation commands

b) According to the curve created, creating the main surface or a large area of a product, establish the modeling features of large model.

c) Use surface & curve shape command, from the curve swept, rounding, and other modeling command to make the transition surface, edit or smoothing processing for the previous a series curves created, and ultimately get the complete product model.

3 Nurbas Modeling Experience Design

Here we borrow an example to experience the 3DS MAX software Nurbs modeling in order to find a number of modeling techniques and modeling ways to better understand the Nurbs modeling. Here we create a pen shape as examples.

First before using Nurbs modeling we need to do some structural analysis of the model object, so that we understand use which modeling method to shape the model, here the shape structure of the pen is composed of three parts, namely cap, pen body and the sharp, first of all start the main part of the object, which is conducive to grasp the whole shape of the object, the pen body is constituted by the regular circular section, body type is very regular, you can first create a Nurbs curve of its profile, and then adjust the curvature of the curve, so as to make the modeling close to the requirements of high proportion and shape style of the pen.

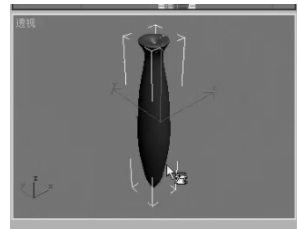


Fig. 3. Model of pen body

Next, select the Nurbs curve tool and draw profile curve, adjusting the curve, you need to select the molding method, 3DS MAX software Nurbs modeling provides a fifteen surface forming methods Figure 2, here we choose the turning surface forming method to create pen body, the final generated model is shown in Figure 3.

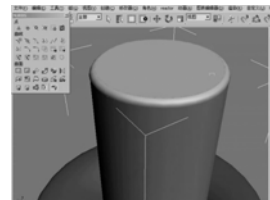


Fig. 4. The model of cap

The design requirement for the cap includes several steps to complete, first is to create two profile round curve, one circle line through Nurbs created surfaces to generate the lower part of the body, another circle line is used to make the lid, and then through Nurbs to create round surface to complete the cap chamfer as shown in Figure 4.

The final tip use the standard geometry modeling to create a sphere on it, then assemble the three parts of the model together to complete the production of the pen model as shown in Figure 4.

4 Summary

In computer three-dimensional software Nurbas surface modeling with its unique modeling features are covered into the major software, such as rhinoceros, UG, MAYA, etc. This shows the ability of its unusual design, its basic model principles

are basically the same, but also exist some important differences between them, they all have their own advantages.

By modeling practice, you can see 3DS MAX software Nurbs Modeling has the following advantages, first, it is characterized by features that it has its own unique set of modeling tools, fit for product appearance design, provides the complex model construction of regular and irregular surface, such as chamfer, trench and special modeling which other industrial products often involve. Second, it can quickly create effect model, modeling function is rich, providing a very good material and rendering, and can set the animation, showing favorable results. But there are shortcomings, it can not achieve a good design parameters, which gives a lot of inconvenience for its later manufacture, in the modeling process to modify some parts, can not achieve the overall parameters change, can not provide effective parameters for post-processing and manufacturing, in particular, it can not meet the integration of detailed design and assembly in the product design process, to better achieve product series and parametric design, through research we also find that only by demonstrate their respective advantages of the software, can we continue to meet different design needs in order to demonstrate their biggest advantages.

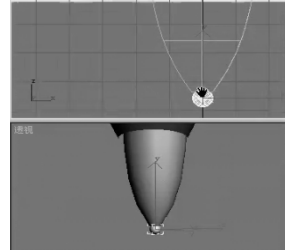


Fig. 5. Model of the nib

References

1. Yu, D.: Three-dimensional modeling examples and techniques. People Posts & Telecom Press Excellent Books, Beijing (2000)
2. Yan, F., Wu, Y.(trans.): A special case of three-dimensional modeling design 3ds max5 completely real. Ocean Press, Beijing (2004)
3. Li, J.: Novice from zero learning 3ds Max. Shanghai Popular Science Press, Shanghai (2008)

Research on Coupling Characters of the Linear Polarized Mode between Two Multi-mode Silica Circular Waveguide

Miao Yu, ZhiQiang Zhang, and JianHua Ren

Beijing University of Posts and Telecommunications, Beijing 100876, China
yumiao42@gmail.com, zqzqzhang@gmail.com

Abstract. Based on fiber coupling equation, this paper discusses the character of linear polarized mode coupling between two multi-mode silica circular waveguides which have the same dopant distribution. The Eigen values of linear polarized mode U, W are calculated based on the Eigen value equations. According to the numerical calculation, coupling coefficient and coupling length in different coupling angles are given, and the method to improve the efficiency of multimode fiber coupling is summarized.

Keywords: silica fiber, multimode fiber coupling, linear polarized mode.

1 Introduction

As lower absorption of light from ultraviolet to near infrared, SiO_2 is considered be the best material for optical transmission. During the 1970s, researchers find that dopants such as GeO_2 and P_2O_5 increase the refractive index of pure silica while materials such as boron and fluorine decrease it. According to the total internal reflection, making them be core and cladding of fiber respectively let the restriction and guiding of light energy be possible. And then, dopants of rare earth ion in core using by modified chemical vapor deposition(MVCD) for fiber amplifiers and lasers are studied, for example, Nd^{3+} gives the wavelength of $1.55\mu\text{m}$ and Er^{3+} gives $1.06\mu\text{m}$. And for pumping of high-power fiber laser, the theory of side coupling between doped silica fibers should be paid more attentions.

Abou[1] deduced the mode coupling coefficient formula, but only provided the coupling coefficients of three low rank modes. His result of simulation reflects that the coefficients of different line polarized modes are different even in the same coupling station. Jacek[2] got use of the experiential formula to prove the relationship of mode quantity and coupling coefficient. They all discovered that the influences of the relative position and geometric parameter of fiber to the coupling efficiency were obvious. However, their researches are restricted to only a few modes and the stacking coupling of modes is ignored. To the coupling of multi-mode fiber, it is essential to consider the mass coupling mode and the different coupling coefficients of the modes. To sum up, it is deficient to discuss several modes only and not enough for the application of mode coupling in practice.

The Eigen values of modes are obtained through the calculation of Eigen value equations and the factors which influence the coupling of multi-mode fiber are analyzed. The methods to improve the efficiency of the multi-mode fiber coupling are present depending on the result of numerical analysis.

2 Theoretical Analyses

In cylindrical coordinates, the electric field distribution of fiber core and clad can be obtained[3]:

$$E_{y1} = \frac{A}{J_m(U)} J_m\left(\frac{U}{a} r\right) \cos m\phi \quad r \leq a \quad (1)$$

$$E_{y2} = \frac{A}{K_m(W)} K_m\left(\frac{W}{a} r\right) \cos m\phi \quad r > a \quad (2)$$

Where A, U, W, a, J_m and K_m are mode amplitude, fiber core transverse propagation constant, fiber clad propagation constant, fiber radius, Bessel's function of order m and modified Bessel's function of order m.

For the LP modes, the following equations can be obtained:

$$U \frac{J_{m+1}(U)}{J_m(U)} = W \frac{K_{m+1}(W)}{K_m(W)} \quad (3)$$

$$U \frac{J_{m-1}(U)}{J_m(U)} = -W \frac{K_{m-1}(W)}{K_m(W)} \quad (4)$$

Eq.3 and Eq.4 are equivalent[3]. The characteristic of transverse field distribution and vertical propagation of the LP modes are fixed when Eigen value U and W are calculated. Each mode can be labeled LP_{mn} . There are the definite physical meanings for the mode ordinal of LP_{mn} . m is the order of Bessel's function while it also fixes the distribution regularity of the field in direction ϕ , where the field changes in $\cos m\phi$. Separately the number of maximum point and zero point is 2m when ϕ changes from 0 to 2π . n reflects the number of extremum in the direction of radius. In the Eigen equations, m represents the order of the equation and n is the ordinal number of the effective solution. Mode LP_{mn} represents the number n root of the equation in order m.

3 Transverse Coupling Analysis of LP Mode

Two coupling fibers A and B are discussed following. A and B have the same dopant distribution, and therefore they have the same refractive index distribution too. They are placed in parallel and α is the angle between the line of two fiber cores and the level. The coordinates of the fiber are shown in Fig. 1

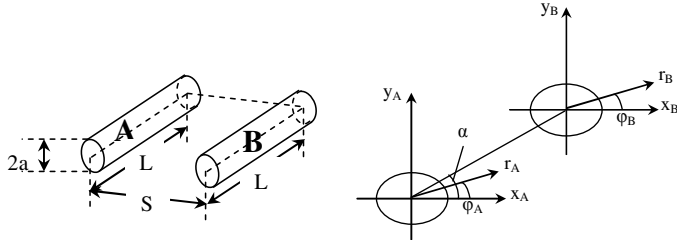


Fig. 1. Transverse coupling of multi-mode fiber

The coupling coefficient can be obtained based on the waveguide coupling equations[4]:

$$K_{AB} = \frac{\omega\epsilon_0}{4} \text{Re} \int_{s_1} E_{2y}^* \cdot E_{1y} (n_1^2 - n_3^2) dx dy \tag{5}$$

$$K_{BA} = \frac{\omega\epsilon_0}{4} \text{Re} \int_{s_2} E_{1y}^* \cdot E_{2y} (n_2^2 - n_3^2) dx dy \tag{6}$$

Integrate K_{BA} in the cross section of fiber A and K_{AB} in the cross section of fiber B. Separately n_1 and n_2 are the core refractive index of fiber A and B. n_3 is the refractive index of the area out of the fiber. According to the Eq.5 and Eq.6, when the geometry structure and electromagnetic parameters of the two waveguides are identical, $K_{21}=K_{12}$.

In ideal situation, E_{1y} and E_{1y}^* are respectively the fields in and out of the fiber A while E_{2y} and E_{2y}^* are the fields around fiber B. They are all the mode field solutions when the fiber exists singly.

Only when the modes of the coupling fibers are identical, the modes in the fibers can couple completely. Not only the Eigen values are uniform, but also m and ϕ are of the same values so that the stable propagation of the standing wave can be formed by the electromagnetic wave in the region of coupling[3].

For $C=K_{AB}=K_{BA}$, converting the coordinate, on the basis of the analysis above, we obtain that:

$$C = \frac{\sqrt{2\Delta} U^2}{a V^3} \frac{K_0\left(\frac{WS}{a}\right) + K_{2m}\left(\frac{WS}{a}\right) \cos(2m\alpha)}{K_{m-1}(W)K_{m+1}(W)} \quad m \neq 0 \tag{7}$$

$$C = \frac{\sqrt{2\Delta} U^2}{a V^3} \frac{K_0\left(\frac{WS}{a}\right)}{K_1^2(W)} \quad m = 0 \tag{8}$$

where $\Delta = \frac{n_1^2 - n_2^2}{2n_1^2}$ is the relative refractive index difference, $V = (2\pi a / \lambda_0) \cdot (n_1^2 - n_2^2)^{1/2}$ is the fiber unitary frequency

The coupling efficiency of the same linear polarized modes[1] is $h = \sin^2(CL)$, where L is the coupling length of the fibers.

4 Numerical Analyses

The radius of multi-mode fiber is $a=100\mu\text{m}$, refraction index of core is $n_1=1.457$, refraction index of cladding is $n_2=1.426$, wavelength is $\lambda_0=850\text{nm}$, the distance of the coupling fiber is $S=2a$, coupling degree is $\alpha=0$. The terms mentioned are the initial conditions for analyzing the coupling of multi-mode fiber[1].

The amount of the LP modes in every coupling direction is shown in Fig.2 on the basis of the regularity of distribution of the LP modes in the fiber cross-section. As a result, there are more modes in some special direction than that in the other one.

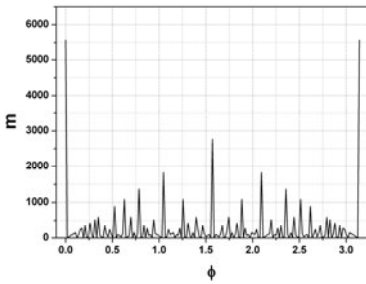


Fig. 2. Mode fields distributing

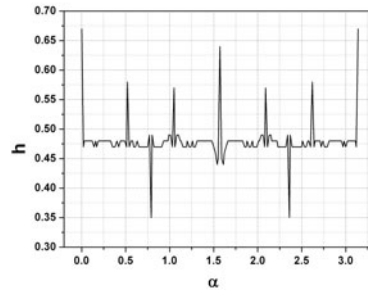


Fig. 3. The influence of geometry angle to coupling efficiency

The influence of the coupling degree to coupling efficiency is shown in Fig.3. At the coupling degree when the modes exist more, as $0, \pi/6, \pi/3$, the coupling efficiency is obviously high. However, there are lots of modes existing in some degrees, but the efficiency is low. After the calculation and analysis, it is the result not only from the distribution of the mode fields, but also the different coupling coefficients with the coupling degree change.

As shown in Fig. 4, with the changes of coupling degree, the coupling coefficient distribution changes a lot. When the degree is $\pi/4$, the modes whose coefficients are $0\sim 5$ take up nearly 50% of all the modes. The coefficients distribute inhomogeneously most compared to the other coupling degree which lead that the coupling efficiency is lower while higher in $\pi/2$ and π result from the coefficients distribute equably.

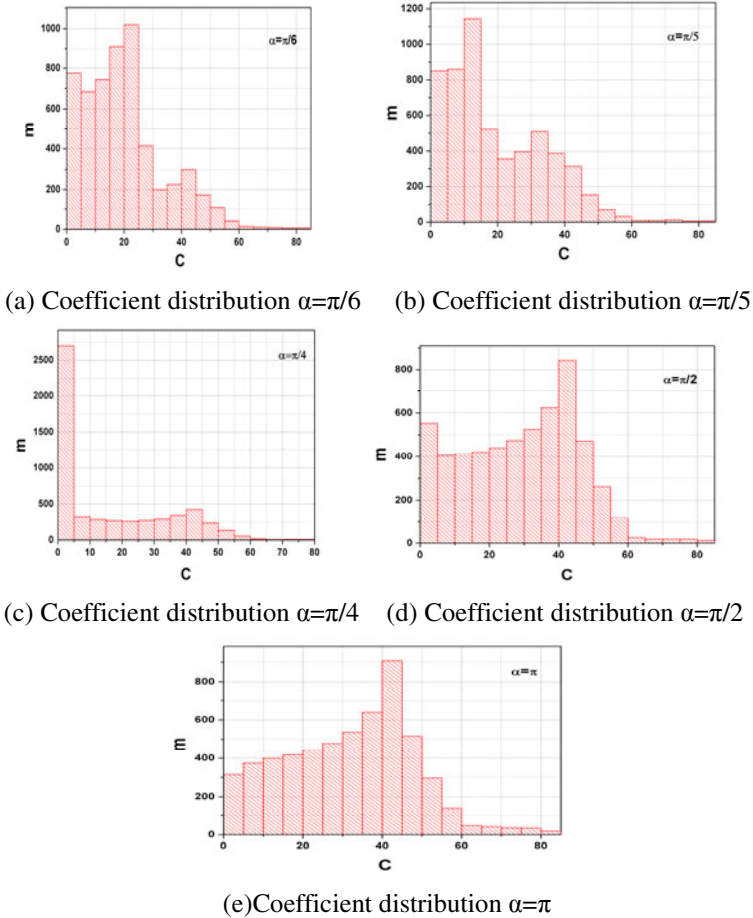


Fig. 4. The change of coupling coefficient with the geometry angle

The influence of coupling length to coupling efficiency is shown in Fig. 5. Fiber coupling efficiency is the average efficiency of all the modes:

$$h = \frac{\sum_{k=1}^N \sin^2(C_k L)}{N} \tag{9}$$

N is the quantity of the fiber modes, k represents the mode number. It is shown that, with the increase of coupling length, the coupling efficiency in the fibers drop to 50% gradually. So the coupling length should be paid attention in order to obtain higher efficiency. The factor influence the coupling length is the value of the coefficient in Eq. 9. Additionally, as the degree is different, the coefficients are also different result of the best coupling lengths is different which is shown in Fig. 6.

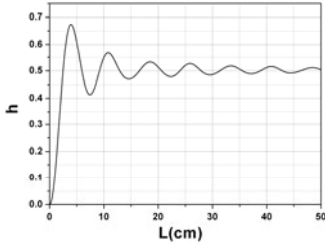


Fig. 5. Average coupling efficiency

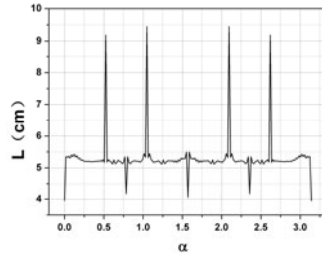


Fig. 6. The influence of geometry angle to coupling length

According to the numerical analysis above, it is known that the coupling efficiency is actually useful only in several special coupling angles. And different angles are followed by a determinate coupling lengths respectively if the best effect needs to be achieved. All these conclusions could be the guide for the fabrication of fiber coupler and combiner. To acquiring more coupling character of silica fiber, the study on the influence of the doping density distribution will be carried out hereafter.

References

1. Abou, E.-F.: Proceeding of 16th National Radio Science Conference, pp. B10/1 – B10/8. NRSC Press (1999)
2. Jacek, K.: Proceeding of SPIE-The International Society for Optical Engineering, pp. 542–547. SPIE Press, San Jose (2004)
3. Li, Y.: Theory and Technology of waveguide. Posts & Telecom Press, Beijing (2002)
4. Liao, Y.: Fiber Optics. Tsinghua University Press, Beijing (2000)

A Study on the Integration of Netblog and English Teaching with Reform of Teaching Materials

Wenlong Wan¹, Ling Zhang², Yuzhuang Lu¹, and Zhen Liu³

¹ Foreign Language Department Henan Institute of Science and Technology,
Henan Xinxiang, China, 453003
wanwenlong@hist.edu.cn, yzh@hist.edu.cn

² Foreign Language School Huanghe Science and Technology College,
Henan Zhengzhou, China, 453003
zhlsqg@hhstu.edu.cn

³ Network Center Henan Institute of Science and Technology, Xinxiang, China, 453003
liuzhen@hist.edu.cn

Abstract. In the past few years, with the reform of teaching materials, NetBlog has been attracting more and more attention as a new assistant approach to foreign language teaching. The integrated model of Netblog and college English Teaching is designed in the study. By the comparison of the traditional college English teaching model to the one based on Netblog with tests and questionnaires, the feasibility and effectiveness of the integration is finally achieved.

Keywords: Netblog, model, humanism, reform of teaching materials.

1 Introduction

In recent years, with the reform of teaching materials, more and more researchers begin to pay attention to and study Netblog, such as Husan Hua, Wang Xiaodong, Xingfu Kun and so on[1,2]. But most researches use qualitative research method, in which the origin and development of Netblog are briefly introduced, and then its application in education is discussed. This study combined qualitative research method with quantitative research method, by means of questionnaires and tests, and then the effect of the integration of Netblog and college English teaching is counted and analyzed to demonstrate the feasibility and effectiveness of integration of Netblog and college English teaching.

2 The Experiment of the Integration of Netblog and the College English Teaching

This experiment, through the setting up of Blog sites, teacher Blog, class Blog and students' personal Blog, establishes an interaction platform between teachers and students, creates a better learning atmosphere, cultivates students' self-learning ability, and improves teachers' teaching methods to achieve self-development[3].

2.1 The Target of the Experiment

The purpose of this experiment is to analyze the feasibility and effectiveness of using NetBlog to achieve teachers guiding, the use of online resources and interactive learning and training in college English teaching, and find out the main factors affecting the use of the Netblog in the experiment.

2.2 The Subjects of the Experiment

The subjects of this experiment are 238 students choosing from eight small classes in Grade 2009 in Henan Institute of Science and Technology. The eight small classes were divided into two large classes, whose English was taught by a same teacher. Each big class had 4 periods of English course per week with the same progress. The teaching material choosing for the two large classes is also same. Trade 091-4 is regarded as the experimental class, a total of 120 people using Blog as a teaching aid; Chinese 091-2, and Section 091-2 as the control class with a total of 118 people, the traditional teaching method “mouthpiece” style-based focusing on knowledge of language. The experiment lasted for two semesters.

2.3 The Experimental Methods and Experimental Tools

The experiment is carried on by means of tests and questionnaires. First, pretest is designed to know whether students from two large classes have the equivalent English, in which grade test scores of non-English major freshmen doing after their enrolment are directly used. The test is taken as the pretest. After two semesters of college English learning, students from the experimental class and control class took part in the English final exam at the end of each semester, and their performance was recorded carefully. The test is taken as the post-test. Finally, test results were counted and analyzed with software SPSS12.0. Second, a suitable scale used in this study was selected with the literature review, and on this basis, the questionnaire was revised through interviews and expert consultation. Then used the pre-test questionnaire to do small-scale issuing and recycling, and did the item analysis of the questionnaire using the data collected, and the formal questionnaire was formed by the deletion of items and the adjustment of the item content. Likert’s 5-point scoring method was adopted in the questionnaire, and the formal scale was formally handed out and recycled. The descriptive statistics analysis of data was done in the use of Excel to complete the study on the relationship of the Blog technology and college English teaching research.

3 The Statistics and Analysis of Experiment Results

3.1 The Analysis of Pre-test Data

The pre-test data was directly isolated from the examination results for graded teaching participated by the freshmen of 2009 after they enrolled for about one week, and independent samples test was done with the test data to analyze whether the English of the experimental group and control group was equivalent before the experiment. (As is seen in Table 1)

Table 1. The analysis of students' English performance before the experiment

	Highest score	lowest score	Average score	standard deviation	Sig. (2-tailed)
experimental class	92	63	76.17	8.14964	.000
Control class	91	65	77.19	8.33378	.000
T value	t=0.27 < 1.645				
P value	P=0.978 > 0.05				

From Table 1, the following can be drawn the English performance of the two large classes of students is considerable when they enrolled very soon, and their t value was $0.27 < 1.645$, while p value was $0.978 > 0.05$, the data showed that Sig. was .000, having no significant differences.

3.2 The Analysis of Post-test Data

The independent sample tests were still adopted in the second step to analyze students' English performance of the two classes. The data was mainly achieved through the two final examination performance during the course of the experiment, and then the data was entered SPSS12.0 for statistical analysis. (Table 2)

Table 2. Analysis of experimental results after the experiment

	First semester final grade		the second semester final grade		Sig.(2-tailed)
	Mean	Standard Deviation	Mean	Standard Deviation	
experimental class	69.06	4.826	78.792	6.814	.001
Control class	67.92	6.601	70.292	8.485	.000
T value	t=0.971		t=2.865		
P value	P=0.334 > 0.05		P=0.005 < 0.01		

The following can be drawn from the above table, there is not big difference between the two classes in their final examination performance in the first semester ($t = 0.971$, $p = 0.334$), which may due to students' not-fully adjustment to this new teaching model after the shorter time of doing the experience. After the experiment lasted for a year, the examination results at the end of the second semester showed that it was significantly different between the experimental class and control class ($t = 2.865$, $p = 0.005$). This shows that the strengths of Netblog Assisted College English teaching gradually revealed, students from the experimental class have greatly improved their interest in learning English, thus contributing to their performance significantly higher than the control classes.

3.3 The Descriptive Statistical Analysis of the Questionnaire

To further understand the experimental results, the research group members conducted a survey of students from the experimental class and control class. The descriptive statistics of data was done with Excel, the results as follows:

Table 3. Statistical analysis of survey data

	Very interested in learning English		more comfortable with verbal communication		equal and harmonious relationship between teachers and students		greatly improved autonomous learning ability	
	Number	Proportion	Number	Proportion	Number	Proportion	Number	Proportion
Experimental Class	108	90%	97	80.8%	113	94.2%	106	88.3%
Control Class	87	73.7%	83	70.3%	88	74.6%	57	48.3%

As can be seen from the above table, after different teaching methods were implemented in two classes, compared to the control class, students in the experimental class have been greatly improved and enhanced in interest in learning English, language ability, teacher-student relationship and self-learning ability and other aspects.

4 The Findings of the Experiment and Countermeasures

First, the education Blog has greatly improved the students' interest in learning by adding sound and video files as resources in teaching and training [4]. Secondly, education Blog increases the amount of training in listening, speaking, reading, writing and translation, thereby improving students' ability of actually using the language[5]. Third, equal and harmonious relationship between teachers and students largely determines the quality of English teaching, while the equal and harmonious relationship between teachers and students is not only affected by the communication between teachers and students in classroom, but also heavily influenced by the exchange of extra-curricular. In the Blog communication, written expression used by students and teachers can conduct a deeper, more comprehensive exchange, which will be helpful to make up for lack of interaction, promote the equal and harmonious development of teacher-student relationship, effectively enhance students' motivation of learning, and greatly improve their enthusiasm for learning. Finally, education Blog created a better learning atmosphere and enhanced the students' self-learning ability.

5 Conclusions

The appearance of Blog marks the Internet beginning to creep across the traditional information-sharing to highlight its infinite value of knowledge. The rise of Blog culture, will affect our approach to learning, teaching, and even the concept of education.

References

1. Husan, H., Wang, X.: The Application of Blog in Education Teaching. *Distance Education Journal* (1), 10–12 (2004)
2. Kun, X.: Blog and Modern Foreign Language Teaching. *Modern Education Technology* (1), 38–41 (2007)
3. Chen, X., Zhang, J.: Blog Culture and Modern Education Technology. *E Education Research* (3), 17–21 (2003)
4. Fu, X.: Blog and the Integration of Modern Education. *Education Information* (1), 47–48 (2005)
5. Mao, I.: Blog will Become an Important tool in Education. *China Distance Education* (1), 73–76 (2003)

A Corpus-Based Study with Corpus Materials on Conjunctions Used by Chinese and English Authors in English Academic Article Abstracts

Wenlong Wan¹, Ling Zhang², Zhen Liu³, and Wenxian Xiao³

¹ Foreign Language Department

Henan Institute of Science and Technology, Henan Xinxiang, China, 453003

wanwenlong@hist.edu.cn

² Foreign Language School

Huanghe Science and Technology College, Henan Zhengzhou, China, 453003

zhlsqg@hhstu.edu.cn

³ Network Center

Henan Institute of Science and Technology, Xinxiang, China, 453003

liuzhen@hist.edu.cn, xwenx@yeah.net

Abstract. On the basis of Halliday's theory of cohesion and achievements of Chinese and English leading scholars in this field, the present writer applies the principles of Chinese traditional textual cohesion --- introduction, elucidation, transition and summing up --- to the study of the use of conjunctions in English abstracts in China's English journals based on two self-built corpora with Corpus Materials. A number of Chinese and English scholars have done researches on the use of conjunctions by contrastive analysis with the rise of corpus linguistics. However, most of the main-stream research waves focused their attention on the functional classification of conjunctions based on Halliday's or Quirk's theories. The research findings would be of practical and instructive significance to Chinese EFL and researchers in writing English abstracts. They might be also helpful to teachers in EAP (English for Academic Purpose) teaching.

Keywords: Conjunctions, English abstract, Corpus Materials, English journal, Corpus-analysis.

1 Introduction

The English academic article abstracts provide the convenience for people to get the main findings. Therefore, the English academic article abstract writing is of vital importance for scholars to demonstrate their research. Traditional studies on English research article abstracts focus on the genre and stylistic analysis of English research article abstracts by native speakers, but few contrastive studies have been made on the textual cohesion between Chinese researchers and English researchers. On the basis of Halliday's theory of cohesion [1] and achievements of Chinese and English leading scholars in this field, by corpus-based analysis with Corpus Materials, the present writer applies the principles of Chinese traditional textual cohesion — introduction,

elucidation, transition and summing up — to the study of the use of conjunctions in academic article abstracts in China's English journals, to see the characters that Chinese authors show when using English conjunctions.

2 Literature Review

“With the advent of abstract databases, many readers will see your abstract separately from the rest of the paper. Therefore, writing an excellent abstract is vital to encourage readers to obtain the full paper, read it, and cite it. [2]” Due to the importance of abstracts, scholars at home and abroad have studied different types of abstracts from different perspectives.

In Western countries, previous studies of academic article abstracts fell into the scope of genre analysis. Hasan, Martin and Ventola all propose their own approaches to the analysis of generic structure[3], of which the most influential one is Hasan's generic structural potential. Salager-Meyer [4] studies medical English abstracts taken from four basic research types and three major text types. Johns [5] compares Portuguese and English versions of Brazilian academic abstracts.

In China, according to the investigation into the journal articles concerning abstract study through computer search, most of them are written for the sake of standardizing academic writing. Among those few written from the linguistic perspective, two articles are worth mentioning. Liu [6] analyzes the structural elements of Chinese research paper abstracts based on the corpus from a wide range of academic fields. While Yu [7] gives a generic structural description of 35 English abstracts presented at an international linguistic conference.

Influenced by Chinese culture and thinking mode, Chinese authors may unconsciously pay much more attention to the writing discipline in Chinese. In order to check the possibility, in this research, conjunctions are classified into four categories according to such writing discipline, that is, introduction, elucidation, transition and summing up.

3 Research Design

3.1 Research Questions

Do Chinese authors use conjunctions at the same frequency as native English authors? Do Chinese authors and the English authors use the same type of conjunctions to express the similar semantic relation? What are the most frequently used conjunctions in CEJ (China English Journal) corpus and NEJ (Native English Journal) corpus respectively?

3.2 Research Method

The basic methodology adopted in this paper is corpus-based, which involves both qualitative and quantitative study. The corpora employed are two self-built mini corpora — CEJ corpus and NEJ corpus. The abstracts in these two corpora are taken from two authoritative Chinese linguistic Journals and two international linguistic

Journals published from the year of 2006 to 2007. AntConc3.2.1 is to be used for concordance analysis and SPSS13.0 for statistics.

3.3 Data Retrieval

With the help of AntConc 3.2.1, we counted the total number of conjunctions in the two corpora, examined the occurrence frequency for each of the conjunctions one by one and provided the concordance for every instance of conjunction in order to assure the maximum precision of occurrence frequency of each conjunction. For each conjunction, the concordance list was screened and, in some cases, the original text was studied. By comparing the overall frequencies, we found the general tendency of the conjunctions used by the two groups of subjects. Next the differences and similarities of the use of conjunctions in the two corpora were explored. According to the frequency of each conjunction, the top ten frequently used conjunctions in each corpus were listed. The Chi-square test was used to test the significance of the differences.

4 Results and Discussion

Firstly, from the overall frequencies of the conjunctions used in CEJ corpus and NEJ corpus, Chinese researchers tend to overuse conjunctions in their abstract writing (71.9:66.3), but from the standard type-token ratio, conjunction density used by Chinese researchers is less than that by the English researchers(31.4: 56), and the difference is significant ($p=.000<.05$).

Table 1. The Overall Frequency of Conjunctions in NEJ and CEJ

	NEJ	CEJ
Total Journal Paper Length (words)	1,10 44	2,34 72
Total Conjunctions (tokens)	732	1687
Frequency: tokens/1,000	66.3	71.9
Types	41	53
Frequency: types/1,000	3.71	2.26

Table 1 exposes that there was a minor difference in overall frequency of conjunctions between Chinese researchers and English researchers (71.9:66.3) which means that Chinese researchers had a tendency to use more conjunctions than English researchers. Each conjunction in CEJ corpus occurred 7.19 times on average, while in NEJ corpus, it occurred 6.63 times on average. Consequently, we can draw a conclusion that Chinese researchers used a large range of vocabulary in their abstracts, while English native researchers employed a smaller vocabulary and a small number of conjunctions. But the types of conjunctions by Chinese researchers were less than those by English researchers.

Secondly, the difference in using elucidation and transition conjunctions by Chinese researchers and English researchers is significant ($p=.000<.05$). However, the difference in using the introduction and summing up conjunctions by Chinese researchers and English researchers is not significant ($p=.083 >.05$, $p=.770 >.05$).

From the comparison of conjunctions in both corpora (see Table 2), we can find Chinese researchers use more summing up conjunctions.

Table 2. Comparison of conjunctions of NEJ and CEJ

	Introduction		Elucidation		Transition		Summing up	
	Total	Type	Total	Type	Total	Type	Total	Type
NEJ	2	2	26	23	17	13	12	6
CEJ	2	2	26	25	17	15	12	12

The differences in using introduction conjunction ($p=.083>.05$) and summing up conjunction ($p=.770>.05$) were not obvious. The use of elucidation conjunction ($p=.000<.05$) and transition conjunction ($p=.000<.05$) was significantly different. This indicates when Chinese researchers and English researchers used a type of conjunction, the difference was quite obvious. However, did it have a significant difference when the four types of conjunction were used on the whole? By SPSS statistic and Chi-square test, we can see that difference was not significant ($\chi^2=7.696$, $p=.053 >0.05$).

In short, as academic English writers, Chinese researchers had internalized the essence of academic argumentation in English and mastered some skills of conjunction use in their English abstracts writing. Moreover, the target readers' comments might also influence Chinese researchers' behavior on conjunctions use in their abstract writing. However, Chinese researchers use more summing up conjunctions and elucidation conjunctions than English researchers.

Thirdly, the top ten conjunctions were used most frequently. The ten conjunctions in each corpus cover only about 1/10 of all conjunctions, and the overall frequency of them is 82.79% in NEJ corpus and 85.06% in CEJ corpus respectively. This shows that both Chinese researchers and English researchers had a tendency to use these high frequency conjunctions to achieve discourse cohesion. And there was a significant difference in the total normalized frequency in both corpora (827.869: 850.623). From the normalized frequency of one particular conjunction in NEJ corpus and CEJ corpus, the Chinese researchers had the tendency to overuse some conjunctions and underuse other conjunctions. Moreover, among the top ten conjunctions in each corpus, seven conjunctions were the same used both by Chinese researchers and English researchers even though the sequence was different. This indicates there existed some similarities and differences in the use of conjunctions.

5 Conclusions

The present research has investigated the similarities and differences between Chinese researchers and English researchers in using conjunctions in English academic

articles' abstracts writings. It also answers the question what features conjunctions show in Chinese researchers' abstract writings. The research findings are a good reference for Chinese learners of English to write better English abstract and thus to make their research articles more easily acceptable by international academic discourse, for teachers in EAP (English for Academic Purpose) to give better guidance and suggestions in writing, and for editors of China's English journals to examine research articles they receive in a more international-standard way.

References

1. Halliday, M.A.K., Hasan, R.: *Cohesion in English*, vol. 9. Foreign Language Teaching and Research Press, Beijing (2001)
2. Martin, P.M.: A Genre Analysis of English and Spanish Research Paper Abstracts in Experimental Social Sciences. *English for Specific Purposes* (1), 25–43 (2003)
3. Paltridge, B.: Genre Analysis and the Identification of Textual Boundaries. *Applied Linguistics* (2), 502–505 (1995)
4. Salager-Mayer, F.: A Text-type and Move Analysis Study of Verb Tense and Modality Distributions in Medical English Abstracts. *English for Specific Purposes* (1), 93–113 (1992)
5. Johns, A.: *Text, Role, and Context*. Cambridge University Press, New York (1997)
6. Liu, S.: *An Outline of the Western Style*. Shandong Education Press, Jinan (2003)
7. Yu, H.: *A Systemic-Functional Approach to Research Paper Abstracts*. Foreign Language Teaching and Research Press, Beijing (2002)

Embedded Fingerprint Identification System Based on DSP Chip

Fuqiang Wang¹ and Guohong Gao²

¹ Network Management Center
Xinxiang University, Henan Xinxiang, China, 453003
wfgwang@163.com

² School of Information Engineer
Henan Institute of Science and Technology, Henan Xinxiang, China, 453003
ggh75@qq.com

Abstract. Fingerprint identification system set pattern recognition, image processing, and database technology in one, suitable for a variety of authentication applications, with a wide range of applications. This article describes the method of DSP microprocessor for the silicon materials manufacturing-based embedded fingerprint recognition system method and specifies the system's hardware and software design process. The system is able to automatically carry out classification, moreover, compare the results with the fingerprint database in real time. Experimental results show that the system can quickly obtain information on the identity of persons to be identified.

Keywords: Image acquisition, Fingerprint feature extraction, Fingerprint identification, DSP chip materials.

1 Introduction

Fingerprint used as a means of identification for a person has other means incomparable superiority. Compared with the other method of identification such as face recognition, iris recognition, fingerprint recognition has the following advantages: (1) the uniqueness of fingerprints, from the current study results, the world does not have two identical fingerprints. Besides, a person's fingerprint determined from the moment of one's birth, and does not change with age. (2) Relatively easy to collect fingerprints. There are various types of fingerprint capture devices, just click with ones, the fingerprint images will be obtained, and it's relatively convenient. (3) The fingerprint recognition algorithm is already quite mature, at present a good fingerprint recognition algorithm's false acceptance rate and false rejection rate can be reached to 1% and 0.1% or less at the same time. On a better performance PC, the time of a fingerprint's recognition does not exceed 0.5 seconds[1].

DSP chip has a strong mathematical ability, besides, the external interface with flexible design; interface circuit is very convenient and cost less and less. This system uses It's TMS320VC5402 as the processing unit of DSP (hereinafter referred to as C5402), with embedded fingerprint identification system[2].

2 Principle of Fingerprint Identification

Fingerprint recognition is a comprehensive study in the area of pattern recognition. The core elements of the fingerprint image are extracted form of organization and order. These elements include the composition of the ridge, flow direction, the center, delta points and minutiae points. As the fingerprints collected and scene fingerprint influenced by the severity of indentation, distortion, deflection and the environment, so that there is relative deformation of fingerprint images, deformity, and noise, resulting in information loss and the appearance of false features. Thus the key of fingerprint image pattern recognition is to seek the method that adapt to image processes and feature's extraction of all kinds of image environment and seek for the image topology model that the relative scale, translation, rotation, affine invariant don't change and the invariable quantity of computer vision. Guided by this approach, the basic processing framework of Automatic Fingerprint Identification usually includes fingerprint collection, preprocessing, feature extraction and classification[3].The algorithm process of fingerprint identification system mainly include:

- (1) image processing - to obtain high-quality binary image;
- (2) lines refinement - to obtain a binary image after thinning;
- (3) details of the extraction - extracting endpoints and shape of the intersection;
- (4) details of the comparison - the details of the input template and the input image;

The purpose of image processing is to enter the gray image into binary image which has better quality. As fingerprint image is a louder noisy image, therefore need image enhancement to reduce the noise and enhance the ridge line.

3 Realization of Fingerprint Identification System

3.1 The Basic Composition of Fingerprint Identification System Hardware

DSP-based fingerprint identification system with the basic same to PC, input and output signals of fingerprint identification system, the only difference is that it constitutes a fingerprint image processing using DSP core, which can from the PC to fingerprint identification[4]. The block diagram shown in Figure 1, DSP-based fingerprint identification system composed by a fingerprint acquisition, DSP unit and memory unit. In addition, since some of the high-performance DSP chip set with flexible external interface, so in order to increase processing capacity of the system, some systems are often includes other management units, such as the fingerprint database, communications, human-machine interface and so on, a number of high-grade fingerprint identification system also requires a Ethernet interface and Internet connectivity.

Fingerprint image acquisition is to get digital fingerprint images that computer can identify. General approach is to "1×1" identify digital fingerprint image into 512×512 pixels (each pixel 8bit) of the array. DSP unit is the core of the fingerprint processing system, is responsible for processing fingerprint images in real time to complete the image preprocessing, extracting fingerprint signatures. And marching the fingerprint

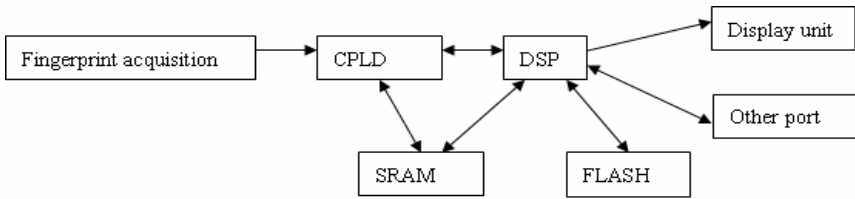


Fig. 1. Principle diagram of fingerprint identification system

feature with the fingerprint database, given the results of discrimination. The unit is composed by main processor of DSP and can be synchronized through the DSP serial port to communicate with other devices. Memory unit consists of SRAM and FLASH memory chip implementation. CPLD (complex programmable logic device) to achieve image acquisition to address generation and the image stored in the SRAM, but also produce other function modules' control signal and a variety of independent timing that system needs or combinational logic circuits. SRAM used for program execution and store temporary data. FLASH used to store boot loader program of DSP, so that the system on the electric start, and contains the fingerprint characteristic data area program.

3.2 Hardware Design of Fingerprint Identification System

Fingerprint identification system adopts TMS320VC5042 processor, produced by TI, as the core processor, the chip is the DSP that TI launched in 1996. Its features are: (1) around eight of bus constitute of enhanced Harvard architecture; (2) a high degree of parallelism and CPU with dedicated hardware logic design; (3) highly specialized instruction system; (4) modular structure design ; (5) advanced IC technology.

Fingerprint acquisition chip adopts FPS200, produced by the Veridical of U.S. MBF200 is capacitive Fujitsu solid fingerprint sensor that can capture the fingerprint images to 500dpi. Its sensors are 256 × 300 sensor array, can be operated in 3.3V ~ 5V wide voltage range.

Fingerprint identification system structure is shown in Figure 2.

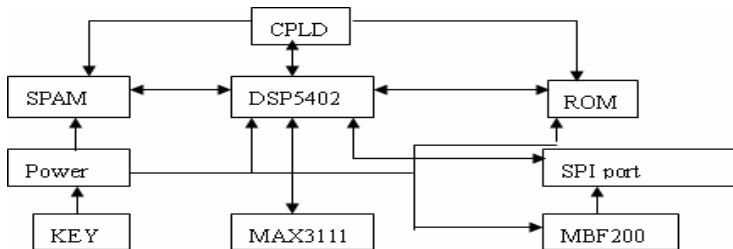


Fig. 2. Fingerprint Identification System structure

When fingerprint collected, the 5402 external expansion RAM and ROM. RAM used to store fingerprint data, ROM to store DSP program. Which, MAX3111 is to provide a RS232 interface, through this interface, fingerprint acquisition system can outward (such as PC) to provide fingerprint data. DSP and MBF200 are 3.3V power supply. MBF200 need no external crystal, but rather use the internal 12MHz oscillator to provide clock.

3.3 Fingerprint Identification System Software Design

Fingerprint Identification System programming, using mixing programming methods, and C language design processing time is not strictly required for the module, design in assembly language requires real-time core algorithm.

MBF200 and 5402 to complete the interface communication between the SPI, still need to run the program on 5402. When the fingerprint data received by 5402, due to before not completed MBF200 in a row, the frame signal must remain in effect, that is to say the length of a frame for 256×8 bits. Therefore, the DMA 5402 can only be used to receive, DMA receive frame size should be configured to 128×16 bits. 5402 part of the assembly procedure is as follows:

/*Open the automatic buffering unit (ABU), open the DMA to 128-word \times 16-bits frame the DMA receiving, channel 0 */

```

STM # DMSRC1, DMSA; set the source address for DRR10
STM # DRR10, DMSDN
STM # DMDST1, DMSA; set the destination address to 3200H
STM # 3200H, DMSDN
STM # DMCTR1, DMSA; set the size of the buffer for 80H a word
STM # 80H, DMSDN
STM # DMSFC1, DMSA
STM # 0001000000000000B, DMSDN
STM # DMMCRI, DMSA
STM # 0101000001001101B, DMSDN
STM # DMIDX0, DMSA
STM # 0001H, DMSDN
STM # 0000001000000011B, DMPREC
...../* INTO interrupt service , used to receive the data of MBF200 */
RET

```

4 Conclusion

Fingerprint identification technology is a kind of relatively mature biometric technology, as to the traditional "ID+password" authentication, it has the advantages of safe and convenient. DSP microprocessor designs adopt fingerprint identification system with fingerprint recognition fast and accurate. This system can automatically carry out classification of fingerprint, besides, comparing the results with the fingerprint database in real time. After testing reach the application requirements.

References

1. Xu, H.-l., Shi, H.-r.: Investigation on S3C2440-based Embedded Fingerprint Identification System. *Instrumentation Technology* (02), 46–48 (2011)
2. Wang, J.: Design of Fingerprint Identification System Based on DSP. *Industrial Control Computer* (03), 65–67 (2010)
3. Pan, J.-j., Zhang, H.-y.: Design of embedded automatic fingerprint identification system. *Journal of Beijing Information Science & Technology University* (01), 62–65 (2010)
4. Ren, L., Chen, L.: Design and Implementation of Fingerprint Verification System Based on Embedded Application. *Science Mosaic* (03), 82–84 (2010)

Temperature Monitoring System Based on AT89C51

Xingrui Liu¹ and Guohong Gao²

¹ Network Management Center
Xinxiang University, Henan Xinxiang, China, 453003
49046838@qq.com

² School of Information Engineer
Henan Institute of Science and Technology, Henan Xinxiang, China, 453003
ggh75@qq.com

Abstract. This paper presents a low cost temperature detection and control design in composite films of the material production based on AT89C51. The system uses nickel-chromium-nickel-aluminum thermocouple as a temperature sensing element, the ICL7135 as the AD converter, displaying the detected temperature through the LED. This paper focuses on the components of the system hardware, the design method of microcontroller interface circuit and software implementation process. After testing, the system is accurate and reliable.

Keywords: AT89C51, Temperature Measurement, ICL7135, Temperature Control, Materials.

1 Introduction

Temperature is one of the main accused parameters in the industrial object, especially in metallurgy, chemical industry, building materials, machinery, food, petroleum and other industries, the furnace, heat treatment furnace and reactor are widely used, so stoves and heating fuel are different, such as gas, natural gas, oil and electricity. The process and the temperatures required are different, and thus the temperature sensors and the temperature methods are different. Product process is different, so the precision of temperature control is also different. Thus the precision of the data acquisition (A/D conversion) and control algorithms are also different. But as concerned the dynamic characteristics of the control system, that is basically the lagging part. For such a link, if delay time is shorter, PID control can be used; if a longer delay time, Dahlin algorithm can be used. If the delay time and time constant changes largely (the part of the approved amount of investment varies greatly), adaptive control algorithm can be used. In the plastic packaging (also known as flexible packaging) industry, it is necessary to put an additional layer of pure white or silver aluminum foil on the back of the exquisite designs of printed plastic, which needs to use tape laminating machine. Its main principle is that after heating it to melt raw materials printed on the back attached to form a protective film to avoid scratching patterns. Laminating machines now are generally universal temperature control devices, and have a large range of temperature control and low accuracy. As the response speed and control accuracy are less than technical requirements, general

temperature control devices on the laminating process will result in the low firm of combined products and poor heat sealing.

This design implements a special temperature control device as the temperature control part for laminating machine. To solve the flexible packaging industry’s laminating processes propylene melting furnace temperature control is to increase reaction speed and control accuracy, thereby improving product quality and enterprise efficiency.

2 System Design

The basic requirements of system design: (1) system should be able to set the desired temperature parameters (the range of parameters: 0-4000C), and be displayed through the LED display; (2) temperature control system should be able to accurately detect the actual temperature of the object and be displayed in the LED display; (3) the system should be able to detect the temperature of the actual parameters of the signal sent to the processor after treatment, the processor should be able to give timely and safe temperature difference between pre algorithm parameters, and give control signals and immediately adjust the temperature; (4) system should be able to store the parameter of the system settings in this value to no re-setting the next time. (5) after the system design is complete, the action should be stable, control action should be correct, control accuracy should be within +5%.

To meet the basic requirements above mentioned, temperature control system uses the AT89C51 microcontroller as the main chip to achieve ICL7135 AD conversion, combined with the external MCU clock circuits mature, high-precision voltage regulator, bus drivers and other devices. As showed in Figure 1.

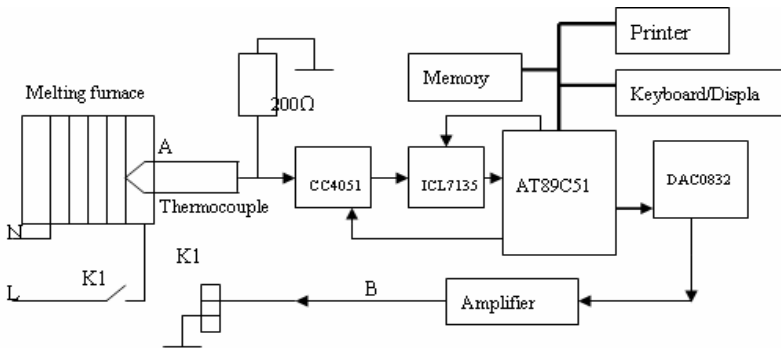


Fig. 1. System structure diagram

In Figure 1, the melting furnace is the controlled object, the control parameter is the melting furnace temperature (system output) y . Changing the gaining and losing state of single-phase of solid power loop (DC4-32V) can control the heat of hot plate and temperature. The temperature is detected by the thermocouple. The thermocouple output is under 100mv, after a signal conditioning circuit into a 0-2V signal, then the A/D converter transfers it into a digital signal send to microcontroller AT89C51. The

microcontroller uses the setted temperature and actual temperature of the furnace system to obtain e , and then uses PID algorithm output to get u_k (digital), which is added to the control Line B by the D/A converter into analog amplification, thereby changing the melting furnace temperature. Temperature range: 0-400⁰C (technical requirement is 0-400⁰C), temperature control accuracy: $\pm 0.5\%$.

EPROM is used for storing programs and forms. RAM is used for storing data temporarily. 8255A is used to extend the parallel port for connecting printers and other external devices. Keyboard or display panel is used for inputting and displaying device parameter and the setting amount. Serial port is used for communicating with other computers.

As the temperature of melting furnace is 0-400⁰C, so the design uses nickel-chromium-nickel-aluminum thermocouple as detection components, sub-degree number is EU, the output signal is 0-41.32mv. Electronic control transmitter uses the transmitter mA, the output is 0-10mA, and then goes through the current - voltage converter circuit to transform into 0-2V signal, then goes to A/D conversion through the A/D conversion circuit. A/D converter adopts double integral A/D converter ICL7135, with a resolution of 1/20000, that is 0.005⁰C, fully meeting product process requirements.

Heat uses single-phase AC220V, 2500W heating plate to supply heat for melting furnace. The control device uses Single-phase 4-32V DC controlled solid-state relays. System master schematic is showed in Figure 2.

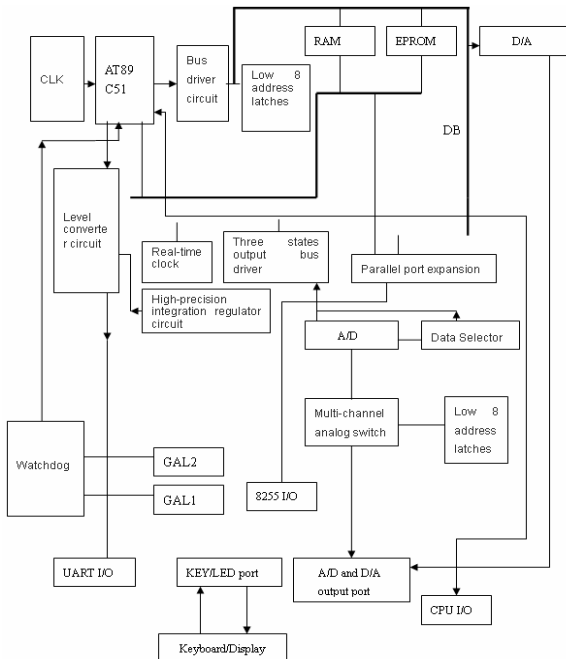


Fig. 2. The main control circuit principle diagram

3 Software Control Algorithm Design

In the design, in order to improve the system precision, the gearshift integral PID control algorithm is adopted. In the hypothesis to keep the temperature for 400C, when the deviation is more than 5%, to abandon integral items totally; when deviation less than 1%, to keep all integral items; when deviation is between 1% to 5%, to increase integral items in diminishing; when the deviation is 1%, equivalent to 4c, corresponding to the binary number B1; when the deviation is 5%, equivalent to 20C, corresponding to the binary number B2. $B2-B1=B3$.

The positional output of increment algorithm of PID control’s gearshift integral differential equation is as follows:

$$\begin{aligned} \Delta u_k &= K_p e_k + N K_i e_k + K_D (E_k - 2E_{k-1} + E_{k-2}) \\ U_k &= U_{k-1} + \Delta U_k \\ N &= 1 \quad |E_k| > B2 \text{ 时}; N = (B2 - E_k) / (B2 - B1) \quad B1 < 1, 1 \leq B2; \\ N &= 0 \quad |E_k| \leq B1 \quad E_k = X - Y_k \end{aligned}$$

$K_i = K_p T / T_1$, T is the sampling period (S), T1 is integral time (S), K is scale coefficients. $K_D = K_p T_D / T$, T_D is differential time (S). E_k is the deviation. X is the binary numbers system given. Y_k is corresponding to the A/D converter’s output binary number. E_{k-1} is the last system deviation, E_{k-2} is the more last deviation. The U_{k-1} is the last U_k value calculation result.

4 System Test Analysis

After the temperature measurement and control system is completed, the whole system is conducted five tests. It can be shown through the test results, in the system allowed set temperature range (0-400⁰C), that the system control precision can be in between -0.5% and +0.5%, which can completely satisfy the product technique requirements. As shown in table 1.

Table 1. The test record results of five times

Times	Set temperature (°C)	Initial temperature (°C)	Display temperature (°C)	Response speed (s)	Control precision
1	218	214	217	30	-0.4%
2	297	278	296	110	-0.3%
3	342	312	343	65	0.2%
4	359	352	361	56	0.27%
5	384	364	385	125	0.26%

5 Conclusion

This design, based on the single chip as the key control parts, adopts advanced temperature measuring element and scientific data acquisition and processing technology and advanced heating components and control method, which is helpful for improving temperature measurement and control precision and effectively improving the response speed of system. What's more, it is beneficial to achieve production requirements, reduce costs and improve efficiency. Due to various reasons, the sensitivity and accuracy of control circuit system are expected to be improved further, and it depends on improving the accuracy of measuring devices, data processing algorithm, and the accuracy of analog digital conversion and the optimization of system control algorithm and software.

References

1. Zhong, X.-w., Song, Z.-c.: Microcontroller-based Design of Laboratory Temperature and Humidity Control System. *Forestry Machinery & Woodworking Equipment* (01), 39–42 (2010)
2. Wang, G., Sun, F., Chen, G.: Design of a new TEC-based constant temperature controller. *Microcomputer Information* (01), 88–91 (2010)
3. Li, H.-p.: Design of AT89S52-Based Shaft Temperature and Humidity Intelligent Control System. *Journal of Jishou University(Natural Sciences Edition)* (01), 70–73 (2010)
4. Hub, O.: Research of Temperature Control System Based on PLC. *Industrial Control Computer* (02), 80–83 (2010)

A Simple Query Mechanism for the Compressed XML in Mobile Circumstance

ShengBo Shi

Institute of Information Technology, Zhejiang Shuren University, Zhejiang, 310015, China
shirleysb@gmail.com

Abstract. Mobile commerce is gradually becoming reality business and XML has become the popular makeup language in mobile circumstance. However, the XML application in mobile network is not very mature. One of the most important issues is how to effectively achieve the compression and query of the XML documents in mobile network. Therefore, this paper combines the development of mobile circumstance and the advantages of XML to study a simple XML query mechanism in the mobile circumstance.

Keywords: SXML, SXQ, XML, mobile circumstance.

1 Introduction

Mobile commerce is gradually becoming reality business. Mobile phones and other wireless devices such as PDA, Pocket PC, and embedded devices are becoming ubiquitous. More and more businesses and customers are increasingly trying to published products information, brown information, communicate to each other and complete the transaction by the mobile network. Besides, XML has the advantages such as flexible, extensible, investment-cheap, widely applicable to make the heterogeneous data among different enterprise applications system to exchange smoothly, automatically and real-time. Recently, the applications of XML have been rapidly developed, including data description, network data exchange, database application and many other fields, and becoming a main form of a new generation of mobile networks data description. However, the XML application in mobile network is not very mature, fragmentary, incomplete and unsystematic. One of the most important issues is how to effectively achieve the compression and query of the XML documents in mobile network.

Therefore, this paper combines the development of mobile commerce and the advantages of XML to study a simple XML query mechanism in the mobile commerce.

2 The Premise of the Simple XML Query Mechanism

The following XML Query Mechanism would not apply to all of XML compressed document, only for the XML documents which have special structure and nature even

after compression. So, before querying, the XML documents should be compressed to be the SXML format.

The Design of SXML Mechanism. To improve the data file transmission and storage efficiency, several of transmission programs and compression mechanisms have been proposed, such as traditional Huffman coding, Lempel-Ziv algorithms, Burrows-Wheeler compression algorithm and XMill compressed model. However, the existing algorithms have been unable to meet the demands for mobile business applications to support a simple and quick query mechanism for the compressed XML. To solve this problem, a new mechanism called as SXML (Simple XML) has been proposed, which can be used in mobile environment to re-encode and to construct new XML documents and make it into more compact data format. Following is a brief description of its basic ideas and implementation.

SXML designed specifically for XML encoding, which can retain the main content of XML document while make data parsing faster than normal. The original XML document will be restructured through SXML mechanism to reduce the storage size and speed up the data processing. Therefore, SXML can keep the advantages of XML and reduce the side-effects to make XML more suitable for mobile circumstances. The detail information about SXML code mechanism is outlined as follows:

Flat XML Structure. Replace the bottom son elements by attributes as keeping XML document extensible. The aim of flattening XML structure is to reduce the memory storage in mobile and don't lose the structure of XML.

Make Tags Concise (Including element, attribute and prefix of namespace). Don't make tag longer than 5 words. Replace longer tag by concise tag which also keeps XML documents extensible. The aim of making tags concise is also to reduce the memory storage.

Order by Content Correlation: Reduce Duplicate Input. The aim of ordering by Content is to change the structure of XML, while no extra memory are consumed and parse more efficient.

Reduce Intervals and Indentation. The aim of reducing intervals and indentation is to save the storage and make the XML file more compressed.

Unify Common Tags. The aim of unifying common tags is make the file more readable and formal to parse.

Above rules reflect the principles of SXML, and they can be added in future to make SXML more perfect for mobile application.

Traditional XML compress methods such as XML compression and XML encoding aim to process the whole document, which will increase the process and response time among several systems, while SXML's purpose is to translate the original XML by streaming and speed up the data processing. So if the focus of mobile system is to reduce the process and response time so as to make users get data more quickly, SXML code mechanism is a good choice.

SXML cannot replace XML compressor, but it can do some pre-treatment before compression. The key character of SXML is that the SXML can reduce the file's size in nature. Its difference from the compression philosophy is that when displaying XML files, SXML doesn't have to decompress them to parse which may also take up large storage.

So the advantages of SXML can be listed as it can reduce the size of XML documents effectively; without too much computing consumption; simplifying the compression processes; provide convenience for further text compression; a new criterion for xml documents that can be used in mobile phones; perfect transplantable performance.; more Easy to understand the syntax.

The Implementation of SXML. SXML focused on processing speed and the structural characteristics of compressed document and the XML document through the pretreatment can reduce the size while improving processing speed. SXML retained the form of XML document specification, which make it different form other compression mechanisms. Although SXML and XMill have some similarities, such as the use of numeric codes instead of element names, they are completely different methods. The following are the code for SXML.

Selecting the XML should be compressed:

```
public class XMLTest extends MIDlet {
    String filepath="/res/order.xml";
    Courseware cw=new Order(filepath);
    String scw=cw.readOrder Read file.
    private Display display;
private Command exitCommand = new Command( "Exit", Command.EXIT,
    1 );
    public XMLTest(){ }
protected void destroyApp( boolean unconditional )
    throws MIDletStateChangeException {
    exitMIDlet();
    }
}
```

The SXML implementation:

```
private String compactString(String str) {
    int linebreak = 0;
    int linestart = 0;
    int strlen = str.length();
    StringBuffer strb = new StringBuffer();
    String strcom=new String();
while(linestart < strlen && (linebreak = str.indexOf("\n", linestart)) >= 0) {
    strb.append(str.substring(linestart, linebreak).trim());
    linestart=linebreak+1 ;
    }
    if (linestart > 0 && linestart < strlen) {
    strb.append(str.substring(linestart).trim());
    }
    strcom = strb.toString();
    return strcom;
    }
}
```

The Characteristic of SXML. SXML specifically designed for mobile circumstance as an XML compression mechanism has some special advantageous, especially in the limited storage space, low bandwidth, high latency and other mobile wireless transmission circumstance. Through the course of preprocessing and compression, respectively, stressed the XML document markup language, markup language specification and the form and structure to maintain after compressing. The following aspects were elaborated for the contribution of SXML to the compression query mechanism.

Normative. In network, a large number of XML file are lack of format and uniform format version. SXML mechanism stresses the normative markup language and makes the compressed XML documents adhere to the rules of XML, and all available XML documents are of uniform structure. Before compression of all the normative documents, form the structure taking the advantages of bringing unity to facilitate SXML mechanism for selective compression, such as starting and ending tags of the separate compression. Under these conditions the compressed XML document can also be maintained as the original structural features, to support for its implementation of the compression check and balance the query response time and comprehensive query.

Structural. Most of the existing mobile business environment based on the compression mechanism does not support compression check was due to their overall compression and compression efficiency over the expense of pursuing the query function. The more the compression is closely the more difficult the query based on its implementation. SXML pretreated good balance of compression rate and compressed structural strength and this will address key issues for step by step transfer.

3 Design of SIMPLE XML Query Mechanisim ——SXQ

Despite the existence of the index structure based on the XML query language used in Web services, but does not query the compress XML files to facilitate the application of mobile phone transmission. Therefore, this article aims to conceive of a query mechanism in the formation of good performance SXML applied on the document, not only to maintain the advantage of the existing XML query language, but also to facilitate users to locate the file that you need and choose to download it in limited bandwidth and mobile network services.

This query mechanism envisaged SXQ (Simple XML query mechanism) of the difficulty lies in the comprehensiveness and balance inquiries, check the flow control, aimed at mobile business environment make it possible for the simple and practical. Network services for mobile phones query mechanism envisaged in the definition of SXQ is in the details, there are modified to support XML query language.

Design of the Key Mechanism. The key to this query mechanism is to form a “Tag Data Dictionary”. Firstly, XML file is pre-optimized using SXML compression, while it is formed the individual “Tag Data Dictionary” based on the structural of XML. Secondly, it is categorized and label according to the content of the “Tag”, and finally, described the content of the XML file with the “Tag Data Dictionary”.

Use the following simple code to explain how the “tag data dictionary” generates.

```

<?xml version="1.0" encoding="gb2312"?>
  <item>
    <title version="EN">Extensible Markup
      Language</title>
    <definition> Extensible Markup
      Language<title>XML</title>
    </definition>
    <kind>Computer</kind>
  </item>
  <edition>Chinese translation edition</ edition >
  <authorname>Chen An</authorname>
  <authorposition>Professor</ authorposition >
  </item>

<?xml version="1.0" encoding="gb2312"?>
  <item>
    <title version="EN">Gone with the
      Wind</title>
    <definition>Gone with the wind</definition>
    <kind> Literature </kind>
  </item>
  <edition>Original edition</ edition >
  <authorname>Michael</authorname>
  <authorhation>America</authorhation>
  </item>
    
```

Fig. 1. Codes for Example

The “Tag Data Dictionary” is generated as the below.

No.	Category	Description
01	title	Extensible Markup Language
02	title	Gone with the Wind

No.	Category	Description
01	kind	Computer
02	kind	Literature

No.	Category	Description
01	authorname	Chen An
02	authorname	Michael

Fig. 2. Data Dictionary

Generally, it is chosen “title” or “author name” for inquiries and occasionally through the “books kind”. Actually, the “Tag Data Dictionary” can be generated to facilitate inquiries according the fact.

The relevant items can be associated by pointer. For example, if it is inquired by choosing “author name” and the key word is “Chen An”, then finding the No.01 and Category “authorname”. The relevant items in the “Tag Data Dictionary” are “Computer” and “Extensible Markup Language”, which are No.01s in Category “kind” and Category “title”. All of these will be returned to user as the query result.

Design of Overall process. Firstly, users select the appropriate query keyword to submit to the server. Then, the server finds the appropriate category tags based on the user-selected keywords, and match the keyword according the “Tag Data Dictionary”. The server will return the relevant tag information for users to choose the exactly XML file to transmit, decompress and other related operations to browse the information he or she want to query.

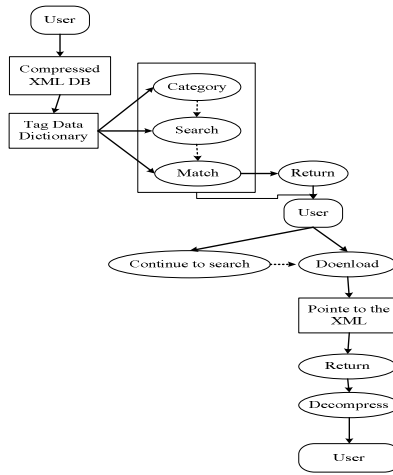


Fig. 3. Overall process

3.1 Design of Specific Incident Response

Search in the “Tag Data Dictionary”. Firstly, it locates in the "Tag Data Dictionary", then inquires the tags in “"Tag Data Dictionary” according to the appropriate keyword. Finally, accesses the match tags and numbers.

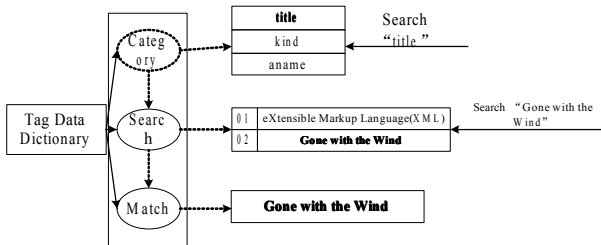


Fig. 4. Search in the “Tag Data Dictionary”

3.2 Return the Query Results

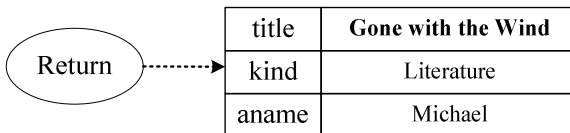


Fig. 5. Return the query results

3.3 Choose to Download the Relevant XML File

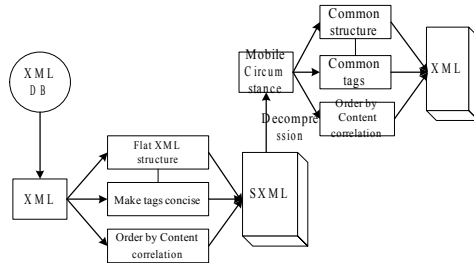


Fig. 6. Choose to download the relevant XML file

4 Conclusion

This article puts forward a simple mechanism (SXQ) for the compressed XML in mobile circumstance, which is the support of XML technology to make its development more quickly. But there are still some limitations in application. Especially, the algorithm needs further modification and improvement. However, these issues will be resolved in the future and SXQ will be used more widely.

References

1. Harrusi, S., Averbuch, A., Yehudai, A.: XML syntax conscious compression. In: Proceedings of the Data Compression Conference, DCC 2006, March 28-30, 10 p (2006)
2. Liefke, H., Suciu, D.: XMill: an efficient compressor for XML data. In: Proceedings of the ACM SIGMOD International Conference on Management of Data, pp. 153–164 (2000)
3. Li, J.B., Miller, J.: Testing the semantics of W3C XML schema. In: 29th Annual International on Computer Software and Applications Conference, COMPSAC 2005, July 26-28, vol. 1, pp. 443–448 (2005)
4. Kotsakis, E., Bohm, K.: XML Schema Directory: a data structure for XML data processing. In: Proceedings of the First International Conference on Web Information Systems Engineering, June 19-21, vol. 1, pp. 62–69 (2000)
5. Adacal, M., Bener, A.B.: Mobile Web services: a new agent-based framework. IEEE Internet Computing 10(3), 58–65 (2006)
6. Shi, S.: SXML, an Enhancement of XML Documents in Mobile Learning. cise 2009, 12 (2009)

Robust Audio Watermarking Algorithm Based on Audio Binary Halftone Pre-process

Huan Li^{1,2}, Zheng Qin¹, XuanPing Zhang¹, and Xu Wang¹

¹ School of Electronics and Information Engineering, Xi'an Jiaotong University
Xi'an, Shanxi, China, 710049
lihuan@dgut.edu.cn

² Department of Computer Science, Dongguan University of Technology
Dongguan, Guangdong, China, 523808

Abstract. Conventional audio watermarking method has the following deficiencies: the embedded watermarking signal bits are too less; the image watermarking pre-process is too simple which reduce the security; the embedded audio watermarking is meaningless binary sequence. To address these problems, we propose a robust audio watermarking algorithm based on audio binary halftone pre-process. The meaningful audio watermarking can be preprocessed to high-fidelity binary audio. The variable dimension operation is used to scramble the host audio. Experiments show the proposed algorithm has big embedding quantity, high security, strong practicability and robustness in enduring common attacks.

Keywords: Robust Audio Watermarking, Audio Binary Halftone, Variable Dimension.

1 Introduction

With the development of computer and network technology, people gradually go into the network and the information age. More and more information resources can be accessed through wired and wireless network, but information security and protection of property rights problem become obviously. In recent years, many digital watermarking algorithms have been proposed for intellectual property right protection of digital media data [1]. The conventional audio watermarking methods have the following deficiencies: 1) the embedded watermarking signal bits are too less; 2) the embedded image watermarking is directly reduced to one-dimensional space and then embedded in audio signals, so the watermarking pre-process is too simple which reduce the security; 3) the embedded audio watermarking is meaningless binary sequence.

To address these problems, in this paper, a robust audio watermarking algorithm based on audio binary halftone pre-process is proposed. The proposed algorithm is based on our early work about audio binary halftone [2], Audio Scrambling Algorithm [3, 4].

2 The Related Definitions

High Dimensional Matrix transformation. For a given $m \times m \times \dots \times m$ (m^n) super cube space, the high dimensional matrix transformation is shown as follow. Where $A_{n \times n}$ is an $n \times n$ integer coefficients matrix and the determinant of $A_{n \times n}$ ($|A_{n \times n}|$) is a relative prime of m .

$$\begin{bmatrix} y1 \\ y2 \\ \vdots \\ yn \end{bmatrix} = A_{n \times n} \begin{bmatrix} x1 \\ x2 \\ \vdots \\ xn \end{bmatrix} \pmod m \tag{1}$$

Binary Halftone Pre-process. According to early work about audio binary halftone [2], meaningful digital audio watermarking is processed to high-fidelity binary audio. Based on Floyd error diffusion algorithm [5], we proposed an Audio Binary Halftone process algorithm. In our method, the error which is caused by waveform conversion from sine wave to a square wave is feedback to follow-up audio sequence. This method is called digital audio binary halftone procedure. The error diffusion model is given in fig.1, where, $m(x)$, $n(x)$, $p(x)$, and $e(x)$ respectively denote input data, output data, input data by preceding step error diffusion, quantization error, $Q(\cdot)$ is threshold quantization, and $W(k)$ is Floyd-Steinberg error diffusion filter.

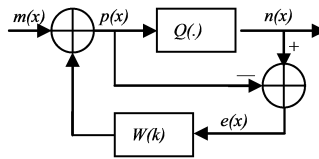


Fig. 1. Error diffusion model

The related computer formulas are as follows:

$$p(x) = m(x) + \sum_k w(k) \cdot e(x - k) \tag{2}$$

$$n(x) = Q(p(x)) = Q(m(x) + \sum_k w(k) \cdot e(x - k)) \tag{3}$$

$$e(x) = n(x) - p(x) \tag{4}$$

The value of $Q(\cdot)$ is selected by practical situation, and the parameters of $W(k)$ are: $W(1)=7/16$, $W(2)=5/16$, $W(3)=3/16$, $W(4)=1/16$.

3 The Realization of Algorithm

Watermarking Embedding Scheme. Let L denote the pre-processed host audio signals length, which was divided to K segments, and each segment has R audio sample points. Let T denote the pre-processed 1-dimensional binary audio watermarking and $B(i) \in [0, 1], 1 \leq i \leq k$; Let $A_i(j)$ denote the audio point in i segment, $A'_i(j)$ denote the embedded sample point, and S is the max of the values that satisfy the Eq.5:

$$A'_i(j) = \begin{cases} A_i(j) - A_i(j) \bmod S + 3S / 4, \text{ if } B(i) = 1; \\ A_i(j) - A_i(j) \bmod S + S / 4, \text{ if } B(i) = 0; \end{cases} \quad (5)$$

Watermarking Extraction Scheme. According to the idea of maximum likelihood decoding, we extract the watermark. Let $B'(s)$ denote the extracted watermark, $\rho(B', B)$ denote the correlation function:

$$\rho(B', B) = \sum_{i=1}^k B'(i), B(i) \quad (6)$$

If exists $\rho(B', B) \geq T$, T denote threshold, we think the watermark is extracted.

The Realization Procedure of Algorithm. The frame diagram of proposed algorithm is given in Fig.2.

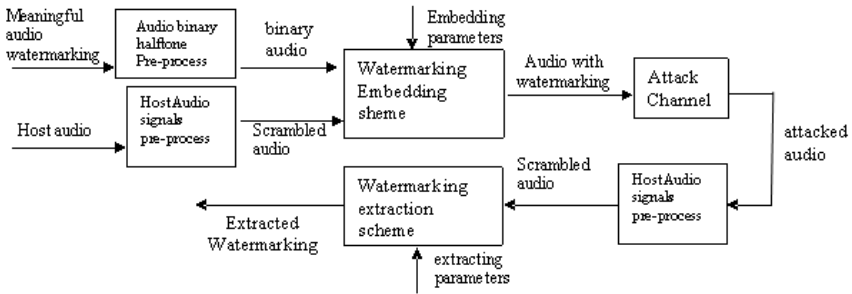


Fig. 2. The frame diagram of the proposed algorithm

1) *Embedding sub-procedure*

Step1: according to audio binary halftone pre-process, the meaningful audio watermarking is pre-processed to binary audio watermark;

Step2: according to the host audio signals pre-process, the host audio is pre-processed to scrambled audio [4];

Step3: according to the Eq.5, embed the binary audio watermark in the scrambled host audio sequence

Step4: get the audio with watermark.

2) *Extracting sub-procedure*

Step1: according to the host audio signals pre-process, the audio signals with watermarking (attacked or non-attacked) is processed to a scrambled audio.

Step2: according to the Eq.6, extract the binary audio watermarking;

Step3: test the performance of the extracted watermarking.

4 Experiment Results and Analysis

In this section, we use 'start.wav' as audio watermarking, and host audio signals sample 'close.wav' (Table1 and Fig.3). For better show performance, we selected 500 points of the 'start.wav' as Fig.4a. From the audio binary halftone pre-process experimrnt (Fig.4), audio watermarking 'start.wav' is processed to high-fidelity binary audio.

Table 1. The Variables of Audio Sample

Name	Length (N)	Time (ms)	File type	Bit	Sample ratio (Hz)	Wave plot
Start	11386	0.516	.Wav	16	22050	Fig.3a
close	183040	1.379	.wav	16	22050	Fig.3b

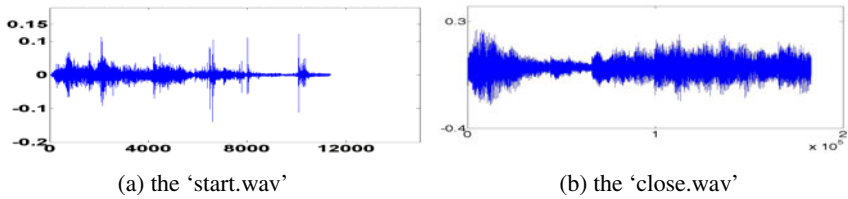


Fig. 3. The wave plots of audio

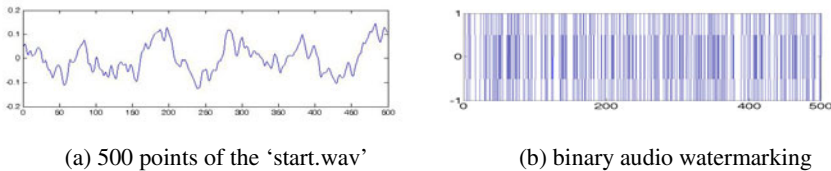


Fig. 4. Audio binary halftone pre-process experimrnt

According to [3], we randomly generated 2 groups of arbitrary high dimensional transform matrices (Fig.5). The pre-processed host audio signal is shown in Fig.5e.

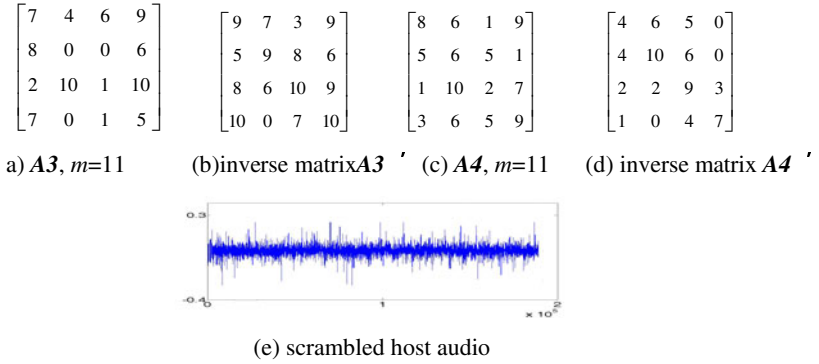


Fig. 5. Host audio signals pre-process experiment

In Fig.6, the audio watermarking embedding experiment is given. From the wave plot of Fig.6b, we can find that it has similar algorithm with the original host audio wave plot. The experiment confirms that the host audio signal with watermarking has good listening performance.

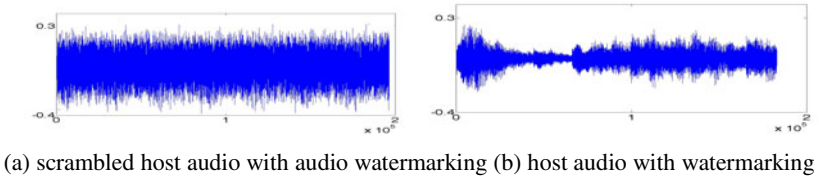


Fig. 6. Audio watermarking embedding experiment

After some different attacks, such as zerocross, Gaussian noise addition, data loss, data amplification and data reduction, etc, the algorithm has good robustness.

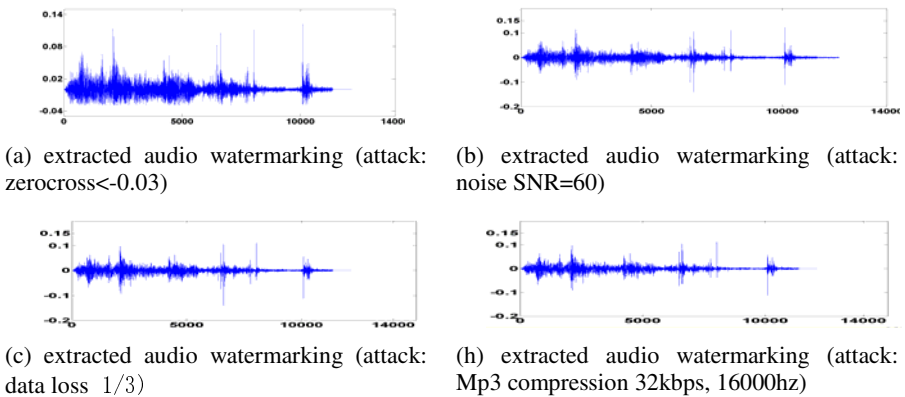


Fig. 7. Extracted audio watermarking from host audio in different attacks

5 Summary

In this study, we proposed a robust audio watermarking algorithm based on audio binary halftone pre-process. Our proposed algorithm is used to solve these problems: the embedded watermarking signal bits are too less; the watermarking pre-process is too simple; and the embedded audio watermarking is meaningless binary sequence. The proposed algorithm pre-processed the audio watermarking and host audio respectively in different method, which increase the security. Experiments show that the proposed algorithm has a wonderful pre-process performance, high imperceptibility, and robustness in enduring common attacks.

Acknowledgment. This work was supported by the National Defense 11th-Five-Year Preliminary Research Project of China under grant (No. 282660008 and N0. 570851613), the Science and Technology Plan Foundation of Dongguan City (No.2008108101001, No. 200910814006).

References

1. Takahashi, A.: Multiple Watermarks for Stereo Audio Signals Using Phase-Modulation Techniques. *IEEE Transactions On Signal Processing* 53(2) (2005)
2. Wang, X.: Research on the Security Algorithm of Auditory Cryptography Based on Auditory Properties of Human Being. Master Degree Thesis of Xi'an Jiaotong University (2010)
3. Shao, L., Qin, Z., Li, H.: Scrambling Matrix Generation Algorithm for High Dimensional Image Scrambling Transformation. In: *IEEE International conference on ICIEA*, pp. 3–5 (2008)
4. Li, H., Qin, Z., Shao, L.: Variable Dimension Space Audio Scrambling Algorithm Against MP3 Compression. In: *IEEE International conference on ICA3PP* (2009)
5. Floyd, R., Steinberg, L.: An adaptive algorithm for spatial greyscale. *Proceedings of the Society for Information Display* 17(2) (1976)

A Virtual Restoration Strategy of 3D Scanned Objects

Guizhen He¹ and Xiaojun Cheng²

¹ Department of Surveying and Geoinformatics, Tongji University, Shanghai, China
yangxin100122@msn.com

² Key Laboratory of Advanced Engineering Survey of SBSM, Shanghai 200092, China
cxj@tongji.edu.cn

Abstract. For creating model, laser scanner is frequently used to sample the object. In practice, due to surface disrepair, certain areas of the object are usually not sampled which will lead holes. This paper presents a strategy for filling holes. First, the k-nearest neighbors of scattered point cloud are found to project to the plane by the method of ALS; then mesh within the plane is divided to extract the boundary; the hole is filled under the constraint of the boundary. Finally, the complete model is built to achieve virtual restoration. The results show that the strategy is more simple and effective with less time costs in contrast to the typical method.

Keywords: virtual restoration, filling hole, scattered point cloud, the hole boundary.

1 Introduction

Reverse engineering can be widely applied to repair broken arts or torn parts in the modern manufacturing field of aviation, aerospace, marine, automotive and mold [1], such as repairing damaged statues and carvings; repair the damaged ship caused by using for years; repair ancient architecture. At this point, the entire prototype is not needed to copy, only the needed repair parts and components are extracted in order to achieve the positioning of empty defects and reverse modeling by means of reverse engineering, which can simulation repair technology of defect objects to achieve the modernization of remediation technologies. In the process of studying repair, point cloud with holes should be studied obtained by the three-dimensional laser scanning technology. In practice, there are different types of holes. According to curvature the holes can be divided into large curvature holes and small curvature holes; by hole size can be divided into large holes and small voids; by the other can be divided into closed and non-closed hollow holes, with characteristic features and without.

The problem of filling holes in range data can essentially be divided into two sub-problems: identifying the holes and finding appropriate parameterizations that allow the reconstruction of the missing parts using the available data. According to different types of holes for different repair methods, this paper mainly studies the large hole for large surface. Currently there are two automatic extraction methods for holes: the first is to identify holes by grid topology based on the surface mesh models. The main idea of this approach: If the mesh has not holes, any edge in the model belongs to only two triangles, and if one belongs to only one triangle, the edge which constitutes the hole

polygon edge is the boundary edge [2, 3]. According to the definition of the boundary edge in the grid model, hole boundaries can be searched just by going through the whole triangular mesh surface. This method is simple, but the premise is that triangular grid model need to be pre-generated, which will overlook features in the generation process of triangular mesh model [4]. The second is directly to identify the boundary points from the scattered point cloud, Gu Yuanyuan [5] proposed a method to identify the hole boundary by judging the uniformity of K neighborhood points, in fact, which will be affected by the interference of noise; Qiu Zeyang [6] proposed a strategy to extract the boundary points by planing the scattered points to the two-dimensional, which is not well applied in surface repair for overlapping projection. To construct the holes, different strategies are employed. Davis [7] presented a volumetric diffusion algorithm, which calculated the distance function of the volume elements near the surfaces and applied a diffusion process to extend this function. Y.Jun[8]proposed a method that can automatically fill complex polygonal holes. Based on the 3D shape of the hole boundary it divided a complex hole into simple holes, and use planar triangulation method filling each simple holes. And smooth and subdivide the newly added hole triangles as the final result. Y.J.Yang etal.[9]proposed N-sided hole filling method to fill n-sided holes which corner is surrounded by rational surfaces (NURBS surfaces) with epsilon-G(1) continuous NURBS patches for vertex blending.

The pleasant result of filling hole method should be immune to the noise points of the hole's edge and be faithful to the true surface with fairly less time-consuming and manual interactive. This paper is organized as follows. First, extraction of the hole boundary is introduced; then hole-filing is presented under the constraint of the boundary, offering the result by building models. Finally, the conclusion is proposed.

2 Hole Boundary Extraction

Extraction of the hole boundary need to use the topological relationships of data near the hole and the projection points of the data in the plane. Specific extraction procedure is shown in Fig 1.

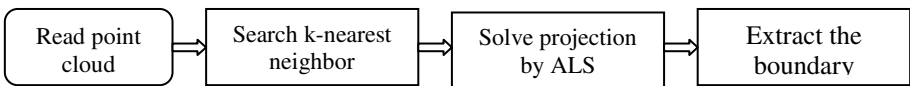


Fig. 1. Flowchart of hole boundary extraction

A. K-Nearest Neighbor Searching

When the hole boundary is extracted from the scattered point cloud, the topological relationship must be established firstly by defining K nearest neighbor which can use the compression octree construction for this strategy. The minimum external cube of the measured surface is regarded as the root of octree model which is divided into eight sub-cubes with the same size regarded as the root of each sub -node to produce 2 power sub-cubes by subdividing space. Octree partition rules: If a sub-cube includes the measurement points (including part of the measured surface), the sub-cube is

recorded as a real node (denoted by black nodes in Figure 2); if the child does not contain a measured point, the sub-cube is denoted as a virtual node (shown by white nodes in Figure 2). The real node is ulteriorly divided to repeat until side length of the sub-cube is less than or equal to a given segmentation accuracy. After dividing $2^n \times 2^n \times 2^n$ octree space, location of any node can be uniquely identified by an octal number for using octal code in Figure 2:

$$Q = q_{n-1}8^{n-1} + q_{n-2}8^{n-2} + \dots + q_k8^k + \dots + q_18^1 + q_08^0 \tag{1}$$

In equation (1), the node q_i is the octal digit to complete show path from each node to the root. The entity node code is {0,00,7,77,774,777} in Figure 2.

It is very easy to determine the parent and sibling nodes based on the node code in cube. If the known coordinates of any point P can obtain the corresponding sub-cube node, 27 sub-cubes can be quickly found according to recurrence relation between the adjacent node code and the node code. K-nearest neighbor of point P can be obtained by fast-tracking octree which can greatly accelerate the search speed and improve the search efficiency.

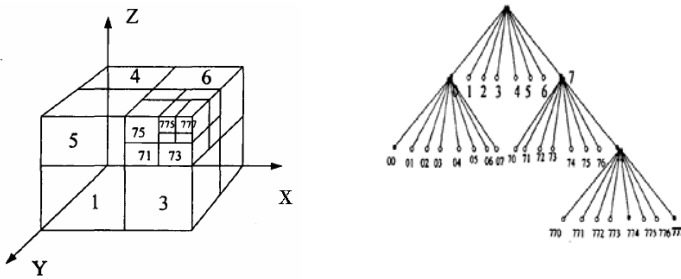


Fig. 2. The establishment and space partition model of octree

B. Projecting by Advancing Layer-Wise Solution

The main idea of this method is to use the characteristic that point cloud in the same level has the same curvature by solving the curvature of K-nearest neighbor point layer by layer. $(Q - P)$ is a vector which any point p directs to the q in its neighbor, then the curvature of the point p along the direction at:

$$k(p, q) = \frac{|Nq - Np|}{|Q - P|} S(p, q) \quad S(p, q) = \begin{cases} 1 & (Np \times Nq) \cdot [Np \times (Q - P)] > 0 \\ -1 & \text{ot her} \end{cases} \tag{2}$$

The basic curvature of any point can be estimated by equation (2). Minimum curvature direction $d1 = q1 - p$; Minimum curvature $k_{min}(p) = k(p, q_1) = \min_{q \in \Omega(p)} k(p, q)$; Maximum curvature direction $d2 = q2 - p$ Maximum curvature $k_{max}(p) = k(p, q_2) = \max_{q \in \Omega(p)} k(p, q)$;

The curvature is greater than the point with threshold γ which is set according to the average curvature, and then calculates middle point c. In order to reflect the

impact of C, each point is given a weight value. The weight function is the Gaussian function:

$$w_m(c) = \exp\left(\frac{-\|p_m - c\|^2}{\sigma^2}\right) \tag{3}$$

$$\bar{p} = \frac{\sum_{p_m \in Nb(c)} w(c) p_m}{\sum_{p_m \in Nb(c)} w(c)} \tag{4}$$

$$CW = \begin{bmatrix} w_1(\bar{p})(p_1 - \bar{p}) \\ \dots\dots\dots \\ w_m(\bar{p})(p_m - \bar{p}) \end{bmatrix}^T \begin{bmatrix} w_1(\bar{p})(p_1 - \bar{p}) \\ \dots\dots\dots \\ w_m(\bar{p})(p_m - \bar{p}) \end{bmatrix} \tag{5}$$

Three feature vectors $\{\lambda_0, \lambda_1, \lambda_2\}$ can be calculated by this matrix to form orthogonal vectors in three-dimensional space. The center \bar{p} and vectors λ_1, λ_2 consist of a projection plane:

$$H = \{x | \langle \lambda_0, x - \bar{p} \rangle = 0, x \in R^3\} \tag{6}$$

K-nearest neighbor of all points are calculated using the above method. the projection of some two points are shown in Figure 3.

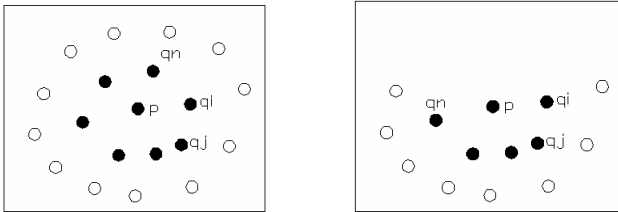


Fig. 3. k-nearest neighbor projection of boundary with hole and without hole

C. Hole Boundary Extraction

The minimum bounding box is found in the projection plane for K-nearest neighbor of all points, which is split by rectangular grid with a certain interval (determined by the K value). The grid is divided into two types: one is a real hole; another empty hole. Each mesh has four adjacent meshes (except the grid boundary). For the real mesh, if its four neighboring meshes have at least one empty or less than 4 meshes, the mesh is defined as

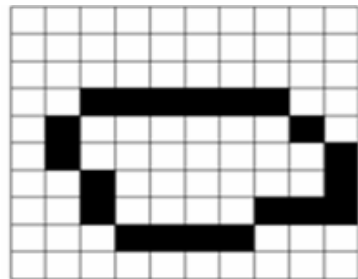


Fig. 4. Extracted boundary grid

the boundary which is signed as black mesh in the grid. All the extracted meshes are connected to obtain the boundary grid.

3 Filling Missing Points

The establishment of the fitting surface under the constraint of point cloud within the boundary grid, these steps is followed:

(1)The triangle ABC is set which can contain all the boundary point cloud p_s' , its original point p_s as the point to fit surface. Firstly calculate surface parameter coordinates (u_s, v_s, w_s) : $u_s=S_{\Delta APs'B}/S_{\Delta ABC}, v_s=S_{\Delta APs'C}/S_{\Delta ABC}, w_s=S_{\Delta BPs'C}/S_{\Delta ABC}$. Taking the p_s coordinates and (u_s, v_s, w_s) into the n times Bezier surface equation can obtain the initial fitting surface.

(2)Obtain the distance vector $d(u,v,w)$ which is from p_s to the surface and partial differential $s_u(u,v,w), s_v(u,v,w), s_w(u,v,w)$, command:

$f(u,v,w)=d(u,v,w)$. $s_u(u,v,w)=0$; $g(u,v,w)=d(u,v,w)$. $s_v(u,v,w)=0$; $h(u,v,w)=d(u,v,w)$. $s_w(u,v,w)=0$;

The above equations are solved based on Newton iterative method using equation

(7): $H\sigma^T = K^T$ Which $\delta_u + \delta_v + \delta_w = 0$,

$$K = -(f(u_s, v_s, w_s), g(u_s, v_s, w_s), h(u_s, v_s, w_s)) \tag{7}$$

$$H = \begin{bmatrix} f_u f_v f_w \\ g_u g_v g_w \\ h_u h_v h_w \end{bmatrix} = \begin{bmatrix} (\|s_u\|^2 + d.s_{uu})(s_v.s_u + d.s_{uv})(s_w.s_u + d.s_{uw}) \\ (s_u.s_v + d.s_{vu})(\|s_v\|^2 + d.s_{vv})(s_w.s_v + d.s_{vw}) \\ (s_u.s_w + d.s_{wu})(s_v.s_w + d.s_{vw})(\|s_w\|^2 + d.s_{ww}) \end{bmatrix}$$

We can obtain $\begin{bmatrix} (\|s_u\|^2 + d.s_{uu})(s_v.s_u + d.s_{uv})(s_w.s_u + d.s_{uw}) \\ (s_u.s_v + d.s_{vu})(\|s_v\|^2 + d.s_{vv})(s_w.s_v + d.s_{vw}) \\ (s_u.s_w + d.s_{wu})(s_v.s_w + d.s_{vw})(\|s_w\|^2 + d.s_{ww}) \end{bmatrix} \begin{bmatrix} \delta_u \\ \delta_v \\ \delta_w \end{bmatrix} = - \begin{bmatrix} f(u_s, v_s, w_s) \\ g(u_s, v_s, w_s) \\ h(u_s, v_s, w_s) \end{bmatrix}$

for $\delta_u + \delta_v + \delta_w = 0$

finally obtaining

$$\begin{bmatrix} (\|s_u\|^2 - s_w.s_u + d.(s_{uu} - s_{uw}))(s_v.s_u - s_w.s_u + d.(s_{uv} - s_{vw})) \\ (s_u.s_v - s_w.s_v + d.(s_{vu} - s_{vw}))(\|s_v\|^2 - s_w.s_v + d.(s_{vv} - s_{vw})) \\ (s_u.s_w - \|s_w\|^2 + d.(s_{wu} - s_{vw}))(s_v.s_w - \|s_w\|^2 + d.(s_{vw} - s_{ww})) \end{bmatrix} \begin{bmatrix} \delta_u \\ \delta_v \end{bmatrix} = - \begin{bmatrix} f(u_s, v_s, w_s) \\ g(u_s, v_s, w_s) \\ h(u_s, v_s, w_s) \end{bmatrix} \text{ for}$$

iterative solution until $m \sum_{s=0}^{m-1} \|d(u_s + \delta u, v_s + \delta v, w_s + \delta w) - d(u_s, v_s, w_s)\| \leq \epsilon$ ϵ is preset accuracy of fitting surface, and then the final fitted surface S' can be determined.

(3) Some points are taken on line which is taken on the surface S' to fill the missing point cloud.

4 The Examination Result

The above strategy is implied and verified, the test results shown in Figure 5. (a) shows a large hole with the original point cloud data, (c) that the method used to filling the hole to build the model shown in (d).

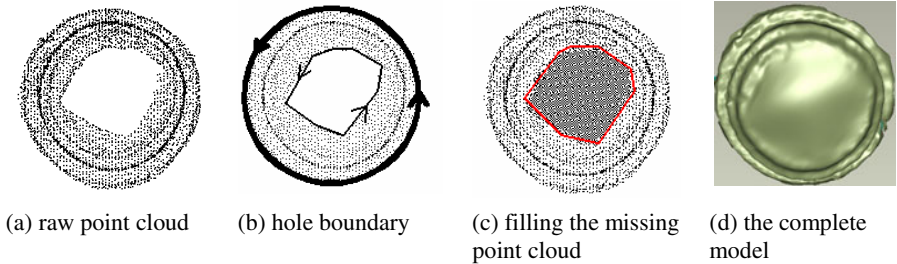


Fig. 5. Virtual restoration

5 Conclusion

In this method, the data uses K-nearest neighbor to calculate planar projection points by ALS for extracting the boundary mesh. The fitting surface is built under the constraint of the boundary to achieve the purpose of filling the missing point cloud. Specific experiment results show that the proposed strategy has strong robustness and adaptability, not only to inhibit the noise, but also not to request "single-value" surface, which can be better to avoid duplication for any complex surface.

References

1. Gu, Y.: Research and Implement of Hole-Repairing Technology for Scatted Points Cloud. Suzhou University, Suzhou (2008)
2. Zhang, L., Zhou, R., Zhou, L.: Research on the Algorithm of Hole Repairing in Mesh Surfaces. *Journal of Applied Sciences* 20(3), 221–224 (2002)
3. Lee, I.-K.: Curve reconstruction from unorganized points. *Computer Aided Geometric Design* 17(2), 161–177 (2000)
4. Wang, D.N., Oliveira, M.M.: A hole-filling strategy for reconstruction of smooth surfaces in range images. In: 16th Brazilian Symposium on Computer Graphics and Image Processing, Sao Carlos, Brazil, pp. 11–18 (2003)
5. Gu, Y., Jiang, X., Zhang, L.: The Boundary Extraction of Point Cloud with Hole in Surface Reconstruction. *Journal of Suzhou University (Engineering Science Edition)* 28(2), 56–61 (2008)
6. Qiu, Z., Song, X., Zhang, S.: A New Method for Extration of Boundary points from Scattered Data points. *Mechanical Science and Technology* 23(9), 1037–1039 (2004)

7. Davis, J., Marschner, S., Garr, M., Levoy, M.: Filling Holes in Complex Surfaces using Volumetric Diffusion. In: Proc. First International Symposium on 3D Data processing, Visualization, Transmission (2002)
8. Jun, Y.: A piecewise hole filling algorithm in reverse engineering. *Computer-Aided Design* 37, 263–270 (2005)
9. Yang, Y.J., Yong, J.H., Zhang, H., Paul, J.C., Sun, J.G.: A rational extension of Piegl's method for filling n-sided holes. *Computer-Aided Design* 38, 1166–1178 (2006)

The Study of Multimedia Transmission IPv6 QoS

Wenxian Xiao¹, Tao Zhang², Wenlong Wan³, and Zhen Liu¹

¹ Network Center

Henan Institute of Science and Technology, Xinxiang, China, 453003

xwenx@yeah.net, liuzhen@hist.edu.cn

² Network Management Center

Xinxiang University, Henan Xinxiang, China, 453003

zht@hstu.edu.cn

³ Foreign Language Department Henan Institute of Science and Technology,
Henan Xinxiang, China, 453003

wanwenlong@hist.edu.cn

Abstract. With the IP network development, streaming media application is more and more, the network can provide effective QoS guarantee, especially to multimedia applications. IPv6 QoS support for reference of new properties, with RSVP agreement and comprehensive service and divisional service integration, and based on this IPv6 network realization based on a guarantee multimedia communication QoS technical plan.

Keywords: IP network, QoS, Multimedia, Distinguish service, Materials.

1 Introduction

With the rise of multimedia services, computers have not only been used for processing according to the number of tools, but more and more close to the life, the computer interaction more real and vivid, the computer network, proposed the corresponding more high to beg. For those who have bandwidth, delay, delay jitter special requirements such as application, it is now some "best" service it is not enough. Although the development of network technology, network bandwidth and network speed are improved tremendously, but need to through the network transmission of data but also by almost the same with network development speed increase, even over the network and the speed of development, this makes the network bandwidth and network speed degrees is still a bottleneck problems. Meanwhile, developed in recent years, some new applications (such as multimedia applications, etc.) not only increased network traffic, more because this some application has altered the Internet flow properties, so they need whole new service requirements. Because do not have service quality guarantee characteristics, can't reserved bandwidth, network time delay, so can limit the current Internet cannot support many new applications, such as remote teaching, distance surgery and academic exchanges.

2 The Related Models Of Qos

2.1 Distinguish between Service Models

Because Int Serv/RSVP body is the extension exhibition deposit sex differences, solid now after miscellaneous such problems, IETF presents a new QoS security machine system namely area points service system structure Diff Serv. Distinguish between service is to adopt the polymerization mechanism will have the same characteristics of several flow together provide services for the entire polymerization flow, and no longer oriented individual traffic. That is to say, in distinguishing the service network boundary on a router maintain each flow state, core router responsible only for packet forwarding and not keep status information. This Core2Stateless knot constitutive has very strong expansibility.

2.2 IPv6 on QoS Support

To Pv6 QoS support mainly reflects in IPv6 Packets to head defined in the two parameters: business types (Ttraffic Class) and agriculture class (Flow Label). Among them, the distribution of agriculture Class 8 Bit, this field can be sent node and the middle of the router definition and recognition. Business category wills IPv6 packet points into different categories or different priority permissions. With the similar To IPv4 and realize real-time service S as speech business and video business) and non-real-time business (such as file transfer, etc) classification, define different priority. In between the router according to different agriculture Class level calls different treatment strategies to ensure the IP network of service quality.

3 Realization of Multimedia Transmission Basing on Ipv6 Network

3.1 Multimedia Application of Network Technology Requirements Analysis

Multimedia data transmission is different from general data transmission; it must request network can provide certain service quality to guarantee the normal application. First of all, should guarantee the certain bandwidth, this is because the multimedia letter, letter interest amount is large, to transmit audio, video data, etc. Must have corresponding network bandwidth. The Times, delay should be controlled in a certain value the following; otherwise staccato audio or video letter number to the user brings intimacy. Again, packet loss rate below a certain value, or in addition to the user bring discomfort outside, still can cause the multimedia information incomplete sex.

3.2 Multimedia Data Transmission Authored QoS Implementation

As stated above, comprehensive service can provide end-to-end services quality assurance. However, due to its extendibility difference, in real application is not used in backbone. And distinguish service is the priority for transmitted in a certain extent, improves the IP network transmission quality of service, at the same time as

scalability, because the appropriate in backbone online application. Figure 3 is considered the various service models of optimal faults brought after the end-to-end multimedia transmission architecture. This architecture is in the edge network with resources reserve technical basis and reference for intraoperative IPv6 support QoS new characteristics (agriculture Class and Flow Label), and combined with a multimedia data points of characteristics of transmission layer research multimedia communication QoS scheme.

3.3 Experimental Analysis

Figure 1, node 1 data transmission to the node 5, node 2 data preach lost node 6. Node 1 and 2 for the sending data nodes UDP bag, the biggest send streaming for 6 M, basic layer for 3M, node 3 to 4 transmission streaming nodes for 10M.

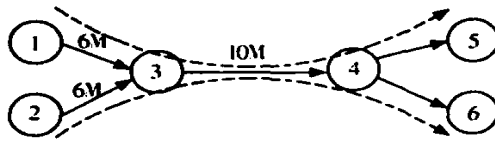


Fig. 1. Network transmission simulation schemes

Testing a fully type resources reserve way validated:

Node 1 first sends a packet, 2 seconds after 2 start sending data nodes in network resources are nodes by 1 residual resources occupied, cannot satisfy the resources needs two nodes resource reserve failure, so there is no way to transmit data. The nodes 1 data sending ended, node 2 resources reserve to build a successful, begin to transmit data.

Test two adaptive resources reserve way validated:

Node 1 open beginning hair, send several according to section 2 seconds after beginning point 2 hair send several according to open. Now although network resources cannot satisfy the node 2 6M data bandwidth requirements, but take the adaptive relegation resources reserve way, node 2 according to the bandwidth demand regular condition net reduced to 4M, insure the resources and the establishment of the reserve data normal transmission.

Test three forced resources reserve way validated:

Node 1 sends data, 2 seconds after 2 starts to send data nodes. Although bandwidth resources do not satisfy the requirements of node, but due to two nodes 2 endowed with high priority, request network nodes in resource allocation shall be strictly guarantee, so in assigned to node 1 resources were forced to drop to 4M below, for node 2 release put bandwidth resources. This solution verified forced resources reserve for multimedia industry-combining the room-service transmission QoS safeguard.

Test using distinguishes service of four data transmission validated:

Node 1 and 2 shall not engage in resource nodes reserved in node 3 and 4 of the distinction between the service for data transmission. Due to the node 1 and node 2

hair sends data than nodes between three and four nodes of data transfer rate, using packet loss to tail method of packs and discarded. In order to test result, lost package in the UD P packages that contain packets priority, from 1 to 3 three levels, and will low-level data and high-level data correlation, simulation I frame, P frame and B frame, adopt the queue with way as the I, B, P, B, I and...

Test five adopts flow tag forwarding processed data transmission validated:

Node 1 and 2 shall not engage in resource nodes reserved node 1 and 2 send packets node is divided into three grades, set in a stream of priority place tags, which he set with test 4. When from node 1 and 2 of the data entered into the section node point 3 when, each will flow tag level to store a queue, while data packets sent out, when prediction congestion occur, from the packet will testing authority from the queue smallest package be deleted.

Test four and test five analysis of results: packet loss rate is almost equal, but to section 5 and 6 of the node receiving data undertakes checking, discover test 4 packet loss of data are basically evenly distributed. 5 and 6 node receiving data every node is basically was a/s, after analyzing that truly useful information not sufficient 2 M/s, basic layer streaming for 3 M, if it's true multimedia data, this can't display properly root. Test 5 found that lost is basically B frame, some less amount of P frame is missing, a computation, basically the streaming in 4M to 5M, the basic layer between more than 3M, eliminate delay the question, can effectively ensure the body as normal playback. It can be seen in edge network through the multimedia business key business is used for special processing flow tags for QoS improvement played an obvious effect

4 Conclusions

With IP network development, with the rise of new network applications, interlocked nets to strengthen QoS support will clearly has the significant real significance is. Support QoS network will distinguish different data streams, to higher-priority data flow give to high-level service, this also is the new USES all sorts of QoS service model of network with the traditional "regular to type" network service model of the fundamental distinction lies. Due to a variety of applications for QoS demand types and levels is endless and same, appeared not with the QoS service model and the related agreement, but from the actual application perspective, each model has certain limitation, both from different starting work area for specific problem and proposed solutions breaches the solution.

References

1. Braden, R., Clark, D., Shenker, S.: Integrated Service sin the Internet Architecture: An Overview. RFC 1633 (1994)
2. Braden, R., Zhang, S., Berson, S., et al.: Resource Reservation Protocol (RSVP) 2 Version 1 Functional Specification. RFC 2205 (1997)
3. Nichols, K., Blake, S., Baker, F., et al.: Definition of the Differentiated Services Field (DSField) int he IPv4 and IPv6 Headers. RFC 2474 (1998)

4. Carlson, M., Weiss, W., Blake, S., et al.: An Architect use for Differentiated Services. RFC 2475 (1998)
5. Deering, S., Hinden, R.: Internet Protocol, Version 6 (IPv6) Specification. RFC 2460 (1998)
6. Rajahalme, J., Conta, A., Carpenter, B., et al.: IPv6 FlowLabel Specification. RFC 3697 (2004)
7. Fgee, E.B., Kenney, J.D., Phillips, W.J., et al.: Implementing an IPv6 QoS Management Scheme Using Flow Label & Class of Service fields. In: Proc. of the 2004 Canadian Conf. on Electrical and Computer Engineering, vol. 2 (2004)
8. Campbell, T., Jian, L., Wei, C.G.: IP network multimedia transmission solutions, (EB/OL) (2004), <http://edu.tmn.cn/html/7/66/200430/81620.html>

Characteristics Recognition of Typical Fractional Order Dynamical Systems via Orthogonal Wavelet Packet Analysis Method

Tao Zhang¹, Wenxian Xiao², Zhen Liu², and Wenlong Wan³

¹ Network Management Center
Xinxiang University, Henan Xinxiang, China, 453003
zht@hstu.edu.cn

² Network Center
Henan Institute of Science and Technology, Xinxiang, China, 453003
xwenx@yeah.net, liuzhen@hist.edu.cn

³ Foreign Language Department
Henan Institute of Science and Technology, Henan Xinxiang, China, 453003
wanwenlong@hist.edu.cn

Abstract. The orthogonal wavelet packet analysis is a method applied on dynamics recognition of fractional order system. Firstly, the signals band was split up into proper levels and the sub signals were gained, which correspond to each frequency band according to the average period of the time series. Then by analysis of sub frequency band power distribution in the signals total power, the chaos in the related signal can be easily identified. Finally, by taking the controlled fractional order Chen's system as an illustration, the results obtained by this procedure agree with power spectrum method. So this new method can be used for dynamics recognition in fractional order systems.

Keywords: Orthogonal wavelet, Packet analysis method, Time series, Fractional order Chen's system, Chaos.

1 Introduction to Wavelet Packet Analysis

Wavelet packet analysis can provide a more precise signal analysis, not only the signal band by multi-level, can not have a breakdown on the resolution of the high frequency part of the further decomposition, thus increasing the frequency resolution rate, can effectively extract the specific frequency components. Thus, by constructing orthogonal wavelet, orthogonal wavelet packet analysis method can effectively solve the high-frequency low-resolution problem.

2 Algorithm Orthogonal Wavelet Packet Analysis Features in the Fractional System Identification

From the beginning of this section, the paper will be a known fractional numerical solution of differential dynamic systems (time series), making use of wavelet packet

delivery side Analysis, identifying the complex dynamics of the system and the traditional power spectrum analysis results were compared to verify the feasibility of this approach.

2.1 Method of Using Wavelet Packet Analysis of Time Series Feature Recognition Steps

This section begins with the literature [1] proposed an orthogonal wavelet packet analysis method for chaotic signal identification feature, the resulting time series analysis of five groups of objects, feature recognition for them. The basic idea of this approach sources are: the theory of wavelet analysis, to select the appropriate wavelet decomposition level, to treat analysis of time series to split the band were fine, and then use the sub-band energy in the band in the distribution of time series, extracted characteristic frequency of chaotic motion, thus identifying chaotic, the distinction between periodic motion, chaotic motion and random motion [2].

The first step: the average duration estimation and band segmentation.

Firstly, the selected object long enough time series and to estimate the average cycle, recorded it as T_{ave} , then its frequency is about $f_i = 1/T_{ave}$ ($i = 1, 2, 3, 4, 5$). By 5 order vanishing moment, supporting a length of 9 wavelet - Daubechies 5 wavelet analysis of time series to be decomposed frequency bands. If the decomposition level is 5, the time series can be divided into 32 sub-band frequency. When time series sampling frequency 1Hz, Nyquis maximum frequency of 0.5Hz. Estimated by the average cycle time series of five groups that approximate the average frequency of less than 0.3Hz, it is of length 05. Segmentation frequency band, enough to reflect the time sequence of the various features. To a length of 0.5 frequency band is divided into 32 sub-bands, each sub-band 0.0156Hz, and each sub-band frequency range of areas such as table1. Which $S5_i$, ($i = 0, 1, 2, \dots, 31$), respectively, of the original signal is decomposed after 5 layers produced on the same scale orthogonal projection signal 32. In addition, this article will present four different periods time series show the frequency of divided and split in Table1 after the corresponding scope of the 32 bands listed, the specific results in Table 1, this result in the power spectrum below is the corresponding. In the selected wavelet packets and the decomposition level, we get the band after the specific time-series data, broken down and reflected in each sub-band decomposition of the time series signal.

Similarly, select 3 - period!, 4 - period!, 2 - period! And one double period! The sequence of analysis, sampling, decomposition of each sub-signal energy distribution shown in Figure 1. Comparison of Figure1 (a), (b), (c), (d), (e) the results easy to find: chaotic time series decomposition of the child despite the uneven distribution of signal energy, but the frequency f_1 at the obvious energy and other prominent; the cycle decomposition of the signal sequence is only a small number of times the energy distribution of sub-paragraph which has frequently focused, reflecting the cyclical nature of the analysis sequence. It can be concluded: the proportion of energy distribution using a histogram can distinguish between chaotic signals and periodic signals.

Overall, the proportion of energy distribution histograms to more accurately reflect the fractional Chen controlled system (1) under different constant controller m presents some of the state of evolution.

2.2 Chaotic Signal (Random) and Random Discussion of the Relevant Comparison

In addition, taking real life into consideration, there are a lot of completely random sequence, easy and chaotic time series, random confusion; the following numerical studies show the use of orthogonal wavelet packet analysis! To identify the fractional differential system dynamic behavior, it can also be effective in identifying the analyzed chaotic or random signal by [1] methods, to generate a time series with the same standard deviation data1 Gaussian white noise sequence (sequencedata1 standard deviation=7.927, a length of 150,000), its sampling, decomposition, to obtain sub-signal analysis of the energy distribution. concrete, when the sampling frequency of 1Hz, the Gaussian white noise of the sampling, orthogonal wavelet packet decomposition, to obtain the energy distribution of sub-signals, such as 2 (d) below. Comparison of Figure 1, easy to find: the latter reflected in the various sub-band power the proportion of the total power signal generally uniform, i.e., the proportion of energy is relatively evenly distributed, no centralized point of power, which in Figure 1 in the chaotic signal sampling, wavelet packet decomposition, the obtained distribution of signal energy sub-significantly different. In fact, as mentioned above, Figure 1 in the chaotic signal characterized by a significant three are in the energy distribution of the relative concentration[3].

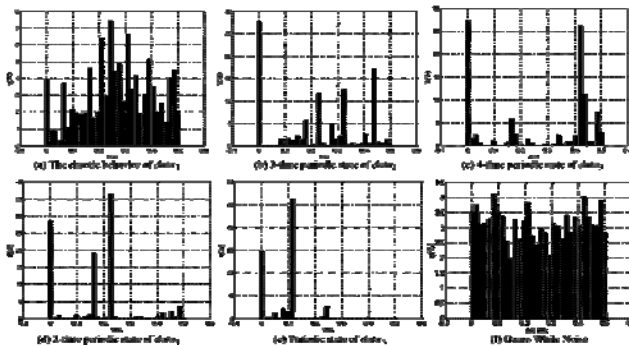


Fig. 1. The Powered Distribute Ion Histogram Of Different Signal Sub- Bands

The method of power spectrum analysis of time series analysis of the aforementioned data ($i = 1, 2, 3, 4, 5$), if the time series of sampling frequency 10Hz, Nyquist frequency 5Hz, from the power spectrum analysis easy to know the results: five time-series average of the corresponding frequencies were $f_1 = 0.1123\text{Hz}$, $f_2 = 0.2719\text{Hz}$, $f_3 = 0.2699\text{Hz}$, $f_4 = 0.2820\text{Hz}$, $f_5 = 0.2919\text{Hz}$, the corresponding results shown in Figure 2 (a) - (e) below. For clarity, the power spectrum of 3 shows only 0 ~ 0.3Hz! Graphics band. The power spectrum shows that: state sequence data1, data2, data3, and data4 and data5 distribution of spectral peaks corresponding to the chaotic

state, 3 - Double period, 4 - double period, 2 - double period! And one double period!, with the literature [8]The bifurcation results and made the first part of the orthogonal wavelet packet analysis of time series features! the results[4].

3 Simulation and Analysis of Results Conclusion and Outlook

Appearing in engineering practice the signal (time series) are mostly chaotic, periodic or random signals mixed form, and chaos, random or periodic signal energy distribution, and wavelet denoising method in the detection of nonlinear time series contains the characteristics of effective application of chaos has some practical significance. This process of analysis and simulation results show that the use of wavelet packet analysis method for chaotic signal feature recognition! The method is feasible. Of course, there are also some of them worthy of further work continue to develop, such as: object-level time series.

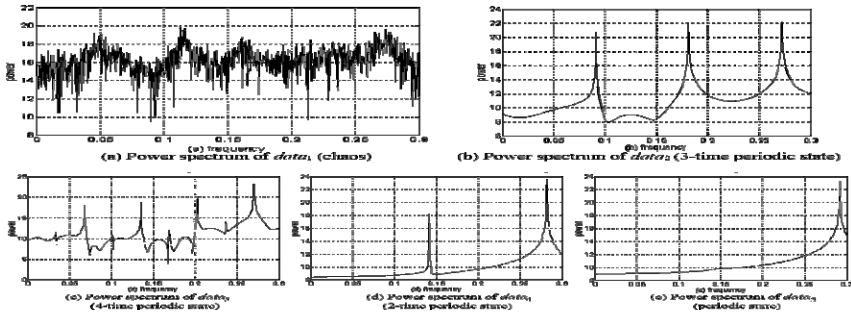


Fig. 2. The local power spectrum of different signals

There are cycles accurately identifying the problem, time series decomposition level corresponding to the selection of standards and so on. In addition, how to power spectral analysis method and how to effectively combine the proposed method, given the time series samples, the energy of the decomposed sub-signal distribution Associated with the cyclical theory of correspondence analysis, are problems to be solved.

References

1. Lu, J.G., Chen, G.: A note on the fractional order Chen system. *Chaos, Solitons and Fractals* 27(3), 685–688 (2006)
2. Diethelm, K., Ford, N.J., Freed, A.D.: A predictor corrector approach for the numerical solution of fractional differential equations. *Nonlinear Dynamics* 29(1), 3–22 (2002)
3. Matignon, D.: Stability results of fractional differential equations with applications to control processing. In: *IEEE-SMC*, pp. 963–968. IMACS, Lille, France (1996)
4. Tavazoei, M.S., Haeri, M.: A necessary condition for double scroll attractor existence in fractional order systems. *Physics Letters A* 367, 102–113 (2007)

5. Donoho, D.L.: De-noising by soft-thresholding. *IEEE Trans. on Inform. Theory* 41(3), 613–627 (1995)
6. Chang, S.G., Yu, B., Vetterli, M.: Adaptive wavelet thresholding for image denoising and compression. *IEEE Transactions on Image Processing* 9(9), 1532–1546 (2000)
7. Wang, A.L., Ye, M., Deng, Q.: *MATLAB R2007 image processing technology and application*, pp. 116–169. Electronic Industry Press, Beijing (2008)
8. Dong, N., Chiang, Xu, F.: Based on second generation wavelet transform image denoising. *Natural Science and Engineering, Yantai University* 20(1), 4 (2007)
9. Liu, J.: Wavelet analysis in fabric pilling objective evaluation of. *Wuhan Institute of Technology* 22(4), 7–10 (2009)

A Novel Method Inpainting Insect Feathered Wing

Minqin Wang

School of Computer Science, Zhaoqing university, Guangdong, China, 526061
wmmq1966@163.com

Abstract. Insects are rich in many types of species. It is very difficult to classify and recognize them, and it is very easy to be damaged for the insects feathered wings, which make it more difficult to be recognized. So inpainting the damaged sample is necessary. The image of insect feathered wing is a kind of texture image with complex restructure. In posed years, Researchers proposed many algorithms which diffused the pixels, which came from the surrounding neighborhood or selected example, into damaged region along isophate direction. Basing on image materials, we advance a novel method which simultaneously inpaints structures and textures of damaged images. The experimental result shows that it is effective to inpaint the insect feathered wing.

Keywords: Image inpainting, Image materials, Texture segmentation, Pulse-Coupled-Neural-Network.

1 Introduction

Insects are the most abundant species, in which there are more than 70 kinds of dangerous fruit flies causing a major threat to fruits and vegetables and other crops. Most of them are the dangerous pest to be prohibiting from entering by Chinese Animal and Plant Quarantine, whereas some other insects are used to make of the specimens for people's appreciation, which has a good economic. Recognition of these insects decide to ban them entering or not. Because there are so many species of insects, insect identification and classification is always plagued researchers and agricultural producers. Whereas the transport causes some insects to be damaged, especially for big feathered wing, which makes identification more difficult. So we should inpaint the feathered wings before recognition.

The algorithm proposed by Bertalmio use the partial differential equations(PDEs) to solve the inpainting problem in 2000[1]. This kind of methods are only fitted for inpainting light scratches, little areas or blots etc, and computing is time consuming. Texture synthesis is also applied to inpaint the image[2]. These methods are effective in replicating consistent texture, but they have difficult to restore images consisting of structures and textures. Some researchers proposed algorithms which simultaneously propagate texture and structure information[3,4]. Reference[4] presented an algorithm which basic idea is to first decompose the image into functions with structure and texture characteristics, and then reconstruct each one of these functions separately with structure and texture recovering algorithms. References[3] proposed example-based

image inpainting method which can simultaneously propagate texture and structure information based on the theory of isophate-driven and the principle of the best matching exemplar patch.

Preceding algorithms perform well on boundaries in damaged image with linear structure and texture. We proposed a new method based on image materials which decomposes the image into two parts. One of them contains the sharp boundary of image and smooth region, while the other contains the texture of image. We inpaint the cartoon image part firstly by boundary reconstruction. Then we do texture synthesis to texture image part guided by boundary reconstruction. The method aims at inpainting structure and texture simultaneously and produces good results for texture with complex structure.

2 Image Decomposition

We segment the image of insect feathered wing. The result is the contour image. The texture image can be got by using the original image to cut the contour.

Texture extraction is key to texture image segmentation. We apply multi-channel Gabor filters to gain eigenvectors describing texture feature, which is used to input into Pulse Coupled Neural Network(PCNN) model to classify the image and finally segment the texture image. For the PCNN-based method is a parallel method, it do good segmentation that combine PCNN-based method with gabor filters based method, which not only make use of the advantage of Gabor filters, but also make use of the parallelism of PCNN model.

2.1 Texture Feature Extraction Based on Gabor Filters

The Gabor wavelet[5] transformation for image u_0 is given by:

$$O_{mn}(x, y) = \iint u_0(x', y') g_{mn}^*(x - x', y - y') dx' dy' \tag{1}$$

Where * stand for complex conjugation operating, g_{mn} is Gabor wavelet kernel. Gabor function is acquired by modeling two dimension Gauss function:

$$g(x, y) = h(x, y) \exp(j2\pi Wx) \\ = \left(\frac{1}{2\pi\sigma_x\sigma_y} \right) \bullet \exp \left[-\frac{1}{2} \left(\frac{x^2}{\sigma_x^2} + \frac{y^2}{\sigma_y^2} \right) + j2\pi Wx \right] \tag{2}$$

Extracted grey image features are presented by mean μ_{mn} and variance σ_{mn} got from modulus of Gabor wavelet transform coefficient. The μ_{mn} and σ_{mn} make of image feature vector.

$$\mu_{mn} = \iint |O_{mn}(x, y)| dx dy \tag{3}$$

$$\sigma_{mn} = \sqrt{\iint (|O_{mn}(x, y) - \mu_{mn}|)^2} \tag{4}$$

For an image of 512×512, if we choose orientations K=4, scale number S=6, we can get feature vector of pixel (i,j):

$$\bar{f}^{(i)} = [\mu_{00}^{(i)} \sigma_{00}^{(i)} \mu_{01}^{(i)} \sigma_{01}^{(i)} \dots \mu_{53}^{(i)} \sigma_{53}^{(i)}]$$

a non-linear function is used to transform the eigenvalues, and then a Gauss smoothing function is applied to implement spatial smoothing, which cause the difference between similar texture become small, while the difference between different texture become large. The non-linear function is given :

$$\psi(t) = \tanh(\alpha t) = \frac{1 - e^{-2\alpha t}}{1 + e^{-2\alpha t}} \tag{5}$$

Where α is a constant. The result is implemented normalization.

Classification the eigenvalues can segmentate image. While the consuming time of traditional clustering methods grows exponentially with the number of categories, we approve a new segmentation based on PCNN, which is a parallel method. The algorithm efficiency is independent with the number of categories.

2.2 Texture Image Segmentation Based on Improved PCNN

A traditional PCN[6] consists of four parts: feeding receptive field, linking receptive field, internal activity field, and the pulse generator. The Feeding receptive field (marked as F_{ij}), in simplified PCNN model, only receive input from outside; while the Linking receptive field (marked as L_{ij}) only receive the pulse output from interconnected PCN. The model is given by:

$$F_{ij}[n] = I_{ij} \tag{6}$$

$$L_{ij}[n] = \sum W_{ijkl} \times Y_{kl}[n-1] \tag{7}$$

$$U_{ij}[n] = F_{ij}[n](1 + \beta L_{ij}[n]) \tag{8}$$

$$Y_{ij}[n] = \begin{cases} 1, & U_{ij}[n] > \theta_{ij}[n] \\ 0, & \text{otherwise} \end{cases} \tag{9}$$

$$\theta_{ij} = \begin{cases} V_k & t = 0 \\ V_k \exp\left(\frac{-(t-t_1)}{\tau}\right) & 0 < t < t_1 \\ V_k & t = t_1 \end{cases} \tag{10}$$

After having computing several times, several firing mode matrixes can be gained. The segmentation boundary can be acquired by performing exclusive or operating on matrixes at matrixes.

For threshold decrease function is exponent, this cause the traditional PCNN model cannot meet various kinds of application. This paper proposes a linear attenuated threshold mechanism and combines the flexibility of the threshold with the simple implementation. Descent gradient of threshold is controlled by the slop of linear function. Then Expression (10) is changed to expression (11):

$$\theta_{ij} = \begin{cases} V_k & t = 0 \\ V_k(1 - \frac{t}{t_1}) & 0 < t < T \\ \infty & t = T \end{cases} \tag{11}$$

Where T is the firing time.

2.3 Image Segmentation Based on Improved PCNN

Since the traditional PCNN is a two dimension matrix and the input image from extracted feature image is a three dimension matrix, we should regulate the PCNN. The input is a pexil in traditional PCNN, which is replaced by a 1-dimention vector. Then the similarity between eigenvectors is valued by a vector distance d(i,j). The distance d(i,j)between eigenvector i and j in feature space is given by :

$$d(i, j) = \sum_m \sum_n d_{mn}(i, j) \tag{12}$$

$$d_{mn}(i, j) = \left| \frac{\mu_{mn}^{(i)} - \mu_{mn}^{(j)}}{\alpha(\mu_{mn})} \right| + \left| \frac{\sigma_{mn}^{(i)} - \sigma_{mn}^{(j)}}{\alpha(\sigma_{mn})} \right|$$

Where $\alpha(\mu_{mn})$, $\alpha(\sigma_{mn})$ is standard variance.

3 Image inpainting

For the bounded variation image u, we use a method which inpaint image based on boundary reconstruction. The algorithm consists of three main steps:

- 1)Segment image and obtain information about edges and regions.
- 2)Reconstruct image structure based on edges repaired.
- 3)Restore image based regions guided by reconstructed image structure.

In the first step, we use a method based PCNN to segement image. We can get the boundary and region information. Fig.2 shows us that the inputs to our algorithm are an original damaged image and a mask which has been detected. Based on the information of boundary and mask, we achieve the edges around the mask, which abide with the principle that an edge must keep one side inside the mask and the other side outside the mask(that means they are interacted with mask.). After calculating their center points, and curvatures, edges are defined as positive edges or negative edges according to their radians(shown as fig.1).

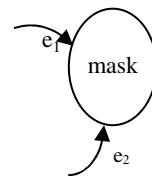


Fig. 1. Edge's direction



(a) 受损图像 (b) 文献 3 修复结果 (c) 文献 4 修复结果 (d) 本文修复结果

Fig. 2. Experimental results

In the second step, edges are distributed to three groups. One group is called matched-edge group, where the two matched edges are strongly related with each other. The second group is called coupled-edge group, where the two coupled edges are moderately related with each other. The third group is called single-edge group, where the edges are not related with each other at all(referred to[7] for more detail). The interpolation is employed when we connect the edges. The point to be interpolated is always affected more by the point near it. Based on this rules, a interpolation function is defined as following:

$$\lambda^{p_i} = \frac{w_1 \lambda^{p_1} + w_2 \lambda^{p_2}}{w_1 + w_2} \tag{13}$$

where λ^{p_i} is the value of a point to be inpainted, $\lambda^{p_j} (j \in \{1, 2\})$ are the value of the end points which connects the edges to be inpainted, and $w_j (j \in \{1, 2\})$ are their powers. W_j are defined as $w_j=1/d_j$, where d_j is the Euclidian distance between point i to j .

In the third step, the algorithm performs inpainting based on interpolation guided by boundary reconstruction. After having inpainted counter image u , we now describe the method inpainting the texture image v . Here we employ the exemplar-based texture synthesis as the main algorithm used to fill-in the region of missing information in v . We use the algorithm developed in[4] to perform texture synthesis. Let I be the image, Ω be the region to be filled in. Let $\partial\Omega$ be the border of Ω , and Ψ be the known region. The image I has been segmented into several region with the edges inpainted. The $p \in \partial\Omega$ is the center of a square block $W(p)$. Choose a block $W(q)$ from the region which is same region as $w(p)$. The q if the center of block $W(q)$. $W(q)$ is similar with $W(p)$. This measure of similarity is calculated by the L2 distance (Euclidean distance) between pixels corresponding to neighborhood window. The function is given by:

$$d(N_1, N_2) = \frac{\sum_{p \in N} (I_1(p) - I_2(p))^2}{n^2} \tag{14}$$

If the $W(q)$ is similar with $W(p)$, We replace p with q . Then choose the next pixel neighbor to p to precede the algorithm until all damaged pixels to be repaired.

4 Experimental Results and Conclusion

We now show the experimental results about our algorithm comparing with the other methods simultaneously inpainting image structure and texture (shown as figure 2). Algorithm [4] decided which patch to be inpainted based on value of patch priority. Since it's an isophote-driven method, the blur is occurred when there is curve structure included in damaged region. Algorithm [3] decomposes the original image into structure image and texture image at first, and then uses the method proposed in [1] to inpaint the structure image. The texture image is restored by exemplar-based method. This algorithm is an isophote-driven method too, so it has the problem during inpainting when the curvature of boundary is variable. The results show that algorithm [3][4] can inpaint the texture, but make the boundary blur, while our algorithm can inpaint the boundary and texture well.

As preceding mention, our algorithm is a method which simultaneously inpaint image texture and structure. The algorithm ensures the boundary to be repaired well. The adaptive texture restoration based on region segmentation gets fast and accurate result.

References

1. Bertalmio, M., et al.: Image inpainting, *Computer Graphics*. In: SIGGRAPH, pp. 417–422 (2000)
2. Efros, A., et al.: Texture synthesis by nonparametric sampling. In: *IEEE Int. Conf. Computer Vision*, pp. 1033–1038 (1999)
3. Bertalmio, M., Vese, L., Sapiro, G., Osher, S.: Simultaneous Structure and Texture Image Inpainting. *Trans. Image Processing* 12(8), 882–889 (2003)
4. Criminisi, A., Pérez, P., Toyama, K.: Region filling and object removal by exemplar-based image inpainting. *IEEE Trans. Image Processing* 13, 1200–1212 (2004)
5. Gabor, D.: *Theory of communication*, vol. 93 (3), pp. 429–457. IEE, London (1946)
6. Ranganath, H.S., Kuntimad, G., Johnson, J.L.: Pulse coupled neural networks for image processing. In: *Proc. 1995 IEEE Southeast Con., Raleigh NC*, pp. 37–43 (1995)
7. Wang, M., Han, G., Tu, Y.: Edge-based image completing guided by region segmentation. In: *CCCM 2008*, vol. 1, pp. 152–156 (2008)

Research on Gender Differences of Trendy Online Behavior Patterns

Tsui-Chuan Hsieh and Chyan Yang

Institute of Information Management National Chiao Tung University
Hsinchu, Taiwan
terrbynctu@gmail.com, Professor.yang@gmail.com

Abstract. The purpose of this article was mainly to investigate gender differences for trendy online behavior patterns. This study applied the latent class analysis model to investigate Internet usage patterns from five trendy online applications among 10,909 Taiwan residents. The results showed that trendy online behavior patterns exhibited gender differences. For instance, females preferred blog service more than males do. Male in general were good at online security issue and mobile service. Gender difference depends on various/heterogeneity application. The findings herein should help Internet service providers form an applicable guideline for developing service strategies of higher service satisfaction between marketing materials, products and users' needs.

Keywords: trendy online application, online behavior, gender difference, latent class analysis.

1 Introduction and Literature Review

The Internet is influencing people's daily lives more so than it did in the past. More and more people are contributing to the generation of online applications, like movies, games, blogs, mobile phones, and e-learning [1]. This study looked at trendy online behavior patterns based on marketing materials include particular issues related to blog, use mobile device, and security.

Typical online activities. What are typical online activities? Internet usage motivates principally by goods-and-information acquisition [2]. The chief purpose of Internet can be sorted into communication, fun, information utility, major life activities, and transactions [3]. The common Internet applications are communicating with friends, browsing news, acquiring general information, support for those with access/mobility problems, entertainment, online education, banking, and shopping [4]. Gross and Leslie exhibited that the new approach applications are blogs, RSS, image hosting, podcasting, social networking, and Wiki [5]. People observe that the risk of information security and privacy for online application strongly relates to use intention [6]. In the Internet world, blog (social network) application, online security, and connect to Internet through mobile device are new issues. This study categorized some online behaviors that frequently occur and chose five of them to analyze. These

five behaviors encompass: browsing blogs, share information, online security using, online security skill, and Internet connection through a mobile device. Personal characteristics, use, and expertise play a role in accounting for variations in the breadth and depth of Internet usage [7], among which demographic variables such as gender has a significant influence [8]. Different genders had a significant impact on online use patterns [9]. Women use the Internet for receiving information, while men preferred career helpful service [4]. This study has referenced the findings from the scholars mentioned above and took gender into the research model to analyze how these personal characteristic variables influence the pattern of trendy online application.

Latent class analysis (LCA). In the social sciences, many research questions have investigated the relationship when both categorical outcomes and predictor variables are latent. Categorical data analysis is very useful in the analysis of sociological data [10]. For an attitude or classification survey, researchers are generally more concerned about the potential groups of samples and the latent class model can provide a better means to categorize data. With an attitude or classification survey, it is more appropriate to use latent class analysis [11, 12]. A latent class model assumes that the population of subjects is divided into a few exclusive latent classes. Latent class analysis (LCA) is a statistical method that identifies subtypes of related cases by using a set of categorical and/or continuously observed variables. These subtypes are referred to as latent classes, which come from multiple observed indicators and are not directly observed [11, 13].

Investigating user behavior patterns. Some studies suggest sorting online use pattern by users' age [1], while others explore the length of experience, access time, and frequency of online use patterns [3]. Another way to examine which people conduct what type of online activities or motives is to explore user typologies. For example, researchers use factor analysis to investigate the online motivated patterns among various users [9]. In online behavior studies, the behaviors of users usually present categorical outcomes and a latent usage pattern. Although the length of experience and frequency of online use help predict which activities people do online, the patterns of online behavior also prove to be a significant predictor. This study tested such a particular relationship of types of online usages. This study took the methodology from previous scholars and applied latent class analysis to investigate user behavior patterns [11-13].

2 Methodology

This study simultaneously applied latent class analysis to attain user segmentation (S). The latent class methodology is available in the computer program LatentGOLD v4.5. This study uses SPSS v12.0 to collate data descriptive statistics and the contingent table.

Sample and Model Fit. In 2009 the average percentage of household Internet access was 78.1%, with average daily time spent on the Internet at 2.95 hours [14]. Therefore, the surveyed data of online application that Taiwanese residents possess

could be a reference to some extent and also offer a good source for service providers to work on Internet products and marketing services. The collected data for all analyses adopted the digital divide survey conducted by the RDEC, which evaluated the situational status of the current digital divide and Internet usage behaviors in Taiwan. This study used five items of categorical variables about online behavior as a research dataset. The data are used in exclusion of missing values for the 10,909 valid samples. Five categorical indicators are used to inform latent class membership (1=yes, 0=no): (1) browsing blogs, (2) online sharing information, (3) online security (such as refusal to open an unknown email), (4) online security skill, and (5) Internet connection through a mobile device. Table 1 shows descriptive statistics for the Internet use sample.

In order to study the similarities and differences between the patterns of online behaviors from five trendy Internet applications among 10,909 users, this study applied the LCA model described beforehand. This paper incorporated effects of gender by means of concomitant variables. Model estimates are obtained for alternative numbers of user segments (S=1...4). Table 2 reports model fit (in particular, the BIC value) for each combination of S and T. The optimal number of user segments applied the minimum BIC [12, 13]. The overall minimum BIC is attained at four user segments (BIC = 62049.59), which this study identified as the most appropriate solution.

Table 1. Descriptive statistics

Online behavior (sample proportion)	%
browsing blogs	76.70
online sharing information	38.55
online security	73.18
online security skill	72.31
Internet connection through a mobile device	28.36
<hr/>	
Gender	%
Female	49.84
Male	50.16

Table 2. Model fit

Number of individual Segments	LL	BIC(LL) ⁽¹⁾	Npar	P-value
1	33394.11	66834.71	5.00	0.00
2	31275.53	62662.64	12.00	0.00
3	31042.80	62262.25	19.00	0.00
4	30903.93	62049.59	26.00	0.00
5	30880.68	62068.18	33.00	0.06

Note: ⁽¹⁾ The lowest BIC overall is boldface and underlined.

3 Results

Do trendy online behaviors exhibit certain identifiable patterns? Table 3 presents trendy online behaviors within each user segment. The table shows that the study acquired conditional probability for this research target, which consists of five users' online behaviors. This paper discovered that the trendy online behavior patterns based

on marketing materials of the Internet consist of four segments (referred to as S1 to S4) that show distinctive usage patterns. Users' online behaviors and thereby membership of user segments are often related to personal characteristic variables such as gender. This paper assessed the effects of gender. The lower part of Table 3 presents the findings for the effects of personal characteristic variables. In order to deduce further interpretation, this paper has referred to the practice by Bijmolt et al. [11]. This paper did not present logic parameters, but instead segmented membership probability per category of each personal characteristic variable, averaged across all categories of the other variables. User segmentation in each model of users' online behaviors is not the same.

Table 3. Model results: user segments

Individual segment	S1	S2	S3	S4
Segment Size	37.74%	27.56%	18.31%	16.39%
Online behaviors	Behaviors probabilities			
browsing blogs	0.99	0.61	0.99	0.27
online sharing information	0.72	0.10	0.45	0.03
online security	0.81	0.81	0.78	0.38
online security skill	0.98	0.90	0.50	0.10
Internet connection through a mobile device	0.66	0.36	0.27	0.12
Gender				
Female	0.35	0.20	0.27	0.17
Male	0.40	0.34	0.10	0.15

4 Discussion

These four user segments showed distinctive online behavior patterns. The S1 segment's members were knowledgeable on various Internet applications. The S2 segment's members relative care about online security and relatively less about online sharing information. The S3 segment's members were good at blogs service and relatively less about mobile service. The S4 segment's members were had a lower use rate of online applications, but they do browsing blog and care about online security.

Do online patterns exhibit gender differences? In order to study the similarities and differences between the online behavior patterns of each gender, this study applied multiple contingency table analysis. Figure 1 presents the findings on the effects of gender differences. The figure shows the conditional probabilities of each of the five types of use behavior within each individual-gender group (SiTj). Each of the eight individual-gender segments shows its own unique profile or combination of five online behaviors. In the figure the dotted line presents the female (F) and the solid line is the male (M). Male in general were good at online security issue, but they

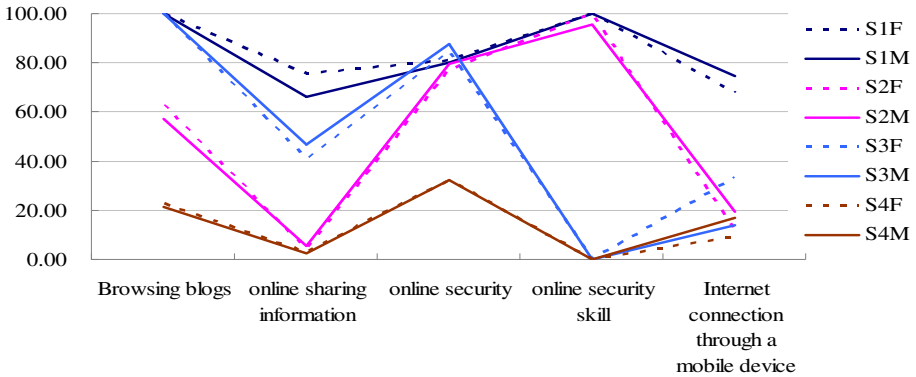


Fig. 1. Gender differences in online behavior patterns

relatively less often used blog service. Traditional researches frequently present those male used online services more often than female. However, in this study confirm that gender difference depend on various/heterogeneity application. This might be attributed to the fast popularization of education and internet application. The needs and motivations affect people of using the Internet service.

5 Conclusions

This study has applied the LCA model to investigate Internet usage patterns from five online applications among 10,909 Taiwan residents. This study took the users' personal characteristic variations into account for analysis, discussing the potential influence behind users' trendy online behaviors, with the goal of aiding service providers in understanding and mastering their target users. These four user segments showed distinct online behavior patterns. The result of the analysis indicates that gender influenced online behaviors. For instance, females used the Internet more often for blog service than males. Male in general were good at online security issue and mobile service. Gender difference depends on various/heterogeneity application. These results showed that gender differences certainly existed within the online behavior patterns based on marketing materials. This paper has suggested that Internet product or service providers could find more appropriate user clusters based on the characteristics of products. For instance, if a service provider is trying to target female users, then it could use trial together with a promotion on a trendy online application, such as blog. If a service provider is trying to target male users, then it should enhance security and could use pre-introduction or a trial together with a promotion on mobile service. With these findings a service provider might identify its potential users in order to design the proper marketing strategies. Service providers can refer to the pattern of online behavior for their own development, which might be helpful to increase fitness and service satisfaction.

References

1. Shah, D.V., Kwak, N., Holbert, R.L.: "Connecting" and "Disconnecting" With Civic Life: Patterns of Internet Use and the Production of Social Capital. *Political Communication* 18(2), 141–162 (2001)
2. Weiser, E.B.: The Functions of Internet Use and Their Social and Psychological Consequences. *CyberPsychology & Behavior* 4(6), 723–743 (2001)
3. Howard, P.E.N., Painie, L., Jones, S.: Days and Nights on the Internet The Impact of a Diffusing Technology. *American Behavioral Scientist* 45(3), 382–404 (2001)
4. Colley, A., Maltby, J.: Impact of the Internet on our lives: Male and female personal perspectives. *Computers in Human Behavior* 24(5), 2005–2013 (2008)
5. Gross, J., Leslie, L.: Learning 2. 0: a catalyst for library organizational change. *The Electronic Library* 28(5), 657–668 (2009)
6. Tsai, Y.H., Yeh, J.H.: Perceived risk of information security and privacy in online shopping: A study of environmentally sustainable products. *African Journal of Business Management* 4(18), 4057–4066 (2010)
7. Livingstone, S., Helsper, E.: Gradations in digital inclusion: Children, young people and digital divide. *New Media & Society* 9(4), 671–696 (2007)
8. Wasserman, I.M., Richmond-Abbott, M.: Gender and the Internet: causes of variation in access, level, and scope of use. *Social Science* 86(1), 252–270 (2005)
9. Teo, T.S.H., Lim, V.K.G.: Gender differences in internet usage and task preferences. *Behavior & Information Technology* 19(4), 283–295 (2000)
10. Goodman, L.A.: Statistical Magic and/or Statistical Serendipity: An Age of Progress in the Analysis of Categorical Data. *Annual Review of Sociology* 33, 1–19 (2007)
11. Bijmolt, T.H.A., Paas, L.J., Vermunt, J.K.: Country and consumer segmentation: Multi-level latent class analysis of financial product ownership. *International Journal of Research in Marketing* 21(4), 323–340 (2004)
12. Horn, M.L.V., Fagan, A.A., Jaki, T.: Using Multilevel Mixtures to Evaluate Intervention Effects in Group Randomized Trials. *Multivariate Behavioral Research* 43(2), 289–326 (2008)
13. Henry, K.L., Muthén, B.: Multilevel latent class analysis: An application of adolescent smoking typologies with individual and contextual predictors. *Structural Equation Modeling: A Multidisciplinary Journal* 17(2), 193–215 (2010)
14. RDEC, Executive Yuan, Taiwan (2009), Digital Divide in Taiwan Survey, <http://www.rdec.gov.tw/mp110.htm> (retrieved)

Study on Affecting Factors of Time Domain Reflectometry Cable Length Measurement

Jianhui Song, Yang Yu, and Hongwei Gao

School of Information Science and Engineering, Shenyang Ligong University,
Shenyang, 110159, P.R. China
hitsong@126.com, yusongh@126.com, ghw1978@sohu.com

Abstract. The theory of the time domain reflectometry(TDR) cable length measurement is investigated. Based on the principle of TDR cable length measurement, the principle error of the TDR cable length measurement is analyzed. The influence of measured cable length, measuring numbers, counting pulse frequency and traveling wave velocity error on measuring accuracy is analyzed. Methods for reducing cable length measurement error are proposed. The simulation results show that the primary task of TDR cable length measurement is to reduce the velocity error. When the velocity errors are small, the length measurement relative error can be significantly improved by increasing the measuring numbers and the counting frequency.

Keywords: TDR, principle error, velocity errors, measuring numbers, counting frequencies.

1 Introduction

All kinds of wires and cables have been widely used with the rapid development of the national economy. The wire and cable industry have developed rapidly, and gradually expanded the production scale and market share. Cable is an important commodity, and its length measurement precision is strictly formulated in the national standard. However, the issue of measuring precision in the wire and cable market becomes more and more prominent. It is significant to measure the cable length precisely, rapidly and economically. Compared with the traditional measurement methods, time domain reflectometry (TDR) technology has an advantage of non-destruction, portability and high-precision, which is an ideal cable length measurement method[1~3]. In order to achieve high cable length measuring precision, the influence of measured cable length, measuring numbers, counting pulse frequency and traveling wave velocity on measuring accuracy is analyzed. Methods for reducing cable length measurement error are proposed.

2 The TDR Cable Length Measurement Theory

TDR is a very useful measuring technology based on high-speed pulse technology. The cable length measuring principle is very simple. The test voltage pulse is injected

into one end of the cable, and the pulse will be reflected at the end of the cable. By measuring the time interval between the injection pulse and the reflection pulse, the cable length can be obtained by assuming the velocity as constant[4,5]. The formula for length measurement is

$$l = \frac{v \cdot \Delta t}{2} \quad (1)$$

Where, l —cable length,

v —signal propagating velocity,

Δt —time interval between the injection pulse and the reflection pulse

At present, the crystal oscillator temperature stability is better than 10^{-9} , therefore the count pulse frequency error can be ignored. At this point the TDR cable length measuring uncertainty u_l can be expressed as

$$u_l = \sqrt{\left(l \cdot \frac{u_v}{v}\right)^2 + \left(\frac{v}{2f\sqrt{n}}\right)^2} \quad (2)$$

Where, u_v —propagation velocity standard uncertainty;

u_f —reference frequency standard uncertainty;

n —number of measurements.

3 Simulation and Analysis

According to formula (2), the influence of measured cable length, measuring numbers, counting pulse frequency and traveling wave velocity on measuring accuracy is analyzed.

When the measured cable length $l=10\text{m}$, the velocity $v=2 \times 10^8 \text{ m/s}$ and the relative error of velocity is 0.1%, the length measurement relative errors of different counting frequencies and different measuring numbers are shown in Fig. 1.

It can be seen from Fig. 1, when the velocity error is constant, the length measurement relative error of different counting frequencies and different measuring numbers are very different. The high measurement accuracy is easy to be achieved when the measuring numbers and the counting frequencies are big. Table 1 is the length measuring relative errors of different counting frequencies and different measuring numbers with $l=10\text{m}$. It can be seen from the table, when the count pulse frequency is constant, the measurement accuracy can be significantly improved by increasing the measuring numbers. But when the measuring numbers is above a certain value, due to the quantization error and system error, continue to increase the measuring numbers to improve the measurement error has little effect. When the measuring numbers are constant, the measurement accuracy can be improved by increasing the measuring numbers. But the improvement is not satisfactory and the high counting frequency is difficult to implement.

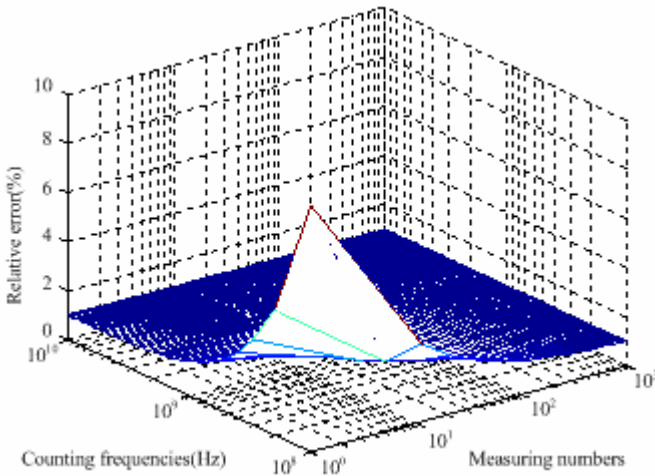


Fig. 1. Length measurement relative errors of different counting frequencies and different measuring numbers

Table 1. Length measuring relative errors of different counting frequencies and different measuring numbers with $l=10\text{m}$ [%]

Measuring numbers	Counting frequencies[GHz]									
	0.5	0.6	0.7	0.8	0.9	1.0	2.0	3.0	4.0	5.0
1	2.00	1.67	1.43	1.25	1.12	1.01	0.51	0.35	0.27	0.22
100	0.22	0.19	0.17	0.16	0.15	0.14	0.11	0.11	0.10	0.10
1000	0.12	0.11	0.11	0.11	0.11	0.10	0.10	0.10	0.10	0.10

When measuring numbers $n = 1$, $v = 2 \times 10^8$ m/s and the relative error of velocity is 0.1%, the length measurement relative errors of different counting frequencies and different measured cable length are shown in Fig. 2.

It can be seen from Fig. 2, when the measuring numbers are constant, the length measurement relative error of different counting frequencies and different cable lengths are very different. The high measurement accuracy is easy to be achieved when the measured cable lengths are long and the counting frequencies are big. Table 2 is the minimum measured cable length of different measuring numbers and different counting frequencies with 0.2% expecting measuring error.

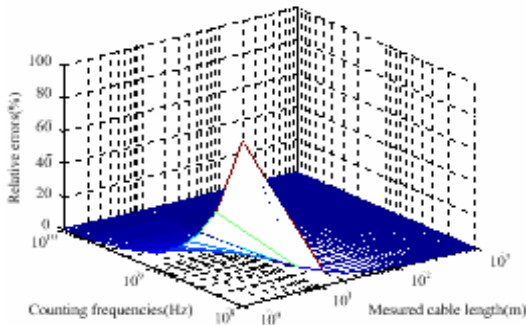


Fig. 2. Length measurement relative errors of different counting frequencies and different measured cable lengths

Table 2. Minimum measured cable length with 0.2% expecting measuring error [m]

Measuring numbers	Counting frequencies[GHz]									
	0.5	0.6	0.7	0.8	0.9	1.0	2.0	3.0	4.0	5.0
1	116.0	97.0	83.0	73.0	65.0	58.0	29.0	20.0	15.0	12.0
100	12.0	10.0	8.3	7.3	6.5	5.8	2.9	2.0	1.5	1.2
1000	3.6	3.1	2.7	2.3	2.1	1.9	1.0	0.7	0.5	0.4

When the measured cable length $l=100$ m, the velocity $v=2\times 10^8$ m/s and the counting frequency is 1GHz, the length measurement relative errors of different velocity error and different measuring numbers are shown in Fig. 3. It can be seen from Fig. 3, when the counting frequency is constant and the velocity errors are small, the length measurement relative error can be significantly improved by increasing the measuring numbers. But when the velocity errors are big, the key segment which affected the measuring precision is velocity. Therefore the measurement accuracy can only be little improved by increasing the measuring numbers.

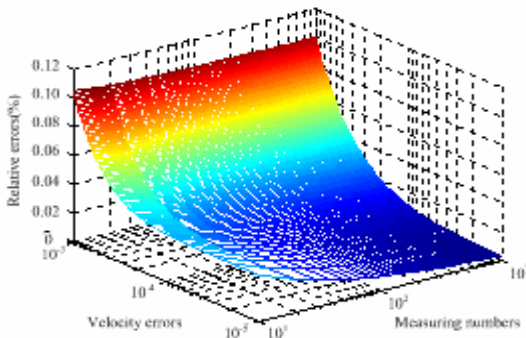


Fig. 3. Length measurement relative error of different velocity errors and different measuring numbers

When the measured cable length $l=100$ m, the velocity $v=2\times 10^8$ m/s and the measuring numbers $n=100$, the length measurement relative errors of different velocity errors and different counting frequencies are shown in Fig. 4.

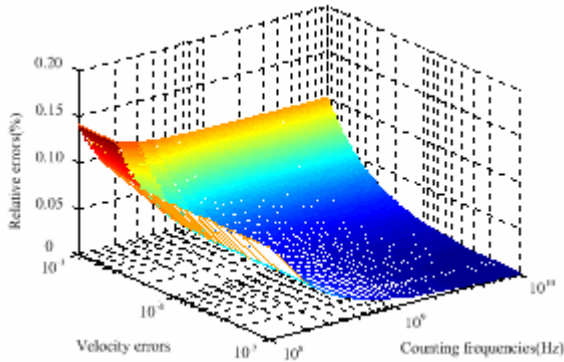


Fig. 4. Length measurement relative error of different velocity errors and different counting frequencies

It can be seen from Fig. 4, when the counting frequency and measured cable length are constant and the velocity errors are small, the length measurement relative error can be significantly improved by increasing the counting frequency. But when the velocity errors are big, the key segment which affected the measuring precision is velocity. Therefore the measurement accuracy can only be little improved by increasing the counting frequency. From Fig. 3 and Fig. 4 it can be concluded that the primary task is to reduce the velocity error.

4 Conclusions

In order to achieve high cable length measuring precision, the influence of measured cable length, measuring numbers, counting pulse frequency and traveling wave velocity on measuring accuracy is analyzed. Methods for reducing cable length measurement error are proposed. The simulation results show that the primary task of TDR cable length measurement is to reduce the velocity error. When the velocity errors are small, the length measurement relative error can be significantly improved by increasing the measuring numbers and the counting frequency.

References

1. Dodds, D.E., Shafique, M., Celaya, B.: TDR and FDR Identification of Bad Splices in Telephone Cables. In: 2006 Canadian Conference on Electrical and Computer Engineering, p. 838 (2007)
2. Du Performance Limits, Z.F.: of PD Location Based on Time-Domain Reflectometry. IEEE Transactions on Dielectrics and Electrical Insulation 4, 182 (1997)

3. Pan, T.W., Hsue, C.W., Huang, J.F.: Time-Domain Reflectometry Using Arbitrary Incident Waveforms. *IEEE Transactions on Microwave Theory and Techniques* 50, 2558 (2002)
4. Langston, W.L., Williams, J.T., Jackson, D.R.: Time-Domain Pulse Propagation on a Microstrip Transmission Line Excited by a Gap Voltage Source. In: *IEEE MTT-S International Microwave Symposium Digest*, p. 1311 (2006)
5. Buccella, C., Feliziani, M., Manzi, G.: Detection and Localization of Defects in Shielded Cables by Time-Domain Measurements with UWB Pulse Injection and Clean Algorithm Postprocessing. *IEEE Transactions on Electromagnetic Compatibility* 46, 597 (2004)

Input-to-Output Stability for One Class of Discontinuous Dynamical Systems

Yang Gao and Wei Zhao

Department of Mathematics, Daqing Normal University, Daqing, Heilongjiang 163712,
People's Republic of China
gy19790607@163.com

Abstract. It is well known that input-to-output stability (IOS) is important in engineering practice. In this paper, IOS problems for one class of discontinuous dynamical systems are considered. Piecewise smooth IOS-Lyapunov functions are adopted. The results for a class of discontinuous dynamical systems' IOS character are shown, naturally. All the research is based on intelligent materials, and it will also serve for the development of modern technology.

Keywords: Discontinuous systems, input-to-output stability, Piecewise nonlinear system, Intelligent Materials.

1 Introduction

During the last twenty years, the notion of input-to-output stability (IOS) became a fundamental concept upon control theory. A lot of good results were obtained. Input to output stability (IOS) means that the output (as opposed to the full state) must be eventually small, no matter what the initial conditions, if future inputs are small ([1,4]). In this paper, IOS problems for one class of discontinuous dynamical systems are considered. Piecewise smooth IOS-Lyapunov functions are adopted. The results for a class of discontinuous dynamical systems' IOS character are shown, naturally. The author has analysed input-to-output stability for one class of discontinuous dynamical systems based on intelligent materials, and he wants to improve discontinuous dynamical systems with the assistance of development of intelligent materials.

2 Main Results

Consider the discontinuous differential equation with outputs:

$$\dot{x}(t) = f(x(t), u(t)), y = h(x) \quad (1)$$

with $x(t) \in \mathbb{R}^n$ and $u(t) \in \mathbb{R}^m$, the state and control input at time $t \in \mathbb{R}_+$, respectively. Assume the output map $h: \mathbb{R}^n \rightarrow \mathbb{R}^p$ is continuous and $h(0) = 0$. For each $\xi \in \mathbb{R}^n$ and each input u , we let $y(t, \xi, u)$ be the output function of the

system i.e. $y(t, \xi, u) = h(t, \xi, u)$. The vector field f is assumed to be a piecewise continuous function from $R^n \times R^m$ to R^n in the following sense

$$f(x, u) = f_i(x, u)$$

when $(x, u)^T \in \Omega_i, i \in \bar{N} = \{1, 2, \dots, N\}$. Here $\Omega_1, \dots, \Omega_N$ form a partitioning of the space $R^n \times R^m$, which satisfies that

1. $\text{int } \Omega_i \cap \text{int } \Omega_j = \Phi$, when $i \neq j$.

2. $\bigcup_{i=1}^N \Omega_i = R^n \times R^m$.

3. $f_i : \Omega_i \rightarrow R^n$ are locally Lipschitz continuous functions on their domains $\Omega_i, i \in \bar{N}$.

Note that $\text{int } \Omega$ denotes Ω 's interior in this paper.

Now recall the definition of extended Filippov solutions for system (1).

Definition 1 [3]. A function $x : [a, b] \rightarrow R^n$ is an extended Filippov solution to system (1) for $u \in L_\infty([a, b] \rightarrow R^m)$, if x is locally absolutely continuous and satisfies $\dot{x}(t) \in C_f(x(t), u(t))$ for almost all $t \in [a, b]$. Here

$$C_f(x(t), u(t)) := \text{co}\{f_i(x, u) \mid i \in I(x, u)\} \text{ and}$$

$$I(x, u) := \{i \in \bar{N} \mid (x, u)^T \in \Omega_i\}.$$

The extended Filippov solutions can be used to discuss the input to state stability for system (1) effectively (W.P.M.H. Heemels and S. Weiland 2008). In this paper, input-to-output stability for system (1) is defined as follows.

Definition 2. The system (1) is said to be input-to-output stability (IOS) if there exist a KL-function β and a K_∞ -function α , K-function γ such that for each initial condition $x(0) = x_0$ and each L_∞ -input function u ,

1. All of extended Filippov solutions x of the system (1) exist on some interval $[0, T_{x_0, u})$.

2. All of output functions satisfy that

$$\alpha(|y(t, x_0, u)|) \leq \beta(|x_0|, t) + \gamma(|u(t)|), \forall t \in [0, T_{x_0, u}).$$

In the study of the IOS characters for systems IOS-Lyapunov function are used usually. We have next definition.

Definition 3. A function V is said to be an IOS-Lyapunov function for the system (1) if

1. V is a piecewise smooth Lyapunov function, which means that

$$V(x) = V_j(x), x \in \Gamma_j, j \in \bar{M} = \{1, 2, \dots, M\}$$

where $\Gamma_1, \dots, \Gamma_M$ form a partitioning of the space R^n and the V_j 's are continuously differentiable functions on some open domain containing Γ_j .

2. V is continuous.

3. There exist functions $\psi_1, \psi_2 \in K_\infty$ such that

$$\psi_1(h(x)) \leq V(x) \leq \psi_2(|x|), \forall x \in R^n.$$

4. There exist K -function σ and a K_∞ -function $\bar{\alpha}$ such that for all $x \in R^n$ and $u \in R^m$

$$\nabla V_j(x) f_i(x, u) \leq -\bar{\alpha}(V(x)) + \sigma(|u|),$$

$$i \in I(x, u), j \in J(x) := \{j \in \bar{M} \mid x \in \Gamma_j\}.$$

Note that, V is continuous which means when $x \in \Gamma_j \cap \Gamma_i$, we have $V_j(x) = V_i(x)$.

Now a key theorem is shown as follows.

Theorem 1. If there exists an IOS-Lyapunov function V for system (1), then for all $u \in L_\infty[R_+ \rightarrow R^m]$ and extended Filippov solution $x : [0, T_{x_0, u}) \rightarrow R^n$ it holds that

$$\frac{d}{dt} V(x(t)) \leq -\bar{\alpha}(V(x(t))) + \sigma(|u(t)|),$$

for almost all time $t \in [0, T_{x_0, u})$.

Proof: Because of V is a locally Lipschitz function and $x(t)$ is locally absolutely continuous. Therefore we have $V(x(t))$ is locally absolutely continuous. In the sequel, $V(x(t))$ is differentiable almost everywhere with respect to

$t \in [0, T_{x_0, u})$. Assume that both $\frac{d}{dt} V(x(t))$ and $\dot{x}(t)$ exist at time t . following from

$$\dot{x}(t) = y \in C_f(x(t), u(t)) = \sum_{i \in I(x, u)} \alpha_i f_i(x(t), u(t))$$

with some $\alpha_i \geq 0$. We have that

$$\begin{aligned} \frac{d}{dt}V(x(t)) &= \lim_{h \downarrow 0} \frac{V(x(t) + hy) - V(x(t))}{h} \\ &= \lim_{h \downarrow 0} \frac{V_j(x(t) + hy) - V_j(x(t))}{h} \end{aligned}$$

for all $j \in \bar{J}(x(t), y) = \bigcap_{h_0 > 0} \bigcup_{0 < h < h_0} J(x(t) + hy) \subseteq J(x(t))$. Therefore, a conclusion can be drawn that

$$\begin{aligned} \frac{d}{dt}V(x(t)) &\leq \max_{j \in J(x(t))} \lim_{h \rightarrow 0} \frac{V(x(t) + hy) - V(x(t))}{h} \\ &= \max_{j \in J(x(t))} \nabla V_j(x(t))y \\ &= \max_{j \in J(x(t))} \sum_{i \in I(x(t), u(t))} \alpha_i \nabla V_j(x(t))f_i(x(t), u(t)) \\ &\leq \max_{i \in I(x(t), u(t)), j \in J(x(t))} \nabla V_j(x(t))f_i(x(t), u(t)) \\ &\leq \max_{i \in I(x(t), u(t)), j \in J(x(t))} -\bar{\alpha}(V(x(t))) + \max_{i \in I(x(t), u(t)), j \in J(x(t))} \sigma(|u(t)|) \\ &= -\bar{\alpha}(V(x(t))) + \sigma(|u(t)|) \end{aligned}$$

Then, the proof is completed.

Following from Theorem 1 and input-to-state stability’s proof method, next theorem is shown.

Theorem 2. If there exists an IOS-Lyapunov function, then system (1) is input-to-output stable.

3 Conclusions

In this paper, IOS problems for one class of discontinuous dynamical systems are considered.

Piecewise smooth IOS-Lyapunov functions are adopted. The results for a class of discontinuous dynamical systems’ IOS character are shown, naturally. The research will be used for the development of modern technology and they will be developed with the development of intelligent materials.

Acknowledgement. This work is supported by Youth Natural Science Foundation of province in Heilongjiang of China under Grant No. QC2009C99.

References

1. Sontag, E.D.: Smooth stabilization implies coprime factorization. *IEEE Trans. Automatic. Contr.* 34, 435–443 (1989)
2. Angeli, D., Sontag, E.D., Wang, Y.: A characterization of integral input-to-state stability. *IEEE Trans. Automatic. Contr.* 45, 1082–1097 (2000)
3. Heemels, W.P.M.H., Weiland, S.: Input-to-state stability and interconnections of discontinuous dynamical systems. *Automatica* 44, 3079–3086 (2008)
4. Sontag, E.D., Wang, Y.: A notion of input to output stability. In: *Proc. European Control Conf.*, Brussels (1997)

Finite Element Analysis of Pump Diesel Engine Connecting Rod

Bin Zheng, Yongqi Liu, Ruixiang Liu, and Jian Meng

School of Traffic and Vehicle Engineering, Shandong University of Technology,
Zibo, Shandong, 255049, China
sdutzb@163.com, sdutzheng@163.com

Abstract. In this paper, with the ANSYS, stress distribution of pump diesel engine connecting rod were analyzed by using 3D finite element method. The results show that the oil-hole of small end of connecting rod shank is the exposed destructive positions at maximum compression condition and maximum stretch condition. Maximum stress value is 371 MPa at maximum compression condition. Maximum deformation value is 0.149mm. Maximum stress value is 69.4MPa at maximum stretch condition. Maximum deformation value is 0.0168mm.

Keywords: Finite Element Analysis, Connecting Rod, Stress Distribution, Pump Diesel Engine.

1 Introduction

Connecting rod is one of the important driving parts of diesel engine. It bears various complex load of periodic change. If it isn't strong enough, endurance failure of connecting rod would be produced easily. So much so that connecting rod fracture. It will lead to engine fault as well as serious outcome. As an effective analysis method, finite element analysis has been used widely in the design of connecting rod [1-7].

With the rapid development of agricultural mechanization, agricultural machinery is applied more and more widely. Pump diesel engines are the main machinery types. In this paper, with the ANSYS, stress distribution of connecting rod of pump diesel engine were analyzed by using 3D finite element method.

2 Model Building

The material of connecting rod is 45 steel. Main performance parameters are shown in Table 1.

Table 1. Main performance parameter

Young's modulus [N/m ²]	Poisson's ration	Breaking point [MPa]	Yield limit [MPa]
2.1e11	0.3	624	377

Building accurate and reliable calculating model is one of the key steps of analysis with finite element analysis. During the process of analysis, the finite element analysis model should be built according to the real one as much as possible. However, if the structure of the object is complex, it can be very difficult, even impossible to build the calculating model in accordance with the real one. Therefore, approximate simplification is necessary. In this paper, big end of connecting rod is simplified. Bearing shell, bushing and bolts of connecting rod are ignored. Big end cover and body of connecting rod are taken as a whole model. In order to avoid the big difference of sizes of finite element mesh which would decrease element quality and calculation accuracy, simplifying treatment is done to the little beveling and circular beads that hardly affected the strength of connecting rod.

In order ensure calculation accuracy, 8-node tetrahedron element SOLID 45 is employed. The method of dividing model is free mesh dividing. As this method is free of manual control, it is necessary to repair the result of mesh dividing. So stress concentrated parts, such as the transition location of small end and connecting rod shank, the transition location of big end and inner sides of I-shaped cross-section of connecting rod shank, are checked. After reparation, there are 65911 meshes on the finite element model of connecting rod. The mesh dividing of connecting rod is shown in Fig.1.

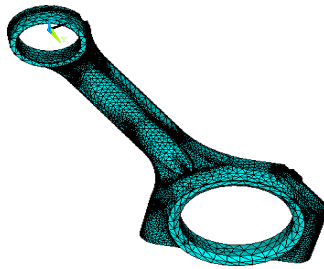


Fig. 1. Mesh of connecting rod

3 Applied Loads

While connecting rod is work, its periodic external force consists of two parts. One is gas combustion pressure transformed by piston crown, which compresses connecting rod. The other is inertia force caused by high-speed moving of piston-connecting rod, which stretches connecting rod. Therefore, during the process of analysis, the main load is maximum combustion pressure, inertia force of piston unit and inertia force of connecting rod unit.

① combustion pressure

Combustion pressure is the gas pressure caused by gas combustion. It presses piston, which will transform the force to small end of connecting rod by piston pin. Gas combustion pressure can be worked out by Eq. 1.

$$F = P_g \frac{\pi D^2}{4} \quad (1)$$

Where P_g is manometer pressure of cylinder and D is diameter of cylinder.

② inertia force of piston unit

Piston unit consists of piston, piston ring, piston pin and piston pin circlip. The mass of piston unit is mass summation of all the parts. Inertia force of piston unit works on piston pin. And it transforms inertia force to connecting rod. The inertia force can be worked out by Eq. 2.

$$F_1 = m_p R \omega^2 (1 + \lambda) \quad (2)$$

Where m_p is mass of piston unit, R is radius of crank, ω is angular velocity of crank and λ is crank link ratio.

③ inertia force of connecting rod unit

Connecting rod unit consists of connecting rod shank, big end cover, bearing shell, bolt and bush. The mass of connecting rod unit is made up of these parts. In order to simplify calculation, the mass of the connecting rod which makes complicated planar movement is divided into two parts. One part concentrates on small end of connecting rod, which is considered to make movement with piston. The other part concentrates on big end of connecting rod, which is considered to make rotary motion with crank. So inertia force of connecting rod consists of reciprocal inertia force on small end and rotary inertia force on big end.

The reciprocal inertia force of small end is calculated by Eq. 3.

$$F_2 = m_1 R \omega^2 (1 + \lambda) \quad (3)$$

The rotary inertia force of big end is calculated by Eq. 4.

$$F_3 = m_2 R (\omega \lambda)^2 \quad (4)$$

Where m_1 is mass of small end of connecting rod, m_2 is mass of big end of connecting rod, R is radius of crank, ω is angular velocity of crank and λ is crank link ratio.

The analysis of connecting rod consists of two conditions, the maximum stretch condition and the maximum compression condition. The load is applied to inner surface of big end and small end. Distributed method is second-degree parabola in axial direction and cosine in radial direction.

Safety factor is calculated by equation (5):

$$n = \frac{\sigma_{-1Z}}{\frac{\sigma_a}{\epsilon_\sigma} + \varphi_\sigma \sigma_m} \quad (5)$$

Where σ_{-1Z} is yield limit, σ_a is stress amplitude, ϵ_σ is surface roughness, φ_σ is fatigue life factor and σ_m is mean stress.

4 Results and Discussion

Stress distribution and deformation of connecting rod at maximum stretch condition are shown in Fig.2. The results show that the oil-hole of small end of connecting rod shank is the exposed destructive positions at maximum stretch condition. Maximum stress value is 69.4MPa at maximum stretch condition. Maximum deformation value is 0.0168mm.

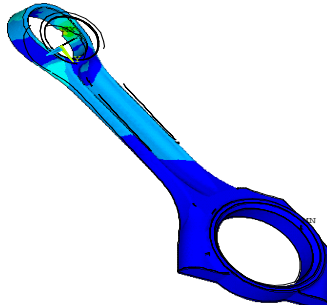


Fig. 2. Stress distribution and deformation of connecting rod at maximum stretch condition

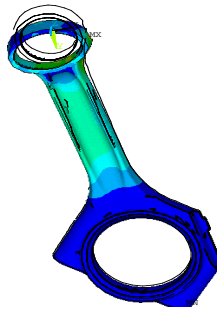


Fig. 3. Stress distribution and deformation of connecting rod at maximum compression condition

Stress distribution and deformation of connecting rod at maximum compression condition are shown in Fig.3. The results show that the oil-hole of small end of connecting rod shank is the exposed destructive positions at maximum compression condition. Maximum stress value is 371 MPa at maximum compression condition. Maximum deformation value is 0.149mm.

5 Conclusions

At maximum compression condition and maximum stretch condition, The oil-hole of small end of connecting rod shank is the exposed destructive positions at. Maximum stress value is 371 MPa at maximum compression condition. Maximum deformation

value is 0.149mm. Maximum stress value is 69.4MPa at maximum stretch condition. Maximum deformation value is 0.0168mm.

Acknowledgment. This work was financially supported by the National High Technology Research and Development Program("863"Program) of China (No.2009AA063202), Shandong Natural Science Foundation (No.Y2006F63) and Zibo Research Programme (No.20062502).

References

1. Zhang, J.C., Li, X.H., Sun, G.: Tractor & Farm Transporter 33, 27 (2006) (in Chinese)
2. Tang, Z.J., Zuo, Z.X., Zhang, R.H.: China Mechanical Engineering 15, 365 (2004) (in Chinese)
3. Dai, W.F., Fan, W.X., Cheng, Z.J.: Small Internal Combustion Engine and Motorcycle 37, 48 (2008) (in Chinese)
4. Ho-Le, K.: Computer Aided Design 20, 27 (1998)
5. Xiong, S.T.: Small Internal Combustion Engine and Motorcycle 30, 22 (2001) (in Chinese)
6. Tu, D.H., Jiang, S.L., Cao, M.L.: Transactions of CSICE 22, 176 (2004) (in Chinese)
7. Wu, H., Wang, F., Gan, H.Y.: Chinese Internal Combustion Engine Engineering 24, 31 (2003) (in Chinese)

A Multiscale Image Edge Detection Algorithm Based on Genetic Fuzzy Clustering

Min Li¹ and Pei-Yan Zhang²

¹ Electromechanics Department, Zhengzhou Tourism College, Zhengzhou450009,
Peoples R China

Limin6808@yahoo.com.cn

² Electromechanics Department, Zhengzhou Tourism College, Zhengzhou450009,
Peoples R China

ZPY1919@163.com

Abstract. This paper presents a new multiscale image edge detection algorithm based on genetic fuzzy clustering. This algorithm reasonably uses the thought of cluster analysis to complete the search of the group of edge points adaptively, without predetermining threshold. And this also has good noise proof ability for having considered the essential distinction between marginal points and noise points by the border feature vector of the wavelet. The result of the experiment suggest that the proposed arithmetic is very effective for edge detection and noise restraining which lay the basis for realizing the defogging of the low-quality image.

Keywords: Genetic Fuzzy Clustering, Multiscale Wavelet, Characteristic Vector of Edge, Edge Detection.

0 Introductions

Edge detection is an important problem in image processing field, which is the basis of further image processing and analyzing. So far, there are many traditional arithmetics, such as Canny operator, Sobel operator and Roberts operator and so on. However, these algorithms are always more sensitive to noise, and don't have the thought of automatic room. In fact, images have different features in different scale.

Since Wavelet transform can provide accurate positioning to measured signal singularities in different scales, what's more, it is not sensitive to noise, so it can obtain better detection results in different scales. As a consequence, it has been widely used in recent years. However, in the use of wavelet transform to extract edge, threshold selection still is its shortcomings for can't use certain value to describe uncertain problems [5]. On the other hand, sceneries in three-dimensional space will lose a lot of information in the process of mapping to two-dimensional space, and the edge, texture and contour information of the scenery tend to be vague. Considering these reasons, it is obvious that we need to find an edge detection algorithm which can adaptively react the marginality of different images, and also has good ability of noise restraining.

1 Genetic Fuzzy Clustering Algorithm

In order to realize the effective partition of image edge points, we need a perfect clustering algorithm. As the most popular kind of fuzzy clustering algorithm, the c-means clustering algorithm (FCM) is widely used in every field. It is a local search algorithm that finds the optimal solution to the research questions through the iterative mountain climbing algorithms. So it is very sensitive to the initialization and easy to fall into the local minimum. Aiming at solving these problems, people have put forward various improvement methods. As a global optimization method, Genetic algorithm, through operating the population made of multiple individuals. And using genetic operator to exchange the information between individuals, so that individuals in groups can evolve from generation to generation, thus gradually approaching optimal solutions. Its main advantages are simple, universal, robust and suitable for parallel processing. So it is a kind of effective method to solve complex problems, and can overcome the problem that FCM is sensitive to initialization.

2 Genetic Fuzzy Clustering Multi-scale Edge Detection

2.1 Multi-scale Wavelet Transform Features

In order to effectively detect the edge points, the features of the edge must be given reasonable description and measurement [8]. In image processing field, gradient information is usually used to characterize the extent of mutation about the pixel, and this is also the most basic feature of edge points. Considering when an image is analyzed in wavelet in multiple scales, each scale provides certain edge information, wavelet transform have the feature of zoom at different scales, and the maxima value in multiple scales can well characterize the singularities of catastrophe points. At the same time, as the maxima value of modulus of the signal and noise in wavelet transform of each scale have distinct transmission characteristics, in other words, the maxima value of modulus of the signal increases as scale increases, while the maxima value of modulus of the noise decrease as scale increases. So based on this characteristics, the coefficients of the wavelet transform multiplied in different scales of the image corresponding to the same space position can make the edge features more outstanding. And in the meanwhile, noise performance weakened. Based on this, the paper selects the product of the multi-scale wavelet as the parameter to represent the gradient characteristics of the edge point.

2.2 Build Image Edge Character Vector

According to wavelet theories given by Mallat [9, 10], when two-dimensional image is $f(x, y)$, and two-dimensional scale function is $y(x, y)$, the corresponding two-dimensional wavelet functions respectively are:

$$\psi^1(x, y) = \partial[\gamma(x, y)] / \partial x \quad (1)$$

$$\psi^2(x, y) = \partial[\gamma(x, y)] / \partial y \tag{2}$$

And then the corresponding wavelet transforms respectively in the directions of x and y in the scale of i are

$$W_{2^i}^1 f(x, y) = f(x, y) * \psi_{2^i}^1(x, y) \tag{3}$$

$$W_{2^i}^2 f(x, y) = f(x, y) * \psi_{2^i}^2(x, y) \tag{4}$$

From the above analyses, we can conclude that the maxima value of modulus of the signal and noise in wavelet transform of each scale have distinct transmission characteristics, and this indicates that the wavelet transformation in each of the dimension has strong correlation, and more strong correlation at the edges, while the wavelet transformation of noise don't have obvious correlation among scales. Base on this characteristic, it is feasible to multiply the wavelet coefficients of adjacent scales to enhance signal directly and reduce the noise.

Definition:

If $Cor_i(x, y) = W_{2^i} f(x, y) \cdot W_{2^{i+1}} f(x, y)$ are corresponding coefficients of adjacent scales i and $i+1$ at the position of point (x, y) , and supposing $i = 1, i = 2, i = 3$, then $Cor_1(x, y), Cor_2(x, y), Cor_3(x, y)$ form the feature vector of the edge point $\{Cor_1(x, y), Cor_2(x, y), Cor_3(x, y)\}$.

2.3 The Algorithm Realization

Considering every pixel of an image as a data sample, due to the grey value of the edge points and the non-edge points can present a bigger difference through multi-scale wavelet transformation, so we use three feature vectors ($Cor_1(x, y), Cor_2(x, y)$ and $Cor_3(x, y)$) to constitute a three-dimensional characteristic vector ($k(x, y)$) to describe the image edge character, here $k(x, y) = \{Cor_1(x, y), Cor_2(x, y), Cor_3(x, y)\}$, and then using genetic fuzzy clustering algorithm to sort the data clustering, one of the descriptions is a class of edge points, so image edge points can adaptively be detected, achieving the purpose of extracting the edge. The realization of the algorithm is as follows:

(1) Creating a data set: converting a $n*n$ grayscale image into a data sets that has $n*n$ points and each of which has three features. Every feature values of every point is the grayscale value of the point via three wavelet operator processing. Like this, a data set to be clustered is obtained.

(2) The genetic encoding: We adopt the coding method of taking clustering center as the chromosomes floating-point.

(3) Genetic fitness calculation: the individual fitness is determined by the mechanism of σ - truncation in this paper.

(4) Genetic choice: we adopt the method of the combination of the optimal elitist and proportion choice to choose. First, at the beginning of every generation, recording the maximum fitness value of the optimal individual in current population, then starting the proportional choice operation and subsequent various operations to create new populations, and selecting the minimum fitness value which is the worst individual, then using the former record individual replace it, then, a new generation population will be created. This operation can not only improve the average fitness value gradually, but also guarantee that the optimal individual fitness value doesn't decrease.

(5) Genetic crossover: adopting arithmetic crossover operator based on the shortest distance genetic match. That is to say, adjust the nearest clustering center to the alleles, and then perform crossover operation on the arithmetic crossover operator.

(6) The Genetic variation: we adopt uniform mutation operator.

(7) The Individual fuzzy, c - mean optimization: because FCM method is a algorithm that has strong local search ability, fuzzy c - mean optimization should be operated after each generation completed the genetic operations, and only groups after optimization will enter the next evolution. By this way, the local search ability of hybrid algorithm can be improved apparently, and its convergence speed can be also enhanced.

(8) Genetic decoding: when genetic operation cycles to the maximum algebra, find out the chromosome with highest fitness and its corresponding clustering center matrix is the optimal solution of hybrid algorithm. With this optimal clustering center, optimal fuzzy classification matrix can be calculated, and then the optimal clustering classification can be determined based on the principle of the maximum membership degree.

3 Experimental Results and Analyses

In order to verify the effectiveness of the edge detection algorithm, this paper made a lot of experiments. Here, two image edge detection effects and contrast experimental results are given.

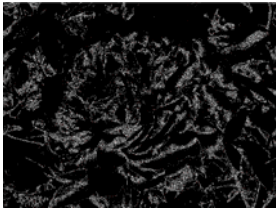
Comparing experimental results in diagrams above, we can see that the algorithm proposed in this paper has better positioning accuracy, and the extracted edge lines are more delicate. Compared with traditional sobel algorithm and Gauss - Laplace edge detection method, it can be seen that in the peony figure, the proposed algorithm do more reservation of the edge of peony, especially in longmen images, detail information between the big Buddha and the little Buddha is more evident in the results with the method proposed in this paper. What's more, contour information in peripheral place is also retained more.



(a) The original image peony



(b) sobel edge detection algorithm



(c) Gauss-Laplace



(d) New algorithm

Fig. 1. Edge detection pictures of every algorithm contrast to the original peony picture



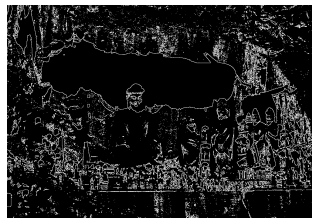
(a) The original image longmen



(b) sobel edge detection algorithm



(c) Gauss-Laplace



(d) New algorithm

Fig. 2. Edge detection pictures of every algorithm contrast to the original longmen picture

4 Conclusions

Based on multi-scale wavelet transform and genetic fuzzy clustering theory, this paper puts forward a new kind of edge detection algorithm. With this method, we can

use genetic fuzzy clustering algorithm to complete the search of the group of edge points without pre-defined threshold, and this also has good anti-noise ability. The experimental results verify that this algorithm can not merely solve the contradiction efficiently between edge available detection and good localization characteristics compared with the traditional algorithm, but also can effectively reduce the noise. So it is a kind of effective edge detection algorithm, and it can be well applied to the processing of real-time video image defogging.

References

1. Canny, J.: A computational approach to edge detection. *IEEE Transaction: Pattern and Order Achine Intelligence* 8(6), 679–698 (1986)
2. Evans, A.N., Liu, X.U.: Morphological Gradient Approach. A Detection. *IEEE to Color Edge dd, 15 allow Transactions on* (6), 1454–1463 (2006)
3. Zhang, L., Paul, B.: Primarily and a wavelet edge detection of - based scale multiplication. In: Google, 16th International Pattern Recognition, vol. 3, pp. 8501–8504 (2002), it hasn't been made clear on 2002
4. Zhang, L., Paul, B., Xiaolin, W.: Primarily for and Detcetion Scale Enhancement Canny Edge. *IEEE Transactions on Multiplication Pattern. Machine Intelligence*, order 27(9), 1485–1490 (2005)
5. Zhang, J.J., Yang, D., Zhang, x.-h., et al.: Based on fuzzy logic multi-scale wavelet edge detection method of. *Chongqing University Journal: natural science edition* 28(10), 62–65 (2005)
6. Shih, M.-Y., Tseng, D.-C.: Multiresolution Wavelet - Based A Detection and Edge Add a Vision Tracking. *Computing, and Singapore -* 451 23 (2005)
7. Mallat, S., Zhong, S.: Characterization of Multiscale Edges. *IEEE - it Transactions on Patten Machine Intelligence* 14(7), 710–732 (1992)
8. Mallat, S., Hwang, W.L.: Singularity Detection and Processing Wavelets. *IEEE Transactions on account* 38(2), guys Information: 1076-145821476 (1992)
9. Stephane, M., Zhong, S.: Characterizing, edges of multiscale it. *IEEE Transactions on Machine Intelligence order Pattern* 14(7), 2131–2132 (1992)
10. Wu, J., Yin, Z., Tiong, Y., Chen, P.X.: Multilevel Fuzzy Edge Detcetion militiamen Fast of Blurry images. *IEEE Allow Signal Letters* 14(5) (2007); 317, 1003 (1981)

Research on Transitional Culture on Impulse Buying Intention in Mainland China

Wang Jian-guo and Yao De-li

School of Economics and Management, Anhui University of Science and Technology,
 Huainan, Anhui, 232001, China
 cancou1005@163.com, dlyao@aust.edu.cn

Abstract. In this paper, structural equation model are used to provide an insight into Chinese transitional culture influence on consumers' impulse buying intention. Results show that, due to rapid economic development and culture transition, impulse buying behavior is becoming a commonplace phenomenon in the mainland China. This paper provides new marketing materials to the research on consumers' impulse buying.

Keywords: Transitional culture, Impulse buying intention, Structural equation model, Marketing materials.

1 Introduction

Impulse buying generates over \$4 billion in annual sales volume in the United States(Kacen, 2002). But previous studies are mainly based on the western culture. We should take into account local market conditions and various cultural forces, which could supply new marketing materials on impulse buying(Kacen & Lee, 2002; Mai et al, 2003; Vohs & Faber, 2007). As Jacqueline & Lee(2002) demonstrated, cultural factors significantly influence consumers' impulsive buying behavior. We find Chinese culture has the following characteristics in Table1: 1) relatively high power distance; 2) tend to collectivism; 3) tend to masculine; 4) the low level of uncertainty avoidance; 5) strongest long-term orientation. However, growing research suggests that Chinese culture is changing(Yu, 2010). Generation X in Mainland China illustrates that these young people are bicultural (Zhang, 2009). The purpose of this paper is to study how the Chinese transtional culture influence on consumers' impulse buying intention(IBM), which provides new marketing materials to the research on consumers' impulse buying.

Table 1. Five dimensions of China Culture index

Dimensins	Power distance	Individualism	Masculinity	Uncertainty avoidance	Long term - orientation
Culture index	63	21	51	49	11

Data source: Hofstede, Across cooperation obstacles: multi-culture and management, 1996

Marketing Materials. Since 1950s, the research on the impulse buying behavior is nearly 60 years. Scholars in the study of impulse buying has made a wealth of marketing materials like the concept of impulse buying behavior, influencing factors, and mechanism models etc. Although some scholars find the small power distance, individualism and femininity are positively related with IBI, few marketing materials show the influence of uncertainty avoidance and short term orientation on impulse buying. Previous studies are mainly based on the western culture. We base on Chinese transitional culture, systematically analyze Hofstede's five culture dimensions influences on consumers' IBI, which enrich the marketing materials on consumers' impulse buying.

2 Overview of the Studies

Impulse buying. Impulse buying is described as more arousing, less deliberate and more irresistible buying behavior compared to planned purchasing behavior (Kacen & Lee, 2002). Based on different perspectives, we can divided the factors influencing impulse buying into firm's factors and consumer's factors. Early research mainly concentrated on the firm's factors. Beginning in the 1990s, researchers began taking a look inside the consumer. From the consumers' perspectives, research into the causes of impulse buying can be separated into two parts: internal, personal-related factors and external environmental influences. The former are: personal factors and mental factors, which include impulse buying trait (Ferrell, 1998; Jones, 2003), self control (Kivetz & Zheng, 2006; Baumeister, 2002), mood and emotions (Rook & Gardner, 1993), and self-identity (Dittmar et al., 1995) etc. The latter are: cultural factors and social factors. For example, peer group pressure (Luo, 2005) and "face" on consumer impulse buying (Zhang & Zhuang, 2008).

Hofstede's culture model and impulse buying. We will analyze the transitional culture on consumers' IBI according to Hofstede's five culture dimensions: power distance, individualism/collectivism, masculinity/femininity, uncertainty avoidance, and long/short-term orientation, which provides new marketing materials to the research on consumers' impulse buying.

Power distance. Power distance is the degree of power disparity that people in a culture expect and accept (Hofstede, 1984). Seeley and Gardner (2003) conclude that people from Eastern cultures are more likely to be perceived as normatively compliant when they can control their impulse urges. So low power distance cultures lead to more impulse buying. Traditional Chinese culture is relatively high power distance. On the basis of this theorizing, we propose the following:

H1: The Chinese culture transition from large power distance to small power distance leads to consumers' more IBI.

Individualism/collectivism. Individualism stands for a preference for a loosely knit social framework in society (Hofstede, 1984). China represents a typical collectivist country (Hofstede, 1980), in which interdependence, emotional control and group needs and desires would seem to discourage impulse buying behavior. However, growing research suggests that the Chinese have become less collectivistic (Yu, 2010). A recent study of Generation X in Mainland China illustrates that these young people are bicultural (Zhang, 2009). From this we conclude the following:

H2: The Chinese culture transition from collectivism to individualism leads to more IBI.

Masculinity/Femininity. Masculinity stands for a preference in society for achievement, heroism, assertiveness, and material success. Femininity, stands for a preference for relationships, modesty, caring for the weak, and the quality of life (Hofstede, 1984). Many previous scholars studied gender on impulse buying, basically come to the same conclusion: women are more impulse than men. Due to the fast economics development, Chinese government even more value the equality of male and female. Female are playing important roles in Chinese families and society. From this we conclude the following:

H3: The Chinese culture transition from masculinity to femininity leads to more IBI.

Uncertainty avoidance. Uncertainty avoidance is the degree to which the members of a society feel uncomfortable with uncertainty and ambiguity. Due to the good economic and political environment, Chinese consumers' shopping value more optimistically and just let them happen. From this we conclude the following:

H4: The Chinese culture transition from strong uncertainty avoidance to weak uncertainty avoidance leads to consumers' more IBI.

Long/short-term orientation. Long versus short-term orientation is the extent to which a society exhibits a pragmatic future-orientated perspective. Many Eastern cultures value the future more than the present (Chen, Ng, and Rao 2005), delayed gratification and restraint are considered the highest virtues. Nowadays more and more Chinese consumption more value the present. From this we conclude the following:

H5: The Chinese culture transition from long-term orientation to short term orientation leads to consumers' more IBI.

We may summarize the characters of Chinese transtional culture as small power distance, high individualism, high femininity, weak uncertainty avoidance, and short-team orientation.

3 Methodology

The model construction. From the perspective of Hofstede's cultural model, we construct the model of Chinese transtional culture on consumers' IBI as follows (Fig1).

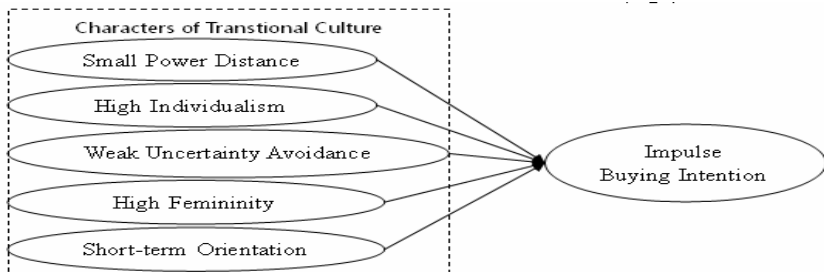


Fig. 1. The model of transitional culture on impulse buying intention

Data sourcing. Participants were 296 undergraduate students from a Chinese university. The sample was divided between male (49.5 per cent) and female (50.5 per cent). Following Rook and Fisher (1995), an imaginary situation was described to the respondents: Mary is a 21-year-old college student with a part-time job. It is two days before Mary receives her next paycheck and she has only \$25 left for necessities. In addition to food, Mary needs to buy a pair of warm socks for an outdoor party this weekend. After work, she goes with her friend Susan to the mall to purchase the socks. As they are walking through M Store, Mary sees a great looking sweater on sale for \$75. After reading their scenario, respondents were instructed to select which one of five decision alternatives would Mary make. These alternative choices were designed to represent varying levels of IBI. From low to high, these alternatives were: (1) buying the socks, (2) desirous of the sweater but not buying it, (3) deciding not to buy the socks, (4) buying both the socks and sweater with a credit card, and (5) buying these plus matching slacks and a shirt, also with a credit card.

4 Model Checking

Reliability testing. In this survey, Cronbach α was used to analyze and SPSS15.0 to calculate. Cronbach α coefficients ranged between 0 and 1. According to Nunally study, when α is greater than 0.8, it indicates an excellent internal consistency, α from 0.7 to 0.8, better, for the minimum acceptable 0.7. The survey shows that all scales of the Cronbach α ranged between 0.803~0.916, indicating a high reliability of the scales.

Validation. Rook and Fisher’s scales has been confirmed by other researchers and each subscale validity is relatively high.

Fitting test. We used AMOS7.0 to perform path analysis for directly observed variables. The fit estimates for the overall model (chi²=187.25, with 104 df (P<0.001), GFI=0.95, AGFI=0.92 RMSEA=0.041, NFI=0.92, CFI=0.96) are within accepted standards. The results of the path analysis appear in Figure2. As expected, positive correlation estimates exist between the five transitional culture dimensions and IBI. This suggests that transtional culture may lead to more impulse buying.

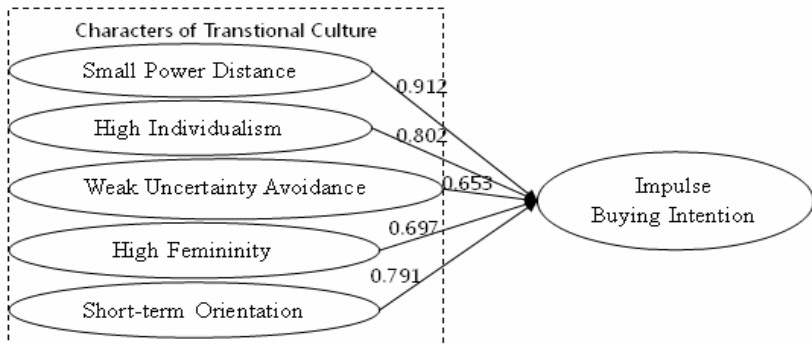


Fig. 2. Path analysis estimates

5 Conclusion

In this research, we demonstrate a relatively novel effect: the influence of culture on impulse buying. Our study of the relationship between transitional culture and IBI reveals all the Hofstede's culture dimensions are positively associated with consumers' IBI. This gives strong evidence to support our proposition. The results of this research suggest that given the changes in the traditional culture and impulse buying behavior is becoming more pervasive and widespread in mainland China, which supply new marketing materials on IBI in non-western culture. This study further verifies culture influence on IBI in the emerging market like China and provides new marketing materials to promote the impulse buying theory development.

Acknowledgment. This article is funded by social science foundation of Anhui province (AHSK09—10D57); The survey objects have done a lot of work for the completion of this article.

References

1. Yu, C., Bastin, M.: Hedonic shopping value and impulse buying behavior in transitional economies: A symbiosis in the Mainland China marketplace. *Journal of Brand Management* 18(2), 105–114 (2010)
2. Hofstede, G.: Cultural Dimensions In Management And Planning. *Asia Pacific Journal of Management* (2), 81–99 (1984)
3. Kacen, J.J., Lee, J.A.: The Influence of Culture on Consumer Impulse Buying Behavior. *Journal of Consumer Psychology* (2), 163–176 (2002)
4. Zhang, W., Mittal: Power distance belief and impulse buying. *Journal of Marketing Research* 10, 945–954 (2010)

Finite Element Analysis of Marine Diesel Engine Crankshaft

Bin Zheng, Yongqi Liu, Ruixiang Liu, and Jian Meng

School of Traffic and Vehicle Engineering, Shandong University of Technology,
Zibo, Shandong, 255049, China
sdutzb@163.com, zhengbin@sdut.edu.cn

Abstract. In this paper, with the ANSYS, stress distribution and safety factor of crankshaft were analyzed by using 3D finite element method. The results show that the exposed destructive position is the transition circular bead location of the crank web and the crankpin. Maximum stress is 112.8 MPa. Safety factor is 3.32. Crankshaft satisfies the design requirement.

Keywords: Finite Element Analysis, Crankshaft, Stress Distribution, Safety Factor.

1 Introduction

Crankshaft is one of the important driving parts of diesel engine. It bears various complex load of periodic change. If it isn't strong enough, endurance failure of crankshaft would be produced easily. So much so that crankshaft fracture. It will lead to engine fault as well as serious outcome. As an effective analysis method, finite element analysis has been used widely in the design of crankshaft [1-7].

Fishery is an important component of agriculture in China. With the rapid development of fishery, fishing boat is applied more and more widely. In this paper, with the ANSYS, stress distribution and safety factor of crankshaft of marine diesel engine were analyzed by using 3D finite element method.

2 Model Building

The material of crankshaft is 45 steel. Main performance parameters are shown in Table 1.

Table 1. Main performance parameter

Young's modulus [N/m ²]	Poisson's ration	Breaking point [MPa]	Yield limit [MPa]
2.1e11	0.3	624	377

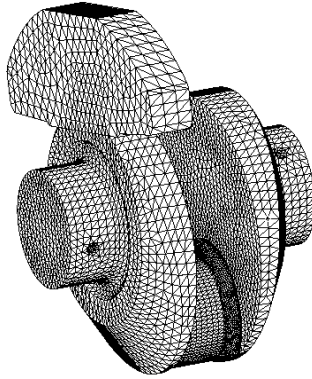


Fig. 1. Mesh of crankshaft

In our investigations the real crankshaft was represented by a model whose structure details, such as chamfer, were ignored. The crankshaft model was created by Pro/ENGINEER software. Then the model was imported to the ANSYS software. According to the structure of crankshaft, the crankshaft model was meshed by 8-node tetrahedron element SOLID 45, which was one of ANSYS solid type. The chamfer of the crankshaft was tessellated. There are 97978 nodes and 30796 meshes on the finite element model. The finite element mesh of the 3-D crankshaft model used ANSYS code is shown in Fig.1.

3 Applied Loads

The boundary conditions are the critical factors for the correctness of calculation. The boundary conditions in the crankthrow model consist of load boundary condition and restriction boundary condition. The mechanics boundary conditions mainly involves: gravity, centrifugal force, crankpin neck surface force, various bending moment and torque, etc. Gravity, centrifugal force, various bending moment and torque can apply to the model with the distributed force, ANSYS software simulates the effects of gravity and centrifugal force itself based on the given gravity accelerative, angular velocity, density and physical dimension. So the load applying on the crankpin neck surface becomes the critical factor of load boundary condition. In the paper, kinetic method is used to calculate load. And the load applying on the crankpin surface is supposed as distributed load. The distributed load along the crankpin axis is a quadratic parabola distribution and along the radial direction within 120° is cosine distribution.

The quadratic parabola load distribution equation along the crankpin axis is assumed by Eq. 1:

$$Q_x = ax^2 + bx + c \quad (1)$$

When $x=\pm L$, $Q_x=0$; when $x=0$, $Q_x=Q_{max}$, the above formula can be written as:

$$0 = aL^2 + bL + c \quad (2)$$

$$0 = aL^2 - bL + c \quad (3)$$

$$Q_{max} = c \quad (4)$$

The a, b, c can be obtained by solving the Eq. 2, 3 and 4. The results are $a=-Q_{max}/L^2$, $b=0$, $c=Q_{max}$. Accordingly, the load distribution along the crankpin axis can be obtained as follows Eq. 5

$$Q_x = Q_{max} \left(1 - \frac{x^2}{L^2} \right) \quad (5)$$

where $x = -L-L$.

The cosine load distribution equation along the radial direction within 120° is supposed by Eq. 6:

$$Q(x, \theta) = Q_x \times \cos k\theta \quad (6)$$

where $\theta = -\pi/3 - \pi/3$. When $\theta = \pi/3$, $Q(x, \theta) = 0$, the k can be calculated by Eq. 7:

$$\cos \frac{\pi}{3} k = 0 \Rightarrow k = \frac{\pi}{2} / \frac{\pi}{3} = \frac{3}{2} \quad (7)$$

Accordingly, the load distribution along the crankpin radial direction within 120° can be written as follows Eq. 8:

$$\begin{aligned} Q(x, \theta) &= Q_x \times \cos \frac{3}{2} \theta \\ &= Q_x \left(1 - \frac{x^2}{L^2} \right) \times \cos \frac{3}{2} \theta \end{aligned} \quad (8)$$

The total load applying on the crankpin neck surface can be caculated by the follow Eq. 9:

$$\begin{aligned} F_c &= \int_{-L}^L \int_{-\frac{\pi}{3}}^{\frac{\pi}{3}} Q(x, \theta) g ds g dx \\ &= \int_{-L}^L \int_{-\frac{\pi}{3}}^{\frac{\pi}{3}} Q_{max} \left(1 - \frac{x^2}{L^2} \right) \cos \left(\frac{3}{2} \theta \right) g R d\theta g dx \\ &= \frac{16}{9} RL \times Q_{max} \end{aligned} \quad (9)$$

where $d_s = Rd_\theta$, R is the crankpin radius. Q_{max} can be expressed in terms of Eq. 9 as the following Eq. 10,

$$Q_{\max} = \frac{9}{16} \times \frac{F_c}{RL} \tag{10}$$

Rewriting Eq. 6 as:

$$Q(x, \theta) = \frac{9F_c}{16LR} \left(1 - \frac{x^2}{L^2}\right) \times \cos \frac{3}{2}\theta \tag{11}$$

where F_c is the total load acting on the crankpin neck surface, x is crankpin load bearing length, $x = -L$ to L . The largest load was used in this paper when the crankpin working at the largest torque.

Based on Eq. 11, equation loaded method was used to exert the load on the crankpin surface. The method to deal with the restriction boundary condition mainly based on the practical situation of crankshaft structure. The degrees of freedom of X, Y, Z direction at the left crankthrow end surface are limited. While at the right crankthrow end surface the motion degrees of freedom of X, Y radial direction are limited.

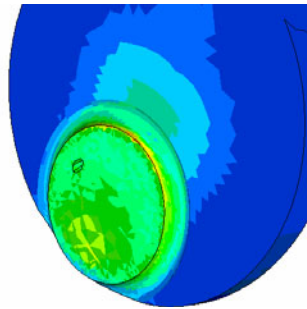


Fig. 2. Stress distribution of connecting rod at maximum compression condition

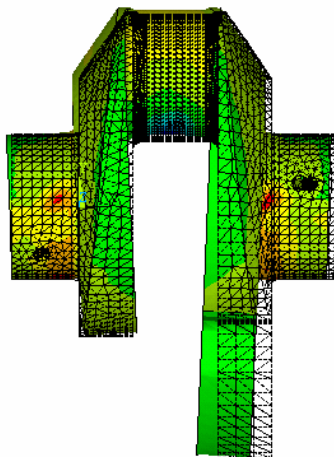


Fig. 3. Stress distribution of connecting rod at maximum stretch condition

4 Results and Discussion

Stress distribution of crankshaft at maximum compression condition and maximum stretch condition are shown in Fig.2 and Fig.3. The results show that the value of stress is the biggest at the transition circular bead location of the crank web and the crankpin. Maximum stress is 112.8 MPa. Safety factor is 3.32. To the whole crankshaft, its safety factor is 3.32, which is bigger than the required value 1.5 of crankshaft design. Therefore, crankshaft satisfies the design requirement.

5 Conclusions

At maximum compression condition, the value of stress is the biggest at the transition circular bead location of the crank web and the crankpin. Maximum stress is 112.8 MPa. Safety factor is 3.32. Crankshaft satisfies the design requirement.

Acknowledgment. This work was financially supported by the National High Technology Research and Development Program("863"Program) of China (No.2009AA063202), Shandong Natural Science Foundation (No.Y2006F63) and Zibo Research Programme (No.20062502).

References

1. Zhang, J.C., Li, X.H., Sun, G.: Tractor & Farm Transporter 33, 27 (2006) (in Chinese)
2. Tang, Z.J., Zuo, Z.X., Zhang, R.H.: China Mechanical Engineering 15, 365 (2004) (in Chinese)
3. Dai, W.F., Fan, W.X., Cheng, Z.J.: Small Internal Combustion Engine and Motorcycle 37, 48 (2008) (in Chinese)
4. Ho-Le, K.: Computer Aided Design 20, 27 (1998)
5. Xiong, S.T.: Small Internal Combustion Engine and Motorcycle 30, 22 (2001) (in Chinese)
6. Tu, D.H., Jiang, S.L., Cao, M.L.: Transactions of CSICE 22, 176 (2004) (in Chinese)
7. Wu, H., Wang, F., Gan, H.Y.: Chinese Internal Combustion Engine Engineering 24, 31 (2003) (in Chinese)

Design of Magnetic Separation Column Data Logger Based on PROFIBUS and USB Bus Control Chip

Ying Sun

Information Engineering Institute Shenyang University
Shenyang 110044, China
sunying_1215@163.com

Abstract. Magnetic separation column is a highly effective concentrate purification equipment. According to field process requirement, its parameters need adjust in practical application. In order to build relationship between the parameters and ore grade, the paper presents a design method of data logger, such as magnetic separation column parameters, running state, current concentration and error code, based on PROFIBUS and CH375B. Moreover, the overall structure of the recorder, hardware circuit and software design flow are described in detail. A fast, efficient and reliable solution is proposed for magnetic separation column parameters recorded.

Keywords: PROFIBUS, CH375B, Magnetic separation Column, data logger.

1 Introduction

Iron mineral processing using magnetic separation has many advantages, such as low energy consumption, pollution, High-grade mineral[1]. Magnetic separation column is a low-field magnetic gravity separation pulse power processing equipment which is combination of gravity and magnetic[2]. It consists of several variable frequency power supply, and generates cycle variation magnetic field in space of magnetic selection, and repeated several times on the magnetic slurry using polymerization - dispersion - Magnetic polymerization way in order to fully separate the mixture of magnetic minerals in the monomer with the living body and gangue to produce up to 67% or more grade iron ore. Recently this technology has used in dozen large iron and steel processing concentrator such as Anshan, Baotou, Benxi Iron and Waitoushan Steel NF. Due to the field environment, the different technical requirements, KSZK separation column automatic control system [3] has many Reserved control parameters such as the frequency inverter power supply, valve opening, and detection parameters such as the separation column underflow concentration, concentration overflow. Control and detection parameters is closely related to field testing process requirements and iron ore grade demand, therefore, recording parameters on the separation column real-time have significance to discover relationship between parameters and iron grade and provide important reference data. The field bus protocol use PROFIBUS.

According to Magnetic Separation Column parameters recording problem, a data recorder design method based on PROFIBUS bus and USB bus controller CH375B. C8051F020 microcontroller used for the design method of the PROFIBUS protocol processing chips based on the PROFIBUS bus communication VPC3 + and U-disk-based data storage CH375B with a RTC (Real-Time clock) clock function of the circuit. It is provide a feasible and effective way for parameters recording and setting of magnetic separation column.

2 Data Logger System Design of Magnetic Separation Column

Figure 1 shows data logger system block of magnetic separation column. Microprocessor selection is C8051F020. RTC chip is DS3231, CH375B is selected as USB controller chip, VPC3+ is used as PROFIBUS protocol chip, HCPL0710 and HCPL0601 are optocoupler respectively, RS-485 converter chip used DS75176. System starting work in VPC3 + after initialization by microprocessor C8051F020, which processing transmission data in PROFIBUS from VPC3+, while detecting the clock chip is working properly, whether USB disk installed. after Peripherals ready microprocessor write the date, time, function code, data, and other data. System parameter settings (such as the current date, time, etc.) implement through the PROFIBUS write specific code. System power supply is DC 24V, and convert several power for chips on board by designed DC /DC convert circuit. isolation module is used for PROFIBUS interface circuit power supply, which can improve system reliability and noise immunity.

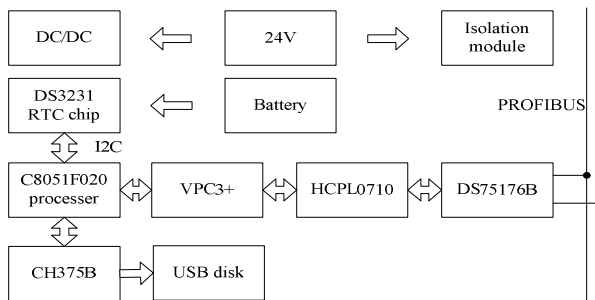


Fig. 1. Data logger system block of magnetic separation column.

3 Separation Column Hardware Design Data Logger

VPC3 + and microcontroller interface design. PROFIBUS is industrial field bus with European standards EN50170 and German DN19245. Features of PROFIBUS are open, intelligent, interoperable, adaptable, decentralized control, data transmission and control which is widely used in industrial automation equipment[4,5]. PROFIBUS-DP is a specification from PROFIBUS. it is a high-speed, long-distance communication way which speed up to 12Mbps and communication distance up to 23.8km. The solution paper present use RS- 485 as the physical layer transmission.

Before communications is established in PROFIBUS-DP communication, it is need that for the following three steps: (1) Master, Slave station self-test, establish the diagnosis of response information. Master monitors token on the bus, and slave waits for the main station parameters set command. (2) Master and slave station initialize communicate. (3) Master, Slave exchange data. After it is into data exchange message state, station will be conducted after the analysis, fault diagnosis and so on. if the PROFIBUS packet processing program use micro-controller. system development cycle is longer and PROFIBUS-DP specification requires a deep understanding. Due to restrictions of the microcontroller UART baud rate, it difficult to achieve 12Mbps communication speed which PROFIBUS-DP required. The paper uses VPC3 + as PROFIBUS-DP protocol processing chip, the chip integrates all the PROFIBUS-DP protocol, thereby reducing the development effort.

The paper selected C8051F020 as microcontroller, which uses CIP-51 microcontroller core, instruction processing speed of up to 25MIPS. The microcontroller integrated memory and 4KB of RAM and 64KB of Flash memory, a lot of external interfaces. when use VPC3+ chip, its port need set. Where MODE is set to 0, the port will work in the Intel mode, Motorola is Available in the port 1. DIVIDER determine CLK2 output frequency, the output frequency is 12Mhz when 0 is set, while the output frequency is 24Mhz when 1 is set. XCTS is the chip select port, RXD, RTS, TXD are data transmission port, moreover, isolation interface circuit between PROFIBUS and SPC3 is need.

Usually there are three transmission mode as physical layer: RS-485, IEC158-2 and fiber. low-cost RS-485 transmission mode is use in the text, the interface circuit shown in Figure 2.

DS75176B is selected as RS-485 level converter chip, which is a high-speed tri-state RS-485 converter chip, drive delay is 22 ns. High-speed communications to meet the requirements of PROFIBUS. Agilent HCPL0710 are for high-speed optocouple of communication. It is used HCPL0601 optocoupler for RTS port. Power isolation module supply power for both sides of optocoupler to improve system reliability.

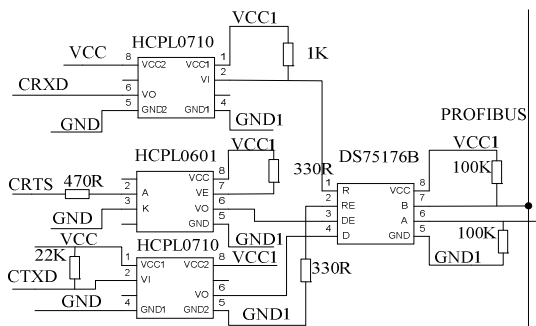


Fig. 2. Interface between VPC3+ and PROFIBUS

Interface design and microcontroller CH375B. Figure 3 shows the interface between microcontroller and CH375B. Set CH375B work as parallel port work mode. TXD ports need to be grounded. Power supply pin to ground need to connect 0.1uF

decoupling capacitor. It is need to connect 100uF capacitor between U disk and VCC port to prevent power suddenly decreases in hot swap. Crystal frequency is 12Mhz, and it is need to connected 20P high-frequency ceramic capacitor in XI, XO ports. RSTI pin is used to reset the chip CH375B.which connect a internal pull-down resistor. There is a 0.47uF capacitance, the reset time is about 100 milliseconds. The chip pin A0 is address \ data set pin, built-in weak pull-up resistor, when A0 = 1 for writing command, when A0 = 0for reading and writing data. Command and control pins WR, RD, CS and INT interrupt key interfaces with the microcontroller are as shown in figure 3.

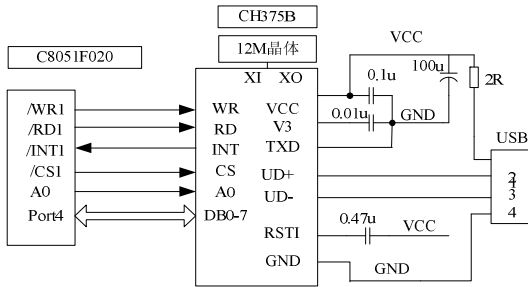


Fig. 3. Interface between CH375B and microcontroller

The recorder has RTC function for record current parameters and detecting data time. DS3231 is a temperature-compensated crystal devices with high-precision mode using I2C RTC chip communication [6], which is for read and write the time of data to the data recorder.

4 Control Processing Design

Figure 4 shows the program flow chart based on PROFIBUS interface. Its function is to read the separation column PROFIBUS parameters and recorded U disk. Specific work process is as follows: (1) After system power-on reset, initialize VPC3 +, and wait for their connection with the main station. if master of its parameters are set correctly, go to the data exchange state, meanwhile, slave station can exchange data with master station.(2) Before system initializes Ch375B, it will detect whether U disk is connect to system. if U disk is ready, it initialize the U disk for receive data. (3) Initialize the DS3231 RTC chip, and set alarm time is 12 hours for file name change. (4) Wait to allow recording command, and start the timer, which is set the period of 1 second. Meanwhile, it is need to read the data in the record before the current time, read cache of VPC3 + magnetic separation column parameter data, query U disk whether is filled. Finally, create TXT files in U disk. The FAT file format is more complex, the paper company called Qin Hang LIB functions that the definition in the CH375HF6.H. (5) Change file name. if SQW port in RTC is low, it will change current filename to avoid data file too large. It will stop recording after receive stop command.

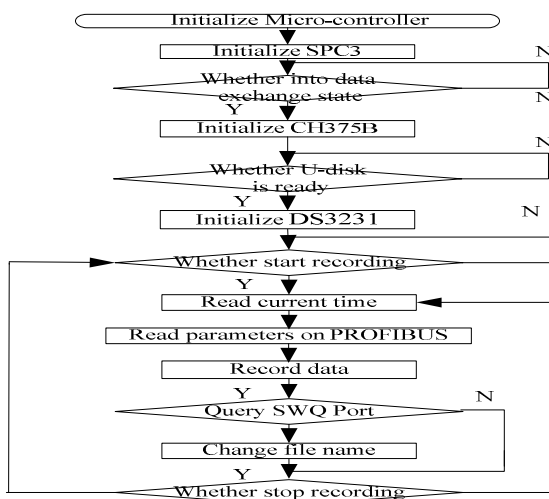


Fig. 4. Interface between CH375B and microcontroller

5 Conclusions

The paper described in detail magnetic separation column based on PROFIBUS bus data logger hardware and software design. VPC3 + chip is used for processing PROFIBUS protocol saving development costs and shorten development cycle. The way reading and writing data to U disk with CH375B has low cost, versatility and other advantages. The recorder hardware is stable and reliable, fully functional, and software ideas clear. Now, it have applied in trial operation of a large-scale concentrator. It is good to meet the mineral processing industry requirements for records on the set parameters, and greatly save labor costs, with a wide range of applications.

References

1. Zhen, C., Liu, B., Zhou: Separation column and its industrial application. *Metal Mine* (9), 30–31, 43 (2002)
2. Chen, G., Quan, F., Xiaofei, G.: Magnetic Current status and development trend. *Magnetic Materials and Devices* 41(3), 10–13, 25 (2010)
3. Wang, A., Guo, M., Xiuping Guo, A.: Implication of KSZK-III magnetic separation column controller system on concentrator. *Magnetic Materials and Devices* 38(2), 77–78 (2010)
4. Pizá, R., Salt, J., Sala, A., Cuenca, A.: Maglev platform networked control: A Profibus DP application. In: *Industrial Informatics (INDIN)*, Japan, pp. 160–165 (2010)
5. Narduci, F.L., Torres, R.D.V., Brandão, D.: Desenvolvimento de um mestre classe 2 pertencente a uma ferramenta de diagnóstico em redes PROFIBUS. In: *Industry Applications (INDUSCON)*, Brazil, pp. 1–6 (2010)
6. Gao, M.-z., Mao, Y.-m., Liu, J.-j.: Interface design of AVR microcomputer with serial clock DS3231. In: *International Electronic Elements*, China, vol. 5, pp. 15–18 (2007)

The Theory of Elastic Thin Plate Stability Problem Analysis with Approximated Daubechies Wavelets

Gao Zhongshe

School of Mathematics and Statistics, Tianshui Normal University,
Tianshui, P.R. China
gaozhongshe@hotmail.com

Abstract. It is mainly introduce the distribution method for stability problem of elastic thin plate with the approximated Daubechies wavelets. The distribution will be discussed in the two Dimensional tensor spaces.

Keywords: wavelet function, the stability problem of thin plate, finite element method.

1 Introduction

These are very important problem in elasticity of plate with later force deflection problem and plate with axial force stability problem. In general, the plate can strength more than critical value, the plate is very thin in plane structure, so study the region of supercritical value is very important. The approximated Daubechies wavelets can be found in reference [4]. The paper is organized by three sections. In the second section, we will introduce the stability problem of elastic thin plate. In the last section, we mainly derive the distribution for stability problem of elastic thin plate.

2 Stability Problem of Elastic Thin Plate

The stability problem of thin plate with axial force on neutral plan can be express by the follow

$$\begin{cases} \nabla^2 \nabla^2 w = \frac{1}{D} (N_x \frac{\partial^2 w}{\partial x^2} + N_y \frac{\partial^2 w}{\partial y^2} + 2N_{xy} \frac{\partial^2 w}{\partial x \partial y}) \\ w|_{\partial\Omega} = 0, M_n|_{\partial\Omega} = 0. \end{cases} \quad (1)$$

When the stability disappear, $w(x, y)$ is series of dual sinusoidal function, where n is boundary out vector of Ω , $w(x, y)$ is deflection of z side,

$M_n(x, y)$ is moment:

$$M_n = M_x \cos^2 \alpha + M_y \sin^2 \alpha - 2M_{xy} \sin \alpha \cos \alpha,$$

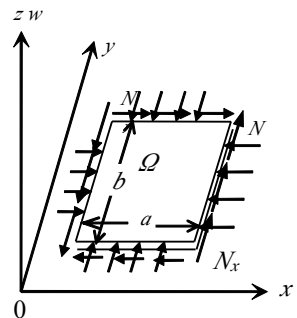


Fig. 1. Simple thin plate

$$M_x = -D\left(\frac{\partial^2 w}{\partial x^2} + \nu \frac{\partial^2 w}{\partial y^2}\right), M_y = -D\left(\frac{\partial^2 w}{\partial y^2} + \nu \frac{\partial^2 w}{\partial x^2}\right),$$

$$M_{xy} = D(1 - \nu) \frac{\partial^2 w}{\partial x \partial y}, \alpha \text{ is angel of the boundary out vector and the positive}$$

of x axis, where $D = \frac{Eh^3}{12(1-\nu^2)}$ s flexural rigidity, E is modulus of elasticity, ν is

Possion ratio, N_x is x aspect pressure, N_y is y aspect pressure, N_{xy} is shear lag around side. When N_x, N_y, N_{xy} work on the neutral plane of thin plate, the potential energy is that when plate bending in equilibration state

$$V = \frac{1}{2} \iint_{\Omega} \{N_x \left(\frac{\partial w}{\partial x}\right)^2 + N_y \left(\frac{\partial w}{\partial y}\right)^2 + 2N_{xy} \frac{\partial w}{\partial x} \frac{\partial w}{\partial y}\} dx dy + \frac{D}{2} \iint_{\Omega} \left\{ \left(\frac{\partial^2 w}{\partial x^2} + \frac{\partial^2 w}{\partial y^2}\right)^2 - 2(1-\nu) \left[\frac{\partial^2 w}{\partial x^2} \frac{\partial^2 w}{\partial y^2} - \left(\frac{\partial^2 w}{\partial x \partial y}\right)^2\right] \right\} dx dy, \tag{2}$$

Since principle of minimum potential energy, equilibrium state displacement with potential energy minimum

$$V = V_{\min} = \text{Minimum value, or } \partial V = 0. \tag{3}$$

3 Distribution for Stability Problem of Elastic Thin Plate

Let cut interval $[0, a]$ of x aspect with equal length:

$$\pi_1 : \dots < x_{\frac{1}{2}} < 0 = x_0 < x_{\frac{1}{2}} < x_1 < \dots < x_{M-\frac{1}{2}} < x_M = a < x_{M+\frac{1}{2}} < \dots; x_j = \frac{j}{2} h_x, h_x = \frac{a}{M}, \tag{4}$$

where the nodes $\dots, x_{\frac{1}{2}}$, and $x_{M+\frac{1}{2}}, \dots$ out of $[0, a]$ are prolong nodes. And let

$$\tilde{\phi}_i(x) = \tilde{\phi}\left(\frac{x-x_{i-1}}{h_x}\right), \tilde{\psi}_i(x) = \tilde{\psi}\left(\frac{x-x_{i-1}}{h_x}\right). \tag{5}$$

Let cut interval $[0, b]$ of y aspect with equal length:

$$\pi_2 : \dots < y_{\frac{1}{2}} < 0 = y_0 < y_{\frac{1}{2}} < y_1 < \dots < y_{N-\frac{1}{2}} < y_N = b < y_{N+\frac{1}{2}} < \dots; y_j = \frac{j}{2} h_y, h_y = \frac{b}{N}, \tag{6}$$

where the nodes $\dots, y_{\frac{1}{2}}$, and $y_{N+\frac{1}{2}}, \dots$ out of $[0, b]$ are prolong nodes. And let

$$\tilde{\phi}_j(y) = \tilde{\phi}\left(\frac{y-y_{j-1}}{h_y}\right), \tilde{\psi}_j(y) = \tilde{\psi}\left(\frac{y-y_{j-1}}{h_y}\right). \tag{7}$$

The following let the deflection $w(x, y)$ of elastic thin plate with transverse load

$$w(x, y) = \sum_{i_1=8}^{2M+8} \sum_{j_1=8}^{2N+8} c_{i_1 j_1} \tilde{\psi}_{i_1}(x) \tilde{\psi}_{j_1}(y) + \sum_{i_2=8}^{2M+8} \sum_{j_2=0}^N d_{i_2 j_2} \tilde{\psi}_{i_2}(x) \tilde{\phi}_{j_2}(y) + \sum_{i_3=0}^M \sum_{j_3=8}^{2N+8} e_{i_3 j_3} \tilde{\phi}_{i_3}(x) \tilde{\psi}_{j_3}(y), \quad (8)$$

The reason of of $i_1, i_2 = 8, 9, \dots, 2M + 8$, $i_3 = 0, 1, \dots, M$, (j_1, j_2, j_3 similarly).

(i) Since $\text{supp } \tilde{\phi} = [0, 9]$, then $\tilde{\phi}(t - (i_3 - 1))$ must be

$i - 1 \leq t \leq 9 + (i - 1)$, when $i = 0$, has $-1 \leq t \leq 8$, when

$i_3 = M$, has $M - 1 \leq t \leq M + 8$. so $i_3 = 0, 1, \dots, M$.

(ii) Since $\text{supp } \tilde{\psi} = [-4, 5]$, then $\tilde{\psi}(t - \frac{i_1 - 1}{2})$ must be

$-4 + \frac{i_1 - 1}{2} \leq t \leq 5 + \frac{i_1 - 1}{2}$, when $i_1 = 8$, has $-0.5 \leq t \leq 8.5$, when $i_1 = 2M + 8$, has

$M - 0.5 \leq t \leq M + 8.5$ (i_2 similarly). So $i_1, i_2 = 8, 9, \dots, 2M + 8$.

Take (8) into (2) do variation, obtain algebra equation sets

$$\begin{aligned} & \iint_{\Omega} \{ \sum_{i_1=8}^{2M+8} \sum_{j_1=8}^{2N+8} c_{i_1 j_1} [D[\tilde{\psi}_{i_1}''(x) \tilde{\psi}_{k_1}''(x) \tilde{\psi}_{j_1}(y) \tilde{\psi}_{l_1}(y) + \tilde{\psi}_{i_1}(x) \tilde{\psi}_{k_1}(x) \tilde{\psi}_{j_1}''(y) \tilde{\psi}_{l_1}''(y) + v(\tilde{\psi}_{i_1}''(x) \tilde{\psi}_{k_1}(x) \tilde{\psi}_{j_1}(y) \tilde{\psi}_{l_1}''(y) \\ & + \tilde{\psi}_{i_1}(x) \tilde{\psi}_{k_1}''(x) \tilde{\psi}_{j_1}''(y) \tilde{\psi}_{l_1}(y) + 2(1-v) \tilde{\psi}_{i_1}'(x) \tilde{\psi}_{k_1}'(x) \tilde{\psi}_{j_1}'(y) \tilde{\psi}_{l_1}'(y) + N_x \tilde{\psi}_{i_1}'(x) \tilde{\psi}_{k_1}'(x) \tilde{\psi}_{j_1}(y) \tilde{\psi}_{l_1}(y) \\ & + N_y \tilde{\psi}_{i_1}(x) \tilde{\psi}_{k_1}(x) \tilde{\psi}_{j_1}'(y) \tilde{\psi}_{l_1}'(y) + N_{xy} [\tilde{\psi}_{i_1}(x) \tilde{\psi}_{k_1}'(x) \tilde{\psi}_{j_1}'(y) \tilde{\psi}_{l_1}(y) + \tilde{\psi}_{i_1}'(x) \tilde{\psi}_{k_1}(x) \tilde{\psi}_{j_1}(y) \tilde{\psi}_{l_1}'(y)]] \\ & + \sum_{i_2=8}^{2M+8} \sum_{j_2=0}^N d_{i_2 j_2} [D[\tilde{\psi}_{i_2}''(x) \tilde{\psi}_{k_2}''(x) \tilde{\phi}_{j_2}(y) \tilde{\psi}_{l_2}(y) + \tilde{\psi}_{i_2}(x) \tilde{\psi}_{k_2}(x) \tilde{\phi}_{j_2}''(y) \tilde{\psi}_{l_2}''(y) + v(\tilde{\psi}_{i_2}''(x) \tilde{\psi}_{k_2}(x) \tilde{\phi}_{j_2}(y) \tilde{\psi}_{l_2}''(y) \\ & + \tilde{\psi}_{i_2}(x) \tilde{\psi}_{k_2}''(x) \tilde{\phi}_{j_2}''(y) \tilde{\psi}_{l_2}(y) + 2(1-v) \tilde{\psi}_{i_2}'(x) \tilde{\psi}_{k_2}'(x) \tilde{\phi}_{j_2}'(y) \tilde{\psi}_{l_2}'(y) + N_x \tilde{\psi}_{i_2}'(x) \tilde{\psi}_{k_2}'(x) \tilde{\phi}_{j_2}(y) \tilde{\psi}_{l_2}(y) \\ & + N_y \tilde{\psi}_{i_2}(x) \tilde{\psi}_{k_2}(x) \tilde{\phi}_{j_2}'(y) \tilde{\psi}_{l_2}'(y) + N_{xy} [\tilde{\psi}_{i_2}(x) \tilde{\psi}_{k_2}'(x) \tilde{\phi}_{j_2}'(y) \tilde{\psi}_{l_2}(y) + \tilde{\psi}_{i_2}'(x) \tilde{\psi}_{k_2}(x) \tilde{\phi}_{j_2}(y) \tilde{\psi}_{l_2}'(y)]] \\ & + \sum_{i_3=0}^M \sum_{j_3=8}^{2N+8} e_{i_3 j_3} [D[\tilde{\phi}_{i_3}''(x) \tilde{\psi}_{k_3}''(x) \tilde{\psi}_{j_3}(y) \tilde{\psi}_{l_3}(y) + \tilde{\phi}_{i_3}(x) \tilde{\psi}_{k_3}(x) \tilde{\psi}_{j_3}''(y) \tilde{\psi}_{l_3}''(y) \\ & + v(\tilde{\phi}_{i_3}''(x) \tilde{\psi}_{k_3}(x) \tilde{\psi}_{j_3}''(y) \tilde{\psi}_{l_3}(y) + \tilde{\phi}_{i_3}(x) \tilde{\psi}_{k_3}''(x) \tilde{\psi}_{j_3}''(y) \tilde{\psi}_{l_3}(y) + 2(1-v) \tilde{\phi}_{i_3}'(x) \tilde{\psi}_{k_3}'(x) \tilde{\psi}_{j_3}'(y) \tilde{\psi}_{l_3}'(y) \\ & + N_x \tilde{\phi}_{i_3}'(x) \tilde{\psi}_{k_3}'(x) \tilde{\psi}_{j_3}(y) \tilde{\psi}_{l_3}(y) + N_y \tilde{\phi}_{i_3}(x) \tilde{\psi}_{k_3}(x) \tilde{\psi}_{j_3}'(y) \tilde{\psi}_{l_3}'(y) + N_{xy} [\tilde{\phi}_{i_3}(x) \tilde{\psi}_{k_3}'(x) \tilde{\psi}_{j_3}'(y) \tilde{\psi}_{l_3}(y) \\ & + \tilde{\phi}_{i_3}'(x) \tilde{\psi}_{k_3}(x) \tilde{\psi}_{j_3}(y) \tilde{\psi}_{l_3}'(y)]] \} dx dy = 0, \quad (k_1 = 8, 9, \dots, 2M + 8; l_1 = 8, 9, \dots, 2N + 8) \end{aligned} \quad (9)$$

$$\begin{aligned} & \iint_{\Omega} \{ \sum_{i_1=8}^{2M+8} \sum_{j_1=8}^{2N+8} c_{i_1 j_1} [D[\tilde{\psi}_{i_1}'(x) \tilde{\psi}_{k_1}'(x) \tilde{\psi}_{j_1}(y) \tilde{\phi}_{l_1}''(y) + \tilde{\psi}_{i_1}(x) \tilde{\psi}_{k_1}(x) \tilde{\psi}_{j_1}''(y) \tilde{\phi}_{l_1}''(y) + v(\tilde{\psi}_{i_1}'(x) \tilde{\psi}_{k_1}(x) \tilde{\psi}_{j_1}(y) \tilde{\phi}_{l_1}''(y) \\ & + \tilde{\psi}_{i_1}(x) \tilde{\psi}_{k_1}'(x) \tilde{\psi}_{j_1}'(y) \tilde{\phi}_{l_1}''(y) + 2(1-v) \tilde{\psi}_{i_1}'(x) \tilde{\psi}_{k_1}'(x) \tilde{\psi}_{j_1}'(y) \tilde{\phi}_{l_1}'(y) + N_x \tilde{\psi}_{i_1}'(x) \tilde{\psi}_{k_1}'(x) \tilde{\psi}_{j_1}(y) \tilde{\phi}_{l_1}'(y) \\ & + N_y \tilde{\psi}_{i_1}(x) \tilde{\psi}_{k_1}(x) \tilde{\psi}_{j_1}'(y) \tilde{\phi}_{l_1}'(y) + N_{xy} [\tilde{\psi}_{i_1}(x) \tilde{\psi}_{k_1}'(x) \tilde{\psi}_{j_1}'(y) \tilde{\phi}_{l_1}'(y) + \tilde{\psi}_{i_1}'(x) \tilde{\psi}_{k_1}(x) \tilde{\psi}_{j_1}(y) \tilde{\phi}_{l_1}'(y)]] \\ & + \sum_{i_2=8}^{2M+8} \sum_{j_2=0}^N d_{i_2 j_2} [D[\tilde{\psi}_{i_2}'(x) \tilde{\psi}_{k_2}'(x) \tilde{\phi}_{j_2}''(y) \tilde{\psi}_{l_2}''(y) + \tilde{\psi}_{i_2}(x) \tilde{\psi}_{k_2}(x) \tilde{\phi}_{j_2}''(y) \tilde{\psi}_{l_2}''(y) + v(\tilde{\psi}_{i_2}'(x) \tilde{\psi}_{k_2}(x) \tilde{\phi}_{j_2}''(y) \tilde{\psi}_{l_2}''(y) \\ & + \tilde{\psi}_{i_2}(x) \tilde{\psi}_{k_2}'(x) \tilde{\phi}_{j_2}''(y) \tilde{\psi}_{l_2}''(y) + 2(1-v) \tilde{\psi}_{i_2}'(x) \tilde{\psi}_{k_2}'(x) \tilde{\phi}_{j_2}'(y) \tilde{\psi}_{l_2}'(y) + N_x \tilde{\psi}_{i_2}'(x) \tilde{\psi}_{k_2}'(x) \tilde{\phi}_{j_2}(y) \tilde{\psi}_{l_2}(y) \\ & + N_y \tilde{\psi}_{i_2}(x) \tilde{\psi}_{k_2}(x) \tilde{\phi}_{j_2}'(y) \tilde{\psi}_{l_2}'(y) + N_{xy} [\tilde{\psi}_{i_2}(x) \tilde{\psi}_{k_2}'(x) \tilde{\phi}_{j_2}'(y) \tilde{\psi}_{l_2}(y) + \tilde{\psi}_{i_2}'(x) \tilde{\psi}_{k_2}(x) \tilde{\phi}_{j_2}(y) \tilde{\psi}_{l_2}'(y)]] \\ & + \sum_{i_3=0}^M \sum_{j_3=8}^{2N+8} e_{i_3 j_3} [D[\tilde{\phi}_{i_3}'(x) \tilde{\psi}_{k_3}'(x) \tilde{\psi}_{j_3}(y) \tilde{\psi}_{l_3}''(y) + \tilde{\phi}_{i_3}(x) \tilde{\psi}_{k_3}(x) \tilde{\psi}_{j_3}''(y) \tilde{\psi}_{l_3}''(y) \\ & + v(\tilde{\phi}_{i_3}'(x) \tilde{\psi}_{k_3}(x) \tilde{\psi}_{j_3}''(y) \tilde{\psi}_{l_3}(y) + \tilde{\phi}_{i_3}(x) \tilde{\psi}_{k_3}'(x) \tilde{\psi}_{j_3}''(y) \tilde{\psi}_{l_3}(y) + 2(1-v) \tilde{\phi}_{i_3}'(x) \tilde{\psi}_{k_3}'(x) \tilde{\psi}_{j_3}'(y) \tilde{\psi}_{l_3}'(y) \\ & + N_x \tilde{\phi}_{i_3}'(x) \tilde{\psi}_{k_3}'(x) \tilde{\psi}_{j_3}(y) \tilde{\psi}_{l_3}(y) + N_y \tilde{\phi}_{i_3}(x) \tilde{\psi}_{k_3}(x) \tilde{\psi}_{j_3}'(y) \tilde{\psi}_{l_3}'(y) + N_{xy} [\tilde{\phi}_{i_3}(x) \tilde{\psi}_{k_3}'(x) \tilde{\psi}_{j_3}'(y) \tilde{\psi}_{l_3}(y) \\ & + \tilde{\phi}_{i_3}'(x) \tilde{\psi}_{k_3}(x) \tilde{\psi}_{j_3}(y) \tilde{\psi}_{l_3}'(y)]] \} dx dy = 0, \quad (k_2 = 8, 9, \dots, 2M + 8; l_2 = 8, 9, \dots, 2N + 8) \end{aligned}$$

$$\begin{aligned}
 & + \sum_{i_2=8}^{2M+8} \sum_{j_2=0}^N d'_{i_2 j_2} [D[\psi_{i_2}^{\phi_2}(x)\psi_{k_2}^{\phi_2}(x)\phi_{i_2}^{\phi_2}(y)+\psi_{i_2}^{\phi_2}(x)\psi_{k_2}^{\phi_2}(x)\phi_{i_2}^{\phi_2}(y)+\nu(\psi_{i_2}^{\phi_2}(x)\psi_{k_2}^{\phi_2}(x)\phi_{i_2}^{\phi_2}(y)\phi_{i_2}^{\phi_2}(y) \\
 & +\psi_{i_2}^{\phi_2}(x)\psi_{k_2}^{\phi_2}(x)\phi_{i_2}^{\phi_2}(y)\phi_{i_2}^{\phi_2}(y)]+2(1-\nu)\psi_{i_2}^{\phi_2}(x)\psi_{k_2}^{\phi_2}(x)\phi_{i_2}^{\phi_2}(y)\phi_{i_2}^{\phi_2}(y)]+N_x\psi_{i_2}^{\phi_2}(x)\psi_{k_2}^{\phi_2}(x)\phi_{i_2}^{\phi_2}(y)\phi_{i_2}^{\phi_2}(y) \\
 & +N_y\psi_{i_2}^{\phi_2}(x)\psi_{k_2}^{\phi_2}(x)\phi_{i_2}^{\phi_2}(y)\phi_{i_2}^{\phi_2}(y)+N_{xy}[\psi_{i_2}^{\phi_2}(x)\psi_{k_2}^{\phi_2}(x)\phi_{i_2}^{\phi_2}(y)\phi_{i_2}^{\phi_2}(y)+\psi_{i_2}^{\phi_2}(x)\psi_{k_2}^{\phi_2}(x)\phi_{i_2}^{\phi_2}(y)\phi_{i_2}^{\phi_2}(y)] \\
 & + \sum_{i_3=0}^M \sum_{j_3=8}^{2N+8} e_{i_3 j_3} [D[\phi_{i_3}^{\phi_3}(x)\psi_{k_3}^{\phi_3}(x)\psi_{l_3}^{\phi_3}(y)\phi_{i_3}^{\phi_3}(y)+\phi_{i_3}^{\phi_3}(x)\psi_{k_3}^{\phi_3}(x)\psi_{l_3}^{\phi_3}(y)\phi_{i_3}^{\phi_3}(y) \\
 & +\nu(\phi_{i_3}^{\phi_3}(x)\psi_{k_3}^{\phi_3}(x)\psi_{l_3}^{\phi_3}(y)\phi_{i_3}^{\phi_3}(y)+\phi_{i_3}^{\phi_3}(x)\psi_{k_3}^{\phi_3}(x)\psi_{l_3}^{\phi_3}(y)\phi_{i_3}^{\phi_3}(y)]+2(1-\nu)\phi_{i_3}^{\phi_3}(x)\psi_{k_3}^{\phi_3}(x)\psi_{l_3}^{\phi_3}(y)\phi_{i_3}^{\phi_3}(y) \\
 & +N_x\phi_{i_3}^{\phi_3}(x)\psi_{k_3}^{\phi_3}(x)\psi_{l_3}^{\phi_3}(y)\phi_{i_3}^{\phi_3}(y)+N_y\phi_{i_3}^{\phi_3}(x)\psi_{k_3}^{\phi_3}(x)\psi_{l_3}^{\phi_3}(y)\phi_{i_3}^{\phi_3}(y)+N_{xy}[\phi_{i_3}^{\phi_3}(x)\psi_{k_3}^{\phi_3}(x)\psi_{l_3}^{\phi_3}(y)\phi_{i_3}^{\phi_3}(y) \\
 & +\phi_{i_3}^{\phi_3}(x)\psi_{k_3}^{\phi_3}(x)\psi_{l_3}^{\phi_3}(y)\phi_{i_3}^{\phi_3}(y)]]dx dy=0 \quad (k_2=8,9,L,2M+8; l_2=8,9,L,2N+8)
 \end{aligned}
 \tag{10}$$

$$\begin{aligned}
 & \iint_{\Omega} \{ \sum_{i_4=8}^{2M+8} \sum_{j_4=8}^{2N+8} c_{i_4 j_4} [D[\tilde{\psi}'_i(x)\tilde{\phi}'_{k_3}(x)\tilde{\psi}'_j(y)\tilde{\psi}'_l(y)+\tilde{\psi}'_i(x)\tilde{\phi}'_{k_3}(x)\tilde{\psi}'_j(y)\tilde{\psi}'_l(y)+\nu(\tilde{\psi}'_i(x)\tilde{\phi}'_{k_3}(x)\tilde{\psi}'_j(y)\tilde{\psi}'_l(y) \\
 & +\tilde{\psi}'_i(x)\tilde{\phi}'_{k_3}(x)\tilde{\psi}'_j(y)\tilde{\psi}'_l(y)]+2(1-\nu)\tilde{\psi}'_i(x)\tilde{\phi}'_{k_3}(x)\tilde{\psi}'_j(y)\tilde{\psi}'_l(y)]+N_x\tilde{\psi}'_i(x)\tilde{\phi}'_{k_3}(x)\tilde{\psi}'_j(y)\tilde{\psi}'_l(y) \\
 & +N_y\tilde{\psi}'_i(x)\tilde{\phi}'_{k_3}(x)\tilde{\psi}'_j(y)\tilde{\psi}'_l(y)+N_{xy}[\tilde{\psi}'_i(x)\tilde{\phi}'_{k_3}(x)\tilde{\psi}'_j(y)\tilde{\psi}'_l(y)+\tilde{\psi}'_i(x)\tilde{\phi}'_{k_3}(x)\tilde{\psi}'_j(y)\tilde{\psi}'_l(y)] \\
 & + \sum_{i_2=8}^{2M+8} \sum_{j_2=0}^N d_{i_2 j_2} [D[\tilde{\psi}'_i(x)\tilde{\phi}'_{k_3}(x)\tilde{\psi}'_j(y)\tilde{\psi}'_l(y)+\tilde{\psi}'_i(x)\tilde{\phi}'_{k_3}(x)\tilde{\psi}'_j(y)\tilde{\psi}'_l(y)+\nu(\tilde{\psi}'_i(x)\tilde{\phi}'_{k_3}(x)\tilde{\psi}'_j(y)\tilde{\psi}'_l(y) \\
 & +\tilde{\psi}'_i(x)\tilde{\phi}'_{k_3}(x)\tilde{\psi}'_j(y)\tilde{\psi}'_l(y)]+2(1-\nu)\tilde{\psi}'_i(x)\tilde{\phi}'_{k_3}(x)\tilde{\psi}'_j(y)\tilde{\psi}'_l(y)]+N_x\tilde{\psi}'_i(x)\tilde{\phi}'_{k_3}(x)\tilde{\psi}'_j(y)\tilde{\psi}'_l(y) \\
 & +N_y\tilde{\psi}'_i(x)\tilde{\phi}'_{k_3}(x)\tilde{\psi}'_j(y)\tilde{\psi}'_l(y)+N_{xy}[\tilde{\psi}'_i(x)\tilde{\phi}'_{k_3}(x)\tilde{\psi}'_j(y)\tilde{\psi}'_l(y)+\tilde{\psi}'_i(x)\tilde{\phi}'_{k_3}(x)\tilde{\psi}'_j(y)\tilde{\psi}'_l(y)] \\
 & + \sum_{i_3=0}^M \sum_{j_3=8}^{2N+8} e_{i_3 j_3} [D[\tilde{\phi}'_i(x)\tilde{\phi}'_{k_3}(x)\tilde{\psi}'_j(y)\tilde{\psi}'_l(y)+\tilde{\phi}'_i(x)\tilde{\phi}'_{k_3}(x)\tilde{\psi}'_j(y)\tilde{\psi}'_l(y) \\
 & +\nu(\tilde{\phi}'_i(x)\tilde{\phi}'_{k_3}(x)\tilde{\psi}'_j(y)\tilde{\psi}'_l(y)+\tilde{\phi}'_i(x)\tilde{\phi}'_{k_3}(x)\tilde{\psi}'_j(y)\tilde{\psi}'_l(y)]+2(1-\nu)\tilde{\phi}'_i(x)\tilde{\phi}'_{k_3}(x)\tilde{\psi}'_j(y)\tilde{\psi}'_l(y) \\
 & +N_x\tilde{\phi}'_i(x)\tilde{\phi}'_{k_3}(x)\tilde{\psi}'_j(y)\tilde{\psi}'_l(y)+N_y\tilde{\phi}'_i(x)\tilde{\phi}'_{k_3}(x)\tilde{\psi}'_j(y)\tilde{\psi}'_l(y)+N_{xy}[\tilde{\phi}'_i(x)\tilde{\phi}'_{k_3}(x)\tilde{\psi}'_j(y)\tilde{\psi}'_l(y) \\
 & +\tilde{\phi}'_i(x)\tilde{\phi}'_{k_3}(x)\tilde{\psi}'_j(y)\tilde{\psi}'_l(y)]]dx dy=0 \quad (k_3=8,9,\dots,2M+8; l_3=8,9,\dots,2N+8)
 \end{aligned}
 \tag{11}$$

Join (9) to (10) can get a inhomogeneous system which have $(2M+1)(2N+1)+(2M+1)(N+1)+(M+1)(2N+1)=8MN+5(M+N)+3$ unknown quantities. Taking in matrix sign

$$\begin{aligned}
 A_x & = \left(\int_0^a \tilde{\psi}_i''(x)\tilde{\psi}_j''(x)dx \right), \quad B_x = \left(\int_0^a \tilde{\psi}_i(x)\tilde{\psi}_j''(x)dx \right), \\
 C_x & = \left(\int_0^a \tilde{\psi}_i'(x)\tilde{\psi}_j'(x)dx \right), \\
 D_x & = \left(\int_0^a \tilde{\psi}_i(x)\tilde{\psi}_j(x)dx \right), \quad O_x = \left(\int_0^a \tilde{\psi}_i(x)\tilde{\psi}_j'(x)dx \right), \text{ index} \\
 & \quad i, j = 8, 9, \dots, 2M + 8.
 \end{aligned}
 \tag{12}$$

$$\begin{aligned}
 E_x &= \left(\int_0^a \tilde{\phi}_i''(x)\tilde{\psi}_j''(x)dx\right), & F_x &= \left(\int_0^a \tilde{\phi}_i(x)\tilde{\psi}_j''(x)dx\right), \\
 G_x &= \left(\int_0^a \tilde{\phi}_i''(x)\tilde{\psi}_j(x)dx\right), \\
 H_x &= \left(\int_0^a \tilde{\phi}_i'(x)\tilde{\psi}_j'(x)dx\right), & I_x &= \left(\int_0^a \tilde{\phi}_i(x)\tilde{\psi}_j(x)dx\right), \\
 P_x &= \left(\int_0^a \tilde{\phi}_i'(x)\tilde{\psi}_j(x)dx\right), & & (13) \\
 P_{2x} &= \left(\int_0^a \tilde{\phi}_i(x)\tilde{\psi}_j'(x)dx\right), \text{ index } i = 0, 1, \dots, M; j = 8, 9, \dots, 2M + 8. \\
 J_x &= \left(\int_0^a \tilde{\phi}_i''(x)\tilde{\phi}_j''(x)dx\right), & K_x &= \left(\int_0^a \tilde{\phi}_i(x)\tilde{\phi}_j''(x)dx\right), \\
 L_x &= \left(\int_0^a \tilde{\phi}_i'(x)\tilde{\phi}_j'(x)dx\right), \\
 M_x &= \left(\int_0^a \tilde{\phi}_i(x)\tilde{\phi}_j(x)dx\right), & Q_x &= \left(\int_0^a \tilde{\phi}_i'(x)\tilde{\phi}_j(x)dx\right), \text{ index} \\
 & & & i, j = 0, 1, \dots, M. & (14)
 \end{aligned}$$

$A_y, B_y, C_y, D_y, E_y, F_y, G_y, H_y, I_y, J_y, K_y, L_y, M_y, O_y, P_y, Q_y$ is matrixes sign which are got from replacing independent variable x with y , a with b , M with N in (12) ~ (14). Again let:

$$r_{11} = (\bar{c}_{i_1 8}, \bar{c}_{i_1 9}, \bar{c}_{i_1 10}, \dots, \bar{c}_{i_1, 2N+8})^T, \bar{c}_{i_1 l_1} = (c_{8l_1}, c_{9l_1}, c_{10l_1}, \dots, c_{2M+8, l_1}), \quad (15)$$

$$r_{12} = (\bar{d}_{i_2 0}, \bar{d}_{i_2 1}, \bar{d}_{i_2 2}, \dots, \bar{d}_{i_2, N})^T, \bar{d}_{i_2 l_2} = (d_{8l_2}, d_{9l_2}, d_{10l_2}, \dots, d_{2M+8, l_2}), \quad (16)$$

$$r_{13} = (\bar{e}_{i_3 8}, \bar{e}_{i_3 9}, \bar{e}_{i_3 10}, \dots, \bar{e}_{i_3, 2N+8})^T, \bar{e}_{i_3 l_3} = (e_{0l_3}, e_{1l_3}, e_{2l_3}, \dots, e_{M, l_3}). \quad (17)$$

After have the front matrix sign, equation (9)~(11) can be expressed simply as:

$$\begin{cases}
 U_{11}r_{11} + U_{12}r_{12} + U_{13}r_{13} = 0 \\
 U_{21}r_{11} + U_{22}r_{12} + U_{23}r_{13} = 0, \\
 U_{31}r_{11} + U_{32}r_{12} + U_{33}r_{13} = 0
 \end{cases} \quad (18)$$

Which

$$\begin{aligned}
 U_{11} &= D[D_y \otimes A_x + A_y \otimes D_x + \nu(B_y \otimes B_x^T + B_y^T \otimes B_x) + 2(1-\nu)C_y \otimes C_x] + N_x D_y \otimes C_x \\
 &+ N_y C_y \otimes D_x + N_{xy}(O_y^T \otimes O_x + O_y \otimes O_x^T), & (19)
 \end{aligned}$$

$$\begin{aligned}
 U_{21} &= D[U_y \otimes A_x + E_y \otimes D_x + \nu(F_y \otimes B_x^T + G_y \otimes B_x) + 2(1-\nu)H_y \otimes C_x] + N_x I_y \otimes C_x \\
 &+ N_y H_y \otimes D_x + N_{xy}(P_{1y} \otimes O_x + P_{2y} \otimes O_y^T), & (20)
 \end{aligned}$$

$$U_{31} = D[D_y \otimes E_x + A_y \otimes I_x + u(B_y \otimes G_x + B_y^T \otimes F_x) + 2(1-u)C_y \otimes H_x] + N_x D_y \otimes H_x + N_y C_y \otimes I_x + N_{xy}(O_y^T \otimes P_{2x} + O_y \otimes P_{1x}), \tag{21}$$

$$U_{12} = D[I_y^T \otimes A_x + E_y^T \otimes D_x + u(F_y \otimes B_x^T + G_y \otimes B_x) + 2(1-u)H_y^T \otimes C_x] + N_x I_y \otimes C_x + N_y H_y \otimes D_x + N_{xy}(P_{2y}^T \otimes O_x + P_{1y}^T \otimes O_x^T), \tag{22}$$

$$U_{22} = D[M_y \otimes A_x + J_y \otimes D_x + u(K_y \otimes B_x^T + K_y^T \otimes B_x) + 2(1-u)L_y \otimes C_x] + N_x M_y \otimes C_x + N_y L_y \otimes D_x + N_{xy}(Q_y \otimes O_x + Q_y^T \otimes O_x^T), \tag{23}$$

$$U_{32} = D[I_y^T \otimes E_x + E_y^T \otimes I_x + u(F_y \otimes G_x + G_y \otimes F_x) + 2(1-u)H_y^T \otimes H_x] + N_x I_y \otimes H_x + N_y H_y \otimes I_x + N_{xy}(P_{2y}^T \otimes P_{2x} + I_y^T \otimes H_x), \tag{24}$$

$$U_{13} = D[D_y \otimes E_x^T + A_y \otimes I_x^T + u(B_y \otimes G_x + B_y^T \otimes F_x) + 2(1-u)C_y \otimes H_x^T] + N_x D_y \otimes H_x + N_y C_y \otimes I_x^T + N_{xy}(O_y^T \otimes P_{2x}^T + O_y \otimes P_{2x}^T), \tag{25}$$

$$U_{23} = D[I_y \otimes E_x^T + E_y \otimes I_x^T + u(G_y \otimes F_x + F_y \otimes G_x) + 2(1-u)H_y \otimes H_x^T] + N_x I_y \otimes H_x + N_y H_y \otimes I_x^T + N_{xy}(P_{1y}^T \otimes P_{1x}^T + P_{2y} \otimes P_{2x}^T), \tag{26}$$

$$U_{33} = D[D_y \otimes J_x + A_y \otimes M_x + u(B_y \otimes K_x^T + B_y^T \otimes K_x) + 2(1-u)C_y \otimes L_x] + N_x D_y \otimes L_x + N_y C_y \otimes M_x + N_{xy}(O_y^T \otimes Q_x^T + O_y \otimes Q_x). \tag{27}$$

Then equation sets (9)~(11) can be remark $UX = 0$. (28)

Sign $A \otimes B$ means the Kronecker product of matrix A and B $A \otimes B = (a_{ij}B)$. (29)

Since $\phi(x) = \tilde{\phi}(x)$ and $\psi(x) = \tilde{\psi}(x)$, they are all polynomial function with correspond supported set and have analytic expression, which can be found in [4], so A_x, \dots, Q_x can be obtained.

For the matrixes A_y, \dots, Q_y , since their form are same as A_x, \dots, Q_x , only replacing h_x with h_y , M with N in A_x, \dots, Q_x . then obtain the non-zero solution by solving the set of equation $UX = 0$, let $|U| = 0$, can obtain the critical force N_x, N_{xy}, N_y .

References

1. Shi, Z.: Spline finite element. *Mathematic Numerical Sinica* (1), 50–72 (1979)
2. Strang, G., Fix, G.J.: *An analysis of the element method*. Academic Press, New York (1973)
3. Zhang, H., Wang, M.: *The Mathematic Theory of Finite Element*. Science Press, Beijing (1991)
4. Gao, Z.: Approximated two dimensional Daubechies wavelets. In: *MIME 2011* (2011)

Design of Low Cost Human ADL Signal Acquire System Based on Wireless Wearable MEMS Sensor

Ying Sun

Information Engineering Institute Shenyang University
Shenyang 110044, China
sunying_1215@163.com

Abstract. The paper presents a design method of human body's ADL signal data acquisition system based on MEMS and LabVIEW for elder person. The system consists of three parts, wearable sensors detection system based on MEMS, wireless data acquisition system based on USB bus and PC software. PC software is developed by LabVIEW with several functions, such as USB data acquisition, data analysis and setting sensor parameters. Experimental results confirm the effectiveness of this design method.

Keywords: MEMS, ADL signal, Wearable sensors.

1 Introduction

Population aging has become a global hot topic. With the advances in medical technology, aging population is increasing every year in proportion of the total population. Moreover, it make the problem of elderly care highlighted for declining birth rate the population, reducing the number of young people, increasing numbers of elderly[1]. With human becoming more and more elder, some researcher introduced the concept of ADL(activity of daily living) is to evaluate the activities of daily living self-care ability of elderly people [2-3]. This paper presents a human body ADL acquisition method, which combines MEMS human posture sensors with RF wireless data transmission mode. It is a practical way to acquire human posture data, which is not only can real-time detected and record the daily activities of the elderly physical behavior, accurately, effectively and safely, but also can understand the trend for the Aged and supply important patients' body function data to rehabilitation doctors. It will educe the burden of doctors or family.

According to ADL signal acquisition problem for elderly, a human body ADL data acquisition method based on MEMS and the LabVIEW is present. Wireless communication module, NRF24L01 with 2.4G bandwidth is used. Wireless wearable human body posture detect system based on MEMS chips and data acquisition system based USB interface and LabVIEW are designed. With the comparison of the traditional vision-based human body gesture recognition system[4,5], it does not need to change the indoor environment, free from light and other environmental factors and has low cost, highly practical features.

2 Human ADL Signal Acquisition System Design

Figure 1 shows the body ADL signal acquisition hardware system diagram. The system consists of three parts respectively, wearable sensors, wireless data acquisition system with USB interface, software on PC. Wearable sensor is fixed on body position shown as Figure 1, which composed of the MEMS sensor, microprocessor, wireless data transceiver modules. MEMS device is MMA7260QT triaxial accelerometer. C8051F310 is used as microcontroller. Wireless data transceiver modules based on nRF24L01 are used. When system start working, wearable fix on human body, MEMS device MMA7260QT detect human current posture signal. Microprocessor C8051F310 converse analogy signal to digital and control RF module for transmitting body posture signals to acquisition system. The acquisition system with USB interface, which used C8051F340 as Micro-control chip transmits received human posture data to host PC. Pc acquisition software is programmed under LABVIEW, which call DLL file to receive and process data.

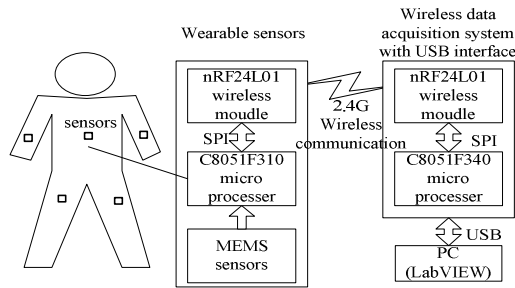


Fig. 1. Body ADL signal acquisition hardware system diagram

3 Design of Wearable Human Posture Detect System

MEMS device detection principle of the human body posture. MMA7260QT is Freescale's three-axis acceleration sensors, which has several features such as low cost, low power consumption, quality, small size, etc, to meet the requirements of the task requirements. It uses its own signal conditioning with a single low-pass filter and temperature compensation function, which improve the reliability of the sensor itself.

Upper body angle will change when human body do daily movement. For example, in the process of walking around the upper body shaking will occur, and lean forward. Thigh's angle will change, either. If three-axis acceleration sensors MMA7260QT is fixed on human body, the sensor's output will follow the human motion, which three-axis direction will be detected. So human body posture(such as walking, standing, lying down, etc.) change will be detected. Detection principle of the human body posture is shown as Fig 2.

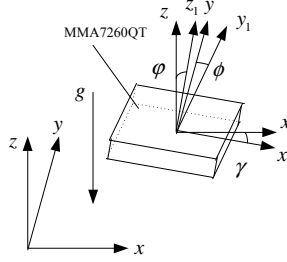


Fig. 2. Detection principle of the human body posture

Global coordinate system is x, y, z . Coordinates of sensor MMA7260QT is x_1, y_1, z_1 . Angle between the direction x is γ . Angle between the direction y is ϕ . Angle between the direction z is ϕ . Gravity in space is g . The sensor output voltage is

$$\begin{cases} V_x = V_0 + V_g \sin(\gamma) \\ V_y = V_0 + V_g \sin(\phi) \\ V_z = V_0 + V_g \sin(\phi) \end{cases} \quad (1)$$

Where, V_x, V_y, V_z are MMA7260QT output x, y, z axis voltage respectively. Sensor sensitivity is selected as 1.5g, and V_0 is 1.65V, V_g is 800mV. V_x, V_y, V_z change with γ, ϕ, ϕ variation.

Design of hardware circuit. Wearable sensor hardware consist of battery DC / DC conversion, wireless communication interface, MMA7260QT sensor A / D conversion, filtering circuit, the reference voltage source circuit. Output power waveform of MMA7260QT have noise. In order to reduce the burden of microcontroller operation, the system uses with the eighth order Butterworth low-pass filter MAX7480 as a filter unit. Respectively, the x, y, z voltage signals is processed by Low-pass filtering. The cut-off frequency f_c from frequency f_{clk} which set by microprocessor clock PCA, which is calculated as

$$f_c = \frac{f_{clk}}{100} \quad (2)$$

wireless communication module is used for 2.4G bandwidth nRF24L01 high-speed transceiver function module. when module work in sent state, it is for transmit human posture data, while in receive state, it is for parameters (such as low-pass cutoff frequency, etc.) setting from host computer.

A acquirement system between USB interface and host computer is designed. The function is send data via USB to the PC for LabVIEW acquisition and processing. Microprocessors use C8051F340. In order to prevent poor or no grounding protection damaging the USB bus interface during hot swap, sn75240 is used as USB protection devices.

4 Software Design

There are three parts software that are wearable sensor signal acquisition and transmission, wireless data acquisition base on USB interface, LabVIEW data acquisition and processing software. As it is shown in Fig 3. It need initialize the microcontroller and wireless modules after boot, set up wireless communication module to receive mode, and test the wireless communication whether successful. After receive start command and it will start AD conversion to collect human body posture data. After conversion, it will set communication module to send mode and send collected data. If it has finished, module will be set receive mode. transmit frequency is 100 milliseconds.

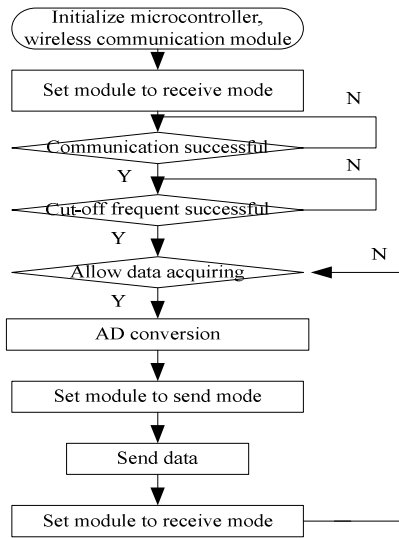


Fig. 3. Flow chart of wearable sensor signal acquisition and transmission software

After Plugged in the USB cable board and initialize microcontroller, wireless communication module and the microcontroller internal USB interface, system will wait for whether USB is successful communication. Then, it will set communication module to sent mode and send test data. If the communication is successful, wait for the host computer to set the cutoff frequency. Then, wait allow acquisition command. If the host computer with LabVIEW program allows attitude acquisition, it will set wireless communication module to receive mode after sent allow acquisition command. Moreover, software wait for data reception, and determine whether there is stop command. After receiving the host computer to stop acquisition command, system sends the command to set the communication module to send mode, while waits for the host computer to allow acquisition command.

PC software includes following parts, USB communication driver, sensor parameters, the next bit machine control, virtual instrument display. Its functions are data collection, analysis, cut-off frequency or other parameters settings. PC software is programmed in LabVIEW, which call SiUSBXp.dll to control USB interface.

5 Experiment and Analysis

Figure 4 is experimental waveforms of human body signals when walking. Wearable sensors fixed on chest, position shown in Figure 1, for the detection of changes in upper body posture. The red curve in Figure 4 is the upper body during walking human horizontal acceleration curve, defined as the x direction curve. Black one is vertical curve, defined as y direction curve. Green curve is defined as the z direction curve. Experiment shows this design method can capture real-time signal the body to walk signal, and verify he effectiveness of this acquisition method.

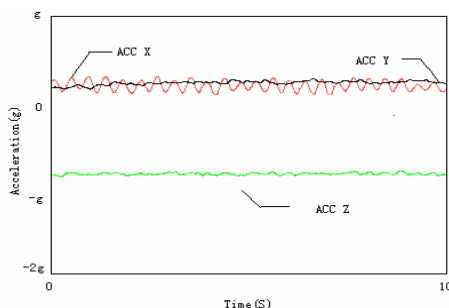


Fig. 4. Experimental waveforms of signals of human walking

6 Conclusions

In this paper, a method which complete human posture signal detection and real-time wireless data collection based on LabVIEW is present. Hardware circuits have small size, light weight, low power consumption, high integration, cost performance features. The software design ideas are clear and structured. Experiments verify he effectiveness of this method. Using this method of detection signals human ADL has broad application prospects.

References

1. Lei, J.-y.: Study on Establishment of the Service System for the Old in An Aged Society. *Journal of Xiangfan University* 30(9), 37–41 (2009)
2. Lee, Y., Kim, J., Son, M.: Implementation of Accelerometer Sensor Module and Fall Detection Monitoring System based on Wireless Sensor Network. In: *Engineering in Medicine and Biology Society EMBS 2007, France*, pp. 2315–2318 (2008)
3. Hua, q.: *Elderly nursing*, pp. 28–29. People Health Press, Beijing (2006)
4. Wang, R., Huang, C.: Landmark image processing for human motion analysis system based on video camera. *Journal of tsinghua university* 39(3), 75–77 (1999)
5. Xu, G.f., Li, B.: Measurement of motion parameters based on the binocular vision model. *Infrared and Laser Engineering* 32(3), 200–202 (2003)

A Fast Plotting Method for 3D Directional Marker

Hongqian Chen, Yi Chen, Yuehong Sun, and Li Liu

School of Computer and Information Engineering, Beijing Technology and Business University, Beijing, 100048, China
chenhongqian1@163.com

Abstract. To improve the plotting performance for the 3D directional marker in virtual environment, propose a fast plotting method based on gradient field. The method can plot the 3D directional terrain-matching marker conveniently on the 3D terrain. The terrain height data are transformed into the gradient field. It obtains the maximum affection region and locates the key position to matching the terrain. The final shape of the markers can be obtained by interpolating these key positions via the Catmull-Rom algorithm. The experimental results denoted that the method can plot the 3D directional marker quickly. The realistic effect can be expressed by the method proposed in the paper.

Keywords: Directional Marker, Gradient Methods, Plotting, Terrain-matching, Catmull.

1 Introduction

With the development of the virtual reality technology, 3D virtual environment becomes one of the most important approach for the information and interaction. 3D virtual environment can provide the intuitional exhibit and the dynamic interaction. The directional marker is the common symbol in the GIS (Geographic Information System). The performance of plotting the marker is the important factor for the efficiency of the simulation system.

Youngseok [1] present the plotting method of the 3D military symbol. The methods express the destination with the composite model and the symbolic cube. Color is adopted to distinguish the friendly or enemy force. The method can achieve unambiguous express effect and the nice visual effect. But the method use too much composite model and lead to low performance.

Dan [2] marked the operational range and plotted the symbols using billboard. Yang[3] mapped the military symbol into the image texture of the billboard. Wang [4] stated the COM component-based technology to accomplish the marking and plotting system. The method renders directly the military symbols using billboard in virtual environment. The method can obtain fast marking, but the authority of symbols is inadequate and unobvious.

The terrain matching is the key technology to improve the authority of the directional markers. Rui [5] and Wang [6] matched the road onto the terrain and achieved the terrain matching. Xu [7] presented three integrate method for combining

GIS and military symbols. These methods can match the static markers and the terrain.

The paper proposes a fast plotting method for 3D directional markers. The method extracts the terrain elevation from the DEM data file. And the elevation data are converted into the gradient field. The key points with the maximum influence factor to the appearance of the terrain are extracted by the processing in gradient field. The final directional markers are achieved by interpolating the key points. The marker can match the appearance of its covered terrain. The method can achieve processing and plotting real time for the dynamic directional markers.

2 Terrain-Matching for 3D Directional Marker

The paper proposes a plotting method for 3D directional markers. The method achieve terrain-matching feature for 3D markers by processing in gradient field. The key points influencing the appearance of the terrain are extracted by processing and simplifying in gradient field. The directional markers are generated via interpolating the key points using spine function. The method can achieve the quickly plotting dynamic markers and matching the feature of the terrain.

2.1 Extracting the Key Points for Terrain-Matching

The directional marker covers one region and matches the appearance of the terrain in the region. The region is expressed in its head position, tail position and width. The head and tail position can be given by the simulation data during simulating.

The elevation data in the covered region are extracted from the DEM data. The terrain elevation data are merged horizontally according to the direction of the marker. The merging procedure is accomplished via obtaining the highest elevation in the perpendicular. The procedure can be expressed by Equ. 1.

$$H_p = \max\{H_x \mid x \in L_{p\perp}\} \quad (1)$$

In Equ.1, $L_{p\perp}$ is the perpendicular of the direction of the marker. H_x is the elevation of the point x in the terrain. H_p is the merging elevation of the point P after processing.

The gradient value can express the changing level of the region around one position. The bigger the absolute gradient value, the more the terrain change in the region. The method converts the original merging elevation data into the gradient field. The key points located the position where has the maximum absolute value in gradient field. The converting procedure can be expressed as Equ.2. ∇_p is the gradient vector of the position P in Equ.2.

$$\nabla_p = \left(\frac{\partial}{\partial x}, \frac{\partial}{\partial y} \right) \quad (2)$$

The method converts the elevation data of the terrain into the gradient vectors. The contribution for the specified direction of the position P can be obtained by the dot product between the direction and its gradient vector. The function of the contribution can be shown as Equ. 3.

$$Cont_p = \overrightarrow{BA} \bullet \nabla_p \tag{3}$$

The key points for the terrain located in the positions with the maximum contribution for the specified direction. The positions with the maximum contribution can be selected by the Equ. 4,

$$Ext_p = \frac{\partial Cont_p}{\partial x} = 0 \tag{4}$$

The key points with the feature $Ext_p = 0$ can be selected by their gradient contribution. They can be shown as Fig.1.

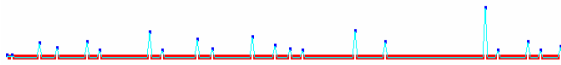


Fig. 1. The key points with the maximum influence for the terrain

2.2 Simplifying the Key Points According to Contribution

The key points can express the feature of the covered terrain. But there are too many points to plotting directly the direction marker. We should simplify them according to its contribution. The simplify procedure can be described as the following steps:

Step 1: Specify the final number of the key points. Set the current setting difference value for decreasing. The initial difference value is 1.

Step 2: Traversal all the key points and get their difference value. The difference value of one key point can be got by the distance to its adjacent key points.

Step 3: Delete the key point when its difference value is smaller than the setting decreasing value. The difference value of the deleted point is added onto its closest key point. The number of key points decreases by 1.

Step 4: Verify the current number of key points. Goto step 2 when it is larger than the specified final number, while finish the procedure when it is smaller

The comparing between the original terrain and the matching curve by connecting the simplified key points is shown in Fig.2.

In Fig.2, the broken line A is the matching curve produced by connecting line of the simplified key points. The curve B is the original terrain. The point line C is the key points with their difference values. The simplified key points can express the feature of its covered terrain in the least number of control points according to Fig.2.

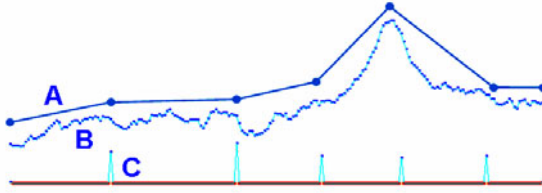


Fig. 2. The comparing between the original terrain and the matching curve.

2.3 Interpolating the Key Points for Smoothing

The final plotting of the 3D direction marker needs the smooth control curve. The Catmull-Rom algorithm is adopted to interpolate the key point and to obtain the smooth curve. The interpolating algorithm arranges each four adjacent points into one group. It can be described as Equ.5.

$$P_t = f_0(t)P_0 + f_1(t)P_1 + f_2(t)P_2 + f_3(t)P_3 \tag{5}$$

In Equ.5, P_t is the interpolating point, $P_0P_1P_2P_3$ is the four adjacent points, and $f_0f_1f_2f_3$ are the interpolating functions, which can be described as Equ.6.

$$\begin{aligned} f_0(t) &= 1/2 * (-t^3 + 2t^2 - t) & f_1(t) &= 1/2 * (3t^3 - 5t^2 + 2) \\ f_2(t) &= 1/2 * (-3t^3 + 4t^2 + t) & f_3(t) &= 1/2 * (t^3 - t^2) \end{aligned} \tag{6}$$

The final directional marker can be obtained by expended horizontally the interpolating curve. The final model is rendered by triangle-strip mode. The marker needs raising a little altitude to prevent the collision between the marker and the terrain.

3 Experimental Result and Analysis

The method can be accomplished by the following step:

- A) Get the DEM data of the terrain and obtain the elevation of the covered region.
- B) Convert the elevation data into the gradient field and extract the key points with the maximum contribution.
- C) Simplify the key points and interpolate the simplified key points with Catmull-Rom algorithm.
- D) Plot the final directional marker model and raise its altitude.

We has accomplished the plotting method in a simulation system. The experimental environment includes Intel Core2 3.0CPU, 1GRAM, WinXP Sp2 OS. The plotting result is shown as Fig.3. The span of the directional marker in Fig.5 is 300 sampling points, 9KM for 30M of each space. The covered width of the marker is 50 sampling points. The result illustrates the method can plot the directional marker with little control points. The plotting algorithm can finish at the time cost with 8ms according to our experiments. It can meet the requirement of simulating in real time.

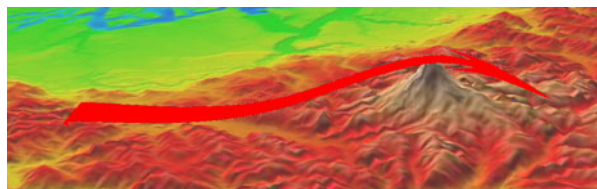


Fig. 3. The plotting result of the terrain-matching directional marker

4 Conclusions

To improve the plotting performance for the 3D directional marker in virtual environment, propose a fast plotting method based on gradient field. The method can plot the 3D directional terrain-matching marker conveniently on the 3D terrain. The contribution of the paper can be concluded as follows: A) Locate the key points quickly via transforming the terrain height data into the gradient field. B) Simplify the sequence of the key points to reduce the complexity of the algorithm. C) Interpolate the key points to obtain the smooth control curve of the directional marker. The experimental results denoted that the method can plot the 3D directional marker quickly.

The future work is aim to resolve the distributed cooperation for plotting the large scale of markers.

Acknowledgement. This work was supported by the Foundation for Youth Teacher and the Fund for the Beijing Key Construction Subjects. We are grateful to our colleagues for their help of proofreading this paper.

References

1. Kim, Y., Kesavadas, T.: Automated Dynamic Symbolology for Visualization of High Level Fusion. Technical Report of State University of New York, Buffalo, USA, pp. 1196–1208 (2004)
2. Hagens, D., Montgomery, J., Moor, C.: Developing custom 3D visualization applications for defense using ARCGIS. In: Proceedings of the 2005 Developer Summit, San Diego, CA, USA, pp. 814–835 (2005)
3. Yang, Q.: Research on Technique of 3D Unit Symbol Building and Situation Protracting. Dissertation of Master in National Defense University, Hunan, P.R.China (2006)
4. Wang, J., Liu, J.-z.: Design and Realization of Military Plotting Component Based on COM. *Journal of Institute of Surveying and Mapping* 4, 308–310 (2004)
5. Rui, X.: Research on the Key Technologies about Visualization of Spatial Information. Dissertation of PhD in Chinese Academy of Sciences (2004)
6. Wang, C.-h., Tang, X.-a., Chen, M., Chen, H.: Adaptive Road Modeling Method Based on Terrain-Matching. *Journal Of System Simulation* 18(10), 2824–2826 (2006)
7. Xu, B.-l., Gong, J.-h., Lin, H., Huang, J.-q., Zheng, C.-w.: The Integration of Geographic Information System and Combat Simulation. *Journal of System Simulation* 18(5), 1149–1152 (2005)
8. Jiang, H.: Design and Implement of 3D Military symbol based on B spine. Dissertation of Master in Jilin University (2009)

A Fast Rendering Method for Dynamic Crowd Scene

Hongqian Chen, Yi Chen, Yuehong Sun, and Jian Cao

School of Computer and Information Engineering, Beijing Technology and Business University, Beijing, 100048, China
chenhongqian1@163.com

Abstract. To render realistically the crowd scene including large-scale motional roles in real-time, proposes a fast rendering method based on image-deformation technology. The role images are adopted to decrease the time cost of deformation and rendering. The motional roles is deformed by the curve-skeleton model according to its motion data. The deformation result is improved by the area-preservation algorithm. The method has been proved feasible and valid to render the large scale crowd scene. It can 30 FPS for the scene containing thousands of dynamic roles by our experiments.

Keywords: Crowd simulation, dynamic rendering, Deformation, image-based rendering.

1 Introduction

The large scale of crowd scene occupy one of the important topics in virtual reality. The crowd simulation can help for the preparation for the emergency, group activities, large-scale operation and etc. But it is a difficult task for rendering a large scale of crowd scene in real-time. One role model in virtual environment maybe reach 5,000 patches. And there are thousands of roles in a large scale of scene. The traditional method can not achieve rendering them in real-time.

There are commonly two method to improve the rendering capacity. They are LOD (Level of Detail) technology and image-based rendering. LOD technology [1,2] can accelerate the rendering by decreasing the number of triangle patches. But the technology could bring down the visualization effect when the simplification processing is excessive. And the technology can not achieve the rendering for thousands of roles.

The image-based rendering method expresses one scene or one model using a set of image and its corresponding depth chart. The image-based method can render the complex scene in a fixed speed. The speed of the rendering is independent of the complexity of the scene. Billboard [3] is one technology of image-based method. It expresses the model with one plane which always toward the viewer. It can achieve the high rendering speed with the technology. But billboard can not render the dynamic model because of its static texture image.

The deformation is the common method to achieve the motional effect for the model. There are several mainstream technologies to solve the deformation. They are

skeleton-based technology [4,5], the FFD technology [6], and physical-based technology. These deformation technologies can deform one or several model in real-time. But they can not process the deformation of hundreds or thousands of model in real-time.

The paper proposes one fast rendering method for motional roles. It can support to improve the performance in large scale of crowd simulation. The method achieve the fast rendering based on the image deformation technology. The role images are adopted to instead of the 3D model and to decrease the time cost of rendering the roles. The deformation for motional roles are achieved by the curve-skeleton model. The method proposed in the paper can accomplish the rendering of the large scale of crowd scene in real-time. It can reach 30FPS for the scene including thousands of dynamic roles in our experiments.

The rest of this paper is organized as follows. The following section states the deformation method for single role in detail. In the next section, the area-preservation parameter are calculated. Section 4 elaborate the procedure of the rendering of the crowd scene. In section 5, we show our experimental results. The conclusion and future work are given in last section.

2 Deformation for Single Role

The deformation for single role is accomplished by the image deformation algorithm. The curve-skeleton model is adopted to deform the role image. The model builds one deform mesh for each joint-point. The deform mesh for one joint-point can be shown as Fig.1(a).

The control curve of the deform mesh is the two connect line between the current joint-point and its adjacent joint-points. The X-axis of the local coordinate for the deform mesh is the angle bisector of the control curve, the two connect line.

The deform region of the current joint-point is defined by two edge curve. The outer edge curve can be expressed by Equ.1. The equation of the inner edge curve is Equ.2.

$$\frac{(X + iX)^2}{r^2} - \frac{Y^2}{(k * r)^2} = 1 \quad (1)$$

$$\frac{(X - iX)^2}{r^2} - \frac{Y^2}{(k * r)^2} = 1 \quad (2)$$

In Equ.1 and Equ.2, r is the hardness factor of the final shape. The larger r is, the harder the deformed shape expresses. Parameter k is corresponded to the angle between two connect line. Parameter iX is the adjust factor to area-preservation.

The vertices of the deformation mesh are scattered in the two edge curve. Their coordinates can be calculated by Equ.3.

$$\begin{cases} y_i = -Y_e + \frac{i}{N} * (2 * Y_e) \\ x_i = k * b * \sqrt{\left(\frac{y_i}{b}\right)^2 + 1} \pm \frac{iX}{2} \end{cases} \quad (3)$$

In Equ.3, N is the whole number of the triangles. Parameter i is the serial number of the current triangle. Y_e is the maximum vertical value of the current edge curve. The value of Y_e is set as Y_{e1} for the outer edge curve, while Y_{e2} for the inner edge curve.

The whole deform mesh for one role can be obtained by connecting all the meshes of each joint-point. The whole deform mesh for one role is shown as Fig.1(b).

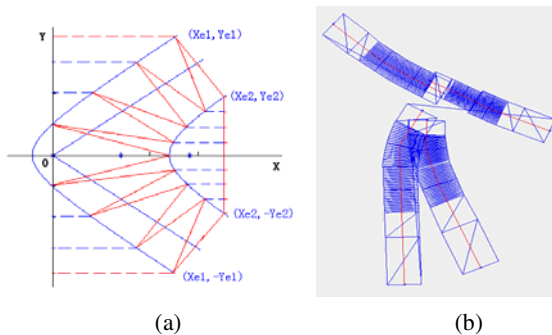


Fig. 1. (a)The deformation for one joint-point, (b) The deformation for one role.

3 The Area-Preservation for Deformation of One Role

Area-preservation is an effective measure to decrease the distortion in 2D image deformation. We preserve the area of each close deform-region via adjusting the parameter iX , the shift distance of the edge curve. An example of the close region named “*emphng*” is shown in Fig.2. The region “*amb*” has equal area with “*dnc*”. The four regions “*aeF*”, “*dgf*”, “*bpk*”, “*chk*” have the same area. We can summarize that the close region “*emphng*” has equal area with the rectangle “*abcd*”.

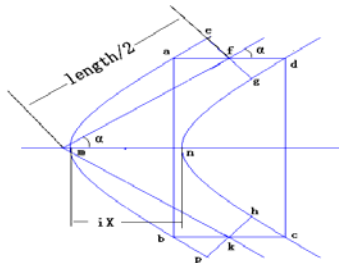


Fig. 2. The sketch map of area-preservation.

The area of the rectangle “*abcd*” can be calculated by Equ.4. Its parameter “*length*” is the length of the shorter bones and “ α ” is slope angle of the upper asymptote. The parameter “*iX*” is the X distance between the two edge curve.

$$\begin{cases} S_{abcd} = height * width \\ height = (length/2) * \sin(\alpha) * 2 \\ width = iX \end{cases} \quad (4)$$

Since the length of the bone is a constant, we set *iX* as Equ.5. The parameter “*BoneWidth₀*” is the width of the bones, and then the region “*emphng*” would have the constant area during deformation even if the angle “ α ” changed.

$$iX = BoneWidth_0 / \sin(\alpha) \quad (5)$$

4 Rendering the Crowd Scene

The crowd scene is assembled by thousands of single role. In our method, each role can be deformed by the upper image-deformation algorithm. The dynamic crowd scene can be obtained via rendering each role according to its own motion data. The procedure of rendering the dynamic crowd scene can be described as following.

Initial operation: A) Load the skeleton data for each role in the dynamic crowd scene. B) Calculate the deform mesh for the current role according its skeleton structure. C) Calculate the parameter *iX* for the area-preservation.

Deformation and rendering operation: A) Load the motion data for all the roles. B) Deform the motional role according to its own motion data. C) Calculate the transform matrix for each role according to the relationship between the position of the current role and the position of viewer. The transform matrix can express the relation between the local coordinate and the global coordinate. D) Rendering the deformation result for each role. The deformation result in any time is obtained according to the motion data in the same time.

5 Experimental Result

We has realized the rendering system according to the method proposed in the paper. The experimental environment includes Intel Core2 3.0CPU, 1GRAM, WinXP Sp2 OS. The plotting result is shown as Fig.3. The deformation result for one role is shown as Fig.3(a), while the rendering result for the large scale of dynamic crowd scene is shown as Fig.3(b).

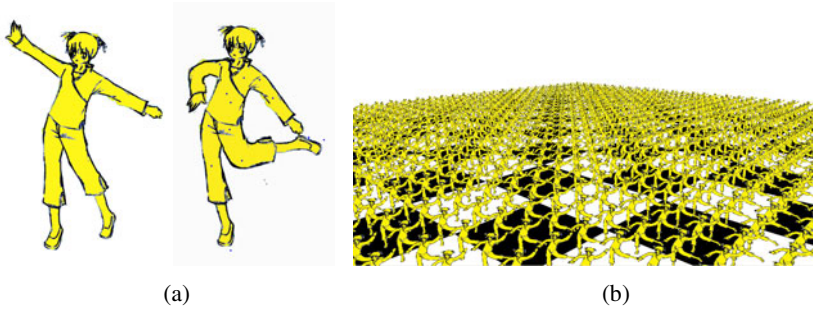


Fig. 3. (a)The deformation result of role. (b)The rendering result for dynamic crowd scene.

6 Conclusions

To improve the performance in large scale of crowd simulation in real-time, proposes a fast rendering method based on image-deformation technology. The method can achieve the fast rendering the crowd scene including thousands of roles. The role images are adopted to instead of the 3D model and to decrease the time cost of rendering each role. The deformation for dynamic roles are achieved by the curve-skeleton model according to the motion data. The deformation result is improved by the area-preservation. The method has been proved feasible and valid to render the large scale crowd scene containing thousands of roles in 30 FPS by our experiments.

The future work is aim to accelerate the rendering processing via hardware-based technology.

Acknowledgement. This work was supported by the Foundation for Youth Teacher and the Fund for the Beijing Key Construction Subjects. We are grateful to our colleagues for their help of proofreading this paper.

References

1. Joshua, L.: Fast View-Dependent Level-of-Detail Rendering using Cached Geometry. In: Proc. of IEEE Visualization, 2002, pp. 259–266 (2002)
2. Tan, K.H., Daman, D.: A review on level of detail. In: Proceedings of Computer Graphics, Imaging and Visualization, 2004, pp. 70–75 (2004)
3. Endo, T., Katayama, A., Tamura, H., Hirose, M., Tanikawa, T., Saito, M.: Image-based walk-through system for large-scale scenes. In: Proceedings of VSMM1998: 4th International Conference on Virtual Systems and Multimedia, vol. 1(1), pp. 269–274 (1998)
4. Capell, S., Green, S., Curless, B., Duchamp, T., Popovic, Z.: Interactive Skeleton-Driven Dynamic Deformations. In: Proc. of 2002 ACM Transactions on Graphics, July 2002, vol. 21(3), pp. 586–593 (2002)
5. Yan, H.-B., Hu, S.-M., Martin, R.: Skeleton-based shape deformation using simplex transformations. In: Nishita, T., Peng, Q., Seidel, H.-P. (eds.) CGI 2006. LNCS, vol. 4035, pp. 66–77. Springer, Heidelberg (2006)
6. Igarashi, T., Moscovich, T., Hughes, J.F.: As-Rigid-As-Possible Shape Manipulation. In: Proceedings of, ACM Transactions on Graphics, vol. 24(3), pp. 1134–1141 (2005)

Human Daily Activity Detect System Optimization Method Using Bayesian Network Based on Wireless Sensor Network

Ying Sun

Information Engineering Institute Shenyang University Shenyang 110044, China
sunying_1215@163.com

Abstract. Human-body daily activity real-time monitoring system design method based on internet of things is proposed, which is able to detect elderly people body posture and biological signal at rehabilitation centers and nursing homes and doctor or their family can know patients' body state through mobile phone or PC. It's possible that number of nodes in each base station increase shapely cause network congestion. A new data transmission algorithm based on Bayesian network is presented, and the sensor under the Bayesian network distribution model and algorithm are built. Finally, experiments results indicate that Bayesian network parameters training method is effective and real-time performance of system is improved.

Keywords: Bayesian, wireless sensor network, ADL, ZigBee.

1 Introduction

With economic development and medical technology advancement, population structure transfer from the young to the old type in china [1]. With human becoming more and more elder, some researcher introduced the concept of ADL(activity of daily living) is to evaluate the activities of daily living self-care ability of elderly people [2-3]. This paper presents a human body ADL acquisition method in things of internet framework. with the combination between monitoring human ADL data and data transmission using things of internet, it's not only can understand the trend for the Aged and supply important patients' body function data to rehabilitation doctors, but also can realize remote and near-range real-time monitoring several patients by one doctor to educe the burden of doctors, health care resources.

ADL data transmission real-time performance of monitoring system for serious patients and patients in accidents is a important indicator with the uncertainty number of child nodes in the network. The application of this system is placed at nursing homes, rehabilitation center. Number of child node in one base station is uncertainty. In traditional design methods, time T is maximum transmission cycle time. It will gets larger when child node increases. It is clearly not monitor the status of ill patients or timely response to emergencies. A real time monitor method of body ADL information using wireless sensor network based on Bayesian network is proposed. It's combined that the Bayesian Networks and, wireless sensor network-based

monitoring system in the human body ADL monitor system, improved traditional network congestion when the network delay is too large to monitor critically ill patients, reduced the system transmission Delay timely treatment of patients. It's significant treatment patients timely.

2 Internet of Things Based on Real-Time Human Daily Living Monitoring System

System framework. The core of things is to achieve things (including people) between the Internet, and realize the active exchange and communications of information in all the things. it would be achieved in a variety of information services and applications that object information through the network to the information processing center. Fig. 1 is block of human ADL acquisition system framework under internet of things [4,5]. It consists of three parts, ZigBee wireless sensor networks [6,7], WLAN bus data transmission network, the monitoring center server and user terminal. ZigBee network includes of low-power low-cost human ADL signal detection sensors and wireless routing nodes. WLAN bus data transmission network, the monitoring center server and user terminal. ZigBee network includes of low-power low-cost human ADL signal detection sensors and wireless routing nodes. Each detect node is for detecting the signal data, controlling wearable sensors, setting parameter instruction and assessment of the human body condition.

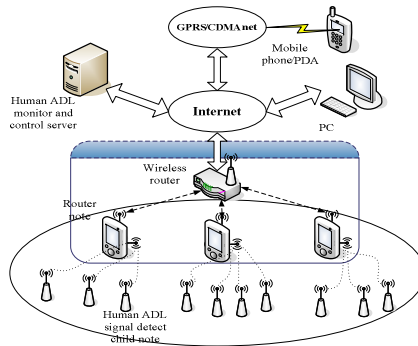


Fig. 1. Human ADL acquisition system framework under internet of things.

Problems in ADL data transmission based on Zigbee wireless sensors networks. Zigbee network have low cost, low complexity, low power consumption features, but the lack of low data rate. If let each node scan cycle 30ms, Cycle time T of Zigbee network in this paper's detection and routing node data can be expressed as,

$$T = 30ms (1 + 2 + 3 + \dots + n) \tag{1}$$

thus, n is the number of nodes. It is obviously than scan period T becomes longer while the number of nodes increases. Assuming that the number of nodes is 20, cycle time will be 40s, and cycle time with the increase in the number of nodes grew up

significantly. In practice, patients in the indoor activity, the number of nodes is uncertain. In case of such a meeting or gathering activities, the burden of route node in network will aggravate, the transmission cycle become long. It is not conducive to the timely detection of accidents. In order to improve the system real-time characteristic, to ensure data transfer rate, this paper presents a optimization of network nodes method based Bayesian network.

3 Optimization Method Based on Bayesian Network

In the whole wireless sensors network which include many child nodes, real time is important for information interaction in the network. When the number of child nodes is excessive or when there are many information to interact, there network happens crowd. It is possible to bring the problem like that: the node B appear abnormal state when the center server is interacting with node A, and T time late center server start to interact with node B, which is a danger situation for the wardship. Therefore effective observation using the wireless sensors network is the key for the patient wardship.

Feature extraction model body posture based Bayesian network. Bayesian Networks describe the combined probability distribution of a set of random variables $X = (X_1, X_2, \dots, X_n)$, and BNs can be formulated using a unit doublet $\langle G, \theta \rangle$, where G is directed and graph, in which the each node is mapped to a random variable in X, X_1, \dots, X_n , and the directed arc expresses the causality and relationship of conditional independence between the nodes, and θ is the set of parameter used to quantized the network. $\theta = \{P(X_i | \pi_i), 1 \leq i \leq n\}$ (π_i is the set of father node of X_i), θ_i is conditional probability table of X_i .

G represents the combined probability distribution qualitatively, which establishes the relationship of conditional independence between the random variables. θ characterize the it quantitatively, which make certain the conditional probability of X_i in the condition tha π_i are konwn. Consequently, according to Bayesian Network the combined probability distribution can be formulated like this:

$$P(X_1, X_2, \dots, X_n) = \prod_{i=1}^n P(X_i | \pi_i) \tag{2}$$

The sensor network of a child node i can be modeled a three-layer BNs as follows: $BN_i = \langle G_i, \theta_i \rangle$ where $G_i = \langle S_i, F_i, RD_i \rangle$, S_i is the set of sensor data of base i , F_i is the set of features, RD_i is set of assessment index. There is a architecture of a wireless sensor network, which include N child node.

Feature extraction model body posture based Bayesian network. Because the topological structure of BNs is definitive, the EM(Expectation Maximization) algorithm can be used to compute the parameters of network, which performs well to default samples and is robust for the whole network. The expectation logarithmic

likelihood function is defined like that $Q(\theta | \theta^t)$, and its maximum is iterated θ using

$$\theta_{ijk}^{t+1} = \begin{cases} \frac{m_{ijk}^t}{\sum_{k=1}^{r_i} m_{ijk}^t}, & \text{if } \sum_{k=1}^{r_i} m_{ijk}^t > 0 \\ \frac{1}{r_i}, & \text{if } \sum_{k=1}^{r_i} m_{ijk}^t \leq 0 \end{cases} \quad (3)$$

where m_{ijk}^t is

$$m_{ijk}^t = \sum_{l=1}^m P(X_i = k, \pi(X_i) = j | D_l, \theta^t) \quad (4)$$

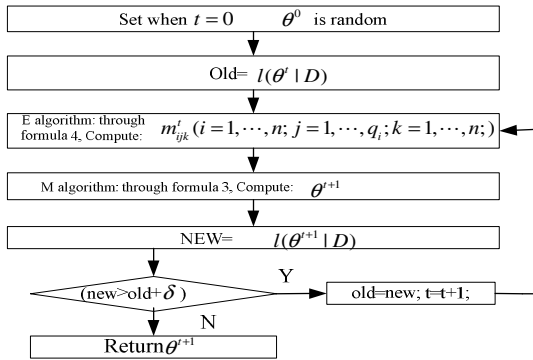


Fig. 2. Structure of three layer Bayesian network

As shown in figure 2. The "old" expresses former state, and the current state is expressed using "new". Fig4 show the flow of this algorithm, where D is the expectation logarithmic likelihood function of(p) that holds invariable in the process of iteration. The stochastic value θ^0 is set in $t = 0$, and the "old" is $l(\theta^t | D)$. The logarithmic likelihood function is computed by E algorithm in t times iteration $Q(\theta | \theta^t)$, and the maximum θ of is computed by M algorithm that is $\theta^{t+1} = \arg \sup_{\theta} Q(\theta | \theta^t)$, obtain θ^{t+1} .

4 Experiment and Analysis

Algorithm comparison results shown in figure 3. Experiments is about a routing node busy test, which is comparison between the use of Bayesian optimization algorithm and the algorithm is not used. In the same routing node, less than 20 test nodes, the

performance of two algorithms is almost the same, but with the increase in the number of nodes detected by Bayesian optimization algorithm performance significantly. In the number of nodes is 100, the cycle time, is only 12% of the used Bayesian optimization algorithm. Experiment results verified the validity of Bayesian optimization algorithm.

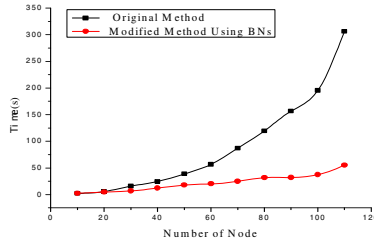


Fig. 3. Algorithm comparison results

5 Conclusions

Error of relationship between body posture characteristics and number of Bayesian network parameters training samples given in the experiment. Algorithm comparison experiment show effectiveness of the proposed Bayesian network based on wireless sensor network information real-time monitoring of human ADL design method. The ADL detect solution, based on the Internet of Things technology, effective solve long-range (or short-range) of the human biological signal acquisition, detection, query problems in rehabilitation centers and nursing home.

References

1. Ching-Lung, L., Hsueh-Hsien, C., Ching-Feng, L.: Design a Telecare E-Marketplace System for Elder People in Elderly Center. In: e-Business Engineering (ICEBE), China, pp. 435–441 (2007)
2. SunLee, B., Minh, K., Sa-kwang, S., Soo-Jun, P.: Toward real time detection of the basic living activity in home using a wearable sensor and smart home sensors. In: Computer-Based Medical Systems, Canada, pp. 5200–5203 (2008)
3. Fleury, A., Vacher, M., Noury, N.: SVM-Based multimodal classification of activities of daily living in health smart homes: sensors, algorithms, and first experimental results. *Information Technology in Biomedicine* 14(2), 274–283 (2010)
4. ITU Internet Reports 2005: The Internet of Things (2005)(unpublished)
5. Zhiyong, S., Kui, L., Shiping, Y., Qingbo, O.: Design and implementation of the mobile internet of things based on td-scdma network. In: Information Theory and Information Security (ICITIS), China, pp. 954–957 (2010)
6. Huang, J., Guoliang, X., Gang, Z., Ruogu, Z.: Beyond co-existence: Exploiting WiFi white space for Zigbee performance assurance. In: Network Protocols (ICNP), China, pp. 305–314 (2010)
7. Guoqiang, L., Shubo, Q., Yuan, X., Qiang, W.: A monitoring system for the condition of storage batteries based on Zigbee. In: Communication Technology (ICCT), China, pp. 163–166 (2010)

Support Vector Machine Based on Chaos Particle Swarm Optimization for Lightning Prediction

Xianlun Tang^{1,2}, Ling Zhuang², and Yanghua Gao¹

¹ Chongqing Institute of Meteorological Science, Chongqing 401147, P.R. China
tangxlun@hotmail.com, gaoyanghua@sina.com

² College of Automation, Chongqing University of Posts and Telecommunications,
Chongqing 400065, P.R. China
zhuangling2000@hotmail.com

Abstract. The learn accuracy and generalization ability of support vector machine (SVM) depend on a proper setting of its parameters to a great extent. An optimal selection approach of support vector machine parameters is proposed based on chaos particle swarm optimization (CPSO) algorithm. Then a lightning prediction model for Shapingba district of Chongqing based on support vector machine is established, and the optimal parameters of the model are searched by CPSO. The upper air data and the ground data of the model are collected from the Micaps system of the national weather service and the actual thunderstorm data are collected from the ground station of Shapingba from year 1998 to 2008. The results show that the proposed prediction model has better prediction results than neural network trained by particle swarm optimization and least squares support vector machine.

Keywords: support vector machine, particle swarm optimization, prediction, lightning.

1 Introduction

With rapid socio-economic development and the improvement of city modernization, especially with the ever increasing development of the information technology and ever increasing fast emergence of tall building in urban construction, the harm degree of lightning and the economic loss caused by it together exert a growing social influence. Lightning prediction has left much to be desired due to the complexity of lightning formation mechanism[1]. In order to improve the veracity and reliability of the lightning prediction results, some artificial intelligence methods such as neural networks have been used. Dohald first made prediction of strong lightning by adopting the multiplayer feed forward neural networks, Manzat trained neural networks by using sounding data and lightning location data, and made predictions of thunderstorm and lightning density[2-3]. While these methods are based on an empirical risk minimization principle and have some disadvantages such as local optimal solution, low convergence rate, obvious “over-fitting”.

Growing efforts are made to explore innovative methods to increase prediction performance. Since the creation of the theory of support vector machines (SVM), rapid development of SVM in statistical learning theory encourages researchers actively focus on applying SVM to various research fields like document classifications, pattern recognitions, data mining and image processing[4-5]. SVM possess great potential and superior performance as is appeared in many previous researches. This is largely due to the structural risk minimization (SRM) principle in SVM that has greater generalization ability and is superior to the empirical risk minimization (ERM) principle as adopted in neural networks[6]. Therefore, it is a promising theory for application to lightning prediction.

The lightning prediction problem can be treated as a binary classification problem based on training pattern from the samples, so SVM can be used for classification. Because the quality of SVM models depends on a proper setting of SVM meta-parameters, the main issue for practitioners trying to apply SVM is how to set these parameter values to ensure good generalization performance for a given data set. Whereas existing sources on SVM give some recommendations on appropriate setting of SVM parameters, there are clearly no consensus and contradictory opinions.

In this paper, we propose a new particle swarm optimization algorithm based on chaos searching (CPSO) to search the optimal parameters of SVM, then a lightning prediction model (CPSO-SVM) is established by using SVM optimized by CPSO. The results show that this model is applicable to lightning prediction and outperforms some previous methods.

2 Support Vector Machine

The basic idea of SVM is to transform the signal to a higher dimensional feature space and find the optimal hyperplane in the space that maximizes the margin between the classes. Traditionally, a SVM is a learning machine for two class classification problems, and learns from a set of l N dimensional vectors x_i , and their associated classes y_i , i.e.

The main idea is to construct a hyperplane to separate the two classes (labeled $y \in \{-1, 1\}$) so that the margin is maximal. It is equivalent to solving the following optimization problem:

$$\min \frac{1}{2}(w \cdot w) + C \sum_{i=1}^l \xi_i$$

with constraints

$$\begin{aligned} y_i((w \cdot x_i) + b) &\geq 1 - \xi_i, \quad i = 1, \dots, l \\ \xi_i &\geq 0, \quad i = 1, \dots, l \end{aligned}$$

where ξ_i is a slack variable giving a soft classification boundary and C is a constant corresponding to the value $\|w\|^2$.

The dual solution to this problem is: maximize the quadratic form (1) under constraints (2) and (3).

$$\max_{\alpha} \sum_{i=1}^l \alpha_i - \frac{1}{2} \sum_{i,j=1}^l y_i y_j \alpha_i \alpha_j K(x_i, x_j) \tag{1}$$

with constraints

$$0 \leq \alpha_i \leq C, i = 1, \dots, l \tag{2}$$

$$\sum_{i=1}^l \alpha_i y_i = 0 \tag{3}$$

where α_i are Lagrange multipliers from the quadratic programming (QP) problem. Kernel function $K(x_i, x_j)$ is used to transform the original input space to a higher dimensional feature space.

Based on the support vectors, the SVM classification can be carried out as follows:

$$f(x) = \text{sgn}[(\sum_{i=1}^l \alpha_i y_i K(x, x_i)) + b]$$

3 Lightning Prediction Based on SVM Optimized by CPSO

Particle swarm optimization. PSO is initialized with a swarm including N random particles. Each particle is treated as a point in a D -dimensional space. The i -th particle is represented as $x_i = (x_{i1}, x_{i2}, \dots, x_{iD})$, x_{ij} is limited in the range $[a_j, b_j]$. The best previous position of the i -th particle is represented as $P_i = (p_{i1}, p_{i2}, \dots, p_{iD})$. The best particle among all the particles in the population is represented by $P_g = (p_{g1}, p_{g2}, \dots, p_{gD})$. The velocity of particle i is represented as $V_i = (v_{i1}, v_{i2}, \dots, v_{iD})$. After finding the aforementioned two best values, the particle updates its velocity and position according to the following equations:

$$v_{id} = \omega v_{id} + c_1 r_1 (p_{id} - x_{id}) + c_2 r_2 (p_{gd} - x_{id}) \tag{4}$$

$$x_{id} = x_{id} + v_{id} \tag{5}$$

where d is the d -th dimension of a particle, ω is the inertia weight, c_1 and c_2 are two positive constants called learning factors, r_1 and r_2 are random numbers in the range of $[0, 1]$ [7].

Chaos particle swarm optimization. Chaos is characterized as ergodicity, randomness and regularity. Because chaos queues can experience all the states in a specific area without repeat, chaotic search becomes a novel tool used as an optimizer[8]. Here, Logistic Equation is employed to obtain chaos queues, which is represented as follows:

$$z_{n+1} = \mu z_n (1 - z_n) \quad n = 0, 1, 2, \dots \tag{6}$$

where μ is the control parameter, suppose that $0 \leq z_0 \leq 1$, when $\mu = 4$, the system of (6) has been proved to be entirely chaotic.

The basic idea of CPSO is described as follows: Generate the chaos queues based on the optimal position searched by all particles until now, and then replace the position of one particle of the swarm with the best position of the chaos queues. The searching algorithm using chaos queues can avoid the search being trapped in local optimum.

Lightning prediction model based on CPSO-SVM. The radial basis function (RBF) is commonly used as the kernel for pattern recognition. For the nonlinear SVM, its generalization performance depends on a good setting of parameters C and the kernel parameter σ . CPSO is used to select these parameters, which are the attributes of each particle, they are set in the range: $C=[0.001,100]$, $\sigma=[0.1,10]$ [5]. The performance of each particle is measured according to the fitness function.

The basic steps of lightning prediction algorithm (CPSO-SVM) are described as follows:

Step 1: Randomly initialize the position and velocity of M particles.

Step 2: for all the particles of the swarm, take the following steps:

1) Using the global best and individual best of each particle, each particle’s velocity and position of weight variables is updated according to (4) and (5).

2) Evaluate the fitness of each particle and compare the evaluated fitness value of each particle to its individual best p_i . If current value is better than p_i , then update p_i as current position.

3) If current value is better than the global best p_g , update p_g as current position.

Step 3: Optimize P_g by chaos search. Firstly, scale $P_{gi} (i = 1, 2)$ into $[0,1]$ according to $z_i = (p_{gi} - a_i) / (b_i - a_i), (i = 1, 2)$, and generate chaos queues $z_i^{(m)} (m = 1, 2, \dots)$ by iteration of Logistic Equation, then, transfer the chaos queues into the optimization variable $p_g^{(m)} (m = 1, 2, \dots)$ according to following equation:

$p_{gi}^{(m)} = a_i + (b_i - a_i)z_i^{(m)}$, upon that the solution set is obtained:

$p_g^{(m)} = (p_{g1}^{(m)}, p_{g2}^{(m)}), (m = 1, 2, \dots)$. Compute the fitness value of each feasible

solution $p_g^{(m)} (m = 1, 2, \dots)$ in the problem space during chaotic search, and get the best solution p^* .

Step 4: Replace the position of one particle selected randomly from the swarm with p^*

Step 5: If one of the stopping criteria is satisfied, then stop, we can get the global optimal that are the value of C and σ . Otherwise, loop to step 2.

Step 6: Establish the decision function of lightning prediction based on the global optimal.

4 Experiment and Analysis

Data Collection. The experiment used surface observing data and upper air data, collected from the Micaps system of the national weather service, along with data of live thunderstorm from 34 ground stations in Chongqing municipality. The upper air data from Shangpingba station is collected at eight o'clock in the morning from 1998 to 2008 on a daily basis. Every upper altitude exploration station collects various kinds of information, including pressure, wind direction, wind speed, temperature and dew-point five elements in 11 different heights of earth atmosphere in lower-to-upper motion. Only pressure, wind direction, wind speed, temperature and dew-point five elements collected from ground stations are needed to establish the predict model, which can predict whether lightning will occur in the next 24 hours. The variables of data collected for lightning prediction have different level of magnitudes from each other, therefore, all variables should be normalized to the range [0,1].

The results of prediction are processed by the code of 1 and -1. 1 represents lightning, and -1 the non-lightning and the forecast validity is 24 hours. The accuracy of prediction is $P = (M_1 + M_2) / M_3$. M_1 are the times of accurate predictions of non-lightning; M_2 are the times of accurate predictions of lightning; M_3 is the total number of testing samples. Terms like vacancy rate, miss rate and forecast accuracy are available to describe the forecast results, in correspond to how the predictions actually turn out. Vacancy rate is used to describe the frequency of mistakenly forecast lightning and miss rate of non-lightning.

Prediction with CPSO-SVM. Fig.1 shows the prediction system developed by C# and SQL Server. A dataset collected from April 1, 2003 to September 30, 2007 is established to train CPSO-SVM and predict lightning. The parameters of CPSO are set as follows: the size of the population $M=30$, the inertia weight ω decreases linearly from 0.9 to 0.4, set learning factors $c_1 = c_2 = 2$, the optimal parameters of SVM searched by CPSO are $C=18$, $\sigma = 1.4$. Using the parameters determined by CPSO and several groups of parameters selected randomly to establish lightning prediction models based on CPSO-SVM, the prediction results are shown in Table 1. Can be seen from Table 1, the model established by the optimal parameters has the best prediction effect.

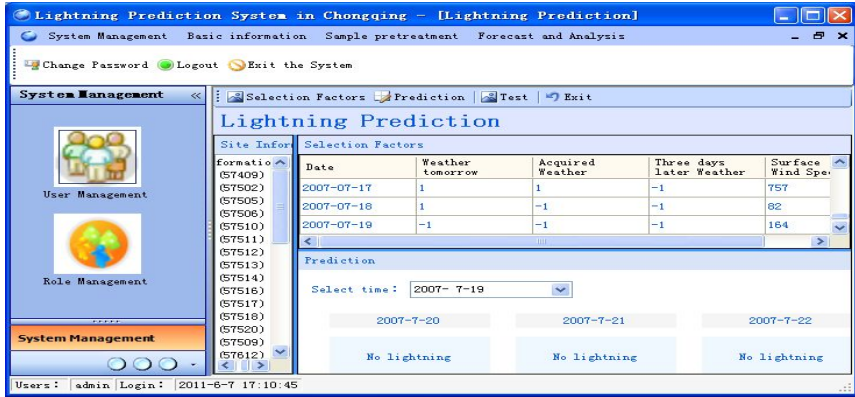


Fig. 1. The lightning prediction systems

Table 1. Prediction results of models with different parameters

Group number	C	σ	Prediction accuracy (%)
1	18	1.4	86.3
2	8.5	0.8	81.4
3	10.5	2.5	83.2
4	1.6	4.2	79.7

In order to compare the prediction accuracy with other methods, apply least squares support vector machine (LS-SVM), neural network trained by chaos particle swarm optimization (CPSO-NN) and CPSO-SVM to establish lightning prediction models. The experiment is repeated 30 times, where the training set and test set are randomly selected without replacement every time. The average experimental results of miss rate and vacancy rate are given in Table 2.

Table 2. Comparison of average prediction results

Group number	LS-SVM		PSO-NN		CPSO-SVM	
	Miss rate (%)	Vacancy rate (%)	Miss rate (%)	Vacancy rate (%)	Miss rate (%)	Vacancy rate (%)
1	21.3	11.3	25.6	12.6	18.3	10.5
2	23.5	12.5	26.4	13.9	19.6	11.6
3	21.9	13.2	23.6	14.8	20.1	9.5
4	24.1	10.4	23.1	11.7	21.5	8.2

From the results of comparison, it is obvious that CPSO-SVM algorithm has better prediction accuracy and stronger stability than that of LS-SVM and CPSO-NN. If more data were applied for LS-SVM training, LS-SVM will have a greater generalization ability and study ability, but this improvement will consume more energy and time, in that sense, CPSO-SVM also has certain advantages that it needs only a small set of training data.

5 Conclusions

In this study, we applied SVM optimized by CPSO in lightning prediction. Results show that SVM can serve as a promising alternative for exiting prediction models. It can be seen from the experiment that the prediction model overcomes the main shortage of artificial neural network without defining network structure and trapping in the local optimum, so it's applicable to lightning formation process with complex relationship between input and output, and it can overcome the interference of noise data. Compared with LS-SVM and CPSO-NN, CPSO-SVM has better performance.

The CPSO-SVM prediction model can be used successfully to make a suggestion to help weather forecasters to make the right decision. In this sense, it is necessary to improve the performance of the system according to deep analysis on mechanism of the prediction model.

Acknowledgments. This work was supported by the National Nature Science Foundation of China (No. 60905066).

References

1. Alwin, J.H.: Thunderstorm predictors and their forecast skill for the Netherlands. *Atmospheric Research* 67(3), 273–299 (2003)
2. Agostino, M.: Sounding-derived indices for neural network based short-term thunderstorm and rainfall forecasts. *Atmospheric Research* 83(3), 349–365 (2005)
3. Agostino, M.: The use of sounding-derived indices for a neural network short-term thunderstorm forecast. *Weather And Forecasting* 20(8), 896–917 (2005)
4. Liu, X.-h.: Computer-aided diagnosis of breast cancer based on support vector machine. *Journal of Chongqing University(Natural Science Edition)* 36(06), 144–148 (2007)
5. Deng, N.Y., Tian, Y.J.: *New method of data mining - support vector machine*. Science Press, Beijing (2004)
6. Vapnik, V.: *The nature of statistical learning theory*. Springer, New York (1995)
7. Kennedy, J., Eberhart, R.C.: Particle swarm optimization. In: *Proc. of the IEEE International Conference on Neural Networks*, pp. 1942–1948. IEEE Press, Piscataway (1995)
8. Fei, C.-g., Han, Z.-z.: An improved chaotic optimization algorithm. *Control Theory & Applications* 23(3), 471–474 (2006)

Extraction of Visual Material and Spatial Information from Text Description for Scene Visualization

Xin Zeng, MLing Tan, and WJing Chen

School of Architecture and Art Central South University, China
zengxin@mail.csu.edu.cn

Abstract. The generation of 3D virtual scene could be greatly simplified by integration of natural language interface. This involves complex task of extracting of visual object, material and their spatial information from language description. The knowledge of visual perception, spatial language, natural language processing and graphic representation can be combined with one another to accomplish the task of generating a virtual scene. This paper first mentions a variety of research in developing language based scene application. This is followed by a brief introduction of natural language processing technology. Some related theories of human visual perception and spatial language are investigated in section 3. A representation formalism based on word-concept-visual information has been proposed by linking the levels of meaning and visualization in section 4. Finally, we draw conclusion and mentioned future work.

Keywords: Virtual Reality, CAD, Material and Spatial Representation, Text Visualization.

1 Introduction

The barriers to productive use of traditional menu-based virtual environment CAD tools have been recognized, and as interactive software tools of the future become more and more complex and knowledge-intensive, the possibilities for integrating a natural language interface and computer graphics by incorporating knowledge of human-to-human interaction has been considered in improved virtual environment user-interfaces. Different types of text to images conversion system have been attempted and considered by many researchers over the last few decades, such as text to static scene based applications [1,2,3,4,5], and text to animation based applications [6,7,8,9].

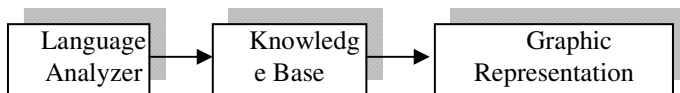


Fig. 1. Architecture of Language-based Graphic Application

All common approach of language-based graphic applications consists of three components as shown in Figure 1. The input sentence is analyzed by the language component, and then the semantic of sentence is mapped into low level parameterized data in the knowledge base component. The output is used by the graphic component and ultimately to construct a virtual scene. The work in this area focuses on how to extract the meaning of the description and represent in a computational virtual scene. This involves complex natural language processing and visualization, and the knowledge of visual perception, spatial language, natural language processing and graphic representation can be combined with one another to accomplish the task of generating a virtual environment.

2 Language Processing and Information Extraction

Natural language processing uses known data about words and predefined rules that show authorized word structures to give the meaning of descriptions to enable communication between people and computers [10]. The general process of natural language processing can be divided into following levels: morphological analysis, lexical tagging, syntactic parsing, and semantic analysis. During the process the knowledge of the real world information need be captured and encoded in databases for aiding language understanding. There are three types of knowledge which are used in natural language processing, namely syntactic knowledge, word-sense knowledge, and world knowledge [11]. When combined, the above three types of knowledge permit to construct a representation of the initial meaning of the sentence. After many years of development and research on natural language processing and understanding, the state-of-art natural language enabled technology is rapidly growing along with development of computer processing power. If we constrain our language interface, this may help us use exist natural language processing techniques to extract information from language description and produce reliable interpretations. In current, each language based graphic application has its own constrained input language to suit its particular objectives. The form of the language created restricts the concepts then can be expressed and, ultimately the scenes that can be generated.

3 Visual Information and Related Theories

When dealing with computational models for integrating natural language and graphic representation, it is useful to examine theories of human visual perception and spatial language to discover what kind of processes and representation lie in between. The integration of visual perception and language understanding is one of the research fields of artificial intelligence and cognitive science that concerned with machine-simulated intelligent [12, 13]. This involves object identification and placement, it also appears very important to areas of computer graphics such as generation of virtual environment and animation. In the research of visual perception, [14] investigate how to use visual information to construct an internal spatial representation of visible objects. An intermediate representation provides the link between language and Marr's computational theory of vision. The object descriptions

similar to Marr's 3D models are associated with classes of objects, thus providing a link between the perceptual system and the conceptual level [15]. Furthermore, both visual imagery and object recognition share the same 3D representation of objects.

Spatial language is a specific subject cognitive linguistics and considers the linguistic structure used for describing configurations as being fundamental for spatial cognition. Within the structure of a state [17], a [PLACES] is normally occupied by a [THING], many prepositions in English—for example, “over; under; on; in; above and between” can be illustrated as a pure place-function as illustrated: *The mouse is under the table.* [Place UNDER ([Thing TABLE])]

Whenever an object location or orientation is depended on some other object, this relationship is called Figure/Ground (foreground vs. background) or primary object/reference object provides an extensive list of other terms used to describe the relationship [18, 19]. The location and orientation of a primary object can be determined in relation to reference objects. Objects can be solely characterized by their spatial properties, such as relevant dimensions, boundary conditions, symmetry vs. distinguish ability of parts. There are three dimensional spatial information is traditionally represented as volumetric representation (each entity is described with the volume it occupies); boundary representation (objects are described by their bounding surfaces that are approximated as polyhedral objects or polylines); representation by symbolic vocabulary (each group of word has a set of parameters to describe its characteristics) [20]. Volumetric representation and boundary representation are often used in computer graphics. Representation by symbolic vocabulary can be used for defining specific object. They are appropriate methods for the purpose to reconstruct the virtual environment based on language input. Object identification (nouns/shape), attribution (material/adjectives), object position (spatial prepositions/adverbs) of the language system are distinguished by “what” (identification) and “where” (localization) channels [21]. To representation of the “where” is a major dimension of narrative processing and involves the determination of the objects to be included in the presentation; selection of object properties and attributes to depict; object positioning [22]. In this paper, we focus on the rigid objects, material and their spatial configuration in a virtual environment, we must consider both visual features (e.g. colour, material, orientation, dimension, shape) and spatial attributes for each entity.

4 Visual Object, Material and Spatial Formalism Definition

In all application of language-based scene generation, the central issue is the correspondence problem, how to correlate visual information with words and context. Conveying the abstract meaning from the words is considered as primitive resource for visualization, and this direct association word-concept-visual is used for knowledge representations. Another issue to be considered is whether the intermediate representation is flexible enough to handle both meaning and visual these two expression modes.

In general, noun associated object in most language-based graphic application is defined explicitly to represent a physical object, each object in the environment corresponding to a related noun and associated with a geometry model in visual object

database. The construction of the 3D scene depends not only on a large number of 3D objects but also on having a large set of visual features of objects and material that affect the environment specified. This involves converting the various semantic elements into parameterized data definition, and the attribute related descriptive adjectives can be redefined in database and the values assigned to these parameters affect the generation of the 3D scene, such as colour, material, sizes, *etc.* These works have been done by our previous research[23].

The interpretation and representation of the spatial relationships of the objects are the most important issues in a conceptual reconstruction of a 3D scene from input language. When we describe spatial relationships with language we often use spatial prepositions. Compare with other two categories (*i.e.* nouns and adjectives), spatial prepositions is more complicated to define because of various situation. [16] defines the spatial system according to configurations and interrelationships of boundaries, masses. We distinguish between structural and spatial properties of objects. The structural properties stand to the spatial attributes within the object, meaning that each object has location, orientation, dimension, and shape as its internal and independent spatial attributes. Spatial properties specify the relationships between objects. Spatial properties of one object to another depend on geometric relations (*i.e.* near, in, on). This is the most common way to express object spatial relations.

The prepositions can be divided into several groups: proximity prepositions (near, far (from), by, next to), directional prepositions (in front, behind, left of, below), and boundary prepositions (in, on, between, across, crossing). In the current system, we use the relative reference frame method of [24] and examine the spatial descriptions that describe the spatial configuration of a located entity with respect to a reference entity. The bounding-box as the boundary to all the objects, the definition of the spatial area of object is obtained by expending the idea of [25] from 2D to 3D. The grey areas shown in Figure 2 illustrate the definition of the spatial area of an object's 6 basic sides. The information such as structural properties of the objects involved, initial position, orientation, axes of rotation *etc.* can be used to semantically parameterize the prepositions according the common situation.

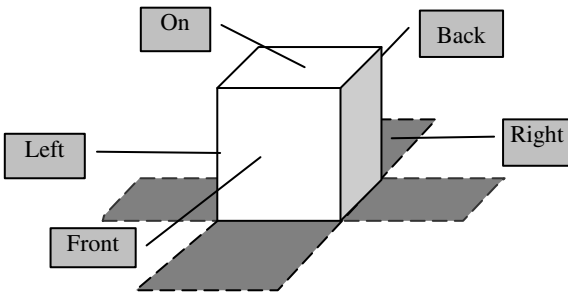


Fig. 2. Definition of the Spatial Area of Object

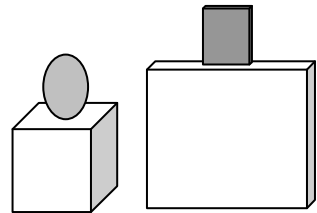


Fig. 3. Common Definition Prep on

The preposition such as *on* is handled by semantic functions that look at the left and right dependents of the preposition (*i.e.* subject and object) and construct a semantic spatial parameterization depending upon their properties as below.


```

<preposition_frame> <position>
<on> <place x_subject ="0.0" y_subject =" + h_subject op(+) + h_object "
z_subject="0.0"/></on>
</position></preposition_frame>

```

The element of the prepositions consists of three attributes; $x_subject$, $y_subject$ and $z_subject$ representing the x, y, and z axis respectively. Each attribute takes different values to indicate the position of the *subject* is determined by both *subject* and *object* associate objects' structural properties; especially the position of *object* is key reference to the *subject*.

However, not all prepositions are one-to-one association, and some problems may appear if the preposition contains more than one geometric description, or the spatial attributes of objects vary in different situations. These will cause the system to fail or present the spatial relations wrongly. For example, the concept of *on* is more complex compared with other prepositions. This definition works well in a common setting of objects, such as *a ball is on a box*. But consider *a picture is on a wall*, and then the output virtual scene would appear odd if this definition were used (see Figure 3). The picture should be placed on the side of the wall rather than on the top of the wall because of the functional dimensionalities of the objects. In order to address this problem, the objects are classified into two different types, i.e. 2D placement and 3D placement. Which one applies is determined by the spatial attributes of the objects. For example, *wall* always appears as 2D, and *box* appears as 3D in many cases. In addition, orientation of the objects is also added as a constraint in the noun associated database. In addition, a filter is created for handling some specific prepositions, like *on*, *in*, *under*, etc. The filter firstly checks the type of the objects, and then identifies if the sentence contains the specific prepositions. In the next stage, there are several different corresponding methods to take care of each case if the prepositions are encountered. Otherwise, it interprets the default and common numerical constraints to complete the whole visualization process. To illustrate the techniques, consider the sentences: *A table is in front of a wall*. *A lake picture is on the table*. *A sky picture is on the wall*.

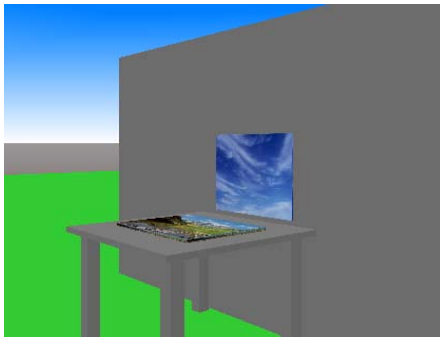


Fig. 4. The Output from Sentences

For the first sentence, the table is 3D and the wall is 2D, *in front of* is the general preposition phrase. There is no need to change any state of the objects. In second sentence, the lake picture is 2D and the preposition *on* in this sentence which is same as its definition in Knowledge Base. The objects are placed in the regular position. Things are different in third sentence as both objects are 2D objects; the preposition *on* belongs to the specific case. The conditions are analyzed and sky picture appears to satisfy the conditions of the

filter. Thus, the orientation of the sky picture is further executed and placed on the surface of the wall. Figure 4 shows the final output from the sentences. The use of the spatial filter enables the system to cope with both common and specific compound

spatial relations. The system obtains the constraints from the knowledge base and then updates the position of the objects by considering the current location of the objects from the virtual scene. In this way the system can handle the spatial relations of the objects in a dynamic environment and makes the real time interaction possible.

5 Conclusion and Future Works

As natural language often describes visual scenes at a high level, the conversion of language description into a virtual scene need to extract and define the meaning from input context into computer understood low-level data. A representation formalism based on word-concept-visual information in Knowledge Base component has been developed by linking between the levels of meaning and visualization. The most important part of visual semantics is to unify various words meanings, and to interpret their associated visual information (such as object shape, material and spatial relation) with computer program functions. Then enable graphic component to create correspond virtual scene. Our first step toward generating a virtual environment based on simplified language approach is promising. Based on this work, it appears that the semantic information is insufficient and would be greatly improved by interpreting more grammatical structures of the descriptions. The graphic component can be more sufficient to achieve both good rendering effect and flexible interactive capabilities.

Acknowledgement. This project is supported by NSFC 60873189.

References

1. Winograd, T.: *Understanding Natural Language*. Academic Press, London (1972)
2. Yamada, A., Yamamoto, T., Ikeda, H.: *Reconstructing Spatial Image from Natural Language Texts*. In: *Proceedings of COLING 1992, Nantes*, pp. 23–28 (1992)
3. Clay, R., Wilhelms, J.: *Put: language-based interactive manipulation of objects*. *IEEE Computer Graphics and Applications* 16(2), 31–39 (1996)
4. Coyne, B., Sproat, R.: *WordsEye: An automatic text-to-scene conversion system*. In: *Proceedings of 28th SIGGRAPH Annual Conf. Computer Graphics and Interactive Techniques, Los Angeles*, pp. 487–496 (2001)
5. Akazawa, Y., Okada, Y., Nijijima, K.: *Automatic 3D object placement for 3D scene generation*. In: *The European Simulation and Modeling Conference*, pp. 316–318 (2003)
6. Kahn, K.M.: *Creation of Computer Animation from Story Descriptions*. AI Technical report 540 MIT. Artificial Intelligence Laboratory, Cambridge (1979)
7. Mukerjee, A., Singh, M., Mishra, N.: *Conceptual description of visual scenes from linguistic models*. *Journal of Image and Vision Computing. Special Issue on Conceptual Descriptions* 18 (2000)
8. Nugues, P.: *Verbal and written interaction in virtual worlds, some application examples*. In: *Proceedings of the Fifteenth Twente Workshop on Language Technology, Universiteit Twente, Enschede*, pp. 137–145 (1999)
9. Glass, K., Bangay, S.: *Constraint-based conversion of fiction text to a time-based graphical representation*. In: *Proceedings of the South African institute of computer scientists and information technologists on IT research in developing countries, New York*, pp. 19–28 (2007)

10. Samad, T.: *A Natural Language Interface for Computer-Aided Design*. Kluwer Academic Publishers, Boston (1986)
11. Allen, J.: *Natural Language Understanding*. Benjamin/Cummings, Menlo Park (1987)
12. McKeivitt, P.: Integration of natural language and vision processing. In: *AAAI-1994. Workshop*, Seattle, WA (1994)
13. Maaß, W.: How spatial information connects visual perception and natural language generation in dynamic environments: Towards a computational model. In: *Proceedings of the International Conference, COSIT 1995*, pp. 223–240. Springer, Heidelberg (1995)
14. Marr, D.: *Vision: a Computational Investigation into the Human Representation and Processing of Visual Information*. Freeman, San Francisco (1982)
15. Jackendoff, R.: On beyond zebra: the relation of linguistic and visual information. *Cognition* 26(2), 89–114 (1987)
16. Talmy, L.: How language structures space. In: Herbert, P., Linda, A. (eds.) *Spatial Orientation: Theory, Research, and Application*, pp. 225–282. Plenum Press, New York (1983)
17. Miller, G.A., Johnson-Laird, P.N.: *Language and perception*. Belknap Press, Cambridge (1976)
18. Herskovits, A.: *Language and Spatial Cognition: An interdisciplinary Study of the prepositions in English*. Cambridge University Press, Cambridge (1986)
19. Retz-Schmidt, G.: Various views on spatial prepositions. *AI Magazine* 9(2), 95–105 (1988)
20. McDermott, V.: Spatial reasoning. In: *Encyclopedia of Artificial Intelligence*, vol. 2. John Wiley & Sons, Chichester (1987)
21. Laudau, B., Jackendoff, R.: What and Where in spatial language and spatial cognition. *Behaviour and Brain Sciences* 16, 217–265 (1993)
22. Fludernik, M.: *Towards a Natural Narratology*. Routledge, London (1996)
23. Zeng, X., Tan, M.L.: The Application of Text to Visualization Technology in Virtual Environment. *Journal of Computer Engineer and Science* (2) (2010)
24. Levinson, S.C., et al.: Returning the tables: language affects spatial reasoning. *Cognition* 84, 155–188 (2002)
25. Logan, G., Sadler, D.: A computational analysis of the apprehension of spatial relations. In: Bloom, P., Peterson, M., Nadel, L., Garrett, M. (eds.) *Language and Space*, pp. 493–529. MIT Press, Cambridge (1996)

The Design of Elevator Control System Based on PLC and Configuration

Shuang Zheng¹ and Fugang Liu²

¹ Heilongjiang Institute of Science and Technology, Harbin, China

² Heilongjiang Institute of Science and Technology, Harbin, China
zs1980225@126.com, liufugang_36@163.com

Abstract. This paper introduced the design and realization of the elevator experimental equipment based on configuration software and PLC. Using configuration software in conjunction with the manipulator's movement in the system gave the most intuitive exhibition and the dynamic imitation. The system can not only supervise and control the manipulator process, but also carry on simulation and imitation control. Also it can make the system easily extend and greatly promote the automation level of monitor and management.

Keywords: king-view, programmable logic controller (PLC), elevator monitoring and control system, imitation.

1 Introduction

Elevator is a complex machine-electronic transportation system. It covers a wide range of subjects to improve the move speed, landing accuracy, comfort and safety and provides convenience for people. In electric automatic control system of elevator, logical control takes the major place. For any elevators, the electric automation system has same functions no matter how fast or automated it is. The best way for single elevator controlling is collective selection control. Using PLC to undertake the controller of electrical system of elevator has been a perfect technology. But the monitoring system is laggard and low its whole performance. The proposed system combines the advantages of PLC and configuration, not only owns real-time, higher stability and flexible accommodation, but also have better system interface, which g can make the system easily extend and greatly promote the automation level of monitor and management.

2 Design of Elevator Control System

Elevator electrical control systems have same function and its basic requirement is: every floor has call button, call light and indicator light. Indicator light is used to demonstrate where the elevator is. No matter in which floor the call button is pressed,

then the call light will bright, which is standing for the elevator going to the calling floor. The call light does not become extinguished until the call receives response. The direction of elevator is made up of up and down button; whether the elevator door open or not depends on door indicating light. When there is unique demand, elevator will go ahead to that floor directly and wait for entering. If it appears many calls for elevator in the same time, it will response to each request in turn, and stop 5 seconds for each waiting for entering. According to these requirements, the system's I/O distribution demonstrates in the Table 1. Its main programmer is presented in Fig. 1.

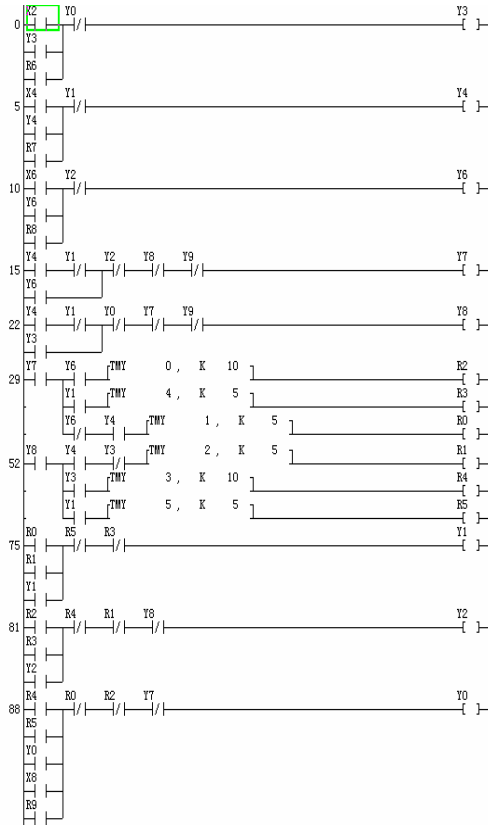


Fig. 1. Main ladder diagram of the system

Table 1. I/O distribution

No.	Function Explanation	I/O style	Remark	No.	Function Explanation	I/O style	Remark
1	first floor calling button	I/O discrete	X2	8	second floor call light	I/O discrete	Y4
2	second floor call button	I/O discrete	X4	9	third floor call light	I/O discrete	Y6
3	third floor call button	I/O discrete	X6	10	up indicator light	I/O discrete	Y7
4	first floor indicator light	I/O discrete	Y0	11	down indicator light	I/O discrete	Y8
5	second floor indicator light	I/O discrete	Y1	12	first floor open door indicator light	I/O discrete	YA
6	third floor indicator light	I/O discrete	Y2	13	second floor open door indicator light	I/O discrete	YC
7	first floor call light	I/O discrete	Y3	14	third floor open door indicator light	I/O discrete	YE

3 PLC Elevator Control System Based on Configuration

Configuration is also called upper computer management software and widely used in industrial field. It offers flexible configuration tools, good human-computer interface and has ability to accomplish all kinds of industrial assignments, such as management control, data collection, continuous control and statistical process control.

The king-view represents the best configuration software. It can provide the situation of PLC control system for customer through collecting data of site, animated cartoon display, alert processing, real-time curve, history data curve, form output and other approaches. Customer can freely combine word, light, ON/OFF button, various active form shape, digital data input, abnormality alert, tranquility demonstration and so on to monitor or deal with the process of multifunctional exhibit which is possible to change at any time [3]. The software can be easily operated. In the method of monitoring system, it can make best use of computer and PLC and make up their disadvantages to be widely used in production.

4 The Achievement of Configuration Project

4.1 Building New Project, Set Communication Configuration

Firstly, build a new project in the Proj-Manager of the king-view. In order to realize the bilateral control, communication should be built between configuration software and PLC. The system chooses RS-232 serial communication. It should be noted that the setting in king-view must comes in line with that in PLC to ensure correct communication.

4.2 Setting the System Imitation Interface

In configuration software, build “elevator operation system” window and set the attribution. Use drawing tool to design each aspect of elevator operation system, choose system control tool to design every floor's buttons, lights and so on, and make use of word label to demonstrate every floor. To make the system easy be understood, we construct the imitation of elevator operation on the right of the surface. Fig. 2 shows the operating system.

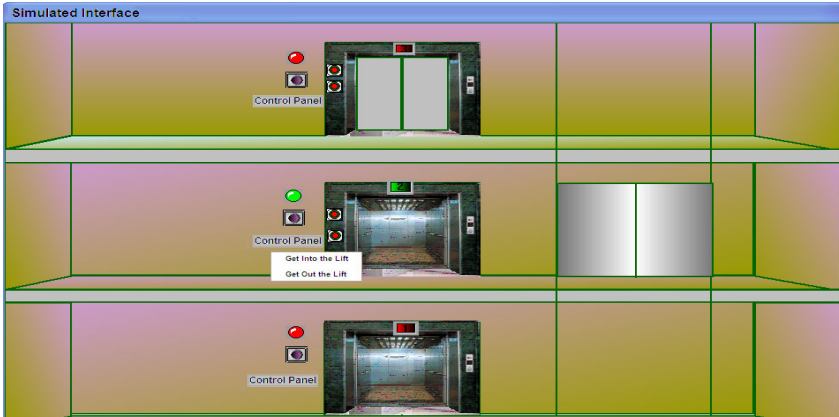


Fig. 2. The imitated interface of system

4.3 Defining Data Variation

As the communication bridge of upper computer and lower operating CPU, database is the core of the king-view. When we operate the king-view software, the situation of industry will show in the screen by animation cartoon and the operator's order must be sent to the spot at the same time.

4.4 Setting Connection of Animation Cartoon

The scene made by the king-view is still. The cartoon is got by changing the variable of database. Setting connection of animation cartoon is building the relation between pixel and variable of database. Consequently, the changing of real data, such as the elevator calling button, the operation light of elevator door, will lead the variables of database to change, and make the pixel of picture move. To strengthen the flexibility of project, for example, the realization of animation cartoon such as up and down of elevator, the right and left button of elevator door, user should have aid of programmable language. Part of the program are as follow:

```

if (\local station\first floor calling light==1&&\local station\down light=
=1&&\local station\direction light 2 = =1)
{\local station\elevator 2→1\local station\elevator 2→1+28;}
if(\local station\second floor calling light= =1&&\local station\down light=
=1)
{\local station\elevator 3→2=\local station\elevator 3→2+24;}
If(\local station\first floor calling light==1&&\local station\down light=
=1&&\local station\direction light 2= =0)
{\local station\elevator 3→1=\local station\elevator 3→1+25;}
if(\local station\up light= =0)
{\local station\elevator 1→2=0;
\local station\elevator 1→3=0;}
if(\local station\down light= =0)
{\local station\elevator 3→2=0;
\local station\elevator 3→1=0;}
if(\local station\direction light 1= =1)
{\local station\elevator 2→3=0;}
if(\local station\direction light 3= =1)
{\local station\elevator 2→1=0;}
if(\local station\first floor open door light= =1)
{\local station\first floor of left light=\local station\first floor of left
light+10;
\local station\first floor of left light=\local station\first floor of left
light+10 ;}
if (\local station\first floor open door light==1)
{\local station\first floor of left light=\local station\first floor of left light-
10;
\local station\first floor of right light=\local station\first floor of right light-
10 ;}

```

5 Conclusion

Based on PLC and the king-view software, elevator control system performs well and stably and has a friendly screen. Compared to traditional control system, it can enhance the efficiency and improve the automation level in some extent. The design is meaningful for other monitoring system.

References

1. Ji, S.-p., Sun, C.-z., Lu, M.: Innovational Teaching Method of PLC and Its Application. Journal of Electrical & Electronic Education 30(02), 122–124 (2008)
2. Wang, Y., Ren, S.-j., Li, Z.-q.: PLC electrical control and configuration design. Electronic Industry Publishing, Beijing (2010) (in press)
3. Beijing Asia-controlled technology company: the king-view software reference manual (2003)
4. Wonder ware Corporation: In Touch 7.0 Advanced, Training Manual (1998)

5. Zhou, M.-l.: PLC electronic control and configuration design. Science Press, Beijing (2003) (in Press)
6. Yu, X.-h., Tao, W.-q., Liu, J.-j.: The Research about the Gaphic Library Model of Configurable Software. *Control & Automation* (3), 60–62 (2005)
7. Zhang, L.-n., Huang, J.-l., Li, S.-g.: Design of Intelligent Elevator Monitoring System Based on Advanced RISC Machine. *Electrotechnics Electric* (1), 25–27 (2009)

Study on Module Partition Method for CNC Lathe Design

ZhiWei Xu and YongXian Liu

School of Mechanical Engineering & Automation, Northeastern University, China
zhwxu@mail.neu.edu.cn, yxliu@mail.neu.edu.cn

Abstract. A multi-dimensional module partition methodology is put forward for CNC lathe, in which not only the functional module partition and the physical structure module partition of CNC machine tools are taken into account, but the characteristics of different stages of in the whole life-cycle of machine tools is considered as well. On the basis of this module partition flow and the principle of module partition for CNC machine tools are presented. The CNC lathe is elaborated on the functional module and structural module. A CNC machine tool company's HTC Series CNC lathes modular design is illustrated as an example.

Keywords: Modular design, Module partition, Modularization, CNC lathe, Variant design.

1 Introduction

Modular design is a kind of advanced design which is widely adopted in recent years. Modular design of the products which transforms small batch production into medium scale production or mass production has great adaptability and flexibility to cater for diverse users and personalized requirements. Modular design technology is one of basic technologies of mass customization production. Modular design method can improve the efficiency and adaptability of machine tool design. Modular design based on product family is the important foundation of variant design or derived design of CNC machine tools. How to scientifically partition the module is essential in the modular design of CNC machine tools. The rational modular partition will greatly affect the general appearance, the performance and the cost of modular products.

In recent years the methodology of functional module partition of the products have made some progress. P.Gu [1] presents an integrated modular design methodology for life-cycle engineering. Su Ming and Chen Wei Fang [2] at Nanjing University of Aeronautics and Astronautics propose a methodology of the NC machine tools modular partition based on the customer demands for innovative modular design. Sun Nuogang [3] at Xi'an Jiaotong University, puts forward a module partition methodology based on the Quality Function Deployment (QFD). An CNC machine tools module partition methodology is presented in this paper.

2 Module Partition Flow

Module partition is the preliminary step of modular design. Based on the study of the existing module partition method, a new product module partition flow model is presented which consists of the following seven phases, as is shown in figure 1 below:

- (1) To Get Access to Customer Needs:
To get access to customer needs refers to acquiring the needs of customers by means of market survey and clarify them to guide the follow-up work
- (2) To Determine the Function:
According to the reports of customer’s needs, the demands of the customer are transformed into explicit product design requirements and product function by means of QFD (Quality Function Deployment), black box or other methods.
- (3) To Determine the Principle:
According to the different phases of product life cycle and different characteristics of each phases, the principle of module partition can be categorized as principle of module partition for design, principle of module partition for manufacturing, principle of module partition for assembly, principle of module partition for maintenance, and principle of module partition for recycling. The principle of module partition is determined by the actual conditions of specific products and market requirements.
- (4) To Partition Functional Module
According to the basic principle of functional module partition, the overall function of product is partitioned reasonably to determine the sub-function modules, and to achieve reasonable function module partition.
- (5) To Partition Physical Structure Module
Modular design is to decompose a product or groups components into separate modules. Based on the functional module partition, according to the structural design requirements, production conditions, and assembly relationship of products, and abiding by the basic principles of structure module partition, the physical structure of the product is partitioned into several modules which consist of parts, components and groups components.
- (6) To Evaluate Scheme
After several module partition schemes have been evaluated by scientific theories and methods, a relatively optimal module partition scheme is selected.

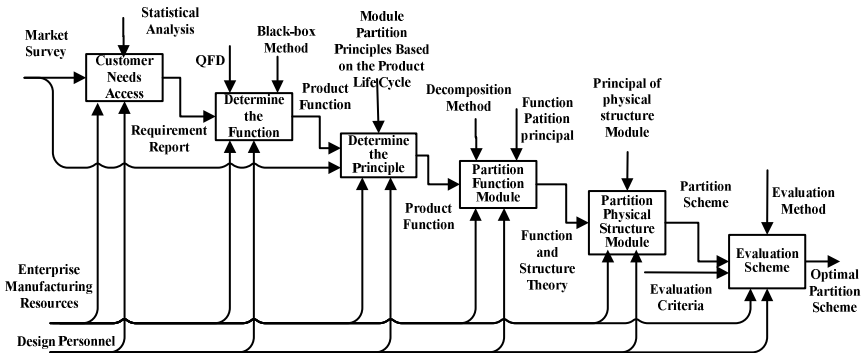


Fig. 1. Product module partition flow model

3 Principle of Module Partition

The principle of structure module partition should take into account the following factors: (1) Composability: (2) Principle of independence: (3) Machinability: (4) Components Principle: (5) Expandability: (6) The Principles of Basic Parts. The principles of module partition should be considered from a multidimensional perspective: taking into account not only the functional module partition and structure module partition of the NC machine tools, but also the different stages of the NC machine life cycle. The product life cycle is marked off as four phases: design, manufacture, maintenance and recycling. According to the specific circumstances of products what phase the module partition focuses on is determined by a few principles.

4 CNC Lathe Module Partition

CNC Lathe Functional Modules. This paper takes CNC lathe as a case study to explore the product module partition. Function analysis including the comprehension of function, decomposition and combination of functions, is an important means of engineering design. Function refers to the attributes of a product that meet customer needs, or the performance, usage and value that a product (or module) has. Based on market survey, the requirements of the CNC machine tools of horizontal series modular design, vertical series of modular design, full range of modular design and cross-series modular design are determined, and their main parameters are also determined accordingly.

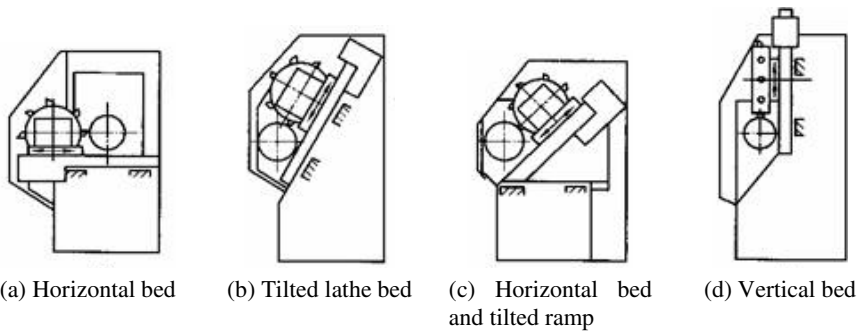


Fig. 2. Four Layout Form of Lathe

CNC Lathe Structure Module. The key of the modular design of CNC lathe lies in physical structure module partition. According to the characteristics of the product structure, the module partition is divided into three levels: level 1, level 2 and level 3 module. Level 1 module refers to the basic module of which the products are composed; Level 2 module refers to the functional modules that are divided on the basis of Level 1; and level 3 module is obtained by analogy. Module hierarchies can effectively expand the application of modular design. Generally, the mechanical structure system of typical CNC lathe consists of the following several level 1 modules:

1. lathe bed and its layout forms, including lathe bed of four layouts form (see figure 2).

2. Spindle Box and Transmission System: It is composed of normal servo motor spindle, high-speed motor spindle, hydraulic spindle and other types of spindle (level 2 module).

3. Feed Transmission System: It includes two types of feed systems: linear motor feed drive and servo motor drive.

4. Chuck System: It is classified into pneumatic clamping chuck, hydraulic clamping chuck, electromagnetic clamping chuck and other types.

5. Tool System: Tool system is composed of turret, tool magazine, automatic tool change device. Turret module includes dual turret, profiling turret, transfer turret, vertical shaft turret, back wheel turret and so on;

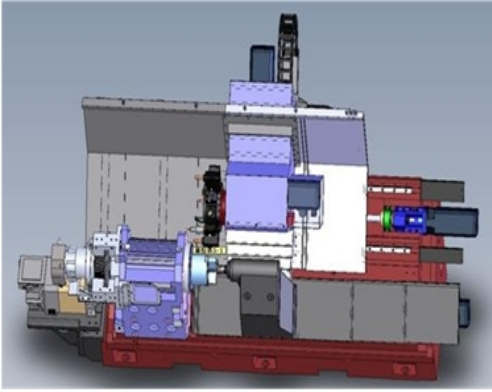
6. Tailstock: It includes mechanical tailstock, pneumatic tailstock, hydraulic tailstock and other types.;7. Lubrication System;8. Cooling System; 9. Chip Systems; 10. Hydraulic Station System

In a CNC machine tools company, the module in a HTC series of CNC Lathe is designed in accordance with the 10 kinds of 1st level module mentioned above. The table below is a series of CNC machine company HTC CNC lathe modular design parameter table.

Table 1. HTC Series CNC Lathe modular design parameters

HTC Series CNC Lathe modular design parameters				
Maximum turning diamete(mm)	160, 250, 320, 450, 630, 800			
Maximum turning length(mm)	350,460,550/960/1000/1500/2000/3000			
Spindle speed range(r/min)	Small lathe: 60-5000;	Medium-sized lathe: 45-4000;	Medium and large lathes 20-1800; 10-1200	
Main motor power	FANUC 0i-Mate kW	FANUC 0i-TC kW	SIMENS 802D kW	SIMENS 810D kW
	7.5/11/15	5.5/7.5/11/22/26/30/ 37/	12/16/21.5/3 0/37/41/51	16/21.5/30/ 37/41/51
Spindle bore diameter(mm)	43/62/70/80/104/130			
NC system	Siemens, Fanuc, GSK			
X-axis, z-axis motor				
guide rail				
X, Z-axis encoder	HEIDENHAIN			
Chuck type	manual chuck, electromagnetic chuck, pneumatic chuck, hydraulic chuck			
Hydraulic chuck	6 ", 8 ", 10 ", 12 "			
Tailstock sleeve diameter(mm)	60/80/100/130/150/180			
Tailstock sleeve taper	MT4, MT5, MT6			
Turret type	Horizontal servo power turret (Horizontal 6-position, horizontal 8-position, horizontal 12-position)			

5 Summary



In the design of CNC lathe, a series of products can be quickly designed through the modular design technology to meet customers personalized and diverse requirements of individual. The modular design can speed up the progress of product development of CNC lathes, shorten the manufacturing cycle, and lower manufacturing costs.

Fig. 3. Modular design of the htc2550 Horizontal CNC Lathe

Acknowledgements. The work presented is based on research supported by the Ministry of Industry and Information Technology of China (project number: 2009ZX04001-062 and 2009ZX04001-053) as well as the Science and Technology Department of Liaoning Province China. (project number: 2010020076-301).

References

1. Gu, P., Sosale, S.: Product modularization for life cycle engineering. *Robotics and Computer Integrated Manufacturing* 15, 387–401 (1999)
2. Su, M., Chen, W.-f.: The Machine module partition method for the client and life cycle. *Manufacture Information Engineering of China* 1(39),1:49–1:52 (2010)
3. Sun, N., Mei, X., Zhang, Y.: Product modular division based on house of quality matrix. *Journal of Xian Jiaotong University* 40(1), 46–49 (2006)
4. Jiang, H., et al.: Research on modular dividing method of machinery products. *Manufacturing Technology & Machine tool* 3, 9–10 (1999)

Risk Control Research on Chang Chun Street Networks with Intelligent Materials Based on Complex Network

Ling Zhang, Fan-sen Kong, and Yan-hua Ma

Institute of Mechanical Science and Engineering, Jilin University, Changchun, China
zlingjlu@yahoo.com.cn

Abstract. Complex network theory is used to study risk control of urban street network, and suggestions are put forward to avoid disaster under different emergency states with intelligent materials, which can improve the ability of information processing and information control. Changchun street network is taken as an example to study, it is found that the connectivity risk of traffic congestion is between random failures and deliberate attacks, which can provide a theoretical basis to improve the emergency response capability and risk control capability.

Keywords: Risk control, Intelligent materials, Street network, Complex Networks, Emergency.

1 Introduction

Facing abrupt accidents, the availability of streets becomes the focus, the reliability of street network is an important research and application of complex network theory in transportation [1, 2, 3, 4]. The connectivity of network is the basis of the research on reliability of street network [5]. The capability of network maintaining connectivity can measure the attack tolerance of network [6]. Connectivity reliability index is an important index when measuring the reliability of street network under emergency [1], and the capability of connectivity is based on the damage extent of key nodes. Albert (2000) considered two attack strategies: one is failure strategy and the other is selective attack strategy [3]. To street network, abrupt accidents include failure of nature disasters, failure of terrorist attacks and probability failure. This thesis intends to start from the measure of key nodes, then combine with the topological structure of different period, uses three failure modes to find out mutation points. Through observing the microcosmic change of nodes, research the discipline of network evolvement and construct basis to improve emergency response capacity.

2 Measure Index

In graph theory, people use parameter of graph connectivity to describe the attack tolerance of network, including the degree of connectivity and clustering coefficient proposed by Frank et al [7]. Connectivity degree is measured by characteristic path

length, and clustering coefficient is measured by density of network. So this thesis adopts characteristic path length, clustering coefficient, degree, degree distribution. Because connectivity efficiency is inverse proportional to shortest path length, so choose the inverse proportion of characteristic path length as efficiency index.

Characteristic Index of Complex Network. Degree is defined as the number of edge connected with nodes directly in undirected graph. Degree distribution $p(k)$ is the proportion of nodes whose degree is k , its expression is $p(k)=n(k)/N$. In above expression, $n(k)$ is the number of nodes whose degree is k properly, N is the number of nodes in the whole network. Degree can describe the wealthy extent of a node. Clustering coefficient C is defined as the average value of the clustering coefficient of each node. Clustering coefficient of a node is the quotient between the number of actual edge and the number of maximum edge. C can be defined as

$$C = \frac{1}{n} \sum_{i=1}^n \frac{l_i}{m_i(m_i - 1) / 2} \tag{1}$$

where l is the number of edge in G_i , and m is the number of nodes which are connected with node i directly. G_i is the subgraph of node i . Clustering coefficient is used to describe the density degree of network.

Characteristic path length L is the average valve of the shortest distance between any two nodes. The distance of two nodes is the number of shortest path edges which connects these two nodes. Characteristic path length is used to describe connectivity extent of network. The shorter L is, the better connectivity extent is. If a network has high clustering coefficient and short characteristic path length, people call it small-world network [8]. If its degree distribution follows power-law distribution, people call it scale-free network [9].

The connectivity efficiency of street network can be defined as

$$E = \frac{1}{N(N - 1)} \sum_{i \neq j \in G} \frac{1}{d_{ij}} \tag{2}$$

where N is the number of nodes in the whole network, d_{ij} is the shortest distance between node i and node j . If there is no path between node i and node j , then $d_{ij}=\infty$, consistently $e_{ij}=0$. E is used to measure connective condition between node i and node j .

Algorithm of Street Network Failure Simulation under Emergency

According to failure probability of the node, the emergency can be divided into three sorts: nature disaster, terrorist attack, traffic congestion. Nature disaster belongs to failure, the destroyed street is selected randomly; terrorist attack belongs to attack, the destroyed street is selected by the importance of node; traffic congestion belongs to probability failure, and the edges connected with node have different probability to fail based on their importance. How to identify the importance of node? We can choose node degree as an index simply [10].

Attack Failure Algorithm. Step 1: Initialize characteristic path length l_0 , the initial size of network is $S(0)=N$, the size of failure node is $SS(0)=0$, where N is the number of nodes in initial network; Step 2: Construct adjacency matrix of street network, if node i is connected with node j , $M(i, j)=1$, if node i isn't connected with

node j , $M(i, j)=0$; Step 3: Calculate and choose node with biggest degree and make it fail. Mark the degree of node i as k_i . If $\max(k)=0$, it means that all edges are deleted. Then algorithm can be stopped and all nodes fail. If $\max(k)\neq 0$, then set $[\max, n]=\max(k)$. It means that node n has the biggest node degree, and we choose node n to make it fail. Make elements in Row n of adjacency matrix M become 0, and make elements in Column n of adjacency matrix M become 0. Then, we obtain new adjacency matrix $M(t)(t=1,2,\dots)$; Step 4: Use floyed shortest distance algorithm to calculate the shortest distances and the shortest paths of network;

(a). Initialize distance matrix D and path matrix $path$, $D=(d_{ij})_{N\times N}=\text{zeros}(N)$, $path=\text{zeros}(N)$;

$$D(i, j) = d_{ij} = \begin{cases} M(i, j), M(i, j) \neq 0 \\ \text{inf}, \text{others} \end{cases} \tag{3}$$

$$path(i, j) = j, d_{ij} \neq \text{inf} \tag{4}$$

(b) Set $D(0)=D$;

(c) Calculate $d_{ij}(s)$ repeatedly, and

make $d_{ij}(s) = \min\{d_{ij}(s-1), d_{ik}(s-1) + d_{kj}(s-1)\}$

If $d_{ik}(s-1)+d_{kj}(s-1)<d_{ij}(s-1)$, then set $paths(i,j)= paths-1(i,k)$. If $D(s)$ and $path(s)$ don't vary any more, we obtain shortest distance matrix $D(t)$ and shortest path matrix $path(t)$; Step 5: Calculate the size of failed nodes and the size of network. If every element of a row in matrix $D(t)$ is inf, then the consistent node fails. Calculate the number of failed nodes and obtain $SS(t)$. Calculate the number of nodes in the biggest subgraph (the size of network). Choose consistent row elements and column elements as new $D(t)$. And $D(t)$ is the distance matrix of biggest subgraph. The size of biggest subgraph is $S(t)=\text{size}(D(t),2)$; Step 6: Calculate characteristic path length

$$L_t = \frac{\sum_{i=1}^{S(t)} \sum_{j=1}^{S(t)} d^t_{ij}}{S^t \times (S^t - 1)} (i \neq j) \tag{5}$$

If all nodes in network have failed, then set $S(t)=0$, and $L_t=0$; Step 7: Calculate network efficiency

$$E_t = \frac{\sum_{i=1}^{S(t)} \sum_{j=1}^{S(t)} \frac{1}{d^t_{ij}}}{S^t \times (S^t - 1)} (i \neq j) \tag{6}$$

If all nodes in network have failed, then set $S(t)=0$, and $E_t=0$; Step 8: Return to execute Step 2.

Probability Failure Algorithm. Step 1 and Step 2 are same to attack simulation; Step 3: Calculate degree of every node, find the biggest node degree value. Then, put all nodes into four levels, set failure probability $p=[0.2,0.4,0.6,0.8]$ (of course, people can adopt different values based on network condition); Step 4: Calculate degree of every node. Set the degree of node i as k_i . If $\sum(k)=0$, then all nodes and edges have failed, and algorithm can be stopped; If $\sum(k)\neq 0$, then choose node with biggest degree to make it fail; Step 5, Step 6, Step 7, Step 8 are same to attack simulation; Step 9: Return and execute step 4.

Random Failure Algorithm. The process of failure simulation: Firstly, choose an edge randomly and make it fail. Then, calculate the size of network, characteristic path length and network efficiency. Then choose an edge randomly and make it fail. Do this operation repeatedly until all nodes are failed.

Simulation Model

Characteristic of Changchun Street Network. This thesis selects a region of Changchun and this region has 59 streets. After calculating, we obtain the basic statistical characteristics of Changchun street network. The top ten shortest path lengths are shown in Table [1]. Then we use software to calculate characteristic path length $L=2.618$, clustering coefficient $C=0.2154$. Because of short L and high C ($C=0.2154 \gg 1/59$), Changchun street network has small-world effect.

Table 1. Basic statistic Features of Street Network

Street	L	degree	C
Jiefang	1.8448	15	0.0762
Renmin	1.8621	17	0.1029
Kaiyun	2.0172	12	0.0758
Nanhu	2.0517	12	0.1061
Xi'an	2.1207	10	0.0667
Gongnong	2.1552	8	0.3214
Yatai	2.1724	10	0.1111
Ziyou	2.1724	10	0.0889
Changchun	2.2414	8	0.2143
Weixing	2.2414	8	0

Figure 1a is the relation between node degree and degree distribution. Figure 1b is the double logarithm relation between node degree and degree distribution. It follows linear relationship nearly. It shows that Changchun street network is a scale-free network, and its degree distribution follows power-law distribution. Through calculating, we obtain that power-law index equals to 1.54. So Changchun street network has small-world effect and scale-free property.



Fig. 1. Relationship Between Degree and Degree Distribution

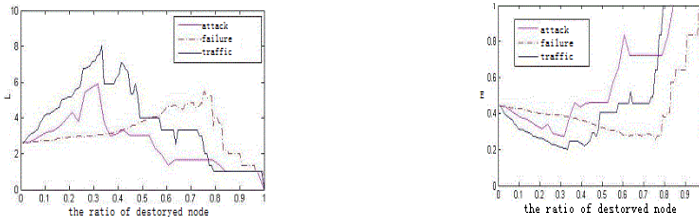


Fig. 2. Comparison of the Characteristic Path Length and Efficiency under Different Failure Mode

Simulation Result Comparison. In Fig.2, compared with failure, network efficiency under attack and traffic congestion varies more quickly. Inflection under attack condition appears much earlier than under traffic congestion. And the variable scale of characteristic path length and network efficiency under attack condition is less than that under traffic congestion. In other words, attack can destroy network more quickly and it gives people less time to response to emergency. The reason is explained as follows: In attack condition, one street is destroyed completely. It means that all edges connected with chosen node are failed. While in traffic congestion, one street is destroyed partly. It means that only few edges connected with chosen node are failed. According to the fact, we think that the intersections of street with more intersections have high failure probability. So in traffic congestion, the characteristic path length becomes longer continuously. In real life, it means that there has new intersection becomes not connected, and it results in that we need to detour other street when arriving at our goals. With the accumulation of time, initial network is divided into several subgraphs. Below, we will study network characteristic of key point. So we can understand destruction extent brought by abrupt accidents clearly and we can improve speediness of emergency response.

3 Conclusion

The theory of complex network is used to research the relationship between the structure of street network and its risk control capability. The Changchun street network is taken as research object, develops three kinds of failure algorithm and analyzes the street network failure risk. Through analyzing and finding important nodes and points, we can improve the risk resistance capability of street network

existed. If the intelligent materials are used in information processing and information controlling of street network, then the intelligent transportation can be formed, which can improve the utility of transportation resources, reduce traffic congestion risk, improve emergency response capabilities when under different emergencies, build targeted prevention and emergency management system, offer references to establish effective emergency rescue plan.

References

1. Deng, Y.J., Yang, Y.F., Ma, R.G.: Highway Network Structure Characteristics Based on Complex Network Theory. *China Journal of Highway and Transport* 23, 98–103 (2010)
2. Callaway, D.S., Newman, M.E.J., Strogatz, S.H.: Network robustness and fragility: Percolation on random graphs. *Phys. Rev. Lett.* 85, 5468–5471 (2000)
3. Albert, R., Jeong, H., Barabási, A.-L.: Attack and Error Tolerance of Complex Networks. *Nature* 406, 387–482 (2000)
4. Gallos, L.K.R., Cohen, P.A.: Stability and Topology of Scale-free Networks under Attack and Defense Strategies. *Phys. Rev. Lett.* 94, 188701 (2005)
5. Yasunori, I.: Basic Concepts and Future Directions of Road Network Reliability Analysis. *Journal of Advanced Transportation* 33, 125–134 (1999)
6. Zhao, J., Guo, P., Wu, J., Deng, H.Z., Tan, Y.J.: Review on the Reliability of Complex Networks. *Journal Of Logistical Engineering University* 26, 72–79 (2010)
7. Frank, H., Frisch, I.T.: Analysis and Design of Survivable Network. *IEEE Transaction on Communication Technology* (18), 501–519 (1970)
8. Watts, D.J., Strogatz, S.H.: Collective Dynamics of Small-world Networks. *Nature* 393, 409–410 (1998)
9. Barabasi, A.L., Albert, R.: Emergence of Scaling in Random Networks. *Science* 286, 509–512 (1999)
10. Tan, Y.J., Wu, J., Deng, H.Z.: Evaluation Method for Node Importance based on Node Contraction in Complex Networks. *Systems Engineering-Theory & Practice* 11, 79–83 (2006)

Research on Semantic Web Services Composing System Based on Multi-Agent

Junwei Luo¹ and Huimin Luo²

¹ College of Computer Science and Technology, Henan Polytechnic University,
Jiaozuo, China

ljwonly@yahoo.com.cn

² School of Computer and Information Engineering, Henan University, Kaifeng, China
hmluo_henu@yahoo.com.cn

Abstract. Nowadays, a huge amount of web services are deployed on the Web and there are a lot of requests that cannot be fulfilled using just one web service. For using web services, composing individual services to create composite web service to fulfill the users' request is necessary in most cases. The Semantic Web Service and Multi-Agent are effective means for fulfilling more and more complex requests. So, it is very important to develop a system built on seamlessly integrating Intelligent Agents and Semantic Web Services for composing and assessing available services automatically and precisely. In this paper we developed a new Semantic Web Service Composing System.

Keywords: Semantic Web Service, Multi-Agent, Web Service Composing.

1 Introduction

According to the user's application requirements, Web service composition, making use of existing web services, aims at forming a new more powerful web service to meet the users' complex needs by automatically selecting other web services in certain rules. The new composite web service meets not only the functional requirements, but also some other special service's requirements, for example: costs, expenses, operating time and so on.

Today, a lot of techniques are proposed for manual service composition. But creating composite services manually is hard and time consuming task for the user. So the automatic composition of web services is a recent trend to deal with the aforementioned problem[1,2]. Methods of automatic composition of web services use semantic technology to describe users' needs and composition rules, and use reasoning, planning and other methods to complete web service composition automatically. A complete web services composing at least should include four phases: demand, composition, assessing and feedback. Only through the cooperation and effective interaction of the four phases, we can build a composite web service to meet users' complex needs.

So, there are some weaknesses in previous studies.

On one hand, previous studies only involves the development phase, referring to web service composition and evaluation phase, does not involve other phases, it is not easy to grasp the user's needs and the situation of dynamic composition.

On the other hand, there is no effective means to help interacting with each other in four phases.

To solve these problems, in this paper, we develop a new Semantic Web Service Composing System which include web service and users' requests collecting, semantic description, web service composing, assessing and feedback.

The joint application of semantic web and web services in order to create intelligent web services is referred to as semantic web services (SWS). SWS are a step forward in the way to a Next Generation Web. They consist in describing web services with semantic content so that service discovery, composition and invocation can be done automatically by, for example, the use of intelligent agents able to process the semantic information provided.

Agent technology appeared in the 70s of the 20th century. Agent can be defined as: an entity has the capacity of calculating, perceiving, reasoning, operating and communicating. Multi-agent system (MAS) can be seen as a system consisting of a group of agents that can potentially interact with each other. MAS present several advantages over isolated agents, such as reliability and robustness, modularity and scalability, adaptivity, concurrency and parallelism, and dynamism[3].

The combination of semantic web service and Multi-agent technology has the following features: (1) Adaptability: Based on the information of users' behaviors in internet, Agent can discover the users' interest, reason the user's needs and establish personalized documentation for each user; (2) Initiative: Agent can initiatively retrieve the corresponding information based on users' demand, and even can monitor the changes of information sources; (3) Collaborative: Agents can share the information with other Agents. For example, a user's Agent can access to a lot of useful information from other users' Agents that have the same data about users' interest[4,5].

This work makes the following contributions:

It presents an overall solution for web service composing. The new complete system of semantic web service composing based on multi-agent is discussed, in which (1)web services provide the more basic level functionality and agents provide higher-level functions by using, combining and choreographing web services, so achieving added-value functions; (2) communication in web services and agents becomes equivalent, so the distinction between them disappears.

The remaining of the paper is arranged as follows. In Section Two we propose the new complete system of semantic web service composing based on multi-agent. In Section Three we discuss the architecture of the system. The paper is concluded in Section Four.

2 Semantic Web Services Composing System Model

W3C recommends a language, named Web Ontology Language for Services (OWL-S), which is becoming more and more popular for creating and annotating semantic web services. It includes three parts. ServiceProfile tells "what the service does" and includes a description of what is accomplished by the service, limitations on service applicability and quality of service, and requirements that the service requester must

satisfy to use the service successfully. ServiceModel tells a client how to use the service by detailing the semantic content of requests, the conditions under which particular outcomes will occur, and, where necessary, the step by step processes leading to those outcomes. It may be used in at least four different ways: (1) to perform a more in-depth analysis of whether the service meets its needs; (2) to compose service descriptions from multiple services to perform a specific task; (3) during the course of the service enactment, to coordinate the activities of the different participants; and (4) to monitor the execution of the service. ServiceGrounding provides the detailed information of how to access the web service like protocols and message format, transport, serialization and addressing[6].

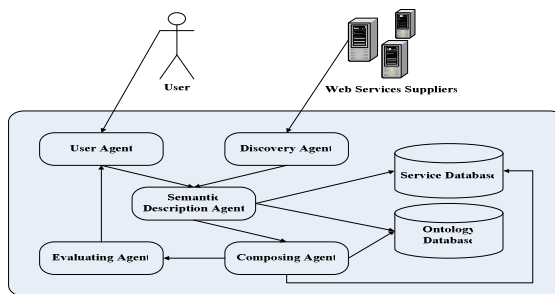


Fig. 1. Semantic Web Services Composing System Model

Generally speaking, the ServiceProfile provides the information needed to discover a service, while the ServiceModel and ServiceGrounding, taken together, provide enough information to make use of a service. The Semantic Web Service Composing system designed utilizes OWL-S and Multi-agent technology as the basis to transform users' queries and web services in internet into semantic pattern as triples: ServiceProfile, ServiceModel and ServiceGrounding, so as to complete composing web services automatically and precisely.

The Semantic Web Services Composing System Model is shown in Fig. 1.

3 Architecture of Semantic Web Service Composing System

3.1 User Agent

User Agent includes Input Module, Memory Base, Knowledge Base, Learning Machine and Output Module (Shown in Fig. 2). The Input module in the User Agent aims at receiving and storing Users' queries. Memory Base records users' personal information, for example, individual's occupation, age, sex, education, hobbies, etc. Knowledge Base includes Statistical model, logistics model, optimization model and so on. Learning Machine is used to summary the behavior of users and formats the information. Output Module outputs the standard queries based on analysis.

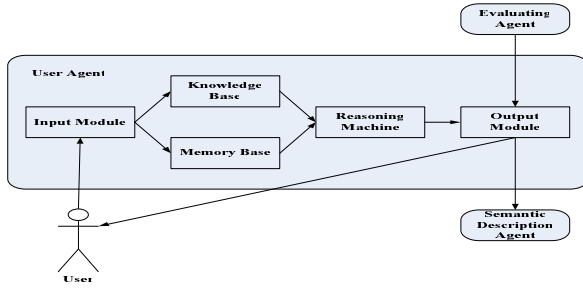


Fig. 2. User Agent

3.2 Discovery Agent

Discovery Agent mainly includes Discovery Module, Discovery Optimization and Module Base. (Shown in Fig. 3). Module Base includes Discovery strategy, Discovery Module and Algorithm. Discovery Optimization includes Optimization module which determine which web service should be searched firstly and which web service should be ignored. Discovery Module is a program that detecting web services in internet based on the Module Base and Discovery Optimization.

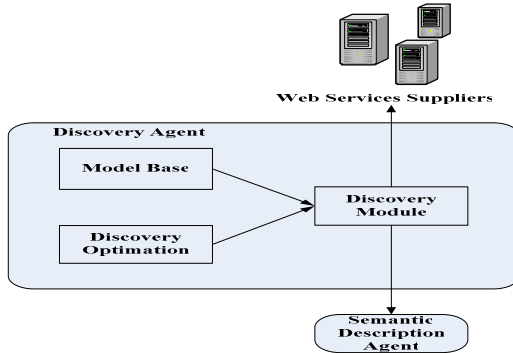


Fig. 3. Discovery Agent

3.3 Semantic Description Agent

Semantic Description Agent (Shown in Fig.4): it aims to mine the semantic features in the users' queries and web services. It will make use of agent technologies, natural language processing technology, ontology technologies and other technologies to analyze the nature of words, structure and association relation in the users' queries and web services to extract semantic features. This module contains the following four components: Content preprocessing: While processing web services, this component will filter the web services in different formats and identify and eliminate the noise content. Web services classification and index web services will be also completed. Semantic Analyzing: This component identified semantics elements like

ServiceProfile, ServiceModel and ServiceGrounding in the content and analyzes their relations. Semantic Extension: This component utilizes latent semantic analysis to create more semantic features for matching and composing. This component solves the problem of query failure due to lack of required keywords in the query sentence even when only limited information of query content is available. Semantic Construction: This component finally will construct the semantic pattern of the content according to Semantic Analyzing and Semantic Extension.

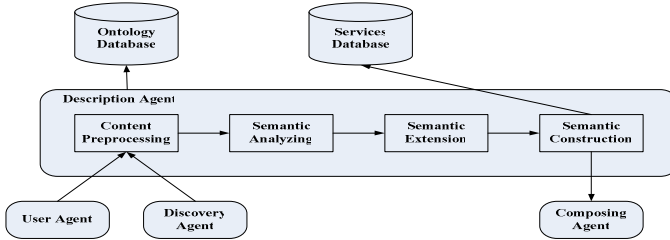


Fig. 4. Semantic Description Agent

3.4 Composing Agent

In the process, matching and composing algorithms are presented to enable fast matching and composing web services. The components included in this module are: Knowledge Base, Model Base, and Composing Module. (Shown in Fig. 5). Knowledge base: It includes the user's personalized information transmitted by the User Agent. When matching and composing, Semantic Matching and composing will make use of users' personalize information (users' gender, users' age, users' occupation, users' search history and so on) to search more accurate and useful web services for users. Model Base: It includes a variety of web service mathing and composing models and algorithms, for example: Bayesian Probability Model, Support Vector Machine (SVM), Neural Network Algorithm and so on. It also includes new algorithms based on semantic pattern which can solve some traditional problems. Composing Module: According to the Model Base and users' queries, this component will chose apposite model and algorithm to matches web services and composing composite web service to fulfill complex tasks.

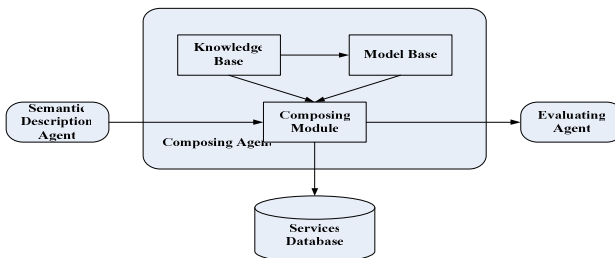


Fig. 5. Composing Agent

3.5 Evaluating Agent

Evaluating Agent includes Model Base, Evaluating Index, Evaluating Module and Results Choosing (Shown in Fig. 6). Model Base: It includes web service evaluating modules. Evaluating Index: It includes Cost, Response Time, Availability, Reliability, Reputation, Security and so on. Evaluating Module: According to Model Base and Evaluating Index, this component will score every composing web service. Results Choosing: This component will sort every composing web service by descending order.

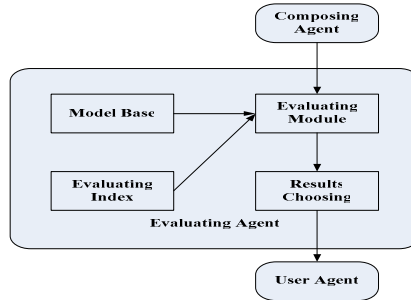


Fig. 6. Evaluating Agent

4 Ontology Database and Services Database

The ontology database supports the communication among the components in the framework. It also includes the knowledge about the environment it possesses. This ontology generally includes knowledge about the assigned tasks and the ontology also contains the semantic description of Web Services are stored.

5 Summary

In this study, a new Semantic Web Service Composing System based on Multi-Agent has been presented to effectively overcome existing defects and constraints of the traditional methods, and help users to obtain composite web service and fulfill complex needs.

References

1. Medjahed, B., Bouguettaya, A., Elmagarmid, A.K.: VLDB Journal 12, 333 (2003)
2. Prashant, D., Goodwin, R., Akkiraju, R., Verma, K.: International Journal of Web Services Research 2, 213 (2006)
3. Maes, P.: Communications of the ACM 37, 31 (1994)
4. Wu, D., Sirin, E., Hendler, J., Nau, D.: Htn: Journal of Web Semantics 1, 112 (2004)
5. Elamy, A.H.: AgentLink News 18, 19 (2005)
6. Information on, <http://www.w3.org/Submission/OWL-S/>

Approach of the Secure Communication Mechanism for the Off-Site Live Virtual Machine Migrations

Xinnian Wang¹ and Yanlin Chen²

¹ School of Computer Science, South-central University for Nationalities,
Wuhan 430074, China

² College of Chemistry and Environmental Engineering, Hubei University of Technology,
Wuhan 430068, China

Caridle@qq.com, Chenyl@126.com

Abstract. The virtual machines of cloud computing platform deployed in the enterprise need remote off-site live migration, but the bandwidth and WAN security factors could cause communication delay and can not penetrate the firewalls two-way, at the same time system has the shortcomings of counterfeiting and vulnerable during communication, so we need a new structure and the communication mechanism of live migration to ensure migration safe and reliable. This paper designs the off-site live migration structure for confidentiality, integrity and penetration requirements, and puts forward a new secure communications protocol underlying SUDP to discuss the authentication and messaging security.

Keywords: Cloud computing, Live virtual machine migration, Secure communication mechanism.

1 Introduction

The virtual machines of cloud computing platform deployed in the enterprise need remote off-site live migration, but the bandwidth and WAN security factors could cause communication delay and can not penetrate the firewalls two-way, at the same system has the shortcomings of counterfeiting and vulnerable during communication, so we need a new structure and the communication mechanism of live migration to ensure migration safe and reliable. Currently the live virtual machine migrations mainly occur on the local area network environment[1,2] without considering the concentration of off-site remote disaster recovery business environment, especially the environment of disaster and WAN requires high speed communication, a small delay and two-way communications to penetrate any protection system for wide area network such as firewalls, the current connection-oriented TCP protocol can not meet this requirements which is a fatal weakness; Another factor is considered to authenticate every function component include the communication to prevent fake, theft and attacks; Finally, we must consider the disaster recovery, the current live migration structure has single migration management center (MMC), if MMC fails, the live migration will fail, so there will be a backup MMC to manage local virtual

machines in the off-site side. In summary, this paper first proposed the live migration structure include the main and backup MMC, and discuss the structure’s communication mechanism.

2 The Off-Site Live Migration Structure

Fig. 1 describes an off-site live virtual machine migration system structure. The structure includes the main MMC, the backup MMC, the local authenticated Migration Agent (MA) and the local authenticated System Monitoring Agent (SMA).

MA and SMA communicate with the MMC and get the corresponding strategy. SMA gets the local server CPU parameter, memory parameter and network bandwidth usage to provide local resources to MMC, MA receives MMC’s migration instructions and executes the actual migration operations.

In a virtual environment, VMM is responsible for scheduling the virtual machine and fetches the relevant virtual devices’ parameters and operations; SMA gets the relevant independent nodes parameters and provides MMC with the corresponding parameters periodically. The relevant parameters can be expressed as $S = \{S_Cpu, S_Mem, S_Net\}$, here, S_Cpu is the virtual machine CPU usage, S_Mem is virtual machine memory usage and S_Net is virtual machine network traffic.

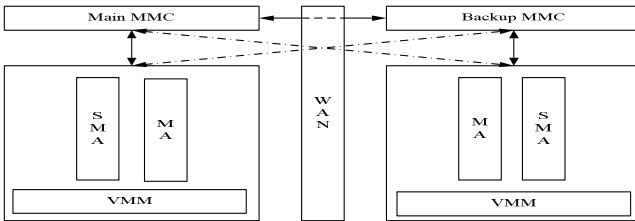


Fig. 1. The off-site live virtual machine migration system structure

MMC masters the use of physical resources as a whole and starts the remote live virtual machine migrations on demand according to the default strategy for load balancing within the platform. MMC has the corresponding management modules to control MA and SMA respectively. MMC gets the parameters via MMC and analyses the relevant parameters S to determine whether and how to start launching the live migration of virtual machines operating. Whether the live virtual machine migration starts, Service-Level Agreements (SLA) can not be met, such as $S_Net <En, En$ is the default bandwidth, $S_Cpu > Up$, Up is CPU utilization scheduled, S_Mem represents whether physical server’s memory swapped out frequently.

All agents and MMCs need to communicate with each other, such as data synchronization strategies, the corresponding messages and data transmitted, which will involve the establishment of secure communication mechanism for the remote live virtual machine migrations in different places. DES encryption and decryption algorithm are applied to ensure the data transmission.

3 The Communication Mechanism

Agent Communication Language[3] is an important content on the communication between agents and MMCs, it includes definition, processing and semantic interpretation[4] of the communication language. KQML is currently the most frequently ACL, it is an interface library and it is not compiled and interpreted language, programmers still need to provide code to deal with each communication primitive, more importantly, KQML does not take into account the requirements of secure communications, it is not suitable for network security system, although some scholars expanded its security on communications in the original language KQML, but they only provided a basis for secure public key system communication model, there was no concrete implementation and application[5,6].

Generally speaking, agent Communication use binary stream socket communications from the kernel of the operator system, certainly it can be used call mechanism of RPC remote procedure[7]. A protocol is constructed based on UDP as a message, code, data transmission security kernel communication architecture, combined with common security technology and agent special applications for safe live migration, this protocol is named as SUDP (Safe UDP) protocol.

In the standard TCP/IP protocol, UDP is much faster than TCP for data transition, the program implementation is relatively simple, its disadvantage is easy to lose data packets, further, it cannot re-sent and assembly packets automatically, it has no data security mechanism and can not send data packets which exceed 2K, Otherwise, occur error. In a complex network communication environment, you may need to send large amounts of data packets (eg, policy data replication) and the communication speed must be ensured, the important data can not be lost, which requires SUDP protocol.

In comparison with TCP, first, it is possible to cross the firewall in the WAN, TCP can not be good through NAT for point to point communication. Second, the communication process does not need to lose some important messages, TCP need to first establish a connection, each packet requires confirmation to lead to a lot slower speed. Finally, using SUDP send any size packet, it can guarantee the package will not lose some important and can easily penetrate the NAT for point to point communication.

SUDP has the following characteristics: Split and assembly packets automatically; Support to send any size packets at one time; Support security control (include AMP messaging protocol); Adjust the communication speed according to the network speed and packet loss rate. Therefore, the communication protocol is mainly based on SUDP, the implementation process as shown in Fig. 2.

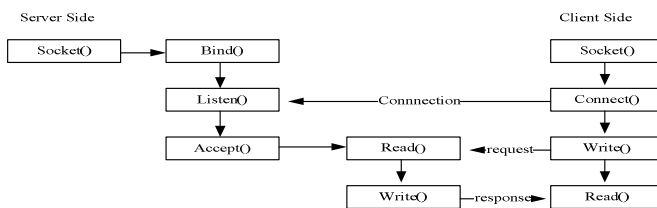


Fig. 2. Message transmission process based on socket

The Agents are sometimes necessary to communicate directly, the transmit message is less and mainly related to the notification message, such as the MMC message notification for MA, a lot of traffic message is relate with a direct communication between the MMCs, which is similar to the Blackboard Model.

Agents communication with the blackboard and obtain the corresponding authentication to make a relation with each other, where the blackboard that is MMC. SMA and MA is very similar to the Blackboard Model, with the MMC board they can better finish the cooperative task between SMA and MA to improve the quality of communication [8].

Message transmit structure, in essence, is based on socket communication, as shown in Fig. 2, SUDP implementation is based on the socket communication, Socket () is a socket function, Bind () binds to the socket on a port, and then activate the detection listening Listen (), Accept () accepts data, Read () and Write () reads and writes data in the buffer accordingly, Connect () is connected to the server's port. Agents communication use message transmit structure, it is a basis of flexible and complex coordinative strategies, in a word, and the virtual machines can be monitored by using the similar blackboard system to reflect the intermediate state between the transmissions of information. Meanwhile, whether agents exist in the network or their identifications can be authorized, MMC on the blackboard is the dispatcher to be shown in form of network message.

4 Agent Authentication

4.1 Agent's Identity Authentication System

In this paper, symmetric key system is used, that is the shared secret key to ensure secure communication between the agents.

Definition 1: The registration code sends connection request to MMC, MMC randomly assigns a string value of M; the registration code is only valid in this connection session, a new one will generate in the next re-connection, therefore, the registration code can be used as the secret key associated with session itself.

Definition 2: Each agent has its own fixed ID number, agent's ID number is relative to the registration key M, Bios_Serial, denoted Agent_Id. Expression is: $Agent_Id = M \parallel Bios_Serial$.

Definition 3: Agent-shared key with the MMC for the registration key M, Bios_Serial of the Hash value, that is, $K = GetHash (Agent_Id)$.

Assumption 1: M is a registration key 128-bit random string, it is can not be cracked by exhaustive list.

Proposition 1: All agents in different domains have different registration number and different Agent_Id, which is unique.

Definition 1 reflects the difference between communication entities. Definition 3 ensures the key's privacy. Assumption 1 is the prerequisite and basis for secure communications of the distributed agents; a registration code is enough long to ensure

that the password brute-force attack is almost impossible. Proposition 1 show the uniqueness of agent; you can record, detect and manage agents through the registration and cancellation.

If agents and MMC communicate to complete collaborative tasks, agents must first be authenticated. Authorized authentication method is a simple way to apply in the promotion of the system. Agents first apply for registration from MMC, and authorized by the administrator in MMC console to obtain a registration code, store it in memory. However, the weakness of this method is: 1) registration code stored in the server side, once stolen, the system passwords are not safe for all users; 2) can not resist the replay attack [9,10,11], the attacker License information can be intercepted to lead to the system threat through legitimate authentication request of license agent to MMC.

MMC does not stored the user's plaintext Agent_Id directly, it stores the ciphertext of one-way hash value to solve the first weakness [11,12], MMC can generate the hash value according to M and the appropriate virtual machine information to store in MMC.

4.2 C-R Certification

Agent must be authenticated in a limited life cycle in communication with MMC, MMC carries out certification using a simple "Challenge-Response(C-R)" approach through the three-way handshake, PPP CHAP protocol is used as authentication method. This certification means that the characteristics of absorption shown in Fig. 3.

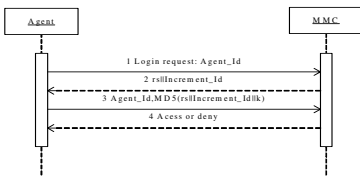


Fig. 3. C-R authentication



Fig. 4. C-R complex and authentication

MMC sends a challenge message and the incremental identifier to the Agent, the challenge message is generally a random number;

Agent sends back a response to the MMC, the response is calculated by the hash function, the input parameters have the identifier of this certification, the secret key and challenge message;

MMC receive a response compared with the hash function value calculated by the identifier, the secret key and the challenge message, if the match is certified to the Agent send a "success" message, or send a "failure" message to cut off the services of the Agent.

The network listener can not get the key plaintext in the certification process because of the content transmission through hash function, such as the MD5 encryption algorithm. In addition, MMC each selected different random challenge number, hacker obtains transmission to get the original contents but replay attack is not certified. Incremental change in Fig. 3 for the MMC host identifier time, the time synchronizes with client time to solve the replay attack.

4.3 The Complex C-R Certification

The complex authentication method is used to solve agent certification with MMC. The process shown in Fig. 4, described as follows:

MMC send a message to agent: "DES (rs, k)". Where, k by the "K = MD5 (Agent_ID)" merger, DES symmetric encryption algorithm. Agent can decrypt "DES (rs, k)" according to Agent_Id, and then calculate rs;

Agent sends back a response to the MMC: "MD5 (rc), DES (rs || rc, k)". Where, the first part of the message is the hash value of the random number rc, other part combines rs with rc, and encrypt using k; only the basic rules library of Agent on MMC retains k value, when MMC receives the response from agent, MMC decrypts and certifies. If rs values match, then MMC trusts agent and sends a message to agent: "DES (rc || ts || LoginState, k)";

Agent with the correct key can decrypt "DES (rc || ts || LoginState, k)", and verify rc. If match, agent trusts MMC, and then adjust LoginState accordingly, and adjust the host time same as MMC ts, this is a trust validation cycles. By improving processes, solving agent and MMC's mutual authentication, it can block hacker attacks launched by the network listener, replay attacks and middle attacks.

5 Summary

The paper proposes a structure for the off-site live virtual machine migrations based on cloud computing platform deployed in the enterprise, this is a good solution to solve remote disaster recovery of virtual machine load balancing, and discusses secure communication problems. The next step will be further testing and optimization on the open source virtualization software, such as the KVM and Xen VMM.

References

1. Ma, F., Liu, F., Liu, Z.: Live virtual machine migration based on improved pre-copy approach. In: 2010 IEEE International Conference on Software Engineering and Service Sciences (ICSESS), July 2010, pp. 230–233 (2010)
2. Hai, J., Li, D., Song, W., et al.: Live virtual machine migration with adaptive, memory compression. In: IEEE International Conference on Cluster Computing and Workshops, CLUSTER 2009, September 2009, pp. 1–10 (2009)
3. Landor, S.E.: Issues in multiAgent systems. *IEEE Expert Mag.*, 18–26 (April 1997)
4. Finin, T., Weber, J.: Draft Specification of the KQML Agent-Communication Language, June 15 (1993)
5. Thirunavukkarasuy, C., Finin, T., Mayfield, J.: Secret Agents-A Security Architecture for the KQML Agent Communication Language. Draft submitted to the CIKM 1995 Intelligent Information Agents Workshop, Baltimore (December 1995)
6. Wong, H.C., Sycara, K.: Adding security and trust to multi-Agent systems. In: Proc. Autonomous Agents 1999 workshop on deception, fraud and trust in Agent societies, pp. 146–161 (1999)
7. Manvi, S.S., Venkataram, P.: Applications of Agent technology in communications: a review. *Computer Communications* 27(15), 1493–1508 (2004)

8. Jiang, Y.C., Xia, Z.Y., Zhong, Y.P., Zhang, S.Y.: An adaptive adjusting mechanism for Agent distributed blackboard architecture. *Microprocessors and Microsystems* 29(1), 9–20 (2005)
9. Lennon, R.E., Matyas, S.M.: Cryptographic authentication of time invariant quantities. *IEEE Trans. Comm.* 29(6), 773–777 (1981)
10. Evans, W.K.: A user authentication scheme for requiring secrecy in the computer. *Comm. ACM* 17(8), 437–442 (1974)
11. Morris, K.T.: Password security: A case history, *UNIX Programmer's manual*, 7 edn., 2B (1979)
12. Giuseppe, R., Antonio, I., Sergio, P.: 802.11-Based Wireless-LAN and UMTS interworking: requirements, proposed solutions and open issues. *Computer Networks* 47(2), 151–166 (2005)

Author Index

- An, Xiaodong 25
- Bai, Xiaoping 561
Bai, Ye 113, 119
Bingqing, Ye 191
- Cai, Yuehua 285, 291
Cao, GuoHua 517
Cao, Jian 715
Chang, Ande 549
Chen, GuoHua 567
Chen, Hongqian 709, 715
Chen, Song 345
Chen, WenLue 179
Chen, WJing 735
Chen, Xiucui 421
Chen, Yanlin 767
Chen, Yi 709, 715
Cheng, Songliang 71
Cheng, XiaoJun 621
Chi, XiaoNi 179
Chu, Mei 539
Cui, Jianzhu 381
Cui, Peng 363
- Dai, ZuCheng 439
De-li, Yao 677
Deng, Chao 169
Deng, ZhiPing 137
Diao, RuiJiang 99
Dong, Shuoqi 25
Dong, ZengShou 339
Du, Honglei 447
- Fang, Liang 39
Feng, Bing 509
Feng, Zhao 387
- Gao, Guohong 595, 601
Gao, Hongwei 653
Gao, Yang 659
Gao, Yanghua 727
Gu, XueJing 99
Gu, Yu 345
Guo, Jiao 567
Guo, Wanli 403
Guoyang, Wu 303
- Han, Dan 327
Han, Jie 169
Hao, YueJun 339
He, Guizhen 621
He, Jia-zhi 357
He, Ling 315
He, LiuJie 83
He, Yi 357
Hsieh, Tsui-Chuan 647
Hu, ChaoJu 251
Hu, YuPing 43
Hu, Zhijuan 131
Huang, Chuanjin 185
Huang, Haiquan 375
Huang, Songbo 453
- Ji, Huawei 13
Jia, JiLin 7
Jiang, Guiyan 549
Jiang, Haining 309, 427
Jiang, Ping 137

- Jiang, Rong 297
 Jiang, YongMing 491
 Jian-guo, Wang 677
 Jiao, Peng 533
 Jing-rong, Dong 393

 Kong, Fan-sen 755

 Li, Feng 467
 Li, HaiYan 439
 Li, Han 39
 Li, Huan 615
 Li, Hui-na 169
 Li, Husong 175
 Li, Jing 197, 381
 Li, Lan 105
 Li, Min 671
 Li, MingYang 333
 Li, Mingzhu 125
 Li, Ning 543
 Li, Qing 99
 Li, Sheng 77
 Li, Wandong 25
 Li, Yan 381
 Li, Yang 543
 Li, Yan Su 227
 Li, Yi 157
 Li, Yongfeng 63
 Li, Zhipeng 381
 Li, Zhong 265
 Li, Zongying 19
 Liang, WenJuan 271
 Lifeng, Han 387
 Lin, Jie 131
 Lin, Yuyuan 375
 Liu, Fugang 743
 Liu, GuoYi 95
 Liu, Huanbin 215
 Liu, Jie 245
 Liu, Jun 251
 Liu, Li 709
 Liu, Man 539
 Liu, Ruixiang 665, 683
 Liu, Shengman 203
 Liu, Shuo 415
 Liu, WeiWei 105
 Liu, Xifeng 185
 Liu, Xingrui 601
 Liu, Ying 447
 Liu, Yongqi 665, 683

 Liu, YongXian 749
 Liu, Yubin 57, 89, 461
 Liu, Yucheng 57, 89, 461
 Liu, Zaiwen 25
 Liu, Zhen 583, 589, 629, 635
 Lou, Xiaodan 277
 Lu, Yuzhuang 583
 Luo, Huimin 761
 Luo, Junwei 761
 Luo, Yuan 485

 Ma, Jian 151
 Ma, Ming 233
 Ma, Yan-hua 755
 Meng, Jian 665, 683
 Meng, Wu Xiao 221, 227
 Miao, XiaoKun 333

 Nan, Tang 221
 Niu, Shifeng 549
 Niu, Xiaoying 433

 Pan, Shaowei 175
 Peng, Guobin 239, 573
 Piao, ShengHua 567
 Pu, Feng Shan 371

 Qian, KaiGuo 439
 Qian, Yuexia 525
 Qiang, Li 387
 Qin, Zheng 615
 Qiu, Taorong 375
 Qu, Qingwen 277

 Rao, Congjun 215
 Ren, JianHua 577

 Sha, Shi 473
 Shen, Jianying 13
 Shi, Hongyan 539
 Shi, Sha 125
 Shi, ShengBo 607
 Shiand, Wei 185
 Song, Jianhui 653
 Song, Qing 485
 Song, RenWang 339
 Song, YuLong 517
 Sun, Haiyi 543
 Sun, Hongxiang 473
 Sun, XiuYing 197

- Sun, Ying 689, 703, 721
 Sun, Yuehong 709, 715

 Tan, HangSheng 491
 Tan, MLing 735
 Tan, Wenxue 51
 Tang, Di 555
 Tang, Minli 315
 Tang, Weiqin 351
 Tang, Xianlun 727
 Tao, Guozheng 525
 Tong, GuoPing 77
 Tu, YongQiu 567

 Wan, Wenlong 583, 589, 629, 635
 Wang, Bing 409
 Wang, Cheng 209
 Wang, Chengjun 277
 Wang, Dongsheng 421
 Wang, Fuqiang 595
 Wang, Guoqing 403
 Wang, Jianqiang 113, 119
 Wang, Jinlin 479
 Wang, Lei 321, 327
 Wang, Minqin 641
 Wang, Ping 381
 Wang, QingTuan 83
 Wang, Tao 539
 Wang, Tingtai 203
 Wang, Xiaoyi 25
 Wang, Xinnian 767
 Wang, Xiping 51
 Wang, Xu 615
 Wang, Yuefen 157
 Wei, Yong 77
 Wen, Qiaoyan 125, 143, 163, 473
 Wu, Hengyu 315
 Wu, Lu 131
 Wu, ShuFang 95

 Xia, Ling 555
 Xia, Liya 433
 Xiao, Weiyue 285, 291
 Xiao, Wenxian 589, 629, 635
 Xiao, Xiao 71
 Xin, Gao Wei 221, 227
 Xing, Guojing 363
 Xu, Chunxiang 185
 Xu, Guozhen 533
 Xu, Jiping 25

 Xu, ShuangYing 151
 Xu, Xiangli 233
 Xu, Xiaorong 51
 Xu, YouSheng 77
 Xu, ZhiWei 749
 Xue, Shan 517

 Yan, Ai Xiao 257
 Yan, Dong 387
 Yan, Guangrong 453
 Yan, Tao 143
 Yan, Zou 393
 Yang, Chyan 647
 Yang, HaiZhu 245
 Yang, Jirong 285, 291
 Yao, Xiaokun 375
 You, Xine 43
 Yu, Miao 577
 Yu, Qing 479
 Yu, Sijia 453
 Yu, Xiaojun 163
 Yu, Yang 653
 Yu, Yunliang 113, 119
 Yu, Zhezhou 233
 Yue, Qiangbin 509
 Yu-Ke, Chen 393

 Zeng, Xin 735
 Zha, Yabing 533
 Zhang, Changhui 479
 Zhang, Chenghui 363
 Zhang, Dong-xue 265
 Zhang, Hangsen 371
 Zhang, Jing 501
 Zhang, Jingchang 203
 Zhang, Lei 151
 Zhang, Libiao 233
 Zhang, Ling 583, 589, 755
 Zhang, LingFeng 43
 Zhang, Liumei 175
 Zhang, Min 501
 Zhang, Pei-Yan 671
 Zhang, Ping chuan 371
 Zhang, Tao 629, 635
 Zhang, Tingting 113, 119
 Zhang, Xiaolan 473
 Zhang, Xiao-yu 433
 Zhang, XuanPing 615
 Zhang, YanE 95
 Zhang, Ying 203

- Zhang, ZhiQiang 577
Zhao, Huihong 363
Zhao, Qian 271
Zhao, Wei 659
Zhao, Xiang 509
Zhao, Xiaoping 25
Zhao, Xingqun 555
Zhao, Yanru 421
Zhao, Yongjian 309, 427
Zhao, YongQiang 1
Zhao, Yu 561
Zhao, Yun 13
Zheng, Bin 665, 683
Zheng, Bo 277
Zheng, JiangBo 33
Zheng, Shuang 743
Zhongshe, Gao 695
Zhou, Chunguang 233
Zhou, Huixiang 163
Zhu, Liping 63
Zhuang, Ling 727
Zou, Cunwei 485